Handbook of Oral Biomaterials

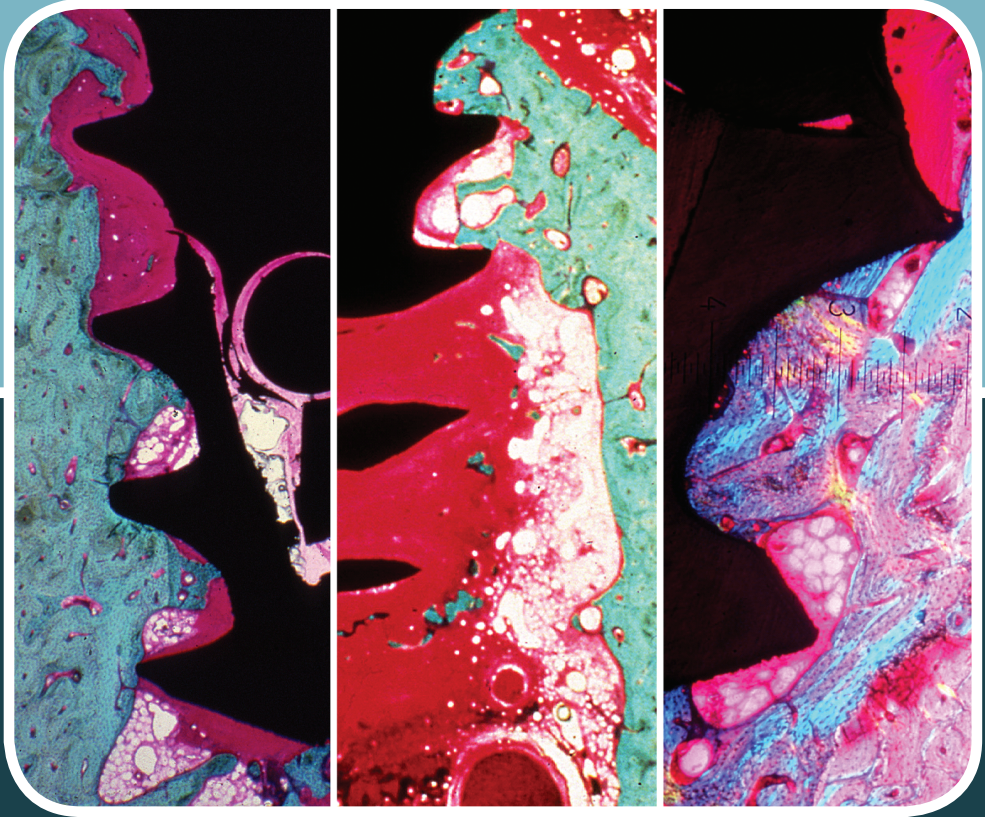

edited by

Jukka P. Matinlinna

Handbook of Oral Biomaterials

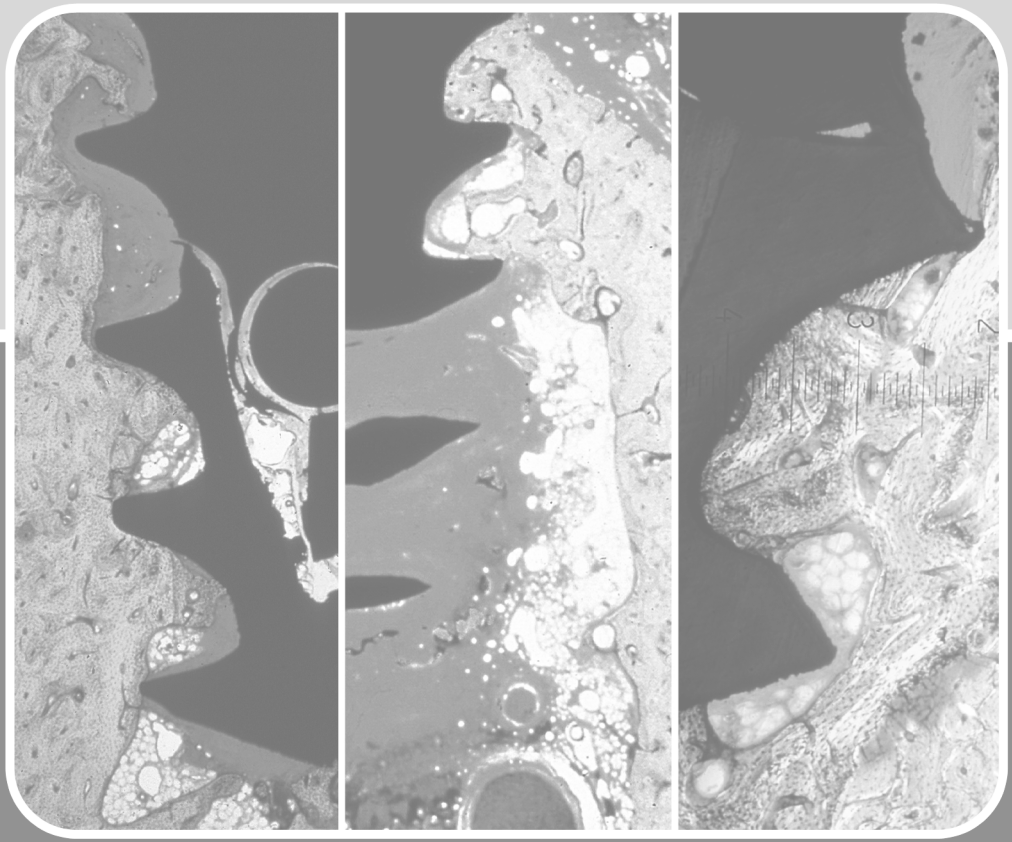

This page intentionally left blank

Handbook of Oral Biomaterials

edited by

Jukka P. Matinlinna

Pan Stanford Publishing

CRC Press
Taylor & Francis Group
6000 Broken Sound Parkway NW, Suite 300
Boca Raton, FL 33487-2742

Version Date: 20140612

International Standard Book Number-13: 978-981-4463-13-3 (eBook - PDF)

Contents

Preface xix

1. Bonding in Dentistry **1**

Bart Van Meerbeek, Kirsten Van Landuyt, Kumiko Yoshihara, André Poitevin, Jan De Munck, and Marleen Peumans

1.1 Introduction 2
1.2 The AD Concept Revisited as a Fundament of Dental Bonding 3
1.3 Adhesive Approaches and Nomenclature (Classification) 6
1.4 Glass Ionomers 7
1.5 Etch-and-Rinse Adhesives 11
1.5.1 The Degradation-Prone E&R Bond to Dentin 18
1.5.2 Strategies to Improve the Resistance of E&R Hybrid Layers against Degradation 22
1.5.2.1 Ethanol wet bonding to improve hybridization 22
1.5.2.2 Application of MMP inhibitors to prevent enzymatic bond degradation 23
1.5.2.3 Biomimetic repair of E&R hybrid layers 25
1.6 Self-Etch Adhesives 26
1.6.1 Major Shortcomings of One-Step SEAs 28
1.6.2 No Use of Strong SEAs 31
1.6.3 Use of Mild SEAs 32
1.6.4 Improved Bond Durability through Chemical Bonding and Interfacial Nanolayering 34
1.6.5 Self-Etching and the Smear Layer 38

1.6.6 Self-Etching Enamel and Recommendation to Selectively Phosphoric-Acid-Etch Enamel 39
1.7 Self-Adhesive Composites 42
1.8 Clinical Performance of Adhesives and Its Prediction in the Laboratory 44
1.9 Conclusion: Today's Most Ideal Adhesive Approach to Achieve Durable Bonding 46

2. Biomineralization and Biodemineralization of Enamel 57
Maisoon Al-Jawad and Paul Anderson
2.1 Introduction 58
2.1.1 Primary and Secondary Mineralization 59
2.1.2 Biologically Controlled and Biologically Induced Mineralization 60
2.1.3 Amelogenesis 61
2.1.4 Remineralization 62
2.1.5 Hierarchical Length Scales in Enamel Structure 63
2.2 Atomic/Molecular Length Scale 64
2.2.1 Chemical Control of Biomineralization 64
2.2.2 Solubility of Calcium Hydroxyapatite 66
2.2.3 Proteins of Enamel Biomineralization 67
2.2.4 Proteins of Saliva 68
2.2.4.1 Proline-rich proteins 69
2.2.4.2 Cystatins 69
2.2.4.3 Histatins 69
2.2.4.4 Statherin 70
2.3 Nanometer Length Scale 70
2.3.1 Nanostructure of Enamel 70
2.3.2 Biodemineralization 73
2.3.3 Iatrogenic Remineralization Strategies 73
2.4 Micrometer Length Scale 73
2.4.1 Enamel Prism Mineralization 73
2.4.2 Enamel Caries 74
2.5 Macroscopic Length Scale 75
2.5.1 Tooth Morphology 75
2.5.2 Medicinal Enamel Mineralization 75
2.6 Conclusions 76
2.7 Further Reading 76

3. Materials in Dentistry **81**

Ammar A. Mustafa and Jukka P. Matinlinna

3.1 Classification of Dental Biomaterials 82
3.1.1 Restorative Dental Materials 83
3.1.1.1 Zinc oxide eugenol cement 85
3.1.1.2 Glass ionomer cement 86
3.1.2 Preventive Dental Materials 87
3.1.2.1 Dentifrices 87
3.1.2.2 Mouthwashes 89
3.1.2.3 Pit and fissure sealants 90
3.1.3 Gypsum 91
3.1.4 Waxes 93
3.1.5 . . . And the Rest 94
3.2 Metals 95
3.3 Ceramics 97
3.3.1 Dental Porcelain 98
3.3.2 Porcelain Fused-to-Metal Restorations 100
3.4 Polymers 104
3.5 Elastic Impression Materials 105
3.5.1 The Hydrocolloids 105
3.5.2 Colloids 105
3.5.3 Reversible Hydrocolloids: Agar 106
3.5.4 Irreversible Hydrocolloids: Alginates 107
3.6 Elastomers 110
3.6.1 Polysulfides 110
3.6.2 Polyether Impression Materials 111
3.6.3 Condensation Silicones 112
3.6.4 Addition Silicones 116
3.6.5 Is Silicon a Biomaterial? 117
3.6.6 Silicones as Biomaterials 118
3.7 Acrylic Materials 118
3.7.1 Denture Repair 123
3.7.2 Denture Rebasing 124
3.7.3 Tissue-Conditioning Liners 125
3.7.4 Orthopedics: Bone Cements 125
3.8 Resin Composites 125
3.9 Adhesion and Bonding 130
3.9.1 Atomic Bonds 130
3.9.2 Adhesion and Cohesion 131
3.9.3 Factors and Mechanisms of Adhesion 133

3.10 Basic Properties of Dental Materials 134
3.10.1 Biomechanical Properties 134
3.10.2 Hardness Tests 137
3.10.3 Physical Properties 138
3.10.4 Thermal and Electrical Properties 138
3.10.5 Rheological Properties 140
3.10.6 Chemical Properties 141
3.10.7 Kinetics and Thermodynamics 142
3.10.8 Biocompatibility 143
3.11 Dental Silver Amalgams 143
3.11.1 Mercury 144
3.11.2 About the Use of Dental Amalgams 145
3.11.3 Some Amalgam Chemistry and Physics 146
3.11.4 A Summary on Amalgams: Disadvantages and Advantages 148
3.12 What Is an Ideal Dental Biomaterial? 149

4. Biomechanics in Dentistry 155
Akikazu Shinya
4.1 Moments Affecting Dental Materials and Tissues 156
4.2 Types of Force 157
4.2.1 Force: Newton's Laws 157
4.3 Bending Moment 158
4.3.1 Section Modulus 160
4.4 Stress and Strain 160
4.4.1 Stress–Strain Diagrams 161
4.4.2 Modulus of Elasticity 161
4.4.3 Proportional Limit 163
4.4.4 Yield Point 163
4.4.5 Ultimate Strength 163
4.5 Tension, Compression, and Shear 164
4.5.1 Tension 164
4.5.2 Compression 164
4.5.3 Shear 165
4.6 Stress (Strain) Distributions and Concentrations 165
4.7 Stress, Strength, and Fracture 167
4.7.1 Fracture Mode 169
4.7.2 Crack Separation Modes 170

4.7.3 Fracture Toughness 170
4.7.4 Stiffness 170

5. Biocompatibility 173
Alexander T. H. Tang
5.1 Introduction and Consensus Definitions 174
5.2 Dose and Host Responses 175
5.2.1 Dose-Response Curve 176
5.2.2 Water Fluoridation 177
5.2.2.1 Dental fluorosis as an adverse effect 177
5.2.2.2 Fluoride dose (*x* axis) 181
5.2.2.3 Quantification of adverse effects (*y* axis) 182
5.3 Non-Paracelsian Adverse Effects of Oral Biomaterials 184
5.3.1 Bis-GMA-Based Resin Composites 185
5.3.2 Hypersensitivity 189
5.3.3 Other Medical Issues 192
5.4 Three Levels of Testing 194
5.4.1 Test Design and Reproducibility 197
5.4.2 Reproducibility and Relevance of in vitro Cytotoxicity 200
5.4.2.1 Assessment of cytotoxicity of the test setting 200
5.4.2.2 Assessment of reproducibility 201
5.4.2.3 Rationalising "relevance" 201
5.4.3 Alternative Pathways in Biocompatibility Studies 202
5.5 Concluding Remarks 203

6. Resin-Based Cements Used in Dentistry 213
William M. Palin and Jack L. Ferracane
6.1 Introduction and Historical Perspectives 214
6.1.1 Evolution of Dental Cements 214
6.1.2 Contemporary Dental Cements 217
6.2 Key Material Properties of Resin Cements 219
6.2.1 Chemistry and Curing Mechanisms 219

6.2.1.1 General composition 219
6.2.1.2 Self-etch and self-adhesive composition 221
6.2.1.3 Initiation chemistry 223
6.2.2 Mechanical and Physical Properties 224
6.2.3 Biocompatibility 227
6.2.4 Clinical Performance 228
6.3 Mechanisms of Adhesion 230
6.3.1 Resin Cements with Adhesives 230
6.3.2 Self-Adhesive Resins 231
6.3.3 Resin Strengthening of Conventional Ceramics 232
6.3.4 Bonding to Polycrystalline Ceramics 235
6.3.5 Metal Adhesion 240
6.4 Future Trends 243

7. Glass Fibers in Fiber-Reinforced Composites 255
Pekka K. Vallittu
7.1 Overview of Fiber-Reinforced Composites 256
7.1.1 Role of the Resin 258
7.1.2 Interface between Glass Fibers and the Polymer Matrix 260
7.1.3 Chemical Composition of Various Glass Fibers 263
7.1.4 Effect of Water on the Properties of FRCs 265
7.2 Clinical Aspects and Use 266
7.2.1 Structure of Dental FRC Devices 266
7.2.2 Removable Dentures 267
7.2.3 Fixed Dental Prostheses 268
7.2.4 Root Canal Posts 271
7.2.5 Fiber-Reinforced Filling Composites 272
7.3 Future Development 273

8. Bioactive Glasses 281
Leena Hupa and Susanne Fagerlund
8.1 Background 282
8.2 Glass as a Biomaterial 285
8.3 Compositions of Melt-Derived Bioactive Glasses 287

8.4 Surface Reactions of Bioactive Glasses 289
8.4.1 Reaction Steps at the Glass Surface 289
8.4.2 In vitro vs. in vivo Surface Layers 292
8.5 Ion Dissolution vs. Cellular Response 293
8.6 Applications in Dentistry 299
8.6.1 Bone Regeneration 299
8.6.2 Treatment of Dental Hypersensitivity 300
8.6.3 Coatings Enhancing Osseointegration 302
8.7 Scaffolds for Tissue Engineering 303
8.8 Clinical Studies in Head and Neck Surgery 304
8.9 Commercial Products 304
8.10 Summary 305

9. Biological Activity of Titanium 317
Yo Shibata and Takashi Miyazaki
9.1 Initial Cell Adhesion 318
9.1.1 Wound-Healing Phenomena 320
9.2 Bone Tissue Responses 321
9.3 Biomechanical Considerations 322
9.3.1 Surface Roughness of Titanium Implants 322
9.3.2 Nanomechanical Evaluation of Biological Tissues 323
9.4 Bacterial Cell Responses 329
9.4.1 Killing Adherent Bacteria on Titanium Implants 330
9.4.2 Preventing Bacterial Cell Adhesion on Titanium Implants 331
9.5 Future Challenges and Directions 332

10. Titanium in Implant Dentistry 339
Niklaus P. Lang and Jukka P. Matinlinna
10.1 Titanium, Its Chemistry, and Biomechanics 340
10.2 Bonding to Titanium 341
10.3 Titanium Alloys 341
10.4 Titanium Oxides 343
10.5 Titanium Surface Properties and Surface Modifications 345
10.6 Surface Charges on Titanium 346
10.7 Oral Implants 348

10.8 Osseointegration 348
10.9 Clinical Aspects of Dental Implant Surfaces 352

11. Surface Pretreatment Methods and Silanization 359
Christie Ying Kei Lung and Jukka P. Matinlinna
11.1 Introduction 360
11.2 Surface Science 360
11.2.1 Interface and Surface Tension 360
11.2.2 Contact Angle 361
11.2.3 Critical Surface Tension 362
11.3 Theories of Adhesion 362
11.3.1 Mechanical Interlocking Theory 363
11.3.2 Wetting Theory 364
11.3.3 Diffusion Theory 364
11.3.4 Weak Boundary Layer Theory 365
11.3.5 Electrostatic Theory 365
11.3.6 Chemical Bonding Theory 365
11.4 Surface Characterization Techniques 366
11.4.1 Infrared Spectroscopy 366
11.4.2 Scanning Electron Microscopy 367
11.4.3 Energy Dispersive X-Ray Spectroscopy 367
11.4.4 Transmission Electron Microscopy 368
11.4.5 Atomic Force Microscopy 368
11.5 Surface Pretreatment Methods Used in Dental Laboratories 369
11.5.1 Hydrofluoric Acid Etching 369
11.5.2 Grit Blasting 370
11.5.3 Pyrochemical Silica Coating 370
11.5.4 Tribochemical Silica Coating 371
11.5.5 Silanization 371
11.6 Current Studies on Other Surface Pretreatment Methods 375
11.6.1 Chemical Treatment 375
11.6.2 Selective Infiltration Etching 376
11.6.3 Laser Treatments 376
11.6.4 Nanostructured Alumina Coating 377
11.6.5 Internal Porcelain Coating 377
11.6.6 Chemical Vapor Deposition 377
11.6.7 Plasma Fluorination 378

11.7 Mechanisms of Surface Pretreatment Methods 378
11.7.1 Hydrofluoric Acid Etching 379
11.7.2 Pyrochemical Silica Coating 379
11.7.3 Grit Blasting and Tribochemical Silica-Coating 380
11.7.4 Silanization 381
11.7.5 Chemical Treatments 384
11.7.6 Selective Infiltration Etching 385
11.7.7 Laser Treatments 386
11.7.8 Nanostructured Alumina Coating 386
11.7.9 Internal Porcelain Coating 387
11.7.10 Chemical Vapor Deposition 388
11.7.11 Plasma Fluorination 388
11.8 Conclusions 390

12. Sol-Gel Coatings on Titanium 399
Andy H. Choi and Besim Ben-Nissan
12.1 Introduction 399
12.2 Coating Techniques for Dental and Biomedical Applications 402
12.2.1 Plasma Spraying 402
12.2.2 Chemical Vapor Deposition 403
12.2.3 Physical Vapor Deposition 403
12.3 The Sol-Gel Technique 404
12.4 Sol-Gel Synthesis of Nanohydroxyapatite 406
12.5 Sol-Gel Synthesis of Hydroxyapatite Micro- and Nanocoatings 407
12.6 Cell Responses and Hydroxyapatite Coatings on Titanium 412
12.7 Mechanical Testing of Thin Films and Coatings 422
12.7.1 Instrumented Nanoindentation 422
12.8 Concluding Remarks 425

13. Internal Fixation in Oral and Maxillofacial Surgery 435
Roger A. Zwahlen
13.1 Introduction 436
13.1.1 Bone 436
13.1.2 Bone Healing 437
13.1.2.1 Indirect bone healing 437

13.1.2.2 Direct bone healing 437
13.1.3 Osteosynthesis 437
13.2 Titanium 439
13.2.1 Mechanical Properties 439
13.2.2 Biocompatibility 440
13.2.3 Clinical Applications 440
13.3 Oral and Maxillofacial Surgery 441
13.3.1 Clinical Applications in Oral and Maxillofacial Fractures 441
13.3.1.1 Mandibular fractures 442
13.3.1.2 Midfacial fractures 445
13.3.2 Clinical Applications in Orthognathic Surgery 447
13.3.3 Titanium Alloy as Substitution for Bone Defects 449
13.4 Alternatives to Titanium for Internal Fixation 451
13.4.1 Adverse Events of Titanium 451
13.4.2 Removal of Titanium Plates after Bone Healing 451
13.4.3 Polyhydroxyacids: Reabsorbable Osteosynthesis Materials 453
13.5 Epilogue 454

14. Zirconia and Implant Dentistry 459
Moustafa N. Aboushelib and Jukka P. Matinlinna
14.1 Zirconium, Alumina, and Zirconia 460
14.1.1 Zirconium Chemistry and Group IV A 460
14.1.2 Zirconia and Alumina 461
14.2 Biomedical Applications of Zirconia 464
14.2.1 Tissue Reactions around Zirconia Implants 464
14.2.2 Zirconia as a Dental Implant Material 465
14.2.3 Difficulties Related to Fabrication of Ceramic Implants 467
14.2.4 New Surface Treatments of Zirconia Implants 468
14.2.5 Future Composite Ceramics for Zirconia Implants 470
14.2.6 Precautions When Using Zirconia Implants and Abutments 470

15. Bonding to Zirconia **477**

Alvaro Della Bona and Jukka P. Matinlinna

15.1 Introduction: Is It Zirconium or Zirconia? 478
15.1.1 Zirconium and Its Alloys 478
15.1.2 Zirconia 480
15.1.3 Alumina 483
15.1.4 Zirconia Restorations and Their Preparation 484
15.2 Porcelain–Zirconia Bonding 486
15.2.1 Surface Treatments and Their Effects: Coloring 487
15.2.2 Sandblasting 487
15.2.3 Some Laboratory Observations 488
15.2.4 Porcelain–Zirconia Bonding Mechanism 489
15.2.5 Laser Methods in Dentistry 490
15.2.6 Zirconia in the Human Body 491
15.2.7 Some Zirconia Properties and Their Effects 492
15.2.8 Cooling Rate 493
15.2.9 More about Veneering 494
15.2.10 Some Clinical Experience and Observations 495
15.3 Resin–Zirconia Bonding 496
15.3.1 Adhesion Mechanisms 497
15.3.2 Bond Strength Tests and Fractography Analysis 502
15.3.3 Clinical Considerations for Resin Bonding to Zirconia 505

16. All-Ceramic Restorations on Implants **517**

Alvaro Della Bona and Marcia Borba

16.1 Introduction: Ceramic Materials 517
16.2 All-Ceramic Restorations 518
16.2.1 Glasses and Porcelains 519
16.2.2 Particle-Filled Ceramics 520
16.2.2.1 Hot-pressed leucite- and lithium disilicate–based ceramics 520
16.2.2.2 Glass-infiltrated ceramics 522

16.3 Polycrystalline Ceramics 524
16.3.1 Alumina-Based Polycrystalline Ceramics 524
16.3.2 Zirconia-Based Polycrystalline Ceramics 525
16.4 Ceramic Implant Abutments 526

17. Finite-Element Analysis in Dentistry 535
Andy H. Choi, Besim Ben-Nissan, and Richard Conway
17.1 Introduction 536
17.1.1 Element Type and Number 536
17.1.2 General Principles 539
17.1.3 Material Properties 541
17.1.4 Nonlinear Analysis 541
17.1.5 Convergence Test 542
17.2 Finite-Element Analysis in Dentistry 542
17.3 Finite-Element Analysis and Indentation in Dentistry 558
17.4 Finite-Element Analysis of Thin-Film Coatings 562
17.5 Concluding Remarks 567

18. Digital Dentistry and Dental Informatics 577
James Kit-Hon Tsoi
18.1 Digital Dentistry: Introduction 577
18.2 Digital Dentistry: Systems and Devices 580
18.2.1 CAD-CAM 581
18.2.2 Dental Imaging and Digital Impression 585
18.2.3 Digital 3D Printing 590
18.2.4 Digital Dental Biomaterials 591
18.3 Dental Informatics 592
18.3.1 Quality Assurance for Information 595
18.3.2 Real and Digital Dental Biomaterials: Interaction 597
18.3.2.1 Case 1: Impression materials simulation 597
18.3.2.2 Case 2: Dental biomaterials science education 599
18.3.2.3 Case 3: Dental drug discovery 600
18.4 Conclusions 604

19. Barrier Membranes for Periodontal Guided Tissue Regeneration Applications **605**

Zeeshan Sheikh, Mohamed-Nur Abdallah, Nader Hamdan, Mohammad Ahmad Javaid, and Zohaib Khurshid

19.1 Preamble 606
19.2 Guided Tissue/Bone Regeneration 607
19.3 Rationale, Biologic Interactions and Advantages of Barrier Membranes for Guided Regeneration Therapy 610
19.4 Ideal Properties of Barrier Membranes 612
19.4.1 Biocompatibility 612
19.4.2 Cell Occlusivity 613
19.4.3 Bioresorption 613
19.4.4 Tear Strength 613
19.4.5 Stiffness 613
19.4.6 Biological Activity 613
19.4.7 Clinical Manageability 614
19.5 Types of Barrier Membranes for Periodontal Guided Tissue Regeneration 614
19.5.1 Nonresorbable Barrier Membranes 617
19.5.1.1 Expanded polytetrafluoroethylene 618
19.5.1.2 Titanium-reinforced polytetrafluoroethylene 618
19.5.2 Resorbable Barrier Membranes 619
19.5.2.1 Natural resorbable barrier membranes 619
19.5.2.2 Synthetic resorbable barrier membranes 623
19.6 Factors Influencing Success of Guided Regeneration Therapy Using Barrier Membranes 626
19.6.1 Plaque Control and Microbial Contamination 626
19.6.2 Defect Morphology and Tooth Anatomy 627
19.6.3 Membrane Exposure 627
19.6.4 Defect Space Maintenance 628

19.6.5 Diabetes 628
19.6.6 Gingival Flap Thickness 628
19.6.7 Smoking 628
19.7 Summary and Future Considerations 629

Index 637

Preface

Congratulations and my most humble thanks to you, our reader! I believe that this reading and learning experience with *Handbook of Oral Biomaterials* is something unique in our scientific community. We, the contributors, wish you to enjoy these 19 brand new and unforeseen chapters that introduce you to and facilitate your understanding of oral biomaterials. *Handbook of Oral Biomaterials* provides you with the latest updates and advances in dental materials and dental biomaterials. This book lays special emphasis on materials used in implant dentistry, but it also covers other clinically vital aspects and indications of dental biomaterials.

What is contemporary dentistry, then? My definition that all my undergraduate and postgraduate students in Hong Kong, since 2008, have heard is that "dentistry is all about adhesion, biochemistry, biocompatibility, biofilms, bioinformatics, biology, biomaterials, biomechanics, biomineralization and beyond." In this book we come across these disciplines, at least concisely.

The initiative for this book came from the Singapore publisher Mr. Stanford Chong of Pan Stanford Publishing Pte Ltd., who contacted me sometime in late 2011. Mr. Chong had paid attention to the serious and continuous lack of a proper updated textbook on titanium and zirconia as materials in dentistry. This invaluable observation was remarkable, as titanium and zirconia are growingly materials of choice in various disciplines in dentistry: implant dentistry, oral and maxillofacial surgery, prosthodontics, endodontics, etc. Hence, special emphasis on these contemporary materials of choice in dentistry was born and now sees daylight.

The chapters aim at going easily and directly to business, without compromising the context. Given this, we may not go deep into details of the physicochemical phenomena behind (but we do take a concise and clinically adequate glance), but then we refer to some other sources. We all may agree that there is a continuous need for a comprehensive but, at the same time, crystallized, easy-to-digest information package for undergraduate and postgraduate students, researchers, mentors, facilitators, clinicians, tutors, and teachers.

This book aims at adding value, with its novelty and updates, to the existing clinical textbooks and textbooks on materials science. Basic sciences are included, as appropriate, to support clinical dental sciences. All the chapters also provide our readers with appropriate and recent references to discover the topics deeper and thus deepen their understanding.

Do we cover *all* dental materials, dental biomaterials, and materials in dental technology in *Handbook of Oral Biomaterials*, then? I am confident that we cover or at least introduce, in addition to some procedures in operative dentistry, restorative materials, and dental cements, ceramic materials, polymers, metal and alloys, bioactive glasses, modern resin composite materials, surface-conditioning approaches, primers and their monomeric components, and modeling approaches. We don't discuss dental instruments, burs, or procedures at dental laboratories—how important they of course are. We refer again to some other existing textbooks by our colleagues. Please, let me know, if I am wrong in saying this, and drop a few lines (or more): jpmat@hku.hk.

Handbook of Oral Biomaterials, with its total 649 pages, is constructed on a principle that certain concepts are handled time after time in different contexts in the book in its 19 chapters. This is why, for example, *adhesion* as a vital dental phenomenon is covered in several contexts and occasions throughout the book. There are some other topics dealt following this principle as well. We believe that this effectively facilitates learning. *Handbook of Oral Biomaterials* is probably the first dental textbook to include a chapter on dental informatics and digital dentistry (Chapter 18). We, the contributors, are building up tomorrow's dentistry. We present the whole "dental chain" from etching enamel and dentin and primer systems (Chapter 1) to mineralization processes (Chapter 2), primers and coupling agents (Chapters 1 and 11), biological activity (Chapter 9), and biocompatibility (Chapter 5), ending with restorative materials (Chapters 3 and 6). Metals, alloys, polymers, waxes, and, in particular, acrylic materials find an easy-to-access platform in Chapter 3. We also go for explaining surface treatments and gaining an understanding of why it is significant (Chapter 11). In addition, the role of biomechanical aspects is covered in Chapters 3, 4, and 17. The oral and maxillofacial world is illuminated in Chapter 13, and periodontal guided tissue generation is dealt with in Chapter 19.

Resin composite–based materials are widely discussed in Chapters 3, 6, and 7. Whilst titanium is discussed in Chapters 9, 10, and 13, bioactive coatings on titanium are summarized in Chapter 12. Glasses in various chemical compositions finding promising applications in dentistry are exhibited in Chapters 7 and 8. Ceramic materials in dentistry, in particular alumina and zirconia, are widely discussed in Chapters 3 and 14–16. Virtually any material in dentistry and dental technology is introduced, at least to a certain extent, in Chapter 3, in addition to clinically important material properties.

As this is the dawn, the first edition, we are obviously collecting the readers' experience and remarks for the content. I am indebted to our Dean, Chair Professor Edward C. M. Lo (University of Hong Kong, People's Republic of China) for his support, Professor Jukka H. Meurman (University of Helsinki, Finland), Professor Nabil Samman (University of Hong Kong, People's Republic of China), and Professor Mohamed Ibrahim Abu Hassan (Universiti Teknologi MARA, Shah Alam, Malaysia) for their reviews of the manuscript and comments on the back cover of this book. With the chapter contributors, we have been a tremendous seamless team, scattered geographically all over the world (from Australia, Belgium, Brazil, Canada, Egypt, Finland, Hong Kong SAR of the People's Republic of China, Japan, Malaysia, Pakistan, Switzerland, UK, and USA), working toward this final outcome. I am deeply grateful to every one of you for your invaluable input and support. Thank you so much from the bottom of my heart, my colleagues and friends Aki, Alex, Alvaro, Ammar, Andre, Andy, Bart, Besim, Christie, Jack, James, Jan, Kirsten, Klaus, Kumiko, Leena, Maisoon, Marcia, Marleen, Mohammad Ahmad, Mohamed-Nur, Moustafa, Nader, Paul, Pekka, Richard, Roger, Susanne, Takashi, Will, Yo, Zeeshan, and Zohaib. Dr. Christie Y. K. Lung (University of Hong Kong) is warmly acknowledged for drawing numerous figures in Chapter 3.

In addition, I want to express my deepest gratitude to Mr. Stanford Chong for accepting the manuscript of *Handbook of Oral Biomaterials* for publication and to his editorial and production team. I am deeply grateful to my dear, sweet daughter, Salli, who timely reminded me of my years-old dream to one day edit a textbook and encouraged me to go for it. Thank you for the initiation, interest, and endless support. Most of all, I am indebted to my dear wife, Suzie, for her dental expertise, unconditional love, never-ending support, partnership, inspiration, and faith in me during this book project.

It is not only for her never-ending technical support in my text creation and editing but also for the time I had to use. Suzie, having you in my life as my partner is God's true blessing.

Dr. Jukka Pekka Matinlinna
Pok Fu Lam, Hong Kong SAR,
People's Republic of China
April 2014

Disclaimer

The material in this textbook, *Handbook of Oral Biomaterials*, whether related to dentistry, medicine, or any other topic, should be verified as to its accuracy, currency, and preciseness by the reader.

It should in no way replace any advice given by a dental or medical professional or any other professional.

None of the information provided here should be a substitute for additional reading advice, experience, or other relevant information in any topic discussed in this book.

This page intentionally left blank

Chapter 1

Bonding in Dentistry

Bart Van Meerbeek, Kirsten Van Landuyt, Atsushi Mine, Kumiko Yoshihara, André Poitevin, Jan De Munck, and Marleen Peumans
KU Leuven BIOMAT, Department of Oral Health Sciences, KU Leuven (University of Leuven) & Dentistry, University Hospitals Leuven, Leuven, Belgium
bart.vanmeerbeek@med.kuleuven.be

Current dental adhesive technology follows either an *etch-and-rinse* or a *self-etch* approach. Although functional monomers in self-etch adhesives are designed to chemically interact with hydroxyapatite (HAp), the structure, size, and orientation of enamel HAp crystals appear to provide insufficient chemical-bonding sites to achieve durable bonding to enamel. At dentin, phosphoric acid (H_3PO_4) may today be less preferred, as the adhesives are generally not capable of enveloping the exposed collagen tight enough, so as to make the relatively thick hybrid layer resistant to hydrolytic and enzymatic degradation processes. Also, the use of matrix metalloproteinase (MMP) inhibitors, to be applied separately or mixed with the primer/adhesive, appeared to retard rather than prevent bond degradation. Another strategy in the search for durable bonding to dentin involves chemical interaction of functional monomers with HAp.

Handbook of Oral Biomaterials
Edited by Jukka P. Matinlinna

ISBN 978-981-4463-12-6 (Hardcover), 978-981-4463-13-3 (eBook)
www.panstanford.com

This chapter will sketch the current status of scientific knowledge regarding bonding approaches to enamel and dentin, thereby also addressing the most recent findings on molecular interaction of diverse functional monomers with HAp and on a new interfacial nanoscale phenomenon termed *nanolayering*.

1.1 Introduction

Teeth, affected by decay or trauma, are today best reconstructed in their function, anatomy, and esthetics using the least invasive restorative procedure [1, 2]. This treatment objective can best be achieved when the restorative material, either composite or ceramic, is bonded to the remaining sound tooth tissue that is no further sacrificed (as it, for instance, is/was needed to hold the amalgam in the prepared cavity). Today, dental adhesive technology is therefore applied for many restorative direct, semidirect, and indirect indications. The current chapter will focus mainly on the use of dental adhesives for direct restorative purposes. As such, contemporary dental adhesives have gradually evolved from systems that require a relatively complex *multistep* application procedure to *simplified* adhesives with user-friendlier application protocols in fewer steps [3]. The current trend is obviously *fast and easy*, although this is not always achievable without significant loss in effectiveness. Most recently, the ultimate form of easy application was reached with the introduction of *self-adhesive* (flowable) resin composites that have been claimed to no longer need any separate adhesive to bond to tooth enamel and dentin [4] (see also Chapter 6).

The main challenge for dental adhesives is to provide an equally effective bond to two hard tissues of different nature. Bonding to *enamel* has been proven to be durable. Bonding to *dentin* is far more intricate and can apparently only be achieved when more complicated application procedures are followed. Moreover, usually a significantly shorter clinical lifetime is achieved than in the case of bonding to enamel. Consequently, today's adhesives are often regarded as technique sensitive, with the smallest error in the clinical application procedure being penalized either by relatively rapid debonding or by early marginal degradation. As a consequence, the

demand for simpler, more user-friendly, and less technique-sensitive adhesives remains high, urging manufacturers into developing new adhesives at a rapid pace.

It is fair to state that glass ionomers (GIs) certainly also should be regarded as self-adhering restorative materials. They have clinically been used already for a very long time since the first paper in 1972 reported on this, at that time, "new translucent cement for dentistry" [5]. Despite the fact that there have recently not been much new developments in GI technology, nearly every contemporary dental practice has GI cements available for restorative bonding, typically to be employed in usually less-moisture-controlled situations.

Different from GIs, current resin-based adhesive technology follows either an etch-and-rinse (E&R) or a self-etch (SE; or *etch-and-dry*) approach. They differ significantly in the manner they deal with tooth tissue [3]. Nevertheless, it should be stated that both approaches have performed successfully in laboratory as well as in clinical research, while obviously there also exists high product dependency.

The objective of Chapter 1 is to sketch the current status of adhesive technology in terms of mechanisms, strengths, and weaknesses, thereby also reporting on their effectiveness in the laboratory as well as clinically in the patient's mouth.

1.2 The AD Concept Revisited as a Fundament of Dental Bonding

To bond to tooth substrate, basically both *micromechanical* as well as *chemical bonding* mechanisms can be employed. While micromechanical interlocking has long been considered the only mechanism involved and probably today still might be the principal mechanism of adhesion, more recent research has definitely highlighted the added value of additional chemical interaction. Obviously, chemical intermolecular interaction at the interface between functional monomers provided with a dental adhesive and primarily the mineral substances of tooth tissue is most intimate and should therefore always be strived for. Chemical bonding is particularly thought to improve bond durability [3].

The way molecules interact with an HAp-based substrate, like tooth enamel and dentin but also bone, has been described well in the so-called *adhesion-decalcification concept*, or the AD concept [6, 7] (Fig. 1.1). In the first phase, an acidic molecule will always ionically interact with Ca^{2+}, abundantly present in HAp (see Fig. 1.1, **phase I**). To keep the surface electroneutral, negatively loaded ions, like hydroxide (OH^-) and phosphate (PO_4^{3-}), will be released from the surface. For **phase II**, two options exist. Whether the molecule will remain bonded (Fig. 1.1, **phase II**, **option 1**) or will debond (Fig. 1.1, **phase II**, **option 2**) depends on the stability of the formed bond to Ca^{2+}, or in other words on the stability of the respective calcium salt.

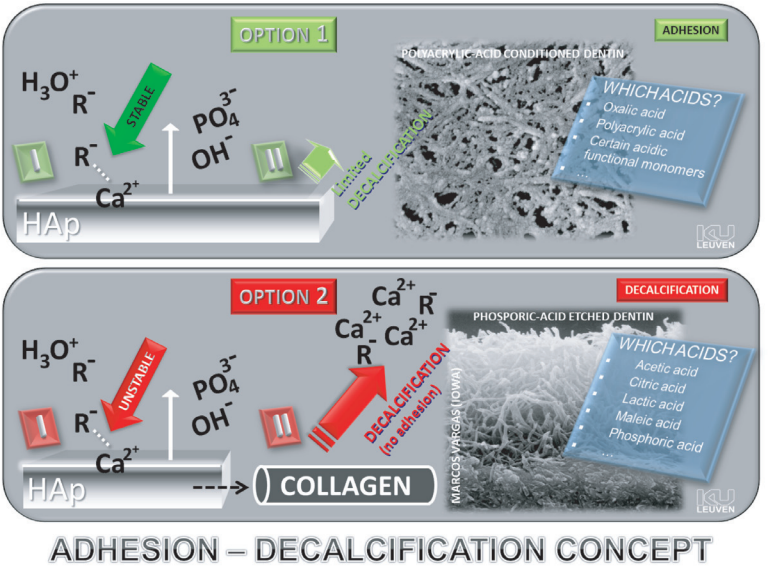

Figure 1.1 Schematic explaining the *AD concept*, consisting of a common phase I and a subsequent **adhesion** route (phase II, option 1; in green), when the initial bond of the acidic molecule to Ca^{2+} of HAp is stable, or a subsequent **decalcification** route (phase II, option 2; in red), in case the initial bond of the acidic molecule to Ca^{2+} of (HAp) is unstable.

When the initial bond is stable (Fig. 1.1, **phase II**, **option 1**), the acidic molecule will remain bonded (**adhesion** route), forming

stable calcium phosphate or calcium carboxylate salts, along with only a limited surface decalcification effect. Indeed, the surface gets only lightly decalcified, like in nature there always exist a kind of balance with, in this case, primarily bonding combined with some decalcification. The latter is beneficial because it will still provide significant micromechanical interlocking that thus is complemented by primary (ionic) chemical bonding. Consequently, the interaction occurs much more superficial (commonly less than 1 μm deep) and will, for instance, at dentin keep collagen covered (protected) with HAp that then serves as a receptor for chemical bonding. This process is imposed by acids like oxalic acid (e.g., commonly used in the form of oxalates for dentin/root hypersensitivity treatment or as an intermediary step in a bonding procedure to prevent postoperative sensitivity), *polyalkenoic acid* (PAA) (as the main active ingredient of GIs), and diverse functional monomers of resin-based dental adhesives as those, for instance, in the "mild" and "ultramild" self-etch adhesives (SEAs) (see below and Chapter 3).

When the bond is not stable (Fig. 1.1b, **phase II**, **option 2**), the initial ionic bond will readily dissociate (actually immediately or even simultaneously so that the bonding phase I hardly can be detected). The negatively loaded acidic molecule (phosphate and/or carboxylate ions) will take the positively loaded (and thus electrostatically attracted) Ca^{2+} from the mineral substrate with it to result in a relatively ample decalcification (**decalcification** route) up to a certain depth depending on the application time. Such surface decalcification or **etching** is induced by acids like acetic acid, citric acid, lactic acid (e.g., during the process of caries produced by bacteria), maleic acid (e.g., having been used a long time ago as a tooth conditioner provided with the very popular Scotchbond Multi-Purpose™, from 3M at that time), and, of course employed almost with each adhesive procedure today, phosphoric acid. Indeed, the most typical and relevant example is phosphoric acid etching as part of the E&R bonding approach (see below) used to provide a means for micromechanical interlocking and thus to produce a highly microretentive surface at enamel and to expose collagen at dentin as a scaffold to be impregnated by resin during subsequent hybridization.

1.3 Adhesive Approaches and Nomenclature (Classification)

To bond to tooth tissue, the above-mentioned basic micromechanical and chemical mechanisms are employed to a different extent by the three different approaches: the GI, the E&R, and the SE approach [3] (Fig. 1.2).

Classifying dental adhesives into different categories is not straightforward because of the great supply and vast turnover of commercially available adhesives. Although a *classification in generations* is still quite often used in certain areas of the world, in scientific as well as commercial literature, this chronological classification is not logical, lacks scientific background with regard to the bonding strategy followed, is often commercially misused, and most importantly does not provide any clear information to practitioners with regard to their correct use [8, 9].

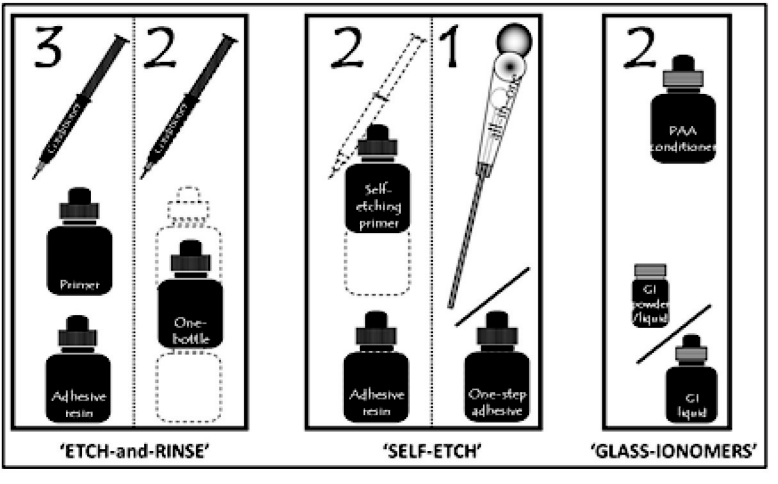

Figure 1.2 Classification of adhesives according to the adhesive approach and the number of clinical application steps. From Ref. [10].

Classifying adhesives into E&R adhesives (E&RAs) and SEAs, as opposed to GIs, is simple, reliable, and consistent and, in particular, better describes the adhesive strategy involved [3]. Further subdivisions are made on the basis of the number of application steps (*one-step*, *two-step*, and *three-step* adhesives), the number

of components (*one-component* or *two-component* adhesives, the latter needing to be mixed), and, especially with regard to, SEAs [8, 10, 11] on the basis of their interaction intensity into *strong* (pH < 1), *intermediately strong* (pH ≈ 1.5), *mild* (pH ≈ 2), and *ultramild* (pH ≥ 2.5) SEAs (Fig. 1.3).

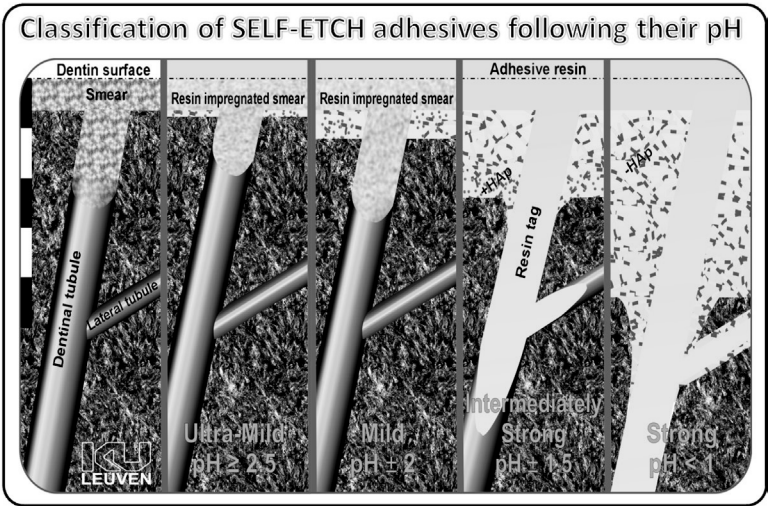

Figure 1.3 Schematic illustrating the interfacial structure produced at dentin by the four classes of SEAs following their pH. Adapted from Ref. [10].

1.4 Glass Ionomers

Conventional and resin-modified (RM) GIs are in principle self-adhering but may suffer from interference of surface debris as they are smeared across enamel and dentin during cavity preparation by a bur (Fig. 1.4). Therefore, clinicians are generally recommended to pretreat the cavity with a PAA conditioner (Figs. 1.2, 1.4, and 1.5). This conditioner has a threefold purpose (Figs. 1.4 and 1.6): **(1)** obviously to clean the surface and remove bur-smear debris, **(2)** to provide rather shallow microretention sites for the primary micromechanical bonding mechanism, and **(3)** to keep HAp around collagen to serve as a receptor for the additional and for GIs' crucial chemical-bonding mechanism (Fig. 1.7).

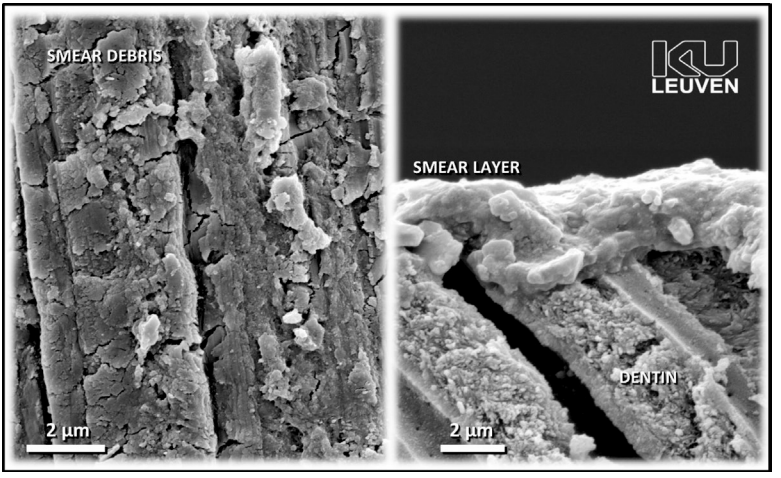

Figure 1.4 SEM photomicrographs showing the deposition of a smear layer on dentin upon cavity preparation using a diamond bur. *Abbreviation*: SEM, scanning electron microscopy.

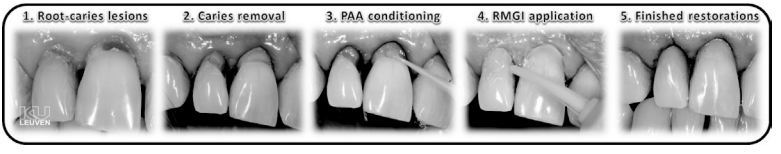

Figure 1.5 Clinical series of typical root caries lesions restored with an RMGI after the surface was conditioned with a PAA conditioner. *Abbreviation*: RMGI, resin-modified glass ionomer.

This PAA conditioner needs still to rinsed off, thus leaving room for improvement regarding ease of use. For RMGIs, an alternative SE conditioner (Self-conditioner™, GC), which does not need to be rinsed off, appeared equally successful; it contains 4-methacryloxyethyl trimellitic acid (4-MET) (see below) as a functional monomer in a 2-hydroxyethyl methacrylate (HEMA)/water/ethanol solution [12]. Unfortunately, this GI SE conditioner is only available in certain parts of the world. Most detrimental to GIs would obviously be to condition the cavity surfaces with phosphoric acid, because then all HAp would be removed (and collagen exposed), losing the chemical-bonding mechanism.

The conditioner also results in hybrid-layer formation of a submicron size, which is typical of GIs (Figs. 1.7 and 1.8). This

hybrid layer is rich in HAp and has no collagen exposed. The unique property of self-adhesiveness of *polycarboxylic acid* based materials has already since long been suggested to involve chemical bonding [5, 13]. Hypothetical models were later suggested that the (self) adhesion is based either on *diffusion* of the PAA into the softened tooth surface [14] or on the formation of *ionic bonds* to the HAp component of the mineralized tissue [15, 16]. Direct evidence of ionic interaction of the functional carboxyl groups of PAA was however only provided using X-ray photoelectron spectroscopy (XPS) by Yoshida et al. in 2000 [17].

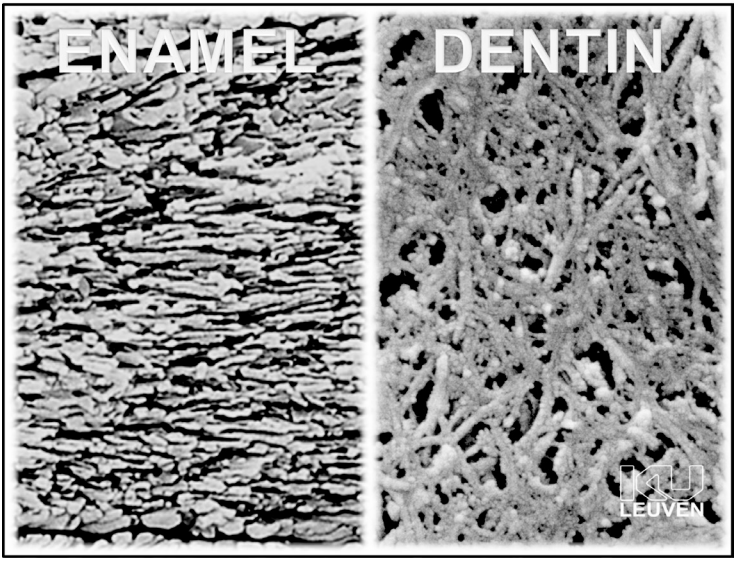

Figure 1.6 SEM photomicrographs illustrating enamel and dentin after treatment with a PAA conditioner.

According to the AD concept [6, 7], PAA is a polymer with a multitude of carboxyl functional groups that as chemical "hands" grab individual Ca^{2+} ions along the mineral substrate, thereby following the AD concept phase II, option 1 (cf Fig. 1.1). This chemical bonding, combined with micromechanical interlocking through shallow hybridization, establishes the unique self-adhesiveness of GIs (even without any form of beforehand treatment but then slightly worse). GIs have clinically indeed been recorded with the lowest annual failure rate with regard to class V adhesive restorations [19].

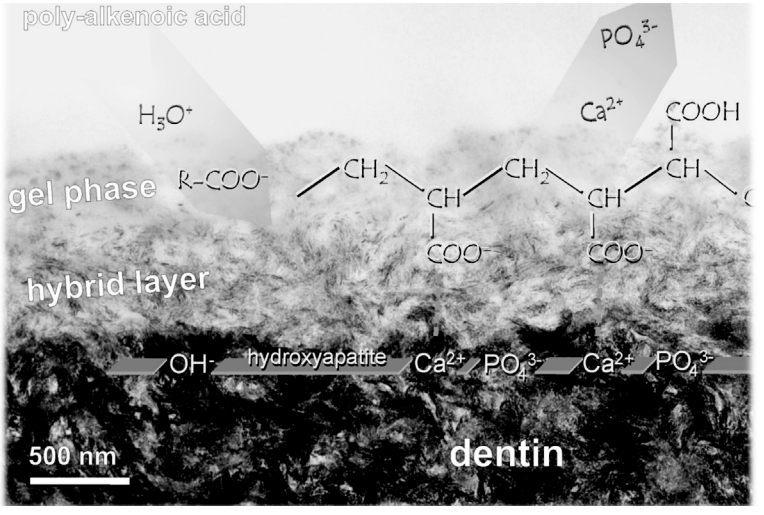

Figure 1.7 TEM photomicrograph illustrating the submicron HAp-rich hybrid layer produced by an RMGI after PAA conditioning and the typical gel phase deposited on top [18]. Within the hybrid layer, sufficient HAp remains available for ionic interaction with the carboxyl groups of PAA as the functional polymer within the GI conditioner and the RMGI restorative material itself. *Abbreviation*: TEM, transmission electron microscopy.

Not very remarkable innovations in GI technology have lately been reported. Heat-curing of conventional (resin-free) GIs using ultrasonic excitation or by heat produced by curing lights was shown to improve the mechanical properties of GIs at an early setting time [20]. This provides a clinically attractive ”command” setting method to conventional GIs, allowing GI restorations to be finished/polished earlier (without the need to wait sufficiently long for the chemical setting) and resulting in surface properties that make the GI restoration more resistant to early wear.

Alternatively, also effective is the use of a separate SE coating to be applied on top of the GI restoration, following the commercialized Equia™ concept (GC). This nanofilled self-adhering GI coating (Equia Coat™, or before marketed as G-Coat™, GC) basically serves a similar purpose as the heat curing above—to protect the GI during early maturation [21, 22]. In addition, it also helps to protect the restoration margins as the coating layer bonds not only to the GI itself but also to the surrounding tooth tissue, thereby providing

an extra seal to the margins. It also helps the practitioner to finish the restoration, as the finished GI surface is covered by a resin gloss, making further polishing needless (Fig. 1.9).

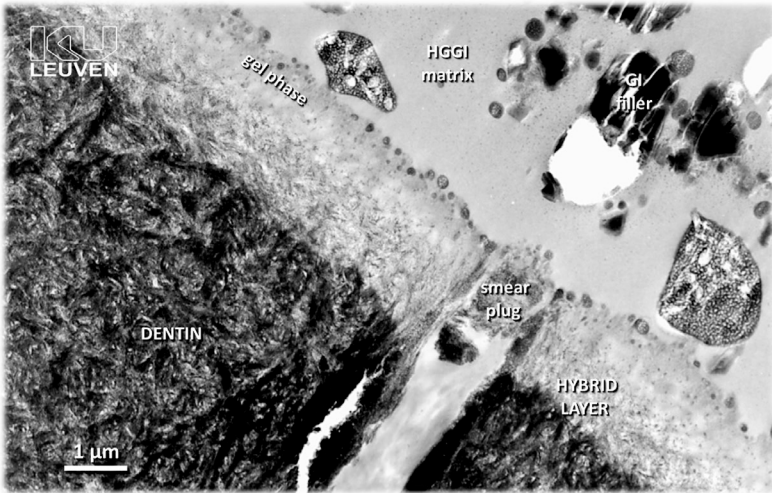

Figure 1.8 TEM photomicrograph illustrating the submicron HAp-rich hybrid layer and gel phase produced by an RMGI.

Future developments in GI technology may be expected with regard to mechanically stronger GIs (perhaps using other stronger filler technology), still better esthetic potential (e.g., better polishability), and more active therapeutic potential in light of tissue mineralization. Conventional GIs are free of resins and remain therefore of interest as a technology for the development of true amalgam alternatives, now that official bodies such as the World Health Organization (WHO) strive for phasing down dental mercury [23], while resin-based restorative materials are also not free of biocompatibility issues.

1.5 Etch-and-Rinse Adhesives

Following an *E&R process*, the fundamental mechanism of bonding to enamel and dentin is essentially based on an exchange process, in which minerals removed from the dental hard tissues are replaced by resin monomers, which upon polymerization become

micromechanically interlocked in the created porosities [9]. This process, which is called *hybridization* on dentin [24], is a process primarily based upon diffusion and thus basically requires monomers that diffuse efficiently a few micrometers deep and into the hydrophilic collagen fibril network. Naturally, besides tight envelopment of the exposed collagen fibrils by resin, the strength and durability of the formed hybrid layer will also depend largely on adequate in situ polymerization of the infiltrated monomers.

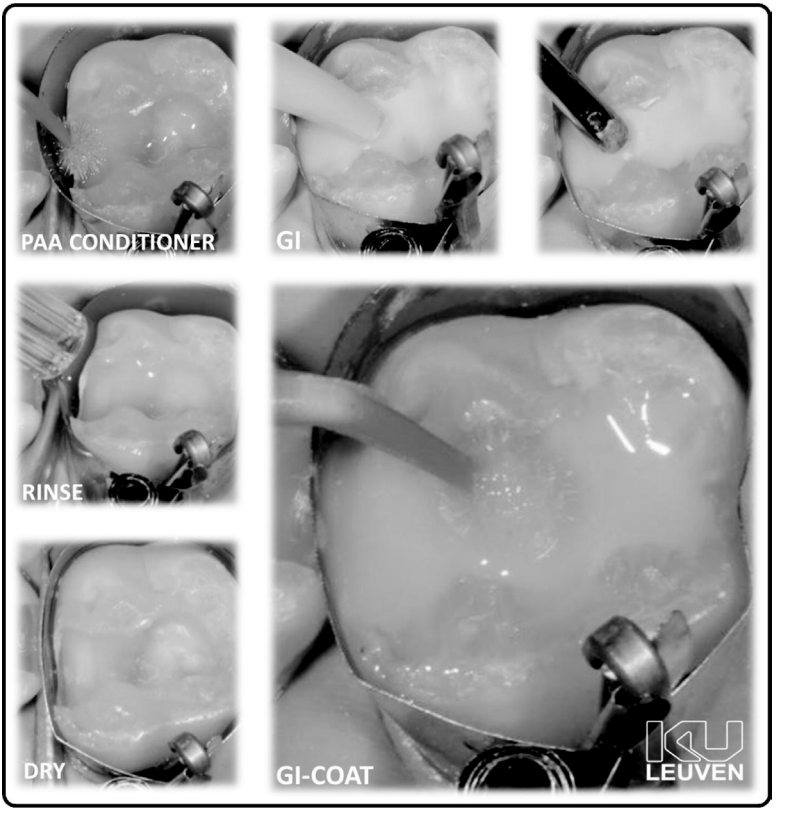

Figure 1.9 Clinical series of a primary molar restored with the conventional GI Equia™ system (GC). It involved as a final step the application of a resin gloss to finish the GI restoration and protect it, in particular, during the early setting phase.

The most commonly used etchant today contains phosphoric acid in a concentration of 30–40%. Following the AD concept [6, 7],

it will initially bond to Ca^{2+} of HAp (AD concept phase I) but will readily debond (AD concept phase II, option 2) and thus *etch* the tooth surface (cf Fig. 1.1).

At the *enamel*, phosphoric acid substantially increases the surface free energy of enamel by partially dissolving the parallel-oriented enamel HAp crystals, producing deep etch pits between neighboring HAp rods (Fig. 1.10). Upon rinsing and (gently) drying, the typical white-frosted pattern appears and gives the clinician a visual indication if enamel was effectively etched (Fig. 1.11). Subsequently, the application of a simple unfilled resin is sufficient to readily infiltrate, as promoted by capillary attraction, the created microretentions. This *acid-etch technique*, as originally invented by R. Buonocore in 1955 is still today without doubts the most effective procedure to durably bond to enamel [25]. This enamel bond has been shown to durably seal the cavity margins and even to protect the weaker adjacent dentin bond [26].

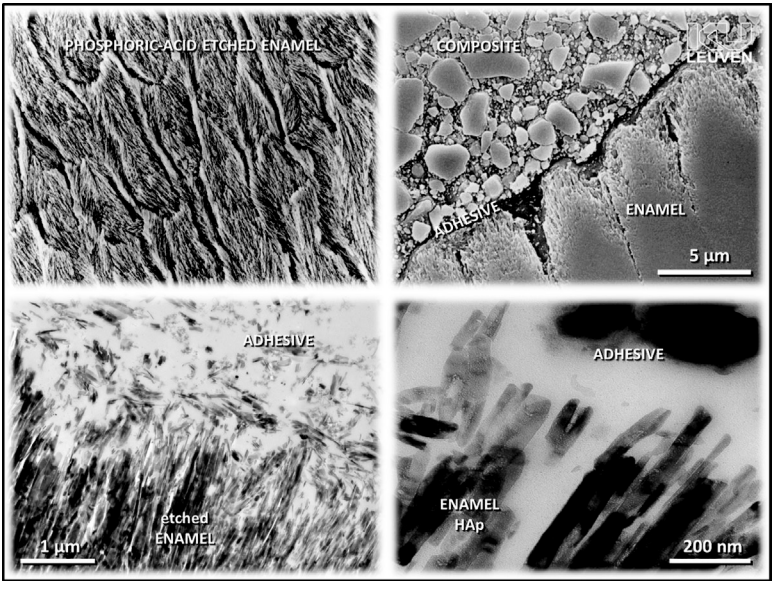

Figure 1.10 SEM photomicrographs illustrating the effect of phosphoric acid etching of enamel and the resultant interfacial TEM ultrastructure upon subsequent application of a particle-filled adhesive resin.

At *dentin*, phosphoric acid completely dissolves the inorganic dentin component (Fig. 1.12). The dissolved calcium phosphates are subsequently removed from the surface upon rinsing off the etchant (Fig. 1.11). Dentinal collagen is exposed up to a depth of 3–5 μm, basically depending on the etching time and concentration of the acid but also on other etchant ingredients like the kind of thickener contained [27]. Hence, only an organic dentin substance is remaining within an E&R hybrid layer (Fig. 1.13). Although some chemical interaction of monomers with collagen has been documented [28, 29], it concerns mainly secondary binding, for example, van der Waals forces and hydrogen bonding (see more in Chapter 3) that will not much contribute to the bond.

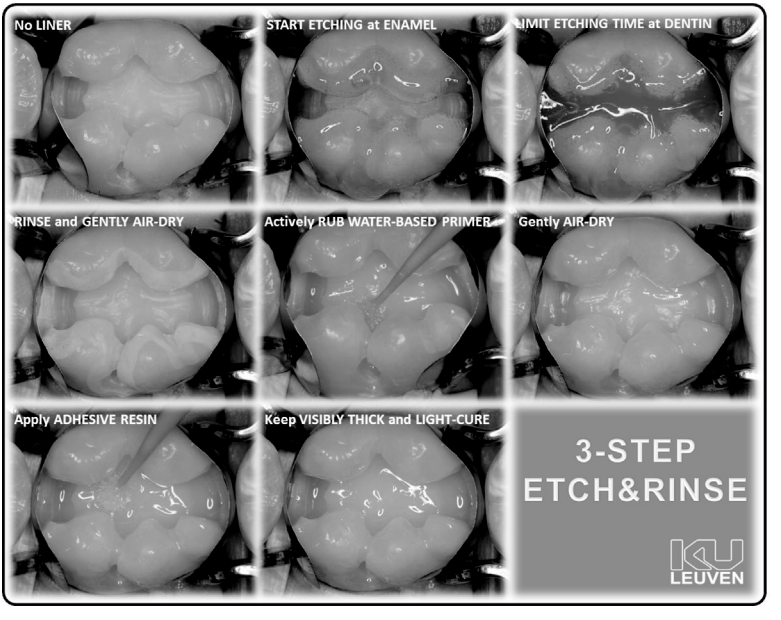

Figure 1.11 Clinical series of a molar on which an adhesive MOD cavity was prepared and that subsequently received a three-step E&RA application. *Abbreviation*: MOD, mesial occlusal distal.

Nevertheless, a recent paper [29] reported, having used nuclear magnetic resonance (NMR), that *10-methacryloyloxydecyl dihydrogen phosphate* (10-MDP) in contrast to 4-MET, two common functional monomers used in SEA (see below), has a relatively stable interaction with collagen, thanks to the hydrophobic interactions

between the hydrophobic 10-MDP moieties and the hydrophobic collagen surface. The authors concluded that such 10-MDP/collagen complexation may contribute to the generally well-performing 10-MDP-based SEAs [30].

In brief, the principal mechanism of bonding to dentin following an *E&R process* is based on micromechanical interlocking through the formation of resin tags in the opened dentin tubules, thereby sealing the relatively direct connection to the dental pulp, and through hybridization or the formation of a relatively thick hybrid layer at intertubular dentin that to a certain extent extends within the tubule orifice walls (see Figs. 1.12 and 1.13).

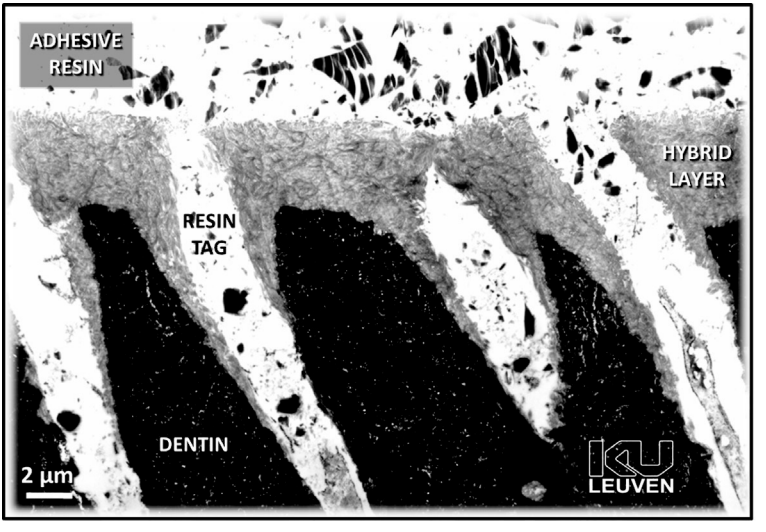

Figure 1.12 Representative TEM photomicrograph illustrating the mainly micromechanical bonding mechanism of E&RAs, consisting of 3–5 µm hybridization at intertubular dentin that extends somewhat into the tubule orifice walls, and resin tag formation into the opened dentin tubules, thereby sealing the relatively direct connection to the underlying pulp.

During cavity preparation, debris is smeared across the enamel and dentin surface (Fig. 1.14). Its composition typically reflects the substrate it is produced on. Self-evidently, any kind of smear layer, even thick and compact, will easily be dissolved by phosphoric acid, following an E&R approach (this in contrast with the milder SEA; see below).

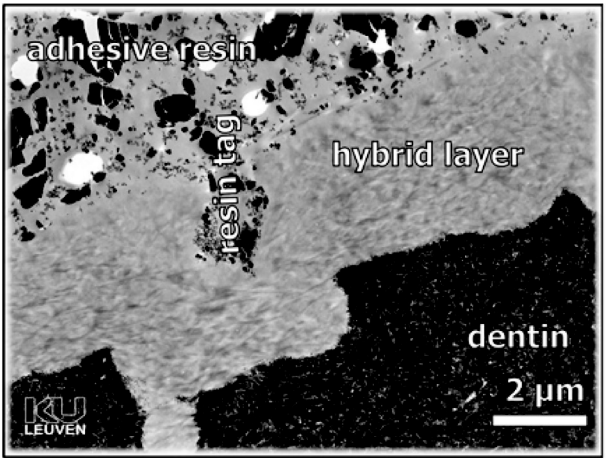

Figure 1.13 Representative TEM photomicrograph illustrating the HAp-free hybrid layer resulting from the relatively aggressive phosphoric acid etching.

After etching, a so-called *wet-bonding* technique (nowadays better referred to as *water wet bonding*, since more recently an "ethanol wet bonding" technique was introduced; see below) is recommended as a standard application technique to promote infiltration of resin within the noncollapsed collagen fibril scaffold [31, 32]. Water wet bonding means that the etched surface should be kept *wet* but not *overwet*, prior to the application of the primer (in the case of 3E&RA)—or the combined primer/adhesive resin (in the case of 2E&RA). While this technique was generally adopted in clinical practice, it has also been documented to be very technique sensitive with regard to the degree of dentin wetness needed [33].

In addition, *wet-bonding primers* typically contain acetone as a solvent because of its excellent water-chasing power, but that due to its high volatility also forced the manufacturer to employ evaporation-resistant plastic or even glass bottles. Furthermore, the dentist is urged to immediately apply the primer to the tooth once dispensed and to reclose the bottle to prevent rapid acetone evaporation.

Applying a wet-bonding protocol, the practitioner also loses the opportunity to check if he or she has etched enamel well that should show its white-frosted appearance. Because of these drawbacks,

a *gently dry-bonding* technique was also recommended. The use of a water-based primer is then mandatory. Given this, it enables automatic rewetting of the air-dried and thus collapsed collagen network to eventually allow the resin to infiltrate effectively [34] (Fig. 1.11). The favorable 13-year clinical effectiveness of the water-based E&RA Optibond FL™ (Kerr), thereby revealing 94% retention in class V, confirms that the in-that-study-applied "gently dry bonding" technique is indeed clinically effective [35] (Fig. 1.14).

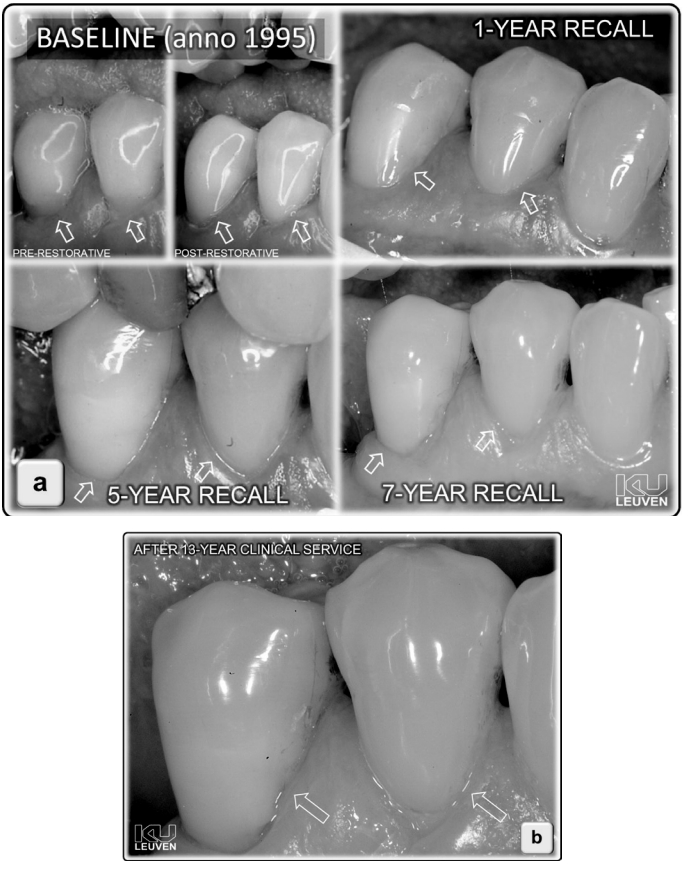

Figure 1.14 (a) Clinical series of two class V composite restorations bonded using the three-step E&RA OptiBond FL™ (Kerr) as part of an up-to-13-year follow-up RCT. At 13 years (b) the two composite restorations are still in excellent condition, with only a slight gingival retraction revealing their presence. *Abbreviation***:** RCT, randomized clinical trial.

1.5.1 The Degradation-Prone E&R Bond to Dentin

Although E&RAs have been proven to effectively bond to enamel and dentin, in laboratory research [36] as well as in RCTs [19, 35], in particular the E&R bond to dentin cannot be considered as very stable and durable in the long term [37]. Clinically, restorations will generally fail first at their margins in dentin, revealing marginal defects and discoloration that eventually may develop in caries recurrence (Fig. 1.15).

Today, the use of phosphoric acid should perhaps be regarded as too aggressive for dentin (in contrast to enamel that requires phosphoric acid etching for durable bonding; see above). Phosphoric acid, even when applied in a short time of 15 seconds, demineralizes dentin deeply and completely, thereby removing the natural protection of collagen, which is HAp (Figs. 1.13 and 1.16).

Figure 1.15 Clinical class V composite restoration from the same 13-year follow-up RCT, as in Fig. 1.14, clearly disclosing marginal defects, discoloration, and perhaps even caries recurrence at the dentin margin, while the margin at enamel does not show any signs of bond degradation.

In addition, the literature documented abundantly that *resin infiltration* within the relatively deeply exposed collagen network is *seldom complete*, making the E&R hybrid layer prone to degradation with time. Collagen molecules keep extracellular fluid bonded, whereby acid-etched dentin gets its highly hydrophilic state.

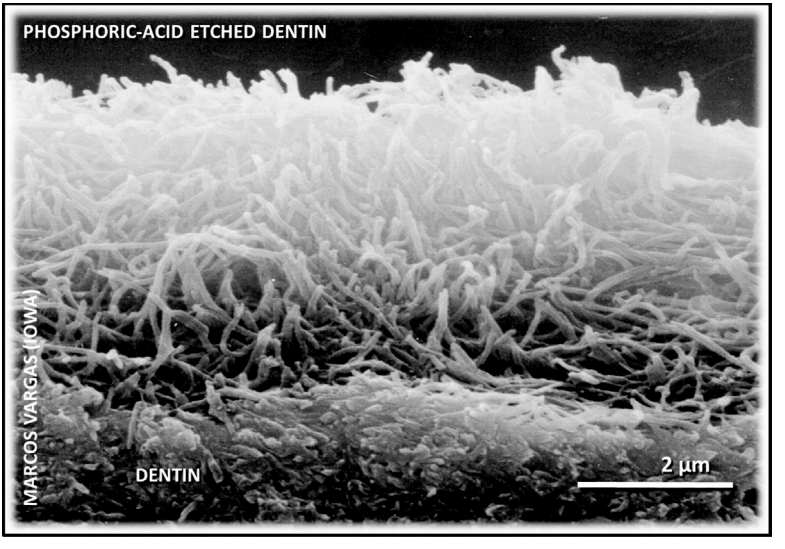

Figure 1.16 SEM photomicrograph illustrating a loosely organized collagen fibril arrangement exposed upon phosphoric acid etching. With courtesy from Marcos Vargas, University of Iowa.

Therefore, although primary chemical bonding is the most stable form of intermolecular interaction and is thus highly desirable, an intrinsically hydrophobic medium like the methacrylate-based dental adhesive can hardly link chemically to this hydrophilic dentinal surface. Some chemical interaction of monomers with dentinal collagen has been demonstrated (see above), but generally the most likely manner to achieve longer lasting E&R bonds is by filling the exposed collagen fibril network with resin as completely as possible.

Such gradual bond degradation appears from the bond strength that decreases with the time the specimens are aged in water (Fig. 1.17), even for some well-known E&RAs. Interfacial characterization revealed clear *nanoleakage channels* as a sign of incomplete resin

envelopment of collagen (Fig. 1.18), thereby proving the relatively high permeability of the E&R hybrid layer, again even shown with one of the best-performing three-step E&RA. The so-called *nanoleakage*, as introduced by Sano et al. in 1994 [38, 39], could be provoked when restored teeth with exposed dentin margins were immersed in silver nitrate ($AgNO_3$) or when this nanoleakage tracer was applied to the pulp chamber (Fig. 1.18).

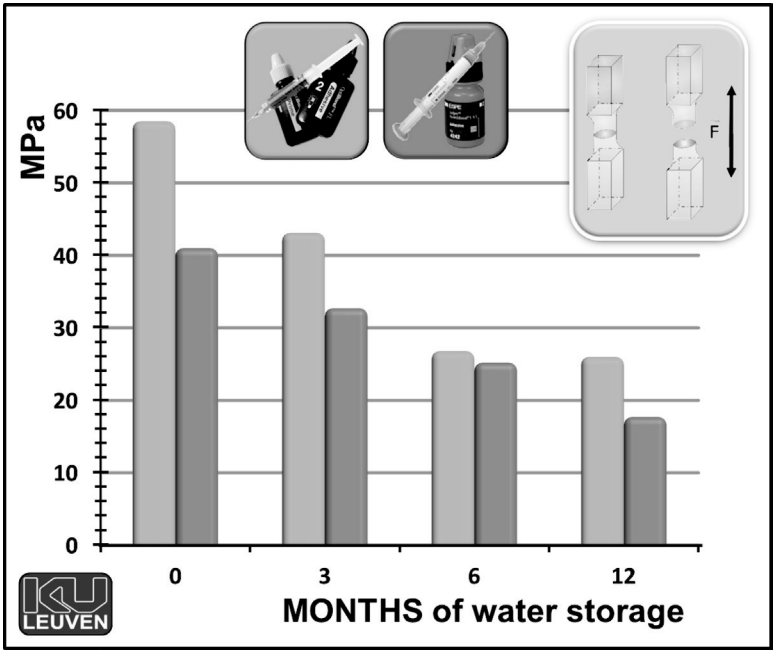

Figure 1.17 Bar graph of microtensile bond strength data, measured at KU Leuven BIOMAT, revealing the gradual decrease in bond strength to dentin with the time of water storage aging.

Recent three-dimensional visualization showed the highly regional variance in nanoleakage within the hybrid layer and resin tags (Fig. 1.19). High-resolution interfacial characterization should therefore be interpreted with care, as zones of nanoleakage could just have been missed, revealing a false-positive impression, or otherwise zones of extreme nanoleakage could give a too negative impression.

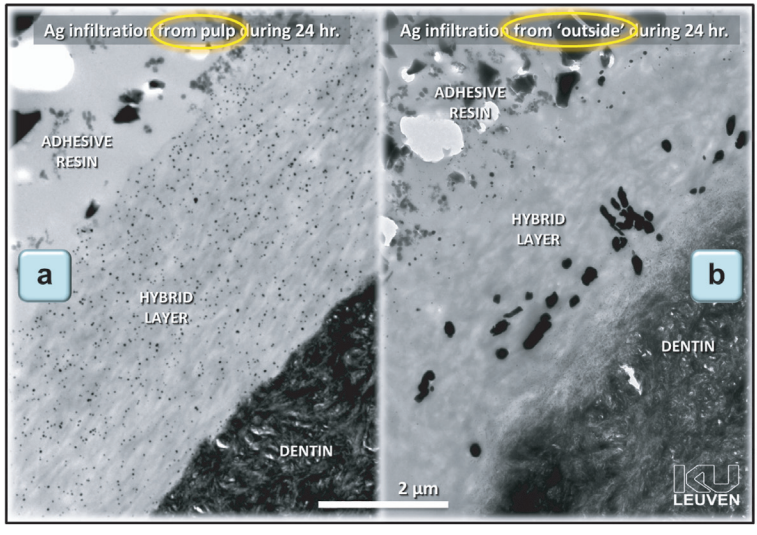

Figure 1.18 TEM photomicrographs showing a so-called spot-like nanoleakage pattern in (a) when the pulp chamber was saturated with silver nitrate (24 hours) that got entrapped within the hybrid layer produced by the three-step E&RA OptiBond FL™ (Kerr), and a clustered nanoleakage appearance in (b) when the whole specimen was immersed within the silver nitrate solution.

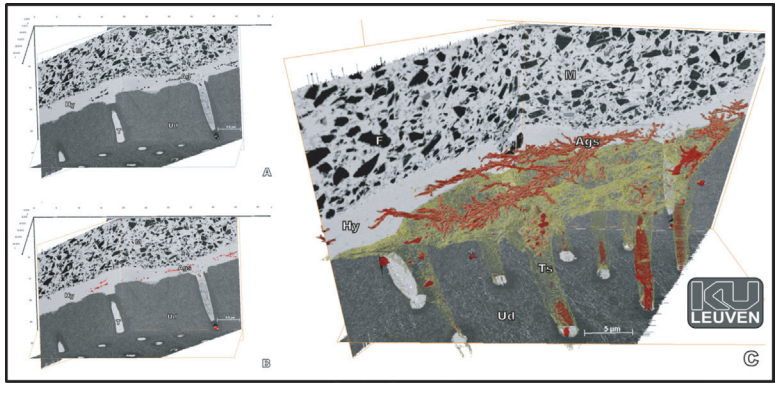

Figure 1.19 Three-dimensional reconstruction (25 μm^3) of the hybrid layer and resin tag complex produced by the three-step E&RA OptiBond FL™ (Kerr), in which the silver nitrate tracer for nanoleakage was marked in red. Nanoleakage can be detected within the hybrid layer as well as within the resin tags and clearly regionally varies substantially.

1.5.2 Strategies to Improve the Resistance of E&R Hybrid Layers against Degradation

1.5.2.1 Ethanol wet bonding to improve hybridization

It is clear that the current E&R bonding protocol requires adhesives that are *hydrophilic* enough to interact with the intrinsically moist acid-etched dentin. This prerequisite is somewhat contradictory, given the need for more *hydrophobic adhesives* to extend bond longevity. Nevertheless, less water will then be absorbed from both the host dentin and the oral environment and render the interface more resistant to water degradation effects [8, 40]. One interesting attempt by Sadek et al. to optimize infiltration of more hydrophobic resins into acid-etched dentin has been introduced as the *ethanol wet-bonding* technique [41].

It basically involves the intermediate application of a *highly concentrated ethanol solution* for at least one minute or, even better, the successive application of ethanol-water solutions with a gradually increasing ethanol concentration up to absolute ethanol (100%) to (gradually) exchange water within the exposed collagen fibril network for ethanol, thereby dehydrating the acid-etched dentin as well as transforming it into a more hydrophobic state. In this way, with ethanol being a better medium (or transporting agent) for resins, the acid-etched dentinal substrate is better prepared to receive more hydrophobic and thus less water-absorbing resin monomers.

Hence, a more hydrophobic resin–dentin interface is formed that is expected to absorb less water over time and offer better resistance against degradation. This unfortunately laborious and therefore perhaps clinically less practical technique originated from the laboratory processing of samples for electron microscopy. In particular for TEM, specimens typically undergo a gradual and thus slow dehydration process using increasing concentrations of ethanol prior to embedding procedures with highly hydrophobic epoxy resins.

As mentioned by the proponents of this technique ". . . the bonding of *bis*-GMA to acid-etched dentin should be viewed as a proof of concept for hydrophobic dentin-bonding, rather than as the development of a clinically applicable bonding technique . . ." [41].

There is a striking similarity in the performance of this experimental ethanol wet-bonding technique with that of the above-mentioned "gold standard" three-step E&RA OptiBond FL™ (Kerr), which also provides an ethanol-/water-based primer. The research on ethanol wet bonding therefore confirms that ethanol is the preferred solvent within an E&R primer. It also confirms the overall superior laboratory and clinical effectiveness of the above-mentioned gold-standard adhesive OptiBond FL™ (Kerr).

1.5.2.2 Application of MMP inhibitors to prevent enzymatic bond degradation

Dentinal collagen exposed by an E&R procedure has been documented to be highly vulnerable to hydrolytic and enzymatic degradation processes [42–44]. The latter *enzymatic degradation of collagen* within the hybrid layer does not occur only due to activity of collagenases produced in vivo by bacteria but also due to host-derived enzymes that are released and iatrogenically activated by specific adhesive procedures (Fig. 1.20). Such collagenolytic and gelatinolytic activities are *triggered by endogenous enzymes*, which are naturally present in the mineralized dentin matrix and known as MMPs.

During bonding procedures, (self-)etching of dentin has been shown to release and activate such MMPs [45–48], which may in part digest collagen fibrils within the hybrid layer that are reachable and thus were insufficiently enveloped with resin.

A relatively simple method to protect the interface against such enzymatic degradation is the use of *MMP inhibitors*. Several MMP inhibitors have been tried out, of which *chlorhexidine* (CHX) is already commonly used in dentistry and seems effective in vitro as well as in vivo [42, 44, 49–51]. However, there does not exist a good consensus in the literature on the actual effectiveness of MMP inhibitors with regard to improving bond durability [44, 46, 52].

Ideally, to avoid having to introduce another intermediate step in the already multistep application procedure of E&RA, for instance, by applying a CHX solution after etching and prior to priming, *building in MMP inhibitors* within, for instance, the primer appears clinically more attractive. Two KU Leuven BIOMAT studies revealed [44, 46] that some degradation-reduction effect was found up to 6-month aging by storage in water, while this positive effect was lost again after 12-month water aging (Fig. 1.21).

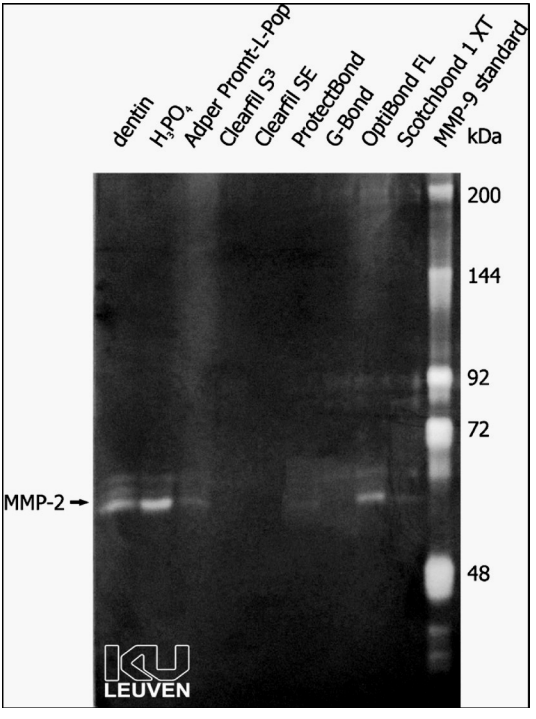

Figure 1.20 Activation of gelatinase (MMP-2) by adhesive treatments, as measured by gelatin zymography of dentin powder and dentin powder exposed for 30 seconds to phosphoric acid and/or to different adhesives (applied following their respective manufacturers' instructions).

Interestingly, one study comparatively investigated the application of the above-mentioned ethanol wet-bonding application technique versus the use of a CHX MMP-inhibiting solution on bond durability for the two well-known E&RAs Scotchbond Multi-Purpose™ and Single Bond 2™ (both 3M ESPE) [41]. The CHX solution prevented the bond strength to dentin to decrease when the specimens were aged by 9-month water storage; this beneficial effect was, however, lost upon 18-month aging. On the contrary, the time-consuming ethanol wet-bonding technique, involving a wet dentin surface being treated with a series of increasing ethanol concentrations (50%, 70%, 80%, 95%) and 100% ethanol applications for 30 seconds each [41], did not result in any significant reduction in bond strength upon 9- and 18-month water aging.

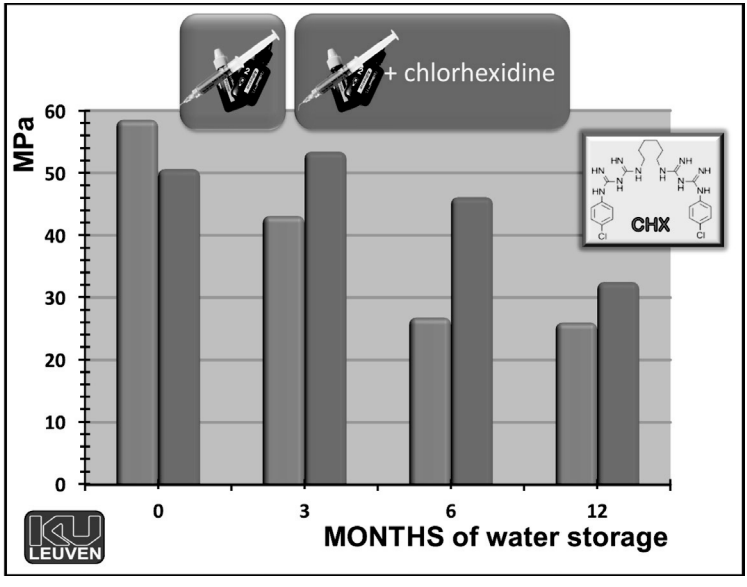

Figure 1.21 Bar graph showing the microtensile bond strength of the three-step E&RA OptiBond Fl™ (Kerr) when it was applied as such or when CHX as an MMP inhibitor was added to the primer. The addition of CHX did not result in a significant decrease in bond strength up to 6-month water storage. However, after 12-month water aging no significant difference in bond strength was found with or without CHX.

While endogenous enzymes appear to contribute more to bond degradation of E&RAs than SEAs [44], *water sorption* of adhesive interfaces and hydrolysis effects most likely remain the principal mechanisms of bond degradation, thereby giving a reason why MMP inhibitors appear to only retard the bond degradation process but are not able to prevent it completely. Noteworthy is also that the levels of such endogenous enzymes gradually decrease with age, commonly disappearing before one reaches the age of 40 years [53], and so even could be employed for age estimation [54].

1.5.2.3 Biomimetic repair of E&R hybrid layers

Another elegant approach to potentially *repair* E&R hybrid layers that are incompletely resin infiltrated has been proposed through the so-called *guided-tissue remineralization* [55, 56]. This technology involves a relatively long exposure of the adhesive interface to a

highly concentrated calcium phosphate remineralization medium. Within two to four months, areas within the hybrid layers that were initially poorly infiltrated by adhesive resins appeared to have remineralized to a certain extent.

However, the *clinical applicability* of such a time-consuming process is today still unclear. Now that the working principle of this guided-tissue remineralization has been proven, research effort is definitely being spent toward development of methodologies that are clinically applicable. Although, for instance, such a remineralization liner could be effective to heal caries tissue that was intentionally left at the cavity bottom (thereby minimizing cavity preparation and potentially avoiding pulp exposure), combining bonding procedures with liners (to repair deficient hybrid layers) appears perhaps clinically less feasible.

Actually, the fact that an E&R hybrid layer can be remineralized, confirms the relatively permeable nature of the resin-impregnated collagen layer and perhaps its consequent instability in the long term.

1.6 Self-Etch Adhesives

Different from E&RAs, SEAs do not require a separate etching step, as they contain acidic monomers that simultaneously *condition* and *prime* the dental substrate. Consequently, this approach has been claimed to be user friendlier (shorter application time, fewer steps) and less technique sensitive (no wet bonding, simple drying), thereby resulting in reliable clinical performance [19, 57–59], though this appeared very product dependent (see below). Another important clinical benefit of SEAs is the absence of or at least lower incidence of postoperative sensitivity experienced by patients as compared to that associated with E&RAs [60, 61]. This should to a great extent be attributed to their less aggressive (with respect to dentin and as compared to phosphoric acid etching) and thus more superficial interaction with dentin, leaving tubules largely obstructed with smear (see below). All these favorable key features have led to the steadily growing popularity of SEAs in today's dental practice.

SE adhesives can come as *two-step* and *one-step* SEAs, depending on whether a self-etching primer and (mostly solvent-free) adhesive

resin are separately provided or are combined into one single solution (Fig. 1.2). SEAs can also be subdivided into *two-component* and *single-component* SEAs. By separating *active ingredients* (like the functional monomer from water), two-component SEAs *theoretically* possess a longer shelf life, but additional and adequate mixing of both components is needed. Single-component one-step SEAs can be considered as the only true *one-bottle* or *all-in-one* adhesives, as they combine *conditioning*, *priming*, and *application of the adhesive resin* and do not require mixing.

To enable (self-)etching, all SEAs contain water as an ionizing medium [62]. The only exceptions are some commercially available water-free SEAs. They, however, require a more technique-sensitive wet-bonding application technique, like that required for acetone-based E&RAs [63]. Sufficient surface water should then indeed be present to enable self-etching, again leading to the question, *how wet should the surface be?* (See more above). In general, SEAs have the advantage to demineralize and infiltrate the tooth surface simultaneously to the same depth, theoretically ensuring complete penetration of the adhesive [3]. With increasing depth, acidic monomers are gradually buffered by the mineral content of the substrate, most likely losing their ability to further etch dentin. The morphological features of the *adhesive–tooth interface* produced by SEAs depend to a great extent on the manner their functional monomers interact with the dental substrate (Fig. 1.3). In part depending on the pH of the SE solutions (Fig. 1.3), the actual interaction depth of SEAs at dentin differs from a few hundreds of nanometers following an *ultramild* SE approach (pH > 2.5; Fig. 1.22a), which sometimes is being referred to as *nanointeraction* [64], an interaction depth of around 1 μm for a "mild" SE approach (pH ≈ 2; Fig. 1.22b), an interaction depth between 1 μm and 2 μm for an "intermediately strong" SE approach (pH ≈ 1.5; Fig. 22c), and to an interaction several micrometers deep for a "strong" SE approach (pH ≤ 1; Fig. 1.22d). Only using strong SEAs, typical resin tags are formed at dentin, while they are hardly formed with mild and ultramild SEAs, or at maximum the smear plugs get slightly demineralized and subsequently resin infiltrated.

The actual bonding performance attained by SEAs varies a great deal, depending not only on the actual class of SEAs (Figs. 1.3 and 1.22) but certainly also on the actual composition and

more specifically on the actual functional monomer included in the adhesive formulation (Fig. 1.23) [62]. See also below for an in-depth discussion on the importance of functional monomers with regard to bonding effectiveness and durability.

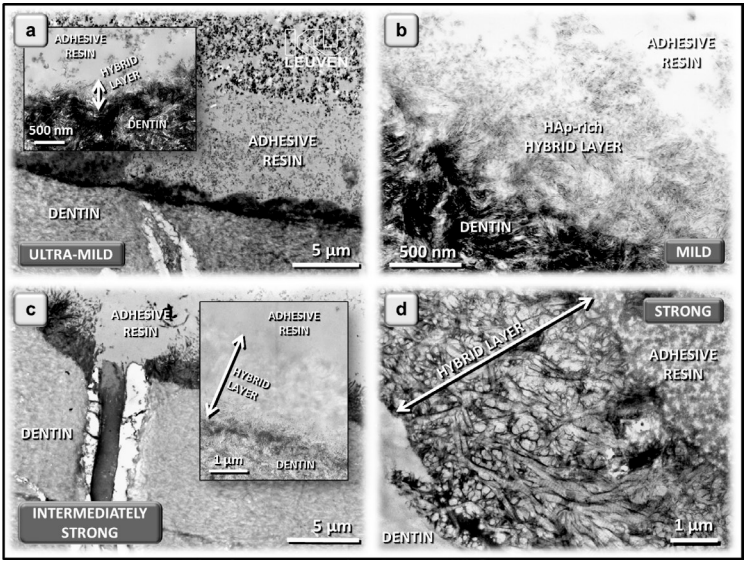

Figure 1.22 Collage of representative TEM photomicrographs of the interfacial ultrastructure produced by an "ultramild" SEA in (a), a "mild" SEA in (b), an "intermediately strong" SEA in (c), and a "strong" SEA in (d).

1.6.1 Major Shortcomings of One-Step SEAs

The latest generation of the most simple-to-use one-step adhesives are intricate mixes of hydrophilic *and* hydrophobic components. These "difficult" mixtures should so far be considered as "compromise" materials that have consequently been *documented with several shortcomings* (Fig. 1.24), as listed below:

(1) Generally, a reduced "immediate" bond strength is recorded in comparison to that measured for multistep adhesives [36].

(2) In addition, any kind of "aging" demonstrates lower long-term bonding effectiveness [8, 10, 36].

(3) Moreover, numerous studies report on increased interfacial nanoleakage [65, 66].

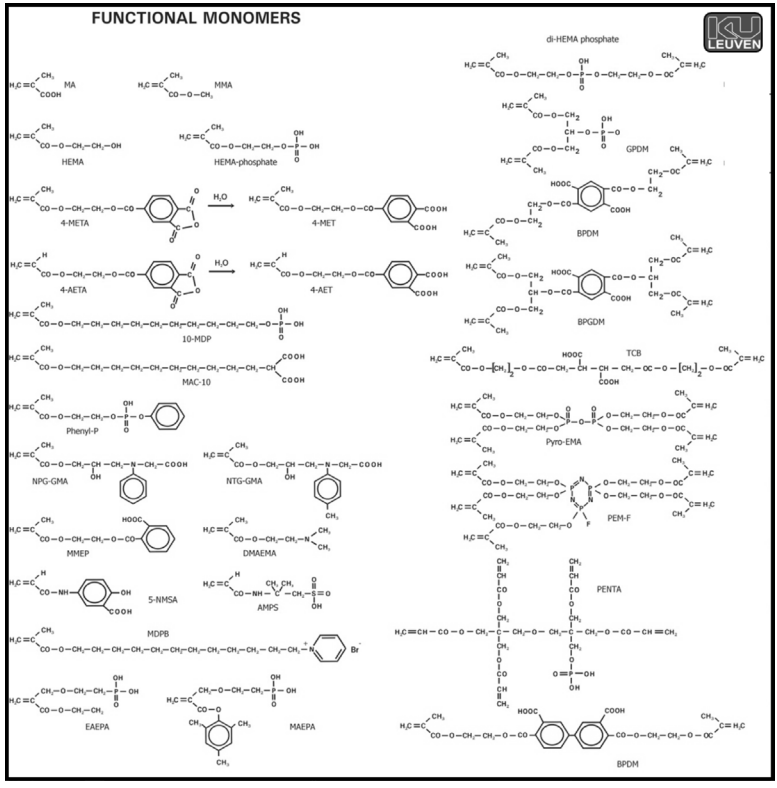

Figure 1.23 Overview of different functional monomers present in commercial adhesives.

(4) One-step adhesives that are rich in HEMA showed enhanced water sorption from the host dentin, in particular when the lining composite is not immediately cured to block these osmosis effects [67] (Fig. 1.25).

(5) On the other hand, typical is also the phase separation described for HEMA-free/HEMA-poor adhesives [62, 67, 68] (Fig. 1.26).

An adapted *strong* air-drying procedure provides a means to remove water (that is separated from the more hydrophobic components) from the interfacial area, theoretically enabling better polymerization. While this technique works on relatively flat surfaces, the water *bubbles* (formed once the

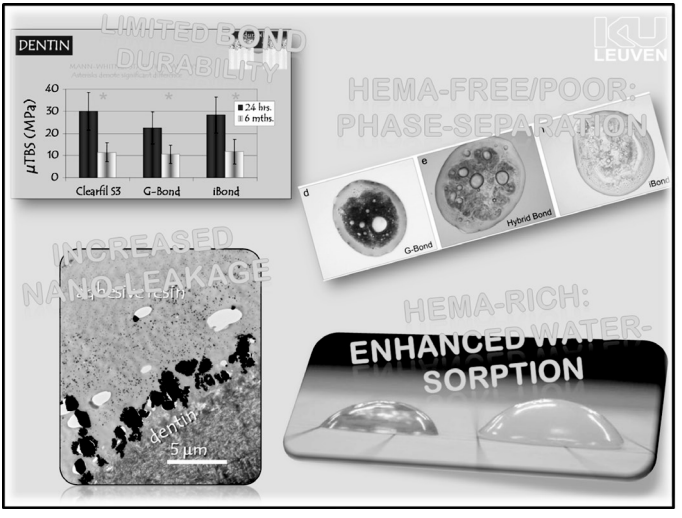

Figure 1.24 The four main shortcomings of one-step SEAs.

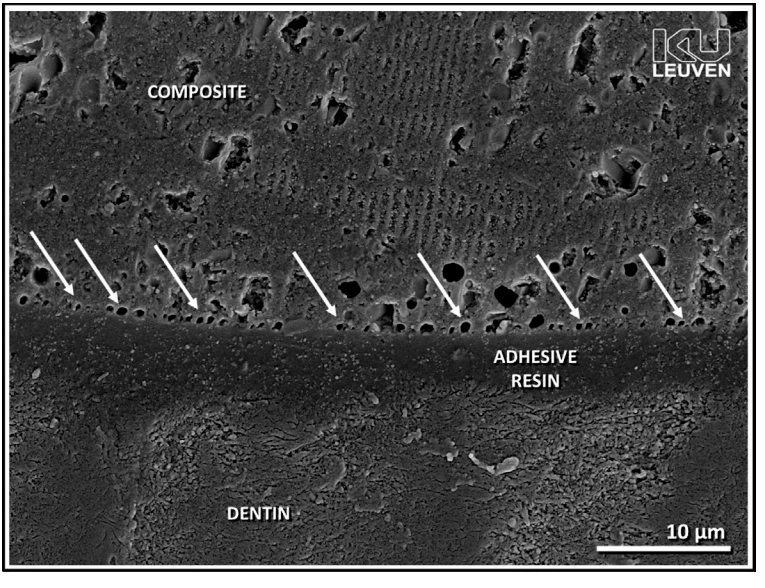

Figure 1.25 SEM photomicrograph showing the adhesive interface produced by a HEMA-rich one-step SEA. The clear layer of pores at the adhesive–composite interface represents water droplets that migrated through osmosis from the host dentin through the hybrid and adhesive layer to the immediately adjacent composite.

solvent starts to evaporate, by which the more hydrophobic monomer components no longer remain in solution) are more difficult to blow away in more complex cavity configurations.

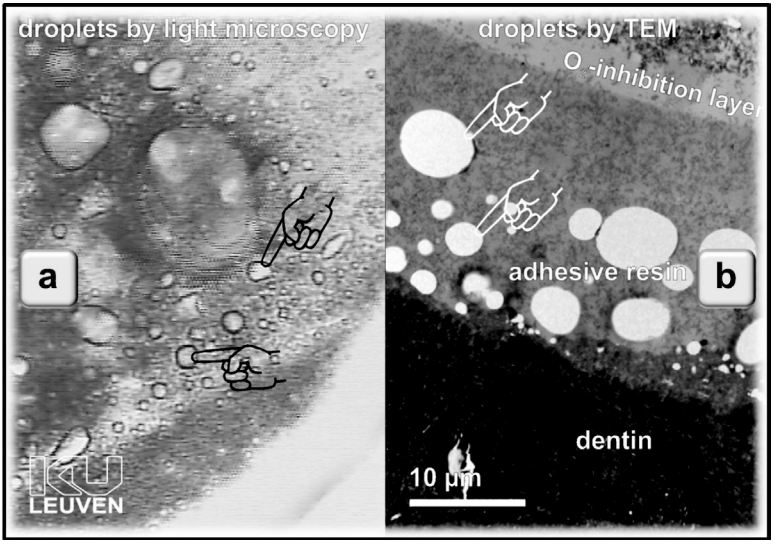

Figure 1.26 Light microscopic image in (a) illustrating phase separation between water and resin once the HEMA-free one-step SEA was dispensed, and a TEM photomicrograph in (b) showing entrapment of pores within the hybrid layer, in particular when the adhesive was not strongly air-dried.

(6) In addition, mixing all ingredients into one bottle has caused shelf life problems [69], though recently some manufacturers solved this issue by using more hydrolytically resistant *acrylamide* monomers [70].

(7) Finally, the inferior clinical performance of one-step SEAs confirmed the less favorable laboratory findings, while it must also be said that the latest generation of one-step adhesives definitely performs better [71].

1.6.2 No Use of Strong SEAs

Strong SEAs present rather deep demineralization effects at both enamel and dentin (Fig. 1.22d). Following the AD concept (phase II,

option 2; Fig. 1.10) [6, 7], the bond of a functional monomer like a (di-)HEMA-phosphate to Ca^{2+} of HAp will readily debond and thus amply *etch* enamel and dentin, similar to what phosphoric acid does. Depending on the *stability and purity* of the functional monomer, some phosphoric acid might be present in the adhesive formulation and obviously contribute to the relatively severe etching effect. Hence, the *interfacial ultrastructures* at enamel and dentin produced by such strong SEAs resemble those of E&RAs (Figs. 1.12 and 1.22d). They, however, differ from E&RAs because like all SEAs they are not rinsed off. All dissolved calcium phosphates are consequently not rinsed away but embedded at the interface. Such embedded calcium phosphates are not very stable in an aqueous environment, thereby seriously weakening interfacial integrity. Laboratory as well as clinical data have both undeniably shown that despite their rather reasonable bonding potential to enamel, strong SEAs generally underperform at dentin, in particular with regard to bond durability and restoration longevity [19]. This data corroborates the AD concept (Fig. 1.1) [6, 7] and should be attributed to the low hydrolytic stability of the embedded calcium phosphates, along with the lack of stable chemical interaction with the exposed collagen.

Although manufacturers have introduced strong SEAs some years ago, especially with regard to their *better etching performance at enamel*, their severely compromised bonding to dentin has apparently pushed the dental industry today more toward the more promising *mild* SE approach.

1.6.3 Use of Mild SEAs

Mild (and *ultramild*) SEAs demineralize dentin only partially, leaving a substantial amount of HAp crystals around the collagen fibrils (Figs. 1.22a,b and 1.27). Following the AD concept [6, 7], a functional monomer like MDP, commonly referred to as 10-MDP, will chemically bond to Ca^{2+} of HAp, thus, according to AD concept phase II, option 1 (Fig. 1.1) [6, 7], forming stable calcium phosphate salts, along with only a limited surface decalcification effect. Like GIs, mild SEAs indeed only superficially interact with enamel and dentin and hardly dissolve HAp crystals but rather keep them in place (within a thin submicron hybrid layer; see below and Fig. 1.27). Advantageous

is the fact that mild SEAs not only keep collagen encapsulated and thus protected by HAp but also provide the potential to chemically interact with HAp [72].

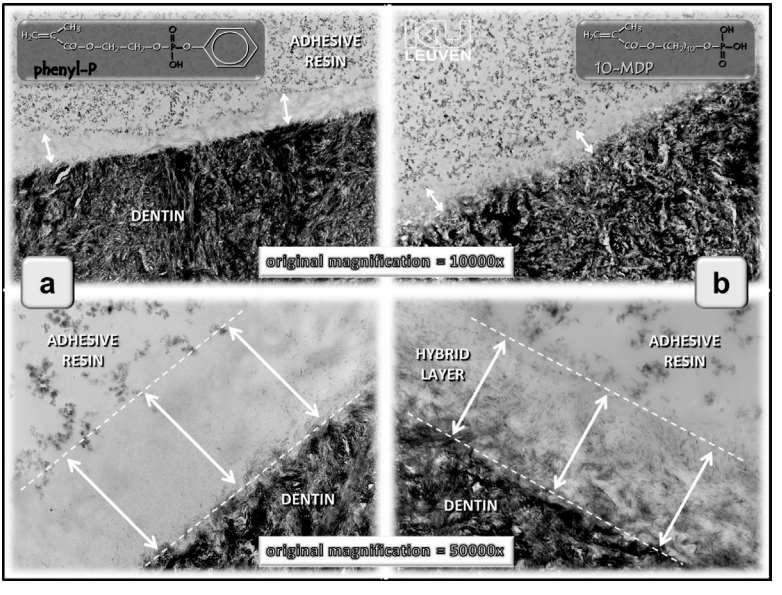

Figure 1.27 TEM photomicrographs showing the adhesive–dentin interface produced by a phenyl-P-based "mild" SEA in (a) and a 10-MDP-based "mild" SEA in (b). Since the functional monomer phenyl-P has only a weak chemical affinity to Ca^{2+} of HAp, it follows the **decalcification** route of the AD concept (Fig. 1.1, AD concept phase II, option 2) with more intense demineralization and exposure of collagen. In contrast, the hybrid layer ultrastructure produced by the 10-MDP-based adhesive shows an HAp-rich hybrid layer because of the high chemical affinity of 10-MDP to HAp Ca, thereby following the **adhesion** route of the AD concept (Fig. 1.1, AD concept phase II, option 1).

The resultant two-fold micromechanical- and chemical-bonding mechanism of mild SEAs indeed closely resembles that of GIs [3, 11]. Both typically present with a submicron hybrid layer that still contains substantial HAp that was not dissolved. In this respect, GIs could even be regarded as a kind of mild SEAs. The basic difference between a resin-based SEA and a GI is that the SEA possesses functional monomers with usually only one or two functional

chemical groups with affinity to HAp (Fig. 1.22b). They provide individual monomers that become upon polymerization a polymer that is linked to HAp, versus GIs that make use of an already existing (PAA) polymer with multiple functional groups that are attached to the polymer backbone and can "grab" Ca^{2+} at different and remote sites. The additional chemical bonding provided by GIs and mild SEAs is believed to be advantageous in terms of bond durability [73].

1.6.4 Improved Bond Durability through Chemical Bonding and Interfacial Nanolayering

More specifically, chemical interaction is achieved through specific functional monomers, such as 10-MDP, 4-MET, and phenyl-P (Figs. 1.23 and 1.27). Ionic bond formation of the carboxylic/phosphate groups of these functional monomers to Ca^{2+} of HAp was first proven by Yoshida et al. in 2004 [72] using XPS. However, the chemical-bonding potential on its own is insufficient; the formed ionic bonds should also be stable in an aqueous environment. In this sense, the chemical bonding promoted by 10-MDP is not only more effective but also more stable in water than that provided by 4-MET and phenyl-P in this order. The dissolution rate of the respective calcium salts of these three monomers, as measured by atomic absorption spectroscopy (AAS), was inversely related to their chemical-bonding potential, as revealed by XPS: the more intense the chemical-bonding potential, the less the resultant calcium salt could be dissolved. This mechanism explains the contrasting ultrastructures of two SE hybrid layers (Fig. 1.27). The hybrid layer produced by the phenyl-P-based adhesive is not only thicker but also demineralized more with exposure of collagen than that produced by the 10-MDP-based adhesive, in which no collagen was exposed and dentin was only partially demineralized, leaving abundant HAp available for chemical interaction.

Confirming this experimental chemical data and hence the AD concept [6, 7], the bond strength to dentin of the 10-MDP-based "mild" two-step SEA Clearfil SE™ (Kuraray Noritake) remained high after long-term thermocycling, while that of Unifil Bond™ (GC) that contains 4-MET significantly dropped (but only after 100,000 cycles), and that of Clearfil Liner Bond II™ (Kuraray Noritake) that contains

phenyl-P gradually decreased the longer the bond was exposed to thermocycling [73]. Clearfil SE Bond™ (Kuraray Noritake) has been proven to yield reliable results in terms of bonding effectiveness and durability when compared to other commercially available SEAs, in the laboratory as well as in clinical research [19, 57].

The functional monomer 10-MDP bonds through its phosphate groups to HAp and peculiarly forms a regularly layered structure at the HAp surface (Fig. 1.28) [11, 74–78]. Both X-ray diffraction (XRD) of HAp powder allowed to interact with 10-MDP and high-resolution TEM of 10-MDP-treated HAp powder revealed the formation of a 4 nm *layered structure* (Figs. 1.28 and 1.29).

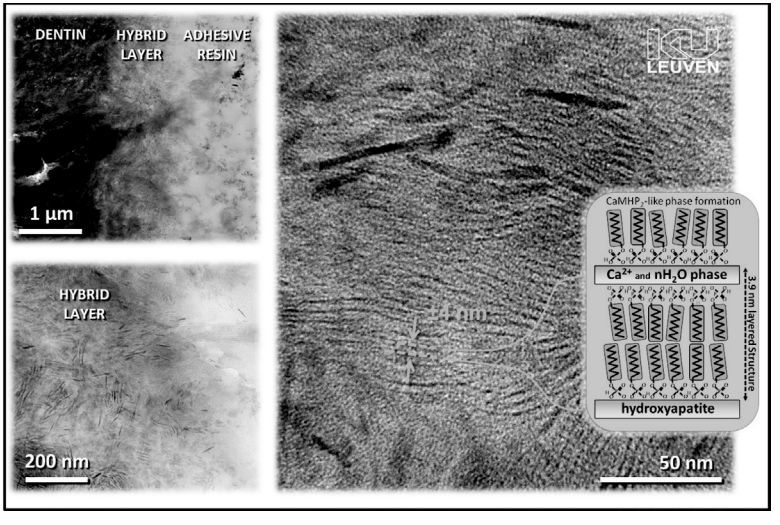

Figure 1.28 TEM photomicrographs illustrating the adhesive–dentin interface produced by the 10-MDP-based "mild" two-step SEA Clearfil SE Bond (Kuraray Noritake). High magnification (100,000x) of the HAp-rich submicron hybrid layer revealed a 4 nm regularly layered structure, being termed **self-assembled nanolayering**. This nanolayering consists of layers each of two molecules of 10-MDP directed in opposite directions; different layers are linked to each other by Ca having ionically interacted with the functional phosphate group of 10-MDP. This typical arrangement is thought to provide more stability and hydrophobicity to the interface, thereby explaining the improved bond durability documented with 10-MDP-based SEA formulations.

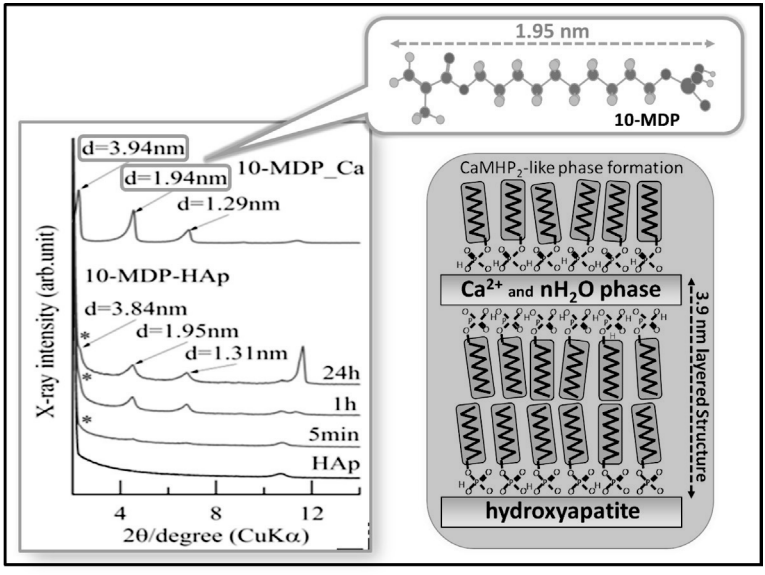

Figure 1.29 XRD of 10-MDP having reacted with HAp powder, revealing a typical three-peak XRD pattern that represents nanolayering. The peak at $2q = 4.56°$ represents a structural arrangement with a dimension of 1.94 nm, which corresponds to the theoretical size of one 10-MDP molecule. The peak at $2\theta = 2.24°$ reveals a dimension of 3.94 nm, thereby corresponding to about the size of two 10-MDP molecules and thus in agreement with the dimension of the nanolayering pattern observed by TEM in Fig. 1.28. Note that HAp powder is significantly less reactive than dentin (and enamel), by which much longer reaction times are needed in contrast to dentin where nanolayering can be disclosed within clinically relevant application times.

Such *nanolayering* could not be detected for the functional monomers phenyl-P and 4-MET. Each layer of this *self-assembled nanolayered structure* consists of two 10-MDP molecules with their methacrylate groups directed toward each other and their functional hydrogen phosphate groups directed away from each other [79]. In between the layers, calcium salts are deposited, basically linking two adjacent nanolayers. This high chemical affinity of 10-MDP to HAp along with nanolayering was first demonstrated on pure synthetic HAp using XRD and later confirmed by NMR. Apatite in natural dentin is carbonated and also contains trace amounts of Na,

Mg, Sr, and Al, among others. Direct evidence of the formation of a nanolayered structure on natural dentin was later provided by TEM (Fig. 1.28) and structurally by XRD of 10-MDP-treated dentin samples [75, 76]. More recent experiments [78] proved that nanolayering occurred at dentin when an experimental 10-MDP-based adhesive (as well as the commercially available Clearfil SE Bond™ of Kuraray Noritake) was applied to dentin, following a clinically relevant application procedure, that is, 20-second application followed by gentle air-drying. Furthermore, rubbing the primer solution on the dentin surface intensified the nanolayering, which may explain why this "active" application technique increases bond strength, as was observed in previous studies. However, nanolayering was clearly less detectable by XRD at enamel, which may be due to the significantly higher crystallinity of enamel, reducing the interaction potential of 10-MDP. Dentinal HAp has not only lower crystallinity, but the crystal rods are also smaller in size and oriented crisscross (versus parallel oriented at enamel).

The important finding that the adhesive performance of an SEA depends on the *functional monomer* included in the adhesive solution and its particular molecular structure and affinity to HAp was confirmed by another study in which the chemical interaction of the three experimental Ivoclar Vivadent (Schaan, Liechtenstein) phosphonate monomers, 2-[4-(dihydroxyphosphoryl)-2-oxabutyl]-acrylate (HAEPA), ethyl 2-[4-(dihydroxyphosphoryl)-2-oxabutyl] -acrylate (EAEPA), and 2,4,6 trimethylphenyl 2-[4-(dihydroxy-phosphoryl)-2-oxabutyl]acrylate (MAEPA), was assessed and compared to that of 10-MDP as the control [76]. The carboxyl group in HEAPA was esterified in EAEPA and MAEPA with an ethyl and a phenyl group, respectively. The bond strength of experimentally prepared adhesive cements that differed only in the functional monomer was inversely related to the dissolution rate of the calcium salt of the respective functional monomer. The latter is according to the AD concept, suggestive of a high chemical-bonding capacity following a "phase II, option 1" profile (Fig. 1.1) [6, 7]. Only a slightly higher dissolution rate was recorded for MAEPA than for the 10-MDP control, while the 10-MDP-based adhesive cement showed only significantly higher bond strength to enamel. Ca-HAEPA was highly hydrolytically sensitive, while the Ca salt of EAEPA was also

significantly more soluble than the Ca salts of MAEPA and 10-MDP. Their respective bonding effectiveness to dentin was correspondingly significantly lower. Recent XRD experiments confirmed that MAEPA formed hydrolytically stable Ca monomer salts that remained attached to the dentin surface despite rinsing [76]. EAEPA also ionically bonded to Ca^{2+} at dentin, but the Ca-EAEPA salt formed did not resist washing with ethanol and water. Finally, no evidence for the formation of the Ca-HAEPA salt was detected by XRD.

Despite the high chemical interaction potential of 10-MDP and the related nanolayering, a recent finding showed that the application of an experimental 10-MDP:EtOH:H_2O self-etching primer followed by the bonding agent of the commercially available Clearfil SE Bond™ (Kuraray Noritake) did not suffice to reach a bond strength comparable to that of the complete Clearfil SE Bond™ system (using also the commercially available 10-MDP-based self-etching primer; Kuraray Noritake) [75]. However, when camphorquinone/amine (CQ/amine) was added as a photoinitiator to the experimental 10-MDP:EtOH:H_2O self-etching primer, an equally high bond strength to dentin was measured like that of Clearfil SE Bond™ (whose self-etching primer also contains CQ; Kuraray Noritake). This finding highlights the need for *adequate polymerization*, hypothetically thought to be very important in case nanolayering produces a relatively thick intermediary layer. This layer can only polymerize and thus resist debonding during bond strength testing when a sufficient photoinitiator is provided locally. Adding CQ/amine to the subsequently applied bonding agent of Clearfil SE Bond™ (Kuraray Noritake) appeared insufficient, most likely because of the less penetrable nanolayering arrangement.

1.6.5 Self-Etching and the Smear Layer

It is well known that during cavity preparation using rotary instruments, the surface to bond to will be covered by a smear layer [80, 81]. Depending on the preparation technique, this smear layer varies significantly in size and structure (Figs. 1.30 and 1.31). Unfortunately, the smear layer is not attached firmly to the tooth surface, and SEAs better interact with surface smear sufficiently to obtain a satisfactory bond to the underlying tooth surface.

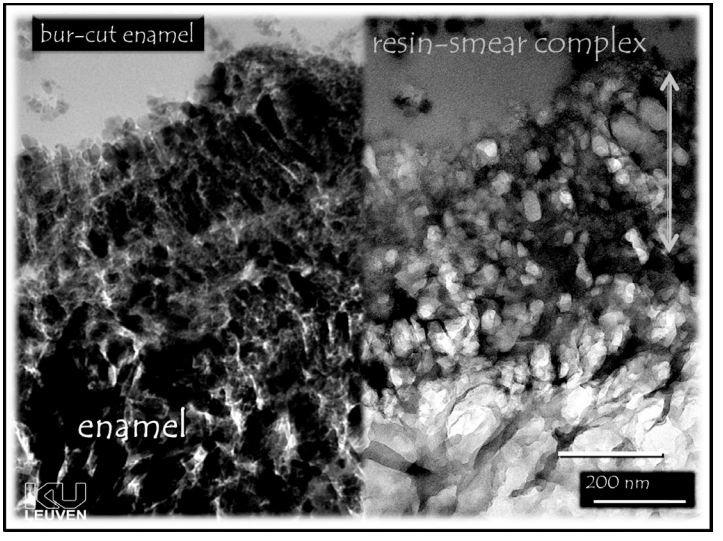

Figure 1.30 TEM photomicrographs illustrating the resin–smear complex formed at enamel upon diamond bur instrumentation.

There are indications that the bonding effectiveness of especially ultramild SEAs may be impaired by thick smear layers [82]. In addition, a recent study revealed that mild SEAs failed predominantly under the hybrid layer after water aging, which may also be the result of insufficient smear removal by current mild SEAs [83]. These studies highlight the importance of the cavity preparation method. It is clear that the main challenge for current SEAs (as well as materials like *self-adhesive composite* (*SAC*) *cements* and actual *self-adhesive* [*restorative*] *composites;* see below and see also Chapters 3 and 6) is to dissolve the smear layer without demineralizing the tooth surface too profoundly and thereby not to remove HAp at the interface. As mentioned above, preserving HAp at the interface not only protects the collagen from external chemical aggression, but the HAp will also provide Ca^{2+} for chemical bonding of the functional monomer.

1.6.6 Self-Etching Enamel and Recommendation to Selectively Phosphoric-Acid-Etch Enamel

At enamel, an E&R approach using phosphoric acid remains the choice of preference, since it not only guarantees the most durable

bond to enamel but also seals and thus protects the more vulnerable bond to dentin against degradation [3, 26]. As mentioned above, while "strong" SEAs generally perform not that unfavorably at enamel, bonding of *mild* SEAs to enamel (and certainly to unground, aprismatic enamel) remains so far unsatisfactorily (Fig. 1.32). Clinical research has clearly revealed that marginal defects at the enamel margins of a composite restoration develop rather rapidly, whereas the dentin margins appear to maintain their marginal integrity much longer [57, 58].

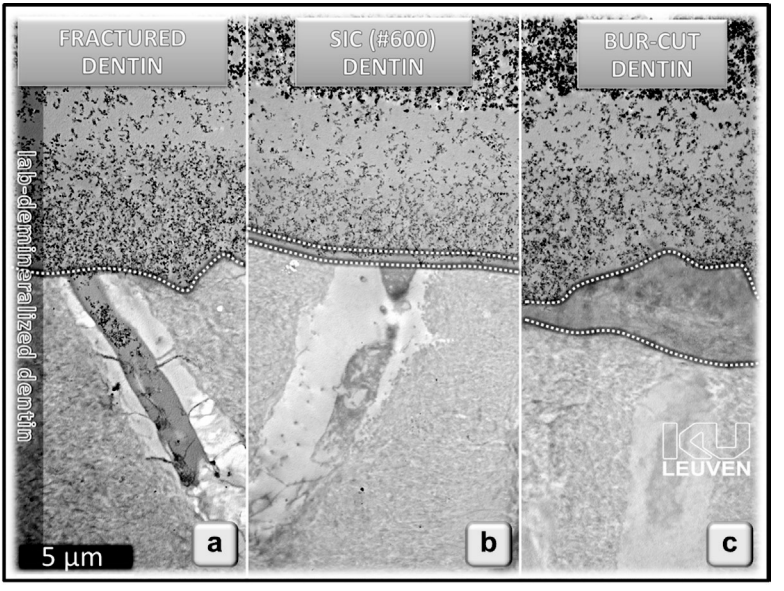

Figure 1.31 TEM photomicrographs illustrating the absence of surface smear when dentin was fractured in (a) and, respectively, the relatively thin smear layer versus a much thicker, more irregular, and compact resin–smear complex formed at dentin upon grinding using 600-grit silicon carbide (SiC) paper in (b) and upon a 100 µm diamond bur preparation in (c).

This is somewhat odd considering that the chemical-bonding potential of functional monomers to HAp (at least with certain functional monomers) should also be beneficial for the bonding effectiveness to enamel that contains even more HAp than dentin does. Recent XRD analysis of interfacial interaction of 10-MDP revealed significantly more intense nanolayering at dentin than

at enamel, both enhanced when the experimental 10-MDP-based self-etching primer was actively rubbed on the surface [74]. Since the nanolayering formed at enamel was not relatively thick, adding CQ/amine to the experimental self-etching primer appeared not necessary (in contrast to bonding to dentin; see above) to reach a bond strength to enamel equally as that achieved by the commercial Clearfil SE Bond™ (Kuraray Noritake).

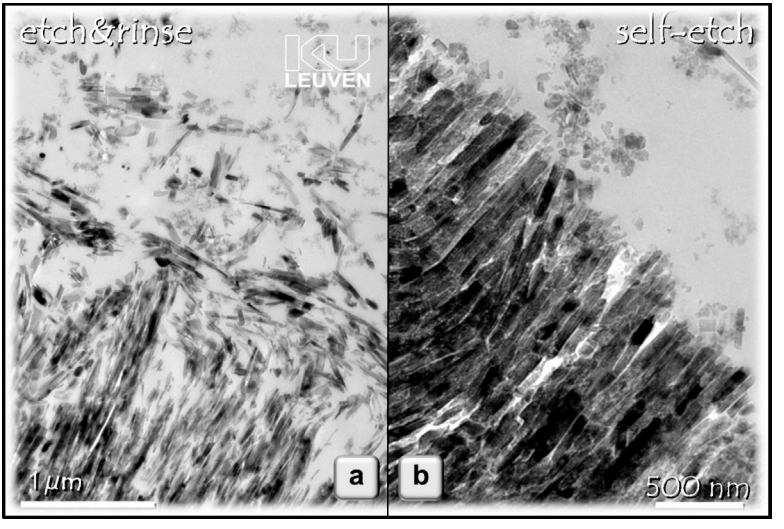

Figure 1.32 TEM photomicrographs illustrating the difference in interaction intensity regarding phosphoric acid etching in (a) and "mild" self-etching enamel in (b). A much deeper interaction can be observed for the E&R approach with deep etch pits and individual HAp rods being partially dissolved versus very shallow interaction and much more solid HAp rods remaining when a mild SE approach was applied.

More recent research investigated to which extent the compromised enamel bonding obtained with (ultra)mild SEAs could be attributed to interference of bur debris smeared across enamel during cavity preparation. Somewhat surprisingly, very little information is available on the morphology of enamel smear layers. In this respect, the interaction of the so-called *ultramild* SEA Clearfil S^3 Bond™ (Kuraray Noritake) with enamel was ultrastructurally studied that was prepared in three ways (Figs. 1.30 and 1.31 above*)* [81], either solely pumice-cleaned and kept uncut **(1)**, ground using

#600-grit silicon carbide (SiC) paper **(2)**, or cut using a medium-grit (100 μm) diamond bur **(3)**. At uncut enamel, the thin aprismatic enamel layer acted as a barrier, which hindered in most areas the adhesive to infiltrate beyond—even though a void-free interface was observed. This aprismatic layer was removed by SiC paper grinding that enabled the adhesive to penetrate deeper and more uniformly, reaching a firmer micromechanical interlock with the formation of a fine reticular resin network. Bur preparation, on the other hand, resulted in a much rougher surface, with numerous subsurface cracks that served as infiltration "highways." A fine reticular mesh, as seen on enamel prepared with SiC paper, was, however, not formed, though the bond to enamel must have been stabilized better than when the adhesive was bonded to uncut enamel.

Altogether, the lower bonding effectiveness of (ultra)mild SEAs to enamel should be ascribed most likely in the first place to *less potential for micromechanical interlocking* (which requires some kind of etching) but also to a lower chemical reactivity (nanolayering in the case of 10-MDP) with enamel HAp.

Therefore, *selective etching of enamel margins* with phosphoric acid is highly recommended to combine a more favorable E&R treatment at enamel with a mild SE approach at dentin (see below).

1.7 Self-Adhesive Composites

As today's adhesives are often regarded as technique sensitive, combining the benefits of adhesive and composite technology into a self-adhesive restorative composite was the next step clinicians have been waiting for [11, 71].

Especially *simplification* in clinical adhesive procedures is a major drive for current research and development efforts in the dental industry. However, the hydrophobic–hydrophilic mismatch between the dental composite and the tooth substrate needs to be overcome to achieve a long-term lasting bond. The introduction of SAC cements [84-87] has led to the development of a new class of (restorative) SACs that are bonded to tooth enamel and dentin *without* a separate adhesive.

Although ultrastructural characterization of the adhesive interface revealed tight interaction at enamel and dentin (Fig. 1.33),

recent bond strength evaluation, however, revealed that the bonding effectiveness of the two flowable SACs underscores that of one-step SEAs and *one gold-standard* three-step E&RA when combined with their proprietary flowable composite (Fig. 1.33). Consequently, routine clinical application of SACs should be very carefully considered, in particular in case no macroretention is provided.

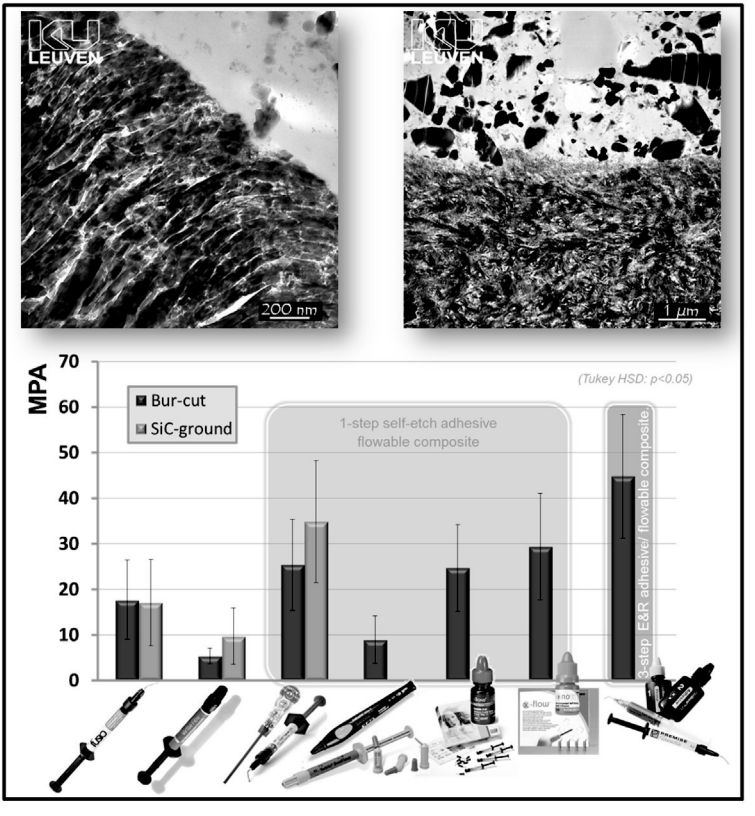

Figure 1.33 Collage of two TEM photomicrographs showing tight interaction of the self-adhesive flowable composite Vertise Flow™ (Kerr) to enamel and dentin. Microtensile bond strength testing showed, however, significantly lower bonding effectiveness to bur-cut and SiC-ground dentin of the SACs Vertise Flow™ (Kerr) and Fusio Liquid Dentin™ (Pentron) than of one-step SEA/flowable composite combinations and in particular the three-step E&RA/flowable composite combination.

1.8 Clinical Performance of Adhesives and Its Prediction in the Laboratory

Despite the importance of laboratory studies attempting to predict clinical performance of biomaterials, clinical trials remain the ultimate way to collect scientific evidence on the clinical effectiveness of a restorative treatment [19]. The popularity of in vitro studies in the field of adhesive dentistry may, in part, be ascribed to the rapid evolution of dental adhesive technology and the resultant high turnover of adhesives. This often tempts manufacturers to release a successor product in the market even before its precursor has been clinically evaluated, at least in the long term. By carrying out in vivo studies, all possible aging factors play at the same time, thereby disclosing whether an adhesive is truly reliable for routine clinical practice. Retention, marginal integrity and clinical microleakage are usually the key parameters recorded to judge the clinical effectiveness of adhesives.

As mentioned before, the best clinical performance with regard to retention (the most objective criterion to judge clinical effectiveness) has so far been achieved by GIs (Fig. 1.34) [19, 71].

Despite their excellent clinical performance in terms of retention, GIs commonly present with lower esthetic features and poorer physicomechanical properties that may clinically require them to be replaced more rapidly than resin-based restorative materials.

Besides GIs, three-step E&RAs have exhibited good clinical effectiveness (Fig. 1.34) [19, 71]. The *clinical durability* of three-step E&RAs confirms their generally superior laboratory results, in which they are considered as the gold standard and employed as a control to compare the performance of new-generation adhesives.

According to the same standard, *mild* two-step SEAs tend to approach three-step E&RAs in terms of low annual failure rates (Fig. 1.34) [19, 71]. Their ability to provide a shallow but uniform hybrid layer, along with their capability to chemically bond to the dentin substrate, seems to play an important role to resist long-term hydrolytic degradation. Commonly, the clinical performance of such SEAs does not vary substantially from one study to another, which is indicative of their rather low technique sensitivity. Considering solely mild SEAs, their annual failure rate happens to be as low as that of GIs [71].

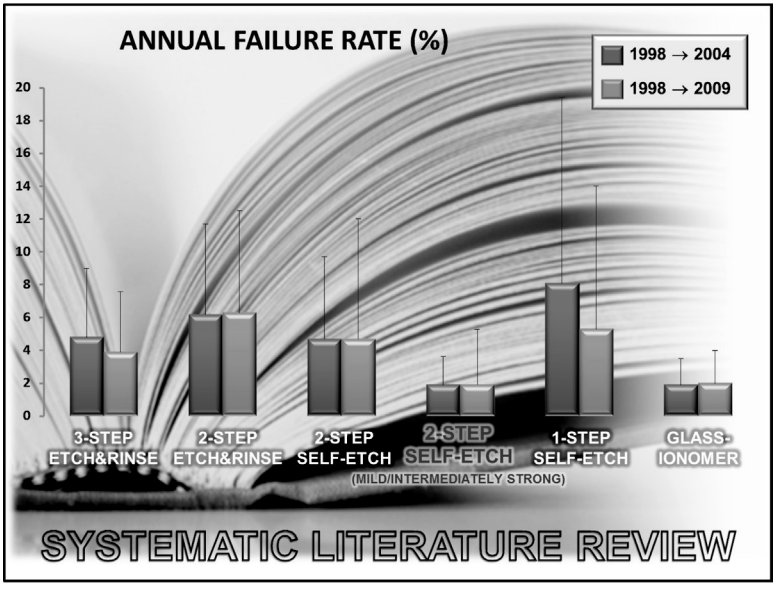

Figure 1.34 Annual failure rates for different classes of adhesives and also for GIs, determined upon a systematic literature review in two periods. When *mild* two-step SEAs are separated from the other two-step SEAs, their annual failure rate equals that of GIs. The annual failure rate of the youngest generation of one-step SEAs is reducing.

In general, two-step E&RAs have performed less favorably than the conventional three-step version [19, 71] (Fig. 1.34). Laboratory studies have corroborated these results, ascribing their poorer performance to their higher hydrophilicity and reduced hybridization potential.

So far, rather inefficient clinical performance has been noted for the newest generation of one-step adhesives [19, 71] (Fig. 1.34). Widely varying retention scores have been recorded, indicating their higher technique sensitivity despite their favorable user-friendliness. Such lower bonding performance must be ascribed to the many concerns advanced earlier. Nevertheless, clearly improved bonding performance with reduced annual failure rates was recorded for the newest generation of one-step adhesives [71] (see Fig. 1.34).

Correlating two extensive systematic literature reviews, having focused on laboratory bond strength testing [36] and on retention rates of class V composite restorations [19, 71], showed that *no significant correlation* was found between "immediate" bond strength and two-year class V retention rates ($r^2 = 0.12$; $p = 0.5056$), while a *significantly* and *relatively good correlation* ($r^2 = 0.58$; $p = 0.0475$) was found between "aged" bond strength and five-year class V retention rates. This finding confirms the definite need to test new adhesive formulations not only *immediately* but also in particular *after a kind of artificial aging*, which appears to predict clinical effectiveness relatively well.

1.9 Conclusion: Today's Most Ideal Adhesive Approach to Achieve Durable Bonding

Micromechanical interlocking is still the best strategy to bond to enamel (Fig. 1.35).

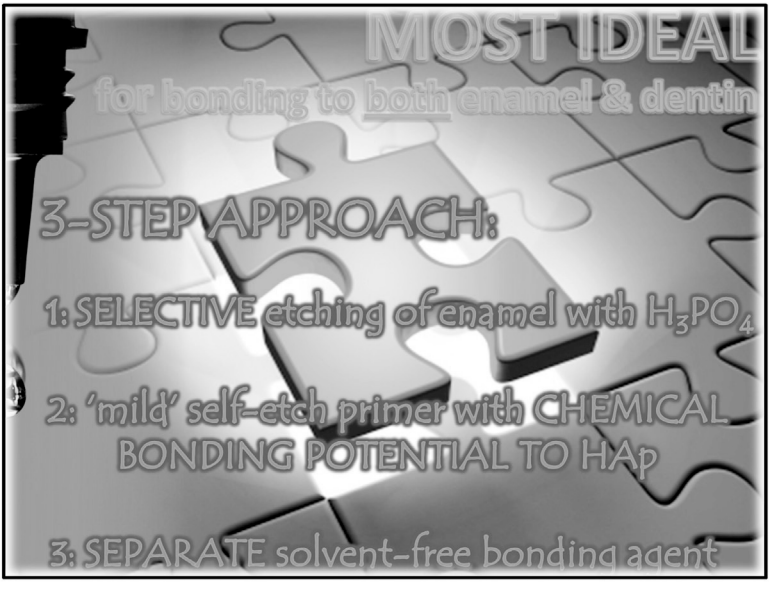

Figure 1.35 The most ideal adhesive approach today to durably bond to enamel and dentin according to KU Leuven BIOMAT.

Selective phosphoric acid etching of enamel cavity margins is therefore today highly recommended as a **first step** in the ideal three-step bonding approach. In the **second step**, a "*mild*" SEA is *recommended* to be applied to both the beforehand-etched enamel and (unetched) dentin. Such a mild SEA should contain a *functional monomer with a high chemical affinity to HAp*. This approach appears to guarantee the most durable bonding performance at dentin, provided that it deals adequately with the debris smeared across the surface by a bur. Phosphoric acid etching of dentin could nowadays be considered too aggressive for dentin, given all the consequences related to exposure of the vulnerable collagen (Fig. 1.36). As a final **third step**, the interface is best sealed by the application of a *solvent-free bonding resin* with adequate polymerization efficiency.

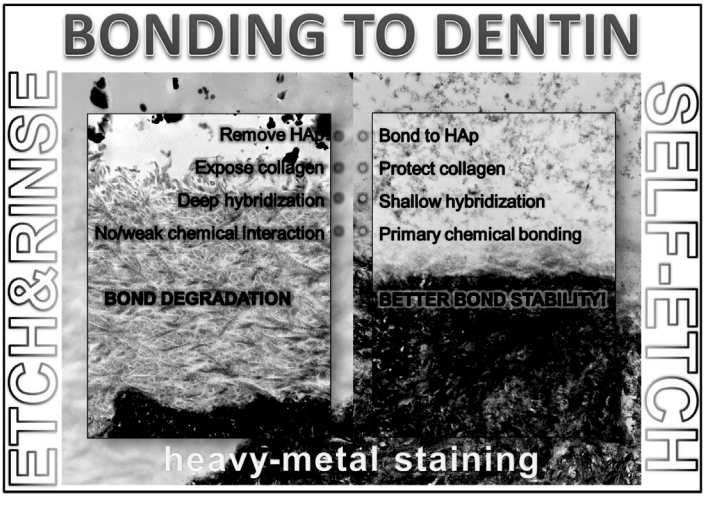

Figure 1.36 The difference in interaction between the E&R and the "mild" SE approach.

Acknowledgments

The authors wish to thank all KU Leuven BIOMAT researchers who have worked on the diverse aspects of bonding to tooth tissue, as was covered in this chapter (Fig. 1.37).

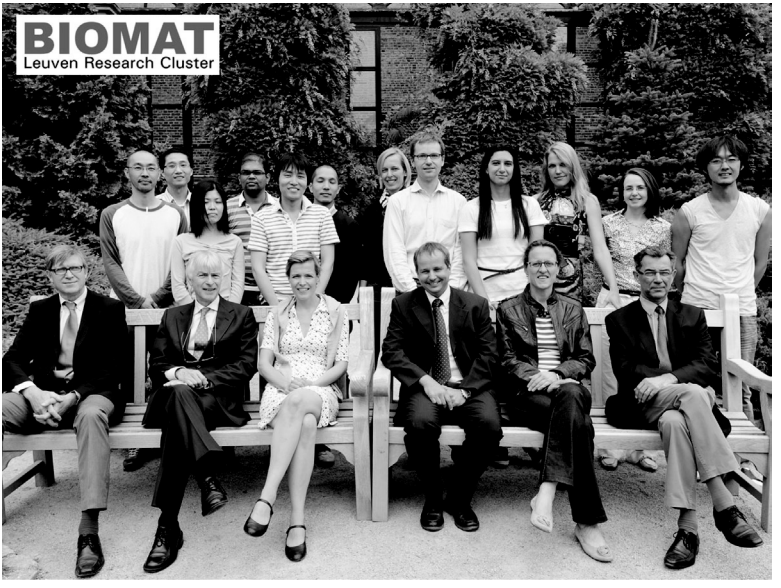

Figure 1.37 The KU Leuven BIOMAT research team.

References

1. Degrange, M., Roulet, J. F. (1997) *Minimally Invasive Restorations with Bonding*, Quintessence, Chicago, IL, USA.
2. Tyas, M. J., Anusavice, K. J., Frencken, J. E., Mount, G. J. (2000) Minimal intervention dentistry: a review. FDI Commission Project 1-97, *Int. Dent. J.*, **50**, 1–12.
3. Van Meerbeek, B., De Munck, J., Yoshida, Y., Inoue, S., Vargas, M., Vijay, P., Van Landuyt, K., Lambrechts, P., Vanherle, G. (2003) Buonocore memorial lecture. Adhesion to enamel and dentin: current status and future challenges, *Oper. Dent.*, **28**, 215–235.
4. Poitevin, A., De Munck, J., Van Ende, A., Suyama, Y., Mine, A., Peumans, M., Van Meerbeek, B. (2013) Bonding effectiveness of self-adhesive composites to dentin and enamel, *Dent. Mater.*, **29**, 221–230.
5. Wilson, A. D., Kent, B. E. (1972) A new translucent cement for dentistry. The glass ionomer cement, *Br. Dent. J.*, **132**, 133–135.
6. Yoshida, Y., Van Meerbeek, B., Nakayama, Y., Yoshioka, M., Snauwaert, J., Abe, Y., Lambrechts, P., Vanherle, G., Okazaki, M. (2001) Adhesion to and decalcification of hydroxyapatite by carboxylic acids, *J. Dent. Res.*, **80**, 1565–1569.

7. Yoshioka, M., Yoshida, Y., Inoue, S., Lambrechts, P., Vanherle, G., Nomura, Y., Okazaki, M., Shintani, H., Van Meerbeek, B. (2002) Adhesion/decalcification mechanisms of acid interactions with human hard tissues, *J. Biomed. Mater. Res*., **59**, 56–62.
8. De Munck, J., Van Landuyt, K., Peumans, M., Poitevin, A., Lambrechts, P., Braem, M., Van Meerbeek, B. (2005a) A critical review of the durability of adhesion to tooth tissue: methods and results, *J. Dent. Res*., **84**, 118–132.
9. Van Meerbeek, B., Yoshida, Y., Van Landuyt, K., Perdigão, J., De Munck, J., Lambrechts, P., Inoue, S., Peumans, M. (2006) Bonding to enamel and dentin, in *Fundamentals of Operative Dentistry. A Contemporary Approach*, 3rd ed. (Ed. Summitt, J. B., Robbins, J. W., Hilton, T. J., Schwartz, R. S.), Quintessence, Chicago, Il, USA, ISBN 0-86715-452-7.
10. De Munck, J., Vargas, M., Iracki, J., Van Landuyt, K., Poitevin, A., Lambrechts, P., Van Meerbeek, B. (2005b) One-day bonding effectiveness of new self-etch adhesives to bur-cut enamel and dentin, *Oper. Dent*., **30**, 39–49.
11. Van Meerbeek, B., Yoshihara, K., Yoshida, Y., Mine, A., De Munck, J., Van Landuyt, K. L. (2011) State of the art of self-etch adhesives, *Dent. Mater*., **27**, 17–28.
12. Coutinho, E., Van Landuyt, K., De Munck, J., Poitevin, A., Yoshida, Y., Inoue, S., Peumans, M., Suzuki, K., Lambrechts, P., Van Meerbeek, B. (2006) Development of a self-etch adhesive for resin-modified glass ionomers, *J. Dent. Res*., **85**, 349–53.
13. Smith, D. C. (1968) A new dental cement, *Br. Dent. J*., **124**, 381–384.
14. Akinmade, A. O., Nicholson, J. W. (1993) GI cements as adhesives. Part I: fundamental aspects and their clinical relevance*, J. Mater. Sci. Mater. Med*., **4**, 95–101.
15. Wilson, A. D., Prosser, H. J., Powis, D. M. (1983) Mechanism of adhesion of polyelectrolyte cements to hydroxyapatite*, J. Dent. Res*., **62**, 590–592.
16. Lin, A., McIntyre, N. S., Davidson, R. D. (1992) Studies on the adhesion of GI cements to dentin*, J. Dent. Res*. **71**, 1836–1841.
17. Yoshida, Y., Van Meerbeek, B., Nakayama, Y., Snauwaert, J., Hellemans, L., Lambrechts, P., Vanherle, G., Wakasa, K. (2000) Evidence of chemical bonding at biomaterial-hard tissue interfaces*, J. Dent. Res*., **79**, 709–714.
18. Coutinho, E., Yoshida, Y., Inoue, S., Fukuda, R., Snauwaert, J., Nakayama, Y., De Munck, J., Lambrechts, P., Suzuki, K., Van Meerbeek, B. (2007) Gel phase

formation at resin-modified glass-ionomer/tooth interfaces, *J. Dent. Res.*, **86**, 656–661.

19. Peumans, M., Kanumilli, P., De Munck, J., Van Landuyt, K., Lambrechts, P., Van Meerbeek, B. (2005) Clinical effectiveness of contemporary adhesives: a systematic review of current clinical trials, *Dent. Mater.*, **21**, 864–881.
20. Kleverlaan, C. J., van Duinen, R. N., Feilzer, A. J. (2004) Mechanical properties of glass ionomer cements affected by curing methods, *Dent. Mater.*, **20**, 45–50.
21. Lohbauer, U., Krämer, N., Siedschlag, G., Schubert, E. W., Lauerer, B., Müller, F. A., Petschelt, A., Ebert, J. (2011) Strength and wear resistance of a dental glass-ionomer cement with a novel nanofilled resin coating, *Am. J. Dent.*, **24**, 124–128.
22. Bonifácio, C. C., Werner, A., Kleverlaan, C. J. (2012) Coating glass-ionomer cements with a nanofilled resin, *Acta Odontol. Scand.*, **70**, 471–477.
23. World Health Organization. (2010) *Future Use of Materials for Dental Restoration. Report of the Meeting Convened at WHO HQ, Geneva, Switzerland (November 16–17, 2009)*, ISBN 978-92-4-150064-7.
24. Nakabayashi, N., Kojima, K., Masuhara, E. (1982) The promotion of adhesion by the infiltration of monomers into tooth substrates, *J. Biomed. Mater. Res.*, **16**, 265–273.
25. Buonocore, M. G. (1955) A simple method of increasing the adhesion of acrylic filling materials to enamel surfaces, *J. Dent. Res.*, **34**, 849–853.
26. De Munck, J., Van Meerbeek, B., Yoshida, Y., Inoue, S., Vargas, M., Suzuki, K., Lambrechts, P., Vanherle, G. (2003) Four-year water degradation of total-etch adhesives bonded to dentin, *J. Dent. Res.*, **82**, 136–140.
27. Perdigão, J., Lambrechts, P., Van Meerbeek, B., Tomé, A. R., Vanherle, G., Lopes, A. B. (1996) Morphological field emission-SEM study of the effect of six phosphoric acid etching agents on human dentin, *Dent. Mater.*, **12**, 262–271.
28. Xu, J., Stangel, I, Butler, I. S., Gilson, D. F. (1997) An FT-Raman spectroscopic investigation of dentin and collagen surfaces modified by 2-hydroxyethylmethacrylate, *J. Dent. Res.*, **76**, 596–601.
29. Nishiyama, N., Suzuki, K., Komatsu, K., Yasuda, S., Nemoto, K. (2002) A 13C NMR study on the adsorption characteristics of HEMA to dentinal collagen, *J. Dent. Res.*, **81**, 469–471.

30. Hiraishi, N., Tochio, N., Kigawa, T., Otsuki, M., Tagami, J. (2013) Monomer-collagen interactions studied by saturation transfer difference NMR, *J. Dent. Res.*, **92**, 284–288.

31. Kanca, J., 3rd. (1992) Resin bonding to wet substrate. 1. Bonding to dentin, *Quintess. Int.*, **23**, 39–41.

32. Gwinnett, A. J., Kanca, J. A., 3rd. (1992) Micromorphology of the bonded dentin interface and its relationship to bond strength, *Am. J. Dent.*, **5**, 73–77.

33. Tay, F. R., Gwinnett, J. A., Wei, S. H. (1996) Micromorphological spectrum from overdrying to overwetting acid-conditioned dentin in water-free acetone-based, single-bottle primer/adhesives, *Dent. Mater.*, **12**, 236–244.

34. Van Meerbeek, B., Yoshida, Y., Lambrechts, P., Vanherle, G., Duke, E. S., Eick, J. D., Robinson, S. J. (1998) A TEM study of two water-based adhesive systems bonded to dry and wet dentin, *J. Dent. Res.*, **77**, 50–59.

35. Peumans, M., De Munck, J., Van Landuyt, K. L., Poitevin, A., Lambrechts, P., Van Meerbeek, B. (2012) A 13-year clinical evaluation of two three-step etch-and-rinse adhesives in non-carious class-V lesions, *Clin. Oral Investig.*, **16**, 129–137.

36. De Munck, J., Mine, A., Poitevin, A., Van Ende, A., Cardoso, M. V., Van Landuyt, K. L., Peumans, M., Van Meerbeek, B. (2012) Meta-analytical review of parameters involved in dentin bonding, *J. Dent. Res.*, **91**, 351–357.

37. Liu, Y., Tjäderhane, L., Breschi, L., Mazzoni, A., Li, N., Mao, J., Pashley, D. H., Tay, F. R. (2011) Limitations in bonding to dentin and experimental strategies to prevent bond degradation, *J. Dent. Res.*, **90**, 953–968.

38. Sano, H., Shono, T., Takatsu, T., Hosoda, H. (1994) Microporous dentin zone beneath resin-impregnated layer, *Oper. Dent.*, **19**, 59–64.

39. Sano, H., Takatsu, T., Ciucchi, B., Horner, J. A., Matthews, W. G., Pashley, D. H. (1995) Nanoleakage: leakage within the hybrid layer, *Oper. Dent.*, **20**, 18-25.

40. Breschi, L., Mazzoni, A., Ruggeri, A., Cadenaro, M., Di Lenarda, R., Dorigo, E de Stefano. (2008) Dental adhesion review: aging and stability of the bonded interface, *Dent. Mater.*, **24**, 90–101.

41. Sadek, F. T., Braga, R. R., Muench, A., Liu, Y., Pashley, D. H., Tay, F. R. (2010) Ethanol wet-bonding challenges current anti-degradation strategy, *J. Dent. Res.*, **89**, 1499–1504.

42. Hebling, J., Pashley, D. H., Tjäderhane, L., Tay, F. R. (2005) Chlorhexidine arrests subclinical degradation of dentin hybrid layers in vivo, *J. Dent. Res*., **84**, 741–746.

43. Tay, F. R., Pashley, D. H., Loushine, R. J., Weller, R. N., Monticelli, F., Osorio, R. (2006) Self-etching adhesives increase collagenolytic activity in radicular dentin, *J. Endod.*, **32**, 862–868.

44. De Munck, J., Van den Steen, P. E., Mine, A., Van Landuyt, K. L., Poitevin, A., Opdenakker, G., Van Meerbeek, B. (2009) Inhibition of enzymatic degradation of adhesive-dentin interfaces, *J. Dent. Res*., **88**, 1101–1106.

45. Nishitani, Y., Yoshiyama, M., Wadgaonkar, B., Breschi, L., Mannello, F., Mazzoni, A., Carvalho, R. M., Tjäderhane, L., Tay, F. R., Pashley, D. H. (2006) Activation of gelatinolytic/collagenolytic activity in dentin by self-etching adhesives, *Eur. J. Oral Sci*., **114**, 160–166.

46. De Munck, J., Mine, A., Van den Steen, P. E., Van Landuyt, K. L., Poitevin, A., Opdenakker, G., Van Meerbeek, B. (2010) Enzymatic degradation of adhesive-dentin interfaces produced by mild self-etch adhesives, *Eur. J. Oral Sci*., **118**, 494–501.

47. Mazzoni, A., Nascimento, F. D., Carrilho, M., Tersariol, I, Papa, V., Tjäderhane, L., Di Lenarda, R., Tay, F. R., Pashley, D. H., Breschi, L. (2012) MMP activity in the hybrid layer detected with in situ zymography, *J. Dent. Res*., **91**, 467–472.

48. Mazzoni, A., Scaffa, P., Carrilho, M., Tjäderhane, L., Di Lenarda, R., Polimeni, A., Tezvergil-Mutluay, A., Tay, F. R., Pashley, D. H., Breschi, L. (2013) Effects of etch-and-rinse and self-etch adhesives on dentin MMP-2 and MMP-9, *J. Dent. Res*., **92**, 82–86.

49. Breschi, L., Martin, P., Mazzoni, A., Nato, F., Carrilho, M., Tjäderhane, L., Visintini, E., Cadenaro, M., Tay, F. R., De Stefano Dorigo, E., Pashley, D. H. (2010a) Use of a specific MMP-inhibitor (galardin) for preservation of hybrid layer, *Dent. Mater*., **26**, 571–578.

50. Breschi, L., Mazzoni, A., Nato, F., Carrilho, M., Visintini, E., Tjäderhane, L., Ruggeri, A Jr, Tay, F. R., Dorigo Ede, S., Pashley, D. H. (2010b) Chlorhexidine stabilizes the adhesive interface: a 2-year in vitro study, *Dent. Mater*., **26**, 320–325.

51. Almahdy, A., Koller, G., Sauro, S., Bartsch, J. W., Sherriff, M., Watson, T. F., Banerjee, A. (2012) Effects of MMP inhibitors incorporated within dental adhesives, *J. Dent. Res*., **91**, 605–611.

52. Lührs, A. K., De Munck, J., Geurtsen, W., Van Meerbeek, B. (2013) Does inhibition of proteolytic activity improve adhesive luting? *Eur. J. Oral Sci*., **121**, 121–131.

53. Martin-De Las Heras, S., Valenzuela, A., Overall, C. M. (2000b) The matrix metalloproteinase gelatinase A in human dentine, *Arch. Oral Biol*., **45**, 757–765.

54. Martin-De Las Heras, S., Valenzuela, A., Overall, C. M. (2000a) Gelatinase A in human dentin as a new biochemical marker for age estimation*, J. Forensic Sci*., **45**, 807–811.

55. Tay, F. R., Pashley, D. H. (2008) Guided tissue remineralisation of partially demineralised human dentine, *Biomaterials*, **29**, 1127–1137.

56. Tay, F. R., Pashley, D. H. (2009) Biomimetic remineralization of resin-bonded acid-etched dentin*, J. Dent. Res*., **88**, 719–724.

57. Peumans, M., De Munck, J., Van Landuyt, K. L., Poitevin, A., Lambrechts, P., Van Meerbeek, B. (2010) Eight-year clinical evaluation of a two-step self-etch adhesive with and without selective enamel etching, *Dent. Mater*., **26**, 1176–1184.

58. Van Landuyt, K. L., Peumans, M., De Munck, J., Cardoso, M. V., Ermis, B., Van Meerbeek, B. (2011) Three-year clinical performance of a HEMA-free one-step self-etch adhesive in non-carious cervical lesions, *Eur. J. Oral Sci*., **119**, 511–516.

59. Ermis, R. B., Van Landuyt, K. L., Cardoso, M. V., De Munck, J., Van Meerbeek, B., Peumans, M. (2012) Clinical effectiveness of a one-step self-etch adhesive in non-carious cervical lesions at 2 years, *Clin. Oral Invest*., **16**, 889–897.

60. Perdigão, J., Geraldeli, S., Hodges, J. S. (2003) Total-etch versus self-etch adhesive: effect on postoperative sensitivity*, J. Am. Dent. Assoc*., **134**, 1621–1629.

61. Van Meerbeek, B., Kanumilli, P., De Munck, J., Van Landuyt, K., Lambrechts, P., Peumans, M. (2005) A randomized controlled study evaluating the effectiveness of a two-step self-etch adhesive with and without selective phosphoric-acid etching of enamel, *Dent. Mater*., **21**, 375–383.

62. Van Landuyt, K. L., Snauwaert, J., De Munck, J., Peumans, M., Yoshida, Y., Poitevin, A., Coutinho, E., Suzuki, K., Lambrechts, P., Van Meerbeek, B. (2007b) Systematic review of the chemical composition of contemporary dental adhesives. *Biomaterials*, **28**, 3757–3785.

63. Van Landuyt, K. L., Mine, A., De Munck, J., Countinho, E., Peumans, M., Jaecques, S., Lambrechts, P., Van Meerbeek, B. (2008) Technique sensitivity of water-free one-step adhesives, *Dent. Mater*., **24**, 1258–1267.

64. Koshiro, K., Sidhu, S. K., Inoue, S., Ikeda, T., Sano, H. (2006) New concept of resin-dentin interfacial adhesion: the nanointeraction zone, *J. Biomed. Mater. Res. B: Appl. Biomater*., **77**, 401–408.

65. Tay, F. R., Pashley, D. H. (2003) Water treeing-a potential mechanism for degradation of dentin adhesives, *Am. J. Dent*., **16**, 6–12.

66. Tay, F. R., Pashley, D. H., Yoshiyama, M. (2002) Two modes of nanoleakage expression in single-step adhesives, *J. Dent. Res*., **81**, 472–476.

67. Van Landuyt, K. L., Snauwaert, J., De Munck, J., Coutinho, E., Poitevin, A., Yoshida, Y., Suzuzki, K., Lambrechts, P., Van Meerbeek, B. (2007a) Origin of interfacial droplets with one-step adhesives, *J. Dent. Res*., **86**, 739–744.

68. Van Landuyt, K. L., De Munck, J., Snauwaert, J., Coutinho, E., Poitevin, A., Yoshida, Y., Inoue, S., Peumans, M., Suzuki, K., Lambrechts, P., Van Meerbeek, B. (2005) Monomer-solvent phase separation in one-step self-etch adhesives, *J. Dent. Res*., **84**, 183–188.

69. Nishiyama, N., Tay, F. R., Fujita, K., Pashley, D. H., Ikemura, K., Hiraishi, N., King, N. M. (2006) Hydrolysis of functional monomers in a single-bottle self-etching primer--correlation of 13C NMR and TEM findings, *J. Dent. Res*., **85**, 422–426.

70. Salz, U., Zimmermann, J., Zeuner, F., Moszner, N. (2005) Hydrolytic stability of self-etching adhesive systems, *J. Adhes. Dent*., **7**, 107–116.

71. Van Meerbeek, B., Peumans, M., Poitevin, A., Mine, A., Van Ende, A., Neves, A., De Munck, J. (2010) Relationship between bond-strength tests and clinical outcomes, *Dent. Mater*., **26**, e100–e121.

72. Yoshida, Y., Nagakane, K., Fukuda, R., Nakayama, Y., Okazaki, M., Shintani, H., Inoue, S., Tagawa, Y., Suzuki, K., De Munck, J., Van Meerbeek, B. (2004) Comparative study on adhesive performance of functional monomers, *J. Dent. Res*., **83**, 454–458.

73. Inoue, S., Koshiro, K., Yoshida, Y., De Munck, J., Nagakane, K., Suzuki, K., Sano, H., Van Meerbeek, B. (2005) Hydrolytic stability of self-etch adhesives bonded to dentin, *J. Dent. Res*., **84**, 1160–1164.

74. Yoshihara, K., Yoshida, Y., Nagaoka, N., Fukegawa, D., Hayakawa, S., Mine, A., Nakamura, M., Minagi, S., Osaka, A., Suzuki, K., Van Meerbeek, B. (2010) Nano-controlled molecular interaction at adhesive interfaces for hard tissue reconstruction, *Acta Biomater*., **6**, 3573–3582.

75. Yoshihara, K., Yoshida, Y., Hayakawa, S., Nagaoka, N., Irie, M., Ogawa, T., Van Landuyt, K. L., Osaka, A., Suzuki, K., Minagi, S., Van Meerbeek, B. (2011a) Nanolayering of phosphoric acid ester monomer on enamel and dentin, *Acta Biomater*., **7**, 3187–3195.

76. Yoshihara, K., Yoshida, Y., Hayakawa, S., Nagaoka, N., Torii, Y., Osaka, A., Suzuki, K., Minagi, S., Van Meerbeek, B., Van Landuyt, K. L. (2011b) Self-etch monomer-calcium salt deposition on dentin*, J. Dent. Res*., **90**, 602–606.

77. Yoshida, Y., Yoshihara, K., Hayakawa, S., Nagaoka, N., Okihara, T., Matsumoto, T., Minagi, S., Osaka, A., Van Landuyt, K., Van Meerbeek, B. (2012a) HEMA inhibits interfacial nano-layering of the functional monomer MDP*, J. Dent. Res*., **91**, 1060–1065.

78. Yoshida, Y., Yoshihara, K., Nagaoka, N., Hayakawa, S., Torii, Y., Ogawa, T., Osaka, A., Van Meerbeek, B. (2012b) Self-assembled nano-layering at the adhesive interface*, J. Dent. Res*., **91**, 376–381.

79. Fukegawa, D., Hayakawa, S., Yoshida, Y., Suzuki, K., Osaka, A., Van Meerbeek, B. (2006) Chemical interaction of phosphoric acid ester with hydroxyapatite*, J. Dent. Res*., **85**, 941–944.

80. Pashley, D. H., Tao, L., Boyd, L., King, G. E., Horner, J. A. (1988) Scanning electron microscopy of the substructure of smear layers in human dentine, *Arch Oral Biol*., **33**, 265–270.

81. Mine, A., De Munck, J., Vivan Cardoso, M., Van Landuyt, K. L., Poitevin, A., Kuboki, T., Yoshida, Y., Suzuki, K., Van Meerbeek, B. (2010) Enamel-smear compromises bonding by mild self-etch adhesives*, J. Dent. Res*., **89**, 1505–1509.

82. Ermis, R. B., De Munck, J., Cardoso, M. V., Coutinho, E., Van Landuyt, K. L., Poitevin, A., Lambrechts, P., Van Meerbeek, B. (2008) Bond strength of self-etch adhesives to dentin prepared with three different diamond burs, *Dent. Mater*., **24**, 978–985.

83. Van Landuyt, K. L., De Munck, J., Mine, A., Cardoso, M. V., Peumans, M., Van Meerbeek, B. (2010) Filler debonding & subhybrid-layer failures in self-etch adhesives*, J. Dent. Res*., **89**, 1045–1050.

84. De Munck, J., Vargas, M., Van Landuyt, K., Hikita, K., Lambrechts, P., Van Meerbeek, B. (2004) Bonding of an auto-adhesive luting material to enamel and dentin, *Dent. Mater*., **20**, 963–971.

85. Goracci, C., Cury, A. H., Cantoro, A., Papacchini, F., Tay, F., Ferrari, M. (2006) Microtensile bond strength and interfacial properties of self-etching and self-adhesive resin cements used to lute composite onlays under different seating forces*, J. Adhes. Dent*., **8**, 327-335.

86. Yang, B., Ludwig, K., Adelung, R., Kern, M. (2006) Micro-tensile bond strength of three luting resins to human regional dentin, *Dent. Mater*., **22**, 45–56.

87. Barcellos, D., Batista, G., Silva, M., Rangel, P., Torres, C., Fava, M. (2011) Evaluation of bond strength of self-adhesive cements to dentin with or without application of adhesive systems, *J. Adhes. Dent.*, **13**, 261–265.

Chapter 2

Biomineralization and Biodemineralization of Enamel

Maisoon Al-Jawad and Paul Anderson
Institute of Dentistry, Barts and The London School of Medicine and Dentistry, Queen Mary University of London, E1 4NS, UK
m.al-jawad@qmul.ac.uk

Biomineralization is an important concept for understanding how enamel is initially formed and subsequently grows. The structure and function of fully mature enamel are determined by these complex processes. Once formed, enamel is in continual contact with the oral environment, particularly saliva and plaque fluids, which bathe the exposed surfaces. Thus, during formation and subsequently when completely formed, enamel is constantly undergoing biomineralization events, which may also influence its destruction during tooth mineral loss events such as caries and erosion. This chapter focuses on the processes occurring at different length scales during the biomineralization and biodemineralization of enamel and on the factors that influence its subsequent preservation.

Handbook of Oral Biomaterials
Edited by Jukka P. Matinlinna

ISBN 978-981-4463-12-6 (Hardcover), 978-981-4463-13-3 (eBook)
www.panstanford.com

2.1 Introduction

Biomineralization is the process by which living organisms construct functioning inorganic mineral material devices out of supersaturated ionic solutions through controlled deposition and regulated growth, leading to a highly specified structure, size, and orientation suited to the functional requirement. Dental enamel biomineralization is unique since it forms the most highly mineralized, most oriented, and strongest biological hard tissue in the mammalian skeleton. Mature enamel is 96% hydroxyapatite (HA) mineral, 3% water, and 1% organic matter by weight. Once fully mature, the enamel tissue is a hierarchical structure with ordered arrangements of units or building blocks present at different length scales. It is comprised of needle-like crystallites, which have a strong preferred orientation along their growth direction. These crystallites bundle into long rod-like structures with cross-sectional dimensions typically of 50 × 25 nm and up to 1 mm long. Typically around 100 HA crystallites are organized and bundled together into larger-scale structures called prisms.

Prisms are approximately 5 μm in diameter and up to several millimeters in length with their long axes at acute angles to, and following the shape of, the enamel–dentine junction (EDJ). The ordering continues to the next length scale as prisms are oriented relative to each other with interprismatic less-ordered enamel in between. Prismatic and interprismatic enamel arrange and grow in the correct conformation to produce the macroscopic shape of the tooth suitable to its function. This intricate and complex hierarchical structure, combined with the small amount of protein in fully mature enamel, explains the particular physicomechanical properties of enamel, allowing it to function as a cutting, grinding, and masticatory tool.

The physical and mechanical properties of enamel need to be considered when designing dental materials including zirconia, since these synthetic materials need to be suitable to replace lost enamel tissue, integrate with remaining healthy tissue, and not damage opposing or neighboring teeth. In addition in dentistry, understanding the biological progression of mineral formation will lead to technological advances in regenerative dentistry. Ideally this could allow the possibility of regrowth of the highly ordered

hierarchical structure of dental enamel using a patient's own cells to control ordered growth from the atomic to the macroscopic scale.

In this chapter the structure and formation of enamel from the point of view of different length scales will be described. A distinction will be made between the initial process of enamel formation, which will be termed "primary" biomineralization, and subsequent remineralization processes in enamel, which happen posteruption in the mouth, termed "secondary" mineralization. The important aspects of "primary" biomineralization are the cellular control and role of proteins secreted by ameloblast cells, including amelogenin, enamelin, ameloblastin, and tuftelin. Once erupted, dental enamel can be lost through different routes, the most common of which are erosion and dental caries. The process of enamel dissolution as a response to changes in the oral environment or "biodemineralization" will be described, together with the role of salivary proteins as an important driver in subsequent remineralization or "secondary" mineralization.

2.1.1 Primary and Secondary Mineralization

The process of primary biomineralization of dental enamel starts in utero for primary dentition and takes several years to complete, varying for each tooth type. Age-linked development of teeth has been comprehensively described on the macroscopic length scale by AlQahtani's "Atlas of Human Tooth Development and Eruption" [1]. This is an invaluable evidence-based resource for accurate age determination from dental remains or dental radiographs.

Once a tooth is fully formed and erupted in the oral cavity, dental enamel will undergo acid attacks, and cyclic demineralization and remineralization regimes exists in the mouth as a function of food or drink challenges. There are drivers that will push the balance toward demineralization, such as poor oral hygiene, which can then lead to dental caries. Conversely there are mechanisms such as the role of saliva and, in particular, salivary proteins that can tip the balance toward faster remineralization of enamel, ensuring that enamel maintains its structure and mechanical efficacy. This remineralization of enamel has been termed "secondary" mineralization so as to be distinct from the initial pre-eruption enamel formation process.

Fully mature enamel does not contain cells and therefore is not able to regenerate itself; therefore secondary mineralization or remineralization is an acellular process relying on chemical and rather than biological control.

2.1.2 Biologically Controlled and Biologically Induced Mineralization

Primary enamel biomineralization is an example of biologically controlled mineralization. Biologically controlled mineralization is a highly regulated process that produces inorganic minerals with reproducible structures and species-specific crystallographic and chemical properties. It produces inorganic minerals that have a specific biological function. Biologically controlled mineralization occurs in many unicellular creatures and many multicellular organisms. Properties of a biologically controlled inorganic mineral include uniform particle sizes, well-defined structures and compositions, high levels of spatial organization, complex morphologies, controlled aggregation, preferred crystallographic orientation, a higher-order assembly, and hierarchical structures. Dental enamel is an excellent example of a biologically controlled mineral structure.

In contrast, in biologically induced mineralization, inorganic minerals are deposited by precipitation arising from secondary interactions with the surrounding environment. For example, in some green algae, calcium carbonate is precipitated from saturated calcium bicarbonate solutions by metabolic removal of CO_2 during photosynthesis. Thus the inorganic mineral can be a by-product of another reaction process. Bacteria typically carry out biologically induced mineralization. Bacteria can precipitate various inorganic minerals by passing OH^- ions across their cell walls. The posteruptive secondary mineralization of dental enamel is an example of biologically induced mineralization since there is no cellular control but chemical control from the environment. The size, shape, structure, composition, and organization of the mineral particles can be poorly defined and heterogeneous. It is often difficult to distinguish biologically induced minerals from those produced synthetically.

2.1.3 Amelogenesis

Dental enamel is the most mineralized of all tissues and forms progressively over extended time periods. "Amelogenesis" is the term used for the formation of enamel. The enamel starts to form at the dentine interface and initially grows away from this interface layer. The hierarchical structure of enamel is achieved by a dynamic process of controlled crystal formation, organization, and growth guided by the organic matrix. It is an excellent example of organic matrix–mediated biomineralization. At the start of the process the tissue is rich in the organic matrix. As the process of mineralization progresses the organic matrix retreats and breaks down, leaving a material that is 96% mineral by weight. In Fig. 2.1 the relationship between the amount of amelogenin protein and the amount of mineral as a function of time during the primary biomineralization process is illustrated.

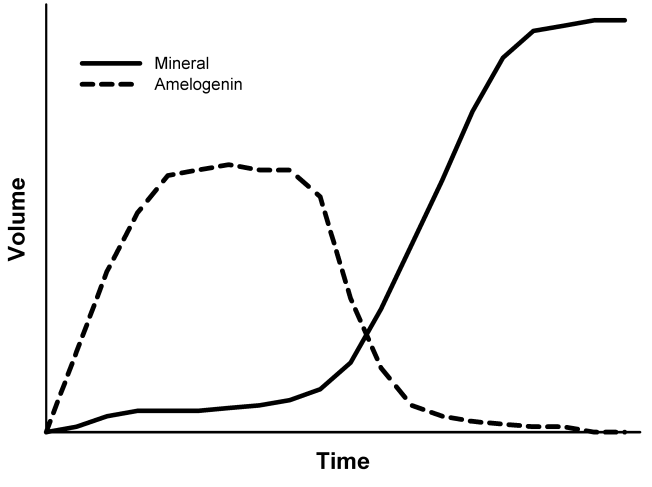

Figure 2.1 Mineral content vs. amelogenin as a function of the enamel development time.

The part of amelogenesis when mineralization occurs can be divided into four distinct stages:

(i) Secretory stage:
At this stage, secretion of the extracellular matrix (predominantly amelogenin proteins) by ameloblast cells

occurs, and nucleation of apatite crystallites begins. The enamel tissue is up to 30% mineralized.

(ii) Self-assembly stage:
Overlapping with the secretory stage, in the self-assembly stage, amelogenin protein self-assembles into nanospheres in order to direct and control the size and shape of mineral crystallites, including the prismatic and interprismatic structures. This results in the formation of elongated, ribbon-like crystallites.

(iii) Transition/resorption stage:
By this stage the organic matrix has stopped being secreted and degradation/removal of protein occurs. The ameloblast cells retreat and are replaced with fluid, generating a porous tissue.

(iv) Maturation stage:
The maturation stage of amelogenesis involves a massive increase in mineral ions to facilitate lateral growth of crystals and almost complete removal of the organic matrix. At the end of this stage the final mineral concentrations are reached and all cells have degenerated.

2.1.4 Remineralization

The term "remineralization" is applied to the process by which enamel mineral can be "repaired" by a process of precipitation of what is often presumed to be enamel, or at least calcium HA.

Remineralization is the mechanism by which enamel that has previously undergone mineral loss by some pathological process can under the right supersaturation conditions subsequently recover mineral and potentially fully repair but is perhaps one of the most misunderstood concepts in the dental literature. Although there is considerable in vitro evidence for partial recovery of mineral from very early-stage artificial carious lesions [2], evidence for significant mineral recovery is very scant indeed and for complete recovery of mineral from all but the very early-stage lesions does not exist. Further, there is little if any evidence that the mineral actually redeposited in artificial remineralization systems is in fact calcium HA, or even HA-like, as it is almost impossible to investigate and identify the mineral phases formed.

It is well established that HA nucleates easily under highly supersaturated conditions. However, HA undergoes very little secondary growth, and therefore it is not likely that either the existing enamel mineral or any newly formed protocrystals will regrow following mineral loss merely by increasing the degree of supersaturation. However, within the oral environment the situation may be very different, where the enamel crystallites are bathed continuously in a supersaturated solution that has originated from saliva but also contains a multitude of salivary proteins, some of which are involved in enamel homeostasis [3]. Thus, the oral environment may be better described as a biomineralization environment in which proteins control enamel crystal growth but are also influential in its destruction. Therefore the in vitro systems described in many reported studies do not fully reflect the in vivo environment. Although the proteins involved in amelogenesis have not been identified in saliva, it is likely that some salivary peptides may play a role in the biomineralization control of remineralization in vivo.

Further, the enamel pellicle, a highly organized organic molecular layer immediately overlying the enamel surface, is likely to be involved in the regulation of enamel HA interface chemistry, thereby controlling both remineralization and demineralization. However, it is also unlikely that at the molecular pellicle level, the interface conditions exist similar to those prevailing during amelogenesis. So although some limited mineral deposition may occur, complete repair of significant lesions does not occur, and therefore "healing" of all but the most early-stage enamel lesions will not be possible merely by transporting huge quantities of calcium and phosphate ions to an enamel surface.

2.1.5 Hierarchical Length Scales in Enamel Structure

It is important to understand the process of enamel formation, the final structure formed, the subsequent demineralization and remineralization processes, and the tissue function at different length scales, since this will give us the greatest insight into this complex hierarchical tissue structure and function. Enamel is a heterogeneous tissue with physical and chemical structural distributions at the atomic, nanoscopic, microscopic, and macroscopic distances, all

of which contribute to the final successful function of this tissue. Therefore, in the remainder of this chapter, the detailed physical and chemical characteristics and processes of the enamel structure and its formation are described at the length scales at which they occur.

2.2 Atomic/Molecular Length Scale

2.2.1 Chemical Control of Biomineralization

It is at the atomic and molecular length scale that the chemical control of the primary biomineralization process of enamel formation occurs. The solubility of the apatite phase is a crucial factor in determining the thermodynamic conditions for precipitation, and lattice substitutions are important in controlling the solubility of biological apatite. Many substitutions are possible on the Ca^{2+} and the PO_4^{3-} and the OH^- sites such as Na^+, NH_4^+, K^+, Mg^{2+}, Fe^{2+}, CO_3^{2-}, and F^-. The carbonate-substituted apatite of dental enamel can be written as:

$$Ca_{10-x}(PO_4)_{6-x}(CO_3)_x(OH)_2$$

Chemical analysis of the distribution of fluoride, carbonate, and magnesium in enamel has been carried out by Robinson et al. [4–6]. The amount of fluoridated apatite was determined by etching the tooth sections and analyzing the fluoride concentration in a postetched buffer solution [4]; the concentration of carbonate was determined by dissolving each piece in acid and measuring the volume of CO_2 emitted [5]; and the concentration of magnesium was found using atomic absorption spectrophotometry [6]. Fluoride concentrations decrease as a function of enamel depth from the surface, while carbonate and magnesium concentrations increase (from 2% to 4–6% and from 0.2% to 0.5%, respectively) across the same distance [7]. In addition, changes in crystallographic lattice parameters in crystallite structure can reveal changes in enamel crystal chemistry. Measured using synchrotron X-ray diffraction analyzed using Rietveld refinement, trends in the lattice parameter changes are shown in Fig. 2.2, relative to the average lattice parameters. It can be seen that the *a* and *c* lattice parameters vary between –0.6% and +0.3% of their average values of $a = 9.5165(6)$

Å and c = 6.9394(2) Å, revealing a systematic variation in the lattice parameters as a function of position within the enamel [8]. It can be seen that there is more variation in the a lattice parameter than in the c lattice. This trend has also been seen in dentine, where the a lattice parameter decreased by 0.5% with increasing distance from the EDJ into the dentine, whereas the c lattice parameter only decreased by 0.1% over the same distance [9].

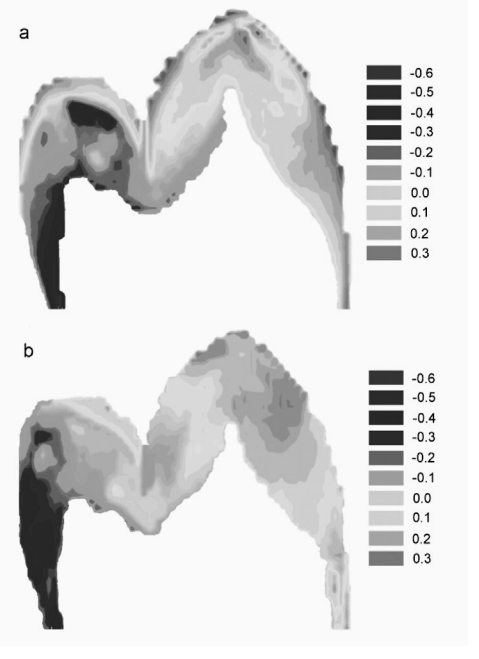

Figure 2.2 (a) The a lattice parameter and (b) c lattice parameter contour maps showing the percentage change in the lattice parameter value at different positions around the tooth.

In addition to a decrease in lattice parameters going from the surface enamel to the EDJ, there is a difference in the lattice parameters on the buccal and lingual sides of the tooth, indicating a change in crystal chemistry on the different sides of the tooth. This could be due to the primary biomineralization process differing on the two sides, perhaps as a response to different mechanical functions of the two sides of the tooth, or due to their slightly different oral environments which would affect the local chemical

environment during post-eruption remineralizing events or due to a combination of both.

2.2.2 Solubility of Calcium Hydroxyapatite

In the oral environment, enamel mineral coexists with saliva, which provides a rich source of calcium and phosphate ions. The concentration of calcium ions in saliva is considered to be about 1 mmol L^{-1} [10]. Thus saliva is very supersaturated with respect to enamel. Considered in inorganic terms alone this should lead to considerable deposition of calcium phosphate mineral were it not for the action of primary and secondary nucleation inhibiting salivary proteins (discussed later).

Figure 2.3 shows the position of the solubility isotherm for HA calculated from speciation software. The exact position of the HA isotherm is dependent on the value for the solubility product of HA used [11]. Unfortunately, the precise value for the solubility product of HA is still a contentious issue, and published values vary [12]. One reason for this, as pointed out by Darvell et al., is that values for the solubility of HA have generally been measured in the presence of bulk (or excess) solid, which often displays incongruent solubility behavior, which leads to variations in the final values. To circumvent these complications, Darvell has reported measurements of the solubility product (K_{Sp}) of HA and related calcium phosphates, and enamel, using an elegant light-scattering method with successively decreasing amounts of solid present so that values can be obtained by extrapolation when no solid remains [13]. For enamel, there is the additional complication that the impurity ion level within the HA lattice can also significantly influence the solubility, and a range of values for K_{Sp} of enamel have been published (e.g., [14–15]). As these values are used in chemical speciation programs [16] this gives rise to variation in the literature about the position of the solubility isotherm of enamel. Therefore, it is advisable to be cautious about reported solubility product values and to take into account the various constraints of each system.

In many dental textbooks, the term “critical pH” is used, defined as the pH at which calcium HA would start to dissolve. From Fig. 2.3, it can be seen that, taking the average concentration of calcium in the oral environment to be 1.0 mmol L^{-1} and the normal oral to be pH 7

(shown by point O on the diagram) and then extrapolating leftward from point O, that is, assuming the calcium concentration remains constant, the pH at which this extrapolation cuts the isotherm is at approximately 5.5, which is the value often seen in many textbooks. However, as discussed the precise value for any given calcium concentration will depend on the value of K_{Sp} used.

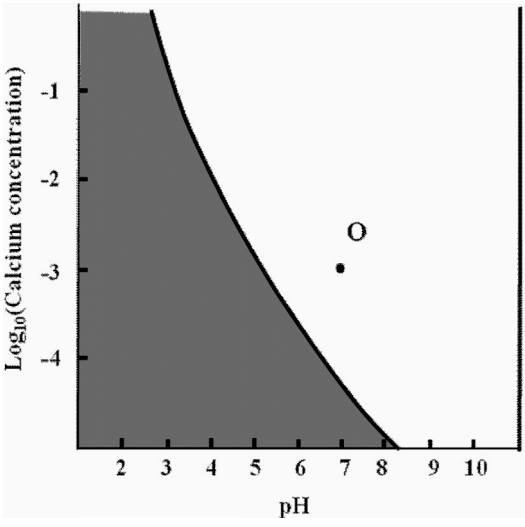

Figure 2.3 Solubility isotherm for calcium HA. Point O represents "normal" conditions within the oral environment.

2.2.3 Proteins of Enamel Biomineralization

Also at the molecular length scale is the role of the extracellular matrix. Dental enamel formation is an example of protein matrix–mediated biomineralization. Enamel proteins comprise predominantly amelogenins, which make up 90–95% of the extracellular matrix, whilst 5–10% are nonamelogenins. Most amelogenin is degraded and removed following maturation. The vast majority of the 1% by weight protein remnant in mature enamel is nonamelogenin protein.

The precise role of each enamel protein is still under exploration since it is a complex system with complicating factors, including a series of degradative changes by proteolytic enzymes during the development of enamel. This results in the accumulation of many smaller enamel proteins and peptides as enamel matures. Briefly, the

evidence to date suggests the following roles for each known enamel protein: dentine sialophosphoprotein initiates mineralization, amelogenin and enamelin control the crystal growth, ameloblastin determines the prismatic pattern, and tuftelin and ameloblastin are likely to be involved in cell signaling.

Amelogenin protein forms an insoluble macromolecular framework that acts as a key mediator in controlling the biomineralization process. Nascent full-length amelogenin is a bipolar macromolecule with high levels of histidine, glutamine, and leucine and has a molecular weight of 25 kDa. It has a highly charged C terminal with an isoelectric point (pI) of approximately 4.2, whilst the remainder of the molecule is hydrophobic with a pI of approximately 8—the overall pI being around 6.5. Research shows that the N terminal is responsible for a self-assembly process through specific interactions between protein segments, causing aggregation into "nanospheres." The C terminal is believed to stabilize nanospheres by being exposed on the surface and thereby hindering further aggregation. A model for the role of amelogenin and enamelin in the guiding and control of crystal growth is the two-component model in organic matrix–mediated biomineralization [17]. This model consists of a structural framework of hydrophobic macromolecules with associated cross-links (in this case amelogenins) onto which are anchored hydrophilic macromolecules acting as active nucleating surfaces to external solutions (in this case enamelins). Organic matrices lower the activation energy of nucleation by reducing interfacial energies and therefore promote crystal nucleation and growth.

2.2.4 Proteins of Saliva

Saliva contains a huge number of proteins and peptides, and well over a thousand have been reported [18]. There are four groups of salivary proteins that are thought to be directly involved in enamel mineral homeostasis. These are proline-rich proteins (PRPs), cystatins, histatins, and statherin.

Many of these peptides have a common evolutionary pathway [19]. Most bind calcium ions and also bind to HA surfaces. It has been proposed that, for example, statherin only binds to the {001} face of HA, suggesting complex, site-specific biomineralization involvement. Many of these peptides are also related to other

proteins involved in biomineralization, for example, the sibling proteins osteopontin and bone sialoproteins [20]. Although it is not clear how these proteins function in enamel homeostasis, it may be that the underlying chemical mechanisms are similar to those involved in enamel biomineralization.

There have been a number of studies exploring the nature of interaction between HA surfaces and salivary proteins, particularly statherin as this binds most readily to the tooth surface, forming the basis of the enamel pellicle. Unfortunately, many of these studies are either computational or solid-state nuclear magnetic resonance (NMR) studies and therefore do not include the impact of water or the solution state, which prevails in the oral environment. Nevertheless, these studies do give considerable insight into the HA–protein interface, and computational studies involving minimum energy calculations are useful in corroborating the experimental evidence obtained [21].

2.2.4.1 Proline-rich proteins

PRPs are about 150 amino acid residues in length and account for approximately 70% of the total protein secreted in saliva [22]. Six different PRPs have been identified. It is understood that their N terminal is involved in inhibition of secondary HA precipitation [23], whereas the C terminal is responsible for adhesion of bacteria enamel surfaces [24]. It has also been confirmed that PRPs are present in the formation of the enamel pellicle [25].

2.2.4.2 Cystatins

Cystatins (121 residues) are present in a wide range of body fluids and tissues [22]. They bind to HA but only about a third as well as statherin [26]. They are also involved in crystal growth inhibition, as well as inhibition of selected bacterial proteases, and the formation of complexes with several viral proteases [27].

2.2.4.3 Histatins

Histatins are a group of 12 low-molecular-weight histidine-rich peptides [27], with histatin 1, histatin 3, and histatin 5 consisting of 38, 32, and 24 amino acid residues, respectively, with histatin 5 being the most common [28]. Histatin 1 is a neutral protein, whereas both histatins 3 and 5 are basic [29]. All adsorb and bind onto HA surfaces

[30]. It is likely that only histatin 1 inhibits secondary precipitation but does not inhibit spontaneous precipitation [30]. Further, histatin 3 does not bind to calcium and only has antifungal and antibacterial functions [31, 32].

2.2.4.4 Statherin

Statherin is a well-studied molecule, which when first discovered was suggested to be important in the inhibition of primary and secondary crystal growth of calcium phosphates in the oral environment [33]. However, more recently, Anderson et al. have reported that it may also be important in the inhibition of dissolution of HA and enamel [34]. From a dental perspective, this means that statherin acts to protect enamel from acidic attack and is therefore part of the natural protection mechanism of oral hard tissues, maintaining enamel integrity [35].

This work confirmed that reported by Makrodimitris et al. who used Monte Carlo and energy minimization computational methods to calculate the adsorption free-energy interactions of statherin binding to HA surfaces. The authors suggested that there is a molecular recognition motif comprising the α helix of statherin at its N terminal binding to the {001} face of HA, reported to be the predominate surface at the enamel–saliva interface [36].

2.3 Nanometer Length Scale

2.3.1 Nanostructure of Enamel

At the nanometer length scale, during enamel formation, HA crystallites are laid down as nanorods with cross-sectional dimensions of 50 × 25 nm and up to 1 mm long. The orientation of these crystallites is important in understanding the structure–function relationship in enamel. The orientation can be measured by synchrotron X-ray diffraction texture analysis—a way to measure the organization in the structure at the nanometer length scale. In Fig. 2.4 the direction that crystallites are oriented as a function of position within a tooth are shown for six serial sections through the enamel of a human premolar. In general the crystallite orientation in enamel is perpendicular to the EDJ.

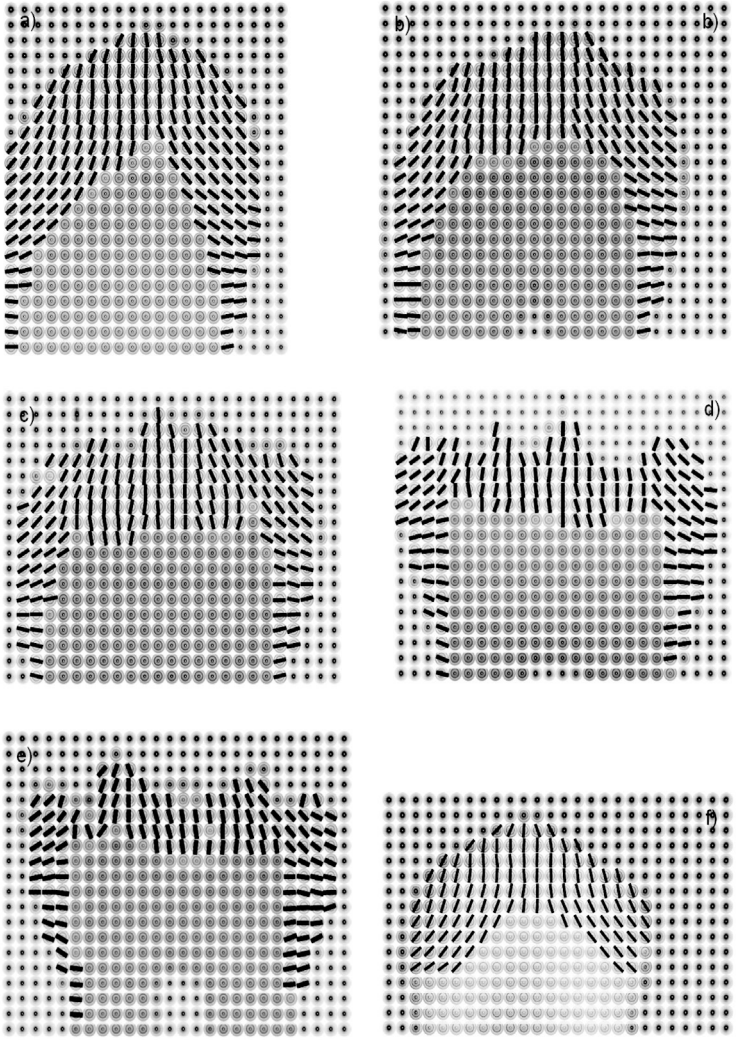

Figure 2.4 Texture orientation from the (002) reflection of HA crystals in enamel for six serial intact tooth sections cut along the mesial–distal plane. (A) Buccal section. (B–E) Central sections. (F) Palatal section.

However, in some parts of the tooth the crystallites run close to parallel to the EDJ. The crystallite arrangement in enamel is highly anisotropic and displays a high degree of intratooth heterogeneity [36]. Figure 2.5 shows individual contour maps of the change in

magnitude of the preferred orientation through the same tooth, revealing the variation in the amount of ordering in the enamel in different regions of a tooth crown. There is less orientation in the surface enamel at both the buccal and palatal sides of the tooth (Fig. 2.5a,f) than in the central mesiodistal slices (Fig 2.5 b,c,e). This indicates a higher degree of preferred orientation at the cusps [37]. It is interesting to note that the points with the highest crystallite alignment correspond to those where the crystallites are directed perpendicular to the occlusal surface and match the expected mastication points for a lower first molar [37]. This would indicate that, as a function of position, biomineralization of enamel varies according to function, whereby regions of enamel structure that are expected to take the largest load contain the most highly ordered crystallites.

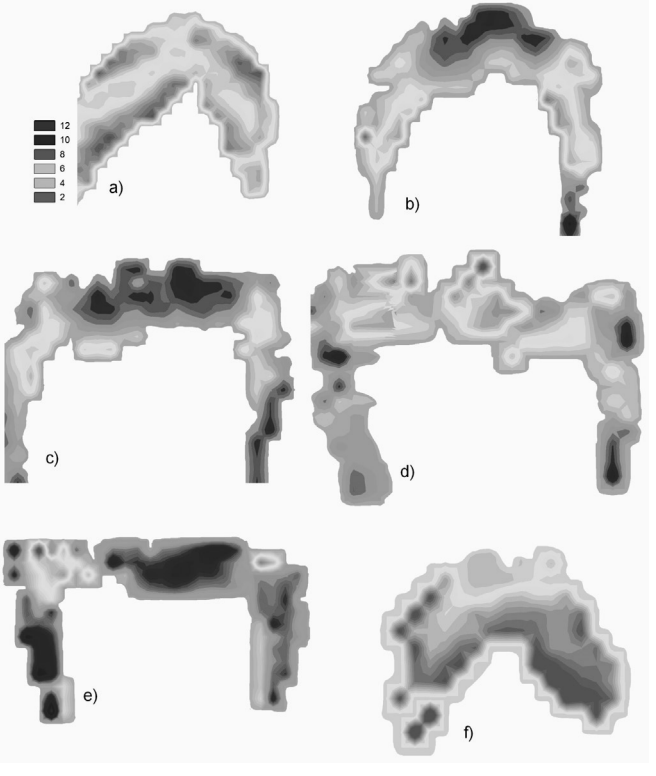

Figure 2.5 Texture maps of enamel, showing the spatial variation in magnitude of the preferred crystallite orientation.

2.3.2 Biodemineralization

The demineralization of enamel has generally been studied under in vitro conditions, which are fundamentally inorganic [38]. However, the real oral environment is far from inorganic, and during a cariogenic or erosivogenic challenge the dissolving enamel tissues are surrounded by organic molecules, mainly proteins, which as described earlier can significantly influence HA crystal dissolution. Thus in vivo demineralization is not a solely inorganic process but would better be described as "biodemineralization." It is true that the driving forces of physicochemical thermodynamic and kinetic conditions [39] will exist, but there will also be many peptides present that will control, modify, and even reverse the effects of the inorganic physicochemical conditions by binding, inhibiting, or promoting crystal growth. Thus, this becomes an extremely complex microenvironment with many organic processes operating simultaneously. Tooth enamel mineral loss is a dynamic process in which both mineral deposition and mineral dissolution happen quasi-simultaneously. It is likely that both processes are under salivary protein control, and hence it is proposed to term this mechanism "biodemineralization."

2.3.3 Iatrogenic Remineralization Strategies

Kirkham et al. [40] have described an elegant method of using self-assembling polymers that undergo one-dimensional self-assembly to form peptides containing β sheets. These form a network of biomimetic scaffolds within carious enamel, capable of HA nucleation.

2.4 Micrometer Length Scale

2.4.1 Enamel Prism Mineralization

At the micrometer length scale enamel crystallites cluster into prisms 5 μm in cross-sectional dimension. The microstructural architecture of enamel varies from species to species, depending on specific requirements, since the enamel structure is the result

of long-term evolution and functional adaptation. Nanoscale HA crystallites have higher strength than bulk materials: from modeling of mineral crystallites of biocomposites a critical crystallite thickness of around 30 nm has been shown to be optimized for stress resistance [41]. This is the same order of magnitude as the size of enamel HA crystallites. A balance is achieved between wear resistance and fracture resistance by having oriented rods to reduce wear by increasing hardness and by having inter-rod structures to halt cracks.

The protein remnant in enamel gives the material better mechanical properties under load—protein macromolecule chains may deform with polymer-like behavior. These are thermodynamically unstable and therefore will return to their initial form and position on release of load elastically.

2.4.2 Enamel Caries

The pathological destruction of enamel mineral observed at the micron scale is the loss of mineral from the enamel prisms, principally along the *c* axis [39]. Acids penetrate through pores in the enamel surface and enter the interprismatic boundaries. However, the conditions of undersaturation will not extend deep into the enamel, and it is unlikely that initial dissolution will occur much below the first few microns. However, diffusive transport of acids into, and calcium and phosphate ions out of, the developing lesion will drive these processes forward as long as there is a source of acid [42]. In natural caries, the loss of enamel does not occur uniformly over the entire exposed enamel surface, whereas in in vitro carious systems, lesion progression occurs at a reasonable uniform rate [43].

The reason for the dissimilarity between artificial lesions and natural lesions in the oral environment may be associated with the varying concentrations inorganic and organic salivary components of the oral environment during demineralization and remineralization [44]. However, the precise chemical mechanism of enamel mineral loss is still not known. Nancollas et al. have suggested that HA demineralization occurs as a result of the coalescence of dissolution pit nuclei, and only if a sufficient number of these sites come together does dissolution continue [45].

2.5 Macroscopic Length Scale

2.5.1 Tooth Morphology

At the macroscopic length scale enamel is grayish or bluish white (it appears yellowish white as it is translucent and reflects the color of underlying dentine). In incisors enamel is up to 2 mm thick, and in molars it can have a thickness of up to 2.6 mm. At the macroscale enamel is selectively permeable (water can travel through at 4 $mm^3\ cm^{-2}\ day^{-1}$) and is soluble in acids. The overall tooth crown morphology varies between tooth types in shape and thickness and is fundamentally controlled by the amount of extracellular matrix laid down during amelogenesis.

2.5.2 Medicinal Enamel Mineralization

Dental enamel formation is a complex biological and physicochemical process, and advances in stem cell research are bringing the possibility of in vivo tooth growth to replace missing whole or partial teeth [46–48]. Synthetic three-dimensional scaffolds to support mineralization processes are already being produced either through manufacturing routes, such as selective laser sintering of polymer-, apatite-, or glass-based structures [49] and protein spinning [50], or through self-assembly processes for regenerative tissue engineering functions. A recent proof-of-concept study has shown that a tooth organ bioengineered using epithelial and mesenchymal cells [51] can be successfully grown onto a plastic structure and transplanted into a mouse model. Other approaches are based on identifying a cell line able to reproduce the function of the embryonic oral epithelium and mesenchyme in order to reproduce the natural processes of embryonic tooth development, rather than build from a scaffold [52]. To offer long-term replacement of a tooth that satisfactorily mimics the structure of natural tissue, artificially grown teeth need to incorporate a hierarchical enamel-like structure into their formation.

2.6 Conclusions

Primary mineralization and secondary mineralization of dental enamel are complex processes driven by a combination of intricate physical, chemical, and biological factors. To understand these processes and the mechanisms that drive them, and to characterize the enamel tissue these processes form, we must look at them on different length scales as we have laid out in this chapter.

Work is ongoing to design more effective caries prevention therapies and design better biomaterials that more closely mimic the in vivo environment in which dental hard tissues are lost.

2.7 Further Reading

For further reading on biomineralization see Mann [53], for enamel demineralization see Robinson et al. [54], and for calcium orthophosphate chemistry see Elliott [11].

References

1. AlQahtani, S. J., Hector, M. P., Liversidge, H. M. (2010) The London atlas of human tooth development and eruption, *Am. J. Phys. Anthropol.,* **142**, 481–490.
2. Guo, T., Rudnick, P. A. and Wang, W., Lee, C. S., Devoe, D. L., Balgley, B. M. (2006) Characterization of the human salivary proteome by capillary isoelectric focusing/nanoreversed-phase liquid chromatography coupled with ESI-tandem MS, *J. Proteome Res.*, **5,** 1469–1478.
3. Gao, X. J., Anderson, P., Davis, G. R., Elliott, J. C. (1993) Scanning microradiographic and microtomographic studies of remineralization of subsurface enamel lesions, *Faraday Trans.*, **89**, 2907–2912.
4. Weatherell, J. A., Robinson, C., Hallsworth, A. S. (1972) Changes in the fluoride concentration of the labial enamel surface with age, *Caries Res.*, **6**, 312–324.
5. Robinson, C., Weatherell, J. A., Hallsworth, A. S. (1971) Variation in composition of dental enamel within thin ground sections, *Caries Res.*, **5**, 44–57.
6. Robinson, C., Weatherell, J. A., Hallsworth, A. S. (1981) Distribution of magnesium in mature human-enamel, *Caries Res.*, **15**, 70–77.

7. Robinson, C., Shore, R. C., Brookes, S. J., Strafford, S., Wood, S. R., Kirkham, J. (2000) The chemistry of enamel caries, *Crit. Rev. Oral Biol.*, **11**, 481–495.

8. Al-Jawad, M., Steuwer, A., Kilcoyne, S. H., Shore, R. C., Cywinski, R., Wood, D. J. (2007) 2D mapping of texture and lattice parameters of dental enamel, *Biomaterials*, **28**, 2908–2914.

9. Zioupos, P., Rogers, K. D. (2006) Complementary physical and mechanical techniques to characterise tooth: a bone-like tissue, *J. Bionic Eng.*, **3**, 19–31.

10. Anderson, P., Hector, M. P., Rampersad, M. A. (2001) Critical pH in resting and stimulated whole saliva in a group of children and adults, *Int. J. Paed. Dent.*, **11**, 266–273.

11. Elliott, J. C. (1994) *Structure and Chemistry of the Apatites and Other Calcium Orthophosphates*, Elsevier Science, Holland.

12. Chuong, R. (1973) Experimental study of surface and lattice effects on the solubility of hydroxyapatite, *J. Dent. Res.*, **52**, 911–914.

13. Chen, Z.-F., Darvell, B. W., Leung, V. W.-H. (2004) Hydroxyapatite solubility in simple inorganic solutions, *Arch. Oral Biol.,* **49**, 359–367.

14. Patel, P. R., Brown, W. E. (1975) Thermodynamic solubility product of human tooth enamel: powdered sample, *J. Dent. Res.,* **54**, 728–736.

15. Larsen, M. J., Jensen, S. J. (1989) The hydroxyapatite solubility product of human dental enamel as a function of pH in the range 4.6-7.6 at 20 degrees C, *Arch. Oral Biol.*, **34,** 957–961.

16. Shellis, R. P. (1988) A microcomputer program to evaluate the saturation of complex solutions with respect to biominerals*, Comput. Appl. Biosci.,* **4**, 373–379.

17. Mann, S., Weiner, S. (1999) Biomineralization: structural questions at all length scales, *J. Struct. Biol.*, **126**, 179–181.

18. Hu, S., Xie, Y. M., Ramachandran, P., Loo, R. R. O., Li, Y., Loo, J. A., Wong, D. T. (2005) Large-scale identification of proteins in human salivary proteome by liquid chromatography/mass spectrometry and two-dimensional gel electrophoresis-mass spectrometry, *Proteomics*, **5**, 1714–1728.

19. Kawasaki, K., Weiss, K. M. (2003) Mineralized tissue and vertebrate evolution: the secretory calcium-binding phosphoprotein gene cluster, *Proc. Natl. Acad. Sci.*, **100**, 4060–4065.

20. Fisher, L. W., Torchia, D. A., Fohr, B., Young, M. F., Fedarko, N. S. (2001) Flexible structures of SIBLING proteins, bone sialoprotein, and osteopontin, *Biochem. Biophys. Res. Commun.*, **280**, 460–465.

21. Masica, D. L., Gray, J. J. (2009) Solution- and adsorbed-state structural ensembles predicted for the statherin-hydroxyapatite system, *Biophys. J.*, **96**, 3082–3091.

22. Lamkin, M. S., Oppenheim, F. G. (1993) Structural features of salivary function, *Crit. Rev. Oral Biol. Med.*, **4**, 251–259.

23. Aoba, T., Moreno, E. C., Hay, D. I. (1984) Inhibition of apatite crystal growth by the amino-terminal segment of human salivary acidic proline-rich proteins, *Calcif. Tissue Int.*, **36**, 651–658.

24. Gibbons, R. J., Hay, D. I. (1988) Human salivary acidic proline-rich proteins and statherin promote the attachment of Actinomyces viscosus LY7 to apatitic surfaces, *Infect. Immun.,* **56**, 439–445.

25. Kousvelari, E. E., Baratz, R. S., Burke, B., Oppenheim F. G. (1980) Immunochemical identification and determination of proline-rich proteins in salivary secretions, enamel pellicle, and glandular tissue specimens, *J. Dent. Res.,* **59**, 1430–1438.

26. Shomers, J. P., Tabak, L. A., Levine, M. J., Mandel I. D., Hay D. I. (1982) Properties of cysteine-containing phosphoproteins from human submandibular-sublingual saliva, *J. Dent. Res.*, **61**, 397–399.

27. Hay, D. I., Bowen, W. H. (1996) *The Functions of Salivary Proteins*, 105–123 (Ed. Edgar, W. M., O'Mullane, D. M., Saliva, Oral Health), British Dental Association, London.

28. Oppenheim, F. G., Yang, Y. C., Diamond, R. D., Hyslop, D., Offner, G. D., Troxler, R. F. (1986) The primary structure and functional characterization of the neutral histidine-rich polypeptide from human parotid secretion, *J. Biol. Chem.*, **261**, 1177–1182.

29. Oppenheim, F. G., Xu, T., McMillian, F. M., Levitz, S. M., Diamond, R. D., Offner G. D., Troxler, R. F. (1988) Histatins, a novel family of histidine-rich proteins in human parotid secretion. Isolation, characterization, primary structure, and fungistatic effects on Candida albicans, *J. Biol. Chem.,* **263**, 7472–7477.

30. Jensen, J. L., Lamkin, M. S., Oppenheim, F. G. (1992) Adsorption of human salivary proteins to hydroxyapatite: a comparison between whole saliva and glandular salivary secretions, *J. Dent. Res.*, **71**, 1569–1576.

31. Lamkin, M. S., Arancillo, A. A., Oppenheim, F. G. (1996) Temporal and compositional characteristics of salivary protein adsorption to hydroxyapatite, *J. Dent. Res.*, **75**, 803–808.

32. Huq, N. L., Cross, K. J., Reynolds, E. C. (1995) A 1H-NMR study of the casein phosphopeptide alpha s1-casein(59-79), *Biochim. Biophys. Acta*, **1247**, 201–208.

33. Shlesinger, D. H., Hay, D. I. (1977) Complete covalent structure of statherin, a tyrosine-rich acidic peptide which inhibits calcium phosphate precipitation from human parotid saliva, *J. Biol. Chem.*, **252**, 1689–1695.

34. Kosoric, J., Williams, R. A. D., Hector, M. P., Anderson, P. (2007) A synthetic peptide based on a natural salivary protein reduces demineralization in model systems for dental caries and erosion, *J. Peptide Res. Ther*., **13**, 497–503.

35. Shah, S., Kosoric, J., Hector, M. P., Anderson, P. (2011) An in vitro scanning microradiography study of the reduction in hydroxyapatite demineralization rate by statherin-like peptides as a function of increasing N-terminal length, *Eur. J. Oral Sci.*, **119**, 13–18.

36. Makrodimitris, K., Masica, D. L., Kim, E. T., Gray, J. J. (2007) Structure prediction of protein- solid surface interactions reveals a molecular recognition motif of statherin for hydroxyapatite, *J. Am. Chem. Soc.*, **129**, 13713–13722.

37. Simmons, L. M., Al-Jawad, M., Kilcoyne, S. H., Wood, D. J. (2011) Distribution of enamel crystallite orientation through an entire tooth crown studied using synchrotron x-ray diffraction, *Eur. J. Oral Sciences,* **119**, 19–24.

38. Berkovitz, B. K. B., Holland, G. R., Moxham, B. J. (2002) *Oral Anatomy, Histology and Embryology*, Mosby, New York, USA.

39. Kim, H., Renato, P., Camata, Chowdhury, S., Vohra, Y. K. (2010) In vitro dissolution and mechanical behavior of c-axis preferentially oriented hydroxyapatite thin films fabricated by pulsed laser deposition, *Acta Biomater.,* **6**, 3234–3241.

40. Kirkham, J., Firth, A., Vernals, D., Boden, N., Robinson, C., Shore, R. C.,Brookes, S. J., Aggeli, A. (2007) Self-assembling peptide scaffolds promote enamel remineralization, *J. Dent. Res.*, **86**, 426–430.

41. Gao, H. J., Ji, B. H., Jager, I. L., Arzt, E., Fratzl, P. (2003) Materials become insensitive to flaws at nanoscale: lessons from nature, *Proc. Natl. Acad. Sci.*, **100**, 5597–5600.

42. Bollet-Quivogne, F. R. G., Anderson, P., Dowker, S. E. P., Elliott, J. C. (2005) Scanning microradiographic study on the influence of diffusion in the external liquid on rate of demineralisation in hydroxyapatite aggregates, *Eur. J. Oral Sci*., **113**, 53–59.

43. Anderson, P., Elliott, J. C. (2000) Rates of mineral loss in human enamel during in vitro demineralization perpendicular and parallel to the natural surface, *Caries Res.,* **34**, 33–40.

44. Cochrane, N. J., Anderson, P., Davis, G. R., Adams, G. G., Stacey, M. A., Reynolds, E. C. (2012) An X-ray microtomographic study of natural white-spot enamel lesions, *J. Dent. Res.,* **91**, 586–591.

45. Wang, L., Nancollas, G. H. (2008) Calcium orthophosphates: crystallization and dissolution, *Chem. Rev.*, **108**, 4628–4669.

46. Bluteau, G., Luder, H. U., DeBari, C., Mitsiadis, T. A. (2008) Stem cells for tooth engineering, *Eur. Cells Mater.,* **16**, 1–9.

47. Kim K., Lee, C. H., Kim, B. K., Mao, J. J. (2010) Anatomically sHAed tooth and periodontal regeneration by cell homing, *J. Dent. Res.,* **89**, 842–847.

48. Oshima, M., Mizuno, M., Imamura, A., Ogawa, M., Yasukawa, M., Yamazaki, H., Morita, R., Ikeda, E., Nakao, K., Takano-Yamamoto, T., Kasugai, S., Saito, M., Tsuji, T. (2011) Functional tooth regeneration using a bioengineered tooth unit as a mature organ replacement regenerative therapy, *PLOS ONE*, **6**, e21531.

49. Duan, B., Wang, M., Zhou, W. Y., Cheung, W. L., Li, Z. Y., Lu, W. W. (2010) Three-dimensional nanocomposite scaffolds fabricated via selective laser sintering for bone tissue engineering, *Acta Biomater*., **6**, 4495–4505.

50. Matthews, J. A., Wenk, G. E., Simpson, D. G., Bowlin, G. L. (2002) Electrospinning of collagen nanofibers, *Biomacromolecules*, **3**, 232–238.

51. Ikeda, E., Morita, R., Nakao, K., Ishida, K., Nakamura, T., Takano-Yamamoto, T., Ogawa, M., Mizuno, M., Kasugai, S., Tsuji T. (2009) Fully functional bioengineered tooth replacement as an organ replacement therapy, *Proc. Natl. Acad. Sci.*, **106**, 13475–13480.

52. Yen, A. H. H., Sharpe, P. T. (2008) Stem cells and tooth tissue engineering, *Cell Tissue Res*., **331**, 359–372.

53. Mann, S. (2001) *Biomineralization: Principles and Concepts in Bioinorganic Materials Chemistry*, Oxford University Press, Oxford.

54. Robinson, C., Kirkham, J. and Shore R. (1995) *Dental Enamel: Formation to Destruction*, CRC Press, Boca Raton, FL, USA.

Chapter 3

Materials in Dentistry

Ammar A. Mustafa[a] and Jukka P. Matinlinna[b]
[a]*Kulliyyah of Dentistry, Prosthodontics and Dental Materials Science, International Islamic University Malaysia, Kuantan Campus, Bandar Indera Mahkota, 25200 Kuantan, Pahang, Malaysia*
[b]*Faculty of Dentistry, Dental Materials Science, University of Hong Kong, Prince Philip Dental Hospital, 34 Hospital Road, Sai Ying Pun, Hong Kong SAR, People's Republic of China*
drammar71@gmail.com, jpmat@hku.hk

Dentists are authorized end users of dental biomaterials. Dental materials and, in general, biomaterials have been developed and initialized globally at dental schools. What different dental materials do we have in clinical use? What are dental biomaterials? What should a dental student know about them all? What is so special in the materials and their properties one is using in dentistry and dental technology? These are some of the questions we try to address, at least briefly. This chapter introduces materials in dentistry and their chemical and physical properties in a concise but comprehensive and contemporary way. We start with an introduction to restorative dental materials and explain what biomaterials are. We also go briefly through material classes and their indications in dentistry,

Handbook of Oral Biomaterials
Edited by Jukka P. Matinlinna

ISBN 978-981-4463-12-6 (Hardcover), 978-981-4463-13-3 (eBook)
www.panstanford.com

which comprise polymeric materials, ceramic materials, and metallic materials. Basic concepts, for example, adhesion, retention, and bonding, of dental restorative materials are also introduced.

3.1 Classification of Dental Biomaterials

In general, *dental materials* are used to restore or help in restoring diseased and traumatized teeth and/or neighboring tooth structures (and tissues) and *rehabilitate the oral milieu*. Dental materials can be classified as restorative materials, preventive materials, and auxiliary materials.

A *bioactive material* elicits a specific biological response at the interface of the material and surrounding tissues. This results in the formation of a biologically active bond of a hydroxyapatite (HAp) layer between the material and the tissues [1–3]—see also Chapters 1, 2, 8, and 19.

The term *bioengineering* is used to refer to the application of methods and concepts of the physical sciences and mathematics in an engineering approach toward solving problems in the repair and reconstruction of lost, damaged, or deceased tissues [4, 5].

Any material that is used for that purpose can be regarded as a *biomaterial.* During the old days, before the consensus meeting organized by Prof. Williams (in 1987), the term *biomaterial* was understood solely as referring to biological materials such as bone, cartilage, and corals. For general clarity, the current use of it referring to man-made materials is preferable [6].

> A biomaterial is a nonviable material used in a medical device, intended to interact with biological systems [7].

Now, if the word *medical* is removed, the definition before becomes more general and still quite useful. On the other hand, if the word *nonviable* is removed, the definition becomes even more general and can address new tissue engineering and hybrid artificial organ applications where living cells are used. Given this, a complementary definition needed to understand an important aspect of biomaterials is that of biocompatibility [6, 7].

Biocompatibility is the capability of a material (a biomaterial) to respond to a specific use. It refers to the ability of a biomaterial to perform its desired, anticipated function with respect to a medical therapy, without eliciting any undesirable local or systemic effects in the recipient or beneficiary of that therapy. It should generate the most appropriate beneficial cellular or tissue response in that specific situation and optimize the clinically relevant performance of that therapy. The desired function of physiochemical and biological interactions between host tissue and the implant surface determine the host's response [8, 9]. More about biocompatibility is found in Chapter 5.

> Biocompatibility is the ability of a material to perform with an appropriate host response in a specific application [7].

Biomaterials science brings together researchers and experts from diverse disciplines. Such areas include inorganic chemistry, bioengineering, esthetics, chemical engineering, dentistry (all fields), electrical engineering, analytical chemistry, mechanical engineering, materials science, physical chemistry, biology, financing, medicine, microbiology, organic chemistry, physics, polymer chemistry, veterinary, ethics, and nursing sciences.

3.1.1 Restorative Dental Materials

Restorative dental materials can be classified according to the principles of direct application as (a) *direct restorative materials* and (b) *indirect restorative materials.* Direct restorative materials such as resin composites (composite resin, filled resins), dental silver amalgams, and glass ionomer cements (GIC) are used directly inside the oral cavity to restore the function of teeth and to increase esthetics. Whereas indirect restorative materials such as porcelain fused to metal (PFM), high-content gold (Au) alloys, nonprecious, i.e., base metal alloys, and indirect resin composites are used extraorally to help in the construction of the restoration or prosthesis for the treatment of damaged or missing teeth.

Restorative dental materials can be classified also as *definitive* (permanent) and *provisional* (temporary) restorative materials. Definitive restorative materials are those materials that are used permanently inside the oral cavity to restore or replace missing

teeth and/or adjacent structures. These materials can be used either permanently like implants and crown/bridgeworks or as long-lasting restorations like reinforced resin composites [9, 10].

A *dental silver amalgam* is a direct definitive restorative material used to restore cavities of decayed permanent posterior teeth. In general, an amalgam is an alloy that contains mercury (Hg) as one of its constituents. Mercury is a liquid metal at room temperature. A dental silver amalgam consists mainly of a combination of a silver-tin (Ag-Sn) alloy and mercury. A dental amalgam alloy powder component mainly consists of silver (Ag), copper (Cu), and tin (Sn), but may also contain palladium (Pd), zinc (Zn), and some other metals to increase handling characteristics and to improve clinical performance.

The process of *amalgamation* (trituration) is the mixing of liquid mercury with one or more metals or alloys to form an amalgam, whereas trituration is the process of grinding powder, especially within a liquid. Amalgamation describes the process of mixing the amalgam alloy particles with liquid mercury in an amalgamator. Mercury is purified by the distillation process to make it suitable for use in dental amalgams. The purification of mercury is performed to ensure the elimination of impurities that may unfavorably affect the setting characteristics [9–11]. More about amalgams is available on p. 143–148.

The shape of *dental amalgam alloy particles* is (a) lathe cut, (b) spherical, or (c) admixed. In lathe-cut powder, the particles are needle-like in shape and they are formed by shaving off an ingot of the alloy by means of a lathe or a milling machine. The resultant particles are sieved to get the proper particle size. Spherical powder or atomized powder is made by melting all the desired elements. The liquid metal is atomized into fine spherical droplets of metal through spray cooling and under high pressure of an inert gas. An *admixed amalgam alloy* is a mixture of lathe-cut and spherical particles [9, 11, 12].

In *amalgamation*, the alloy particles are dissolved in mercury to produce an amalgam paste, which is a moldable restoration into a prepared cavity. During the amalgamation process silver, Sn, and Cu atoms are dissolved in the Hg, where they start forming different precipitates. These precipitates form a matrix that retains the remaining partly dissolved amalgam alloy particles. The amount of

mercury needed to wet all powder particles and occupy the space between the particles range from 40–60% mercury by weight. In early low-copper amalgams, the amalgamation reaction produced tin-mercury as a product, which is also known as gamma-2 (γ_2). Nowadays, the reaction of high-copper amalgams produces no γ_2 product, which has an effective impact on increasing corrosion resistance and marginal creep in class II cavities [11–13]. The reaction of amalgams in general can be summarized by the following equation (see more about setting at the end of this chapter):

$$\text{Ag alloy } (\gamma) + \text{Hg} \rightarrow \text{Ag alloy (unreacted)} + \text{Ag-Hg } (\gamma_1) + \text{Cu-Sn} \quad (3.1)$$

Provisional dental materials are used for a limited planned period of time, which may be a few days to a few weeks. In dentistry not all times can the dentist directly accomplish treatment with the application of a permanent device or restoration. In some occasions, the dentist needs time to decide the definitive treatment. For example, treatment of very deep cavities with shallow dentin covering the pulp may require the application of a zinc oxide eugenol (ZOE) temporary filling until the decision of making a permanent filling or proceeding with root canal therapy. On other occasions, a prepared tooth may need to be covered with a temporary crown made of acrylic resin while waiting for the definitive crown to be finished by the dental laboratory [10].

3.1.1.1 Zinc oxide eugenol cement

One of the best examples of a provisional dental material is the use of zinc oxide (ZnO) *eugenol* cement (aka ZOE). ZOE is a low-strength cement characterized with its strong *sedative effect* and used usually as a *provisional* treatment. It consists of a powder and a liquid, where the powder usually consists of zinc oxide (70 wt%). A resin is added to reinforce the cement and to reduce the brittleness of the set cement, zinc stearate is added as a plasticiser, and zinc acetate is added to improve strength.

In a polymer-modified ZOE formulation, beads of poly(methyl methacrylate), PMMA are added (approx. 20 wt%) to strengthen the cement. In some other types, aluminum trioxide (Al_2O_3) particles are added (approximately 30 wt%) to reinforce the cement. The liquid component consists of eugenol (HE) and small amounts of olive oil. In the ZOE type using aluminum trioxide–reinforcing particles, the

liquid contains 65% ethoxybenzoic acid (EBA) with approximately 35% eugenol [12, 13].

Eugenol (4-allyl-2-methoxyphenol, $C_{10}H_{12}O_2$, aka *allylguaiacol* and *eugenic acid*, abbr. HE*)* is a colorless to pale-yellow oily liquid (boiling point 255°C), and it is extracted from certain essential oils, in particular from cinnamon, nutmeg, and clove oil. It is practically insoluble in water but soluble in alcohols, ether, oils, and chloroform [14, 15]. Eugenol thickens and darkens on exposure to air. Eugenol has a clove-like, spicy aroma, a pungent taste, and analgesic and antiseptic effects. The general setting reaction consists of two steps, Eqs. 3.2 and 3.3:
Firstly:

$$ZnO + HE \xrightarrow{\text{Water}} Zn(OH)_2 + HE \quad (3.2)$$

Secondly:

$$Zn(OH)_2 + 2HE \rightarrow ZnE_2 + 2H_2O \quad (3.3)$$

3.1.1.2 Glass ionomer cement

A GIC is a restorative material that consists of a powder and a liquid, which produces a plastic mass when mixed and then sets to a rigid solid. A GIC has the ability to *bond chemically to enamel and dentine* and also is able to release fluoride ions (F^-) from the glass component. GICs have been used mainly for restoration of abrasion and erosion lesions and as a luting agent for crown and bridge reconstructions. Recent indications also include the restoration of proximal lesions, occlusal restorations in deciduous dentitions, cavity bases, and liners. The main composition includes glass powder, the polyacid (PA) component, water, and *tartaric acid* (2,3-dihydroxybutanedioic acid) [9, 12].

The glass component employs the glass system of Al_2O_3-CaF_2-SiO_2. A *suitable* amount of each is needed for optimal mechanical and esthetic properties. The term *polyacid* describes a wide range of chemical analogues. Some copolymers of PA, such as acrylic acid–co-itaconic acid and acrylic acid–co-maleic acid, are now commonly used in dentistry. Tartaric acid is used to adjust the setting time. In short, the GIC setting reaction can be generally described as a *three-overlapped-stage* process: (a) *dissolution,* (b) *gelation*, and

(c) *hardening* [12, 16–19] (see Eqs. 3.4–3.10). Acrylic materials in dentistry are discussed later in this chapter.

Dissolution: hydrolysis of glass, release of Ca^{2+} and silicate (SiO_4^{4-}):

$$PA + H_2O \rightarrow H_3O^+ \text{ (i.e., } H^+) + (PA)^- \quad (3.4)$$

$$\text{Glass} + H^+ \rightarrow Ca^{2+} + SiO_4^{4-} \quad (3.5)$$

Gelation: silicates form silica gel, and the Ca^{2+} ions chelate with $(PA)^-$:

$$SiO_4^{4-} + 4n\ H^+ \rightarrow (SiO_4)_n \cdot 2n\ H_2O \text{ (silica gel)} \quad (3.6)$$

$$Ca^{2+} + 2PA^- \rightarrow Ca(PA)_2 \text{ (initial set)} \quad (3.7)$$

During *hardening* hydrolysis continues and further release of silicate and Al^{3+} ions takes place. Al^{3+} can chelate with $(PA)^-$ and also take up Ca^{2+} in the chelation (final set):

$$\text{Glass} + H^+ \rightarrow Al^{3+} + SiO_4^{4-} \quad (3.8)$$

Final setting:

$$Al^{3+} + 2PA^- \rightarrow Al(PA)^{2+} + PA^- \quad (3.9)$$

$$Al^{3+} + Ca(PA)_2 \rightarrow Al(PA)^{2+} + Ca^{2+} + PA^- \quad (3.10)$$

3.1.2 Preventive Dental Materials

Plaque is a naturally occurring biofilm on tooth surfaces. It is soft, white yellow, and mainly bacterial. It is formed by a process of bacteria and protein adsorption to the tooth surfaces. *Van der Waals forces* play a major role in creating adhesion to the tooth surface. Plaque can be removed through the use of a toothbrush/water and flossing, whereas *pellicles* need the use of a proper detergent, together with an appropriate abrasive.

Dental calculus cannot be successfully removed by ordinary brushing. The objective of using dentifrices is to obtain a clean substrate. However, modern dentifrices such as those in the form of pastes or powders contain a variety of components, which may include anticariogenic, antidentine hypersensitivity and antibacterial ingredients.

3.1.2.1 Dentifrices

Dentifrices are materials used together with a toothbrush to remove adhered plaque and stained pellicle layers from teeth. The most

essential dentifrice that is recommended by dentists is toothpaste. In addition to water, the *general ingredients* of modern toothpastes are:

(a) *Humectants* are used to stabilize the composition of the dentifrice through preventing desiccation of the material by reducing water evaporation. Humectants are short-chained polyalcohols such as glycerol (propane-1,2,3-triol), which is hygroscopic in nature and soluble in water.

(b) *Colloidal binders* (thickening agents) are long-chained molecules used as binders to prevent the separation of solids during dentifrice preparation and during storage. They delay the gravity-induced movement of solids toward the bottom of the tube during storage. Sodium alginate, Na-carboxy methylcellulose, or hydroxylethylcellulose may be used as an active ingredient.

(c) *Surfactants* (detergents), Na-lauryl sulfate, Na-sarcosinate, and Na-dodecylbenzene sulfonate, are usually used to lower the surface tension of the solution so that the dentifrice can contact the teeth more easily to remove debris from surfaces.

(d) *Abrasives* are required for the effective removal of tenacious plaque, stains, pellicle and simple calculus. Calcium carbonate ($CaCO_3$, i.e., chalk) is a common abrasive in dentifrices, and also calcium phosphate ($Ca_3(PO_4)_2$), sodium hydrogen carbonate ($NaHCO_3$), and amorphous silicon dioxide (SiO_2) may be used, too. The degree of dentifrice abrasive capability depends on the hardness of the abrasive particles, the morphology of the abrasive particles, and the concentration of abrasive in the paste.

(e) *Preservatives* such as sodium benzoate and potassium sorbate are commonly used to inhibit bacterial growth within the dentifrice material.

(f) *Therapeutic agents* such as some fluoride, antidentine hypersensitivity and/or antibacterial agents, are widely used in modern dentifrices. The use of fluoride, mostly in the form of stannous fluoride, that is, tin(II)fluoride (SnF_2), can improve the resistance of enamel and dentin to demineralization, and at the same time it can (to a certain extent) remineralize

decayed tooth surfaces. Antihypersensitivity agents are used to prevent or to reduce the sensitivity originating from exposed dentin, especially in cervical areas. Potassium nitrate (KNO_3), calcium hydroxide ($Ca(OH)_2$), and glutaraldehyde $CH_2(CH_2CHO)_2$ are commonly used as antihypersensitivity agents. Another therapeutic agent can be incorporated into the formula of dentifrices, namely, antimicrobial agents such as *Zn-citrate trihydrate, triclosan* (polychloro phenoxy phenol), and *hexetidine*, that is, 1,3-bis(2-ethylhexyl)-5-methylhexahydropyrimidin-5-amine).

As it is generally understood, SnF_2 acts as to convert the calcium hydroxyapatite in tooth enamel into fluorapatite, $Ca_5(PO_4)_3F$, which makes enamel more resistant to acid attacks generated by bacteria. In toothpastes containing Ca minerals, NaF becomes ineffective over time, while SnF_2 keeps its effect in strengthening tooth enamel. Some modern toothpaste formulations contain strontium chloride ($SrCl_2$), which is reported to plug open dentinal tubuli and pores on exposed roots [20, 21].

3.1.2.2 Mouthwashes

Mouthwashes (mouth rinses) are liquid solutions that are used as an oral rinse to improve oral health by inhibiting plaque formation. They can also bring breath freshness.

In general, mouthwashes are composed of three main ingredients:

(a) An active agent such as chlorhexidine gluconate
(b) Alcohol (ethanol, CH_3CH_2OH [EtOH]) to dissolve ingredients and to act as a preservative
(c) Surfactants to remove debris from teeth surfaces and to lower the surface tension of the solution

Chlorhexidine (CHX) is a cationic bis-biguanide, and it has an optimal antimicrobial action ranging from pH 5.5 to 7.0. CHX is active against a wide range of microorganisms, for example, gram-negative and gram-positive bacteria, bacterial spores, yeasts, dermatophytes, and lipophilic viruses.

The criteria of selecting active ingredients are based on their ability to act as antimicrobial agents or to perform as antiplaque formation agents [22].

3.1.2.3 Pit and fissure sealants

Pit and fissure sealants are used to prevent caries formation in the deep pits, grooves, and fissures of natural teeth that cannot be reached by the bristles of a toothbrush (Fig. 3.1) [23]. Bacteria can be easily accumulated in these unreachable areas; hence they can produce acids, which may lead later to demineralization. These materials are available either as the resin component of dental composite, GIC, or flowable resin composite sealants.

Figure 3.1 Deep pits and fissures.

An important factor that should be considered during the manufacturing of sealants is the coefficient of penetration. The *coefficient of penetration* is known as the ability of any fluid to penetrate micropores. The higher the coefficient of penetration, the deeper the penetration (Fig. 3.2).

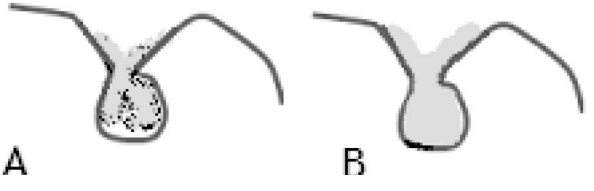

Figure 3.2 Sealant with a low coefficient of penetration (A) compared to sealant with a high coefficient of penetration (B).

Such sealants are composed of diluted bisphenol-A-glycidyl methacrylate (bis-GMA), or sealants may comprise also urethane dimethacrylate (UDMA, aka UEDMA) (see later for more about bis-GMA).

The difference between the *organic matrix* of a sealant and the one for a dental resin composite is that the former one should be more fluid to easily penetrate the deep pits and fissures as well as the

etched areas on enamel (Fig. 3.2). Pit and fissure sealants have the same composition as the organic matrix of dental resin composites, but for sealants, the organic matrix should be more dilute so as to increase the *flowability* of the material to deeply penetrate the pits and fissures. Light-cure sealants are activated by a *diketone* and an *aliphatic amine*.

Chemical-cure sealants consist of a two-container system: one contains bis-GMA resin and benzoyl peroxide as the *initiator*, and the other contains bis-GMA with 5% organic amine as the *accelerator*. The polymerization reaction occurs by mixing equal drops of two liquids containing activators (organic amine) and initiators (peroxides).

Retention of a resin-based sealer to the tooth substrate is highly dependent on micromechanical bonding to etched enamel. The more the sealant retention to the tooth surface, the more the success and durability of the sealer material (Fig. 3.3) [23–25].

Figure 3.3 Visibility of the sealant is important for accurate placement and better evaluation during recall visits.

3.1.3 Gypsum

Gypsum products are one of the most important classes of material in dentistry and dental technology. They are used for taking

impressions and casting investments. Obviously, models of dentition provide the basis of the majority of restorative treatments. Gypsum, which has the common mineralogical name calcium sulfate dihydrate, $CaSO_4 \cdot 2H_2O$ (aka *alabaster, selenite*, and *terra alba)*, is used in cement production, in soil treatment, for artificial marble and plaster casts, etc.

The *dehydrated product* of gypsum, calcium sulfate hemihydrate ($CaSO_4 \cdot ½H_2O$), forms the basis of commonly used materials, that is, *plaster (plaster of Paris)* and *artificial stone*. Calcium sulfate hemihydrate is a fine, odorless, and tasteless powder and is used for wall plasters, tiles, and blocks as well. The natural form of anhydrous calcium sulfate ($CaSO_4$) is known in nature as the mineral *anhydrite*, *karstenite*, *muriacite*, and *anhydrous gypsum.* It is also used as a paper filler and in some cement formulations [9, 12].

Many dental restorations and appliances are constructed extraorally using models, dies (one tooth), and casts for replicas of the patient's teeth. Gypsum materials are combined with deionized water (don't use tap water!) and spatulated to create a slurry, a mixture that is then poured into a dental impression. Gypsum-based materials rely on the reaction of calcium sulfate hemihydrate with water to produce the less soluble calcium sulfate dehydrate. The reaction is *exothermic*:

$$CaSO_4 \cdot ½H_2O + 1½\ H_2O \rightarrow CaSO_4 \cdot 2H_2O\ \Delta H < 0 \qquad (3.11)$$

It is highly important that the *water-to-powder* ratio (mixing proportion) be accurately measured according to the values recommended by the manufacturer. This is vital because the added distilled water must at least fill the spaces between the gypsum powder particles while the mixture is being stirred. Excess water affects the strength of the gypsum cast products adversely.

Because the relative volume of the reaction products is less than that of the reactants on setting, the material should in principle go through a volumetric shrinkage. In practice, there is always observed an overall *expansion* on gypsum setting. This may be explained by the pressures of crystal growth.

Now, if the mixture is immersed in water during setting, *hygroscopic expansion* would also be observed. The dimensional change on setting must be controlled: this is important for the accuracy of models and impressions. Dimensional changes may be

controlled by additions of so-called modifiers. K_2SO_4 accelerates the setting, and addition of NaCl both shortens the setting reaction and increases the setting expansion. Na-citrate retards setting, and borax ($Na_2B_4O_7$) is a retardant for the setting reaction—and a strengthener for hydrocolloids [10–15].

3.1.4 Waxes

Historically, waxes have been classified according to their origin: (a) mineral, (b) insect, (c) plant, and (d) animal. *Dental waxes* may be composed of natural and synthetic waxes, gums, fats, fatty acids, oils, and natural and synthetic resins and pigments.

The *required working characteristics* of each wax are achieved by blending appropriate natural and synthetic waxes and resins and other additives. The color, produced by coloring agents, would provide good contrast and allows feather edges and other undesirable extensions of the pattern to be shown. The chemical components of both natural and synthetic waxes impart characteristic physical properties to the wax [9, 12].

The two principal groups of organic compounds contained in waxes are hydrocarbons and esters. Some of the waxes also contain free alcohols and acids. Waxes differ from fats and oils in that they are simple monoesters of fatty acids. On the other hand, waxes are more brittle, harder and, less greasy than fats. The length of straight and branched carbon chains governs the melting point of the material. As waxes are normally blends of long-chain alkanes (e.g., $C_{27}H_{56}$, $C_{29}H_{60}$), esters, alkanols, or alkanoic acids, a sharp and distinct melting point usually cannot be obtained. Melting points of waxes vary. Manufacturers of waxes usually mix various types of waxes so that the melting range can fit the final application [9, 11, 12].

Waxes are used in dentistry in taking impressions, forming an inlay pattern, blocking out undercuts on models, cementing models, detecting bites, making lost-wax casting patterns, and making acrylic denture baseplate patterns (Fig. 3.4). All these applications rely on one or a few of the characteristic properties of wax. Important properties of waxes include melting range, thermal expansion, mechanical properties, residual stress, flow, and ductility [10].

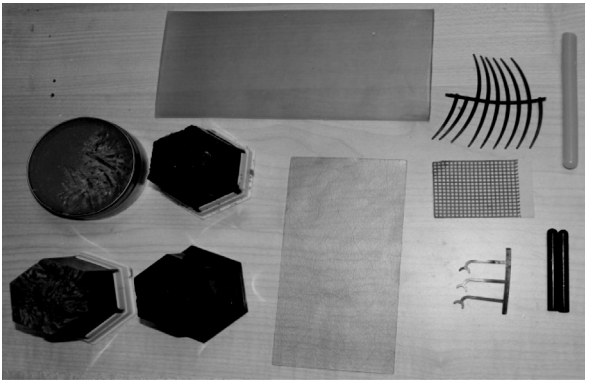

Figure 3.4 Dental waxes are used in the construction of different dental prostheses and devices in dental laboratories.

The so-called *baseplate wax* is used for denture base patterns; *inlay wax* is used for patterns of inlays, crowns, and bridges. *Impression wax* can be used for taking bite registration in edentulous patients, etc. The *flow of waxes* is important, not simply as part of the necessary molding process, but also as an undesirable aspect after the pattern or impression has been made, so the rheology of this material has to be studied in detail. The *high coefficients of thermal expansion* of waxes also directly affect the accuracy of the pattern created [9, 10, 12].

Impression waxes need to have considerable flow at oral temperature to function. The effects due to thermal expansion depend on the temperature at which the pattern was created and the temperature at which it was invested.

3.1.5 . . . And the Rest

Auxiliary dental materials are materials that are used and involved in the construction of dental prostheses and finalized restorations, for example, but do not become part of finalized prostheses or restorations. Some examples of such auxiliary materials other than those discussed in this chapter are acid-etch (*ortho*-phosphoric acid, H_3PO_4) solutions or gels for intraoral tooth tissue etching (cf Chapter 1) and finishing and polishing abrasives. Dental instruments and burs naturally belong to this class but are not included in this presentation [9–14].

Mineral trioxide aggregate (MTA) has been popular as a retrograde apical sealant material over the past decade. Interestingly, Portland cement contains the same chemical elements as MTA, such as certain silicates, ferrites, and aluminates. It has been shown that Portland cements and MTA have no cytotoxic effects in mouse lymphoma cells, which reinforces support to the use of MTA (and Portland cement) in endodontics [26].

For these and other dental materials not discussed in this chapter we ask the readers to consult other sources [26] such as references of this chapter. Examples of such materials may be involved in endodontics, implantology, orthodontics, paediatric dentistry, periodontology etc.

3.2 Metals

Metallurgy is a field of materials science that deals with the physical and chemical behavior of metallic elements, their intermetallic compounds, and their alloys. It is also known as the technology of metals that deals with the way in which science is applied to the practical use of metals and alloys. Metals have crystalline structures in the solid state in which the aggregated atoms are closely packed together. Any combination of metals is known as alloy. If an alloy is composed of two basic metals, it is called a *binary alloy*. Mixing three metals will result in a *ternary alloy* and so on [9–12, 13, 27].

Metals are generally ductile, nontransparent, malleable, lustrous, and hard (except, e.g., Na, K, Hg, and Ga). Metals are typically silvery white (save copper and gold), opaque in nature, and the best conductors of both heat and electricity, with pure gold as the uppermost conductor. Metals reflect light. Metals in general have high strength, yet they are characterized by low elasticity and high plasticity because of their high aptitude of ductility and malleability.

Metals and *alloys* have a vast amount of applications in dentistry [26]. Steel alloys are commonly used for the construction of dental instruments, temporary crowns, and wires for orthodontics. High-content gold (Au) alloys, medium-content gold alloys, and cobalt-chromium (Co-Cr) alloys are used for making crowns, inlays, and denture metal base frameworks. A dental silver amalgam is a

mercury (Hg)-containing alloy, and it is the most widely used dental filling material (discussed later in this chapter) [9, 12, 15, 26].

In dentistry, shaping of metals to have the planned finalized design can be achieved via *three methods*: (a) cold work (e.g., wire bending), (b) casting (e.g., metal crowns), and (c) amalgamation (e.g., amalgam filling). The so-called *cold work* is defined as the mechanical reshaping of highly ductile and malleable metals or their alloys at relatively low temperature. *Casting* implicates the melting of metals or their alloys, followed by pouring into an already prepared mold by a wax pattern so as to take the required shape of the mold. *Amalgamation* involves the mixing (trituration) of alloy powder with liquid metal (Hg) to form a plastic, condensable mass, followed by a condensation process to take the shape of the prepared tooth cavity [12, 28].

In studying the structure of metals, it is basically understood that *all metals are crystalline solid structures* with their atoms regularly arranged. Crystallization is the transformation from liquid status to solid status, and it needs two consecutive stages to occur—nucleation and growth. Metals should be heated beyond their melting points and then casted into molds and cooled to form crystalline solids. By heating and melting the metals a melt is formed in which the atoms are now loose and possess high energy. During the *melt-cooling process*, a solidification process occurs in which the atoms start to slow down to reach low energy. In the case of no impurities present in the melt to accomplish crystallization, undercooling is highly needed so as to bring down the melt to form a stable nuclei or crystal that is known as *homogeneous nucleation* [9, 10, 12, 14].

The need for impurities to accomplish crystallization is known as *heterogeneous nucleation*. In dentistry, it is common to have heterogeneous nucleation as impurities can be incorporated from the inner surfaces of the mold. Upon cooling of the molten metal, impurities will scatter in the melt, and hence metal atoms will deposit on these impurities and crystals start to form.

Crystal growth occurs in the form of 3D *dendrites* or *spherulites*. These 3D dendrites and spherulites are better described as protruding fingers or projections originating from the central nuclei. These crystals will continue to grow because of extra deposition of metal atoms until the metal is completely solidified. The crystals are also known as grains, and the area between each two grains is known as a grain boundary.

Grain size is determined by the number of stable nuclei per unit volume of a crystal. The crystallized grains have the same dimensions in each direction, measured from the central nucleus. In a crystalline structure, the atoms are arranged in repeating structures known as unit cells. The unit cells form a larger 3D array, a lattice, or a crystal [9–13].

In general, in materials science, a **martensitic transformation** refers to a phase transformation involving shear without diffusion.

On the other hand, a so-called **austenitic transformation** is defined as a phase transformation involving a solid solution of carbon (C) in face-centered-cubic (fcc) iron (Fe), which is stable at high temperature.

Metals and alloys have several applications in dentistry, such as PFM gold alloys, high-content gold alloys, medium-content casting gold alloys, cobalt-hromium alloys (Co-Cr), nickel-chromium (Ni-Cr) alloys, noble metal alloys, for example, gold alloys, silver-palladium (Ag-Pd) casting alloys, the so-called white gold, and high-content palladium casting alloys, and, finally, silver amalgam alloys.

3.3 Ceramics

Ceramics are nonmetallic solid materials formed by a firing process. They may consist of, for example, *metal* oxides (see also Chapter 16). They are characterized by having a high melting temperature and very low electrical and thermal conductivity. They have high compressive strength but very low tensile strength (brittle materials) and can resist chemical erosion. In addition, ceramic materials are relatively inert [26] and insoluble in water, and in fact, all ceramics have the same basic composition. From this composition point, they can be defined as this class of materials that is composed of *metallic oxide compounds* such as *feldspar* (which are of the type $KAlSi_3O_8$-$NaAlSi_3O_8$-$CaAl_2Si_2O_8$), *quartz* (flint, SiO_2), and *kaolin* (clay, China clay), $Al_2Si_2O_5(OH)_4$. Ceramics are crystalline in structure or partially crystalline, or they may be amorphous (as is glass). They are typically brittle materials [9, 12].

Ceramics (porcelains) as restorative materials in dentistry are widely used because of their a) high biocompatibility and b) esthetics. Ceramic materials have *three major indications* in contemporary dentistry [26, 29–32]:

(a) Ceramic-metal crowns and fixed partial dentures
(b) All-ceramic restorations consisting of short-span anterior bridges, crowns, onlays, inlays, and veneers
(c) Ceramic denture teeth

A ceramic veneer (a laminate) is used to cover an unsightly area by bonding to the facial surface of the tooth. It is noteworthy that no contraindications have been reported for ceramics [12, 13, 26, 29–31].

3.3.1 Dental Porcelain

Dental porcelain is composed of 60–80% feldspar, 15–25% quartz or flint, and 0–5% kaolin, which is hydrated aluminosilicate (Al_2SiO_5) and is used to increase the workable competence of unfired porcelain and to impart radiopacity. Feldspars are minerals, such as *potassium feldspar* ($KAlSi_3O_8$), *albite* ($NaAlSi_3O_8$), and *anorthite* ($CaAl_2Si_2O_8$). Structurally they are tectosilicates. Feldspars fuse at around 1300°C, and they are added to serve as the amorphous phase that brings silica (SiO_2) crystals together. Quartz, which is a form of silica, is added to act as a strengthening agent [10, 12, 32].

Fluxes like boron trioxide (B_2O_3) can be added to decrease the fusion temperature needed during the firing process of porcelain. *Pigments* such as selected transition metal (e.g., Fe, Cr, Pr, Ti, Cu, Mn) oxides and salts can also be added to the porcelain powder to better control the required shade for matching the natural tooth structure. For esthetic reasons, pigments and opacifiers are added to porcelains used in dentistry. In contemporary dental porcelains, kaolin is not contained in their formula anymore as kaolin requires controlled firing time and temperature to achieve satisfactory results. Modern dental porcelains can be described as a feldspathic amorphous phase with crystalline inclusion of silica [9, 12, 15, 32].

Dental porcelain powder is a mixture of already fired porcelain powder and other ingredients like metal oxides, which are very stable and cannot be decomposed by the high fusion temperature (Fig. 3.5). The resulted melt is poured into a water container by a *quenching* process. This melt will scatter in water into small irregular ingots, forming what is called frit, and the process is called *fritting*. These ingots go through crushing, milling, and lastly sieving with a

certain mesh size to control the particle size [9–15]. Production of dental porcelain goes into three consecutive technical stages: (a) compaction, (b) firing (sintering), and (c) glazing.

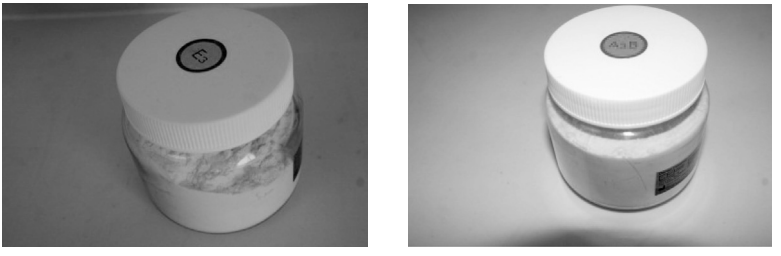

Figure 3.5 Dental porcelain powders: (left) porcelain powder for enameling, usually white in color, and (right) porcelain powder for the body of the crown, usually available in different shades.

In compaction, porcelain powder is mixed to a *slurry* with water, starch, and glycol. Before applying the slurry onto a die of a prepared tooth, a platinum matrix should be applied and adapted well on the die. The slurry is then stacked on the *die* by the use of a brush, or it may be molded in cases of inlays and onlays. Then condensation is a very important step to get rid of water from the slurry. It can be achieved by careful tapping of the applied mass on the die. The stacked porcelain is then *dried slowly* near an open oven to remove water and hence prevent porosity. *Sintering* is the formation of a coherent mass object from powders by heating without melting [9, 10, 12].

Glaze is a low-fusing transparent glass that has the same thermal expansion as porcelain. Glazing improves appearance and strength. Glazing also covers the porosities and voids that are formed during the firing process of porcelain; otherwise these porosities and voids can be very good areas for plaque stagnation, stains, and even a source for crack propagation [12, 29–32].

Indications of dental porcelain are numerous, such as inlays, onlays, laminates, crowns, and denture teeth.

Direct bonding of ceramic to natural teeth is inadequate because ceramic does not have a natural affinity to teeth. To obtain sufficient adhesion, it is vital to etch the tooth enamel with phosphoric acid

(H_3PO_4) before priming and cementation. The porcelain surface should be first etched with hydrofluoric acid (HF). Next, the surface must be rinsed and dried and a *silane coupling agent* applied. When the surface is *silanized*, the luting resin cement is able to penetrate the surface pores and ensure adequate bonding between the ceramic restoration and the flowable resin composite cement [31–33].

Computer-aided design/computer-aided manufacturing (CAD/CAM) is a new computer technology based on a method of fabricating all-ceramic restorations by making a 3D restoration design that imitates all the required specifications of the planned inlay, onlay, or single-unit crown (see Fig. 3.6; see also Chapter 18).

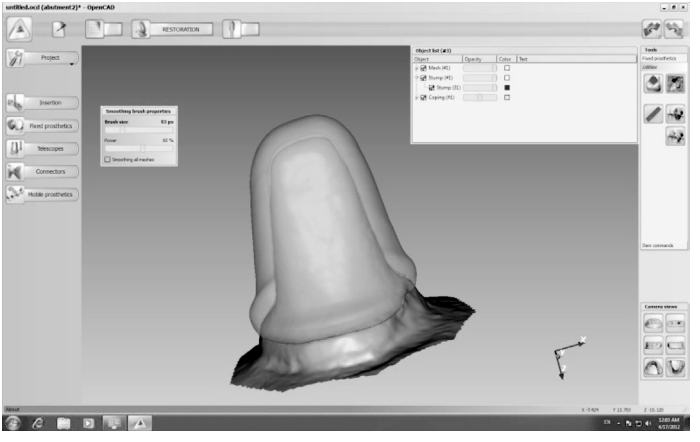

Figure 3.6 CAD/CAM technology is nowadays used in constructing milled dental porcelain restorations.

Dental porcelain, pretreatments such as silanization, and ceramic systems are also discussed in Chapters 11, 14–16, and 18.

3.3.2 Porcelain Fused-to-Metal Restorations

Metallo-ceramic restorations, in other words PFM restorations, are based on ceramic-metal systems. They combine the superior esthetic properties of dental porcelain and the attractive biomechanical properties of dental cast alloys by the so-called enameling technique that comprises the fusion of a thin layer of dental porcelain to a cast metal alloy coping (Figs. 3.7. and 3.8) [9–11].

Figure 3.7 Typical PFM, that is, metalloceramic, dental porcelain bridge.

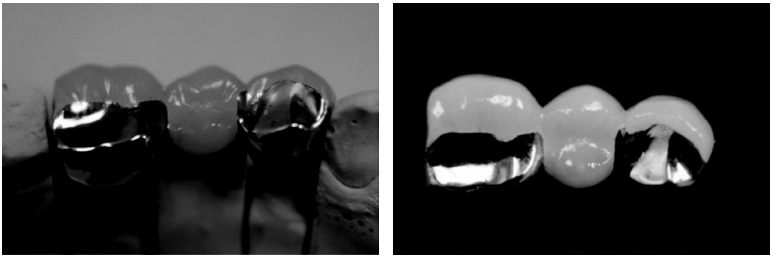

Figure 3.8 PFM dental bridge.

In general, PFM restorations are strong, rigid, and durable restorations. They are compatible with soft tissues and provide usually good esthetic properties. On the other hand, PFM restorations are brittle and with poor transverse strength. They can cause wear to the opposing natural teeth, and they need extra preparation efforts in the laboratory to achieve successful results. *Final designing of PFM restorations* is critical because of the material thickness consideration over the occlusal surfaces. There should be also enough space between the occlusal surface of the prepared tooth and the opposing dentition to provide adequate thickness for the alloy, as well as enough space for the porcelain, to produce excellent esthetic properties [9–15, 31].

The *coefficient of thermal expansion* of the porcelain must be suitably matched with that of the coping cast alloy. The thermal expansion of dental porcelain is 13.0–14.0 × 10^{-6}/°C, which is slightly

parallel to that of most metals, 13.5–14.5 × 10^{-6}/°C. After cooling, the porcelain is in a *slight compression*, which promotes bonding to the metal substrate. At the same instance, the coping alloy must have a high fusion temperature compared to the low fusion temperature for dental porcelain so as to avoid any distortion that may occur to the coping alloy during the construction of the PFM restoration [9–12].

The melting temperatures and melting range of alloys must be considerably higher than the firing temperature of dental porcelain. The melting range of the coping cast alloy must be raised appropriately above the fusion temperature of the porcelain to achieve a successful enameling operation [31].

The consideration of *bonding dental porcelain to metal coping* is a crucial requirement in the ceramic-metal system. Dental porcelain should be compatible to the coping cast alloy. The metal coping should form a strong bond to ceramic without melting or undergoing fatigue during porcelain firing. It is widely accepted that bonding is based upon *chemisorption* by diffusion between surface oxides on the alloy and in the dental porcelain [9–14].

Prior to the bonding process, the surface of the metal coping should be clean and dry and fully free of impurities to achieve successful bonding. It is important to permit the dental porcelain slurry to wet the alloy readily so as to prevent void formation at the interface. Metal oxides are formed during wetting on the metal coping and during the firing process of porcelain. The formation of metal oxides requires the use of *base metal alloys* that contain elements such as nickel (Ni), chromium (Cr), and tin (Sn), which can form oxides easily during the firing process.

On the other hand, *noble metals* are resistant to metal oxide formation, which means that inclusion of other ingredients, such as nickel and indium, should be implemented. It is important that the alloy *not* contain components that form colored oxides, at the interface, or that give rise to *color effects* within the porcelain. This is why, for example, copper is not used in porcelain-bonding gold alloys [9–15].

There are *two bonding mechanisms* whereby dental porcelain can be retained to the structure of a metal casting: (a) *mechanical interaction* (retention, interlocking) and (b) *chemical bonding* (adhesion). The mechanical bonding of dental porcelain with metal

coping results from fusion of the porcelain into undercuts in the metal surface. Grit blasting of the coping surface can *increase the surface area* and create suitable undercuts for mechanical bonding. Given this, metal surfaces should be thoroughly clean, degreased, and empty of impurities; otherwise, the porcelain will not wet the surface evenly and cracks may nucleate into the porcelain where contact with the metal is poor (see also Chapter 11).

Chemical bonding of porcelain to metal is obtained by fusion of the porcelain to a *metal oxide layer* on the surface of the casting. Ideally, this film of the oxide layer should be extremely thin and continuous with the underlying metal structure. Hence, it is unlikely to obtain direct chemical bonding of porcelain to metal. On the other hand, certain metal ions can be merged into dental porcelain, outside of the chain network, in the form of *network-modifying oxides*. This incorporation of network-modifying oxides is especially applied if there is a possibility of development of a *passive oxide layer*. If these metal ions are obtained from the surface of the metal coping, a slow and steady structural transition between pure oxide and pure metal may be achieved. With such conditions chemical bonding can be achieved successfully between the ceramic and the underlying metal coping [9, 10, 12, 31].

The main observed *modes of failure* in PFM restorations can be classified as failure within the porcelain, failure at the metal-porcelain interface, and/or failure within the metal oxide layer (Fig. 3.9). For PFM restorations with a gold alloy framework, the failure usually takes place within the porcelain [10–15, 29–31].

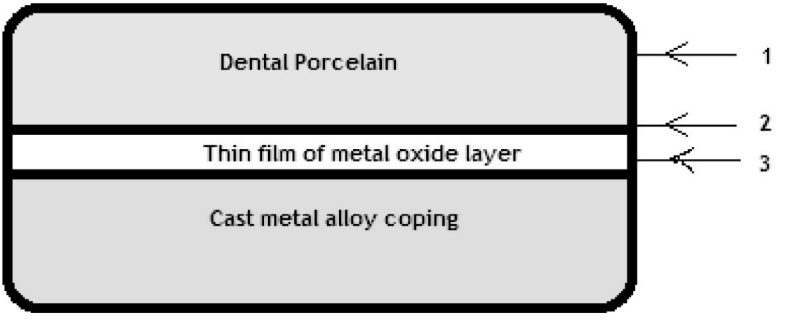

Figure 3.9 The three main modes of failure in PFM restorations. 1: failure takes place within the porcelain; 2: failure at the metal–porcelain interface; and 3: failure within the metal oxide layer.

3.4 Polymers

Polymer molecules are large macromolecules consisting of long and flexible chains with a string of carbon (C) atoms as a *backbone*. Polymers may also consist of a –Si–O–Si–O–Si– type of backbone as in *silicones*, that is, *polysiloxanes.* In general, polymers can also be defined as any of various solid or semisolid, amorphous, natural organic substances that are usually transparent or translucent and brown to yellow [10, 29] and usually formed in plant secretions. They are soluble in organic solvents but not water and are used chiefly in varnishes, inks, plastics, and medicines. They are also found in many dental impression materials [9–14, 26, 35].

In general, the term *polymer* is used to outline and explain natural or synthetic substances that form plastic materials after polymerization. They are named according to their chemical composition, physical structure, and means for activation of polymerization. *Copolymers* are polymers with at least two different types of repeat molecular units (monomers) [9, 12, 35, 36].

Polymerization consists of three consecutive reactions: (a) *induction* (i.e., initiation), which is controlled by two processes, activation and initiation; (b) *propagation*; and (c) *termination*. On the other hand, an *autopolymerizing* resin is a resin whose polymerization is initiated by a chemical activator [9, 29].

> In dentistry, the polymerization process is usually activated by one of three energy sources: (a) heat, (b) chemicals, and (c) light.
>
> In addition to these sources, there is another system consisting of at least two reactants that can generate free radicals when mixed together. In *self-cured materials*, an activator (tertiary amine) and an initiator (benzoyl peroxide) are mixed together at room temperature to initiate polymerization. These two materials should be kept separated during storage to avoid the induction of reaction.

The final molecular weight (chain length) of a polymer is controlled by relative rates of the induction, propagation, and termination steps of polymerization.

Next we'll take a concise look at the applications of polymers in clinical dentistry.

3.5 Elastic Impression Materials

Polymeric elastic impression materials may be classified as follows [36]:

(a) Aqueous elastomeric impression materials (*hydrocolloids*):
   1. Alginate irreversible hydrocolloids
   2. Agar reversible hydrocolloids

(b) Nonaqueous elastomeric impression materials:
   1. Polysulfide materials
   2. Polyether materials
   3. Condensation-polymerizing silicones
   4. Addition-polymerizing silicones

3.5.1 The Hydrocolloids

A *colloid* is a material in which fine particles of less than 1 μm in diameter are suspended in a liquid. This material is known as a *hydrocolloid* when the mixing liquid is water. Two important characteristic features should be considered when dealing with hydrocolloids, which are *syneresis* and *imbibition*. Syneresis is the expulsion of water droplets from the hydrocolloid material surface. Imbibition is the absorption of water by the hydrocolloid material and is usually accompanied by expansion [9–12].

3.5.2 Colloids

In general, c*olloids* contain material that is present in particles of the size of 1–1000 nm (i.e., invisible to the naked eye). There are *three types of colloids* (Table 3.1): (a) insoluble disperse particles, called lyophobic (e.g., colloidal Au, S in H_2O); (b) large molecules with van der Waals bonding in between (e.g., agar, alginate hydrocolloid impression materials); and (c) association colloids (i.e., aggregates of smaller molecules). Examples of the group (c) are surface-active agents such as detergents and soap that consist of long hydrocarbon chains with a small, charged polar entity at one end (e.g., Na-palmitate). Aggregates formed by these molecules are called *micelles* [12–14].

Table 3.1 Classification of colloids

Dispersed phase	Continuous phase	Type
Solid (s)	Liquid (l)	Sol
Solid (s)	Gas (g)	Aerosol (smoke)
Liquid (l)	Liquid (l)	Emulsion
Liquid (l)	Gas (g)	Aerosol (fog)
Gas (g)	Liquid (l)	Foam
Gas (g)	Solid (s)	Foam

3.5.3 Reversible Hydrocolloids: Agar

Agar is based on derivatives of seaweed. It is actually a galactose sulfate, which is a polysaccharide and which forms a colloid when mixed with water. It is a reversible hydrocolloid because it can liquefy to a solution (*sol state*) upon heating and return to rubber (*gel state*) upon cooling by a process known as gelation. This change is an extremely physical change and is not accompanied by any chemical reaction. The agar liquefaction temperature is ranged between 70°C and 100°C, and it sets to a gel again between 30°C and 50°C (Figs. 3.10 and 3.11).

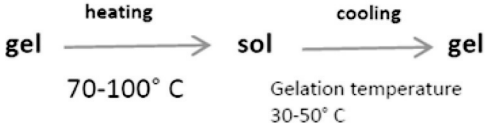

Figure 3.10 Agar liquefaction temperature is ranged between 70°C and 100°C.

The active ingredient of a hydrocolloid impression is agar, which constitutes 8–15% of the total weight, whereas the major constituent (by weight) is water, which constitutes more than 80% of the total weight. Small amounts (0.2%) of borax (disodium tetraborate, $Na_2B_4O_7{\cdot}10H_2O$) are added to improve the strength of the gel. Potassium sulfate (K_2SO_4) is added (ca 1.7%) as an accelerator to counteract the retarder effect of borax on gypsum setting. An alkyl benzoate compound can be added in trace amounts (0.1%) to prevent the growth of mold during storage. *Thymol* (2-isopropyl-5-methylphenol) is a natural monoterpene phenol, and it is used

as a bactericidal. Glycerol (propane-1,2,3-triol, i.e., glycerin) is used as a plasticizer and may be added to the hydrocolloid. Also, some coloring agents and flavors are usually included as well [9–15, 29, 36].

Figure 3.11 Upper master cast for constructing a metal framework is prepared for duplication (left); duplicating impression for the master cast by agar material to produce a refractory cast (right).

3.5.4 Irreversible Hydrocolloids: Alginates

An *alginate* is a hydrocolloid consisting of alginic acid (in sol state) that is changed to an insoluble and elastic Ca-alginate by an irreversible

chemical reaction. *Alginic acid* is an anionic polysaccharide derived from marine seaweed named *algae*.

Alginate powder contains either sodium or potassium alginate (12–18 wt%) and calcium sulfate dihydrate (8–14 wt%) so as to provide calcium ions as reactants. Also, ca 2 wt% sodium phosphate (Na_3PO_4) is added to alginates to act as a retarder to control working time. Adding sodium phosphate in different ratios can control the alginate impression material to be either regular or fast in setting. Around 10% of potassium sulfate (K_2SO_4) is added to control the setting of the gypsum model after pouring. Reinforcing fillers are usually diatomaceous earth in 56–70% to control the consistency of the set material. *Coloring* and *flavoring* additives are contained as trace materials [9–15, 29, 36].

Reaction and cross-linking: when the powder is mixed with water, two main reactions occur. Firstly, a 3D network is formed by cross-linking the polymer chain. This reaction is considered irreversible because the 3D network cannot be broken. Sodium phosphate is reacting with calcium sulfate first to afford a suitable working time. At this stage of the reaction, Ca^{2+} ions are released from calcium sulfate dihydrate.

The chemical reaction at this *first stage* is:

$$2Na_3PO_4 + 3CaSO_4{\cdot}2H_2O \rightarrow Ca_3(PO_4)_2 + 3Na_2SO_4 + 2H_2O \quad (3.12)$$

Calcium sulfate dihydrate provides Ca^{2+} ions that are necessary to change the material from the sol state to the gel state. These ions react preferentially with phosphate ions (from sodium phosphate) to form insoluble calcium phosphate [9–12, 29].

The *second stage* of the reaction is manifested by a reaction between the sodium sulfate with the remaining calcium sulfate:

$$\text{Na-alginate} + CaSO_4{\cdot}2H_2O \rightarrow \text{Ca-alginate} + Na_2SO_4 \quad (3.13)$$

Alginates are used to make impressions for single prepared crowns, removable partial dentures, and orthodontic cases and for primary impressions for completely edentulous arches, especially when there are soft tissue and bony undercuts. Alginate impression materials have good elastic properties. A proper water-to-powder ratio should be used because proper mixing may lead to better control of the setting time and to a homogenous mix to accurately register the surface's fine details. Like other elastic materials, it can

register the undercuts of teeth and their neighboring structures. Gypsum casts are poured *directly* into the impression material, with no need for a separating medium (Figs. 3.12 and 3.13) [9–15, 29, 36].

Figure 3.12 A container of alginate dental impression material. The container of powder should be fluffed before use to get an even distribution of alginate powder constituents.

Figure 3.13 Alginate impression material and its handling.

Alginate as an impression material doesn't have enough body to support itself, so the amount of impression material coming out of the impression tray should be only a few millimeters to avoid tearing of the borders. In addition, a minimum of 3 mm thickness is needed between the tray and the teeth and/or oral structures.

A delay in pouring the impression material mass may cause a dimensional change with shrinkage due to loss of water. If time is needed between impression making and cast pouring, it is advisable to cover the impression with wet gauze or tissue to avoid evaporation of water [9, 11, 14, 29].

3.6 Elastomers

3.6.1 Polysulfides

Polysulfides are a type of elastomeric impression material. Their setting reaction involves cross-linking under the influence of oxidizing agents such as lead dioxide (PbO_2). Polysulfides are also known as *thiokol rubbers* because they are derivatives of thiols (–SH, aka mercapto group), which are the sulfur (S) analogues of alcohols (cf an alcohol –OH, a thiol –SH).

Polysulfides are available in low, medium, and high viscosities, and they are supplied in base and catalyst (accelerator) paste tubes. The base paste, which is usually white, contains a low-molecular-weight polysulfide polymer with a molecular weight of ca 2000–4000 g mol^{-1}. The liquid polymer is converted to a paste by mixing it with fillers like titanium dioxide (TiO_2), which is an inert reinforcing filler and acts to provide the required strength. In addition, the paste can be made thicker by mixing it with silica [9–14].

Dibutyl phthalate is used as a plasticizer to impart the most suitable viscosity to the paste material (i.e., low, medium, or high viscosity). A small quantity of sulfur can be used to accelerate the polymerization reaction. The catalyst paste contains mainly lead dioxide, which gives the catalyst paste its characteristic brown color. PbO_2 is also responsible for the characteristic odor of the polysulfide impression material and for staining the skin if it comes in contact with the paste.

The catalyst paste contains dibutylphthalate (or dioctyl phthalate) as a *plasticizer*, along with Mg-stearate or oleic acid (which is a fatty acid) ($CH_3(CH_2)_7CH{=}CH(CH_2)_7COOH$) as a retarder, to prolong the rate of the setting reaction [9–14, 29, 36].

Other substances like deodorants can be added to the catalyst paste. The polysulfide polymer has terminal and pendant mercapto

(–SH) groups. Lead dioxide is acting as an oxidizing agent to induce polymerization between the terminal and pendant –SH groups with –SH groups on other molecules, resulting in lengthening of the chain and cross-linking. By this, the material is changed to the rubbery state. Water is a by-product of this reaction. The polymerization reaction of polysulfides is *exothermic*, with a temperature rise between 3°C and 4°C. Increases in temperature and humidity can accelerate this reaction process [10–12, 36].

Polysulfides are considered good impression materials to reproduce fine details. They have a long working time, good flowability before setting, good registration of the undercut areas, and high flexibility, and they are probably the most economic material among elastomers [9–15, 29, 36].

3.6.2 Polyether Impression Materials

Polyethers are compounds with more than one *ether* group, R-O-R'. A polyether impression material may be characterized by a short working time and by being among the stiffest of all elastomers when set. Because of this its use is confined to situations where only few remaining teeth are present. Taking an impression of the full dentition is usually difficult with a polyether. They are supplied in low, medium, and heavy body consistency, and they are available in a two-paste system, with a base and a catalyst. The base consists of a polyether, a plasticizer such as phthalate or triglycerides, and colloidal silica as an inert filler [9, 11, 12, 29, 36].

The *catalyst* paste consists of an aromatic sulfonic ester (which increases further polymerization and cross-linking), a *plasticizer*, and a *thickening agent* such as silica inert fillers. *Coloring agents* are added to the base and the catalyst to better differentiate between the two pastes. A sulfonic ester is of the type R'-SO_2O-R". The reaction starts upon mixing the two pastes together. The elastomer is formed by cationic polymerization by opening the reactive terminal rings of the *ethylene imine* group and chain extension. There is no by-product formation in this reaction. However, a polyether tends to absorb water if stored in a moist environment for a long period of time. The formation of a polyether impression material is demonstrated as follows:

$$\text{Polyether} + \text{Sulfonic ester} \rightarrow \text{Polyether rubber} \quad (3.14)$$

Polyether impression materials are easy to manipulate and to mix. They are more accurate than polysulfides in reproducing the very fine details of the teeth and adjacent tissues. They can be kept up to one week if kept dry [9–15, 36].

Polyethers are relatively expensive materials. They have short working and setting times; hence they are limited to professional use only. They are characterized by high stiffness after setting. Polyether impression materials are very sensitive to moisture, so they should be kept dry after setting. Immersion in disinfection solution should be for a very short time. In addition, polyether impression materials have a *bitter taste*, which makes them objectionable to many patients.

3.6.3 Condensation Silicones

Condensation silicone rubber impression materials are made of *silicone polymers*. In general, silicones are inert, synthetic inorganic-organic polymer compounds with a variety of forms and uses. The name *silicone* saw daylight in 1901 by analogy with ketones. Silicones contain *direct* Si–C bonds (exactly like *silanes*, cf Chapter 11), and their general formula is $(R_2SiO)_n$. Both the extent of the *cross-linking* and the nature of the *substituent* determine the nature of silicones. Silicones range from oily liquids and gels to rubbery solids. They are all *hydrophobic* (water repellent). They are also heat resistant, electrically and thermally insulating, and chemically inert. Various silicones find applications as adhesives, lubricants, sealants, and insulation [12, 26].

Silicone synthesis consists of several steps, for example, starting form methylchloride (CH_3Cl) and Si with 5–20% of Cu (which is acting as a catalyst) [36, 37]:

$$CH_3Cl + Si \xrightarrow{Cu} (CH_3)_nSiCl_{4-n} + (CH_3)_nSiCl_{4-n} + (CH_3)_xSi_yH_zCl_w \quad (3.15)$$

This chemical reaction is *one* pathway to synthesize direct Si–C bonds. Out of curiosity, the simplest way might be *hydrosilylation*, starting with the element *silicon*, Si, and hydrochloric acid, HCl. Silicon can be first reduced from silica (e.g., quartz sand) with carbon in an *endothermic* reaction:

$$SiO_2\,(s) + C\,(s) \rightarrow Si\,(s) + CO_2\,(g)\ \Delta H > 0 \quad (3.16)$$

$$\text{Si (s)} + 3\text{HCl} \rightarrow \text{H-SiCl}_3 \rightarrow \text{H-C-C-SiCl}_3 \quad (3.17)$$

>C=C<

It has been reported that over 100 species may be formed in the reaction in Eq. 3.15. This reaction may be optimized to produce *substituted* Si chlorides, such as $(CH_3)_2SiCl_2$ and CH_3SiCl, which are widely used precursors in silicone synthesis [36, 37]. In general, hydrolysis of alkyl (such as CH_3)- or aryl (e.g., C_6H_5)-substituted Si-chlorides produces silicones (Fig. 3.14).

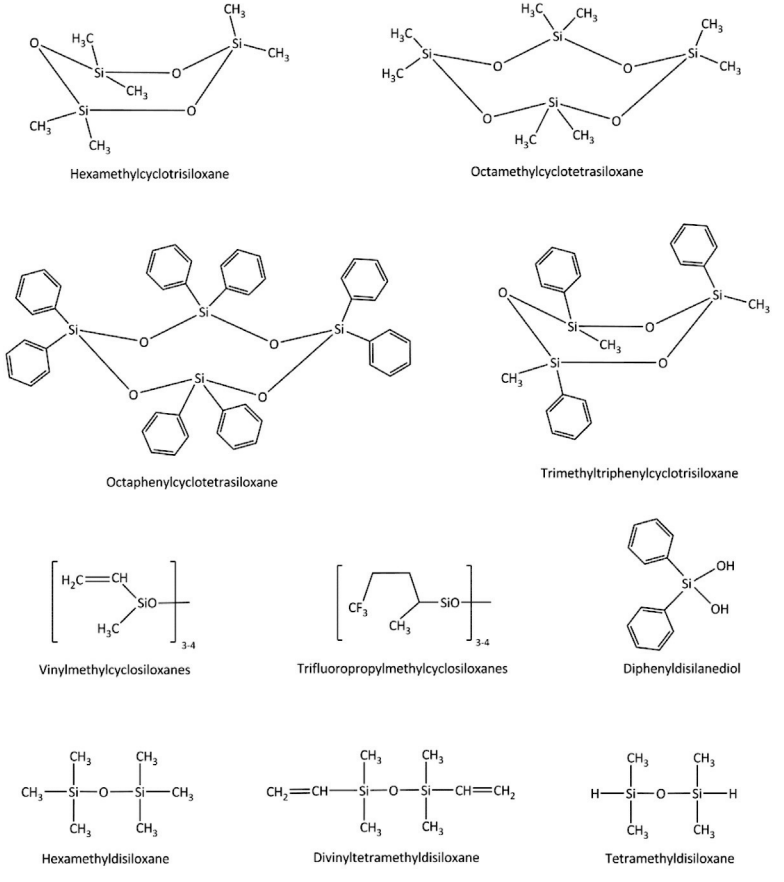

Figure 3.14 Some silicone monomers and terminators.

Hydrolysis of $(CH_3)_3SiCl$ produces *trimethyl silanol*, $(CH_3)_3SiOH$. Through a condensation reaction trimethyl silanols condense and form a *disiloxane* (18):

$$2(CH_3)_3SiOH \rightarrow (CH_3)_3Si\text{-}O\text{-}Si(CH_3)_3 \quad (3.18)$$

A silicone-chain compound is produced in hydrolysis of $(CH_3)_2SiCl_2$, and hydrolysis of CH_3SiCl_3 leads to a 3D cross-linked chain system compound (Fig. 3.15).

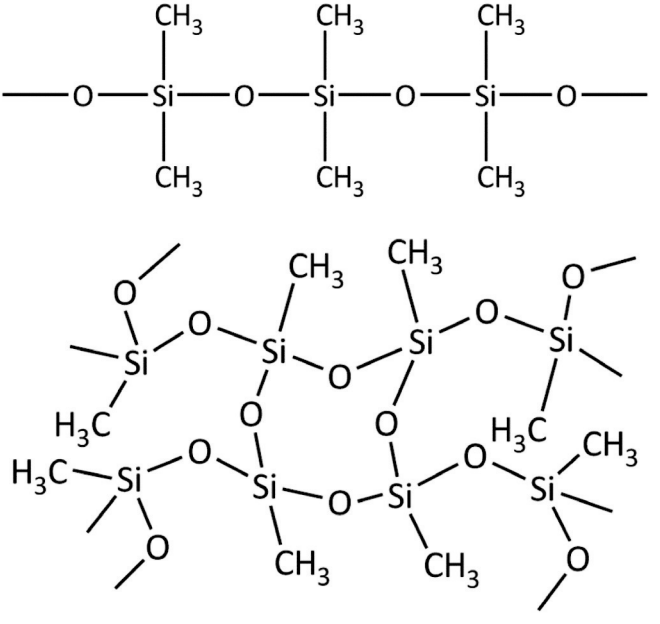

Figure 3.15 Above: Hydrolysis of $(CH_3)_2SiCl_2$ gives a chain-structured compound. Below: Hydrolysis of CH_3SiCl_3 gives a cross-linked system.

In dentistry silicones are used mainly for impressions of implants, fixed partial dentures, and single-unit inlays and onlays [12, 26]. There are four silicone cross-linking (or curing) systems employing *four catalytic systems* (Fig. 3.16).

They are available in low, medium, high, and very high viscosities in a form of a putty (Fig. 3.17) and are usually supplied in a two-paste system or a paste-liquid catalyst system [9–14, 29, 39].

Condensation silicone rubber impression materials are based on a linear polydimethylsiloxane, which has reactive terminal hydroxyl (–OH) groups. Viscosity is controlled by the amount of fillers such as calcium carbonate or silica, which may range from 30–40% for low viscosity to 75% for putty viscosity [11, 29, 39].

Peroxides:

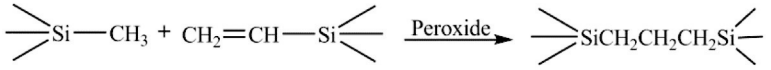

Metal salt:

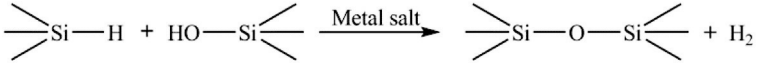

Condensation:

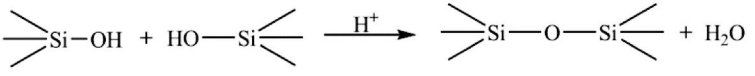

Vinyl addition:

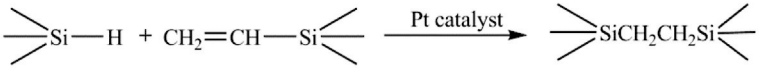

Figure 3.16 Silicone-curing systems.

Figure 3.17 A two-component putty silicone impression material.

Both pastes of the two-paste system polymer contain a liquid silicone polymer made from polydimethylsiloxane. The base paste also contains orthoethylsilicate (i.e., orthoethoxy silane), which is a hybrid inorganic-organic molecule and has a direct influence on the

polymer chain to be cross-linked. The catalyst paste contains a Sn-octate suspension and alkyl silicate and fillers to provide thickening to the paste.

Cross-linking (curing) of this material is achieved by a reaction of tri- and tetraethyl silicate in the presence of Sn-octate. To achieve a cross-linking network, a 3D network is formed. Ethanol is a common by-product of this reaction with a rise in temperature of 1°C. The release of alcohol as a by-product comprises the storage stability. The shrinkage that may occur in the set material in 24 hours ranges from 0.2% to 1.0%, with half of this shrinkage taking place in the first hour after setting of the elastomeric material [9–15, 42].

Condensation silicones are not messy during manipulation and work. They have high elasticity, which makes them acceptable by operators and patients (Fig. 3.18). Mechanical characteristics can be fully achieved if the catalyst amount is carefully controlled to avoid incomplete elastomer cure. The two-step putty-wash impression technique is used favorably to reduce polymerization shrinkage.

Figure 3.18 A complete denture impression can be made by using light-body, low-viscosity silicone impression materials.

3.6.4 Addition Silicones

Addition silicones are usually available in base and catalyst systems of two equal-size tubes, often in an automix dispenser cartridge gun. The base-to-catalyst ratio is 1:1. The *base* mainly consists of

a vinyl-terminated polydimethylsiloxane polymer; a platinum salt as a *catalyst*, usually chloroplatinic acid, $H_2PtCl_6{\cdot}(H_2O)_6$; silica as a filler; and a hydrophilic agent as a surfactant. The catalyst paste consists of a vinyl-terminated polysiloxane polymer, a cross-linking agent, a filler, and a silicone oil to adjust viscosity properties of the impression material (cf Fig. 3.16 before) [9, 10, 29].

Addition silicone impression materials are very stable with nearly zero dimensional changes. They have good tear strength, convenient working and setting times, and excellent wettability. Hydrogen gas (H_2) is a by-product of the addition reaction as the Pt catalyst may release H_2 from water. Another reported effect is the –OH groups in silicone may cause bubbles on a gypsum model, and so it is preferable to pour the cast after one hour of making the impression. Furthermore, it is noteworthy that addition polymerization is *inhibited* by latex gloves or some astringents such as sulfur and heavy metals [9–14, 29, 39].

3.6.5 Is Silicon a Biomaterial?

The earth's crust consists of 25% of the element Si, silicon. Silicon (melting point 1420°C; boiling point 2700°C) is a semiconductor, is a metalloid, is chemically more reactive than carbon, and occurs extensively in numerous forms of SiO_2, silicates, and aluminosilicates. Silicon is gray, hard, crystalline and commercially prepared by heating silica with carbon (Eq. 3.16 before). Silicon can be purified by so-called *zone refining* until the impurity content is less than 10^{-7}%. This form of Si is not toxic but not biocompatible either, and so far this has prevented its use in vivo. Interestingly, the porous form of Si is tolerated by the body's immune system.

Devices based on Si semiconductors are available for *biosensing* applications. Such bulk Si-based integrated *circuits* need a biocompatible carrier material when linked to living tissues. *Bionic implants* mimic the original function very closely, or even surpass it. Currently, there are promising ongoing studies on, for example, electronic sensing devices, to replace damaged eyes, hear sounds, and check body chemistry to monitor disease, drug dosage, or pain. *Nanostructured porous* Si (PS) has reported to be a promising biomaterial for such sensing devices linked to the human biological system.

Some organo-Si compounds, certain silanes, are best known as biologically compatible substances to serve human health. Areas of the present-day applications include cancer therapy, dementia, epilepsy, wound healing, hair growth, Alzheimer, Parkinson, some barbiturates, muscle relaxants, hypolipidemic activity, and enzyme inhibition [38]. Obviously, novel organosilane structures with biological activity are to be identified for applications in medicine.

3.6.6 Silicones as Biomaterials

Silicones are one of the most widely used and one of the most studied biomaterials. In general, silicone polymers are of relatively recent invention, and their commercial-scale production was initiated in the 1940s. By the mid-1950s biomedical applications of silicones had greatly increased, and many studies of the biological properties of these materials were undertaken.

In the 1990s there were claims that the silicone gel used in breast implants was responsible for a number of systemic health problems, including autoimmune diseases. However, it has been reported that women with silicone breast implants are no more likely to develop systemic illness than women without breast implants. Silicone breast implants may rupture, and thereafter silicone can migrate. Nonetheless, the use of silicone breast implants has been approved by several national health authorities worldwide.

In addition, silicones find a wide range of biomedical applications as antireflux cuffs, artificial lungs, brain membranes, chins, contact lenses, ear frames, Eustachian tubes, extracorporeal dialysis, finger joints, hip implants, intra-aortic balloon pumps, oviductal plugs, orbital floors, tibial cups, toe joints, total artificial hearts, tracheal stents, tracheostomy vents, urethral cuffs, vaginal stents, wrist joints, etc. [36]. We may conclude that silicones and silane monomers have a huge potential in biomaterials science and its applications.

3.7 Acrylic Materials

Acrylic acid (i.e., 2-propenoic acid) is a corrosive liquid and the simplest unsaturated carboxylic acid (with a functional –COOH group), and it has the formula CH_2=CHCOOH (Fig. 3.19). Acrylic acid has a so-called *vinyl* group connected directly to a carboxylic acid

terminus. In chemistry vinyl (IUPAC name: ethenyl) is the functional group $–CH=CH_2$ and is a derivative of the *ethene* (ethylene) molecule $H_2C=CH_2$. The name "vinyl" is also used for any compound containing that group, namely, $R–CH=CH_2$, where R is any other group of atoms, for example, Cl. An industrially important example is, indeed, *vinyl chloride*, $Cl–CH=CH_2$, a precursor to poly(vinylchloride) (PVC), $-[CH_2-CHCl]-_n$, a plastic commonly known as vinyl. Acrylic acid liquid is a colorless liquid and has a characteristic acrid smell (melting point 14°C; boiling point 141°C). It is miscible with alcohols, chloroform, ethers, and water. It polymerizes readily in the presence of oxygen. An *acrylate polymer* belongs to a group of polymers that in general may be referred to as plastics. They are noted for their resistance to breakage, transparency, and elasticity. They are also commonly known as *acrylics* or *polyacrylates*.

The term *methacrylate* refers to ester derivatives of *methacrylic acid* (i.e., 2-methyl-2-propeonic acid) (MAA), $CH_2C(CH_3)COOH$ (see in Fig. 3.19).

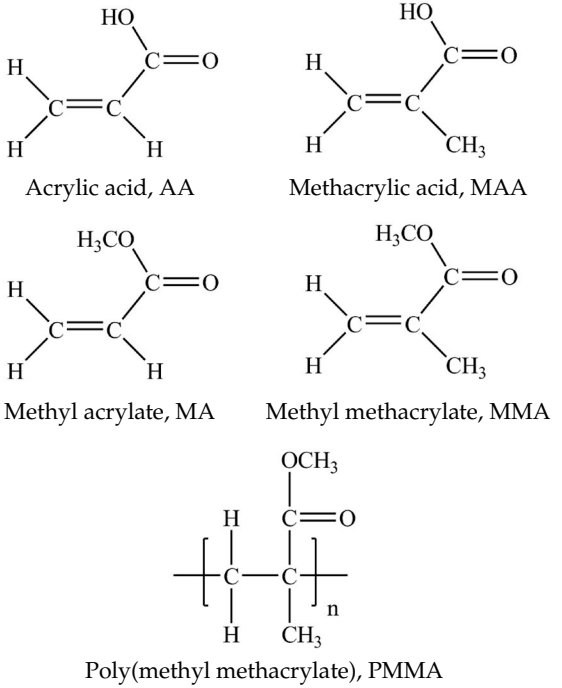

Figure 3.19 Various acrylic compounds.

This corrosive, colorless, and viscous liquid is also a carboxylic acid with a repulsive, acrid odor. MAA is soluble in cold and warm water and miscible with most organic solvents. Its melting point is 16°C and boiling point 163°C. MAA occurs naturally in small amounts in the oil of Roman chamomile (*Chamaemelum nobile*). MAA is produced industrially on a large scale as a precursor to its *esters*. Methacrylate derivatives include the parent acid MAA and salts such as $CH_2C(CH_3)COO^-Na^+$; esters such as *methyl methacrylate* (*MMA*), $CH_2C(CH_3)COOCH_3$; and *polymers* of these species. *Methacrylates* are common monomers in plastics. Methacrylates easily form polymers because the double bonds are very reactive. They have numerous uses, most notably in the manufacture of polymers with trade names, for example, Lucite™ and Plexiglas™. They are used as the monomer resin, for example, in some windscreen repair kits and as *bone cement* for fixing prosthetic devices in orthopedic surgery [9, 26, 39].

In this context we may go back to bis-GMA, bis-glycidyl dimethacrylate. Its systematic IUPAC name is 2-hydroxy-3-[4-[2-[4-[2-hydroxy-3-(2-methylprop-2-enoyloxy)-propoxy]-phenyl]propan-2-yl]-phenoxy]-propyl]-2-methylprop-2-enoate). The cheapest and most convenient starting point for resins used a vast majority of resin composites is bisphenol A, 4,4'-(1-methylethylidene)-bisphenol (often abbr. BPA), $(CH_3)_2C(C_6H_4OH)_2$ [12]. Bisphenol A, a colorless solid, melting point 150°C–155°C, has two hydroxyphenyl functionalities, and it is produced industrially from *acetone* (2-propanone, aka dimethyl ketone) and *phenol*, C_6H_5OH, (*hydroxybenzene*, aka *carbolic acid*):

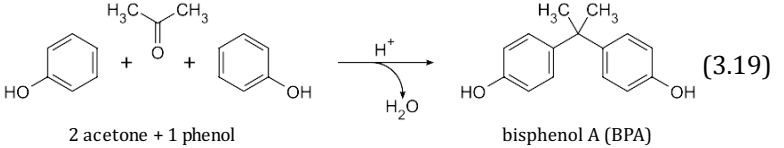

(3.19)

2 acetone + 1 phenol bisphenol A (BPA)

Bisphenol A is a monomer used in various plastics and for *epoxy* resins and polycarbonate. Such plastics are clear and tough and used to manufacture, for example, baby bottles, sports equipment, and DVDs and CDs. Bisphenol A containing epoxy resins are applied in producing thermal papers and protective coatings on the inside of many beverage and food cans. The usefulness of bisphenol A lies in its *rigid* molecular structure due to some steric hindrances to rotation

(cf Eq. 3.19 before). Bisphenol A is claimed to exhibit hormone-like properties, that is, estrogenic activity. This has raised concern about its suitability in food containers. Toxicity aspects are discussed in details in Chapter 5. There are two ways to synthesize bis-GMA, and they are presented in Fig. 3.20.

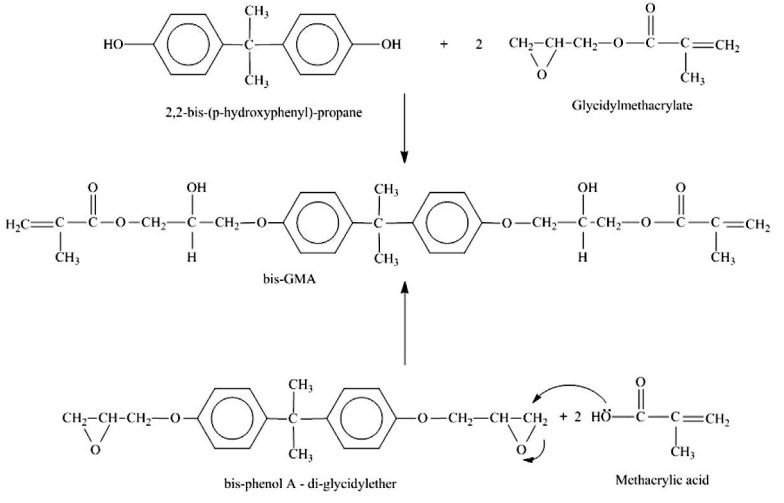

Figure 3.20 Two synthetic pathways to produce bis-GMA.

Bis-GMA is very viscous and it is used as a common basis for the matrix of resin composites. As this resin has two vinyl functional groups it would be highly cross-linked and also very rigid. Bis-GMA may be polymerized by any of the usual initiator-activator systems, for example, benzoyl peroxide and an alkyl borane [12]. Some other bis-GMA "family members," such as *iso*-bis-GMA, ethoxylated bisphenol-A dimethacrylate (bis-EMA), propoxylated bisphenol-A dimethacrylate (bis-PMA), and bis-MA that are, or have been, of interest in dental materials research are presented later in Fig. 3.21.

An acrylic polymer, poly(methyl methacrylate), PMMA, is an acrylate polymer material that was introduced in the market as a *denture base material* in 1937 (see Fig. 3.19). Previously, synthetic materials such as nitrocellulose, vulcanite, phenol formaldehyde, porcelain, and vinyl plastics were used for denture bases. In 1946, already 98% of all denture bases were constructed from MMA polymers (or copolymers).

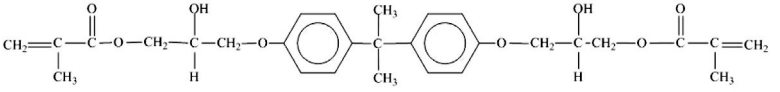

bis-GMA = 2, 2-bis-4(2-hydroxy-3-methacryloxy-propyloxy)-phenyl-propane

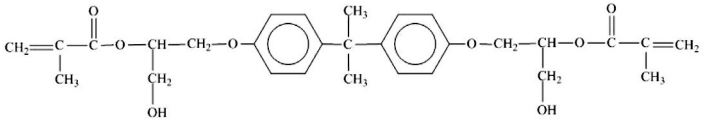

iso-bis-GMA = 2, 2-bis-4(2-hydroxymethyl-3-methacryloxy-ethyoxy)-phenyl-propane

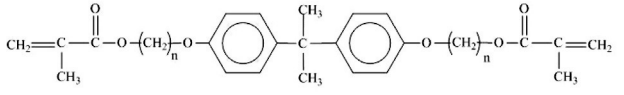

n=2 bis-EMA = 2, 2-bis-4(2-methacryloxy-ethoxy)-phenyl-propane

n=3 bis-PMA = 2, 2-bis-4(3-methacryloxy-propoxy)-phenyl-propane

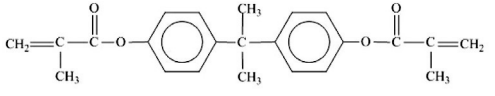

bis-MA = 2, 2-bis-(4-methacryloxy-phenyl)-propane

Figure 3.21 Molecule structures of bis-GMA, iso-bis-GMA, bis-EMA, bis-PMA, and bis-MA.

PMMA, an acrylate polymer familiar to consumers, is the clear, break-resistant "acrylic glass" or sheeting sold in hardware stores under the trade name Plexiglas™. Acrylic polymers have a vast amount of applications in dentistry: denture bases, artificial teeth, denture repair materials, soft liners, impression trays, provisional restorations, and maxillofacial appliances (e.g., for skeletal defects) [9, 12, 26, 39].

There are certain *requirements* [10, 26, 39] for a clinically acceptable denture base material: processing accuracy, strength and durability, dimensional stability, satisfactory thermal properties, chemical stability, absence of odor and taste, insolubility and low sorption properties, biocompatibility, natural appearance, color stability, and adhesion to plastics, metals, and porcelain. In addition, the material should be easy to fabricate and repair [1, 3, 9, 10, 26].

There are *two types of polymers based on MMA*, (a) heat-cure acrylics and (b) cold-cure acrylics.

Acrylic is prepared by an *addition polymerization reaction*, which involves *three steps:* (a) initiation reaction, (b) chain propagation, and (c) chain termination. The initiation reaction is usually triggered by a radical. In this case, benzoyl peroxide is split into benzoyloxy radicals and then further into phenyl radicals. In a *heat-cure acrylic*, the initiator is activated by raising the temperature. On the other hand, in a *cold-cure acrylic*, the initiator is activated by chemical activators (usually a tertiary amine) [9–12, 36]—about this, see also Chapter 6.

3.7.1 Denture Repair

In the case of *denture fracture*, the fractured pieces can usually be easily approximated because brittle failure has occurred. Then, if the (properly cleansed) pieces cannot be realigned, that is, permanent deformation has taken place, it is vital to carefully check the adaptation of the denture to soft tissues. If the cause of breakage is not corrected (e.g., fit and/or faulty occlusion) repairs usually will fail, and this is regardless of which repair material was used [9–11, 39]. *Acrylic repair materials* are commonly the powder-liquid type, similar to those used for denture bases [9]. They are either chemically accelerated to set or heat-accelerated to set. Light-activated and microwave-cured acrylics are fast and effective repair materials. The actual *material of choice* will depend on certain factors, such as (a) the length of the time required for making the repair, (b) the flexural strength obtainable with the repair material, and (c) the degree to which dimensional accuracy is maintained during repair [9, 12, 29, 39].

One technique for making a repair requires holding, or luting, the broken (and cleansed from grease, oil, saliva, blood, etc.) pieces together with *sticky wax*, then pouring a stone model on the inside of the denture, and then investing the model and denture in a flask. Then, the wax is removed and the fracture line is opened with a bur [9, 28]. This is to allow a reasonable amount or repair acrylic to enter. The ground surfaces are painted with a monomer or a 4:1 mixture of a monomer and a polymer. Acrylic dough is then packed into the

area being repaired, and the material is cured, cooled, deflasked, and finished. If a heat-cure acrylic is used, the denture should be completely flasked, and curing of the repair material preferably should be carried out at temperatures not exceeding 74°C–77°C for eight hours or longer [9, 29].

3.7.2 Denture Rebasing

Rebasing a denture refers to a technique in which occlusal relations of the teeth are maintained and the entire denture base is replaced. In general, this technique is as costly and time consuming as fabricating a completely new denture. The method is sometimes used when there are many discrepancies in the adaptation of the denture-bearing area to the oral mucosa that cannot be resolved with the *reline.* Another reason may be that the denture is relatively new [9–14, 29, 39].

Soft or plasticized acrylic, vinyl polymers, and copolymers (as well as natural and silicone rubber products) are used as *denture liners* for patients with irritation of the denture-bearing mucosa, areas of severe undercuts, or congenital or acquired defects of the palate. Some of the liner materials are designed to be cured in situ, and others are designed for dental laboratory processing.

It has been reported that some products have an inhibitory effect on the growth of *Candida albicans*. Conventional mouth-cured soft liners are used to improve the comfort and retention of dentures that are used as interim prostheses. After several weeks they may begin to foul—and debond from the denture [9, 26, 29]. They are mixed chairside, added to the impression surface of the denture, and seated inside the patient's mouth until they polymerized, which generally takes a few minutes.

Actually, there are *three types* of denture-rebasing materials:

(a) Addition silicone elastomers
(b) Powder (poly[ethyl methacrylate] and peroxide initiator) + liquid (aromatic esters, ethanol, tertiary amines)
(c) Powder (poly[ethyl methacrylate], plasticizers such as ethyl glycolate, and a peroxide initiator) + liquid (MMA and tertiary amines)

It is noteworthy that both tissue conditioners and chairside soft liners may *leach out significant amounts* of alcohol and phthalate esters [9, 26, 28].

3.7.3 Tissue-Conditioning Liners

Tissue-conditioning liners are soft elastomers that are used to treat an irritated mucosa supporting a denture. These materials will conform to the anatomy of the residual ridge, gel in that position, and continue to flow slowly after application. Tissue-conditioning liners are used to provide time for healing of the soft tissues or as a diagnostic tool to assess the patient's tolerance of new occlusal schemes or the occlusal vertical dimension. Tissue-conditioning liners are mixed chairside, placed in the denture, and seated in the patient's mouth. Tissue-conditioning liners should be replaced every three to five days because they are indicated only for short-term use [9–14, 26, 29, 39].

3.7.4 Orthopedics: Bone Cements

It is useful to know that in *orthopedics,* acrylic bone cements are used to fix a hip joint prosthesis to femoral bone. A typical current bone cement comprises a liquid component (typically predominantly MMA) and a powder component, PMMA. Due to certain shortcomings, such the released heat during the setting reaction, some promising bone cement modifications are currently under active research [40].

3.8 Resin Composites

In dentistry the term *composite* is usually used to describe dental resin-based composite restorative materials. On the other hand, on the basis of the *definition*, dental silver amalgam is also a composite material.

Generally speaking, *composite materials* are a range of structural materials that, compared to the previously manufactured materials, are generally lighter, stiffer, and stronger. As *natural composite materials*, we may mention wood (a composite consisting of cellulose and lignin), bone (made of soft protein collagens combined with

hard, brittle Ca-hydroxyapatite mineral), muscles, and, of course, enamel, dentin, and cementum [1, 3, 12, 14].

Resin composites (filled resins) in dentistry consist usually of five structural components:

(a) An organic resin matrix (a blend of monomers, dimers, etc.)
(b) Inorganic fillers
(c) An activator-inhibitor system
(d) Pigments
(e) A silane coupling agent

The plastic resin forms the *matrix* of the resin composite (aka filled resin) material, and at the same time it binds the inorganic filler particles. The inorganic fillers are reinforcing pebble-like particles that are scattered in the matrix. These inorganic fillers are bonded to the matrix by the third component, the *silane coupling agent*, which functions to promote adhesion between the resin matrix and the fillers. The resin matrix is actually the active component of the dental composite restoration, and it is a fluid monomer that can be transformed to a rigid polymer by an addition reaction. The resin matrix in the mainstream of dental composites is typically based on bis-GMA or urethane dimethacrylate (UEDMA). These are high-molecular-weight liquid monomers of high viscosity. Bis-GMA is derived from a reaction between bisphenol A and glycidylmethacrylate [26, 41].

Low-viscosity resins such as triethylene glycol dimethacrylate (TEGDMA), dodecanidiol dimethacrylate (DDDMA), and polycarbonate dimethacrylate (PCDMA) are used to lower viscosity and improve the cross-linking density of composites and sealant materials. Other ingredients of the matrix are an activating agent for light or chemical curing and stabilizers for shelf life and pigments of esthetics. Recently, the use of ethoxylated bisphenol A dimethacrylate (EPPADMA), which is a monomer of low water sorption, as a partial or complete substitute to bis-GMA, has further improved the water sorption characteristics of dental composites [9–14, 39, 41]—resin composites are discussed in details in Chapter 6.

Inorganic fillers are incorporated into the resin matrix to strengthen the resin matrix by improving mechanical properties like hardness and compressive strength (Fig. 3.22). These fillers can also help in the reduction of polymerization shrinkage of the matrix

because these fillers are not involved in the polymerization process, so the more are the fillers in the matrix, the less is the polymerization shrinkage. Ceramic inorganic fillers have a coefficient of thermal expansion similar to that of the tooth structure, so their use helps in reducing the thermal expansion of the methacrylate matrix, which has a very high coefficient of thermal expansion (~ 80 ppm/°C). Inorganic fillers help also in reducing water sorption by the matrix. In addition, fillers affect handling characteristics and may impart radiopacity, that is, X-ray contrast (e.g., Ba-based fillers) [9–14, 39, 41]. Fiber-reinforced composites (FRCs) [42, 43], a new promising group of dental biomaterials, are discussed in Chapter 7.

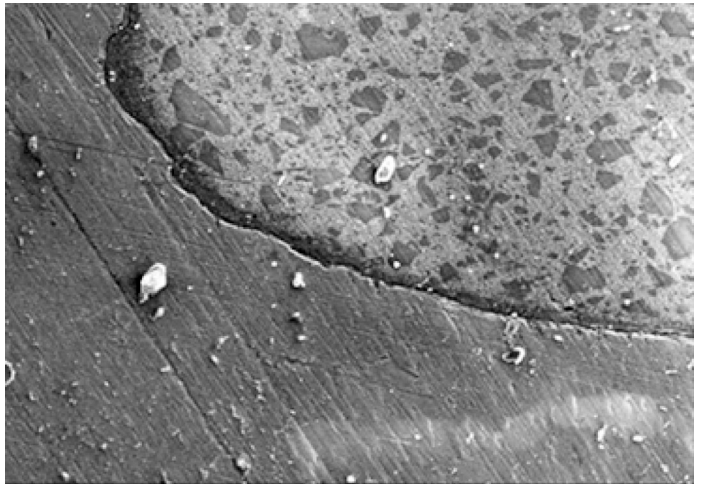

Figure 3.22 Inorganic fillers in a dental resin composite filling material.

As a fact, a resin matrix is *hydrophobic,* whereas, on the other hand, silica-based fillers are *hydrophilic* because of the surface hydroxyl groups. This means that there is no affinity between the matrix phase and the inorganic filler phase. This lack of affinity indicates the use of a silane coupling agent [41] between the two phases [10, 14, 41].

A bond between the filler particles and the matrix is achieved by the use of so-called *coupling agents* [44]. Bonding is obtained by treating the surface of the fillers before mixing them with the oligomer matrix. The most commonly used silane coupling agent is 3-methacryloxypropyltrimethoxysilane (MPTS, MPS, ϒ-MPS, or

3-MPS). Other examples of organosilanes are 3-acryloxypropyltrimethoxysilane, 3-isocyanatopropyltriethoxysilane, and styrylethyltrimethoxysilane (Fig. 3.23).

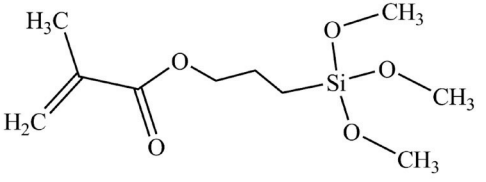

3-Methacryloxypropyltrimethoxysilane

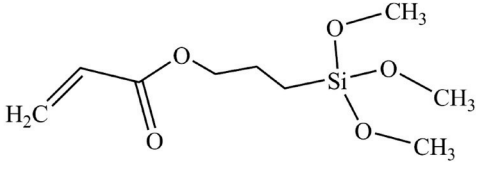

3-Acryloxypropyltrimethoxysilane

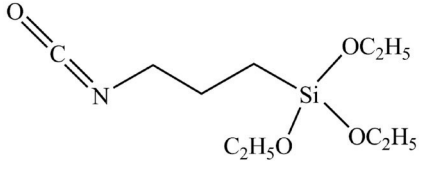

3-Isocyanatopropyltriethoxysilane

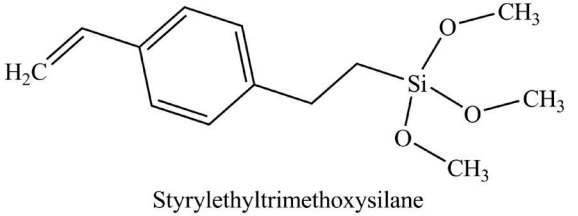

Styrylethyltrimethoxysilane

Figure 3.23 Various silane monomers, which are also called and used as silane coupling agents [44].

The silane coupling agent molecule contains (usually) one silicon atom (Si) in the centre and an organo functional group (R), for example, vinyl, amino, epoxy, and functional hydrolysable groups (X), for example, methoxy, ethoxy, etc. The functional group R will bond with an organic resin material, while the functional group X will attach to an inorganic material [26, 41, 44]. By this, the coupling effect can be attained (Fig. 3.24).

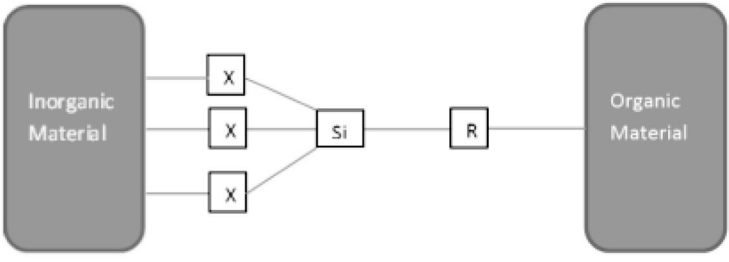

Figure 3.24 The silane molecule can contain one silicon (Si) atom in the centre and an organofunctional group (R), for example, vinyl, amino, or epoxy, and a functional hydrolyzable group (X), for example, methoxy. The functional group R will bond with an organic resin material, while the functional group X will attach to an inorganic material [44].

Silanes form a large group of synthetic organic compounds that essentially contain a silicon (Si) atom or atoms. Silanes bear a resemblance to orthoesters, and they can be bifunctional, that is, they have dual reactivity. The organic functional part, for example, vinyl ($CH{=}CH_2$), allyl ($-CH_2CH{=}CH_2$), amino ($-NH_2$), or isocyanato ($-N{=}C{=}O$) (Fig. 3.23), can polymerize with an organic matrix. The alkoxy groups (e.g., methoxy $-O-CH_3$, ethoxy $-O-CH_2CH_3$) can react with an inorganic substrate, in both cases forming covalent bonds between the matrices [33, 41, 43].

Generally, silanes may or may not contain reactive groups. A reactive group can also be, for example, chloride (–Cl). There is usually a *propylene link* ($-CH_2CH_2CH_2-$) between Si and the organic functionality, especially when the silane is used for, for example, metal pretreatment [44], as discussed in detail in Chapter 11.

To be able to act as coupling agents in the interface between organic-inorganic substances, silanes must first be hydrolyzed

(activated) and condensed. In an aqueous solution, their alkoxy groups react with water to form reactive, hydrophilic, acidic silanol groups, Si–OH, and release alcohol as side products [45].

Flowable resin composites are modified hybrid composites characterized by low viscosity, reduced filler amount, and narrower particle size distribution. These characteristics enable the material matrix to flow easily around the prepared cavity. This flowable consistency makes these materials difficult to handle easily. They have more polymerization shrinkage and lower wear resistance than the other types because of the reduced amount of inorganic fillers. They are more suitable for cervical lesions, non-stress-bearing restorations, and very small cavities [9–13, 39, 41]—read more in Chapter 6.

Laboratory resin composites find application in lab processing for indirect restorations, that is, crowns, inlays, and veneers (laminates) bonded to metal copings. They can be reinforced by fibers [42] and usually bonded with a resin composite cement.

Packable resin composites are characterized by very high viscosity and a low surface thickness. They are used for posterior restorations because of their good mechanical properties and high filler content. They have low polymerization shrinkage, low wear rate, and high light-curing depth [9–15, 41].

Provisional resin composites are mainly used on temporary bases such as an immediate chairside temporary crown after tooth preparation [41].

3.9 Adhesion and Bonding

3.9.1 Atomic Bonds

The basic understanding of the behavior of dental materials is based on their states, phases, and, hence, atomic structure. Properties of materials are dependent on the atomic arrangement. *Interatomic forces* are forces that hold atoms together, and these are classified as primary or secondary bonding.

The structure of materials is determined by the arrangement of their atoms and molecules.

The phases of matter are solid, liquid, gas, and plasma.

Primary bonds are strong bonds, and they are of *three types*: (a) ionic, (b) covalent, and (c) metallic. The bond energy in primary bonds is much higher than that in secondary bonds [12].

A *covalent bond* is characterized by sharing pairs of electrons between atoms. It is stable and considered as the simplest and strongest bond, such as the Si–O bond in porcelain. *Ionic bonds* are formed between the mutual attractions of two oppositely charged ions. An example of an ionic bond is the bond that exists in the crystalline phase of gypsum. A *metallic bond* is formed when there is a large aggregate of atoms. The outer shell of electrons of most metals is characterized by being less than half full. In metals each atom donates one or more electrons to be shared as a *cloud* of mobile electrons. This property explains, for example, why metals are opaque and reflect light [9, 10, 12, 46].

The fact that metal ions are held together is based on their mutual attraction to the electron cloud. These electrons are shared in common by all the metal atoms, which have become positively charged ions as a result of giving up electrons.

In **solid matter** the molecules are very close together and cannot move around easily and are only limited to a local vibration as there is great resistance to movement by molecules.

In **liquids**, the molecules are close together and move around slowly. Their resistance to movement is considerably less than that of solids. Liquid molecules are able to move around each other.

In **gases**, the molecules are widely separated. They move around freely at high speeds depending on the temperature.

Plasma is a state of gas where it is (partially) ionized.

3.9.2 Adhesion and Cohesion

In general, when two substances are brought into intimate contact with each other, the molecules of one substance may adhere to the molecules of the other. *Adhesion* is the physical attraction of dissimilar molecules to remain in close proximity. It can be described as bonding of unlike materials by physical attraction between their atoms or molecules. The material that is used to attach two surfaces (substrates) together producing the interface is called an *adhesive*,

while the initial substrate is known as an *adherend. Cohesion* is the attraction of similar molecules of the same material [10–12, 46].

Adhesion can be defined as *the strength of the interface of two dissimilar materials*. Two dissimilar materials that are held together by intimate interfacial contact can allow work to be transferred across the interface. The interfacial forces holding the two phases together may arise from weak *van der Waals forces*, chemical bonding, or electrostatic attraction [47]. This enables a way to distribute stresses more uniformly across a greater area. By accommodating the differences in the thermal expansion coefficients of the adherends, *adhesives* essentially play an important role in situations where temperature variations are encountered. *Sealing* is also another important function of adhesives [9–14, 46].

Mechanical interlocking (retention), electrostatic, diffusion, and adsorption/surface reaction are theories that have been proposed to describe mechanisms of adhesion [47]. However, it is difficult to fully ascribe the adhesive bonding to an individual mechanism and usually a *combination of different mechanisms* is responsible for bonding. The extent each mechanism may vary for different adhesive systems. Hence, the scale of action is shown in Table 3.2.

Table 3.2 Current adhesion theories

Mechanism	Scale of action
Mechanical interlocking	Microscopic
Electrostatic	Macroscopic
Diffusion	Molecular
Wettability	Molecular
Chemical bonding	Atomic
Weak boundary layer	Molecular

Mechanical interlocking (macro- or microretention) of the adhesive is achieved in the presence of surface irregularities. The ability of the adhesive to readily penetrate the irregularities is governed by the viscosity of the adhesive, the wettability of the substrate by the adhesive, the morphology of the substrate, and the setting time of the adhesive [9–12].

The enhanced adhesion after *surface roughening* can be due the formation of a clean surface, the formation of a highly reactive surface, and an increase in the contact surface area. However, it is debatable whether mechanical interlocking is responsible for strong bonds or the other mechanisms associated with the increase in the adhesive contact area. For example, increased wetting and chemical bonding can be expected as a consequence of increased contact area (cf Chapter 11).

3.9.3 Factors and Mechanisms of Adhesion

Wettability is a measure of the affinity of a liquid for a solid, as indicated by the spreading of a drop. It indicates the ability of a liquid adhesive to contact a substrate. *Cohesive forces* within the liquid cause the drop to develop a sphere and avoid contact with the surface. The *contact angle* (θ) represents a quantitative method to evaluate the capability of liquid adhesives to wet a substrate surface. The contact angle is the angle formed by the adhesive with the substrate (adherend) at their interface. The contact angle is used to determine the ability of any adhesive to wet the surface of an adherend. The tendency for a liquid to spread on a substrate increases as the contact angle decreases [48, 49]. Low values of contact angle indicate high wettability, while high values of contact angle indicate low wettability. For an adhesive to readily wet a solid substrate surface, the adhesive requires a surface tension lower than the critical surface tension of the substrate surface. Good wetting allows the adhesive to flow into cracks and crevices on the substrate surface. Poor wetting results in bridging over the crack. This can potentially lower the overall strength of bond as the actual contact area is reduced [12, 47–49].

Viscosity is the resistance of a liquid against external forces that have a tendency to cause this liquid to flow. Adhesive materials with higher viscosity have more resistance to flow under force, which will lead to less possibility of this adhesive to spread out on the substrate surface.

Surface morphology is an important factor in adhesion. Wetting a solid surface with an adhesive material brings the material into intimate contact with that surface. Here, both the initial substrate (adherend) and the adherent should be flawless and smooth. By

this, the prospective area for bonding is increased. In fact, surface smoothness for the naked eye may be very rough if seen under the microscope. Using adhesive materials with high viscosity and poor wettability on rough surfaces (even microscopically rough) can cause entrapment of air, causing void formation, which then may cause deficiency in adhesion effectiveness [9–14]. The formation of these voids will ensure the prevention of adhesive materials from flowing smoothly into the crevices and irregularities to achieve full wetting of the surface by the adhesive material (see Figs. 3.25 and 3.26).

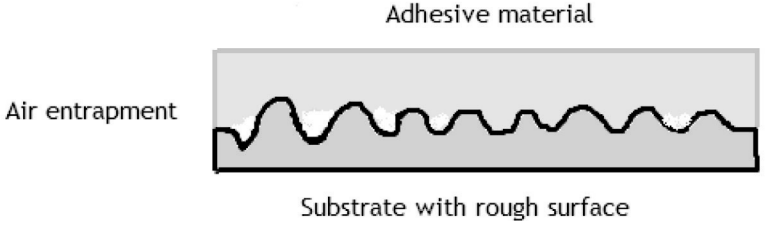

Figure 3.25 Void formation as a result of using a viscous bonding agent.

Two mechanisms of adhesion exist, (a) mechanical adhesion and (b) chemical adhesion. *Mechanical adhesion* is depending on mechanical interlocking surface irregularities and/or penetration of one material into another material. *Chemical adhesion* involves bonding at the atomic or molecular level. In many situations in adhesive dentistry, mechanical and chemical adhesions take place together. A dental composite is bonded to dentine by first etching the dentine surface with orthophosphoric acid (37%), and then a bonding agent is applied to penetrate the opened dentinal tubuli, providing an interlocking mechanism of adhesion[12, 46–50] (see also Chapter 1).

3.10 Basic Properties of Dental Materials

3.10.1 Biomechanical Properties

We make here a brief overview—*biomechanical properties* [9–12, 15, 34, 39, 51–53] are discussed further in Chapter 4.

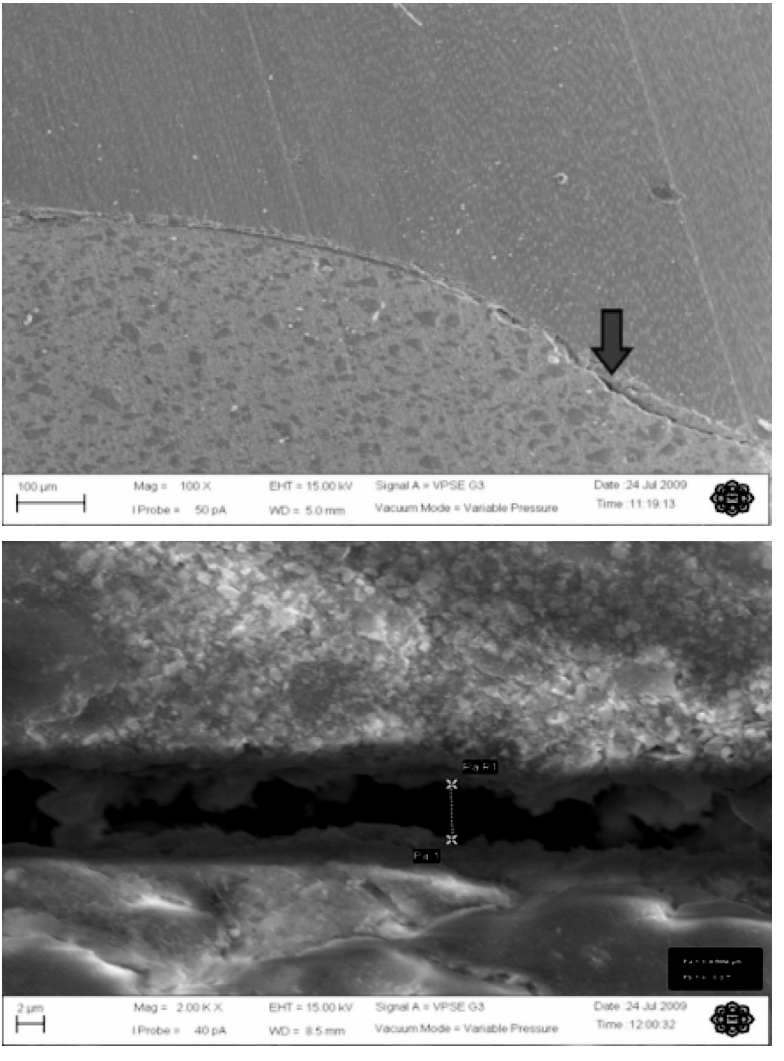

Figure 3.26 SEM image showing the formation of voids between a resin composite and dentin. *Abbreviation*: SEM, scanning electron microscope.

Stress and strain: Force is any effect that can cause any object either to move or to deform. Stress is the force per unit area, whereas strain is the dimensional change in objects caused by stress. When a force is applied on any material object, this material develops an

internal resistance, which is equal in magnitude to the applied force and opposite in direction.

Compressive force (compression) causes the material to decrease in length along the direction of the applied force. The property of any material to resist a compressive force is known as compressive strength of that particular material.

Tensile force (tension) is any force that results in an increase in length (elongation) along the direction of the applied force.

Tensile strength is the property of any material to resist stretching apart by the effect of tensile forces (tension). Application of compression and tension on material objects could be unilateral or bilateral. The tensile strength test is used to measure the elasticity and plasticity behaviors of materials. The compressive strength test is used mainly to measure the ability of dental materials to withstand occlusal forces.

Shear is any force that causes a sliding displacement of one side of a structure compared to the other side, and the ability of any material to resist shear force is known as shear strength [9–14].

Proportional limit is the limit of proportionality of stress to strain. It is labeled on the stress–strain curve when stress ceases to be linear. Beyond the proportional limit, the material starts to deform permanently.

Yield strength is exactly the point coming beyond the proportional limit. It is the point of the first noticeable deviation from proportionality of stress to strain on the stress–strain curve. After the proportional limit a little additional stress is enough to cause permanent deformation in the material, which is represented by yield point.

Ultimate tensile strength is the maximum amount of stress that a material can tolerate without suffering fracture or rupture. So it is exactly below the fracture point on a material. It can be applied to compressive, tensile, or shear stresses.

Fracture strength is the amount of stress required to produce material fracture or rupture.

Ductility is the amount of deformation that a material (metals, alloys) under tensile stress can withstand before fracture or rupture. It is presented in terms of percentage elongation.

Malleability is the amount of deformation that a material (most metals and alloys) under compressive strength can withstand

before fracture or rupture. It is presented in terms of percentage compression.

Brittleness is the characteristic of any material to fracture without noticeable plastic deformation. Brittle materials (such as porcelain, ceramics) have low ductility on which their ultimate strength is the same as their elastic limit.

Fatigue refers to the fact that when materials are subjected to cyclic loading, they will undergo failure below the ultimate tensile strength than they normally would if they were not under cyclic loading. Subjecting any material to repeated stress causes tiny cracks to be generated in the material structure.

Impact strength is quoted in units of energy, and it is the resistance of any material to the sudden application of force.

Resilience is the inherent property of any material (several polymers) to resist permanent deformation. It is represented under the area of elastic limit in the stress–strain curve.

Toughness is the inherent property of any material to resist fracture. It is represented by both elastic and plastic areas of the stress–strain curve.

Fracture toughness is the inherent property of any material to resist the propagation of an existing crack or flaw.

Hardness is the resistance to permanent indentation on a material surface. There are several tests to measure the hardness of various dental materials, such as the Brinell, Vickers, Knoop, and Rockwell tests [11–15, 39, 51–53].

3.10.2 Hardness Tests

The *Brinell hardness test* employs a hardened steel ball that is applied under a certain load to the material being tested to form a round, permanent dent on the surface (must be flat) of the test material. The Brinell hardness number (BHN) value is the measure of the diameter of the dent. This test is highly applicable to ductile materials.

The *Vickers hardness test* employs a pyramid-shaped diamond indenting tool with a square base that applies a constant load to the material being tested. The Vickers hardness number (VHN) is obtained by measuring the diagonals of the square-shaped indentation and then taking the average of the two dimensions. The

Vickers hardness test is used mainly for brittle materials but still can be used for ductile materials.

The *Knoop hardness test* employs a diamond-shaped indenting tool with a rhomboidal base. The diamond-shaped indenting tool can also be described as having one diagonal much longer than the other. This test is ideal for testing the hardness of elastomeric materials. The Knoop hardness number (KHN) is obtained by measuring the long diagonal only.

In the *Rockwell hardness test* the indenters used are either diamond cones or steel balls. The main advantages are that it is a quick test, taking only 10–15 seconds. To get the Rockwell hardness value, a minor load is first applied on the surface, followed by the application of a major load. The test essentially measures the distance from the limit line of the minor load indentation to the bottom of the major load indentation [10–14, 51, 54].

3.10.3 Physical Properties

Working time is the time calculated from the start of mixing until the material becomes so thick that it cannot be manipulated any longer. Whereas *setting time* is the time calculated from the start of mixing until the material reaches a specific degree of setting appropriate to its application, but this amount of setting does not indicate the completion of reaction.

Film thickness is the height of the space between two surfaces that are separated by a thin-film layer of a luting cement. The combined thickness of two pieces of glass is usually measured and then measured again after addition of the luting cement with the application of a certain load (before, Fig. 3.27). The film thickness is the difference between the two measurements [9–12, 39, 51].

3.10.4 Thermal and Electrical Properties

We do have also some other properties determining biomaterials [9–14, 39]. *Heat flow* through materials is measured in terms of either the relative rate of heat conduction (*thermal conductivity*) or the amount of heat conduction per unit time (*thermal diffusivity*).

Thermal conductivity (*K*; unit: $W\ m^{-1}\ K^{-1}$) is simply known as the ability of any material to transmit heat or cold. Thermal conductivity

of solid materials can be defined as the rate of heat transferred through a material by conductive flow.

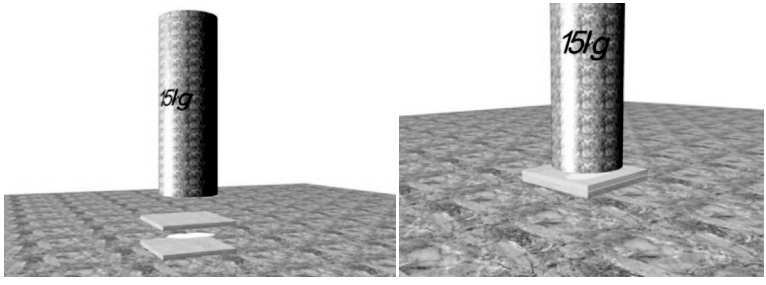

Figure 3.27 The combined thickness of two pieces of glass is usually measured and then measured again after the addition of a luting cement with the application of a certain load.

Coefficient of thermal conductivity (κ) is measured when the temperature difference across a unit cube of material is 1°C. Heat transfer across materials of high thermal conductivity occurs at a higher rate than across materials of low thermal conductivity. *Conductors* are materials with high thermal conductivity, while *insulators* are those materials with low thermal conductivity. Polymers and cements have very low thermal conductivity compared to metals. In general, low thermal conductivity is preferred in restorative materials that are used on teeth, whereas high thermal conductivity is required where the material covers soft tissue.

Specific heat (c) is the heat needed to raise the temperature of 1.00 g of a material by 1°C. The relationship between heat and temperature change is usually expressed in the form $Q = c \times m \times \Delta T$, where Q is heat added, m = mass, and ΔT is the change in temperature.

Thermal diffusivity (Δ; unit: m^2s^{-1}) of any material controls the m^2s^{-1} time rate of temperature change as heat passes through the material. It is measured by calculating the thermal conductivity divided by specific heat multiplied by density.

The volumetric *coefficient of thermal expansion* (α; unit: in 10^{-6}/K) can be measured for all substances of condensed matter (i.e., solid state and liquids). Linear thermal expansion can only be measured in the solid state and is common in engineering applications. During temperature rise, more frequent atomic

motions stretch bonds and produce a net expansion. Given this, during a decrease in temperature, solids undergo contraction. The relative rate of change is called the coefficient of thermal expansion or contraction. If it is referenced to a single dimension, it is called the linear coefficient of thermal expansion. When a restorative material such as amalgam expands more than the tooth, there will be ledge formation at the tooth–filling interface, and this will cause food stagnation and bacterial accumulation. If the same filling contracts more than the tooth, there will be underfilling, causing gap formation, which will lead to microleakage.

Electric resistivity (ρ; unit: Ω m) and *conductivity* (σ; unit: S m^{-1}): The property of any material to conduct an electric current is known as either specific conductivity or, conversely, specific resistivity. Dentin has lower resistivity than enamel, and also sound and carious enamel differ in resistivity [9–14].

3.10.5 Rheological Properties

Rheology is the study of the flow or deformation of materials. Rheology is applicable to liquids as well as solids. Rheological properties have great influence on the handling characteristics of dental materials. *Viscosity* (η; unit: Pa s *or* kg s^{-1} m^{-1}) is a specific property of fluids when a liquid is resistant to flow. The value of viscosity is temperature dependent in such a way that any rise in temperature causes a significant decrease in viscosity.

Thixotropic liquid is any viscous liquid that becomes less viscous under the application of repeated pressure like shaking, stirring, patting, or vibration.

Viscoelastic material combines both elastic and viscous behavior. Elastic impression materials have viscoelastic behavior; conversely, metals and brittle cements have very low viscoelastic properties. Viscoelasticity is highly influenced by the type and rate of load applied, for instance, a putty siloxane impression material does not exhibit any viscosity unless there is a load to be applied so as to cause the putty to flow. This load is important to differentiate between elastic and viscoelastic materials.

Elastic materials have mechanical properties independent of loading rate, whereas viscoelastic materials have mechanical properties dependent on loading rate [9–14, 39].

3.10.6 Chemical Properties

Solubility and disintegration of dental cements can be measured by immersing two disks (20 mm in diameter and 0.1 mm in thickness) in water for more than 24 hours at 37°C. Solubility of materials inside the oral cavity is very important for applied dental materials as some types of dental cements may have high solubility and henceforth they cannot be used as luting agents for a definitive crown treatment but can be applied only on temporary bases. Generally, *brittle dental cements* lack strong consistency (they are weak in tension), and therefore they are more susceptible to be soluble in oral cavity. *Sorption* is simply known as the uptake of fluids by materials.

A very common example in dental technology is the *discoloration of porcelain* because of sorption between metal and the porcelain interface on PFM restoration. In addition, water sorption into *polymers* causes the water to diffuse into the structure of polymers, for example, the diffusion of water into the acrylic denture base for a certain period of time can cause warp of the denture base. This water sorption of a material can be explained in two stages: first the water is adsorbed onto the surface of the material, and second it is absorbed deep into the body of the material. During the second phase it may diffuse into the structure of this material, causing dimensional changes that may lead to material defect. This is especially true if the sorption occurs during manipulation and before the final setting of the material.

Tarnish is the surface reaction of metals in the mouth, with components from food or saliva forming a thin, dull film on these surfaces without attacking the metal itself. Tarnish involving this dull film consists of hard and soft deposits such as chlorides and sulfides. Tarnish can be removed easily by polishing metal surfaces.

In contrast, *corrosion* is the attack on the metal surface that involves the loss of material. It is described as dissolution of metals in the oral cavity. In metals, the corrosion process is normally *electrochemical* as it involves the loss of electrons by an oxidation reaction with the metal becoming a positively charged ion. Corrosion can be a consequence of galvanic action, where the metal restoration is in contact with another restoration of different metal. In the oral cavity, this occurs in the presence of saliva and results in the formation of surface roughening and pitting [9–14, 39].

NB: We preferably should say that metals and alloys *corrode*, but glasses and polymers and resin composites *degrade* (leading to *degradation*).

3.10.7 Kinetics and Thermodynamics

The *surface* is an extremely important factor influencing corrosion, because the surface composition is almost always different from that of the bulk metal/alloy [14, 55, 56]. *Rust*, FeO(OH), layered on iron usually grows to be much thicker and so is not considered passivation. This is because this mixed (and usually brittle) oxidized layer is not protective. This effect is in some sense a property of the material, and it serves as an indirect *kinetic* barrier: the reaction is often quite rapid unless and until an impermeable layer forms [9, 12, 39].

> *Thermodynamics* = a set of laws relating to the paths and driving forces of processes in terms of the energy changes occurring in a system [12]
>
> *Kinetics* = the time-dependent behavior of a system with regard to the rates of chemical reactions [12]

Given the right conditions, a thin passive film of corrosion products can form on a metal's surface, preventing further corrosion (Al, Ti, Cr). The effect of pH on corrosion is essential, but many other factors are influential. Some conditions that inhibit passivation include low pH or the presence of chloride ions for stainless steel and high temperature for Ti (in which case the oxide dissolves into the metal). Exposure to a hot solder or to a liquid metal (Hg) can often circumvent passivation mechanisms. The materials that are most resistant to corrosion are those for which corrosion is *thermodynamically* unfavorable.

Some metals (Mg, Zn and Cd) have naturally slow reaction kinetics, even though their corrosion is thermodynamically favorable. This means that corrosion of Mg, Zn, and Cd is continuous and it happens at a slow rate [10–12, 57, 58].

The four laws of thermodynamics:

0. If two systems are in thermal equilibrium with a third system, they are also in thermal equilibrium with each other.
1. Energy is conserved: heat and work are interconvertible.

2. Heat may not be transferred from a cooler body to a hotter body without some effect elsewhere.
3. The absolute zero (0 K = –273.15°C) of temperature is unattainable.

3.10.8 Biocompatibility

Biocompatibility of dental materials (see Chapter 5) is a very crucial factor to be considered before the introduction of any new material. Dental materials should be successful enough to be used inside the oral cavity, while causing no or minimal response.

3.11 Dental Silver Amalgams

Dental amalgams were introduced in the beginning of this chapter. Dental silver amalgam is one of the most commonly used restorative filling materials. It has served as a convenient and durable direct restorative material for more than 160 years. An amalgam generally is an *alloy of mercury* with other metals. In dental practice, mercury and a silver-based alloy are mixed into a paste, which then sets hard. Amalgam fillings have been used extensively for a long time. They have many advantages, including low cost and high durability. For a vast majority of people they are likely to be completely safe.

Yet, the type of mercury released from amalgam fillings is toxic when sufficient exposure occurs. While exposure appears to be very low, minimal safe levels have not been established. Although amalgams have not been proven to be safe, they have not been proven to cause disease either. On the other hand, amalgams and lichen planus are heavily interrelated. Amalgam is a *composite material.* A composite material, in general, is a combination of two (or more) materials, often designed to replicate naturally occurring materials [9–15, 39].

Amalgam = an alloy of Hg with any metal

Amalgamation = the process of forming an amalgam

Amalgamator = triturator = a machine for mixing dental silver amalgams

Alloy = the result of a combination of different metallic elements melted together or of metals with nonmetals when the result is metallic

3.11.1 Mercury

Mercury (Hg, hydrargyrum, "liquid silver," quicksilver) is obtained by roasting *cinnabar* mineral (HgS). Mercury is slightly volatile at room temperature, melting point –38.9°C, when pure. It doesn't tarnish on exposure to air at ordinary temperatures, but when heated to its boiling point (356.7°C), Hg slowly oxidizes to HgO. Mercury dissolves to form amalgams with gold, zinc, and many other metals. Because iron is an exception, iron flasks have been traditionally used to trade mercury. Other metals that do not form amalgams with mercury include tantalum (Ta), tungsten (W), and platinum (Pt). When heated, mercury also reacts with oxygen in air to form mercury oxide (HgO), which then can be decomposed by further heating to higher temperatures.

Mercury is a heavy, dense, silvery-white metal. As compared to other metals, it is a poor conductor of heat but a fair conductor of electricity. Hg has an exceptionally low melting point for a *d*-block metal. A complete explanation of this fact requires a deep excursion into quantum physics (which we have to omit, *alas!*). Elemental Hg, a volatile form of the liquid metal, is referred to as Hg(0). Hg is stable in two other oxidation states, Hg^{+} and Hg^{2+}, and is able to form inorganic compounds, such as mercuric chloride ($HgCl_2$) which is a poison, and mercurous chloride, calomel (Hg_2Cl_2), which was used in medicine. Hg is able to form a variety of organic compounds, including *methylmercury*, that is, a *monomethylmercuric cation* [9–14, 36].

Elemental Hg may be converted to soluble inorganic forms, which may be methylated in aquatic systems, especially by microorganisms, leading to formation of methylmercury. Methylmercury may easily enter the food chain and accumulate in the tissues of large predatory fish. Methylmercury exposure in adults has also been linked to increased risk of cardiovascular disease, including myocardial infarction. Methylmercury is readily and completely absorbed by the gastrointestinal tract. It is noteworthy that each form of Hg has its own toxicological profile. The toxicity of these forms is highest with organic mercury compounds, followed by elemental Hg and its inorganic compounds. In individuals, Hg can be detected in human milk, blood, urine, and hair for testing [26, 56, 57].

Hg is inevitably present at low concentrations in human tissues.

It has been concluded that the two major sources of the Hg body burden include:

(a) dietary intake of methylmercury, and
(b) intake of elemental mercury from dental amalgams.

3.11.2 About the Use of Dental Amalgams

The current situation is that the use of an amalgam as a dental filling material is expected to decrease, at least in the Western countries. It has been banned in some Scandinavian countries. Some of the proposed reasons to abandon amalgam are:

(a) concern about environmental Hg pollution;
(b) improvement and development of various tooth-colored filling materials; and
(c) the nonesthetic, dark appearance of amalgam.

Moreover, when cavities need to be filled, the preparation of a cavity for an amalgam filling often means loss of healthier tooth substance (which is rather invasive) than if resin composite or GIC were to be used instead. There is still a reason to abandon amalgams, at least in the U.S. and Sweden, perhaps surprisingly, a decreased caries frequency.

The main types of *amalgam failure* are marginal breakdown and fracture, and other deficiencies to be mentioned are *tarnish, corrosion, marginal leakage*, etc. In general, a dental amalgam is weak in tension, as a result of the low tensile strengths of the reaction products, as well as the presence of porosity. The *strength of an amalgam* of a given brand and type is dependent mainly upon manipulation and mixing procedures. When an amalgam restoration is of poor quality, for example, due to the presence of porosity, it can be mainly attributed to improper handling procedures. The speed of amalgam handling before it sets, the mixing time, and the pressure used in condensation are critical to mechanical strength [9–14, 39].

About *toxicity* we should know and bear in mind that mercury readily absorbs via the respiratory tract (in the form of free Hg and dust), intact skin, and gastrointestinal tract. *Acute exposure* to soluble Hg salts may violently corrode skin and mucous membranes and cause severe nausea, abdominal pain, vomiting, and bloody diarrhea. *Chronic exposure* may lead to inflammation of the mouth and gums, excessive salivation, loosening of teeth, kidney damage, muscle tremors, personality changes, depression, and irritability [26, 59, 60].

The Hg body burden of dental personnel is normally higher than in the general population. In its noteworthy that exposure to Hg is cumbersome to measure, and it is normally obtained by measuring Hg levels in the blood and urine of individuals. Data dealing with blood and urine mercury is considered relevant as it reflects actual exposure. It has been reported that the mean urine Hg levels in dental teams range between 3 μg/L and 22 μg/L, when the normal range is 1–5 μg/L. This increased body burden is attributed to dental personnel mixing and applying dental amalgams and *removing amalgam restorations*. Indeed, most dental chairside team personnel do not touch dental amalgams during mixing and placement [9–14, 39, 59, 60].

It is considered that the main sources of Hg exposure are *aerosols*, created in the immediate working environment during, in particular, the *removal of restorations of dental amalgam*, and exhaust air from dental vacuum systems.

3.11.3 Some Amalgam Chemistry and Physics

What happens with amalgam capsules, and what do they contain:

(1) Liquid mercury
(2) Alloy

} An amalgamator to mix and produce a pliable mass

As for amalgam types, we have a conventional (low-copper) amalgam, and its setting proceeds as [12]:

$$Ag_3Sn\ (\gamma) + Hg \rightarrow \underbrace{Ag_2Hg_3\ (\gamma_1)}_{\text{= Amalgam matrix}} + Sn_{7-8}Hg\ (\gamma_2) + Ag_3Sn\ (\gamma) \quad (3.20)$$

Mercury is a limiting reactant. Theoretically, the set amalgam is free of Hg. If free Hg exists, then the resultant amalgam would be unsafe, rather weak, and unserviceable. Cu is often added in a small amounts (0–6%) to increase strength and hardness of the amalgam. Zinc (Zn) is presented in small amounts as a result of initial production of the Ag-Sn alloy. Up to 2% of Zn may be added to scavenge the oxygen and sulfur content in the alloy. In principle, Zn may also react with water in saliva and induce pores in the matrix [9, 10, 12]:

$$Zn + 2H_2O \rightarrow Zn(OH)_2 + H_2 \quad (3.21)$$

If hydrogen gas is produced inside amalgam, it may result in delayed expansion of the amalgam. Thus, it makes the amalgam mixture more ductile and easy to handle. Nevertheless, the gas produced at the margins would induce pores and thus destroy the marginal stability.

Υ_2 alloys have some problems because they are:

(i) weak in tensile strength → this lowers the amalgam tensile strength.

(ii) more electropositive (i.e., they have the ability to donate electrons) → they act as an anode → this leads to corrosion:

$$Sn_{7-8}Hg + \text{Oxygen (from oral environment)} \rightarrow \text{Sn oxides} + Hg \quad (3.22)$$

This is why so-called high-copper amalgams were developed, by adding Cu or its alloy, to reduce the content of Υ_2 [9, 12, 39].

In the case of admixed Cu, eutectic Ag-Cu particles are included:

$$Sn_{7-8}Hg\ (\gamma_2) + \text{Ag-Cu} \rightarrow Cu_6Sn_5\ (\eta') + Ag_2Hg_3\ (\gamma_1) \quad (3.23)$$

Ag-Cu is not a single compound, but it is actually a two-phase alloy. The phase Cu_6Sn_5 is less corrosive; also the crystals act as small pins that hinder the Υ_1, that is, Ag_2Hg_3, grains to slip when the material is loaded, thus reducing the creep of the high-copper amalgam [12].

A unicompositional Cu-based amalgam is an alloy composed of Ag-Sn-Cu and is used to allow it to react with Hg:

$$Ag_3Sn\ (\gamma)\text{-}Cu_3Sn\ (\varepsilon) + Hg \rightarrow Ag_2Hg_3\ (\gamma_1) + Cu_6Sn_5\ (\eta') + Ag_3Sn\ (\gamma)\text{-}Cu_3Sn\ (\varepsilon) \quad (3.24)$$

Initially, Hg would react with the Υ-phase Ag_3Sn and then forms Υ_1 and Υ_2 solid species. Then, solid Cu_3Sn would react with Υ_2, that is, $Sn_{7-8}Hg$:

$$Sn_{7-8}Hg\ (\gamma_2) + Cu_3Sn\ (\varepsilon) \rightarrow Cu_6Sn_5\ (\eta') + Hg \quad (3.25)$$

This is a very slow process due to the solid-state nature. The product Hg would then immediately react with the remaining Υ-phase Ag_3Sn. The higher the copper content (>25%), the lower the amount of Ag; thus the amalgam type may have a higher possibility for free Hg remaining after setting [9–14].

3.11.4 A Summary on Amalgams: Disadvantages and Advantages

The reported disadvantageous aspects of dental silver amalgams include [9–14, 39, 59, 60]:

- Some destruction of sound tooth tissue (i.e., not minimally invasive)
- Poor esthetic qualities
- Long-term corrosion at the tooth–restoration interface, resulting in "ditching," leading to replacement
- Existence of galvanic response potential
- Local allergic potential and predisposition to oral disease
- Concern about possible mercury toxicity
- Marginal breakdowns

Given this, the reported advantageous aspects of dental silver amalgams include the following attributes [9–14, 39, 59, 60]:

- Durability
- Least-sensitive technique of all restorative materials
- Applicability to a broad range of clinical situations
- Newer formulations having greater long-term resistance to surface corrosion
- Good long-term clinical performance
- Ease of manipulation by dentists
- Minimal placement time compared to other materials
- Initially, sealing of the tooth–restoration interface and prevention of bacterial leakage by corrosion products
- One-appointment placement (direct material)
- Long lasting if placed under ideal conditions
- Ability to be repaired at least in some cases
- Economy

3.12 What Is an Ideal Dental Biomaterial?

At the end of this chapter, we may certainly agree and opine that *dental materials* should possess certain criteria to be accepted, validated, and certified for use inside the mouth, and the same applies to *dental biomaterials*. These materials obviously should carry certain ideal properties and features.

We believe the properties of any ideal dental biomaterial should be confined in the following list. Ergo, an ideal dental material should (most of these features next on the list may apply, if not all):

- Be inert
- Be biocompatible
- Be not cytotoxic
- Be not an irritant
- Be dimensionally stable
- Be insoluble in oral fluids
- Be cleanable
- Possess adequate biomechanical properties
- Be easily manipulated by operators
- Be repairable
- Be accepted by patients
- Be with ultimate esthetic properties
- Have adhesion to tissues
- Have long-lasting restoration in the oral cavity
- Have regeneration ability for neighboring tissues (osseointegration)
- Be cost effective
- Have long storage shelf life
- Induce a fast healing process
- Be not carcinogenic or mutagenic

References

1. Park, J. B. (1980) *Biomaterials: An Introduction*, Plenum Press, New York, USA.
2. Hench, L. L., Jones, J. R., Sepulveda, P. (2002) Bioactive materials for tissue engineering scaffolds, in *Future Strategies for Tissue and Organ Replacement*, 3–24 (Ed. Polak, J. M., Hench, L. L., Kemp, P.), Imperial College Press, London.
3. Hench, L. L. (1998) Biomaterials: a forecast for the future, *Biomaterials,* **19**, 1419–1423.
4. Cheung, K. H. (2010) Natural fiber composites in biomedical and bioengineering applications, in *Multifunctional Polymer Nanocomposites*, 283–308 (Ed. Leng, J., Lau, A. K. T.), CRC Press.
5. Cheung, H. Y. M., Lau, M. P., Cardona, K. T., Hui, F. D. (2009) Natural fibre-reinforced composites for bioengineering and environmental engineering applications, *Compos. Part B,* **40,** 655–663.
6. Buddy, D., Ratner, A., Hoffman, S., Schoen, F. J., Lemons, J. (2004) *Biomaterials Science: A Multidisciplinary Endeavour*, 2nd ed., Elsevier, USA.
7. Williams, D. F. (1987) *Definitions in Biomaterials*, Elsevier, Amsterdam, the Netherlands.
8. Anderson, J. M. (2001) Biological responses to materials, *Annu. Rev. Mater. Res.,* **31**, 81–110.
9. Powers, J. M., Sakaguchi, R. L. (2006) *Craig's Restorative Dental Materials*, 12th ed., Mosby, Elsevier.
10. Anusavice, K. J. (2003) *Philips' Science of Dental Materials*, 11th ed., Elsevier.
11. McCabe, J. F., Walls, A. W. G. (2008) *Applied Dental Materials*, 9th ed., Blackwell, Oxford, UK.
12. Darvell, B. W. (2009) *Materials Science for Dentistry*, 9th ed., Woodhead, Cambridge, UK.
13. Von Fraunhofer, J. A. (2010) *Dental Materials at a Glance*, 1st ed., Wiley-Blackwell.
14. Ferracane, J. L. (2001) *Materials in Dentistry: Principles and Applications,* 2nd ed., Lippincott Williams and Wilkins, Philadelphia.
15. van Noort, R. (2007) *Introduction to Dental Materials*, 3rd ed., Mosby Elsevier, Edinburgh.
16. Wilson, A. D. (1974) Alumino-silicate polyacrylic acid and related cements, *Br. Polym. J.,* **6**, 165–179.

17. Wilson, A. D., Kent, B. E., Clinton, D., Miller, R. P. (1972) The formation and microstructure of dental silicate cements, *J. Mater. Sci.,* **7**, 220–238.
18. Lohbauer, U. (2010) Dental glass ionomer cements as permanent filling materials? Properties, limitations and future trends, *Materials,* **3**, 76–96.
19. Fleming, G. J. P., Farooq, A. A., Barralet, J. E. (2003) Influence of powder/liquid mixing ratio on the performance of restorative glass-ionomer dental cement, *Biomaterials,* **24**, 4173–4179.
20. Axelsson, P. (2002) *Preventive Materials Methods and Programmes*, Quintessence, Chicago, IL, USA.
21. Hiremath, S. S. (2011*) Textbook of Preventive and Community Dentistry*, 2nd ed., 424, Elsevier, New Delhi, India.
22. Remington, J. P. (2006) *The Science and Practice of Pharmacy*, 21st ed., Lippincott Williams and Wilkins, Baltimore, MD, USA.
23. Hiiri, A., Ahovuo-Saloranta, A., Nordblad, A., Mäkelä, M. (2010) Pit and fissure sealants versus fluoride varnishes for preventing dental decay in children and adolescents, *Cochrane Database Syst. Rev.*, **17**(3), CD003067.
24. Levy, S. M. (2012) Pit-and-fissure sealants are more effective than fluoride varnish in caries prevention on occlusal surfaces*, J. Evid. Based Dent. Pract.,* **12,** 74–76.
25. ADA Council on Scientific Affairs. (2006) Professionally applied topical fluoride: evidence-based clinical recommendations, *J. Am. Dent. Assoc.,* **137,** 1151–1159.
26. Mallineni, S. K., Nuvvula, S., Matinlinna, J. P., Yiu, C. K. Y., King, N. M. (2013) Biocompatibility of various dental materials of contemporary dentistry: a narrative insight, *J. Invest. Clin. Dent.,* **4**, 9–19.
27. Smith, C., Smith. R. (2009) *Chemistry for Dental Students Volume I Qualitative Analysis and Dental Metallurgy*, 4th ed., John Wiley & Sons, New York, USA.
28. Davis, J. R. (2009) *Handbook of Materials for Medical Devices*, ASM International, USA.
29. Powers, J. M., Wataha, J. C. (2008) *Dental Materials: Properties and manipulation,* 9th ed., Mosby Elsevier, Edinburgh.
30. Schmalz, G., Arenholt-Bindslev, D. (2009) *Biocompatibility of Dental Materials*, Springer, Berlin, Germany.
31. Della Bona, A. (2009) *Bonding to Ceramics: Scientific Evidences for Clinical Dentistry*, Artes Medicas, Sao Paulo.

32. Ho, G. W., Matinlinna, J. P. (2011) Insights on porcelain as a dental material. Part I: ceramic material types in dentistry, *Silicon*, **3**, 109–115.

33. Ho, G. W., Matinlinna, J. P. (2011) Insights on porcelain as a dental material. Part II: chemical surface treatments, *Silicon*, **3**, 117–123.

34. Academy of Prosthodontics. (1995) Glossary of prosthodontics terms, *J. Prosth. Dent.,* **94**, 10–92.

35. Rosenstiel, S. F., Land, M. F., Fujimoto, J. (2006) *Contemporary Fixed Prosthodontics*, 4th ed., Mosby Elsevier, St. Louis, MO, USA.

36. Arkles, B. (1983) Look what you can make out of silicones, *Chemtech,* **13**(5), 542–555.

37. Lung, C. Y. K Matinlinna, J. P. (2013) Silanes for adhesion promotion and surface modification, in *Silanes: Chemistry, Applications and Performance*, 87–109 (Ed. Moriguchi, K., Utagawa, S.), Novapublishers, ISBN 978-1-62257-432-2.

38. Englebienne, P., Van Hoonacker, A., Herst. V. (2005) The place of the bioisosteric sila-substitution in drug design, *Drug Des. Rev. Online,* **2**, 467–483.

39. O'Brien, W. J. (2008) *Dental Materials and Their Selection*, 4th ed., Quintessence, Chicago, IL, USA.

40. Puska, M., Lassila, L., Närhi, T., Yli-Urpo, A., Vallittu, P. (2004) Improvement of mechanical properties of oligomer-modified acrylic bone cement with glass-fibers, *Appl. Compos. Mater.*, **11**, 17–31.

41. Ferracane, J. (2011) Resin composite: state of art, *Dent. Mater.*, **27,** 29–38.

42. Zhang, M., Matinlinna, J. P. (2012) E-glass fiber reinforced composites in dental use, *Silicon*, **4**, 73–78.

43. Zhang, M., Matinlinna, J. P. (2011) The effect of resin matrix composition on mechanical properties of E-glass fiber reinforced composite for dental use, *J. Adhes. Sci. Technol.,* **25**, 2687–2701.

44. Lung, C. Y. K., Matinlinna, J. P. (2012) Aspects of silane coupling agents and surface conditioning in dentistry: an overview, *Dent. Mater.,* **28**, 467–477.

45. Ammar, A. M., Matinlinna, J. P., Choi, A. H., Razak, A. A. A. (2013) Fracture strength and fractographic analysis of zirconia copings treated with four experimental silane primers, *J. Adhes. Sci. Technol.*, **1**, 68–80.

46. Limburg, W. H. (1997) *The Principles of Adhesion*, Stanford University Press, Palo Alto.

47. Ebnesajjad, S. (2008) *Surface Treatment of Materials for Adhesion Bonding,* 2nd ed., William Andrew, USA.
48. Baier, R. E. (1992) Principles of adhesion, *Oper. Dent*., Suppl 5, 1–9.
49. De Gennes, P. G. (1985) Wetting: statics and dynamics, *Rev. Mod. Phys.,* **57**, 827–863.
50. Swift, E. J., Heymann, H. O., Perdigão, J. (1995) Bonding to enamel and dentin: a brief history and state of the art, *Quintess. Int.,* **26,** 95–110.
51. Mustafa, A. (2012) *A Novel Composition for Glass Ionomer Cements,* PhD thesis, Faculty of Engineering, International Islamic University Malaysia, Kuala Lumpur, Malaysia.
52. British Standard 9917 (1994) *Specifications for Compressive Testing Regime for Water-Based Cements.*
53. Ritter, J. E., Bandyopadhyay, N., Jakus, K. (1981) Statistical reproducibility of the dynamic and static fatigue experiments, *Ceram. Bull.,* **60,** 798–806.
54. Fischer-Cripps, A. C. (2011) Nanoindentation testing, in *Nanoindentation. Mechanical Engineering Series,* 3rd ed., Vol. 1, 21–37.
55. Leinfelder, K. F., Lemons, J. E. (1998) *Clinical Restorative Materials and Techniques*, 139–159*,* Lea and Febiger, Philadelphia.
56. American Society for Metals. (1973) *Metallography, Structures and Phase Diagrams. Metals Handbook*, Vol. 8*,* Metals Park, Ohio, USA.
57. Guggenheim, E. A. (1985) *Thermodynamics. An Advanced Treatment for Chemists and Physicists,* 7th ed., North Holland, Amsterdam.
58. Kondepudi D. (2008) *Introduction to Modern Thermodynamics,* Wiley, Chichester.
59. American Dental Association. (2009) Council on Scientific Affairs, April 2009, www.ada.org.
60. FDI World Dental Federation and World Health Organization. (1997) A consensus statement, www.fdiworldental.org.

This page intentionally left blank

Chapter 4

Biomechanics in Dentistry

Akikazu Shinya
Department of Crown and Bridge, School of Life Dentistry at Tokyo,
Nippon Dental University, 1-9-20 Fujimi, Chiyoda-ku, Tokyo 102-0071, Japan
Department of Biomaterials Science, Institute of Dentistry,
BioCity Turku Biomaterials Research Program, University of Turku, Finland
akishi@tky.ndu.ac.jp, akikazu.shinya@utu.fi

New materials, new techniques, and new theories . . . plenty of new things are coming up in the clinical fields of dentistry. These new things help clinicians, scientists, and also patients. However, to master the new materials, very high technical sensitivity, well-established handling, and/or knowledge of basic sciences are recommended. Every year dentists meet a plethora of new dental materials introduced by dental manufacturers. Sometimes the dentists may use these materials without learning their background. Of course, new materials may have a lot of advantages based on many reported experiments—and evidence. However, all the mechanics behind oral functions are controlled by the laws of physics. They are not dominated by "something new." Obviously, the physical

Handbook of Oral Biomaterials
Edited by Jukka P. Matinlinna

ISBN 978-981-4463-12-6 (Hardcover), 978-981-4463-13-3 (eBook)
www.panstanford.com

phenomena of oral function have not changed dramatically over the years! In other words, one can conclude that all new technology is based on the knowledge of basic natural sciences and technology, built on the legendary "gold standards."

4.1 Moments Affecting Dental Materials and Tissues

Dentists have to understand deeply and be best friends with the biomechanical, physical, chemical, and biological backgrounds and facts behind dental materials. This is vital as they will be hands on with the materials. Given this, it is also the only way to establish safe, secure, and standardized treatment procedures in clinical dentistry.

Biomechanical basic concepts necessary for the clinician are introduced in this chapter. What is biomechanics, then? The application of principles of mechanical engineering to biomaterials is called "biomechanics." Structures such as a dental prosthesis are constructed by many different materials, and these are designed to ageist the stress when force is applied, without any failures of structure.

The *resulting moments* in all dental structures (and tissues) are observed from different types of stress:

- Bending
- Compression
- Tension
- Shear
- Twist and torsion while in functional movement (Fig. 4.1)

Moreover, in this moment, under force, different directions of stress (i.e., tensile, compression, and shear) are observed as a complex stress distribution in the same area as well. These phenomena are the main topics on strength considerations of dental materials. These moments are seen at the same time in one structure, and this makes the problem a complex matter for designing of dental prostheses. Under the law of statics, all rigid bodies have to be elastic bodies because every structure will deform under the force until the starting of rupture [1].

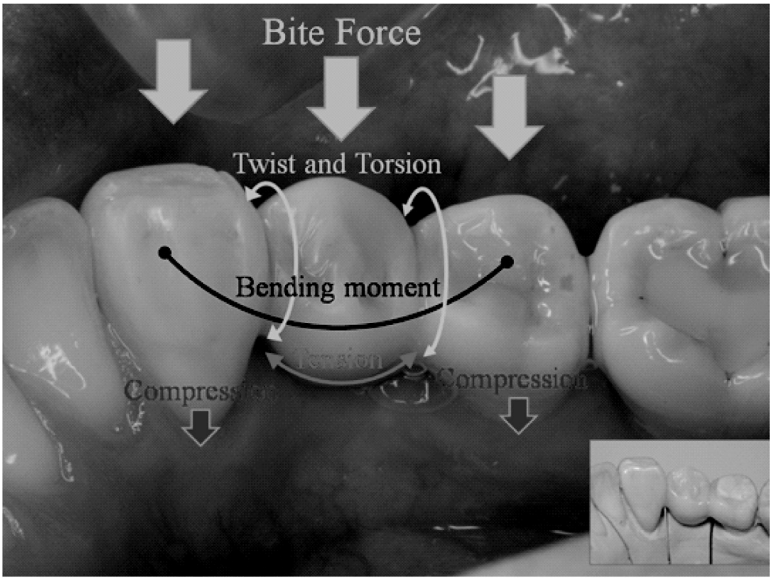

Figure 4.1 Different types of stress on dental structures in the oral milieu.

4.2 Types of Force

In the dental field and its applications, *force* is basically applied from mastication movement (i.e., from the vertical direction, the lateral direction, and a combination of vertical and lateral), parafunctional oral dyskinesia, and accidental trauma. Normally, the force in mastication in human beings is under the *maximum occlusal force* because periodontal tissue should be protected by direct load. The direction and amount of force depend on the tooth (i.e., anterior, posterior, upper, or lower). The maximum occlusal force in the anterior region is around 154 N and in the posterior areas 629 N. It is noteworthy that the maximum occlusal force is applied both to teeth and to periodontal tissue.

4.2.1 Force: Newton's Laws

As it is defined, *force* is an influence of a structure that may cause another structure to change the movement status or to deform. The Englishman Sir Isaac Newton (1642–1727) postulated key laws for

classical mechanics known as the "three laws of motion." For statics Newton's law of reciprocal action plays the major role [2].

Newton's three laws are:

First law: *Every object in a state of uniform motion tends to remain in that state of motion unless an external force is applied to it.*

Second law: *The relationship between an object's mass (m), its acceleration (a), and the applied force (F) is:*

$$\mathbf{F} = m\mathbf{a} \tag{4.1}$$

Acceleration and force are vector quantities (as indicated by their symbols being displayed in bold font); in this law the direction of the force vector is the same as the direction of the acceleration vector.

Third law: *For every action there is an equal and opposite reaction.*

4.3 Bending Moment

Figure 4.2 shows images of a *bending moment*. Bending on a beam and/or a cantilever is the most common moment in dental structures. A bending moment represents the behavior of a beam to a lateral load. External forces (such as loading force and fixed reactions) cause *three* notable forces inside the beam, namely, compression, tension, and shear. The minimum principal stress (mainly of compressive nature) is observed mainly at the uppermost edge of the beam, while the maximum principal stress (mainly of tensile nature) is located at the lower edge of the beam. Since the stresses between these two opposing maxima vary linearly, there therefore exists a point where there is no bending stress. The locus of these points is the neutral axis. In a cross section of the beam is the neutral axis identical with the centre of gravity of the cross section. This is also known as the *second moment of area*, which is a geometrical property of an area that reflects how its points are distributed with regard to a neutral axis [3].

Bending stress is a complex combination of tensile, compressive, and shear stresses (and also strains). There is an important difference in the estimation of deformation between compressive, tensile, and share stresses on one side and the bending moment on the other side [1].

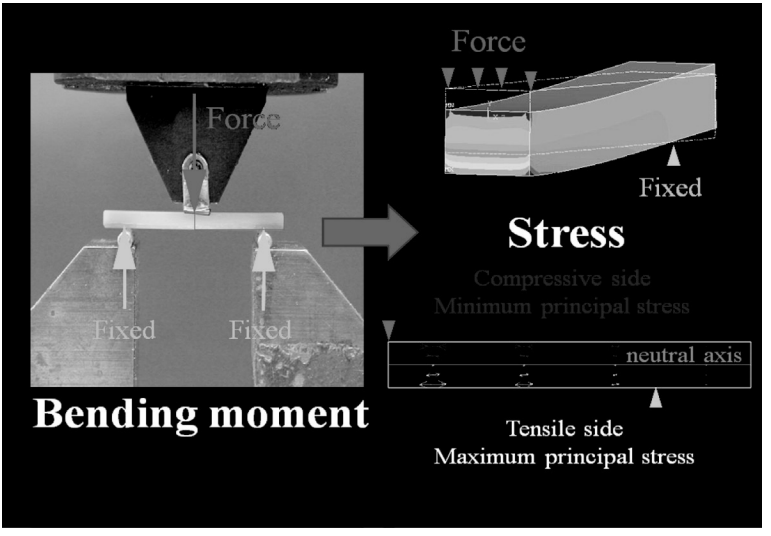

Figure 4.2 Stress distribution under a bending moment.

Furthermore, the shape of the beam structure in a dental prosthetic restoration is recommended not only for optimum shape against the stress but also for the *anatomical form*, which is based on sanitary and esthetic reasons. Basically, stress distribution and stress concentration are affected by the shape, material properties, and boundary conditions [4] (Fig. 4.3).

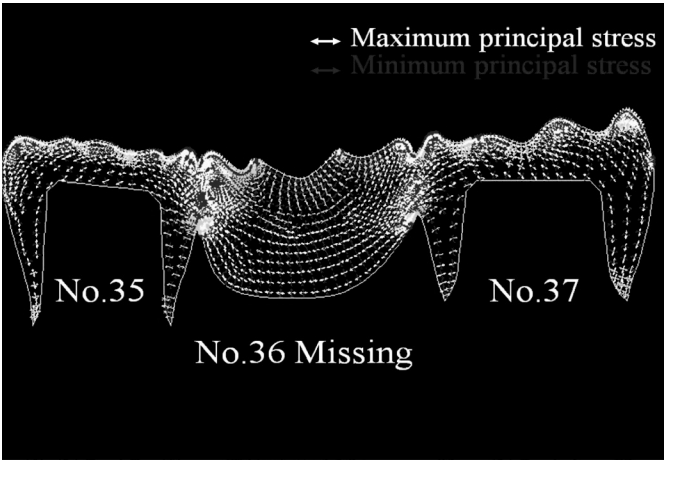

Figure 4.3 Different directions of stress on a three-unit bridge.

4.3.1 Section Modulus

The section modulus is a measure of the flexural strength of a beam that is subjected to bending stress. It is given by the moment of inertia of the area of the cross section of a structural member divided by the distance from the centre of gravity to the farthest point of the section.

4.4 Stress and Strain

Stress is defined as the average force per unit area that some particle of a body exerts on an adjacent particle, across an imaginary surface that separates them:

$$\text{Stress } (\sigma) = \text{Force } (\mathbf{F})/\text{Area } (A) \tag{4.2}$$

The unit for stress (σ) is therefore N/m^2, which is also called Pa (pascal). This unit represents a very small stress. Usually the unit used is in megapascal (MPa), that is, 1 MPa = 1,000,000 Pa.

Deformation in continuum mechanics is the transformation of a body from a reference configuration to a current configuration. A configuration is a set containing the positions of all particles of the body. Contrary to the common definition of deformation, which implies distortion or change in shape, the continuum mechanics definition includes rigid body motions where big shape changes. Deformation may be caused by external loads, body forces, or temperature changes within the body (specimen). Deformation is given by, for example, (1) elasticity modulus and the area of cross section of the specimen beam for basic stresses by forces and (2) forces, elasticity modulus, and the area of cross section and its shape for bending stress [1].

Strain is a description of deformation in terms of the relative displacement of particles in the body and is a normalized measure of deformation representing the displacement between particles in the body relative to a reference length.

Figure 4.4 shows the difference between stress and strain. In this finite element (FEM) calculation, a single Ti implant treatment in the premolar region was simulated. A 100% osseointegration was assumed for boundary conditions, and a force of 50 N was applied at 45° measured from the vertical tooth axis. Material properties,

boundary conditions, design, and shape were exactly the same. From the results, distributions of *strain*, from the left, and *stress*, in the right, can be seen. It can be concluded that the trends in stress and strain are completely different [5].

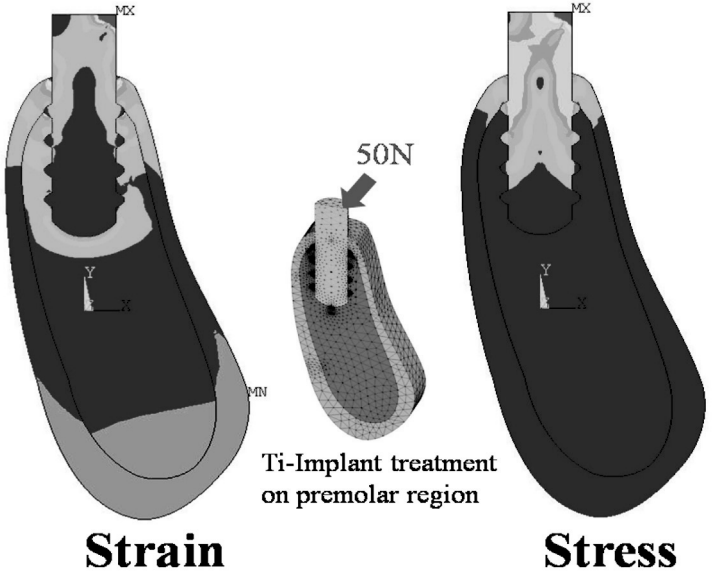

Figure 4.4 Stress and strain distributions of bone around a dental implant.

4.4.1 Stress–Strain Diagrams

The relationship between stress and strain is known as that material's stress–strain diagram (Fig. 4.5). It is found by recording the amount of deformation at distinct intervals of loading. This diagram reveals many of the properties of a material, including data to establish the modulus of elasticity. Stress–strain diagrams of various materials may vary widely. Various tensile tests conducted on the same material yield different results, depending upon the temperature of the specimen and the speed of the loading [1, 6].

4.4.2 Modulus of Elasticity

The letter "E" in the figure above refers to the elastic modulus, which is the resistance of the material to deformation by an applied stress:

Elastic modulus (E) = Stress/Strain (4.3)

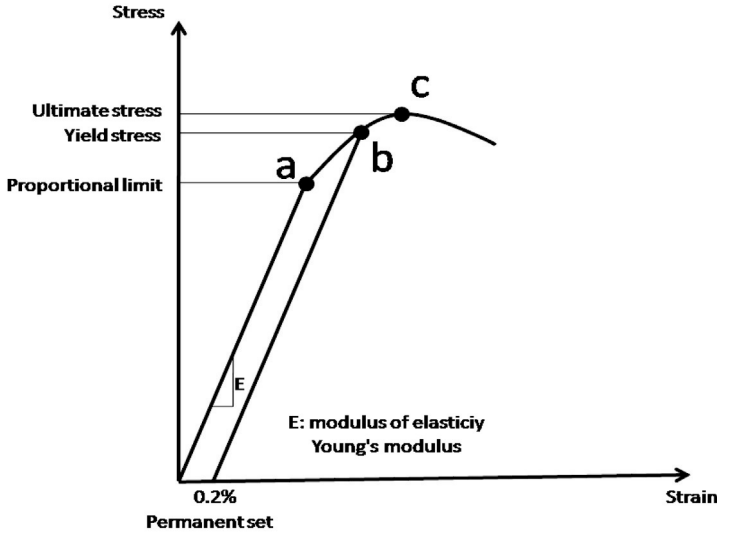

Figure 4.5 Stress–strain diagram.

There are *three primary elastic moduli*, each describing a different kind of deformation:

- Young's modulus (E) describes tensile elasticity.
- The *shear modulus* or *modulus of rigidity* (G) describes an object's tendency to shear.
- The *bulk modulus* describes volumetric elasticity (K), which is the tendency of an object's volume to deform under pressure.

For an *isotropic elastic material* the elastic moduli are interrelated. Typically a material has three mutually perpendicular planes of elastic symmetry. An example of an orthotropic material is organic and/or inorganic fiber-reinforced composite (FRC) material. A typical FRC material has different properties along the directions of fibers (see also Chapter 7).

Isotropic material properties: The property of being independent of direction, it means homogeneity in properties in all directions.

Anisotropic material properties: The property of being directionally dependent as opposed to isotropy.

Orthotropic material properties: The property of an orthotropic material of having two or more planes along which material properties are constant.

4.4.3 Proportional Limit

In Fig. 4.5., at point a, stress is proportional to strain (*Hooke's law*), so the stress–strain diagram is a straight line and the gradient will be equal to the elastic modulus of the material.

4.4.4 Yield Point

In Fig. 4.5., at the point denoted by "b," the *yield point* (stress, strength) is defined in engineering and materials science as the stress at which a material begins to deform plastically. Prior to the yield point the material will deform elastically and will return to its original shape when the applied stress is removed.

Once the yield point is passed, some fraction of the deformation will be permanent and nonreversible. An offset yield point is arbitrarily defined. The value for this is commonly set at 0.2% of the strain. Knowledge of the yield point is vital when designing a component, since it generally represents an upper limit to the load that can be applied. It is also important for the control of many materials production techniques such as forging, rolling, and pressing. In structural engineering, this is a soft failure mode, which does not normally cause catastrophic failure or ultimate failure unless it accelerates buckling [1, 3].

4.4.5 Ultimate Strength

In Fig. 4.5., point c refers to a point showing the *ultimate strength*. It is the maximum stress that a material can withstand while being stretched or pulled before breaking. Some materials will break sharply, without deforming, in what is called a *brittle failure*. Others, which are more ductile, including most metals, will stretch some; rods or bars shrink or neck at the point of maximum stress as that area is stretched out [1, 3].

4.5 Tension, Compression, and Shear

Figure 4.6 shows images describing tension (tensile forces), compression (compressive forces), and shear (shear forces) affecting a material (a body). Under biting forces, stress (and strain) was observed in the dental structure such as a tooth, periodontal tissue, bone, temporomandibular joint, and off cause dental prosthetics. Tensile, compression, and shear stress and strain are also combining everywhere in the structures (cf Figs. 4.3 and 4.4) [1, 6].

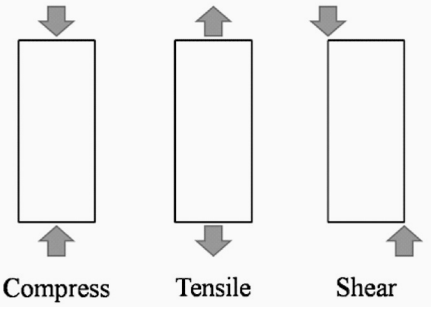

Figure 4.6 Compressive, tensile, and shear forces.

4.5.1 Tension

Tension is the direction of a stress (strain) that tends to produce stretching of a material by the application of axially directed pulling forces. Any material that falls into the elasticity category cannot generally tolerate high tensile stresses, while materials such as ceramics (or composites) are very susceptible to failure under the same conditions. If a material is stressed beyond its limits it will start with microcracks around from a sharp edge, internal defect (air bubbles and/or insufficient adhesion of filler and matrix), and higher difference of material properties in between. The failure mode is based mostly on the microstructure of the material [1, 6].

4.5.2 Compression

Compression is defined as the direction of a stress (strain) that tends to produce pressing of a material by the application of axially directed pushing forces (basically the direction is opposite to tensile

stress). A simple case of compression is the uniaxial compression induced by the action of opposite pushing forces. *Compressive strength* for brittle materials is generally higher than that of tensile stress, but the specimen *geometry* is very important in the analysis, as compressive stresses can lead to buckling in thin members [1, 6].

4.5.3 Shear

Shear stress (strain) is caused when force is applied to produce a sliding failure of a material along a plane that is parallel to the direction of the applied force [1, 6].

4.6 Stress (Strain) Distributions and Concentrations

Stress distribution under a three-point bending test as an example of stress distribution and stress concentration can be seen in Fig. 4.7. The upper bar specimen shows the maximum principal stress, and the stress is concentrated in the lower side of the specimen, under the loading point. The lower part of the beam specimen shows the minimum principal stress, and the stress is concentrated in the upper side, around the loading point. Smooth continuity stress distributions are observed in both of them.

Basic stress analysis calculations assume that the components are smooth, have a uniform section, and have no irregularities. In practice, virtually all components have to go through changes in section, shape, or material, creating areas of discontinuity. Discontinuities change in the stress distribution in the vicinity of the discontinuities, and local increase of stress is referred to as stress concentration [6].

Stress concentration is a location in an object where stress is concentrated. An object is strongest when force is evenly distributed in it, but an area of stress concentration results in a localized increase in stress at that location. A material can *fail*, via a propagating crack, when the concentrated stress exceeds the material's theoretical cohesive strength. The real fracture strength of a material is always lower than the theoretical value because all materials contain small cracks that concentrate stress [1, 8].

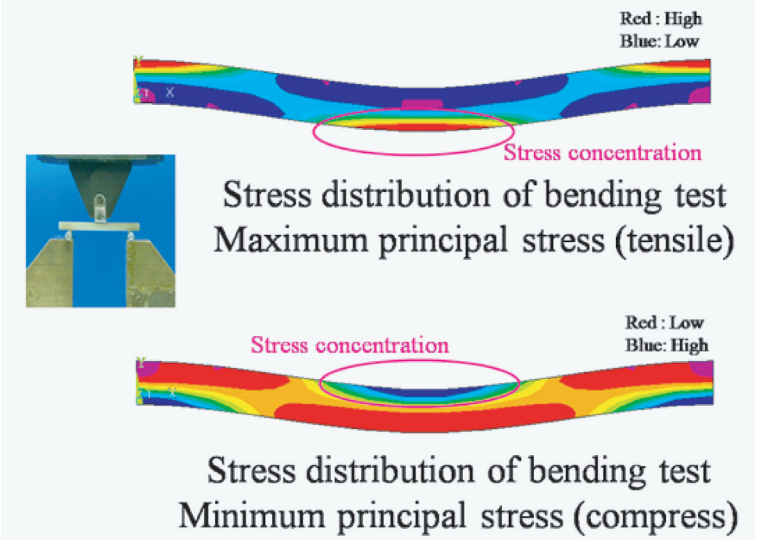

Figure 4.7 Stress distribution in the three-point bending test.

Geometric discontinuities cause an object to experience a local increase in the intensity of a stress field. Material mismatch in the structure has the same effect on stress concentration as geometric discontinuities. Material mismatch means sharp changes in the mechanical properties of materials used in structure.

In implant dentistry, bone growth, remodeling, and adaptation all are believed to be partly regulated by the mechanical properties of the tissue. This phenomenon has been hypothesized to be driven by microscopic damage that stimulates bone adaptation to reconfigure optimal bone strength (*Wolff's law*). A significant modification of the bone's local stress and strain distribution is attained after reconstruction of occlusion with oral implants. The extent and nature of the remodeling process depends partly on the shape and rigidity of the occlusal scheme. The influence of occlusal loads on bone-remodeling phenomena around implants is very important factor for long-term survival rates. The biomechanical relationship between an implant material and different bone qualities under a mastication force should be well known for planning of implant therapies. An understanding of mechanical phenomena is extremely useful to control the stress and strain in implant diagnosis, such as a no-cushioning artificial root (Fig. 4.4) [5].

4.7 Stress, Strength, and Fracture

Many materials have different strengths in tension, compression, and shear. The strength is a limit state of tensile (compressive, shear) stress, which leads to a tensile (compressive, shear) failure. Well-known examples are brittle materials, such as porcelain. Porcelain has, in general, greater *compressive strength* but its *tensile strength* is much lower than the compressive strength. It leads to the necessity of *reinforcement* of porcelain structures that are subjected to tensile stresses. Some metal wires or meshes are used for reinforcement. Metals have much greater strength in tension than porcelain, and metals are able to carry tensile stresses in the structure [7, 8].

Different strengths of material under different stresses are the reasons why the concept of *composite materials* is so successful in nature—and in contemporary dental applications as well. In addition, the anatomical form and composite design of natural teeth are the results of eight-million-year-long optimization of evolution of organisms.

One example of designing metal-free composite bridges [9–11] is shown in Fig. 4.8. Tooth 36 is missing; on teeth 35 and 37 an abutment-supported fixed bridge is assumed and calculated with FEM analysis (see also chapter 17). For boundary conditions, a maximum biting force of 629 N and a mastication force of 250 N are applied, and the bottom of the abutment root is fixed in all directions (Fig. 4.9). A maximum principal stress distribution of the bridge is shown in Fig. 4.10. The reason why the maximum principal stress is selected in this analysis is that the tooth color materials have brittle mechanical properties. Thus, the tensile strength is suitable for comparison. The stress is concentrated around the connector and the bottom of the pontic.

In Fig. 4.11 can be seen the *vector indication* of stress, and different directions of stresses are observed in the same area. Figure 4.12 shows the maximum principal stress in a three-dimensional model with two different forces. The upper bridge is subjected to the maximum force, and the lower bridge is assumed to a mastication force. From this distribution, stress is concentrated around the connector and the pontic. The maximum stress value is comparative to the tensile strength of the assumed material.

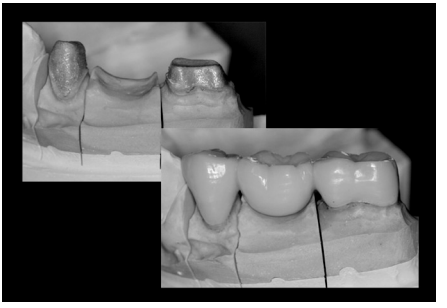

Figure 4.8 Construction of a three-unit metal-free bridge for the molar region.

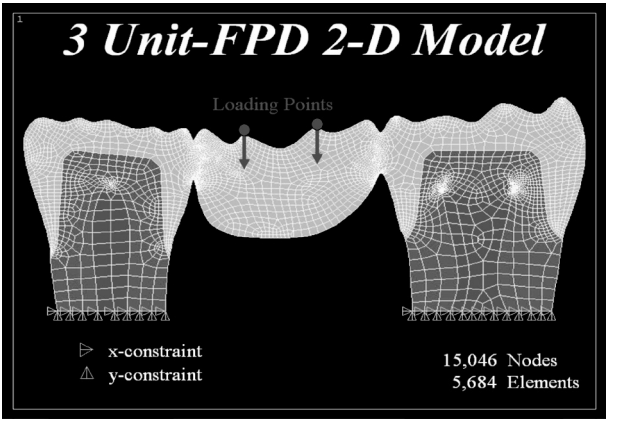

Figure 4.9 Boundary conditions in a three-unit bridge with a pontic.

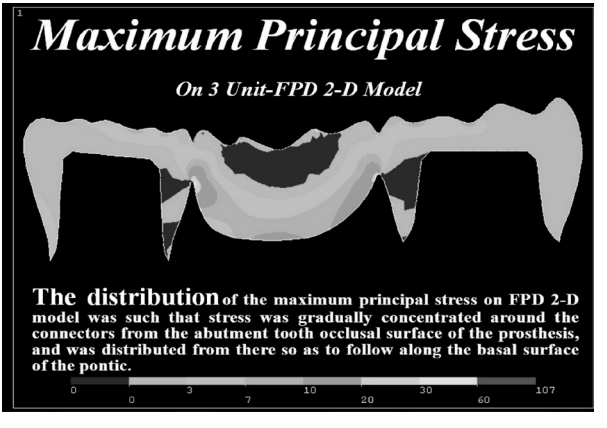

Figure 4.10 The maximum principal stress distribution on a bridge.

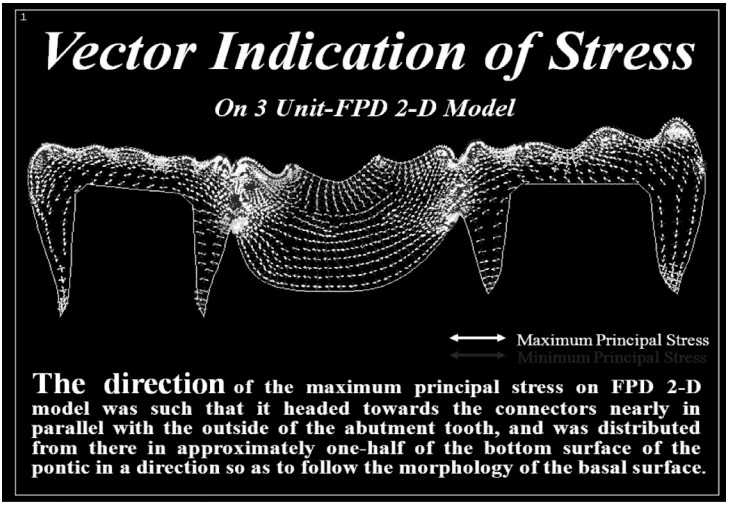

Figure 4.11 A vector indication of stresses in a bridge.

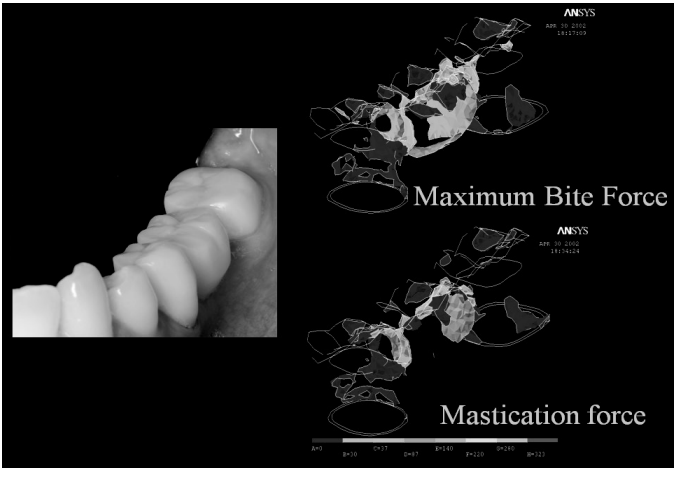

Figure 4.12 The maximum principal stress distributed on a bridge under different applied forces.

4.7.1 Fracture Mode

Fracture is the separation of a body under the higher load of material strength affected with variable stress (strain). There are *two types of fracture mechanisms* [8]:

(a) *Brittle fracture*: No apparent plastic deformation takes place before fracture. Brittleness is a property showing little tendency to deform before fracture.
(b) *Ductile fracture*: Extensive plastic deformation takes place before fracture. Ductility is a property of being capable of sustaining large plastic deformation without fracture.

Fracture is caused by crack initiation followed by crack propagation. These fracture modes are based on the fairer low of principal stress theory. In mathematical computational dynamics, well known as FEM analysis (cf Chapter 17), the calculation value of the stress (tensile, compressive, and shear) is comparable to the mechanical strength applied from the corresponding directions. Normally, in a ductile material, such as virtually all metals, a compressive test is used for prediction of failure. For a brittle material such as ceramics, failure is tested with the application of tensile force [1].

4.7.2 Crack Separation Modes

There are *three modes of fracture*: Mode I is characterized by a stress normal to the crack faces. Mode II is the sliding mode or forward shear mode and has a shear stress normal to the crack front. Finally, Mode III is the tearing mode, with a shear stress parallel to the crack front [1, 6].

4.7.3 Fracture Toughness

Toughness is a property that describes the ability of a material containing a crack to resist fracture. It is defined as the amount of energy that a material can absorb before rupturing (unit: J/m^3). *Fracture toughness* (unit: $MN\ m^{3/2}$) is a quantitative way of expressing a material's resistance to brittle fracture when a crack is present. If a material has a large value of fracture toughness it will probably undergo ductile fracture. Brittle fracture is very characteristic for materials with a low fracture toughness value [1, 6].

4.7.4 Stiffness

Stiffness (k) is the resistance of an elastic body to deformation by an applied force. The stiffness of a body that deflects a distance (δ) under an applied force (P) is:

$$k = P/\delta \tag{4.4}$$

The unit is n/m. Stiffness is a property of a body, while elastic modulus is a property of the material. The stiffness of a body depends on the material, shape, and boundary conditions of the body [1, 6].

References

1. Timoshenko, S., Young, D. H. (1968) *Elements of Strength of Materials*, 5th ed., Van Nostrand Campany, NJ, USA.
2. Feynman, R. P., Leighton, R. B., Sands, M. L. (1965) *The Feynman Lectures on Physics,* Vol. 1, 5th ed., 122–141, Addison-Wesley, MA, USA.
3. Truesdell, C., Noll, W. (2004) *The Non-Linear Field Theories of Mechanics*, 3rd ed., Springer, New York, USA.
4. Shinya, A., Matsuda, T., Shinya, A., Nakasone, Y. (2004) Hybrid resin fixed partial dentures reinforced with glass fiber: optimum posterior fiber frame design with finite element analysis, *Jpn. J. Dent. Mater.,* **23**, 186–192 (in Japanese).
5. Shinya, A., Ballo, A. M., Lassila, L. V., Shinya, A., Närhi, T. O., Vallittu, P. K. (2010) Stress and strain analysis of the bone-implant interface: a comparison of fiber-reinforced composite and titanium implants utilizing 3-dimensional finite element study, *J. Oral Implantol.*, **37**, 133–140.
6. Beer, F., Johnston, R., Dewolf, J., Mazurek, D. (2009) *Mechanics of Materials,* 2nd ed., McGraw-Hill, New York, USA.
7. Vinson, J. R., Sierakowski, R. L. (2002) *The Behaviour of Structures Composed of Composite Materials,* 2nd ed., 1–53, Springer, New York, USA.
8. Gordon, J. E. (1978) Structures: why things don't fall down, in *Strain Energy and Modern Fracture Mechanics*, 2nd ed., 70–109, Da Capo Press, MA, USA.
9. Aida, N., Shinya, A., Yokoyama, D., Lassila, L. V., Gomi, H., Vallittu, P. K., Shinya, A. (2011) Three-dimensional finite element analysis of posterior fiber-reinforced composite fixed partial denture Part 2: influence of fiber reinforcement on mesial and distal connectors, *Dent. Mater. J.,* **30**, 29–37.
10. Shinya, A., Lassila, L. V., Vallittu, P. K., Shinya, A. (2009) Three-dimensional finite element analysis of posterior fiber reinforced composite fixed partial denture: framework design for pontic, *Eur. J. Prosthodont. Restor. Dent.,* **17**, 78–84.

11. Ootaki, M., Shinya, A., Gomi, H., Shinya, A. (2007) Optimum design for fixed partial dentures made of hybrid resin with glass fiber reinforcement on finite element analysis: effect of vertical reinforced thickness to fiber frame, *Dent. Mater. J.,* **26**, 280–289.

Chapter 5

Biocompatibility

Alexander T. H. Tang
Department of Orthodontics, University of Hong Kong, Prince Philip Dental Hospital, 34 Hospital Road, Sai Ying Pun, Hong Kong SAR, People's Republic of China
athtang@hotmail.com

Biocompatibility is often referred to as appropriate host response to biomaterials. The absence of acute adverse effects of oral biomaterials is a result of a wide safety margin of these materials in their hosts. Beyond the safety level of the dose, adverse effects in host(s) or appropriate animal model(s) follows a dose-dependent pattern, that is, the higher the dose of biomaterials, the stronger the adverse effects. Below the safety level of acute adverse reactions, some biomaterials may cause low-dose adverse reactions, for example, hypersensitivity, in a small group of patients. Recent research in endocrine-disrupting chemicals at an extremely low dose, for example, bisphenol A, has given rise to controversies in the safety of some oral biomaterials. Whilst biomaterials do not seem to compromise the life span of human beings, low-dose effects of some oral biomaterials warrant further investigation.

Handbook of Oral Biomaterials
Edited by Jukka P. Matinlinna

ISBN 978-981-4463-12-6 (Hardcover), 978-981-4463-13-3 (eBook)
www.panstanford.com

5.1 Introduction and Consensus Definitions

Biomaterials serve to restore/promote health, function, and/or esthetic appearance of patients. To fulfill such purposes, they are designed to work within their hosts. Such a relationship between biomaterials and host responses has long been loosely described as biocompatibility.

The definition of the term "biocompatibility" may resort to highly philosophical and lengthy debates before any agreeable definitions can be arrived at [1]. In other words, this aspect of biomaterials is very confusing. Definitions of the term "biocompatibility" had varied between authorities [2, 3], dictionaries [4–6], encyclopedias [7, 8], personal preferences [1], etc., until 1986, when a consensual definition emerged in a conference held in Chester, UK [9]. The same issue was reassessed in 1991 in a conference, again in Chester, UK, where experts in this issue agreed that their 1986 definition of biocompatibility had stood challenges over the years and should be upheld as the consensual definition of biocompatibility, as follows [10]:

Biocompatibility is defined as the ability of a material to perform with an appropriate host response in a specific situation [9].

This consensual definition of biocompatibility includes the terms "material" ("biomaterial" to be more precise) and "host response." The consensual definitions of these two terms had also been drawn in the 1986 Chester conference.

A **biomaterial** is defined as a nonviable material used in a medical device, intended to interact with a biological system [9].

A **host response** is defined as the reaction of a living system to the presence of a material [9].

These definitions have not ceased to evolve with time. As technology advances and our understanding in biomaterials and host responses expands, the transition from a material-based to an application-based component was suggested for the definition of biocompatibility [11, 12]. After extensive and vigorous discussion in the Chester conference in 1991, the term "biomaterials" was one of the five definitions updated.

A **biomaterial** was redefined as a material intended to interface with biological systems to evaluate, treat, augment, or replace any tissue, organ, or function of the body [10].

Despite the dynamic nature of these consensual definitions, biocompatibility [9], host response [9], and biomaterials [10] are reasonable definitions as starting points for our purpose.

Biomaterials and their biocompatible properties seem remote to our daily life. However, the *role of fluorides in drinking water* to fight caries makes artificially optimally fluoridated water a biomaterial. In this sense, biocompatibility of biomaterials (e.g., drinking water) is part of our daily life. In fact, fluoridated water and dental composite are convenient examples in elaborating a few basic concepts of biocompatibility. They are dose and host responses, non-Paracelsian adverse effects of oral biomaterials, and the three levels of biomaterial testing.

5.2 Dose and Host Responses

The father of modern toxicology, Paracelsus (born Philippus Aureolus Theophrastus Bombastus von Hohenheim, 1493–1541), aptly pointed out that "in all things there is a poison. It depends only on the dose whether a poison is poisonous or not" [13]. *Cholesterol* is an often-quoted example of the Paracelsian paradigm. The human body needs a small amount of cholesterol as the building block of the cell membrane, but more than enough of it is detrimental to health. The dose–response relationship is, therefore, the fundamental issue in the biocompatibility aspect of the design of biomaterials (Fig. 5.1).

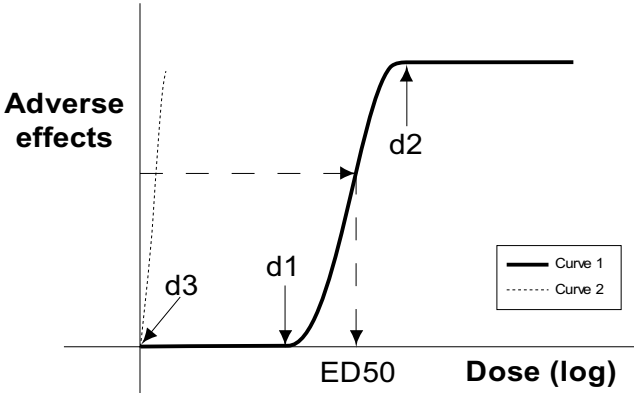

Figure 5.1 A schematic representation of a host dose–response curve.

5.2.1 Dose-Response Curve

Although they are often called dose–response curves, they are, in fact, graphic plots of "host responses or adverse effects" (*y* axis) versus "dose" (*x* axis, usually in the log scale). They may be individual or population based [14]. Each curve represents the variation of one kind of response of a medicine or biomaterial to the dose. The classic dose–response curve is sigmoidal shaped, which is usually analyzed by dividing it into three parts [14]. Take curve 1 of Fig. 5.1 as an example: From dose zero (d0) to d1, an increase in the dose does not give rise to any observable adverse effect of the biomaterial in the host. Biomaterials with a dose of d1 or below are usually regarded as the safety dose—depending on the purpose, d1 may stand for no-observable-effect level (NOEL), no-observable-adverse-effect level (NOAEL), occupational exposure level (OEL), or acceptable daily intake (ADI). Now, from d1 to d2, an increase in the dose of such a biomaterial produces a sharp rise of an adverse effect. Beyond d2, a further increase in the dose does not make much difference in the damage caused by the biomaterial's adverse effect. If the curve is on a population basis or as an animal experiment report, halfway up between *no effect* and *maximum effect* one may project from the *y* axis to the curve and then the *x* axis to give the effective dose at which 50% individuals/animals respond (ED50).

On the other hand, if the lethal effect of medicines or biomaterials is studied, "median lethal dose" is a more appropriate term to use (also known as LD50, the dose required to kill half of a tested population). Most of the time, d1 and the events happen from d1 to d2 of a biomaterial that determine its toxicology. In the design of biomaterials, the safety level d1 is obviously of great interest. The specific nature and intensity of adverse effects that happen from d1 to d2 are also important for risk evaluation and the cost-effectiveness of avoiding such adverse effects.

The construction of such a curve is a much bigger job than it seems. On the *y* axis, the specific side effect of a biomaterial needs to be identified, characterized, and classified (ideally also calibrated for reproducibility and relevance). On the *x* axis, the dose stands for the concentration of the "active ingredient" and host exposure. Concentration depends on the preparation of the biomaterials (toxicodynamics).

Host exposure is related to absorption (oral, respiratory, and skin for oral biomaterials), distribution, metabolism, and excretion (or ADME) (toxicokinetics), thereby determining the duration of exposure and target tissue exposure of the host to the "active ingredient." It is tempting to assume that the retained amount of the "active ingredient" in the host is simple arithmetic between excretion and absorption. However, the distribution and metabolism parts of ADME may make the clinical study of such a dose–response curve more complicated than it seems. Toward d2, the higher end of a toxic dose, the study of the toxicology of an oral biomaterial would inevitably involve ethical issues, population or animal studies alike. Fortunately, in oral biomaterials, fluoride may serve as an example to elaborate at least part of the Paracelsian model of biomaterial toxicology.

5.2.2 Water Fluoridation

One interesting example of oral biomaterials, applying the principles of dose–response curves, is the optimization of the water fluoridation level in caries prevention. In fact, its anticaries property was discovered as a result of the observation of its side effects—mottled teeth (Table 5.1) [15].

5.2.2.1 Dental fluorosis as an adverse effect

From Table 5.1, the path to the identification and characterization of fluoride in drinking water as the cause of dental fluorosis took place between 1901 and 1931—a three-decade-long and tortuous quest.

One key fact in tackling mottled teeth is the noticing of the caries-resistant nature of mottled teeth, by McKay and Black, when caries was rampant and widespread at that point of human history. On the basis of this finding, a possible opportunity of minimizing the unsightly mottled teeth and maximizing the anticaries effect of the "active ingredient" in water became a prevailing vision.

After fluoride was identified as the anticaries material, Dean worked vigorously on the epidemiology data of fluorosis and the fluoride concentration in water in different parts of the U.S. Although a 1 ppm level of water fluoridation regime was proposed and implemented earlier in the U.S., it was not scientific until a pharmacology professor, Harold C. Hodge, made use of the data from

Dean's studies to sketch the dose–response curves (Figs. 5.2 and 5.3) [16].

Table 5.1 Chronicles of the discovery of fluoride's anticaries effect

Year	Events
1901	Dr. Frederick Summer McKay moved from the East Coast to Colorado Springs, Colorado, USA. He observed mottled teeth as a general phenomenon of the native inhabitants of Colorado Springs.
1909	Dr. G. V. Black attended the Conference of Colorado Springs Dental Society to listen to McKay's epidemiological finding of mottled teeth in Colorado Springs.
1909–1915	A collaboration of Black and McKay led to two conclusions before Black passed away in 1915. First, mottled enamel is a developmental condition. Second, mottled enamel is resistant to dental decay.
1923	McKay identified water as the cause of mottled teeth in Oakley, Idaho, USA.
1931	The chief chemist of the Aluminum Company of America (ALCOA), H. V. Churchill, and his assistant identified a high fluoride concentration in the water of Bauxite, Arkansas, USA, related to mottled teeth of residents there.
1931–late 1930s	Dr. H. Trendley Dean, head of the Dental Hygiene Unit, NIH, studied the epidemiology of mottled enamel in USA. Dr. Elias Elvove, senior chemist, NIH, developed a method to measure the water (F^-) level to 0.1 ppm accuracy. Dean concluded from his epidemiology data and water F^- levels around USA that 1.0 ppm of F^- did not cause fluorosis to most but to a small percentage of people.
1945	Grand Rapids, Michigan, USA, started optimal artificial water fluoridation.
1956	Dean announced a >60% drop in the caries rate in the 30,000 school children studied after water fluoridation had started.

Abbreviation: NIH, National Institutes of Health.

The dose–response curve (Fig. 5.2) of Hodge represented the region of interest close to the d1 level (NOAEL) of our schematic drawing in Fig. 5.1. His entire purpose was to identify the water fluoridation level to maximize its anticaries effect without sacrificing unnecessarily the dental appearance of the US population to dental fluorosis. From Fig. 5.2, the increase in Dean's index of fluorosis underwent only negligible increase up to about 1 ppm of fluoride concentration in water.

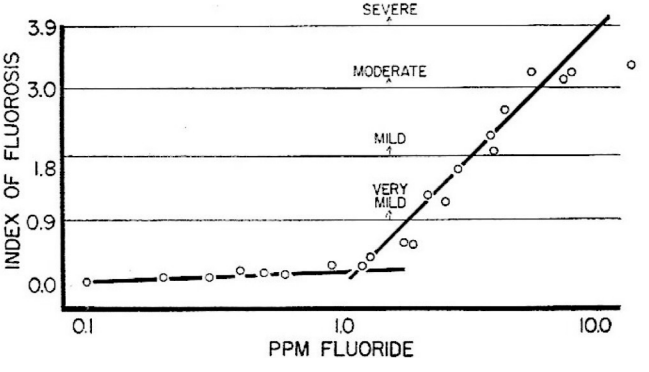

Figure 5.2 Dose–response curve of dental fluorosis vs. water fluoride concentration on the basis of studies of 22 US cities. Studies were conducted with Dean's index of fluorosis and Elvove's method of water-fluoride-level estimation [16]. A complete sigmoidal curve of Dean's data, 1942, can be found in Ref. [17]. Dean's index of fluorosis underwent only a negligible increase up to about 1 ppm of the fluoride concentration in water. (Permission of use of this figure was obtained from *J Am Dent Assoc* via copyright.com.)

After 1 ppm of the fluoride concentration in water, a further increase in the water fluoride level led to a steady and significant increase in dental fluorosis in US populations to a severe level, as recorded by Dean's dental fluorosis index.

The dose–response curve would not be complete without the charting of caries prevalence versus water fluoride concentration. Hodge's curve (Fig. 5.3) recorded an impressive drop in dmft, from around 8 per person at 0.1 ppm (F^-) to about 2 per person at 1.0 ppm (F^-). A further increase in the fluoride level above 1.0 ppm did not seem to reduce dmft to a level significantly below 2 dmft per person. The hypothetical benefit of 1 ppm of fluoride in water was estimated to be a 75% reduction of caries. This estimation was a bold claim in

1950 as the fight against caries had lasted for more than a century without much success.

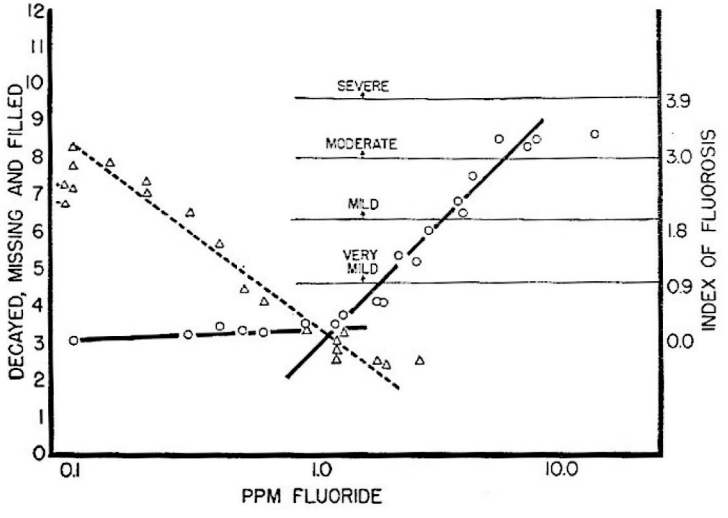

Figure 5.3 Dose–response curve of dental fluorosis vs. water fluoride concentration on the basis of studies of 22 US cities. Caries prevalence (by dmft) was also plotted against the water fluoride level on the same dose–response curve [16]. (Permission of use of this figure was obtained from *J Am Dent Assoc* via copyright.com.) *Abbreviation*: dmft, decayed, missing, and filled teeth.

It turned out to be not very far away from the epidemiology of Dean in 1956, when he claimed a more than 60% reduction in caries among the 30,000 school children who were exposed to 1 ppm fluoride in their drinking water (Table 5.1). Taking into account the errors in the diagnostic criteria of caries and dental fluorosis and the measurement error of the water fluoride content in the 1930s, the dose–response curves of Hodge had quite accurately forecasted the study result of Dean on 30,000 school children.

The residual 2 dmft per person seemed to be beyond the control of optimally fluoridated water. In fact, a further increase in the fluoride level did not seem to be able to lower dmft further in the U.S. in the 1930s to the 1950s. What caused the residual 2 dmft to persist cannot be figured out in Hodge's dose–response curves. However, his curves had indicated a valuable and economical tool to fight 75%

of caries in US populations, and additional research was needed to fight the residual 25% of caries.

Even if a single cause of an adverse effect can be identified, it takes time to collect data to construct a dose–response curve for the oral biomaterial and additional time to testify it. Conclusive evidence to quantify the implementation of water fluoridation as an anticaries biomaterial had taken more than another 20 years to emerge.

5.2.2.2 Fluoride dose (*x* axis)

It is important to point out here that the log transformation of dose on the *x* axis of dose–response curves serves to enable easier detection of the adverse effect(s) by condensing the adverse effects over a range of doses in a shorter scale. In other words, the condensation of data on the *x* axis allows easier identification of d1 in Fig. 5.1. The steep slope of curve 1 from d1 to d2 in Fig. 5.1 is also a condensation of adverse effects to dose. For this reason, cautious interpretation of adverse effects from a dose–response curve with respect to the scale of the *x* axis is always desirable.

Also, the definition of the *x* axis, that is, dose, deserves special attention as it depends on both toxicodynamics and toxicokinetics of the biomaterial. Routes of fluoride uptake in humans are gastrointestinal (GI) and respiratory. For GI uptake of fluoride, the dose of fluoride may arise from a single source, for example, drinking water. More often than not, individuals are exposed to fluoride doses from multiple sources, for example, baby formula or maternal milk, food, dentifrices, fluoride supplements like fluoride tablets, salt, water, and gel. In modern society, the quantification of fluoride doses is not so clear-cut.

To complicate the scenario further, the fluoride level in a particular source may differ by its age, for example, older tea leaves are known to release more fluoride than younger ones into tea beverages [18]. Free fluoride ions available in a certain food source are often estimated by the amount of NaF added to it. Interaction of fluoride may happen with other food components like calcium ions, Ca^{2+} [19]. Free fluoride ions available in fluoridated milk, for example, are difficult to estimate as a result of chelation between the calcium and fluoride ions. The frequency of consumption of a fluoride-containing fluid may be increased as a result of hot climate, dry weather, and geographic locations. Such error in the *x* axis may be highly individualized, further complicating the plotting of a population-based dose–response curve.

Breathing is another possible route of fluoride uptake that may confuse the picture of the overall fluoride uptake [20]. It is usually a minor route of fluoride uptake. In special circumstances, like indoor heating generated by coal burning without appropriate ventilation, industrial production of pesticides, aluminum, and fertilizers, or fumes from a volcano eruption, the inhalation of fluoride compounds may contribute more than usual to the overall systemic fluoride uptake.

Other than the sources of fluoride, individual/population exposure to the dose is also a function of absorption, metabolism, and excretion [19]. Calcium-rich, or any bivalent or trivalent cation-rich, diets tend to chelate fluoride ions to produce a sparingly soluble CaF_2 salt [19]. This reduces the amount of GI absorption of fluoride ions but increases the fecal content of CaF_2 [19].

It is obvious that the complicated nature of the *x* axis of the dose–response curve is difficult to standardize. In Hodge's dose–response curve of dental fluorosis, however, the *x* axis had water fluoride content as the only fluoride source to give rise to dental fluorosis. If Dean's study and Hodge's dose–response curve would be repeated today, this fluoride exposure picture of humans probably cannot be easily defined. Nonetheless, Hodge's curve serves well as a simple and straightforward way to understand this basic concept of the dose–response relationship of oral biomaterials.

5.2.2.3 Quantification of adverse effects (*y* axis)

Dean's index of dental fluorosis served to classify the clinical severity of this condition in Hodge's dose–response curve [21]. Since 1942, at least two other recognized dental fluorosis indices had been used extensively [22, 23]. They represented very much different approaches to classify the clinical severity of dental fluorosis (Table 5.2).

Table 5.2 is by no means a complete list of differences in fluorosis indices. A clinical classification of the severity of dental fluorosis in a study sample may clearly vary according to the choice of indices used on the *y* axis. In a dose–response curve of oral biomaterials, the validity of the *y* axis may directly affect the NOAEL dose, that is, 1 ppm in water fluoridation.

Another relevant aspect of the *y* axis is the nature of the clinical classification of adverse effects. Dean's index is not a continuous

quantitative scale [22]. Categorical data of this kind cannot be averaged into index scores with decimal place(s) [23]. It is at best qualitative data, that is, the number stands for a meaning but cannot be calculated mathematically. In Dean's index, 0 = normal, 0.5 = questionable, 1 = very mild, 2 = mild, 3 = moderate, and 4 = severe; 0.5 may easily mislead its application on the *y* axis. Obviously, Hodge was one of the misled who plotted 0.0, 0.9, 1.8, 3.0, and 3.9 on the *y* axis of his dose–response curve. Statistical analysis of such data can only make use of nonparametric methods.

Table 5.2 A few differences in the three commonly used indices of enamel fluorosis

Indices	Dean's [21]	TFI [22]	TSIF [23]
Scale	0–4	0–9	0–7
Index teeth recorded	Not specified	2 teeth with most severe fluorosis	2 anterior and 3 posterior teeth with most severe fluorosis
Dentition examined	Mixed	Adult	Mixed
Detail description of enamel fluorosis	No	Yes	Yes
Clinical photographs used for index calibration	Nil	Nil	Available
Histopathology of hypomineralization related to the index scale	No	Yes	No
Clinical dental fluorosis classified on the basis of water fluoride content	Up to 14.1 ppm	Up to 21 ppm	Up to 4 ppm
Reproducibility assessment of the index scale	No	No	No
Interexaminer's reproducibility assessment	No	Yes	No

Abbreviations: TFI, Thylstrup and Fejerskov index of fluorosis; TSIF, tooth surface index of fluorosis.

Despite error sources in both *x* and *y* axes, the dose–response curve remains the foundation of the study of biocompatibility of drugs and biomaterials. If Paracelsus were alive today, he might have been surprised to see his comment on poison has evolved into a specialty of pharmacology with a score of subspecialties. He might have been more surprised that each dose-dependent toxicology curve takes a tremendous amount of effort to draw and carries with it much scientific meaning. Yet, he might have been most surprised to see the toxicology of biomaterials at a very to extremely low dose that does not exactly obey his law of dose-dependent toxicology.

5.3 Non-Paracelsian Adverse Effects of Oral Biomaterials

Not all adverse effects can be classified as dose-dependent effects, as Paracelsus once assumed. Some undesirable effects of oral biomaterials fall outside the scope of Paracelsian toxicology.

Hypersensitivity and a variety of medical issues have been attributed to the side effects of bisphenol A (BPA) and its derivatives. Hypersensitivity requires only an extremely low dose of an allergen to trigger an exaggerated response that is not at all dose dependent, for example, d3 in curve 2 of Fig. 5.1. The controversial estrogen-mimicking role of BPA at an extremely low dose in a number of medical conditions makes the construction of dose–response curves difficult if not impossible [24]. These controversies had attracted public concern in recent years and had occupied an unproportionally large coverage in one report to the president of the U.S. in the President's Cancer Panel of the NIH [25].

BPA is a nonvolatile solid at room temperature. It is photodegradable but not easily hydrolyzed. It is used in the manufacturing of polycarbonate plastic and epoxy resins [26]. As much as 6 billion pounds was produced in 2003 worldwide [27]. Food packaging, baby bottles, and dental resinous materials are major sources of human exposure to BPA [28]. They account for roughly 5% of BPA's total production [26]. In the U.S., 95% of the population is exposed to BPA in a random urine test of 394 individuals [29]. A study showed in a group of volunteers that consumed 12 oz of canned soup per day for 5 days has about 19 times higher BPA concentration in urine than volunteers who consume 12 oz of fresh soup per day for 5 days [30]. BPA's uses in the food packaging and medical industries are under the regulation of the Food and Drugs

Administration (FDA) in the U.S., which works in close collaboration with a few other US agencies that are responsible for the regulation of the other 95% production of BPA [26].

In the dental context, a bisphenol A diglycidyl methacrylate (bis-GMA)-based dental resin composite may be used to illustrate the non- Paracelsian adverse effects of oral biomaterials.

5.3.1 Bis-GMA-Based Resin Composites

Today's typical resin composite roughly contains a battery of components, as listed in Table 5.3 (see also chapters 3 and 6).

Table 5.3 Components and purposes of a resin composite

Component	Purpose
Bis-GMA	Monomer for matrix polymerization
TEGDMA	Diluent of thick bis-GMA monomer
Silane coupling agent	Enabler of the blending of matrix and filler
CQ	Photoinitiator in light-cured composite
BP	Initiator in chemically cured composite
Tertiary amine	Activator
Silica	Filler
Others	Comonomers, radio-opaquer, coloring(s), etc.

Abbreviations: TEGDMA, triethylene glycol dimethacrylate; CQ, camphorquinone; BP, benzoyl peroxide.

The matrix of a dental resin composite is made up of a polymerized network of a mixture of bis-GMA and comonomers, for example, bisphenol A dimethacrylate (bis-DMA) and TEGDMA, the filler content is silica. Depending on the filler size, the filler content of a resin composite accounts for roughly 60% to 80% of the material by weight.

The polymer matrix is formed in a subdued in vivo environment. Upon polymerization, C=C double bonds of monomers cross-link to form a polymer network. The percentage of reduction of the C=C double bond is termed the *conversion rate of polymerization*. In such a subdued intraoral environment, the conversion rate of monomers was reported to be in a range between 35% and 77% [31–33]. The low conversion rate may be attributed to the monomer's steric hindrance, the presence of filler content, and poor penetration of the

light source. The heavy steric hindrance of the two benzene rings per monomer limits the mobility of bis-GMA for effective cross-linking, although it is also the reason for the superior mechanical strength of bis-GMA. The filler content also seems to obstruct somewhat the cross-linking between monomers, although, again, it promotes mechanical properties of the resin composite. In addition, the lack of light intensity at a thickness of ≧2 mm of the resin composite plays another role in the low conversion rate of in vivo polymerization [34].

Other than these factors, atmospheric oxygen also compromises the conversion rate of a resin composite (Fig. 5.4) [35]. Unlike the assumptions of most reports, an oxygen-inhibited layer (OIL), a mixture of monomers and short-chain polymers, does not exist only on the surface of a resin composite. Report has shown that a vast number of air bubbles exist in the bulk of a resin composite [36]. All of them are lined by OIL (Fig. 5.5). Contrary to the initial belief of easy removal of OIL from the surface of a resin composite, the toxic contribution of OIL from air bubbles inside a resin composite cannot be ruled out. When and how it may leach out are unknown quantities.

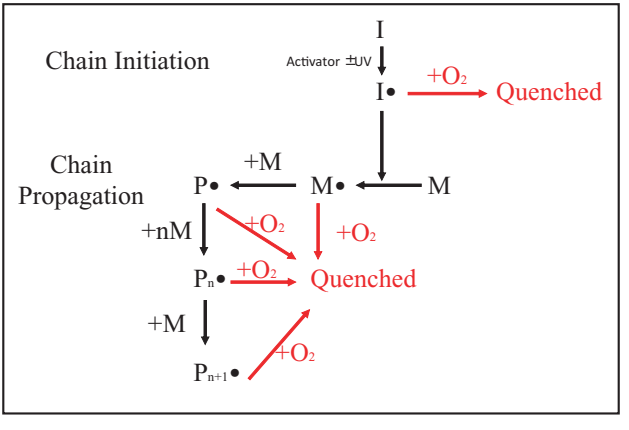

Figure 5.4 Schematic representation of oxygen's (O_2) role in the in vivo polymerization of a dental resin composite. The red routes are much more favourable routes of chemical reaction. *Abbreviations:* I, initiator; I•, free radical of initiator; M, monomer; M•, free radical of monomer; P•, free radical of short chain polymer; P_n•, free radical of short chain polymer with n units; P_{n+1}•, free radical of short chain polymer with n+1 monomer unit.

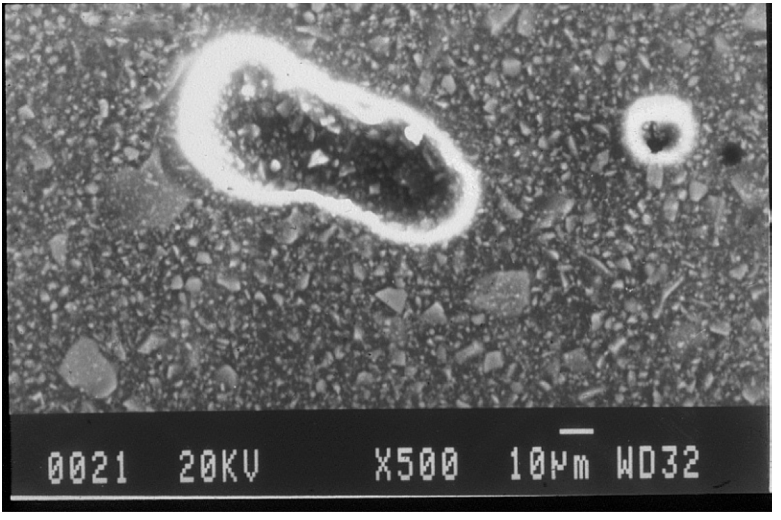

Figure 5.5 OIL lining the air voids inside the bulk of a resin composite [36]. (Kind permission was given by Annals of Royal Australasian College of Dental Surgeons to re-use this figure.)

Liquid resin adhesives used in enamel adhesion contribute another important source of monomers to the toxicology profile of resin composites. It is of special interest as they are usually unfilled, giving rise to 100% monomer content, and more vulnerable to oxygen's inhibition effect on polymerization [37].

Elusion studies have identified a large number of chemical species of residual monomers [38]. The identities and amount of chemical species of these in vitro studies obviously depend on the leaching medium, duration of the experiment, and the condition to degrade the composite, for example, thermocycling [38]. Of our interest in this discussion is, of course, BPA, which had been identified from dental resin composites [39].

In theory, any chemical used in the manufacturing of bis-GMA may be found as a residual component in the resin composite. At least one major manufacturer claimed that BPA was not used in the production of its product, and the American Dental Association (ADA) had cited such a claim in its statement [40, 41]. However, BPA has a role in the manufacturing of the raw material of the alternative BPA-free pathway of bis-GMA production (Fig. 5.6). Also, it was reported that the copolymer bisphenol A dimethacrylate (bis-DMA) of a dental resin composite may degrade to produce BPA [42].

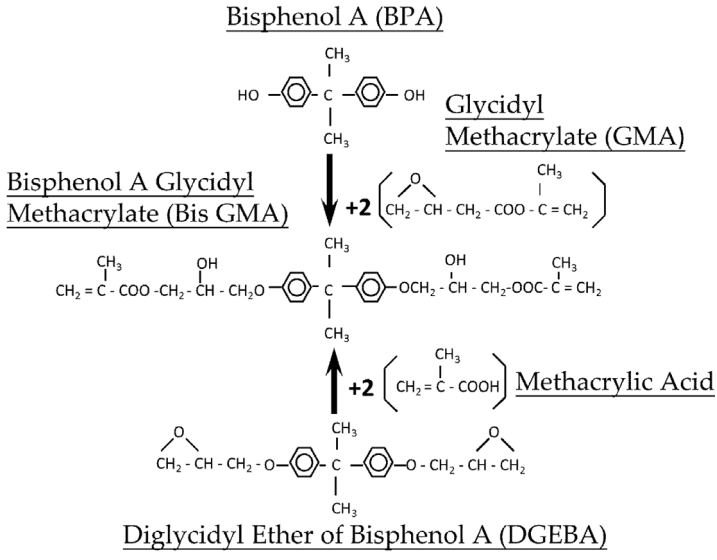

Figure 5.6 Two commonly used routes of industrial manufacturing of bis-GMA. BPA may react with two GMA to produce bis-GMA. DGEBA is a reaction product of BPA and epichlorhydrin. Then, DGEBA is used as a raw material to react with two methacrylic acid to produce bis-GMA. *Abbreviation*: DGEBA, bisphenol A diglycidyl ether.

To simplify the scenario, we may take our minds off the chemicals for a moment. Resin composites may be divided into structural compartments. Studies in a calibrated in vitro experimental design suggested the liquid resin used in enamel adhesion is the most irritating component of a resin composite, followed by OIL in the first six days after the resin composite is cured [43, 44]. The leaching of residual monomers of a resin composite plays a lesser role in the early toxic profile of the resin composite [44]. In other words, if BPA is to be found in a minute concentration in a dental composite, it is most likely to be found in the liquid resin, followed by OIL and leaching components of the resin composite [37].

From a structural point of view, we may assume that the unpolymerized chemicals, including BPA, identified in dental composites are from the three structural sources below. They are listed according to their abundance and availability of unpolymerized chemicals [37]:

- Liquid resin
- OIL on the outside surface of the dental composite
- Leaching residual components and possibly OIL lining the air bubbles inside the bulk of the dental composite

5.3.2 Hypersensitivity

A hypersensitive reaction may be graphically represented by curve 2 in Fig. 5.1. With a minute dose of an allergen, for example, d3, an exaggerated response may be provoked. BPA and DGEBA are potent allergens [45, 46]. A type IV hypersensitivity reaction is possible to be elicited by these chemicals in "at risk" patients and dental personnel (Fig. 5.7). It is characterized by eczematous lesions on the skin, classically appearing a few days after direct contact of the skin to the allergen [47].

Figure 5.7 Allergic contact dermatitis happened on the back of the right hand of a sensitized clinician. The hand instrument was clean on the back of the gloved hand. Allergic contact dermatitis happened a few days later. Clinical presentations include redness, swelling, breach of the skin barrier to secondary infection, and intense itchiness. Due to secondary infection, topical steroids cannot be used to cure the lesion. The clinical had to abstain from work for three weeks to allow healing of the lesion in the absence of the allergen.

Sensitization of an individual requires the contact allergen to penetrate the skin epithelium as low-molecular-weight haptens

and to bind to a small carrier protein in the skin epithelium [48]. Langerhans cells in the skin epithelium may phagocytose the complete antigen and present it to the immune system [48]. Complex cellular and humoral reactions give rise to sensitized T lymphocytes [48]. Direct skin contact to even a minute dose of the allergen will activate an overwhelming immune response. However, the clinical presentation of a type IV reaction may vary (Fig. 5.8). One of the reasons is the incomplete understanding of hypersensitivity reactions. The broad classification of all allergies into four types inevitably gives rise to eccentric clinical signs and symptoms that may not fall into any of these four classes (Fig. 5.8). Another hypothesis suggested long-term low-grade irritation may stimulate skin epithelial cells to secret cytokines to recruit T cells to mediate tissue damage similar to that of the classical hapten-carrier protein sensitization pathway of type IV reactions [49]. However, clinical allergic contact dermatitis is characterized by a delayed reaction, a minute amount of the provoking agent, and a positive patch test result to the allergen [48].

Figure 5.8 Ten years later, recurrence of allergic contact dermatitis happened in a remote location from the hands in the same clinician, that is, left and right eyelids. Accidental fingertip contact with a dental resin was quickly cleaned with a detergent. A delayed type IV reaction happened a few days later. It is not sure if the allergens were carried to the eyelids from the fingertips or via other pathways. The condition was cured with a brief period of 1% hydrocortisone ointment, topical application two times per day.

In Northern European countries, where allergies are prevalent, allergic contact dermatitis is much more readily observed among dental personnel [50–52]. In these countries, occupational dermatoses once happened in 43% of workers in the epoxy industry [53]. On a population basis, there was an increasing trend of epoxy allergy among the population of Malmö over a 20-year period [54].

Almost 20% of dental technicians were reported to suffer from dermatitis in Sweden, Finland, and Denmark [55, 56]. In Norway, a stratified series of studies indicated that 20–27% of general dentists and periodontists suffered from dermatitis on their hands [57]. Now, 40–43% in the same condition were reported to be dental technicians and orthodontists [57]. Although dry weather and hand scrubbing with soap may explain the skin problems of general dentists and periodontists in Norway, the extra incidence of such problems among dental technicians and orthodontists can only be explained by their daily use of polymeric biomaterials, especially dental resin composites [37].

Mucosal lichenoid lesions in patients had been related to resin composites [58]. Occasional patient case reports had demonstrated positive bis-GMA and epoxy resins and negative nickel and latex patch test results [59]. Only two case series of 41 and 7 patients were reported to relate to bis-GMA and epoxy resins [60, 61]. The significantly lower incidence of type IV reactions among patients other than Scandinavian clinicians is assumed to be related to the protective buffering effect and continuous flow of saliva [37].

Hypersentivity refers to a full-blown disease trigger by a tiny amount of allergen in sensitized individuals. This clinical picture apparently does not fit Paracelsian toxicology. Allergy, as a non-Paracelsian side effect of a dental resin composite, makes the identification of the allergen very difficult. Diagnosis is usually by exclusion of negative patch test results to common allergens. Even if the allergen is identified as BPA or DGEBA, at present, it is not known if resin composite triggered hypersentivity still follows a dose-dependent effect at an extremely low dose range, that is, from 0 to d3 in Fig. 5.1, but beyond the detection of modern technology OR the mechanism of hypersensitivity due to BPA and/or DGEBA requires a different strategy to study.

5.3.3 Other Medical Issues

Whilst it is clear-cut that a tiny dose may trigger the maximum effect in hypersensitivity of sensitized individuals, some controversial medical issues of BPA are best examples of long-term low-dose side effects of biomaterials in a larger population. These medical issues are often denied by experts in their clinical fields with the dose-dependent reasoning, that is, a dose below NOAEL is not going to cause any problem [62].

BPA is manufactured and used worldwide. It is known since the 1930s as a weak estrogen mimic [63]. NOAEL is set at 50 mg/kg/day in humans [62]. In humans, BPA may exist in blood as free BPA and glucuronic acid (in the liver)–conjugated BPA (BPAG) [26]. Free BPA is the active form that mimics estrogen's hormonal activity. BPAG is hormonally inactive. In animals, BPA is not conjugated. However, this protective mechanism in human infants is not as efficient as in adults [64].

The salivary extract of patients with dental resins was found to cause estrogenic proliferation in breast cancer cells in vitro [65]. The same group of researchers later detected BPA content in commercial products of dental resin composites in their laboratory [39].

Recent controversies around BPA started in 1997, when a research group, on an NIH grant, reported significant prostate enlargement in male mice offspring whose mother had been fed 2 μg/kg/day during pregnancy [66]. The same group repeated the study on pregnant mice with 10 μg/kg/day with a similar result [67]. The group concluded that acceleration in the rate of proliferation of the prostate epithelium during fetal life by small amounts of estrogenic chemicals could permanently disrupt cellular control systems and predispose the prostate to disease in adulthood [67]. In another study, 2.4 μg/kg/day of BPA was fed to pregnant mice from day 11 to 17 of gestation [68]. Female offspring become significantly overweight and started their first vaginal estrus significantly earlier compared to controls. An independent study on a nematode model suggested that BPA interfered with certain DNA repair processes and also damaged chromosomes in sex cell precursors [69].

Another independent study in mice at peripubertal age fed with 0.025–0.25 μg/kg/day of BPA resulted in persistent morphological alterations of two sites of mammary glands where cancer arises in

humans and rodents [70]. An epigenetic study of female mice fed with BPA before conception, during pregnancy, and during nursing of their offspring resulted in their giving birth to a significantly higher proportion of obesity-, diabetes-, and cancer-prone traits of mice [71]. BPA brought changes in the mother mice's germ line cells before conception, although BPA's effect can be reversed by dietary folic acid or genistein [71].

Statistical analysis of the National Health and Nutrition Examination Survey (NHANES) 2003–2004 data of 1455 adults with measurements of urinary BPA content had also suggested that higher BPA content is related to cardiovascular disorders, diabetes, and abnormal liver enzyme levels [72]. Although the method used in this study to study diabetes was in dispute, this group analyzed NHANES 2005–2006 data and concluded that high BPA exposure is consistently associated with reported heart disease in the general adult population of the U.S. [73].

In animals, these studies suggested the estrogen-mimicking effect of BPA may mediate carcinogenesis of breast and/or other cancers, offspring mutation, and metabolic disorders.

A relatively small number of studies have opposite findings. Tyl et al. reported no effect of BPA on the reproductive process in three generations of CD Sprague–Dawley rats [74]. Six years later, they reported no effect of BPA on the reproductive process in two generations of CD-1 mice [75].

Vom Saal argued that BPA as xenoestrogen works to modify cellular activities at an extremely low dose, not in the range of parts per billion but parts per trillion [76]. Another expert also voiced her worry of the potential relationship between the ever-increasing incidences of estrogen-related illness and widespread exposure of humans to BPA at a low dose [24].

Realms of papers had investigated the effect of BPA in animals at an extremely low dose as if it is in the range of hormone concentration in the human bloodstream. Such papers had reached a number that a meeting, called by the NIH, the Environmental Protection Agency, the National Institute of Environmental Health Science, and the National Institute of Dental and Craniofacial Research, was held at Chapel Hill, North Carolina, USA, in 2006 to allow 38 BPA experts to review existing evidence of BPA's adverse effects. They reviewed more than 700 studies of low-dose BPA.

The conclusions were as follows [77]:

- Molecular mechanisms of BPA in humans and animals are essentially identical.
- Human and animal cells respond to very low doses of exposure because of BPA's interaction with estrogen receptors on the cell membrane at or below a BPA dose range of parts per trillion.
- BPA doses, in animals, related to health issues are lower than the free-BPA level in human blood by enzyme-linked immunosorbent assay (ELISA) testing and mass spectrometry.

So far, the FDA has announced insufficient evidence to prompt for the regulation of human exposure to BPA [78].

Controversies of this sort would require a lot more research to settle. The National Institute of Environmental Health Sciences had allocated $30 million in research to clarify the controversies around BPA [25, 26]. Even the FDA announced no health threat related to BPA, France and Denmark banned baby milk bottles made of a BPA-leaching polycarbonate, due to the immature protection mechanism of infants to BPA [28]. This ban was endorsed by the European Union (EU) in 2011 to all EU member countries [28].

Canada had banned BPA-leaching baby bottles for the same reason in 2009 [26]. To date, a number of states in the U.S. have banned BPA-leaching baby bottles [26]. However, Oregon has not banned BPA-leaching baby bottles [26]. The ADA's standpoint on the BPA issue in dental resin composites is the same as the FDA's [41].

5.4 Three Levels of Testing

This part of biocompatibility is confusing. It includes a legal component and a technical testing component. The legal part of testing may vary between countries. Tests have, however, for a long time been summarized into three levels, that is, primary (in vitro test), secondary (animal test), and usage (clinical trial) [79, 80]. Unfortunately, no part seems to fit the study of dose-dependent or low-dose effects. It is not the intention here to go into the technical details of all these tests. Details of the techniques of these tests can be found in 20 directives of ISO 10993 [81].

The *three rationales* behind testing biomaterials are suggested as follows [80]:

- To identify those untoward reactions that may lead to material failure or that may express themselves in the form of clinical disease
- To determine whether devices constructed of new materials function, as they are designed to, under simulated conditions of use
- To test new concepts

For these reasons, it was believed nine areas of the biological properties of biomaterials are worth to assess (Table 5.4) [80].

Table 5.4 Summary of tests available for the untoward effects of oral biomaterials

Untoward effects	Suggested tests	Level	Relevance/ reproducibility[I]
1. Irritation[II]	Animal or human cell culture, animal	1°	–/?
	skin test, ocular irritation test , e.g., rabbit, oral epithelial test in humans	2°	+/?
		3°	++/?
2. Inflammation[III]	Tissue implantation tests in animals, e.g., rat, rabbit	2°	+/?

[I]Little is known of the reproducibility of all these tests.

[II]This is probably the most widely published part of biocompatibility testing. Mouse and human fibroblasts and/or epithelial cell cultures are often used. The cell viability of cell culture assessed by a variety of assays is usually reported as cytotoxicity of biomaterials after their exposure to cell culture. Animal skin and ocular studies are more costly than cell culture, and they need an ethical approval. Relevance of animal studies is higher, yet it is not as good as clinical trials, making ethical implications of animal studies questionable. Human studies are relevant, costly, and time consuming, and the data may be difficult to interpret due to the existence of a large number of possible confounding factors.

[III]Different animal models are good for different aspects of inflammatory reactions, for example, rat for polymorphonuclear cells and rabbit for mononuclear cell reactions. Depending on the site of implantation, the inflammatory response of the same material may give rise to different pathohistological results. Bearing in mind that humans have a lower inflammatory response than rabbits and with experienced interpretation of test results, they may give relevant meaning to the inflammatory potential of biomaterials.

(*Continued*)

Table 5.4 (*Continued*)

Untoward effects	Suggested tests	Level	Relevance/ reproducibility[I]
3. Pyrogenicity[IV]	Rabbit test, LAL test	2°	–/?
4. Systemic toxicity[V]	Animal study of acute LD50	2°	–/?
5. Sensitization[VI]	Lymphocyte inhibition tests in animals for nickel allergy	2°	+/?
	Patch test in animals or humans	2°–3°	+/?
6. Mutagenicity[VII]	Ames test, HPRT test	1°	–/?
7. Carcinogenicity[VIII]	Rodent animal model	2°	–/?

[IV]Pyrogenicity means the property of a biomaterial to cause fever. It refers not to the mild elevation of temperature due to inflammation but to bacteria- or virus-induced fever. A biomaterial that tends to trap fever-inducing agents may be assessed this way. Tests listed in Table 5.4 have little relevance to humans as rabbits are much less sensitive to fever than humans. LAL is the clotting of horse shoe crab's blood by microorganisms. These test results need careful interpretation for their meaning.

[V]Systemic toxicity is usually assessed by acute LD50 of a biomaterial in an animal model. Due to ethical reasons, only animals can be used after careful planning and ethical approval of the appropriate organization. Extrapolation of the dose leading to LD50 to humans is only based on a hypothetical model.

[VI]The sensitization test for Ni (nickel) is based on the fact that sensitized animals show significantly more inflammatory cells and macrophages than unsensitized animals in the presence of nickel. In extreme cases, nickel may cause tissue necrosis and lymphocyte migration inhibition. A patch test on the skin of animals and humans may be performed not only with nickel but also with all sorts of possible allergens.

[VII]The mutagenic potential of a biomaterial is believed to demonstrate a change in the molecular activity at the DNA level. The Ames test makes use of histidine-deprived cell culture to support bacteria. Upon stimulation of a mutagenic biomaterial, bacteria may mutate to be able to grow into colonies in the absence of histidine. HPRT is an enzyme encode by a gene. Alteration of the HPRT gene by a mutagen will give rise to a change in the production level and quality of the enzyme. However, mutagenicity based on isolated parts of the genome, of bacteria, cell cultures, or animals, cannot be a complete picture of the mutagenic potential of a biomaterial in humans.

[VIII]Carcinogenicity of biomaterials may be demonstrated by implantation of a biomaterial into a rodent animal model. The life span of rodent is long enough to show such change. Cancerous development around the biomaterial may imply the carcinogenic property of that biomaterial. However, in general, humans are much more resistant to cancer development than rodents.

Untoward effects	Suggested tests	Level	Relevance/ reproducibility[I]
8. Interaction with blood[IX]	Lee–White clotting time	1°	–/?
9. Reaction to foreign particles[X]	Animal study on all aspects of foreign bodies, including inflammatory, sensitization, acute, and chronic systemic toxicities	2°	–/?

[IX]The blood reaction to a biomaterial is usually relevant only to a biomaterial in contact with blood in situ, for example, prosthetic heart valves or dental implants. The aim is to assess the biomaterial's properties to induce hemolysis, thrombosis, and embolism. The Lee–White test is the classic way, with many other modifications, which rolls whole blood on a biomaterial surface and measures the time required for gelling of the blood. This test usually gives a more exaggerated result than reality as the blood-clotting cascade is activated the moment it is drawn out of the body of animals or humans.

[X]Foreign-body reactions in all fronts are studies in animal models with a larger amount of foreign bodies. This happens in surgical packing of deeper wounds. It is not easy to identify suitable animal models and is more difficult to sort out all reactions to foreign bodies.

1° = primary test; 2° = secondary test; 3° = usage test; ++ = relevant; + = relevant in a specific aspect only; – = not relevant; and ? = uncertain.

Abbreviations: LAL, *Limulus* amebocyte lysate; HPRT, hypoxanthine-guanine phosphoribosyltransferase.

5.4.1 Test Design and Reproducibility

The regulations of biomaterials started in the 1930s in the U.S., the 1950s in Japan, and slightly later in Australia and New Zealand [80]. Regulations of the EU started since its inception, and it is still evolving. Most of the technical aspects of biocompatibility tests remain similar to that of the 1980s. Relevance of primary and secondary tests is often compromised by conflicting data [44, 82]. Reproducibility of tests is not usually addressed. Cytotoxicity tests based on agar onlays (sometimes call agar overlays) are a good starting point (Fig. 5.9) to illustrate the deficiencies of primary and secondary tests and to seek for solutions to these problems.

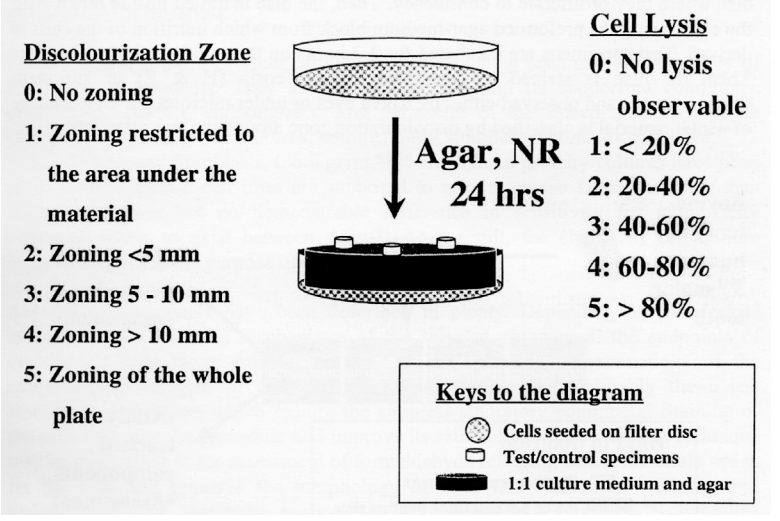

Figure 5.9 Schematic representation of the agar onlay test. Cells are seeded in a petri dish and allowed to proliferate to confluency under appropriate conditions. The culture is stained with NR. A warm agar medium mixture is syringed into the petri dish, where it solidifies. The test specimens are incubated on the agar for at least 24 hours. The cytotoxic property of the test material may be classified arbitrarily by the discoloration zone around the material or the extent of cell lysis under the microscope in the discoloration zone. *Abbreviation*: NR, neutral red.

The agar onlay test (Fig. 5.9) is easy to use and costs less than animal or human studies [83]. However, NR is a phototoxin. The laboratory procedure has to be carried out in dark. Although low-temperature agar has replaced the hot agar used in the past, the elevated temperature of molten agar may still pose a threat to the cell viability of the agar onlay test. The weight of agar on the cells is not a desirable feature of this early widely used technique in the study of the irritation potential of oral biomaterials. At least, these three factors may contribute to a certain degree of inherent cytotoxicity. It seems that the background cytotoxicity is exposed equally much to all test and control groups of the biomaterial, resulting in a still fair and scientific comparison between the test and control groups of the tested biomaterial. However, it is unreasonable to adhere strictly to the conventional agar onlay test instead of making use of modern

technology to overcome weight-, dye-, and heat-induced cytotoxicity. In fact, the Millipore™ test (Fig. 5.10) was an attempt to get rid of, at least part of, background cytotoxicity.

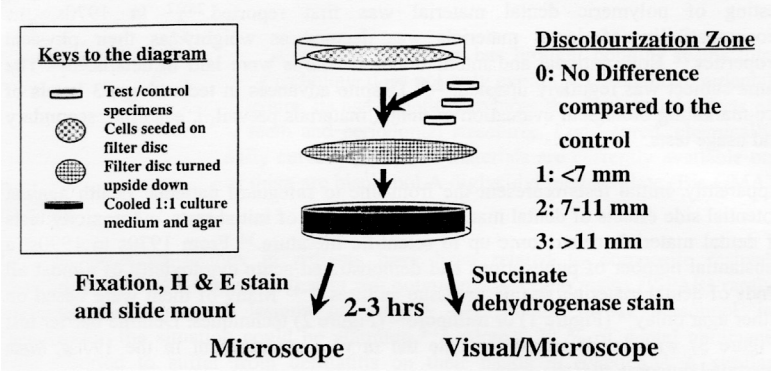

Figure 5.10 Schematic representation of the Millipore™ test. Cells are seeded on a millipore disc, where they proliferate to confluency. Then, the disc is turned upside down, with the cells facing the preformed agar medium block from which nutrition of cells is derived. Test specimens are incubated for two to three hours on the cell-free side of the disc. Then, the disc is stained by hematoxylin and eosin or succinate dehydrogenase for eyeballing or microscopic examination. The cytotoxicity of oral biomaterials is classified by the discoloration zone around the biomaterials.

The Millipore™ test had avoided the heat issue of molten agar [84]. There is also an alternative dye to the phototoxic NR. However, the weight of the oral biomaterial directly rests on the cells via the Millipore™ filter. Then, another attempt was made to handle the weight issue and simulate an in vivo environment (Fig. 5.11).

The dentine barrier test had overcome the weight problem in agar onlay and Millipore™ tests [85, 86]. However, its use is limited to restorative dental biomaterials and by the availability of human or bovine teeth. Its attempt to simulate the in vivo oral environment is also compromised by the lack of pulpal pressure, odontoblasts, nerves, and blood vessels, which have significant buffering effects in vivo.

Again, all these cell culture tests are not sufficiently assessed for their reproducibility.

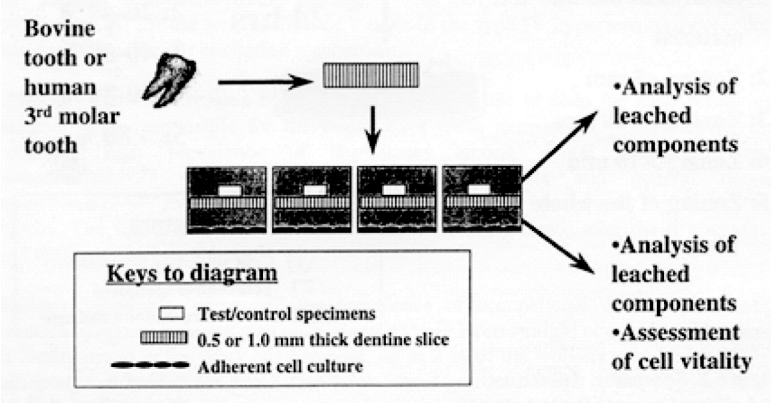

Figure 5.11 Schematic representation of the dentine barrier test. Extracted human third molars or bovine teeth are cut into slices 0.5 mm or 1.0 mm thick. They are used as partitions between two compartments of a cell culture, where test specimens are placed in one compartment and the cell culture in the other. A culture medium is used to fill the chambers. Upon assaying, both leached components and cell viability may be assessed.

5.4.2 Reproducibility and Relevance of in vitro Cytotoxicity

Most in vitro tests should regard reproducibility as the top priority in their design [37]. The cell culture in use should not be toxic in the first hand [37]. It is not only that background cytotoxicity is undesirable in a cytotoxicity test, but it also may invite errors and variations in the data obtained, thereby compromising reproducibility of the test [37].

An in vitro cell culture study had taken the following steps to calibrate an in vitro test before its use in the cytotoxicity testing of a resin composite [43]. It may not be the only way to tackle the reproducibility and relevance issues of cytotoxicity, but it is a convenient, economical, and relatively quick way to obtain some baseline data of the irritation potential of oral biomaterials.

5.4.2.1 Assessment of cytotoxicity of the test setting

To plan solid-phase cytotoxicity testing, direct contact of a fibroblast cell culture with an inert control material above and below the

fibroblasts, the same inert material placed in a filter-like tissue culture insert above the cell culture was compared to a plain fibroblast cell culture [43]. Cell culture plastic was used to plate monolayer fibroblasts to confluency. A cell culture insert with an 8 μm pore size perforated membrane at its bottom is in close proximity to the monolayer fibroblast culture. Both the plastic and fibroblasts are convenient and economical to keep and to use. Assessment of the cell viability make use of the ^{3}H-thymidine incorporation assay (^{3}H-TdR), the 3-[4,5-dimethylthiazol-2-yl]-2,5 diphenyl tetrazolium bromide (MTT) reduction assay, and the NR uptake assay.

It was found that both ways of direct contact of an inert control material with the cells, even below the cells, led to significant reduction in cell viability by NR and ^{3}H-TdR [43]. The solid inert control material in the tissue culture insert had comparable cell viability with a plain fibroblast cell culture. This implies a noncytotoxic experimental setting for cytotoxicity testing of biomaterials [43].

5.4.2.2 Assessment of reproducibility

Statistical comparison of data is one of the many ways to assess the reproducibility of a cell culture test [37]. In this study the coefficient of variation (CV) was used [37]. CV is equal to standard deviation divided by the mean cell viabilities by all three different types of assays. It turns out that the CV of the MTT assay in the tissue culture insert setting has the lowest value among all test settings, that is, roughly 8%, which is a good number for cell culture studies [37].

5.4.2.3 Rationalising "relevance"

First, limit our ambition [37]. In vitro experiments can never resemble in vivo environments to a satisfactory extent. To claim a material cytotoxic or noncytotoxic in vitro is not realistic. It is better to define goals of the in vitro study than seek for clinical relevance, which can never be established. One sensible way to deal with this problem is to "divide and conquer" [37]. The cytotoxic response of cell culture to solid-phase oral biomaterials depends on the relative size of the material to the number of cells, that is, cytotoxicity is the study of dose-dependent toxicology of biomaterials. The larger the material, the more likely it is cytotoxic and vice versa. If the goal is to obtain baseline data of the irritation potential of an oral

biomaterial, the size of the oral biomaterial must be titrated to give a borderline cytotoxicity to the cell culture. Then, different test groups are different structural components of the same biomaterial for cytotoxic comparison in a calibrated cell culture. Alternatively, if a biomaterial has different commercial preparations, its toxicodynamic contribution to irritation potential can be studied.

A resin composite, for example, can be divided into "inside" and "outside" compartments for its unpolymerized irritating chemical species. The "inside" holds the unpolymerized leaching components. The "outside" is a layer of OIL of unpolymerized chemicals. By assessing their relative contribution to irritation potential in a calibrated cell culture test [43, 44], this study tells that OIL gives rise to 37% extra irritation potential of the resin composite without OIL.

By comparing a light-cured resin composite and two-paste chemically cured resin composites to a liquid paste chemically cured resin composite, the former two materials without OIL are relatively "inert." In other words, a liquid resin gives rise to a substantial amount of irritation potential.

One shouldn't forget that most biomaterials are not irritating in vivo [37]. This sort of baseline data of the relative irritation potential of different compartments and/or preparations of a biomaterial is only filed for record purpose [37]. Usually, and hopefully, it shall never be of any use. If, for example, there is a need to seek for a certain chemical from unpolymerized parts of resin composites, for example, BPA, this record will enable the worker to search for this chemical in a liquid resin first, followed by OIL and leaching components. This sort of baseline data may also serve to improve on clinical techniques and modify the quality of biomaterials and/or its production [37]. Again, limit our ambitions in their applications.

5.4.3 Alternative Pathways in Biocompatibility Studies

If we see primary, secondary, and clinical trials as a normal pathway of biomaterial testing, a retrograde approach may be a relevant, cost-effective way to study the biocompatibility of oral biomaterials. This approach makes use of a voluntary patient-reporting system to a biomaterials' adverse effect database. Norway started it in 1993, Sweden in 1996, and the U.K. in 1999 [87–89]. Reporting is made easier by the recent development of Internet technology [89].

The same approach had been used for decades in the study of side effects of medicine, especially rare side effects. At the back of the country-based yearly drug book, for example, the British National Formulary, there are forms to fill out to report suspected unusual side effects of commonly used drugs. If the report is valid, the new adverse effects will be filed in the updated version of the yearly drug book.

The pitfalls that may undermine true reports to the registry are education of the population to be aware of adverse effect(s), motivation of the population to report to the registry, diagnoses of adverse effects, establishment of a cause–effect relationship of biomaterials and adverse effects, and exclusion of confounders in the cause–effect relationship of biomaterials and adverse effects. This kind of registry is more realistic in small populations that are well educated and motivated.

5.5 Concluding Remarks

Back to the definition of biocompatibility as the ability of a material to perform with an appropriate host response in a specific situation [9], biocompatibility seems to imply an appropriate host response as the only effect of oral biomaterials in hosts. Most oral biomaterials certainly obtain appropriate host responses. However, there is no mentioning of any tolerance of neither the nature nor the extent of any undesirable effects of biomaterials in this definition. Is zero tolerance assumed, then?

The toxicology study of oral biomaterials falls broadly into two categories, that is, dose-dependent and non-dose-dependent adverse effects.

Dose-dependent adverse effects of oral biomaterials are time consuming and costly to study. Amalgam, resin composites, glass ionomer materials, luting cements, etc., may be assumed to have a wide safety margin on the dose–response curve as a result of their prolonged, widespread clinical use without major acute adverse effects. To date, the use of oral biomaterials in humans does not seem to compromise the life span of the human population. In fact, the 2009 data of the World Health Organization indicated that the average life span of mankind at birth is 68 years, and if they live

up to 60 years of age, their life span on average is 79 years [90]. Most populations of developed countries, where modern dentistry is practiced on a larger scale, have been reported to have their population life span prolonged with time [90].

However, the low-dose adverse effects of oral biomaterials have not yet been studied adequately. In fact, well-established strategies or philosophies resembling those of Paracelsian toxicology for the study of low-dose adverse effects of oral biomaterials are lacking. Controversies of materials' biocompatibility often arise from contradictory evidence of Paracelsian (dose-dependent) and non-Paracelsian (low-dose) studies. Much more research with relevant strategies of biocompatibility is needed.

To fit the new challenges of discoveries in oral biomaterials, for example, BPA, the current three levels of testing of oral biomaterials need extensive updates in technological and philosophical terms.

We may conclude from these facts that at least the use of oral biomaterials does not have observable detrimental effects on the human life span. The low-dose adverse effects of oral biomaterials, especially in "at risk" individuals, are still poorly understood.

References

1. Black, J. (2006) Biocompatibilities: definitions and issues, in *Biological Performance of Materials: Fundamentals of Biocompatibility*, 3–15, (Ed. Black, J.), CRC Press, Taylor and Francis Group, Boca Raton, USA.
2. Willaims, D. (1990) *Concise Encyclopedia of Medical and Dental Materials*, 51–59 (Ed. Williams, D.), Pergamon Press, Oxford.
3. American Society of Testing and Materials, http://www.astm.org/ (Accessed on Aug. 28, 2012).
4. Williams, D. F. (1999) *The Williams Dictionary of Biomaterials*, 40 (Ed. Williams, D. F.), Liverpool University Press, Liverpool.
5. *Merriam-Webster Dictionary*, http://www.merriam-webster.com/dictionary/biocompatibility (Accessed on Aug. 28, 2012).
6. *Dorland's Medical Dictionary*, http://www.dorlands.com/wsearch.jsp?searchtype=words&searchterm=biocompatibility (Accessed on Aug. 28, 2012).
7. Wikipedia, http://en.wikipedia.org/wiki/Biocompatibility (Accessed on Aug. 28, 2012).

8. *Encyclopedia Britannica Online*, http://www.britannica.com/EBchecked/topic/65815/biocompatibility (Accessed on Aug. 28, 2012).
9. Williams, D. F. (1987) Definitions in biomaterials, in *Proceedings of a Consensus Conference of the European Society for Biomaterials*, *ESB*, Elsevier, Amsterdam.
10. Doherty, P. J., Williams, R. L., Willaims, D. F., Lee, A. J. C. (1992) Consensus report, in *Biomaterial: Tissue Interfaces. Advances in Biomaterials*, 525–533 (Ed. Willaims, D. F., Black, J., Doherty, P. J.), Elsevier, Amsterdam.
11. Williams, D. (2003) Revisiting the definition of biocompatibility, *Med. Device Techn.*, **14**(8), 10–13.
12. Williams, D. F. (2008) On the mechanisms of biocompatibility, *Biomaterials*, **29**(20), 2941–2953.
13. Roberts, M. D. (2002) *Nothing Is Without Poison*, 1, Chinese University Press, Hong Kong.
14. Gilbert, S. G. (2012) An introduction of risk assessment, in *A Small Dose of Toxicology: The Health Effects of Common Chemicals*, 257–265 (Ed. Gilbert, S. G.), Healthy World Press, Seattle, USA.
15. National Institute of Dental and Craniofacial Research, National Institute of Health. *The Story of Fluoride*, http://www.nidcr.nih.gov/oralhealth/topics/fluoride/thestoryoffluoridation.htm (Accessed on Sep. 3, 2012).
16. Hodge, H. C. (1950) The concentration of fluorides in drinking water to give the point of minimum caries with maximum safety, *J. Am. Dent. Assoc.*, **40**(4)**,** 436–439.
17. Health and Ecological Criteria Division, Office of Water, US Environmental Protection Agency. (2010) Appendix B, benchmark dose analysis of severe fluorosis dataset of Dean 1942, in *Fluoride: Dose-Response Analysis for Non-Cancer Effects,* 127–130, USEPA, Washington DC, USA.
18. Fung, K. F., Zhang Z. Q., Wong, J. W. C., Wong, M. H. (1999) Fluoride contents in tea and soil from tea plantations and the release of fluoride into tea liquor during infusion, *Environ. Poll*, **104**, 197–205.
19. Ekstrand, J. (1996) Fluoride metabolism, in *Fluoride in Dentistry*, 55–68 (Ed. Fejerskov, O., Ekstrand, J., Burt, B. A.), Munksgaard, Copenhagen.
20. Fawell, J., Bailey, K., Chilton, J., Dahi, E., Fewtrell L., Magara, Y. (2006) Environmental occurrence, geochemistry and exposure, in *Fluoride in Drinking-Water*, 5–28, IWA, London.

21. Dean, H. T., Arnold, F. A., Elvove, E. (1942) Domestic water and dental caries, *Pub. Health Rep.*, **57**, 1151–1194.
22. Thylstrup, A., Fejerskov, O. (1978) Clinical appearance of dental fluorosis in permanent teeth in relation to histological changes, *Commun. Oral Epidemiol.*, **6**, 315–328.
23. Horowitz, H. S., Driscoll, W. S., Meyers, R. J., Heifetz, S. B., Kingman, A. (1984) A new method for assessing the prevalence of dental fluorosis: the tooth surface index of fluorosis, *J. Am. Dent. Assoc.*, **109**, 37–41.
24. Trubo, R. (2005) Endocrine-disrupting chemicals probed as potential pathways to illness, *J. Am. Med. Assoc.*, **294**, 291–293.
25. Reuben, S. H. (2010) *Reducing Environmental Cancer Risk: What We Can Do Now*, 1–240, US National Institute of Health.
26. US Environmental Protection Agency. *Bisphenol A Action Plan*, 1–22.
27. Welshons, W. V., Nagel, S. C. vom Saal, F. S. (2006) Large effects from small exposures. III. Endocrine mechanisms mediating effects of bisphenol A at levels of human exposure, *Endocrinology*, **147**, S56–S69.
28. European Union. (2011) *Commission Directive 2011/8/EU Amending Directive 2002/72/EC as Regards the Restriction of Use of Bisphenol A in Plastic Infant Feeding Bottles: Report No.: L 26/11*, 1–3, European Union, Brussels.
29. Calafat, A. M., Kuklenyik, Z., Reidy, J. A., Caudill, S. P., Ekong, J., Needham, L. L. (2005) Urinary concentrations of bisphenol A and 4-nonylphenol in a human reference population, *Environ. Health Perspect.*, **113**, 391–395.
30. Carwile, J. L., Ye, X., Zhou, X., Calafat, A. M., Michels, K. B. (2011) Canned soup consumption and uninary bisphenol A: a randomized crossover trial, *J. Am. Med. Assoc.*, **306**, 2218–2219.
31. Antonucci, J. M., Toth, E. E. (1983) Extent of polymerization of dental resin by differential scanning calorimetry, *J. Dent. Res.*, **62**, 121–125.
32. Asmussen, E. (1982) Factors affecting the quantity of remaining double bonds in restorative resin polymers, *Scand. J. Dent. Res.,* **90**, 490–496.
33. Chung, K., Greener, E. H. (1988) Degree of conversion of seven light-cured posterior composites, *J. Oral Rehabil.*, **15**, 555–560.
34. Ruyter, I. E., Øysæd, H. (1982) Conversion in different depths of ultra-violet and visible light activated composite materials, *Acta Odontol. Scand.*, **40**, 179–192.
35. Ruyter, I. E. (1981) Unpolymerized surface layers on sealants, *Acta Odontol. Scand.*, **39**, 27–32.

36. Tang, A. T. H., Björkman, L., Ekstrand J. (2000) New filling materials: an occupational hazard to dental staff, *Ann. R. Australas. Coll. Dent. Surg.*, **15**, 102–105.

37. Tang, A. T. H. (2000) *The Role of Liquid Resin in Orthodontic Bonding: Toxicological, Bond Strength and Clinical Aspects*, 1–37, PhD thesis, Karolinska Institutet, Stockholm.

38. Geurtsen, W. (2000) Biocompatibility of resin-modifies filling materials, *Crit. Rev. Oral Biol. Med.*, **11**, 333–355.

39. Pulgar, R., Olea-Serrano, M. F., Novillo-Fertrell, A., Rivas, A., Pazos, P., Pedraza, V., Navajas, J. M., Olea, N. (2000) Determination of bisphenol A and related aromatic compounds released from bis-GMA-based composites and sealants by high performance liquid chromatography, *Environ. Health Perspect.*, **108**, 21–27.

40. Donovan, W. J. (2010) *Letter to dental professional*, 1, 3M ESPE, St. Paul.

41. American Dental Association. (2010) *Bisphenol A and Dental Materials*, http://www.ada.org/1766.aspx (Accessed on Dec. 30, 2012).

42. Fleisch, A. F., Sheffield, P. E., Chinn, C., Edelstein, B. L., Landrigan, P. J. (2010) Bisphenol A and related compounds in dental materials, *Pediatrics*, **126**, 760–768.

43. Tang, A. T., Li, J., Ekstrand, J., Liu, Y. (1999) Cytotoxicity tests of in situ polymerized resins: methodological comparisons and introduction of a tissue culture insert as a testing device, *J. Biomed. Mater. Res.*, **45**, 214–222.

44. Tang, A. T., Liu, Y., Bjorkman, L., Ekstrand, J. (1999) In vitro cytotoxicity of orthodontic bonding resins on human oral fibroblasts, *Am. J. Orthod. Dentofac. Orthop.*, **116**, 132–138.

45. Cronin, E. (1980) Plastics, in *Contact Dermatitis*, 575–663 (Ed. Cronin, E.), Churchill Livingstone, Edinburgh.

46. Fregert, S., Thorgeirsson, A. (1977) Patch testing with low molecular oligomers of epoxy resins in human, *Contact Dermatitis*, **3**, 301–303.

47. Fregert, S. (1986) Contact allergens and prevention of contact dermatitis*, J. Allergy Clin. Immunol.,* **78**, 1071–1072.

48. Rozman, T. A., Straube, M., Rozman, K. K. (2008) Organ toxicology: the skin, in *Toxicology and Risk Assessment: A Comprehensive Introduction*, 279–294 (Ed. Greim, H., Snyder R.), John Wiley & Sons, West Sussex.

49. Patrick, E., Maibach, H. I., Burkhalter, A. (1985) Mechanisms of chemically induced skin irritation. 1. Studies of time course, dose response, and components of inflammation in the laboratory mouse, *Toxicol. Appl. Phamacol.*, **81**, 476–490.

50. Jacobsen, N., Aasenden, R., Hensten-Pettersen, A. (1991) Occupational health complaints and adverse patient reactions as perceived by personnel in public dentistry, *Commun. Dent. Oral Epidemiol.*, **19**, 155–159.

51. Jacobsen, N., Hensten-Pettersen, A. (1989) Occupational health problems and adverse patient reaction s in orthodontics, *Eur. J. Orthod.*, **11**, 254–264.

52. Kallus, T., Mjör, I. A. (1991) Incidence of adverse effects of dental materials, *Scand. J. Dent. Res.*, **99**, 236–240.

53. International Labour Office. (1971) *Encyclopedia of Occupational Health and Safety*, 469, McGraw-Hill, New York, USA.

54. Edman, B. (1988) *Computerized Patch Test Data in Contact Allergy*, 1–112, PhD thesis, University of Lund, Sweden.

55. Lönnroth, E.-C., Shahnavaz, H. (1998) Hand dermatitis and symptoms from the fingers among Swedish dental personnel, *Swedish Dent. J.*, **22**, 23–32.

56. Munksgaard, E. C., Hansen, E. K., Engen, T., Holm, U. (1996) Self-reported occupational dermatological reactions among Danish dentists, *Eur. J. Oral Sci.,* **104**, 396–402.

57. Hensten-Pettersen, A., Jacobsen, N. (1990) The role of biomaterials as occupational hazards in dentistry, *Int. Dent. J.*, **40**, 159–166.

58. Lind, P. O. (1988) Oral lichenoid reactions related to composite restorations. Preliminary report, *Acta Odontol. Scand.,* **46**, 63–65.

59. Connolly, M., Shaw, L., Hutchinson, I., Ireland, A. J., Dunnill, M. G. S., Sansom, J. E. (2006) Allergic contact dermatitis from bisphenol-A-glycidyldimethacrylate during application of orthodontic fixed appliance, *Contact Dermatitis*, **55**, 367–368.

60. Kanerva, L., Jolanki, R., Estlander, T. (1986) Occupational dermatitis due to an epoxy acrylate, *Contact Dermatitis*, **14**, 80–84.

61. Lee, H. N., Pokorny, C. D., Law, S., Pratt, M., Sasseville, D., Storrs, F. J. (2002) Crossreactivity among epoxy acrylates and bisphenol F epoxy resins in patients with bisphenol A epoxy resin sensitivity, *Am. J. Contact Dermat.*, **13**(3)**,** 108–115.

62. Degen, G. H., Owens, J. W. (2008) Toxicity of selected chemicals: xenoestrogen and xenoantiandrogens, in *Toxicology and Risk Assessment: A Comprehensive Introduction*, 583–603 (Ed. Greim, H., Snyder R.), John Wiley & Sons, West Sussex.

63. Dodds, E. C., Lawson, W. (1936) Synthetic oestrogenic agents without without the phenanthrene nucleus, *Nature*, **137**, p. 996.

64. Calafat, A. M., Weuve, J., Ye, X., Jia, L. T., Hu, H., Ringer, S., Huttner, K., Hause, R. (2009) Exposure to bisphenol A and other phenols in neonatal intensive care unit premature infants, *Environ. Health Perspect.*, **117**, 639–644.

65. Olea, N., Pulgar, R., Perez, P., Olea-Serrano, F., Rivas, A., Novillo-Fertrell, A., Pedraza, V., Soto, A. M., Sonnenschein, C. (1996) Estrogenicity of resin-based composites and sealants used in dentistry, *Environ. Health Perspect*, **104**, 298–305.

66. Nagel, S. C., vom Saal, F. S., Thayer, K. A., Dhar, M. G., Boechler, M., Welshons, W. V. (1997) Relative binding affinity-serum modified access (RBA-SMA) assay predicts the relative in vivo bioactivity of the xeno-estrogens bisphenol A and octylphenol, *Environ. Health Perspect*, **105**, 70–76.

67. Timms, B. G., Howdeshell, K. L., Barton, L., Bradley, S., Richter, C. A., vom Saal, F. S. (2005) Estrogenic chemicals in plastic and oral contraceptives disrupt development of the fetal mouse prostate and urethra, *Proc. Natl. Acad. Sci.*, **102**, 7014–7019.

68. Howdeshell, K. L., Hotchkiss, A. K., Thayer, K. A., Vandenbergh, J. G. vom Saal, F. S. (1999) Exposure to bisphenol A advances puberty, *Nature*, **401**, 763–764.

69. Allard, P., Colaiácovo, M. P. (2010) Bisphenol A impairs the double-strand break repair machinery in the germline and causes chromosome abnormalities, *Proc. Natl. Acad. Sci.*, **107**, 20405–20410.

70. Munoz-de-Toro, M., Markey, C. M., Wadia, P. R., Luque, E. H., Rubin, B. S., Sonnenschein, C., Soto, A. M. (2005) Perinatal exposure to bisphenol-A alters peripubertal mammary gland development in mice, *Endocrinology,* **146**, 4138–4147.

71. Dolinoy, D. C., Huang, D., Jirtle, R. L. (2007) Maternal nutrient supplementation counteracts bisphenol A-induced DNA hypomethylation in early development, *Proc. Natl. Acad. Sci.*, **104**, 13056–13061.

72. Lang, I. A., Galloway, T. S., Scarlett, A., Henley, W. E., Depledge, M., Wallace, R. B., Melzer, D. (2008) Association of urinary bisphenol A concentration with medical disorders and laboratory abnormalities in adults, *J. Am. Med. Assoc.*, **300**, 1303–1310.

73. Melzer, D., Rice, N. E., Lewis, C., Henley, W. E., Galloway, T. S. (2010) Association of urinary bisphenol A concentration with heart disease: evidence from NHANES 2003/06, *PLOS 1*, http://www.plosone.org/article/info%3Adoi%2F10.1371%2Fjournal.pone.0008673 (Accessed on Dec. 30, 2012).

74. Tyl, R. W., Myers, C. B., Marr, M. C., Thomas, B. F., Keimowitz, A. R., Brine, D. R., Veselica, M. M., Fail, P. A., Chang, T. Y., Seely, J. C., Joiner, R. L., Butala, J. H., Dimond, S. S., Cagen, S. Z., Shiotsuka, R. N., Stropp, G. D., Waechter J. M. (2002) Three-generation reproductive toxicity study of dietary bisphenol A in CD Sprague-Dawley rats, *Toxicol. Sci.*, **68**, 121–146.

75. Tyl, R. W., Myers, C. B., Marr, M. C., Sloan, C. S., Castillo, N. P., Veselica, M. M., Seely, J. C., Dimond, S. S., van Miller, J. P., Shiotsuka, R. N., Beyer, D., Hentges, S. G., Waechter, J. M. (2008) Two-generation reproductive toxicity study of dietary bisphenol A in CD-1 (Swiss) mice, *Toxicol. Sci.*, **104**(2), 362–384.

76. Keuhn, B. M. (2007) Expert panels weigh bisphenol-A risks, *J. Am. Med. Assoc.*, **298**, 1499–1503.

77. vom Saal, F. S., Akingbemi, B. T., Belcher, S. M., Birnbaum, L. S., Crain, D. A., Eriksen, M., Farabollini, F., Guillette, L. J., Jr., Hauser, R., Heindel, J. J., Ho, S. M., Hunt, P. A., Iguchi, T., Jobling, S., Kanno, J., Keri, R. A., Knudsen, K. E., Laufer, H., LeBlanc, G. A., Marcus, M., McLachlan, J. A., Myers, J. P., Nadal, A., Newbold, R. R., Olea, N., Prins, G. S., Richter, C. A., Rubin, B. S., Sonnenschein, C., Soto, A. M., Talsness, C. E., Vandenbergh, J. G., Vandenberg, L. N., Walser-Kuntz, D. R., Watson, C. S., Welshons, W. V., Wetherill, Y., Zoeller, R. T. (2007) Chapel Hill bisphenol A expert panel consensus statement: integration of mechanisms, effects in animals and potential to impact human health at current levels of exposure, *Reprod. Toxicol.*, **24**, 131–138.

78. Mitka, M. (2012) Endocrine Society seeks better testing to determine endocrine disruptor health risks, *J. Am. Med. Assoc.*, **308**, 556–557.

79. Williams, D. F. (1986) Introduction to biocompatibility testing, in *Techniques of Biocompatibility Testing*, Vol. 1, 1–4 (Ed. Williams, D. F.), CRC Press, Boca Raton, FL, USA.

80. Lord, G. H. (1986) Regulations and reasons for biocompatibility testing, in *Techniques of Biocompatibility Testing*, Vol. 1, 5–34 (Ed. Williams, D. F.), CRC Press, Boca Raton, FL, USA.

81. International Organization for Standardization. *ISO 10993-1 to 10993-20. Biological Evaluation of Medical Devices*, ISO, Geneva.

82. Jagdish, N., Padmanabhan, S., Chitharanjan, A. B., Revathi, J., Palani, G., Sambasivam, M., Sheriff, K., Saravanamurali, K. (2009) Cytotoxicity and degree of conversion of orthodontic adhesives, *Angle Orthod.*, **79**, 1133–1138.

83. Guess, W. L., Rosenbluth, S. A., Schmidt, B., Autian, J. (1965) Agar diffusion method for toxicity screening of plastics on cultured cell monolayers, *J. Pharm. Sci.*, **54**, 1545–1547.

84. Wennberg, A., Hasselgren, G., Tronstad, L. (1979) A method for toxicity screening of biomaterials using cells cultured on millipore filters, *J. Biomed. Mater. Res.*, **13**, 109–120.
85. Tyas, M. J Browne R. M. (1977) Biological testing of dental restorative materials, *J. Oral Rehabil.*, **4,** 275–290.
86. Browne R. M., Tyas, M. J. (1979) Biological testing of dental restorative materials in vitro: a review, *J. Oral Rehabil.*, **6**, 365–374.
87. Norwegian Dental Biomaterials Adverse Reaction Unit. *Dental Biomaterials: Reporting of Adverse Reactions; Information on Reporting of Adverse Reactions (Side-Effects) Observed with Dental Materials*, http://www.uib.no/ood/advrep/MAIN-Advrep.html (Accessed on Dec. 30, 2012).
88. Swedish Medical Products Agency. *National Register on Side-Effects of Dental Materials*, http://www.lakemedelsverket.se/english/ (Accessed on Dec. 30, 2012).
89. UK Adverse Reaction Reporting Project. *National Survey of Adverse Reactions to Dental Materials*, http://arrp.group.shef.ac.uk/ (Accessed on Dec. 30, 2012).
90. World Health Organization. *Life Expectancy Data*, http://apps.who.int/ghodata/?vid=710 (Accessed on Sep. 2, 2012).

This page intentionally left blank

Chapter 6

Resin-Based Cements Used in Dentistry

William M. Palin[a] and Jack L. Ferracane[b]
[a]*Biomaterials, University of Birmingham, College of Medical and Dental Sciences, School of Dentistry, St. Chads Queensway, Birmingham, B4 6NN, UK*
[b]*Department of Restorative Dentistry, Division of Biomaterials and Biomechanics, Oregon Health & Science University, 611 S.W. Campus Drive, Portland, OR 97239, USA*
w.m.palin@bham.ac.uk, ferracan@ohsu.edu

A dental cement must exhibit key properties that are essential for acceptable performance in situ. The cement material should deliver structural integrity to the entire restoration by providing reliable bond strengths through micromechanical retention and/or chemical adhesion with appropriate low film thickness. Adequate mechanical properties such as high tensile/compressive strengths and fracture toughness and resistance to cyclic loading are required in order to withstand stress transfer without subcritical crack formation within the cement bulk and failure at the tooth–restoration interface. The material should also have low solubility in the oral environment and not illicit pulpal or postoperative sensitivity. Good rheological and handling properties are important to reduce technique sensitivity, which, alongside superior esthetic quality, is one reason for the

Handbook of Oral Biomaterials
Edited by Jukka P. Matinlinna

ISBN 978-981-4463-12-6 (Hardcover), 978-981-4463-13-3 (eBook)
www.panstanford.com

popularity of modern light-activated, single- or two-paste resin cement formulations.

6.1 Introduction and Historical Perspectives

Modern dental cements are vital to the success of indirect restorations and act as luting agents to fix prostheses to tooth tissue, including inlays, onlays, crowns, fixed partial dentures (FPDs), and orthodontic appliances. The development of cement technology has allowed great versatility for numerous applications, and as a result, the term "cement" is somewhat misleading, since these materials also act as cavity liners and bases to protect the pulp, as well as being used as direct filling restoratives.

Since the inception of cement materials in the later stages of the nineteenth century, there has been much development to improve their key material properties. From silicates and zinc phosphates to self-adhesive resins, this chapter aims to review the importance of resin-based cements—from setting chemistry, mechanisms of adhesion, physical properties, and clinical performance to future perspectives of resin technology and their possible advantages for dentistry.

6.1.1 Evolution of Dental Cements

Since the introduction of viable restorative materials such as amalgam, gold, and porcelain crowns, dental cements have been an important addition to the practitioner's armamentarium of dental materials. The first types of cements date back to the mid- to late nineteenth century, with the introduction of *zinc oxychloride* [1] later replaced by *zinc oxide eugenol* (ZOE) [2]. The work of Ames and Fleck developed the first *zinc phosphate cement*, which provided significantly improved durability and reduced pulpal irritation and similar formulations remain in use today [3, 4]. At the turn of the nineteenth century, Steenbock and Schoenbeck developed popular silicate cement types from the initial work of Fletcher in 1873, and by the 1920s, the use of silicate, zinc phosphate, and ZOE was commonplace in dental practice.

Silicate cements were also the first direct filling material that resembled the appearance of teeth and were the most commonly used anterior restorative for many decades [5] until the introduction of methyl methacrylate (MMA) polymer in the late 1940s, which, in turn, was superseded by resin-based composites in the 1960s. However, the esthetic quality of silicates was far from ideal, and high solubility resulted in poor restoration longevity. In terms of their long-term clinical history, zinc phosphate cements are considered the gold standard and remain in use as luting agents for metallic restorations and long-span FPDs, although with recent improvements of resin cement technology, they are becoming far less popular. As with most cement types, zinc phosphates are formed by the interaction of an acid, or anions in solution, with a metal oxide capable of releasing cations to form stable salt complexes (a classic acid–base reaction). Here, zinc oxide reacts with a buffered phosphoric acid solution to produce a zinc phosphate matrix (Fig. 6.1) containing ~2-8 μm diameter unreacted zinc oxide particles. A freshly mixed slurry of zinc phosphate is highly acidic (pH < 2) and will demineralize the hydroxyapatite crystals surrounding the collagen fibril network of dentinal tissue, although a typical hybrid layer (associated with effective resin-dentine adhesion) cannot be formed due to phase separation and lack of particle penetration within fibrillar interstices [6]. Thus, zinc phosphate has no adhesive affinity, and its initial acidity has also been reported to lower the reliability of strength data of feldspathic glass by extending pre-existing flaws (section 6.3.3; [7]). Moreover, the low pH (<2 newly mixed, which may take up to 48 hours to neutralize) may cause pulpal irritation. Further shortcomings include a lack of antibacterial properties, inferior solubility, and high brittleness compared to modern cementation options.

The chemistry of dental cement technology remained relatively unchanged until the pioneering work of Smith [8] and Wilson and Kent [9] and the subsequent introduction of *polyacid cements*, namely, *zinc polycarboxylate* and *glass polyalkenoate* (more commonly referred to as "glass ionomer") cements (Fig. 6.1). Polyacid matrix structures provide effective chemical bonding to tooth structure through the displacement of calcium ions in hydroxyapatite and subsequent chelation with acidic functional groups of the cement.

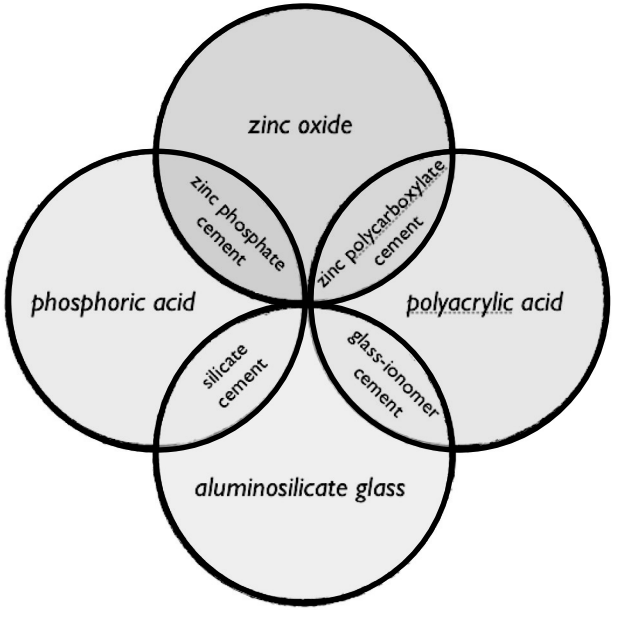

Figure 6.1 Constituents of traditional and contemporary water-based cements used in dentistry.

The formation of polycarboxylate (or polyacrylate) involves the reaction of high-molecular-weight polyalkenoic acids (~30–40%) and water with zinc oxide powder (in the case of zinc polycarboxylates) or a fluoroaluminosilicate glass (for glass ionomer cements [GICs]). Ionization of the acid attacks the zinc oxide or glass particles, creating cations that cross-link the polyacid chains to form a polycarboxylate matrix. The initial viscosity of the setting mixture is higher than that of zinc phosphate because of the high-molecular-weight organic acids, although an acceptable film thickness is achieved due to the pseudoplastic nature of the mixture. Glass ionomers exhibit superior strength characteristics and lower solubility, and their improved antibacterial properties, long-term fluoride release, and increasing cariostatic potential provide a more reasonable choice of luting agent compared to zinc polycarboxylate, especially in patients who are more susceptible to caries [10].

Several review articles have been written addressing the composition, properties, and indications for use of conventional and

resin-based cements, and the reader is referred to these for more in-depth information [11] and comprehensive review [12]. More recently, additional review articles have been written with more up-to-date information about newer resin-based cements [10, 13–15].

6.1.2 Contemporary Dental Cements

Dental cements like zinc phosphate, ZOE, zinc oxide noneugenol, and polycarboxylate are still commercially available, but the two main types of contemporary dental cements are glass ionomers and resin-based systems. Within each category are two options. Glass ionomers consist of the so-called "conventional" material, which comprises an ion-leachable glass that is mixed with a polyacrylic acid ionic polymer, or the resin-modified version, produced by essentially adding a polymerizable monomer to the conventional material. Both types of glass ionomers are capable of chemical adhesion to enamel or dentin tooth structure, although resin-modified ionomers produce a stronger bond compared to conventional types. Each of these materials has certain advantages and disadvantages, and the distinctions between them have been clarified in a recent publication [16].

Resin-based cements are essentially dental composites designed specifically for fixing indirect restorations to teeth. These materials are not chemically adhesive to the tooth structure and are typically used in conjunction with a resin-based dentin-bonding system. In contrast, the newer self-adhesive resin cements are designed to chemically and physically interact directly with the tooth, without the need for the application of a separate adhesive material. Several comprehensive reviews of these materials have been published, each providing guidance regarding their clinical use [17–19].

There is another type of cement, called compomer or polyacid-modified resin, which has properties intermediate to glass ionomers and resin-based cements. These cements behave most similarly to resin composite cements and should be used in conjunction with a dentin adhesive. These materials have been marketed for years but have achieved only limited popularity with clinicians. There are numerous brands of each type of contemporary dental cement (Table 6.1).

Table 6.1 Brands of contemporary resin-based dental cements

Resin Composite Cements		
Product	**Manufacturer**	**Cure mode**
Bistite II DC	Tokuyama	Dual
Calibra	Dentsply/Caulk	Dual/light
C&B Cement	Bisco	Self
Choice 2	Bisco	Light
Duo-link	Bisco	Dual
Duo Cement Plus	Coltene Whaledent	Dual
Illusion	Bisco	Dual
LinkMax	GC	Dual
Multilink	Ivoclar Vivadent	Self
NX 3 Nexus	Kerr	Dual/light
Panavia 21	Kuraray	Self
Panavia F 2.0	Kuraray	Dual
ParaCem	Coltene Whaldent	Dual
RelyX ARC	3M ESPE	Dual
Super Bond C&B	Sun Medical	Self
Variolink II	Ivoclar Vivadent	Dual
Self-Adhesive Resin Cements		
Product	**Manufacturer**	**Cure mode**
BisCem	Bisco	Dual
Bifix SE	Voco	Self/light
Breeze	Pentron	Dual
Clearfil SA	Kuraray	Dual
Embrace WetBond	Pulpdent	Dual
GCem	GC	Dual
iCem	Heraeus	Dual
Maxcem Elite	Kerr	Dual
Monocem	Shofu	Dual
Multilink Sprint	Ivoclar Vivadent	Dual
RelyX Unicem	3M ESPE	Dual
seT	SDI	Dual
Smart Cem 2	Dentsply	Dual
Speed Cem	Ivoclar Vivadent	Self/light

6.2 Key Material Properties of Resin Cements

6.2.1 Chemistry and Curing Mechanisms

6.2.1.1 General composition

The first types of resin cement were developed to improve handling characteristics and setting properties of contemporary acid–base materials. Conventional resin cements have been used since MMA-based materials in the 1950s and remain popular due to their ability to provide reliable adhesion between tooth and restoration and versatility with indirect procedures. Cementation of metal, ceramic, and polymer composite prostheses for crowns, fixed partial dentures (FPDs), inlays, onlays, posts, veneers, and orthodontic appliances with adhesive resin cements are routinely used in dental practice today.

Conventionally, resin cements consist of mono- or dimethacrylate monomers, similar to those used in resin composite restoratives and their counterpart adhesive systems: bisphenol-A glycol dimethacrylate (bis-GMA), ethoxylatedbisphenol-A glycol dimethacrylate (bis-EMA), and 1,6-bis(methacryloxy-2-ethoxycarbonylamino)-2,4,4-trimethylhexane (UDMA) are combined with lower-molecular-weight resins such as triethyleneglycol dimethacrylate (TEGDMA), diethyleneglycol dimethacrylate (DEGDMA), and MMA to control the degree of conversion, shrinkage, and handling properties. Some hydrophilic properties are required to allow for suitable wetting of tooth tissue. Quartz, colloidal silica, silicate glass, and ytterbium fluoride fillers are included as a 30–65% volume fraction to adjust paste rheology, provide radiopacity, leach ions (either fluoride release or to adjust pH of self-adhesive cements on setting), and provide general improvement of mechanical and physical properties of the cured cement layer.

As with resin composite adhesive systems, an important driver of cement technology development remains simplification of the application procedure to satisfy the time-efficient demands of the dentist. Composition of the cement "system" varies greatly, and key properties of the cemented prosthesis will depend upon how the cement adheres to tooth tissue. Such systems either use (1) an etch and rinse adhesive and cement, (2) a self-etching adhesive and cement, or (3) single-step "self-adhesive" cements.

Resin cements are typically "dual-curable" materials, which contain a photoinitiator (PI) system and a self-cure component that enhances their versatility and are intended to overcome the risk of undercuring in situations where effective light transport through opaque prostheses to the cement site is restricted. Separate light and chemically cured systems are available but far less common, and their selection should be entirely dependent upon the application. As with the base monomers of resin cements, conventional PI systems are used for the light-curing reaction. Generally, the Type II PI, camphoroquinone, and a tertiary aliphatic or aromatic amine coinitiator such as 2-(dimethylamino) ethyl methacrylate (DMAEMA) or ethyl 4-dimethylaminobenzoate (EDMAB) are used.

Pigments and dyes provide esthetic quality but, as with resin composite restoratives, will significantly affect curing efficiency, as they are effective light absorbers.

The redox reaction of the self-cure chemistry precludes single-paste formulations of light-cure resin cements. Traditionally, base and catalyst components were proportioned by eye and mixed together by hand. However, modern dispensers include dual syringes with a static spiral mixing lattice to reduce waste and allow reliable mixing, encapsulated systems that are mechanically mixed prior to application or a "clicker" device that dispenses accurate proportions prior to spatulation (Fig. 6.2).

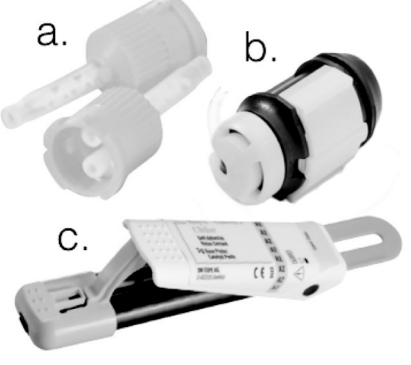

Figure 6.2 Examples of typical resin cement–dispensing devices to improve proportioning and mixing, which include (a) spiral mixing lattices, (b) capsules that are activated and mechanically mixed, and (c) a "clicker" device that dispenses a set quantity of each base and catalyst paste (3M ESPE).

6.2.1.2 Self-etch and self-adhesive composition

As well as base monomers and lower-molecular-weight crosslinking resins from the general composition, for "adhesive" resins, self-etching acid-functionalized monomers are also included to significantly reduce pH and demineralize tooth tissue to promote micromechanical adhesion. Common formulations include methacrylate monomers modified with carboxylic or phosphoric acid groups (Fig. 6.3), such as 4-methacryloyloxyethyl trimellitic anhydride (4-META) and 10-methacryloyloxydecyl dihydrogen phosphate (MDP). The first types of adhesive monomers were introduced in the 1980s by modifying bis-GMA with 4-META (e.g., C&B Metabond, Parkell, USA) and MDP (e.g., Panavia, Kuraray, Japan) and remain a popular choice for luting resin-bonded FPDs. Further examples of acid-modified methacrylate phosphates include glycerol dimethacrylate ester of phosphoric acid (GDMP), methacryloyloxyethyl hihydrogen phosphate (MEP), pentaacryloyl dipentaerythrytol dihydrogen phosphate (Penta-P), and 2-methacryloxyethyl phenyl hydrogen phosphate (Phenyl-P). Other carboxylic acid monomers include 4-methacryloyloxyethyl trimellitic acid (4-MET) and pyromellitic glycerol dimethacrylate (PMGDM).

These class of monomers are able to provide ionic and covalent interaction between the cement and the enamel and/or dentine, which may then form a salt complex between calcium and the acid-modified monomer. However, the hydrolytic stability of this chemical interaction is highly dependent upon the hydrophobicity of the resin [18, 20].

Unsurprisingly, self-adhesive resin cement chemistry is very similar to that used in self-adhesive resin composite bonding systems. Consequently, it is likely that much of the innovative research into acidic monomers for self-adhesive systems will be translated and used for resin cement development, which focuses on increasing hydrolytic stability at the tooth–adhesive interface, especially under acidic conditions. Examples include water-soluble methacrylamide-based adhesives that exhibit lower cytotoxicity and improved hydrolytic stability compared to hydrophilic dimethacrylate-based formulations [21, 22] and novel phosphonic acid monomers that decrease water uptake and improve bond strength to hydroxyapatite [23].

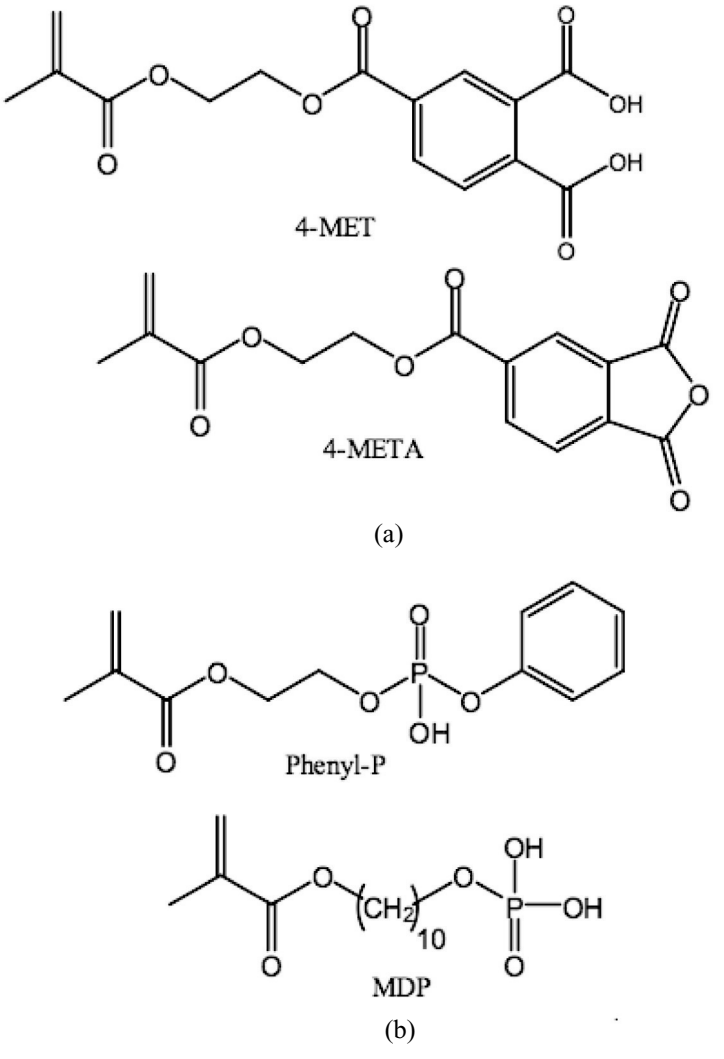

Figure 6.3 Chemical structures of (a) carboxylic acid monomers and (b) phosphate functional groups used in self-etching and self-adhesive dental resin cements.

There exists a plethora of research into the development of related chemistries, and three recent reviews provide an excellent overview of the state of the art [18, 22, 24]. In terms of the key requirement of a resin cement to provide a strong and durable bond

to a variety of adherends (enamel, dentine, base and noble metals, feldspathic glass, highly crystalline ceramics), the development of novel multipurpose self-etching adhesives that contain novel dithiooctanoate and phosphonic acids [25] might represent a significant step in the development of a universal bonding material.

6.2.1.3 Initiation chemistry

The combination of complex chemistries in dual-cured materials within acidic and aqueous conditions may result in unwanted effects that may lead to premature reactions or hinder effective polymerization. The amine coinitiators required for light-responsive polymerization undergo an acid–base reaction with the acid-modified monomer, which results in protonation of the amine, lowers radical concentration, and decreases polymerization [26]. The presence of water, which is an important solvent to provide adequate wettability with tooth tissue, has also been reported to reduce the reactivity of conventional CQ-amine initiator systems [27]. In that work, *N*-phenylglycine (NPG) coinitiators were reported to undergo a different reaction mechanism with the PI and allow increased reactivity in aqueous acidic conditions compared to aromatic amines [27]. Further, the use of NPG has been shown to significantly improve thermal stability, dark storage, and the subsequent shelf life of a methacrylate monomer [28]. Many commercial resin cements contain acid-sensitive chemistries, and in these cases, the amine should be separated from the acidic component prior to mixing.

Another approach to improving reactivity of light-curable and acidified resins is the use of alternative PI systems to the classic CQ-amine combination. Whereas for Type II PIs, which require a co-initiator for clinically effective polymerization, Type I PIs such as monoacylphosphine oxide (MAPO) exhibit high molar absorptivity and an electron donor is not necessary, albeit through thin material sections [29]. However, if MAPO is used in commercial formulations, it is usually in combination with a CQ-amine due to shorter wavelength absorption of the former and incompatibility with single blue diode (470 nm) curing units. However, the introduction of so-called third-generation light-emitting diode (LED) curing units that contain blue (~470 nm) and violet (~400 nm) diodes may lead to the introduction of adhesives and/or resin cements that only contain MAPO of similar Type I PIs.

Other adhesive resin systems have been explored that use a [3-(3,4-dimethyl-9-oxo-9H-thioxanthen-2-yloxy)-2-hydroxylpropy] trimethylammonium chloride (conveniently shortened to QTX) PI [30]. The combination of QTX with the iodonium salt diphenyliodonium hexafluorophosphate (DPIHP) has been reported to effectively initiate the polymerization of acidic monomers, although it remains ineffective for nonacidic formulations [31].

Although the previous descriptions highlight the inefficiencies of photoinitiated systems in acidic environments, decreased activity of the initiator and amine coinitiator is more prevalent in the redox polymerization of dual- or self-cured cements [32].

The chemistry of autocuring components in dual-cured resin cements includes benzoyl peroxide (BPO) and tertiary amines such as *N,N*-dihydroxyethyl-*p*-toluidine (DEPT); however, for self-etching or self-adhesive types of cement, its low pH will cause the oxidant to form radicals, resulting in premature polymerization and decreasing the reducing capacity of the coinitiator. Previous research has investigated the use of an amine-*p*-toluenesulfinic acid sodium salt (*p*-TSNa) in a ternary, self-cure initiating system of BPO-DEPT-*p*-TSNa when used with an acid-modified monomer and reported significantly enhanced reactivity and tensile bond strength to metal alloys compared with that using BPO-DEPT alone [33]. Other research has attempted to develop less acid-sensitive redox initiators such as cumene hydroperoxides used in combination with thiourea-based reducing agents [21]. Barbituric acid derivatives have also been used in alternative initiator systems due to their enhanced polymerization efficiency and the requirement for only a low concentration of amine [24]. A recent study highlighted the inhibitive effect of the acid-functionalized monomer (MAC-10) on a conventional PI system containing an amine; however, the degree of conversion was not affected using a novel borate/iodonium salt PI with the same monomer [34].

6.2.2 Mechanical and Physical Properties

Studies exist in the literature reporting on a variety of physical and mechanical properties of dental cements. The clinical relevance of some of the properties is questionable, but certain properties have been identified as being important for determining the acceptability

of a dental cement and have been incorporated in specifications and standards that manufacturers can use during the development and marketing of their materials. ANSI/ADA specification No. 96 for water-based cements and ISO 9917 [35] examine film thickness (a measure of viscosity and flow), setting time, compressive strength, and erosion and solubility in acids. ISO 4049 [36] is a standard for polymer-based filling and restorative and luting materials and requires testing of flexural strength, radiopacity, and solubility in water. The standards are meant to provide expectations for minimum (e.g., strength) or maximum (e.g., solubility) levels for a specific property for the cement to be considered acceptable. They do not claim to predict clinical success.

It is obvious that a cement must be strong enough to resist the forces of occlusion transferred to it via the overlying restoration, lest it fracture leading to loosening. It is logical to expect that an evaluation of compressive strength is appropriate, as the forces tend to compress the cement between the restorative material and the underlying tooth. This may help to explain why compressive testing is part of the original standard test regime for water-based cements, the first to be available. However, another explanation may be the fact that these materials are very brittle and more difficult to test via other modalities, such as tension and flexure. Because most intraoral forces are complex, due to the geometry of the tooth–restoration complex, compressive forces are typically distributed as tensile and/or shear forces within the cementing material. For this reason, the mechanical test for resin-based cements is flexure, which produces tensile as well as compressive stresses within the material. This test method is also relatively easy to conduct.

A recent review article has compared the literature on the flexure strengths of composite cements and self-adhesive resin cements and generally concluded that as a class, the strength of self-adhesive resin cements was equivalent to or slightly lower than that of composite cements [18]. A similar relationship has been reported for flexure modulus of the two types of cements [37]. It is important to note that both these resin-based cements are stronger than conventional water-based cements [38, 39]. In addition, when tested as self-cure only versus dual cured, nearly all cements are stronger and have higher elastic modulus when dual-cured [40, 41] (Fig. 6.4).

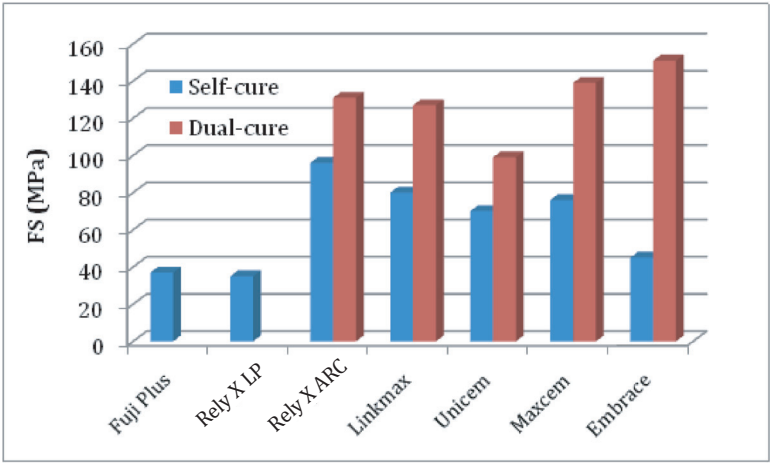

Figure 6.4 Flexure strength of cements in self-cure mode (blue) and dual-cure mode (red). Fuji Plus and Rely X LP are resin-modified glass ionomers. Rely X ARC is a resin cement. Linkmax, Unicem, Maxcem, and Embrace are self-adhesive resin cements. Adapted from Ref. [41].

The strength of the cement, as well as its bond to the tooth, is responsible for its ability to remain fixed on the preparation under typical oral conditions. At least one study has shown that resin-based cements have greater retention than conventional cements and are likely better choices when preparations have less than ideal retention, that is, are overtapered [42]. Studies testing in vitro crown retention were recently reviewed, and it was concluded that in general, retention is better with resin-based cements compared to conventional cements, though many variables affect the outcome of these studies [43].

Perhaps more important to the cement and the restoration as a whole is the fatigue strength. Yoshida et al. [44] used the staircase method to measure the flexural fatigue strength of resin-based dental cements and found that the results followed the same relationship as those of the static flexural strength of the cements. Further, the fatigue strength was in the range of 50–70% of the static flexural strength, and solely light-cured cements were higher than dual-cured versions. This ratio of fatigue to static strength is consistent with that for restorative dental composites tested under the same conditions.

Other properties of composites are often tested, such as microhardness. The clinical relevance of microhardness testing of cements is not clear, though one could argue that it may relate to wear at the margins of restorations on occlusal surfaces. But likely of more importance is the fact that hardness provides an indication of degree of cure of the cement, as has been shown for resins [45]. Further, the degree of cure affects mechanical properties and wear resistance of dual-cure cements [46]. Therefore, the degree of cure is an important parameter, especially as cements must be cured beneath a definitive restoration. While this is not a concern for self-cure materials, polymerization of light-cure or dual-cure materials is adversely affected by the need to transmit light through an opaque restorative material, such as a ceramic. Borges et al. [47] have shown that direct exposure of a dual-cure cement provides a far more extensive cure, as measured by microhardness, than simply allowing the cement to self-cure.

The application of light through a variety of ceramics produced variable results in terms of the extent of cure but was always poorer than that achieved by the direct application of light. Further, this study showed that light penetration, and ultimately cure of the cement, is poorer through ceramics with higher crystalline composition. In any case, a recommendation can be made that whenever a dual-cure cement is used, the clinician should expose as much of the cement as possible to the curing light to maximize cure and properties, as well as adhesion to the substrate [48]. It is important that the practitioner attempt to remove excess cement prior to final curing, however, because resin cements are harder, stronger, less brittle, and more difficult to visualize than water-based cements, making complete removal of the excess difficult [49].

6.2.3 Biocompatibility

There is an obvious need for dental cements to be biocompatible with the dental pulp as well as gingival tissues. Further, since degradation of the material over time is possible, long-term effects on oral tissues, as well as systemic effects from the ingestion of eluted components, are all reasonable considerations. There are relatively few studies on the biocompatibility of resin-based cements themselves. However, since these materials are closely related in composition to dental

composites, and to the components of dentin-bonding agents, consideration of the literature for these materials provides excellent guidance on the biocompatibility of resin cements and self-adhesive resin cements. In general, the monomer components of resin-based dental cements can elicit a pulpal response, and direct contact of the cement with pulpal tissue should be avoided. This conclusion is based on studies of direct pulp-capping agents showing a less than ideal outcome in human studies and trials when adhesives and conventional cements are used as compared to intermediary materials such as calcium hydroxide or mineral trioxide aggregates. For a full review of this literature, see Hilton [50] and also Chapter 5 of this book.

Cell culture studies have shown a difference in cytotoxicity for resin-based cements. In general, dual-cured cements show less cytotoxicity when light-cured as opposed to self-cured cements, due to the enhanced cure produced by the additional light curing, and resin composite cements show less cytotoxicity than self-adhesive resin cements [51]. The latter outcome does not seem to be related to the lower pH of the components of the self-adhesive cement. Further, the cytotoxicity of resin-based cements was similar to that of water-based conventional cements tested (polycarboxylate, glass ionomer, and zinc phosphate).

The incidence of allergy to resin-based dental cements is likely rare, but reports of allergic reactions to dental composites and adhesives exist in the literature, and therefore, the possibility remains exists.

The formation of recurrent caries at the margins of dental restorations is a bioincompatible reaction, and the presence of antimicrobial properties in a dental material to combat this situation is desirable. Resin-based dental cements are typically not antimicrobial. However, when used in conjunction with an adhesive containing a microbial agent, such as Clearfil Protect Bond (Kuraray), the possibility exists that an effect may be achievable. It is likely that as this field becomes more developed and as new compounds are investigated, antimicrobial resin-based dental cements will be forthcoming.

6.2.4 Clinical Performance

The clinical success of a cement itself is difficult to assess. Studies typically survey for overall failures of restorations and then often

provide specific reasons for the failures. Clinical failures directly attributed to the cement would include loosening and/or loss of the restoration or prosthetic from the remaining tooth structure or implant, washout of the cement at the margins that leads to staining and recurrent caries or loosening, and cement discoloration that makes an esthetic restoration clinically unacceptable.

Conventional cements used for fixed prosthodontics have been shown to be very reliable, with failure rates derived from meta-analyses being less than 2% annually [52]. A recent study comparing the short-term (two years) clinical performance of metal ceramic crowns luted with zinc phosphate compared to those bonded with a self-adhesive cement, Rely X Unicem (3M ESPE), showed essentially no difference in clinical performance between the two cements [53]. In another study reporting slightly longer than three-year results, the outcome for FPDs luted with zinc phosphate was equivalent to those bonded with the same self-adhesive resin cement, Rely X Unicem [54].

However, the cementation of ceramic restorations, specifically those not based on high-strength materials such as zirconia, have been shown to perform much better when luted with resin cements [55], and strengthening of ceramics with resin-based cements is discussed further in section 6.3.3. Ohlmann et al. [56] compared Panavia-F and Multilink (Ivoclar Vivadent) used to cement inlay-retained FPDs made from zirconia cores (with a pressed veneer) after they had been air-abraded with silica-coated alumina particles (tribochemical treatment) and silane-treated. A variety of problems were noted, but the authors concluded that adhesive problems contributed to failures, independent of the type of resin cement. Kramer et al. [57] reported no difference in the clinical behavior of pressed ceramic inlays luted with two resin cements, Definite and Variolink Ultra, though both showed similar evidence of marginal degradation. Frankenberger et al. [58] compared the same two cements for inlays made from the same glass ceramic placed by two different practitioners and similarly did not show a clinical difference between the cements, though there was a large difference in the outcomes for the two dentists. Kramer et al. [59] compared Compolute (3M ESPE) and Variolink II (Ivoclar Vivadent) resin cements for inlays and onlays at eight years and showed no difference between them in terms of overall success (10% rate of

failure in 8 years), though wear at the margins was significantly greater for Compolute.

In an earlier study by this group [60], the wear of the resin cement Variolink (Ivoclar Vivadent) at six years was clinically compared to the more highly filled Tetric (Ivoclar Vivadent) composite applied with an ultrasonic technique around leucite-reinforced inlays. Wear increased significantly with time, and there was overall no difference in the two cements. The limited clinical data on direct comparisons of resin cements for prosthetic restorations does not provide any definitive information, other than the concerns over inlay-retained FPDs.

6.3 Mechanisms of Adhesion

6.3.1 Resin Cements with Adhesives

For dual- or self-cured cements, the placement method can significantly affect material properties, specifically, the inhibition of self-curing resin cements underneath an opaque indirect restoration as a result of contact between the cement and the self-etching adhesive layer. For a two-step resin cementation technique, where a self-etching adhesive is placed prior to the cement, the resin requires an acid-functionalized monomer that has sufficiently low pH in order to demineralize the tooth surface. Following placement and light polymerization of the acidic primer, an upper superficial layer will remain uncured due to contact with air and oxygen inhibition. The tertiary amine contained within the self- or dual-cured cement layer will be consumed by the uncured H^+ ions of the adhesive and reduce copolymerization between the two layers [32, 61]. Consequently, inferior bond strengths are observed when the self-etching adhesive layer contacts the resin cement that is cured without light energy [62, 63]. It is the sodium sufinate salt coinitiators (described in section 6.2.1.3) included as a separate activator solution in many self-etching adhesive systems that overcome curing incompatibilities with dual- or self-cured resin cements. In a previous study, a sodium sulfinate salt activator applied following placement of a self-etching adhesive significantly improved the degree of conversion of a dual-cured resin cement when light activation was either not used or attenuated [64].

However, the use of the sodium sulfinate salt activator could not replicate the curing extent of the cement when direct light exposure was used [64], which highlights the critical requirement of clinicians to understand the limitations of resin cementation. Furthermore, the clinical environment will significantly affect curing characteristics that may exacerbate any incompatibility between the adhesive layer and the cement. For instance, self-etching adhesives may act as semipermeable membranes that draw water from dentinal tubules under osmotic pressure, leading to water-filled channels within the adhesive layer, which will significantly deteriorate bond strengths [65].

Regardless of the inhibition of resin cements used in combination with simplified adhesive systems, there have been many investigations on the effect of the curing method on the properties of dual-cured cements. Some studies report no difference in material properties between dual-curing and curing without light activation [66] or even inadequate cure as a result of the light-curing reaction inhibiting the self-cure mechanism [13, 67]. However, it is generally accepted that significantly improved material properties are achieved where the combination of light activation and self-cure mechanisms are compared with self-cure alone [68–70]. The effects of using different curing protocols between commercial products highlights the critical need for a proper selection and placement procedure according to the clinical situation, especially for cementation through opaque indirect restorations (see also Chapters 1 and 3).

6.3.2 Self-Adhesive Resins

The first commercial development of a self-adhesive luting cement was RelyX Unicem (3M ESPE, St. Paul, MN, USA), which was introduced to the market in 2003 and is the subject of most investigations that study bonding mechanisms of this class of material. It follows that the use of acid-modified monomers in the cement, namely, a methacrylated phosphoric ester (section 6.2.1.2), will provide low pH to demineralize and infiltrate tooth tissue. However, there exists a body of evidence to suggest that there is only superficial interaction between the cement and the tooth tissue without any morphological features such as demineralization or prominent

hybrid layer formation normally associated with that of self-etching adhesives [71–74]. Within the literature, the apparent agreement in the lack of demineralization following application of Unicem was initially surprising, given that the manufacturers claim that initial acidity is very low (pH < 2). More recent research has reported an initial pH greater than 2 [41, 75], which may suggest that the demineralization potential is not as effective as the manufacturers suggest. It should be noted, however, that in vitro pH measurements are not fully standardised and that temperature, electrolyte volume, and whether specimens are rinsed (thereby removing acidic components) will affect the measured pH value. Furthermore, any acid neutralization between the cement and the tooth substrate are not usually considered.

A significant chemical interaction of RelyX Unicem cement and calcium in the surrounding hydroxyapatite and the formation of complex calcium salts has been previously reported [76], which may partially explain its generally favorable bonding properties (given that demineralization and hybrid-layer formation are not supported). The acid-soluble filler, calcium hydroxide, contained within the cement and possibly the neutralizing capacity of the surrounding tooth structure increase pH relatively quickly and improve the stability of the material (Fig. 6.5).

The reduction in acidity and the increasing pH profile following placement of self-adhesive resin cements will vary considerably between products and the curing mode, which may have a significant effect upon immediate and long-term material properties. Resin cements that exhibit less efficient pH neutralization processes may experience curing inhibition, especially if light-curing reactions are prevented and the material is allowed to set by the self-cure process in a dual-cured material [41]. Any lack of neutralization may also compromise long-term hydrolytic stability of the adhesive junction, as water sorption within acidic systems will be increased.

6.3.3 Resin Strengthening of Conventional Ceramics

The use of contemporary cements such as zinc phosphate is still advocated as a luting agent for traditional ceramic crowns. However, zinc phosphate only acts as a space filler and has only weak micromechanical retention between the overlying ceramic and the

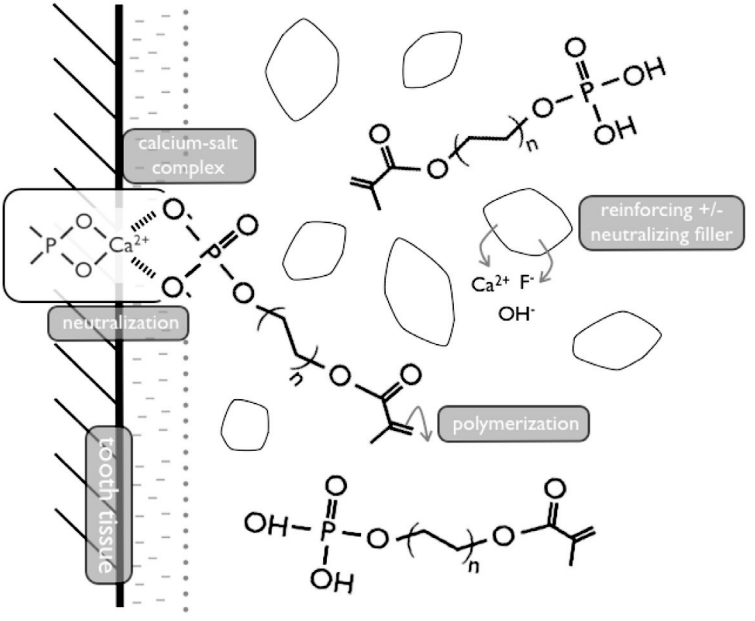

Figure 6.5 Schematic diagram showing the use of an (phosphoric) acidified dimethacrylate monomer resin that may result in the formation of a calcium salt complex and adhesion at the tooth–cement interface. Ion dissolution from reinforcing fillers coupled with any neutralizing effect of the tooth will increase pH following setting.

underlying tooth structure. The main disadvantages of traditional ceramic dental restorations such as feldspathic glass are low tensile strength and inadequate fracture toughness. All-ceramic restorations tend to fail from the internal, "fit" surface of the restoration as a result of crack extension from a pre-existing defect population [77–79]. Even with the introduction of zinc polycarboxylate and glass polyalkenoate cements, which exhibit adhesive properties to tooth tissue, it has been shown that their low initial pH following mixing and placement may extend pre-existing flaws and lead to a reduction in strength and longevity of ceramic restorations [7]. The introduction of resin-modified GICs was designed to improve the setting characteristics of conventional glass ionomers; however, significant water uptake into the cement layer has been reported

to result in premature failure of ceramic restorations [80]. Resin-based cements have become increasingly popular and provide many advantages over traditional cementation techniques, not only in terms of improved bonding potential, but also in terms of lower solubility, adequate mechanical properties, superior esthetic quality, and significantly improved handling and setting characteristics.

Precementation surface roughening of the ceramic is an important step in achieving a reliable bond to the resin cement and is usually carried out by surface grinding, grit blasting, or acid etching. For modern ceramics, where, for example, the crystalline phase has been substantially increased (to improve strength characteristics), traditional surface preparation techniques may not be suitable (section 6.3.4). However, for conventional feldspathic glass or other similar ceramic types with a heterogeneous crystal-glass microstructure, aggressive acid etching (with, e.g., hydrofluoric acid [HF]) results in the preferential dissolution of the different crystal and glass phases. Etching provides a unique etch pattern and surface irregularities that are amenable to resin infiltration in order to create an intimate bond between the tooth and restoration. The reliability of acid etching and/or surface abrasion can be problematic due to the formation of suitable undercuts in the ceramic surface, and therefore the application of an organofunctional silane is usually advised prior to cementation of a silicaceous ceramic restoration [81].

As previously mentioned, the presence of subcritical flaws at the surface of ceramic materials may cause premature restoration failure, and it is the infiltration of the resin cement that has been proposed to strengthen the system. Previous investigations have suggested that the penetration of resin fills pre-existing defects, effectively reducing the crack length and stress intensity at the crack tip [82]. An alternative hypothesis is that polymerization shrinkage of the resin cement imparts a compressive stress at the defect site, increasing the energy requirement to extend the crack under tensile load [83]. However, no significant correlation has been made between system strengthening and shrinkage stress generation as a consequence of resin cement shrinkage [84]. Furthermore, it has been demonstrated that resin strengthening of feldspathic materials is independent of defect size and severity [85, 86] and that increased strength characteristics are associated with macroscopic roughness

of the ceramic surface and that resin infiltration creates a "resin–ceramic hybrid layer," fundamentally modifying stress patterns throughout loading [86]. From these observations, it was suggested that significant strengthening acts over the entire defect population rather than by modifying individual flaws by healing or stabilization [87].

Resin strengthening of ceramics is a complex mechanism, and although the development of resin cement materials focuses predominantly on improving adhesion to both the ceramic and the tooth structure, the mechanical response of the ceramic-cement system under loading has significant clinical relevance. The effect of acidic, self-adhesive resin cements on the performance of ceramic restorations has yet to be fully elucidated but may shed more light on the importance of adhesive strength at the tooth-restoration interface.

6.3.4 Bonding to Polycrystalline Ceramics

The use of polycrystalline ceramics for dental restorations, specifically alumina and zirconia, has increased dramatically in recent years due to their high strength and perceived durability. The higher strength of zirconia has made it the leader in this category. The use of the material as a monolithic structure, without the application of an esthetic porcelain veneer, has become commonplace in an attempt to address concerns over chipping and fracture of the veneer. The optical qualities of dental zirconia remain somewhat of a concern as they are relatively opaque. This allows them to block out the underlying discoloured tooth structure but minimizes their use in highly esthetic situations.

The choice of cement for polycrystalline ceramics is of great interest and has been extensively studied. Lacking a glass matrix, these materials are not readily etched with HF to produce enhanced retention sites, as has been typical for porcelains and glassy matrix or glass-infiltrated ceramics. Thus, alternative surface treatments are required when using resin-based materials for cementation of polycrystalline ceramics. While it became apparent that failure of glassy matrix ceramics was somewhat enhanced when conventional cements were used, this was predominantly due to the low strength and fracture toughness of the ceramic used in the study [55]. Silica-

based ceramic inlays have shown higher failure rates when luted with conventional, water-based cements [88, 89]. Partial glass-matrix ceramic crowns luted with resin-modified GICs showed higher leakage and fracture in vitro compared to resin-cemented restorations [90], possibly due to increased water uptake and expansion for the former. Some have argued that the literature does not show clear evidence of the superiority of resin-based cements over conventional water-based cements for fixed restorations [91], while others have strongly suggested that there is clear evidence for resin cements, citing numerous supportive in vitro and clinical studies [92]. It would seem that cement choice may be very important for silica-based ceramics, and the safest choice when conditions are appropriate would be to use resin cements. The resin cement strengthening of these glassy ceramic materials, which was discussed in the previous section, is not a requirement for zirconia ceramics due to their very high mechanical properties [93]. Thus, conventional cements, such as glass ionomers or resin-modified glass ionomers are acceptable choices. However, resin cements are also acceptable and provide strong bonds when used appropriately.

Bonding to alumina or glass-infiltrated alumina has been achieved by first air-abrading the surface to create retention sites, because the materials cannot be etched with HF since they do not contain any or sufficient glass. In a recent study, two different resin cements used with adhesives, Variolink II and Panavia, and two different self-adhesive resin cements, Rely X Unicem and Multilink, were compared when bonding to a glass-infiltrated alumina (In-ceram Alumina, Vita Zahnfabrik) and a polycrystalline alumina (AllCeram, Procera) with sandblasting or tribochemical treatment followed by silane treatment [94]. The results showed that under the same conditions, Variolink II bonded better to the polycrystalline alumina than Panavia and that silicoating always improved bond strength as compared to air abrasion only. The self-adhesive cements had lower bond strength than Variolink, though Unicem was similar to Panavia. The Multilink cement had the lowest bond strength. The bond to the glass-infiltrated alumina was generally higher for the same cement than to the polycrystalline alumina, but bonding to a control of HF-etched lithium disilicate was the strongest of all.

Oyague et al. [95] showed that pretreatment of the surface of glass-infiltrated alumina with a neodymium-doped yttrium

aluminum garnet (Nd:YAG) laser improved bond strength and enhanced resistance to bond degradation for Panavia and Rely X Unicem self-adhesive cements when challenged in bleach. In another study of glass-infiltrated alumina, resin cement adhesion after erbium, chromium:yttrium–scandium–gallium–garnet (Er,Cr:YSSG) laser treatment followed by silane was equivalent to that obtained by silicoating and silane [96]. The durability of the bond between Panavia and glass-infiltrated alumina has been shown to be more stable than that of a conventional resin cement (Rely X ARC, 3M ESPE) in another study [97]. Thus, it appears that silicoating followed by silane treatment is the most supported method for achieving adhesion of resin cements to high-alumina-content ceramics.

Zirconia is most commonly used in the polycrystalline form for dental restorations (see also Chapters 14–16). Many studies have been conducted to determine the optimal way of promoting adhesion to these materials with resin cements, including air abrasion, tribochemical treatment, organic surface primers, and combinations of the above. Because these materials do not contain silica, the standard protocol of air abrasion followed by silane treatment is not sufficient. Thus, early studies attempted to produce bonding to polycrystalline zirconia (yttrium oxide partially stabilized zirconia [YPSZ]) using the same methods as were successfully used for glass-infiltrated zirconia, that is, tribochemical treatment and silane coupling followed by a bis-GMA-based resin composite, but found that the high initial bond strengths fell drastically during aging in water [98]. The lack of durability of the commonly used silane agents (3-methacryloyloxypropyltrimethoxysilane [γ-MPS]) for bonding of bis-GMA resins to zirconia treated tribochemically has been shown by others [99]—and see also Chapters 3 and 11.

In the Kern and Wegner study [98], the best and most durable bonds were created to air-abraded YPSZ with Panavia cement containing the MDP monomer, emphasizing the importance of a chemical interaction with the surface via a water-stable linkage. The tribochemical process further enhances this bond with MDP-containing resin cements [100]. The superior performance of MDP- or 4-META-containing resin cements versus several self-adhesive resin cements was reinforced in another study, which also reported that air abrasion was useful for enhancing the bond of all self-adhesive cements to zirconia [101]. The concern with air abrasion

is that it should be performed under mild conditions, that is, low pressure [102], to avoid imposing sufficient stress on the intaglio surface of the restoration to force the tetragonal-to-monoclinic phase transformation that is responsible for the toughening effect in these materials. While this transformation may immediately toughen the surface, there is the potential for damage to be created by the air abrasion process that may leave significant flaws and areas of higher stress concentration on this surface. Future load applications would then create stresses that would no longer be blunted by the transformation-toughening mechanism, since this has already occurred. Thus ultimately the surface may be left weakened. There is some evidence for the fact that the surface flaws created by the air abrasion process override any strengthening effect and leave the air-abraded surface weaker to static and cyclic stresses [103]. However, other evidence suggests this surface is actually strengthened by the air abrasion process, as well as enhancing bond strength to resins [104], and that air abrasion with silica-coated alumina particles of 30 μm size (CoJet Sand, 3M ESPE) is recommended for most zirconia ceramics [105, 106]. Thus, it is likely that the beneficial effect of air abrasion, in particular that achieved with the tribochemical process, outweighs the potential risks, and the process can be recommended for zirconia.

Novel methods to alter the zirconia surface for enhanced bonding have been reported by numerous investigators. Piascik et al. [107, 108] modified the surface of zirconia by $SiCl_4$ vapor deposition or gas-phase fluorination to enhance resin bonding, reporting evidence of chemical modification of the surface and reasonable adhesion. A subsequent study showed that the bond formed to the vapor deposition surface was as durable as that to tribochemical-treated or primed zirconia, but in all cases, the bond was less stable than that of traditional etched and silane-treated silica-based ceramics [109].

Others have shown that the use of tribochemical treatment followed by silane application enhances the bond strength with different resin-based cements (SuperBond, Sun Medical, and Panavia F 2.0, Kuraray) tested after aging in water for three months as compared to the manufacturers' instructions for placing these cements [110]. This work followed an earlier study by this group that showed that following the manufacturers' instructions for four

different resin cements led to a total loss of adhesion after thermal cycling in water [111], thus emphasizing the lack of stability of the bond to unmodified zirconia surfaces when aged in water.

Bond stability of the resin cement to zirconia has been evaluated in numerous studies. Wolfart et al. [112] compared the adhesion of Variolink II with Panavia F to air-abraded zirconia (Cercon, Dentsply) after 3 and 150 days and found Panavia to have two to three times' greater bond strength initially (maximum 45 MPa) and after aging (39 MPa). While the bond failed prior to testing for Panavia and Variolink II specimens bonded without prior air abrasion, Variolink II also showed no bond strength after aging to an air-abraded surface. In another study with Panavia F 2.0, bond stability to zirconia (Lava, 3M ESPE) after different surface treatments and primer applications was compared after thermal cycling [113]. In this case, tribochemical treatment and air abrasion followed by priming with three different commercial primers produced equivalent results, all being in the range of 8–12 MPa. Oyague et al. [114] compared the bond of three resin cements, Clearfil Esthetic (Kuraray), Calibra (Dentsply), and Rely X Unicem, to zirconia (Cercon, Dentsply) with no treatment, air abrasion, and silicoating. They found generally better bonding with Clearfil Esthetic initially, and the bonds after aging for six months in water were equivalent or greater for this cement compared to those achieved by RelyX-Unicem. Calibra only had appreciable adhesion to the air-abraded surface, but this was not stable when aged in water. In another study, Passos et al. [115] reported enhanced adhesion of several cements to zirconia, including Panavia F 2.0, Variolink II, Rely X Unicem, and Maxcem (Kerr), when the surface was tribochemically (silicacoat) and silane treated (γ-MPS) (Fig. 6.6).

The many studies investigating the best method to achieve adhesion with resin cements to non-silica-based ceramics lead to the conclusion that the issue is not totally resolved. In a recent review by Thompson et al. [116], the authors concluded that traditional methods for adhesion do not work well enough and that "the ability to chemically functionalize the surface of zirconia appears to be critical." Techniques for this purpose are being investigated. At the present, perhaps the most well-accepted method for bonding to zirconia is through the use of MDP-containing resin cements, such as Panavia, with the aid of air abrasion, in part because these cements appear to achieve the greatest level of hydrolytic durability. Ceramic materials are discussed also in Chapters 3 and 14–16.

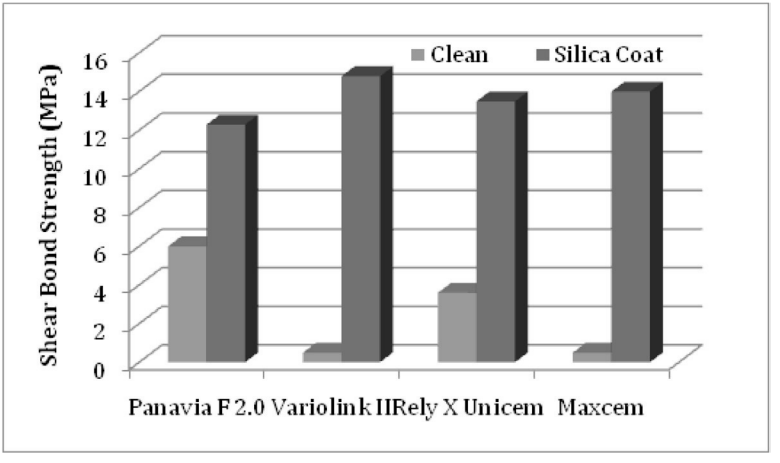

Figure 6.6 Shear bond strength of four resin cements to zirconia after cleaning with alcohol vs. tribochemical (silicacoat) and silane treatment. Adapted from Ref. [115].

6.3.5 Metal Adhesion

Conventional cements have been used for decades for luting restorations with great success. The use of resin cements for full crowns or inlay/onlay restorations made from gold or other alloys would seem to be desirable to maximize retention with less tooth structure removal, that is, the need for less retentive preparations [93]. Unfortunately, there does not appear to be much literature specifically evaluating this.

The adhesion of resin cements to metals includes noble, high noble, and predominantly base metal alloys, including titanium. In each case, there is a need for some pretreatment of the metal surface to establish or enhance its adhesion to the resin. Some cements or adhesives for cements contain molecules that can chemically interact with oxides. Thus, it is important that the alloy form critical oxides for this interaction to occur. This has been accomplished through the addition of oxidizing elements to gold alloys, such as In, Zn, and Sn [117]. Adhesives containing 4-META, a molecule with carboxylic acid groups, that has been used in a variety of dental adhesives [118], show chemical interaction to the oxides produced by these

additions. One of the most popular resin cements for bonding to alloys has been Panavia, a cement with a phosphate-methacrylate monomer (MDP) adhesive system, as previously described. But even with the alloy primer, this resin cement showed better adhesion to gold alloys when they were tin-plated or air-abraded, and this adhesion was equivalent to that to an air-abraded (aluminium oxide particles) nickel-chromium alloy [119].

Numerous primers with various chemistries for bonding to metal surfaces have been developed and tested over the years, showing their ability to enhance adhesion to noble as well as predominantly base metal alloys [25, 120–125]. Simpler systems based on resin cements containing adhesive molecules as an included component as opposed to being applied as a separate adhesive or primer were being pursued simultaneously. This has led to the development of self-adhesive resin cements, all of which contain acid-functionalized monomers based on carboxylic acid or phosphoric acid groups [18].

Previous studies have shown strong adhesion of resin cements to nickel-chromium alloys containing beryllium after etching to provide retention sites [126]. Other studies have shown that resin cements can be bonded to metal surfaces after a laboratory technique called "silicoating" (Heraeus Kulzer), in which a silica-rich layer is applied to the metal surface by a heating process and bonding is achieved with a silane coupling agent [81]. Another popular laboratory method to treat metal surfaces for bonding with resins is the Rocatec system (3M ESPE), in which the surface is treated by air abrasion with particles of aluminum oxide that are coated with silica. These particles become transferred or embedded in the surface, thus making it amenable to silane treatment for bonding with resins. As previously mentioned, an intraoral system, Cojet (3M ESPE), containing particles of approximately 30 μm, was developed with a special delivery system to facilitate this process clinically [127].

Adhesion of resin cements to titanium surfaces that have been silicoated has been enhanced through the application of commercial silane agents, with the level of enhancement being dependent upon the particular brand [128, 129]. In previous work, this same group found that a new silane (3-isocyanatopropyltriethoxysilane) produced better adhesion to air-abraded titanium than the more

common γ-MPS. Taken together, these studies showed the important effect of silica coating prior to silane treating. Recently, a group tested the adhesion of self-adhesive resin cements (G-Cem, G-C, and Rely X Unicem) to titanium surfaces pretreated in a variety of chemical baths as an alternative to air abrading, including methylene chloride, hydrogen peroxide, and HF [130]. The highest bond strengths were obtained with the HF etch, though it was equivalent for both cements (see also Chapter 9).

Adhesion of resin cements to noble or predominantly base metal alloys can be accomplished in a variety of ways, but it appears that the following guidelines should be followed. Noble alloys are best treated by tin plating. Predominantly base metal alloys like Ni-Cr should be chemically etched. Titanium should be air-abraded, preferably with tribochemical treatment followed by the application of a silane coupling agent. Table 6.2 provides a summary of the recommended methods for preparing restorative surfaces for bonding with specific types of cements.

Table 6.2 Cement options for crowns and FPDs

Crown/FPD substrate	Cement option
Noble metal	Conventional
PFM metal	Conventional
Porcelain	Resin cement with HF etch + silane
Lithium disilicate	Resin cement with HF etch + silane
Alumina (polycrystalline or glass infiltrated)	Conventional (resin-modified GIC) Tribochemical abrasion + silane with resin cement Air abrasion + self-etching (or self-adhesive) resin cement
Monolithic zirconia (polycrystalline or glass infiltrated	Conventional (resin-modified GIC) Tribochemical abrasion + silane with resin cement Air abrasion + self-etching (or self-adhesive) resin cement*

*Optimal results have been shown for systems with MDP monomers.
Abbreviation: PFM, porcelain fused to metal.

6.4 Future Trends

The future development of dental cements will undoubtedly include efforts to enhance adhesion to substrates, such as zirconia and other new ceramic formulations, enhance the durability of the cement itself and the adhesive bond to tooth and restoratives, and enhance the material's ability to act as an anticaries and remineralizing agent. The inclusion of calcium and phosphate compounds, or perhaps bioactive glasses, has the potential for both remineralization in a biological fluid environment, as well as some anticaries potential. Many experimental versions of calcium-phosphate-containing cements have been proposed, showing various levels of bioactivity, though commercialization has not been rapid. At least one commercial material containing calcium aluminate and an ionic polymer (similar to that contained in a glass ionomer) currently exists on the market that claims these qualities (Ceramir, Doxa).

A recent study reported the effect of adding titania nanotubes to a resin cement to enhance mechanical properties [131]. Doubtless there are many other potential additives that can be tried, though their effect on handling (i.e., whiskers are precluded due to their effect on viscosity) and cost may make them prohibitive. The strength of the cement may not need to be substantially altered, however, as it is likely that the adhesion durability and solubility resistance are more likely the key properties. As more self-adhesive, hydrophilic technologies develop, this will continue to be a significant issue. It may be that some "marginal sealing" agent that penetrates the cement surface and fills defects at the margin, while making the interface more hydrophobic, would be a possible solution. This approach was somewhat successful for sealing dental composite restorations [132].

One may also expect new delivery systems for cements that ensure more even distribution of cement on the restoration surface, as well as modifications that enhance the clean-up of excess cement. Cements, which set in stages, allowing clean-up before maximum hardening occurs, have existed and will likely continue to be pursued with current self-adhesive formulations.

Finally, cements for use under any type of minimally translucent restoration whose polymerization reaction can be initiated by minimal light or other means, such as mechanical vibration or ultrasound, may be a future possibility.

References

1. Sorel, S. (1855) *Compt. Rend. Hebdomadaire. Seances. Acad. Sci.,* **41**, 784.
2. Flagg, F. (1875), cited from Smith, D. C. (1998) Development of glass-ionomer cement systems, *Biomaterials,* **19**(6), 467–478.
3. Ames, W. V. B. (1892) A new oxyphosphate for crown setting, *Dent. Cosmos.,* **21**, 696.
4. Fleck, D. J. (1902) The chemistry of oxyphosphates, *Dent. Items. Int.,* **24**, 906.
5. Gilmore, H. W. (1967) The use of tooth colored restorative materials, *Dent. Clin. N. Am.,* **11**(1), 203–212.
6. Nakabayashi, N., Pashley, D. H. (1998) *Hybridization of Dental Hard Tissues*, Quintessence, Chicago.
7. Fleming, G. J. P., Narayan, O. (2003) The effect of cement type and mixing on the bi-axial fracture strength of cemented aluminous core porcelain discs, *Dent. Mater.*, **19**(1), 69–76.
8. Smith, D. C. (1968) A new dental cement, *Br. Dent. J.,* **124**, 381–384.
9. Wilson, A. D., Kent, B. E. (1971) The glass ionomer cement: a new translucent dental filling material, *J. Appl. Chem. Biotechnol.,* **21**, 313–320.
10. Hill, E. E. (2007) Dental cements for definitive luting: a review and practical clinical considerations, *Dent. Clin. N. Am.*, **51**(3), 643–658.
11. Diaz-Arnold, A. M., Vargas, M. A., Haselton, D. R. (1999) Current status of luting agents for fixed prosthodontics, *J. Prosthet. Dent.*, **81**(2), 135–141.
12. Rosenstiel, S. F., Land, M. F., Crispin, B. J. (1998) Dental luting agents: a review of the current literature, *J. Prosthet. Dent.*, **80**(3), 280–301.
13. Pegoraro, T. A., da Silva, N. R. F. A., Carvalho, R. M. (2007) Cements for use in esthetic dentistry, *Dent. Clin. N. Am.,* **51**(2), 453–471.
14. Hill, E. E., Lott, J. (2011) A clinically focused discussion of luting materials, *Aust. Dent. J.*, **56**(Suppl 1), 67–76.

15. Haddad, M. F., Rocha, E. P., Assunção, W. G. (2011) Cementation of prosthetic restorations: from conventional cementation to dental bonding concept, *J. Craniofac. Surg.*, **22**(3), 952–958.
16. Mount, G. J., Tyas, M. J., Ferracane, J. L., Nicholson, J. W., Berg, J. H., Simonsen, R. J., and Ngo, H. C. (2009) A revised classification for direct tooth-colored restorative materials, *Quintess. Int.*, **40**, 691–697.
17. Radovic, I., Monticelli, F., Goracci, C., Vulicevic, Z. R., Ferrari, M. (2008) Self-adhesive resin cements: a literature review, *J. Adhes. Dent.*, **10**(4), 251–258.
18. Ferracane, J. L., Stansbury, J. W., Burke, F. J. T. (2011) Self-adhesive resin cements—chemistry, properties and clinical considerations, *J. Oral Rehab.,* **38**, 295–314.
19. Manso, A. P., Silva, N. R., Bonfante, E. A., Pegoraro, T. A., Dias, R. A., Carvalho, R. M. (2011) Cements and adhesives for all-ceramic restorations, *Dent. Clin. N. Am*., **55**(2), 311–332.
20. Van Landuyt, K. L., Yoshida, Y., Hirata, I., Snauwaert, J., De Munck, J., Okazaki, M. (2008) Influence of the chemical structure of functional monomers on their adhesive performance, *J. Dent. Res.,* **87**, 757–761.
21. Moszner, N., Salz, U. (2007) Recent developments of new components for dental adhesives and composites, *Macro. Mater. Eng.,* **292**, 245–271.
22. Salz, U., Bock, T. (2010) Adhesion performance of new hydrolytically stable one-component self-etching enamel/dentine adhesives, *J. Adhes. Dent.* **12**(1), 7–10.
23. Ikemura, K., Tay, F. R., Nishiyama, N., Pashley, D. H., Endo, T. (2007) Multi-purpose bonding performance of newly synthesized phosphonic acid monomers, *Dent. Mater. J.* **26**, 105–115.
24. Ikemura, K., Endo, T. (2010) A review of our development of dental adhesives: effects of radical polymerization initiators and adhesive monomers on adhesion, *Dent. Mater. J.* **29**(2), 109–121.
25. Ikemura, K., Jogetsu, Y., Shinno, K., Nakatsuka, T., Endo, T., Kadoma, Y. (2011,) Effects of a newly designed HEMA-free, multi-purpose, single-bottle, self-etching adhesive on bonding to dental hard tissues, zirconia-based ceramics, and gold, *Dent. Mater. J.*, **30**, 616–625.
26. Dietliker, K. (1998) *Photoinitiators for Free-Radical Cationic and Anionic Polymerisation*, 2nd ed., Vol. 3, SITA Technology, London.
27. Ullrich, G., Burtscher, P., Salz, U., Moszner, N., Liskw, R. (2006) Phenylglycine derivatives as co-initiators for the radical

photopolymerization of acidic aqueous formulations, *J. Polym. Sci: A. Polym. Chem.,* **44**, 115–125.

28. Kim D., Scranton, A. B., Stansbury, J. W. (2009) Effect of the electron donor structure on the shelf-lifetime of visible-light activated three-component initiator systems, *J. Appl. Polym. Sci.,* **114**, 1535–1542.
29. Leprince, J. G., Hadis, M., Shortall, A. C., Ferracance, J. L., Devaux, J., Leloup, G., Palin, W. M. (2011) Photoinitiator type and applicability of exposure reciprocity law in filled and unfilled photoactive resins, *Dent. Mater.,* **27**, 157–164.
30. Hayakawa, T., Kikutake-Sugiyama, K., Nemoto, K. (2005) Development of self-etching primer adhesive in all-in-one bonding system, *Dent. Mater. J.,* **24**, 251–256.
31. Guo, X., Peng, Z., Spencer, P., Wang, Y. (2009) Effect of initiator on photopolymerization of acidic, aqueous dental model adhesives, *J. Biomed. Mater. Res. A,* **90**, 1120–1127.
32. Suh, B. I., Feng, L., Pashley, D. H. (2003) Factors contributing to the incompatibility between simplified-step adhesives and chemically cured or dual cured composites. Part III. Effect of acidic resin monomers, *J. Adhes. Dent.,* **5**, 267–282.
33. Ikemura, K., Endo, T. (1999) Effect on adhesion of new polymerization initiator systems comprising 5-monosubstituted barbituric acids, aromatic sulfinate amides and tert-butylperoxymaleic acid in dental adhesive, *J. Appl. Polym. Sci.,* **72**, 1655–1668.
34. Oguri, M., Yoshida, Y., Yoshihara, K., Miyauchi, T., Nakamura, Y., Shimoda, S., Hanabusa, M., Momoi, Y., Van Meerbeek, B. V. (2012) Effects of functional monomers and photoinitiators on the degree of conversion of a dental adhesive, *Acta Biomater.* **8**, 1928–1934.
35. International Organization for Standardization. *Dentistry: Water-Based Luting Agents,* ISO Standard 9917.1991.
36. International Organization for Standardization. *Dentistry: Polymer-Based Filling, Restorative and Luting Materials*, ISO Standard 4049.2000.
37. Irie, M., Maruo, Y., Nishigawa, G., Suzuki, K., Watts, D. C. (2010) Physical properties of dual-cured luting-agents correlated to early no interfacial-gap incidence with composite inlay restorations, *Dent. Mater.*, **26**(6), 608–615.
38. Piwowarczyk, A., Lauer, H. C. (2003) Mechanical properties of luting cements after water storage, *Oper. Dent.*, **28**, 535–542.

39. Nakamura, T., Wakabayashi, K., Kinuta, S., Nishida, H., Miyamae, M., Yatani, H. (2010) Mechanical properties of new self-adhesive resin-based cement, *J. Prosthodont. Res*., **54**, 59–64.

40. Hofmann, N., Papsthart, G., Hugo, B., Klaiber, B. (2001) Comparison of photo-activation versus chemical or dual curing of resin-based luting cements regarding flexural strength, modulus and surface hardness, *J. Oral Rehab.*, **28**, 1022–1028.

41. Saskalauskaite, E., Tam, L. E., McComb, D. (2008) Flexural strength, elastic modulus, and pH profile of self-etch resin luting cements, *J. Prosthodont.,* **17**(4), 262–268.

42. Johnson, G. H., Lepe, X., Zhang, H., Wataha, J. C. (2009) Retention of metal-ceramic crowns with contemporary dental cements, *J. Am. Dent. Assoc.*, **140**(9), 1125–1136.

43. Heintze, S. D. (2010) Crown pull-off test (crown retention test) to evaluate the bonding effectiveness of luting agents, *Dent. Mater*., **26**(3), 193–206.

44. Yoshida, K., Condon, J. R., Atsuta, M., Ferracane, J. L. (2003) Flexural fatigue strength of CAD/CAM composite material and dual-cured resin luting cements, *Am. J. Dent.*, **16**(3), 177–180.

45. Ferracane, J. L. (1985) Correlation between hardness and degree of conversion during the setting reaction of unfilled dental restorative resins, *Dent. Mater*., **1**(1), 11–14.

46. Peutzfeldt, A. (1995) Dual-cure resin cements: in vitro wear and effect of quantity of remaining double bonds, filler volume, and light curing, *Acta Odontol. Scand.*, **53**(1), 29–34.

47. Borges, G. A., Agarwal, P., Miranzi, B. A., Platt, J. A., Valentino, T. A., dos Santos, P. H. (2008) Influence of different ceramics on resin cement Knoop hardness number, *Oper. Dent.,* **33**(6), 622–628.

48. Manso, A. D., Gonzalez-Lopez, S., Bolanos-Carmona, V., Mauricio, P. J., Felix, S. A., Carvalho, P. A. (2011) Regional bond strength to lateral walls in class I and II ceramic inlays luted with four resin cements and glass-ionomer luting agent, *J. Adhes. Dent.*, **13**, 455–465.

49. Mitchell, C. A., Pintado, M. R., Geary L, Douglas, W. H. (1999) Retention of adhesive cement on the tooth surface after crown cementation, *J. Prosthet. Dent.*, **81**(6), 668–677.

50. Hilton, T. J. (2009) Keys to clinical success with pulp capping: a review of the literature, *Oper. Dent.*, **34**(5), 615–625.

51. Schmid-Schwap, M., Franz, A., König, F., Bristela, M., Lucas, T., Piehslinger, E., Watts, D. C., Schedle, A. (2009) Cytotoxicity of four categories of dental cements, *Dent. Mater*., **25**, 360–368.

52. Creugers, N. H., Kayser, A. F., van't Hof, M. A. (1994) A meta analysis of durability data on conventional fixed bridges, *Comm. Dent. Oral. Epidemiol.,* **22**, 448–452.

53. Piwowarczyk, A., Schick, K., Lauer, H. C. (2012) Metal-ceramic crowns cemented with two luting agents: short-term results of a prospective clinical study, *Clin. Oral Investig.*, **16**, 917–922.

54. Behr, M., Rosentritt, M., Wimmer, J., Lang, R., Kolbeck, C., Bürgers, R., Handel, G. (2009) Self-adhesive resin cement versus zinc phosphate luting material: a prospective clinical trial begun 2003, *Dent. Mater.,* **25**, 601–604.

55. Malament, K. A., Socransky, S. S. (2001) Survival of Dicor glass-ceramic dental restorations over 16 years. Part III: effect of luting agent and tooth or tooth-substitute core structure, *J. Prosthet. Dent.,* **86**(5), 511–519.

56. Ohlmann, B., Rammelsberg, P., Schmitter, M., Schwarz, S., Gabbert, O. (2008) All-ceramic inlay-retained fixed partial dentures: preliminary results from a clinical study, *J. Dent.*, **36**, 692–696.

57. Kramer, N., Reinelt, C., Richter, G., Frankenberger, R. (2009) Four-year clinical performance and marginal analysis of pressed glass ceramic inlays luted with ormocer restorative vs. conventional luting composite, *J. Dent.*, **37**, 813–819.

58. Frankenberger, R., Reinelt, C., Petschelt, A., Kramer, N. (2009) Operator vs. material influence on clinical outcome of bonded ceramic inlays, *Dent. Mater.*, **25**, 960–968.

59. Kramer, N., Taschner, M., Lohbauer, U., Petschelt, A., Frankenberger, R. (2008) Totally bonded ceramic inlays and onlays after eight years, *J. Adhes. Dent.*, **10**, 307–314.

60. Kramer, N., Frankenberger, R. (2000) Leucite-reinforced glass ceramic inlays after six years: wear of luting composites, *Oper. Dent.*, **25**, 466–472.

61. Rueggeberg, F. A., Margeson, D. H. (1990) The effect of oxygen inhibition on an unfilled/filled composite system, *J. Dent. Res.*, **69**, 1652–1658.

62. Arrais, C. A., Giannini, M., Rueggeberg, F. A., Pashley, D. H. (2007) Effect of curing mode on microtensile bond strength of dual-polymerizing cementing systems to dentin using different polymerizing modes, *J. Prosth. Dent.,* **32**, 37–44.

63. Giannini, M., De Goes, M. F., Nikaido, T., Shimada, Y., Tagami, J. (2004) Influence of activation mode of dual-cured resin composite cores and low-viscosity composite liners on bond strength to dentin treated with self-etch adhesives, *J. Adhes. Dent.,* **6**, 301–306.

64. Arrais, C. A., Giannini, M., Rueggeberg, F. A. (2009) Effect of sodium sulfinate salts on the polymerization characteristics of dual-cured resin cement systems exposed to attenuated light activation, *J. Dent.,* **37**, 219–227.

65. Tay, F. R., Pashley, D. H., Peters, M. C. (2003) Adhesive permeability affects composite coupling to dentin treated with a self-etch adhesive, *Oper. Dent.,* **28**, 610–621.

66. Pereira, S. G., Fulgencio, R., Nunes, T. G., Toledano, M., Osorio, R., Carvalho, R. M. (2010) Effect of curing protocol on the polymerization of dual-cured resin cements, *Dent. Mater.,* **26**, 710–718.

67. Arrais, C. A., Rueggeberg, F. A., Waller, J. L., De Goes, M. F., Giannini, M. (2008) Effect of curing mode on the polymerization characteristics of dual-cured resin cement systems, *J. Dent.,* **36**, 418–426.

68. Oliveira, M., Cesar, P. F., Giannini, M., Rueggeberg, F. A., Rodrigues, J., Arrais, C. A. (2012) Effect of temperature on the degree of conversion and working time of dual-cured resin cements exposed to different curing conditions, *Oper. Dent.*, **37**(4), 370–379.

69. Kitzmuller, K., Graf, A., Watts D. C., Schedle, A. (2011) Setting kinetics and shrinkage of self-adhesive resin cements depend on cure-mode and temperature, *Dent. Mater.,* **27**(6), 544–551.

70. Vrochari, A. D., Eliades, G., Hellwig, E., Wrbas, K. T. (2009) Curing efficiency of four self-etching, self-adhesive resin cements, *Dent. Mater*., **25**(9), 1104–1108.

71. De Munck, J., Vargas, M., Van Landuyt, K., Hikita, K., Lambrechts, P., Van Meerbeek, P. (2004) Bonding of an auto-adhesive luting material to enamel and dentine, *Dent. Mater.,* **20**, 963–971.

72. Al-Assaf, K., Chakmakchi, M., Palaghias, G., Karanika-Kouma, A., Eliades, G. (2007) Interfacial characteristics of adhesive luting resins and composites with dentine, *Dent. Mater.,* **23**(7), 829–839.

73. Monticelli, F., Osorio, R., Mazzitelli, C., Ferrari, M., Toledano, M. (2008) Limited decalcification/diffusion of self-adhesive cements into dentin, *J. Dent. Res.,* **87**(10), 974–979.

74. Vaz, R. R., Hipólito, V. D., D'Alpino, P. H., Goes, M. F. (2012) Bond strength and interfacial micromorphology of etch-an-rinse and self-adhesive resin cements to dentin, *J. Prosthodont.,* **21**(2), 101–111.

75. Zorzin, J., Petschelt, A., Ebert, J., Lohbauer, U. (2012) pH neutralization and influence on mechanical strength in self-adhesive resin luting agents, *Dent. Mater.,* **28**(6), 672–679.

76. Gerth, H. S., Dammasschke, T., Züchner, H., Schäfer, E. (2006) Chemical analysis and bonding reaction of RelyX Unicem and Bifix composites: a comparative study, *Dent. Mater.*, **22**(10), 934–941.

77. Kelly, J. R. (1999) Clinically relevant approach to failure testing of all-ceramic restorations, *J. Prosthet. Dent.* **81**, 652–661.

78. Quinn, J. B., Quinn, G. D., Kelly, J. R., Scherrer, S. S. (2005) Fractographic analyses of three ceramic whole crown restoration failures, *Dent. Mater.* **21**(10), 920–929.

79. Scherrer, S. S., Quinn, J. B., Quinn, G. D., Kelly J. R. (2006) Failure analysis of ceramic clinical cases using qualitative fractography, *Int. J. Prosthodont.* **19**(2), 185–192.

80. Sindel, J., Frankenberger, F., Kramer, K., Petschelt, A. (1999) Crack formation of all-ceramic crowns dependent on different core build-up and luting materials, *J. Dent.,* **27**(3), 175–81.

81. Lung, C. Y.K, Matinlinna, J. P. (2012) Aspects of silane coupling agents and surface conditioning in dentistry: an overview, *Dent. Mater.*, **28**(5), 467–477.

82. Marquis, P. M. (1992) The influence of cements on the mechanical performance of dental ceramics, *Bioceramics*, **5**, 317–324.

83. Nathanson, D. (1993) In *Porcelain and Composite Inlays and Onlays: Esthetic Posterior Restorations*, 23–32 (Ed. Gaber, D. A., Goldstein, R. E.), Quintessence, Chicago, IL, USA.

84. Addison, O., Marquis, P. M., Fleming, G. J. P. (2007a) Resin elasticity and the strengthening of all-ceramic restorations, *J. Dent. Res.*, **86**(6), 519–523.

85. Fleming, G. J., Maguire, F. R., Bhamra, G., Burke, F. M., Marquis, P. M. (2006) The strengthening mechanism of resin cements on porcelain surfaces, *J. Dent. Res*., **85**(3), 272–276.

86. Addison, O., Marquis, P. M., Fleming, G. J. P. (2007b) Resin strengthening of dental ceramics: the impact of surface texture and silane, *J. Dent.*, **35**(5), 416–424.

87. Fleming, G. J. P., Addison, O. (2009) Adhesive cementation and the strengthening of all-ceramic dental restorations, *J. Adhes. Sci. Technol.,* **23**, 945–959.

88. Van Dijken, J., Horlund-Aberg, C., Olofsson, A.-L. (1998) Fired ceramic inlays: a 6 years follow up, *J. Dent.*, **26**, 219–225.

89. Gemalmaz, D., Ozcan, M., Alkumru, H. N. (2001) A clinical evaluation of ceramic inlays bonded with different luting agents, *J. Adhes. Dent.*, **3**, 273–283.

90. Federlin, M., Schmidt, S., Hiller, K. A., Thonemann, B., Schmalz, G. (2004) Partial ceramic crowns: influence of preparation design and luting material on internal adaptation, *Oper. Dent.*, **29**, 560–570.

91. Pospiech, P. (2002) All-ceramic crowns: bonding or cementing? *Clin. Oral Invest.*, **6**, 189–197.

92. Burke, F. J. T., Fleming, G. J. P., Nathanson, D., Marquis, P. M. (2002) Are adhesive technologies needed to support ceramics? An assessment of the current evidence, *J. Adhes. Dent.,* **4**, 7–22.

93. Edelhoff, D., Ozcan, M. (2007) To what extent does the longevity of fixed dental prostheses depend on the function of the cement? *Clin. Oral Impl. Res.*, **18**(Suppl 3), 193–204.

94. Román-Rodríguez, J. L., Roig-Vanaclocha, A., Fons-Font, A., Granell-Ruiz, M., Solá-Ruiz, M. F., Amigó-Borrás, V., Busquets-Mataix, D., Vicente-Escuder, A. (2010) In vitro experimental study of bonding between aluminium oxide ceramics and resin cements, *Med. Oral Patol. Oral Cir. Bucal*., **15**, 95–100.

95. Oyague, R. D., Osorio, R., da Silveira, B. L., Toledano, M. (2011) Comparison of bond stability between dual-cure resin cements and pretreated glass-infiltrated alumina ceramics, *Photomed. Laser Surg*., **29**, 465–475.

96. Eduardo CdeP, Bello-Silva, M. S., Moretto, S. G., Cesar, P. F., deFreitas, P. M. (2012) Microtensile bond strength of composite resin to glass-infiltrated alumina composite conditioned with Er,Cr:YSGC laser, *Lasers Med. Sci.*, **27**, 7–14.

97. Blatz, M. B., Sadan, A., Arch, G. H., Jr., Lang, B. R. (2003) In vitro evaluation of long-term bonding of Procera AllCeram alumina restorations with a modified resin luting agent, *J. Prosthet. Dent.,* **89**, 381–387.

98. Kern, M., Wegner, S. M. (1998) Bonding to zirconia ceramic: adhesion methods and their durability, *Dent. Mater*., **14**, 64–71.

99. Matinlinna, J. P., Heikkinen, T., Ozcan, M., Lassila, L. V., Vallittu, P. K. (2006) Evaluation of resin adhesion to zirconia ceramic using some organosilanes, *Dent. Mater*., **22**, 824–831.

100. May, L. G., Passos, S. P., Capelli, D. B., Ozcan, M., Bottino, M. A., Valandro, L. F. (2010) Effect of silica coating combined to a MDP-based primer on the resin bond to Y-TZP ceramic, *J. Biomed. Mater. Res. B: Appl. Biomater*., **95**, 69–74.

101. Blatz, M. B., Phark, J. H., Ozer, F., Mante, F. K., Saleh, N., Bergler, M., Sadan, A. (2010) In vitro comparative bond strength of contemporary self-adhesive resin cements to zirconium oxide ceramic with and without air-particle abrasion, *Clin. Oral. Invest.,* **14**, 187–192.

102. Re, D., Augusti, D., Augusti, G., Giovannetti, A. 92012) Early bond strength to low-pressure sandblasted zirconia: evaluation of a self-adhesive cement, *Eur. J. Esthet. Dent*., **7**, 164–175.

103. Zhang, Y., Pajares, A., Lawn, B. R. (2004) Fatigue and damage tolerance of Y-TZP ceramics in layered biomechanical systems, *J. Biomed. Mater. Res. B: Appl. Biomater.*, **71**, 166–171.

104. Qeblawi, D. M., Muñoz, C. A., Brewer, J. D., Monaco, E. A., Jr. (2010) The effect of zirconia surface treatment on flexural strength and shear bond strength to a resin cement, *J. Prosthet. Dent.*, **103**, 210–220.

105. Scherrer, S. S., Cattani-Lorente, M., Vittecoq, E., de Mestral, F., Griggs, J. A., Wiskott, H. W. (2011) Fatigue behavior in water of Y-TZP zirconia ceramics after abrasion with 30 μm silica-coated alumina particles, *Dent. Mater*., **27**:e28–e42.

106. Senyilmaz, D. P., Palin, W. M., Shortall, A. C., Burke, F. J. (2007) The effect of surface preparation and luting agent on bond strength to a zirconium-based ceramic, *Oper. Dent.,* **32**(6), 623–630.

107. Piascik, J. R., Swift, E. J., Thompson, J. Y., Grego, S., Stoner, B. R. (2009) Surface modification for enhanced silanation of zirconia ceramics, *Dent. Mater.*, **25**, 1116–1121.

108. Piascik, J. R., Wolter, S. D., Stoner, B. R. (2011) Enhanced bonding between YSZ surfaces using a gas-phase fluorination pretreatment, *J. Biomed. Mater. Res. B: Appl. Biomater.*, **98**, 114–119.

109. Smith, R. L., Villanueva, C., Rothrock, J. K., Garcia-Godoy, C. E., Stoner, B. R., Piascik, J. R., Thompson, J. Y. (2011) Long-term microtensile bond strength of surface modified zirconia, *Dent. Mater*., **27**, 779–785.

110. Ozcan, M., Cura, C., Valandro, L. F. (2011) Early bond strength of two resin cements to Y-TZP ceramic using MPS or MPS/4-META silanes, *Odontology*, **99**, 62–67.

111. Ozcan, M., Kerkdijk, S., Valandro, L. F. (2008a) Comparison of resin cement adhesion to Y-TZP ceramic following manufacturers' instructions of the cement only, *Clin. Oral Invest.*, **12**, 279–282.

112. Wolfart, M., Lehmann, F., Wolfart, S., Kern, M. (2007) Durability of the resin bond strength to zirconia ceramic after using different surface conditioning methods, *Dent. Mater*., **23**, 45–50.

113. Ozcan, M., Cura, C., Valandro, L. F. (2008b) Effect of various surface conditioning methods on the adhesion of dual-cure resin cement with MDP functional monomer to zirconia after thermal aging, *Dent. Mater. J*., **27**, 99–104.

114. Oyague, R. C., Monticelli, F., Toledano, M., Osorio, E., Ferrari, M., Osorio, R. (2009) Effect of water aging on microtensile bond strength of dual-

cured resin cements to pre-treated sintered zirconium-oxide ceramics, *Dent. Mater.*, **25**, 392–399.

115. Passos, S. P., May, L. G., Barca, D. C., Ozcan M, Bottino, M. A., Valandro, L. F. (2010) Adhesive quality of self-adhesive and conventional adhesive resin cement to Y-TZP ceramic before and after aging conditions, *Oper. Dent.*, **5**, 689–696.
116. Thompson, J. Y., Stoner, B. R., Piascik, J. R., Smith, R. (2011) Adhesion/cementation to zirconia and other non-silicate ceramics: where are we now? *Dent. Mater.*, **27**(1), 71–82.
117. Ohno, H., Yamane, Y., Endo, K., Araki, Y., Iizuka, Y. (1998) Adhesion of adhesive resin to dental precious metal alloys. Part I. New precious metal alloys with base metals for resin bonding, *Dent. Mater. J.*, **17**, 275–284.
118. Chang, J. C., Hurst, T. L., Hart, D. A., Estey, A. W. (2002) 4-META use in dentistry: a literature review, *J. Prosthet. Dent.,* **87**, 216–224.
119. Parsa, R. Z., Goldstein, G. R., Barrack, G. M., LeGeros, R. Z. (2003) An in vitro comparison of tensile bond strengths of noble and base metal alloys to enamel, *J. Prosthet. Dent.*, **90**, 175–183.
120. Kadoma, Y. (2005) Adhesive properties and kinetic polymerization behaviour of resins containing adhesion promoting monomers for precious metals, *Dent. Mater. J.*, **24**, 335–341.
121. Kadoma, Y., Kojima, K. (2005) Water durability of resin bond to precious metal alloys using adhesive resins containing adhesion promoting monomers, *Dent. Mater. J.*, **24**, 494–502.
122. Kadoma, Y., Kojima, K., Tamaki, Y, Nomura, Y. (2007) Water durability of resin bond to pure gold treated with various adhesion promoting thiirane monomers, *Dent. Mater. J.*, **26**, 29–37.
123. Tanaka, J., Stansbury, J. W., Antonucci, J. M., Suzuki, K. (2007) Surface treatment with N,N'-dimethacryloylcystine for enhanced bonding of resin to dental alloys, *Dent. Mater. J.*, **26**(4), 514–518.
124. Ikemura, K., Fujii, T., Negoro, N., Endo, T., Kadoma, Y. (2011a) Design of a metal primer containing a dithiooctanoate monomer and a phosphonic acid monomer for bonding of prosthetic light-curing resin composite to gold, dental precious and non-precious metal alloys, *Dent. Mater. J.*, **30**, 300–307.
125. Ikemura, K., Kojima, K., Endo, T., Kadoma, Y. (2011c) Effect of novel dithiooctanoate monomers, in comparison with various sulfur-containing adhesive monomers, on adhesion to precious metals and alloys, *Dent. Mater. J.*, **30**(1), 72–78.

126. Livaditis, G. J., Thompson, V. P. (1982) Etched castings: an improved retentive mechanism for resin-bonded retainers, *J. Prosthet. Dent.*, **47**, 52–58.

127. Bertolotti, R. L. (2007) Adhesion to porcelain and metal, *Dent. Clin. N. Am.,* **51,** 433–451.

128. Matinlinna, J. P., Lassila, L. V., Kangasniemi, I., Vallittu, P. K. (2005) Isocayanto- and methacryloxysianes promote Bis-GMA adhesion to titanium, *J. Dent. Res.*, **84**, 360–364.

129. Matinlinna, J. P., Lassila, L. V., Vallittu, P. K. (2006) Evaluation of five dental silanes on bonding a luting cement onto silica-coated titanium, *J Dent.*, **34**, 721–726.

130. Elsaka, S. E., Swain, M. V. (2012) Effect of surface treatmnets on the adhesion of self-adhesive resin cements to titanium, *J. Adhes. Dent.*, epub ahead of print.

131. Khaled, S. M. Z., Miron, R. J., Hamilton, D. W., Chapentier, P. A., Rizkalla, A. S. (2010) Reinforcement of resin based cement with titania nanotubes, *Dent. Mater.*, **26**, 169–178.

132. Ramos, R. P., Chimello, D. T., Chinelatti, M. A., Dibb, R. G., Mondelli, J. (2000) Effect of three surface sealants on marginal sealing of class V composite resin restorations, *Oper. Dent.*, **25**, 448–453.

Chapter 7

Glass Fibers in Fiber-Reinforced Composites

Pekka K. Vallittu
Department of Biomaterials Science and Turku Clinical Biomaterials Centre (TCBC), Institute of Dentistry, University of Turku, Turku, Finland
pekka.vallittu@utu.fi

Fiber-reinforced composites (FRCs) are a novel group of dental materials that are characterized by the filler of the fiber form. The function of the fibers is to transfer loads from the weaker polymer phase to the more durable reinforcing fibers. In dentistry, the use of glass fibers is justified because of their good cosmetic-esthetic properties and due to fact that they can properly be bonded to resins by using silane coupling agents. The glass fiber–polymer matrix surface interface is influenced by many factors of the hostile environment of the oral cavity. Glass fibers of various compositions and surface treatments provide reliable adhesion and retention of physical properties also in a longer perspective.

Handbook of Oral Biomaterials
Edited by Jukka P. Matinlinna

ISBN 978-981-4463-12-6 (Hardcover), 978-981-4463-13-3 (eBook)
www.panstanford.com

7.1 Overview of Fiber-Reinforced Composites

There has been considerable development of synthetic composite materials in recent decades, particularly those containing fibers in a *polymer matrix*. The idea to use high-strength fibers to strengthen a cheap matrix is not new. The practice to embed straw in mud bricks very likely predated the reference to Hebrew slaves under the pharaoh in the Bible. The first evaluations to use FRCs in dentistry were made in the early 1960s, but more extensive research started in the early 1990s [1]. The introduction of new products for the dental market occurred on a larger scale at the end of the 1990s. Presently, there is a great number of FRC products on the market, and most of them are based on glass fibers.

A dental glass FRC is used in a demanding environment regarding chemical stability and mechanical loading conditions. An FRC consists of reinforcing fibers, most typically glass fibers of various kinds. The function of the fibers is to provide load transfer from a weaker polymer matrix to the reinforcing fibers [2, 3].

Parameters that influence the properties of FRCs include:

(i) physical properties of fibers vs. the matrix polymer;
(ii) length and direction of fibers;
(iii) adhesion of fibers to the matrix;
(iv) quantity of fibers in the matrix; and
(v) impregnation of fibers with the resin.

In dentistry, the most suitable fibers have been found to be glass fibers, although other fibers such as carbon/graphite, aramid, and polyethylene fibers have also been used [4, 5]. A combination of fibers and a polymer matrix provides a reinforced composite, which has physical properties between the most durable phase (fiber) and the weakest phase (polymer) (Fig. 7.1).

Although the best glass FRC is comparatively corrosion-resistant material, corrosion, that is, surface leaching of fibers or the polysiloxane interphase to the polymer matrix, can take place due to the moist and frequently acidic environment of the oral cavity. Pathogenic oral microbes, for example, *Streptococcus mutans* and *Lactobacillus*, are well known to produce acids, which locally can lower the pH of the tooth surface to the level of 5.4–4.4, which is a critical value where significant amounts of enamel dissolve. Thus,

although the polymer matrix of FRCs protects the fibers from the direct influence of pH decrease, the FRCs are prone to corrosion by leaching.

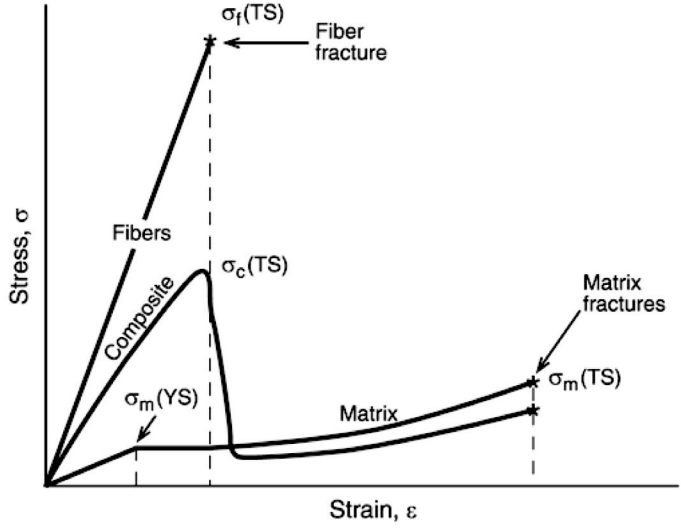

Figure 7.1 Mechanical properties of FRCs are related to properties of the fibers and matrix. The figure shows stress–strain curves for fibers, the matrix, and the composite (TS = tensile strength; YS = yield strength). Modified from Ref. [6].

Biomechanically, loading conditions are also demanding. Oral biomechanics originates from the function of muscles of the masticatory system and their application of force to teeth and restorations and finally to jawbones. Forces are controlled or modulated by the sensory apparatus. Prosthodontic and restorative devices must be designed to resist the same forces than affect natural teeth. A prosthesis requires both static and dynamic strength as well as a number of other mechanical properties to resist the necessary transmission of forces over its many years in the mouth. Maximal biting forces measured unilaterally may be as high as 850 N, but in normal mastication function, forces are considerably lower, around 50–80 N. FRCs are generally not isotropic (independent of the direction of the applied load) but rather are often anisotropic (different depending on the direction of the applied load). Anisotropicity of FRCs plays a significant role in planning and

designing devices used in dentistry, since the loading conditions by the masticatory system produce loads and stresses of various magnitudes and types, that is, bending, shear, tensile, compression, and torque [7–9].

Anisotropicity of FRCs has been demonstrated to occur in terms of

(i) mechanical properties;
(ii) thermal properties;
(iii) optical properties;
(iv) polymerization contraction; and
(v) surface physical properties.

Although FRCs are relatively corrosion-resistant materials, degradation of the polymer resin matrix, glass fibers, and their interface may occur in an aggressive medium. The medium can diffuse into the polymer and reduce the properties by corrosion. Damage mechanisms in cross-linked thermosetting resin FRCs relate to the chemical composition, structure, and cross-link density as well as fibers and other fillers in the composite. It is known that diffusion of water, acids, and bases thorough the polymer matrix is relatively slow, but they proceed quickly along the glass fibers, where the silane-promoted adhesion between fibers and polymer matrix is located. Silanes are discussed in detail in Chapters 3 and 11.

7.1.1 Role of the Resin

Resin systems in thermosetting FRCs are based on polyesters, vinylesters, epoxides, phenols, and furanes, which have different chemical resistance toward the effects of acids and alkaline solutions and aliphatic and aromatic solvents [10]. Resistance can be tested by immersing the polymer in a medium for a certain period of time and following the changes in the physical properties. In thermosetting resins, cross-links between the polymer backbones are covalent in nature, and there dissolving of the resin matrix does not occur. The medium can, however, cause swelling of the resin matrix and cause reversible changes in the physical properties. Swelling increases mobility of the macromolecules, which plastizises the matrix, lowers the modulus of elasticity, and reduces surface hardness. Transport of the medium into the matrix is influenced by diffusion, which

depends principally on the structure of the resin, the temperature, and the type and viscosity of the medium.

Of polymers, polyester resins are widely used. The weak point of polyesters is the ester group, which can be deteriorated by hydrolysis. However, by introduction of an aromatic ring in the resin chain, the resistance against water increases considerably. Polymers that are polymerized from monomer systems based on bisphenol derivates show good resistance toward the effects of water and alkaline solutions. This is an important aspect, which relates to the FRCs used in dentistry and surgery, because bisphenol A glycidyl dimethacrylate (bis-GMA)-based resin systems are widely used. Another commonly used resin system is epoxy resins, which also demonstrate good chemical resistance. Dental FRCs utilize resin systems that are based on bis-GMA, triethylene glycol dimethacrylate (TEGDMA, aka TEGMA), and urethane dimethacrylate (UDMA, aka UEDMA). All these can produce highly cross-linked thermoset polymer matrices for FRCs. To increase toughness of the matrix and surface-adhesive properties, amounts of a linear polymer of *poly*(methyl methacrylate) (PMMA) have been added to the matrix. A mixture of a cross-linked polymer and a linear polymer is the so-called *semi-interpenetrating polymer network* (semi-IPN).

Currently, IPNs are used in denture base polymers, denture teeth, FRCs, and, very recently, restorative composite resins [11]. There are several kinds of IPN structures, which differ in terms of structure. These are [12]:

(i) sequential IPNs;
(ii) gradient IPNs;
(iii) thermoplastic IPNs;
(iv) semi-IPNs; and
(v) simultaneous IPNs.

Dental IPNs are predominantly semi-IPNs in which one or more polymers are cross-linked and one or more polymers are linear or branched. Dimethacrylate monomers or multifunctional monomers and *dendrimers* are typically forming the cross-linked part of the semi-IPN, and PMMA is forming the linear part of the semi-IPN system. The IUPAC Commission on Macromolecular Nomenclature–based name for the semi-IPN made of bis-GMA, TEGDMA, and PMMA

is *net*-poly(methyl methacrylate)-*inter-net*-copoly(bis-glysidyl-A-dimethacrylate)-triethyleneglycol dimethacrylate.

The polymerization reaction of monomer systems of thermoset and semi-IPN polymers is based on free-radical (vinyl) polymerization. Initiation of the polymerization is made by radiation of blue light or by increasing temperature. Normally, light-initiated polymerization is based on activation of an initiator camphorquinone and an activator amine. Heat-induced polymerization is based on activation of a benzoyl peroxide initiator by increasing temperature. If the monomer system is aimed to be cured without temperature increase or light radiation, an activator, such as a tertiary amine, is added to the initiator system. Examples of these autopolymerizing resins are PMMA and p-bis-GMA-pTEGDMA bone cements and PMMA denture rebasing and repair resins (where p = the polymerized form).

Autopolymerization and light-curing polymerization result in a polymer with a lower degree of monomer conversion than that of a polymer cured by increased temperature. Lower monomer conversion also increases the quantity of leachable residual monomers and thus reduces the biocompatibility of the polymer. Leached monomers of the polymer are replaced by molecules of the surrounding medium, in this context by water, which diffuse into the polymer matrix of FRCs and reach the surface of glass fibers. Light-cured polymers can be postcured by heat after initial curing, which increases considerably the degree of monomer conversion, reduces th equantity of residual monomers, improves biocompatibility, and reduces water sorption. The optimal postcuring temperature is close to the glass transition temperature where there is enough thermal energy in the system to create free volume, which enables unreacted carbon–carbon double bonds to form free radicals and react with each other. The glass transition temperature for p-bis-GMA-pTEGDMA is 144°C and for multiphase denture PMMA 110–120°C (see also Chapter 6) [14, 15].

7.1.2 Interface between Glass Fibers and the Polymer Matrix

Adhesion of reinforcing glass fibers to the polymer matrix is of great importance for durability of FRCs. Load transfer from the weaker polymer matrix to the reinforcing fibers is happening through the

adhesive interface (Fig. 7.2) [13]. Adhesion is obtained with the help of silane coupling agents, which increases surface wettability of the glass fibers, resulting in better physical attachment of the resin system to the surface of glass, and on polycondesation of hydrolyzed silanols to the hydroxyl groups on the surface of glass fibers (see also Chapter 11) [16–18].

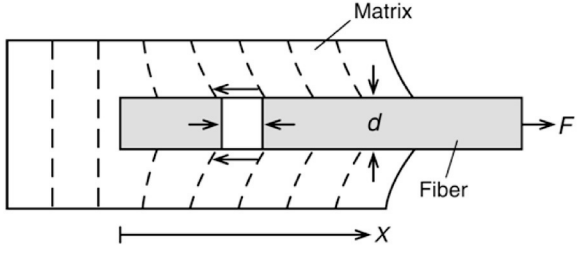

Figure 7.2 Adhesive interface between the fiber and the polymer matrix transfers load when a force (F) is applied to the fiber. The diameter of the fiber (d) and interfacial adhesion influence load transfer to and shear stress formation on the fiber and the interface (arrows). Modified from Ref. [6].

The mechanisms of actions of silane coupling agents are thus based on surface wettability and chemical-bonding theories. A third suggested mechanism of action is the so-called restrained layer theory, which utilizes the elasticity of the polycondensated siloxane layer to even the stress peaks between the polymer matrix and the glass fiber of a higher modulus of elasticity during loading conditions.

The adhesive interface between the reinforcing fiber and the polymer matrix influences also the reinforcing efficiency of short fibers. Long, continuous, unidirectional fibers provide the highest possible reinforcing efficiency in the direction of stress. Depending on the fiber length, short fibers have a reinforcing efficiency between long fibers and the particulate filler. The critical fiber length (l_c) is a parameter of minimum length at which the center of the fiber reaches the ultimate strength when the matrix achieves the maximum shear strength. The critical fiber length can be determined, for example, by a single fiber fragmentation test, where the length of fiber fragments in the polymer matrix can be used to determine the critical fiber length (Fig. 7.3).

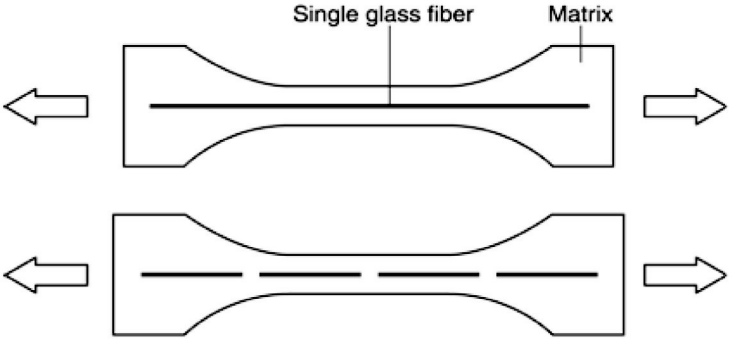

Figure 7.3 The single fiber fragmentation test can be used to determine the critical fiber length, which is the minimum length fibers can provide a reinforcing effect to the polymer. The length of the pieces of fragmented fibers inside the polymer matrix represents the critical fiber length of the particular fiber–matrix system. Arrows show the direction of tensile stress, which elongate the specimen and cut the fiber.

The critical fiber length is related to the elongation at the break of the polymer matrix and fibers and to a large extent on the adhesion of fibers to the polymer matrix. An example of the influence of the length of fibers on reinforcing efficiency is shown in Fig. 7.4.

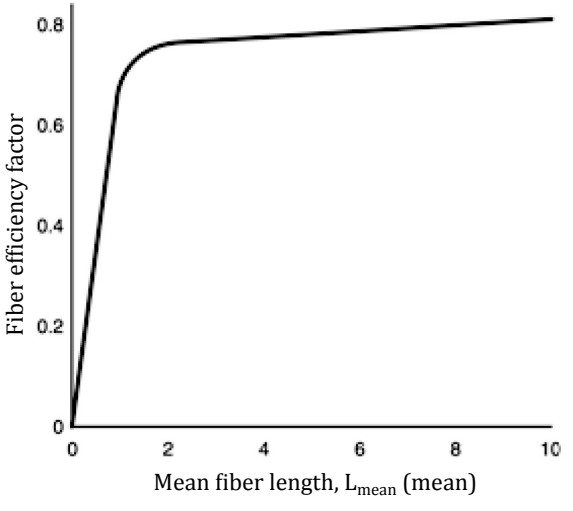

Figure 7.4 Example of the relationship between the fiber length (mm) and reinforcing efficiency.

A good-quality and well-polymerized FRC undergoes hardly any permanent changes of properties by the influence of water [10]. However, the molecular bonds at the interface between glass fibers and the silane coupling agent are a potential place of attack for hydrolytic degradation. Degradation may occur at the polysiloxane network or at the surface of glass fibers. The latter is influenced by the chemical composition of glass fibers and their surface treatment prior to sizing and silanization.

If the medium, water or saliva, can come into contact with glass fibers by exposing the glass fibers during finishing the restoration, by cracks or microcracks in the composite, the proceeding of the saliva or water along the interface is much greater than the diffusion through the polymer matrix. This is due to the capillary effect of the glass fibers, which may exist in the laminate. Shrinkage of the resin by polymerization may also cause capillaries between the fibers and the polymer matrix, as is shown to happen especially with resin systems of high polymerization shrinkage, namely, monomers of methyl methacrylate [19, 20]. It is also possible that manually impregnated fibers with dental resin systems may contain poorly impregnated regions, that is, voids containing air [21]. Oxygen of the air inhibits free-radical polymerization to occur in the polymer surface close to the void and causes increased penetration of water, not only into the voids by capillary forces, but also into the polymer matrix by diffusion.

7.1.3 Chemical Composition of Various Glass Fibers

The composition of glass is playing a decisive role in manufacturing of fibers and in the chemical stability of fibers against the effects of water. It has been shown that chemical resistance of glasses toward glass corrosion relates to the composition, the state of the glass surface, the amount and type of the attacking solvent medium, the temperature, and the time. In the presence of water, the strength of the fibers may be reduced, especially with glass fibers of high alkali metal oxide content [10]. There are several types of glasses used in glass fibers, and of those, the most suitable to be used in dental and medical applications are so-called alkali-free glasses (Table 7.1).

Table 7.1 Nominal composition (%) of certain glass fibers [10]

Component	Type of glass					
	E	**A**	**C**	**R**	**S**	**M**
SiO_2	53–55	70–72	60–65	60	62–65	53
Al_2O_3	14–16	0–2.5	2–6	25	20–25	–
CaO	20–24	5–9	–	6–9	–	13
MgO	20–24	1–4	1–3	6–9	10–15	9
B_2O_3	6–9	0.5	2–7	–	0–1.2	–
K_2O	<1	1	0–8	0.1	–	–
Na_2O	<1	12–15	0–16	0.4	0–1.1	–
Fe_2O_3	<1	0–1.5	0.3	0.3	0.2	0.3
BaO	–	–	1	–	–	–
BeO	–	–	–	–	–	8

Certain glass-forming agents, including B_2O_3, are leached from the surface of glass fibers, and thus, the supporting glass network can be split at different places. The process of production of glass fibers may contain elimination of easy-leaching oxides, which can increase stability of fibers. If leaching occurs in an acidic environment, the external areas of glass fibers are leached quicker than the inner ones. The chemical composition of glass fibers is different on the fiber surface that in the inner part of the fibers. The surface of E-glass may be enriched with boron and calcium. The glass composition has a considerable effect of resistance of the fibers against the influence of acids, as can be seen from Fig. 7.5.

Continuous and short glass fibers in dental FRC products are usually made of alkali-free glass (up to 1% $Na_2O + K_2O$), known as E-glass. E-glass is based on a SiO_2-Al_2O_3-CaO-MgO system, which has a good glass-forming ability. Because of the high calcium oxide content, a glass similar to this composition shows poor resistance to acidic solutions. For this reason, the composition of E-glass is modified by introducing boron oxide (B_2O_3) and by decreasing the CaO content. The other type of glass used in dental FRCs is S-glass, which provides slightly higher tensile strength than that of E-glass (Table 7.2.). For bioactive glasses, see Chapter 8.

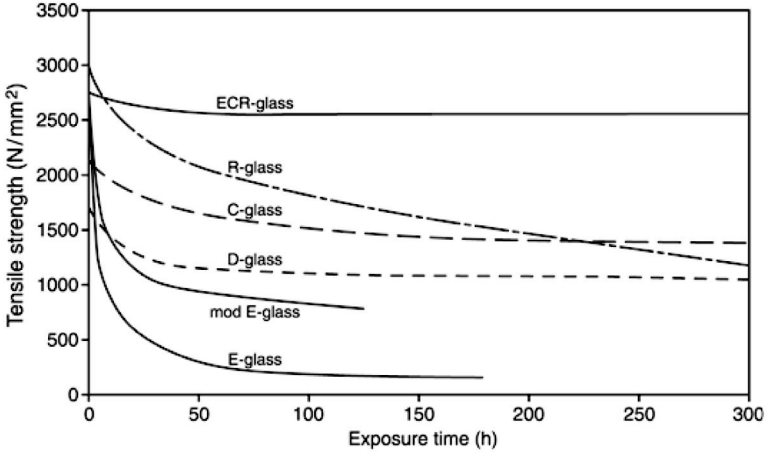

Figure 7.5 Tensile strength of glass fibers of various types plotted against the exposure time in 5% H_2SO_4. Modified from Ref. [10].

Table 7.2 Some physical properties of glass fibers [10]

Property	Type of glass					
	E	A	C	R	S	M
Density (g/cm^3)	2.54–2.59	2.48	2.45–2.49	2.5	2.49	2.89
Tensile strength (10^{-2} N/mm^2)	25–34	24–31	31–34	44–48	49	35
Young's modulus (10^{-3} N/mm^2)	73–77	70–71	70–71	86	86	117

7.1.4 Effect of Water on the Properties of FRCs

The static strength (ultimate flexural strength) of an FRC is dependent on the fiber quantity to the level of approximately 70 vol%. A high-quality glass FRC material with high fiber quantity provided high flexural properties (with continuous unidirectional E-glass at 1250 MPa) [22]. Water sorption of the polymer matrix reduced the strength and modulus of elasticity of the FRC of a semi-IPN polymer matrix by approximately 15% within 30 days' water storage time at 37°C [23, 24]. A positive correlation exists between water sorption of the polymer matrix and the reduction of flexural properties [25]. For

instance, high water sorption of a polyamide (nylon) matrix causes reduction of over 50% in the strength of an FRC. The reduction of flexural properties was reversible, that is, dehydration of the FRC restored the mechanical properties [26]. No significant reduction of flexural strength and modulus, even in long-term water storage (at 10 years), occurred. Consequently, to the present knowledge, a glass FRC made of good-quality E-glass fibers provides a stable composite structure in a water-containing environment of the oral cavity. Devices used in the oral cavity are also designed to have veneering or other coverage of the FRC framework by another polymer, which protects the glass fibers of the FRC framework mechanically and from the effect of water. This is structurally analogous to the gel coats of the FRCs used in engineering composites.

7.2 Clinical Aspects and Use

7.2.1 Structure of Dental FRC Devices

Development of an FRC with a new type of resin system and an understanding of the designing principles behind constructing devices have led to the use of FRCs in a variety of disciplines and applications: removable prosthodontics, fixed prosthodontics, restorative dentistry, periodontology, orthodontics, and repairs of fractured porcelain veneers. The most recent application for FRCs is in fillings of teeth. In dental appliances of relatively small size, the quality of the load-bearing FRC substructure is of importance. From this perspective, all of the factors that influence the properties of FRCs must be carefully taken into consideration. This is especially important because the masticatory system produces cyclic loads to the dental appliances.

Therefore, not only adequate static strength of the appliance but also adequate dynamic (fatigue) strength is needed. It should also be noted that dental constructions are multiphase in nature. For example, an FRC-reinforced root-canal-post system consists of dentine, a composite resin cement, a core buildup composite resin, and, as a load-bearing material, the FRC root canal post. All of these phases need to have adequate strength, and the phases needs to be adhered well to each other. Water absorption from the saliva will

occur on the FRC and the overlaying veneering composite, which causes reduction of some extent of the strength and stiffness of the FRC device. To keep the water penetration and sorption as low as possible, the device should be well polymerized and should not contain any microvoids in the structure.

Dental FRC devices are multiphasic. Adhesion of a particulate filler composite (PFC) resin (resin luting cement, veneering composite) plays an important role in load transfer from the surface of the device to the FRC framework and tooth. An FRC as a bonding substrate contains different types of materials from polymers to inorganic glass fibers and even particulate fillers.

7.2.2 Removable Dentures

Research on dental FRCs started in the early 1960s when the first experiments on using glass fibers in denture base polymers were made. Besides using glass fibers, some tests were made to reinforce denture base polymers by carbon/graphite fibers. Little attention was paid during that time to the low reinforcing effect of any fibers when they were used with powder-liquid-type denture base resins. In the 1990s studies were published that showed that a highly viscous resin mixture of PMMA powder and a monomer liquid was not able to adequately impregnate the fibers. The use of excess of the monomer liquid to lower the viscosity of the resin mixture did not solve the problem. The higher quantity of monomer liquid in the resin mixture caused void formation in the composite by polymerization contraction. This led to the development of a *preimpregnation* system of the reinforcing fibers with porous PMMA. Porous PMMA between the silanized glass fibers behaves as a polymer powder in the acrylic resin mixture. It lowers the polymerization shrinkage of the resin between the fibers.

The fiber reinforcements in denture bases are divided into two categories. Ladizesky et al. reported a method where fibers were distributed through the entire denture base [27–29]. On the other hand, the approach by Vallittu is based on the concept that only the weakest part of the denture base (location of fracture initiation) is reinforced by fiber reinforcement. Two reinforcing concepts are total fiber reinforcement (TFR) and partial fiber reinforcement (PFR) [30, 31]. Clinical studies have been performed with FRC-reinforced

removable dentures, and they suggested that PFR offers an effective method to eliminate fractures in a denture base.

The successful use of PFR requires correct positioning of the fibers in the denture base. The fibers should be placed in the region on the denture base where the fracture most likely begins. The correct place of the fibers in upper complete dentures is close to the denture teeth, and fibers should be directed along the ridge lap in a horseshoe shape. Continuous unidirectional fibers offer the highest resistance against midline fractures.

In removable partial dentures, where the fracture likely occurs in the anterior margin of the denture, fibers in the form of woven fabric are preferred. An average of a 10 mm wide FRC-reinforced region with woven glass fibers eliminates denture fracture initiation and propagation. Maxillary dentures are also reinforced with woven fibers to eliminate fractures of the denture base polymer closed to precision attachments of dentures. It has been suggested that FRCs can also lower the number of loosening parts of precision attachments.

7.2.3 Fixed Dental Prostheses

FRCs can be used to produce definitive fixed partial dentures (FPDs). On the basis of current clinical results, it is reasonable to expect FRC FPDs to attain good longevity. FPDs made of FRCs are classified into surface-retained FPDs, inlay-/onlay-retained FPDs, full-coverage crown-retained FPDs, and hybrid FPDs [32–41]. The latter type is a combination of various retaining elements according to the specific need of the dentition. FRC FPDs can be made directly or indirectly. Implant-supported FPDs have been fabricated from carbon/graphite FRCs and glass FRCs. All permanent-type, indirectly made tooth-supported FRC FPDs have to be luted with composite resin luting cements, although there are reports in which conventional luting cements were tested. Direct FRC FPDs can be bonded to a tooth by polymerization of restorative composite resins. Adhesive properties of FRCs bonded directly to the dentine and enamel have been studied by Tezvergil et al., showing that only minor differences could be found between adhesive properties of FRCs and PFCs [42, 43]. In FRC FPDs, the framework between the abutments is made of continuous unidirectional fibers, which offer high flexural

strength. The crowns can be reinforced with woven fibers or in some fabrication concepts by making a fiber loop of unidirectional fibers to surround the abutment. Recent clinical studies have shown that an FRC framework needs to provide support for the veneering composite resin and, therefore, additional fibers are needed to be placed inside the pontic. There are also studies that emphasize the importance of fiber geometry of the FRC framework for the strength of the FPD construction.

Surface-retained resin-bonded FPDs made of metals are normally supported and bonded from one end only to a diminished number of debondings. In the case of surface-retained FRC FPDs, the bridgework can be supported from both ends because of better bonding characteristics and minor flexibility of the FRC framework. The flexibility allows abutment teeth movement to occur to some extent without loosening the FPD. In surface-retained FRC FPDs, the location of the bonding wing in the vertical dimension of the abutment is important. Fibers of the bonding wing should be placed close to the incisal edge to eliminate the momentary forces for dislodgement. On the other hand, the bonding wing needs to cover largely the bonding surface. The bonding wing is placed most often on the oral surfaces of abutments but labial and buccal surfaces can also be used. To protect the fibers of the bonding wing, a layer of PFR is placed to cover the wing. In this, good interfacial adhesion between the FRC framework and the PFC resin is important to avoid chipping of the composite resin. In connectors, the continuous unidirectional fibers should have a cross-sectional design, which offers good resistance against occlusal forces. It has been shown that the thickness of the connector versus the width of the connector is an important parameter when stiffness and strength are optimized. Normally the cross section of the connector has the maximum quantity of fibers, but if there is excess of space, the highest strength is provided by placing the fibers on the tension side. Surface-retained FRC FPDs are used in anterior and premolar regions. Recent laboratory investigations have suggested that optimally designed FRC FPDs made on nonprepared abutments can provide even higher load-bearing capacity than conventional porcelain fused to metal FPDs.

Inlay-/onlay-retained FPDs are made by combining the cavities of the abutments by continuous unidirectional fibers. The FPDs

can be made indirectly or directly. In the case of indirect FPDs, cementation is made with composite resin luting cements, which contain a regular adhesive resin, which is used to activate the bonding surface for secondary-IPN bonding. Self-adhesive cements do not provide optimal bonding. In canines, it is recommended to add an additional bonding wing buccally or palatinally to the framework to avoid loosening of the inlay in cuspid-protected articulation. In the case of existing old fillings, removal of the fillings totally or partially provides space for the FRC framework and veneering composite resin. Vertical support against occlusal loads is needed, and in intact teeth, an approximal box preparation in depth of more than 1 mm provides support for the FPD if the fibers are accurately placed in the box. The load-bearing capacity of such an FPD is higher than the maximum biting forces in the molar region. Veneering of the FRC framework is made by a laboratory veneering composite resin or by a restorative composite resin. The optimal thickness of the veneering composite resin on the occlusal surface of the FRC framework is more than 1.5 mm.

Full-coverage crown-retained FPDs are made by layering woven FRCs on prepared abutments. Abutments are connected with continuous unidirectional fibers, adding additional pieces of FRCs to support cusps of the pontics. Veneering is made with a laboratory PFC resin. The FRC framework is intended to be fully covered by the veneering composite resin in order to obtain a polishable and tooth-colored surface. Special attention needs to be paid to the interproximal regions. If the FRC framework is not properly covered by the veneering composite resin, or preferably opaque paint, the darkness of the oral cavity can be transmitted through the connectors and cause cosmetic/esthetic problems. Computer-aided design/computer-aided manufacturing (CAD/CAM)-processed FRC blocks made of short, random fiber-oriented FRCs in a polyamide matrix (nylon) are also available for FRC framework fabrication.

Mechanical properties of short FRCs are considerably lower than those of continuous unidirectional FRCs. The water sorption of polyamide causes reduction of the FRCs by up to 60% in 30 days. Use of full-coverage crowns as retaining elements of FPDs does not allow treatment according to the principles of minimal invasiveness. FRCs can also be used as reinforcements of provisional FPDs during fabrication of conventional FPDs.

7.2.4 Root Canal Posts

The use of FRC in root canal posts to anchor cores and crowns has rapidly increased. FRCs can be used in root canals as prefabricated solid posts and individually formed posts [44–50]. Prefabricated posts are made of reinforcing fibers (carbon/graphite, glass, quartz), and finally a polymerized resin matrix between the fibers forms a solid post with a predetermined diameter. Individually formed posts are made of nonpolymerized fiber–resin prepregs, consisting typically of glass fibers and a light-curing resin matrix. The rationale for an individually formed FRC post is to fill the entire space of the root canal by FRC material. The increased fiber quantity, especially in the coronal part of the root canal, increases the load-bearing capacity of the system, and the biomechanics of a tooth can better be simulated because the fibers are located closer to the dentine, where the highest stresses exist. A tooth restored with root canal posts should be able to withstand cyclic loading of high magnitude for a long period of time without catastrophic failure or marginal breakdown of the crown, which can predispose one to secondary caries. The load-bearing phase of the root canal post system, that is, the FRC root canal post, should withstand loads and the crown margins should remain intact. Repeated stress cycles cause microscopic cracks mainly in the tension side of the construction, and after a period of time, the cracks increase to such a size that a sudden fracture can occur even with a low stress level. Clinically, the material-based weakness in fatigue resistance is compensated by designing and dimensioning the cast metal or FRC post and core correctly, thus increasing the quantity of reinforcing fibers in the cervical part of the tooth. This approach can be taken into consideration by fabricating an individually formed post instead of using a prefabricated post.

Fabrication of prefabricated FRC root canal posts is based on impregnation of fibers with thermoset resins, like dimethacrylate or epoxy resins. Thermoset resins forming a cross-linked polymer between the fibers do not allow good bonding of the post to the resin cement. To overcome the problem of adhesion, some manufacturers have added serrations to the post for mechanical retention to the cement. On the other hand, if a semi-IPN polymer matrix is

used between fibers, like in the case of individually formed posts, adhesion of the post to the cement is good. It has been shown by radioactive-labeled resins that monomers of an adhesive resin diffused to the semi-IPN polymer matrix of a post at a depth of 25 μm in a few minutes [51, 52]. The resins should also enable complete impregnation of fibers. There are some prefabricated FRC root canal posts on the market that do not entirely fulfill the requirements of complete impregnation, and thus the strength of the posts is lower than expected from the constituents.

7.2.5 Fiber-Reinforced Filling Composites

Utilization of fibers in filling composites has been tested for years. Reasons for poor success have been selection of too short fibers, which were not able to increase the strength and toughness of the composite resin, and the concept of bulky filling material, which resulted in a poorly polishable surface for the filling. The current concept of using FRCs in fillings is based on using an FRC base with relatively long cut fibers and then veneering the base with a conventional particulate filling composite resin [53–56]. It has been shown that fiber orientation perpendicular to the axial walls of a cavity reduces polymerization contraction of the composite. In dental fillings, the concept of using fiber-controlled polymerization contraction is based on using cut fibers with a length of 1–3 mm. Packing the fibers to the cavity forces the fibers to be orientated randomly in the plane and, thus, perpendicular to the axial walls of the cavity. The FRC base of the filling is veneered with a regular hybrid composite resin (Fig. 7.6). On the basis of the three-dimensional anisotropicity of the FRC, polymerization contraction occurs in the vertical direction rather than horizontally.

Another benefit of using an FRC base for filling composites is the increase of the toughness of the composite filling. Toughness and other physical properties are superior compared to the properties of conventional filling composites. The function of the FRC base for filling composites is to support the filling composite layer and serve as a crack prevention layer (Fig. 7.7). Resin composites are discussed in Chapters 3 and 6.

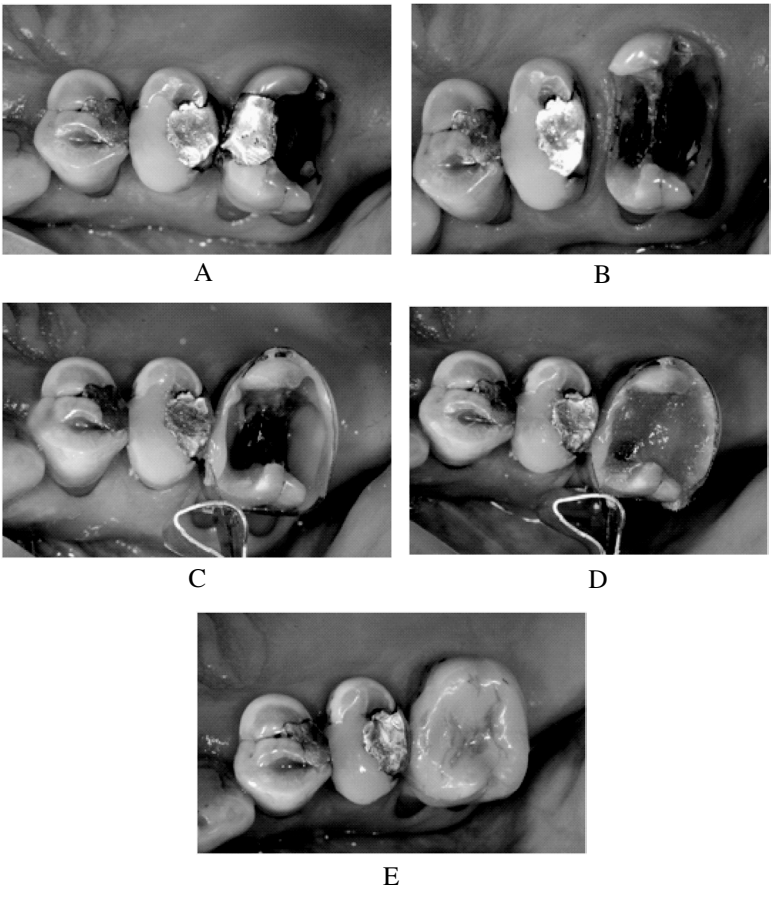

Figure 7.6 A short-fiber FRC is used to toughen large composite fillings. (A) a fractured amalgam filling to be replaced, (B) a removed filling, (C) a matrix band placed and margins sealed with a flowable composite resin, (D) a short FRC applied to replace dentin, and (E) a hybrid composite resin used to veneer the FRC base.

7.3 Future Development

A variety of dental glass FRC materials is available, and they provide improvements in the mechanical strength of resins and PFCs. The light-curing resin-impregnated continuous unidirectional

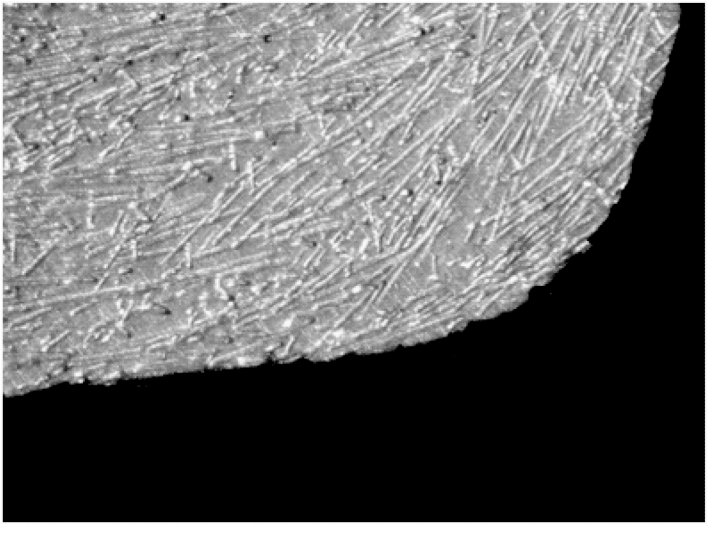

Figure 7.7 Longitudinal section of a short FRC-reinforced filling. Black regions represent dentin, and fibers toughen the filling and control polymerization contraction. The original magnification is 40×.

FRC materials may provide high mechanical strength, which is predictable also in a longer perspective in oral conditions. The future development of glass FRCs in dentistry and medicine will occur in improving the *design* of FRC devices and in developing the *reinforcing fiber–matrix system*. This also includes research to improve even more *adhesion* between glass fibers and the polymer matrix. Attempts to use the semi-IPN polymer matrix short glass FRC for *filling material applications* have been made. This is one field of future development for dental FRCs. Another field where FRCs are being utilized is *implantology*. There are promising results of using bioactive glass-modified FRCs as oral, orthopedic, and head-and-neck implants.

References

1. Smith, D. C. (1962) Recent developments and prospects in dental polymers, *J. Prosthet. Dent.*, **12**, 1066–1078.
2. Kolbeck, C., Rosentritt, M., Behr, M., Lang, R., Handel, G. (2002) In vitro examination of the fracture strength of 3 different fiber composite and

1 all-ceramic posterior inlay fixed partial denture systems, *J. Prosthod.,* **11**, 248–253.

3. Vallittu, P. K. (1997) Glass fiber reinforcement in repaired acrylic resin removable dentures: preliminary results of a clinical study, *Quintess. Int.,* **28**, 39–44.
4. Vallittu, P. K. (1997) Ultra-high-modulus polyethylene ribbon as reinforcement for denture polymethyl methcarylate. A short communication, *Dent. Mater.,* **13**, 381–382.
5. Goldberg, A. J., Burstone, C. J., Hadjinikolaou, I., Jancar, J. (1994) Screening of matrices and fibers for reinforced thermoplastics intended for dental applications, *J. Biomed. Mater. Res.,* **28**, 167–173.
6. Ohring, M. (1995) *Engineering Materials Science*, 1st ed., 475–477, Academic Press, USA.
7. Vallittu, P. K. (1999) Flexural properties of acrylic polymers reinforced with unidirectional and woven glass fibers, *J. Prosthet. Dent.,* **81**, 318–326.
8. Tezvergil, A., Lassila, L. V. J., Vallittu, P. K. (2003) The effect of fiber orientation on the thermal expansion coefficients of the fiber reinforced composites, *Dent. Mater.,* **19**, 471–477.
9. Abdulmajeed, A. A., Lassila, L. H., Vallittu, P. K., Närhi, T. O. (2011) The effectof exposed glass fibers and particles of bioactive glass on the surface wettability of composite implants, *Int. J. Biomater*., **607971**, epub 2011 Dec. 27.
10. Cheremisinoff, N. P. (1990) Corrosion phenomena in glass-fiber-reinforced thermosetting resins, in *Handbook of Ceramics and Composites*, 231–268 (Ed. Ehrenstein, G. W., Schmiemann, A., Bledzki, A., Spaude, R.), Marcel Dekker, USA.
11. Vallittu, P. K. (2009) Interpenetrating polymer networks (IPNs) in dental polymers and composites, *J. Adhes. Sci. Technol.*, **23**, 961–972.
12. Sperling, L. H. (1994) Advances in chemistry series; 239, in *Overview of IPNs. Interpenetrating Polymer Networks*, 4–6 (Ed. Klempner D, Sperling, L. H., Utracti, L. A.), American Chemical Society, USA.
13. Bouillaguet, S., Schutt, A., Alander, P., Vallittu, P. K., Schwaller, P., Buerki, G., Michler, J., Cattani-Lorente, M., Krejci I. (2006) Influence of hydrothermal and mechanical stress to interfacial bond strength glass fibers to polymer matrix, *J. Biomed. Mater. Res. B,* **76**, 98–105.
14. Kilambi, H., Cramer, N. B., Schneidewindm, L. H., Shah, P., Stansbury, J. W., Bowman, C. N. (2009) Evaluation of highly reactive mono-(meth)

acrylates as reactive diluents for Bis-GMA-based dental composites, *Dent. Mater.,* **25**, 33–38.

15. Ruyter, I. E., Öysaed, H. (1982) Conversion in denture base polymers, *J. Biomed. Mater. Res.,* **16**, 741–754.
16. Rosen, M. R. (1978) From treating solution to filler surface and beyond. The life history of a silane coupling agent, *J. Coat. Technol.,* **50**, 70–82.
17. Matinlinna, J. P., Areva, S., Lassila, L. V. J., Vallittu, P. K. (2004) Characterization of siloxane films on titanium substrate derived from three aminosilanes, *Surf. Interface Anal.,* **36**, 1314–1322.
18. Vallittu, P. K. (1993) Comparison of two different silane compounds used for improving adhesion between fibers and acrylic denture base material, *J. Oral. Rehabil.,* **20**, 533–539.
19. Vallittu, P. K. (1995) The effect of void space and polymerisation time on transverse strength of acrylic-glass fiber composite, *J. Oral. Rehabil.,* **22**, 257–261.
20. Vallittu, P. K. (1998) Some aspects of the tensile strength of unidirectional glass fiber-polymethyl methacrylate composite used in dentures, *J. Oral. Rehabil.,* **25**, 100–105.
21. Vallittu, P. K. (1997) Oxygen inhibition of autopolymerization of polymethylmethacrylate-glass fiber composite, *J. Mater. Sci. Mater. Med.*, **8** 489–492.
22. Lassila, L. V. J., Tanner, J., LeBell, A.-M., Narva, K., Vallittu P. K. (2004) Flexural properties of fiber reinforced root canal posts, *Dent. Mater.,* **20**, 29–36.
23. Vallittu, P. K., Ruyter, I. E., Ekstrand, K. (1998) Effect of water storage on the flexural properties of E-glass and silica fiber acrylic resin composite, *Int. J. Prosthodont.,* **11**, 340–350.
24. Vallittu, P. K. (2000) Effect of 180 weeks water storage on the flexural properties of E-glass and silica fiber acrylic resin composite, *Int. J. Prosthodont.,* **13**, 334–339.
25. Lassila, L. V. J., Nohrström, T., Vallittu, P. K. (2002) The influence of short-term water storage on the flexural properties of unidirectional glass fiber–reinforced composite, *Biomaterials,* **23**, 2221–2229.
26. Lastumäki, T., Lassila, L., Vallittu, P. K. (2001) Flexural properties of bulk fiber-reinforced composite DC-Tell used in fixed partial dentures, *Int. J. Prosthodont.,* **14**, 22–26.
27. Ladizesky, N. H., Chow, T. W., Ward, I. M. (1990) The effect of highly drawn polyethylene fibres on the mechanical properties of denture base resins, *Clin. Mater.,* **6**, 209–225.

28. Ladizesky, N. H., Ho, C. F., Chow, T. W. (1992) Reinforcement of complete denture bases with continuous high performance polyethylene fibers, *J. Prosthet. Dent.,* **68**, 934–939.

29. Ladizesky, N. H., Chow, T. W., Cheng, Y. Y. (1994) Denture base reinforcement using woven polyethylene fiber, *Int. J. Prosthodont.,* **7**, 307–314.

30. Vallittu, P. K. (1997) Glass fiber reinforcement in repaired acrylic resin removable dentures: preliminary results of a clinical study, *Quintess. Int.,* **28**, 39–44.

31. Narva, K., Vallittu, P. K., Yli-Urpo, A. (2001) Clinical survey of acrylic resin removable denture repairs with glass-fiber reinforcement, *Int. J. Prosthodont.,* **14**, 219–224.

32. Freilich, M. A., Duncan, J. P., Alarcon, E. K., Eckrote, K. A., Goldberg, A. J. (2002) The design and fabrication of fiber-reinforced implant prostheses., *J. Prosthet. Dent.,* **88**, 449–454.

33. Ahlstrand, W. M., Finger, W. J. (2002) Direct and indirect fiber-reinforced fixed partial dentures: case reports, *Quintess. Int.,* **33**, 359–365.

34. Behr, M., Hindelang, U., Rosentritt, M., Lang, R., Handel, G. (2000) Comparison of failure rates of adhesive-fixed partial dentures for in vivo and in vitro studies, *Clin. Oral. Invest.,* **4**, 25–30.

35. Göhring, T. N., Mormann, W. H., Lutz, F. (1999) Clinical and scanning electron microscopic evaluation of fiber-reinforced inlay fixed partial dentures: preliminary results after one year, *J. Prosthet. Dent.,* **82**, 662–668.

36. Meiers, J. C., Freilich, M. A. (2000) Conservative anterior tooth replacement using fiber-reinforced composite, *Oper. Dent.,* **25**, 239–243.

37. Rosentritt, M., Behr, M., Lang, R., Handel, G. (2000) Experimental design of FPD made of all-ceramics and fibre-reinforced composite, *Dent. Mater.,* **16**, 159–165.

38. Vallittu, P. K., Sevelius, C. (2000) Resin-bonded, glass fiber reinforced composite fixed partial dentures: a clinical study, *J. Prosthet. Dent.,* **84**, 413–418.

39. Nohrström, T. J., Vallittu, P. K., Yli-Urpo, A. (2000) The effect of position and quantity of glass fibers on the fracture resistance of provisional fixed partial denture, *Int. J. Prosthodont.,* **13**, 72–78.

40. Dyer, S. C., Lassila, L. V. J., Vallittu, P. K. (2004) The effect of internal fiber arrangement on the delamination failure in hybrid composite dental prostheses, *J. Phys. Mesomech.,* **7**, 119–122.

41. Dyer, S. R., Lassila, L. V. J., Jokinen, M., Vallittu, P. K. (2004) Effect of fiber position and orientation on fracture load of fiber-reinforced composite, *Dent. Mater.,* **20**, 947–55.

42. Tezvergil, A., Lassila, L. V. J., Vallittu, P. K. (2003) Strength of adhesive-bonded fiber-reinforced composites to enamel and dentine substrates, *J. Adhes. Dent.,* **5**, 301–311.

43. Tezvergil, A., Lassila, L. V. J., Vallittu, P. K. (2005) The shear bond strength of bidirectional and random-oriented fibre-reinforced composite to tooth structure, *J. Dent.,* **33**, 509–516.

44. Le Bell, A.-M., Tanner, J., Lassila, L. V. J., Kangasniemi, I., Vallittu, P. K. (2004) Bonding of composite resin luting cement to fibre-reinforced composite root canal post, *J. Adhes. Dent.,* **6**, 319–325.

45. Le Bell, A.-M., Lassila, L. V. J., Kangasniemi, I., Vallittu, P. K. (2005) Bonding of fibre-reinforced composite post to root canal dentin, *J. Dent.,* **33**, 533–539.

46. Le Bell-Rönnlöf, A.-M., Lassila, L. V., Kangasniemi, I., Vallittu, P. K. (2005) Load-bearing capacity of human incisor restored with various fiber-reinforced composite posts, *Dent. Mater.,* **27**, 107–115.

47. Nagase, D. Y., Takemoto, S., Hattori, M., Yoshinari, M., Kawada, E., Oda, Y. (2005) Influence of fabrication techniques on retention force of fiber-reinforced composite posts, *Dent. Mater. J.,* **24**, 280–285.

48. Island, G., White, G. E. (2005) Polyethylene ribbon fibers: a new alternative for restoring badly destroyed primary incisors, *J. Clin. Ped. Dent.,* **29**, 151–156.

49. Qualthrough, A. J., Mannocci, F. (2003) Tooth-colored post systems: a review, *Oper. Dent.,* **28**, 86–91.

50. Hatta, M., Shinya, A., Vallittu, P. K., Shinya, A., Lassila, L. V. J. (2011) High volume individual fiber post versus low volume fiber post. The fracture load of the restored tooth, *J. Dent.,* **39**, 65–71.

51. Mannocci, F., Sheriff, M., Watson, T. F., Vallittu. P. K. (2005) Penetration of bonding resins into fiber posts: a confocal microscopic study, *Endodont. J.,* **38**, 46–51.

52. Wolff, D., Geiger, S., Ding, P., Staehle, H. J., Frese C. (2012) Analysis of the interdiffusion of resin monomers into pre-polymerized fiber-reinforced composites, *Dent. Mater.,* **28**, 541–547.

53. Garoushi, S. K., Vallittu, P. K., Watts, D. C., Lassila, L. V. J. (2008) Polymerization shrinkage of experimental short glass fiber reinforced composite with semi-interpenetrating polymer network matrix, *Dent. Mater.,* **24**, 211–215.

54. Garoushi, S., Vallittu, P. K., Lassila, L. V. J. (2008) Depth of cure and surface microhardness of experimental short fiber-reinforced composite, *Acta Odontol. Scand.,* **66**, 38–42.

55. Garoushi, S. K., Lassila, L. V., Vallittu, P. K. (2007) Direct composite resin restoration of an anterior tooth: effect of fiber-reinforced composite substructure, *Eur. J. Prosthod. Rest. Dent.,* **15**, 61–66.

This page intentionally left blank

Chapter 8

Bioactive Glasses

Leena Hupa and Susanne Fagerlund
Department of Chemical Engineering, Åbo Akademi University, Turku, Finland
leena.hupa@abo.fi, susanne.fagerlund@abo.fi

Bioactive glasses are feasible implant materials since they not only adhere to tissue but also have the ability to form firm chemical bonds with biological apatite crystals in both bone tissue and teeth. In the human body environment, dissolution and precipitation reactions of the glass lead to the forming of apatite crystals on the glass surface. The crystals on the glass are capable to bond with biological apatite crystals in the living tissue. However, the brittle nature of glasses restricts their use as implant materials in load-bearing applications, such as molar teeth with strong bite forces. The ions dissolved from the glass have been found to trigger and support the body's own capability to actually heal and regenerate human tissue. The most recent research within the field of bioactive glasses has been on tissue engineering devices based on the aforementioned bioactive features.

Handbook of Oral Biomaterials
Edited by Jukka P. Matinlinna

ISBN 978-981-4463-12-6 (Hardcover), 978-981-4463-13-3 (eBook)
www.panstanford.com

8.1 Background

Bioactivity is often defined as the ability of a material to bond chemically with biological tissue. The strength of a chemical bond between a bioactive material and biological tissue is of the same order or higher than that of the chemical bonds within the bioactive material or the biological tissue [1]. A requirement for the formation of a strong bond between an inorganic and amorphous substance, a bioactive glass, and a living tissue is that an interaction at the molecular level has to occur between these two distinctly different materials.

Recent research in this field focuses on using bioactive glasses in bone tissue contact in such a way that bone injuries are healed and growth of new bone tissue is supported, restored, and even regenerated. The phenomena of tissue restoration and regeneration are not directly linked with the ability of a glass to simply bond with biological tissue. Rather, these phenomena occur because biological tissue responds in a certain way to contact with the man-made material. The terms "osteoconduction," "osteoinduction," and "osteostimulation" are used to describe the aforementioned influences of bioactive glasses on bone tissue regrowth.

In general, bioactive materials are defined as materials that induce a specific biological activity [2]. First-generation biomaterials, such as metal prostheses, were used in replacing biological tissue with as small a toxic response as possible. The term "second-generation biomaterial" refers to substances that possess the ability to chemically bond with living tissue. The development of bioactive glasses gave rise to second-generation biomaterials. Third-generation biomaterials evolved from the second generation in such a way that the third-generation materials affect tissue growth on genetic and cellular levels, which is a prerequisite for tissue engineering and tissue regeneration [3].

It is noteworthy, however, that the most important single requirement for any bioactive glass implant is its biocompatibility. The term "biocompatibility" means the ability of a material to generate a beneficial host response in a given situation [4].

Bioactive glasses are said to be discovered by Professor Larry Hench in the late 1960s. To be exact, though, Professor Hench's glasses were a result of a purposeful development of an implant

material that would not be surrounded by fibrous tissue but instead be chemically compatible with bone tissue [5]. Since the first successful in vivo studies, the development of bioactive glasses has been a journey of exploration for novel biological responses and applications of this special family of glasses. Despite wide research over the past four decades, bioactive glasses still have only a few commercial applications. Figure 8.1 gives the timeline of important milestones in the research and development of melt-derived bioactive glasses. Increasing the utilization of bioactive glasses is limited in part by the brittle and rigid nature of glass and in part by problems of the formability of the glass into product forms other than small monoliths, particles, or powdered glass.

Melt-derived bioactive glasses crystallize easily when drawn into continuous fibers or when sintered into porous implants and tissue-engineering scaffolds [6, 7]. Bioactive glasses that allow versatile forming methods have been developed through adjusting and optimizing the composition, thus allowing forming operations based on viscous flow of the molten glass [6, 8, 9]. Thin films, nanoparticles, nanofibers, or mesoporous structures are manufactured through other forming methods than those typical for traditional melt-quenching. Jones [10] presents an excellent and detailed summary of the development of bioactive glasses from melt-quenched silicates into bioactive glass/polymer hybrids. Future utilization of bioactive glass–based devices in tissue engineering scaffolds having the capability to activate genes essential for tissue regeneration calls for a detailed understanding of the influence of glass composition and morphology on the dissolution kinetics and degradation rate of the devices.

> Glasses can be utilized in many fields of medicine: fiber optics for endoscopy, thermometers, insoluble porous carriers for antibodies and enzymes, fillers in resin composite materials, bioactive implants, fillers in bioabsorbable composite structures, and tissue engineering scaffolds [1, 11–14].

Figure 8.2 depicts examples of some products of bioactive glasses from the research at the Åbo Akademi University in Åbo (Turku), Finland. The glass products in the figure have been developed through national and international collaboration between several other research groups active in this field. The figure shows glass

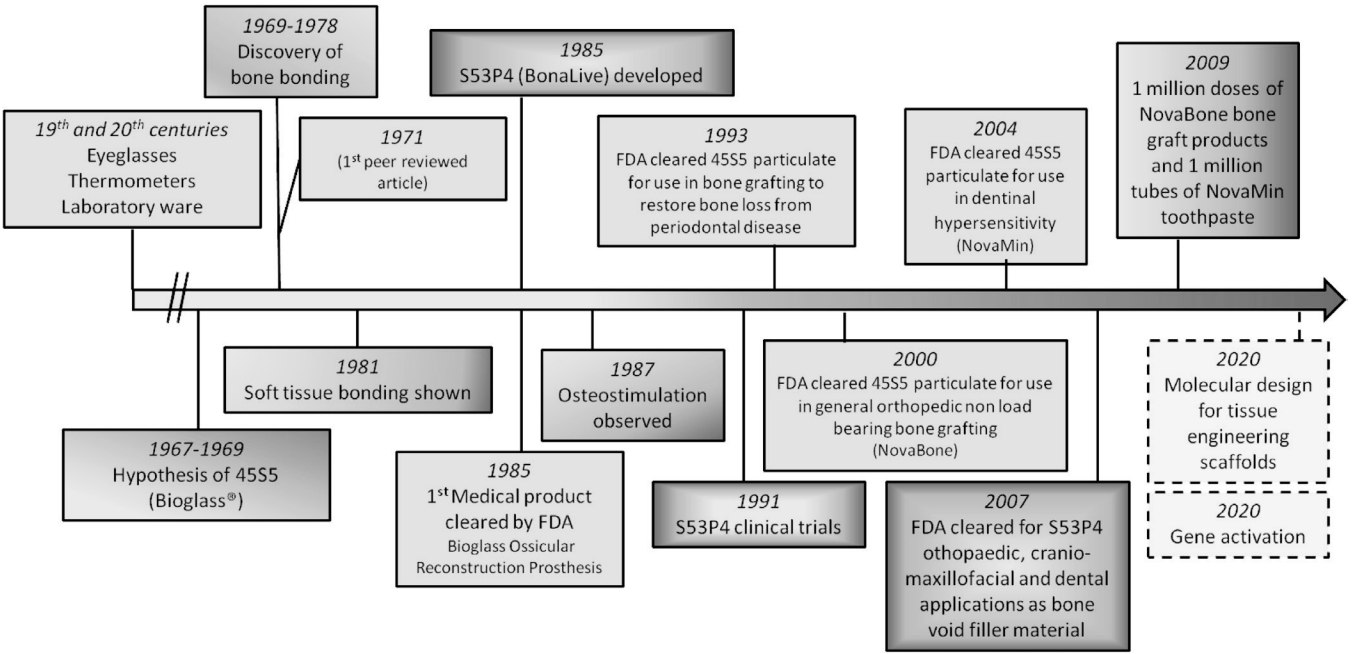

Figure 8.1 Timeline of milestones in the research and development of bioactive glasses into commercial products.

plates, powdered fractions, sintered porous glass implants, porous scaffolds manufactured by the polymer foam replication technique, sol-gel-derived structures, a dense composite of glass particles and polylactic acid, and thin fibers. The fibers can then be used alone or in composite structures. Details of the various requirements placed upon glass composition for successful manufacture of versatile product forms will not be presented here but can be found in other literature [6, 8, 9, 12, 15–21].

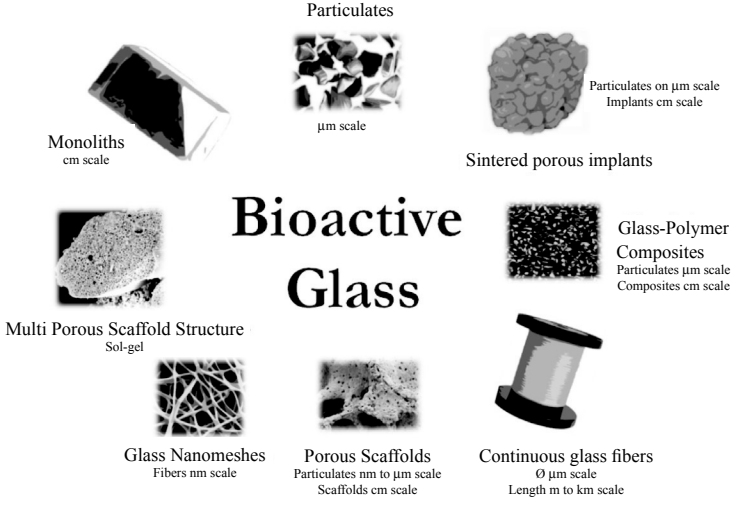

Figure 8.2 Examples of product forms manufactured from bioactive glasses with various methods [18–21].

The research and development of bioactive glasses for medical devices is highly interdisciplinary. Therefore various aspects of materials science, materials manufacture, the environment of the human body, and the requirements of a safe and easily applicable product have to be considered. The most important research on the usage of melt-quenched bioactive glasses mainly in dentistry is reviewed below.

8.2 Glass as a Biomaterial

Bioactive glasses were originally developed to bond chemically with bone tissue and then gradually resorb as new bone tissue grows

and replaces the glass implant. Bone tissue consists of organic components, mainly collagen fibers, inorganic hydroxyapatite (HAP) crystals, $Ca_{10}(PO_4)_6(OH)_2$ around the collagen fibers, and bone cells. HAP is the main inorganic material also in enamel, dentine, and cementum. The amount of HAP in bone tissue and dentine is about 70 vol%, yet in tooth enamel the amount of the HAP crystals is 99 vol%. Two of the major functions of bones are to provide structural support for the body and to provide protection for vital organs within the body, and these suggest that strength is an important property for a graft. The tooth enamel may also be heavily loaded. Why would glass be a material of choice for synthetic bone grafts or dentistry? As a first approximation, glass is a strong material but it fails via brittle fracture with fracture strength highly sensitive to surface and bulk flaws. The risks accompanied with strength may be partly avoided by using the bioactive glass as a powder, particles, or small monoliths in nonloaded or moderately loaded applications. Thin glass fibers and small particles may find use in increasing the overall strength of mechanically less durable polymer composites.

In contrast to their unfavorable strength properties silicate glasses possess a very interesting characteristic: certain amounts of oxides of almost all elements can be incorporated into the glass structure. The backbone of silicate glasses consists of a three-dimensional network structure of *silica*, SiO_2. The building unit of the network is the ion $[SiO_4]^{4-}$, which is bonded in the shape of tetrahedra sharing the O^{2-} corners with each other. Adding modifying oxides, for example, Na_2O and CaO, breaks some of the oxygen bonds and reduces the network connectivity of the glass structure. The strength of the individual modifying ion–oxygen bond together with the amount of the modifying oxides determines several glass properties. Glasses with lower network connectivity are easier to be manufactured into various product shapes than pure silica glasses. The bonding strength of the Na^+ and Ca^{2+} ions to the network is weaker than the bonding within the silicate ion. As the cross-linking of the network decreases, the dissolution of ions from glasses in aqueous solutions increases. When the effect of the oxide on the properties is known, the glass composition may be tailored to show desired properties by merely adjustment of the composition.

Professor Hench had the ingenious starting point of selecting glasses containing *sodium oxide* (Na_2O), *calcium oxide* (CaO), *phosphorus pentoxide* (P_2O_5), and *silica* (SiO_2) for a novel implant material for bone healing and repair [5].

All the elements in these glasses are abundant in the human body, thus minimizing the risk of toxicity or other harmful effects by the implant. The same oxides we may also find in more traditional glasses used in tableware products, windows, containers, etc. It was not only the choice of the oxides but also their amounts in the glass that made these studies a success story. In traditional glasses the silica content is around 65 wt% to 80 wt%, while the glasses studied for implants have clearly lower silica contents, from around 40 wt% to 60 wt%. Accordingly, the contents of Na_2O, CaO, and P_2O_5 are higher. Bioactive glasses should react in the human body, while glass containers are used, for example, to distribute and store medicines and preparations without any mutual interaction. By suitably adjusting the oxide composition, glasses can be tailored from formulations dissolving totally already in mild conditions to compositions that sustain attack of aqueous solutions and gases in severe environments. Controlled dissolution of ions with subsequent HAP surface layer development is the most important individual property.

8.3 Compositions of Melt-Derived Bioactive Glasses

Bioactive glasses have been developed within three systems:

(i) Glasses based on silicates (SiO_2)
(ii) Glasses based on phosphates (P_2O_5)
(iii) Glasses based on borates (B_2O_3)

The main manufacturing methods are the traditional melt-quenching technique and sol-gel synthesis. Although the phosphate- and borate-based glasses show several interesting features and effects, the discussion in this chapter is limited to the melt-derived silicate glasses.

The glasses are manufactured by melting a carefully mixed batch of crystalline raw materials such as *quartz sand* (SiO_2), *sodium*

carbonate (Na_2CO_3), *calcium carbonate* ($CaCO_3$), etc., at elevated temperatures of around 1400°C. The volatile compounds, carbonates, moisture, etc., are eliminated, and the batch forms a homogenous oxide melt. When cooling the melt to room temperature, a special time–temperature schedule is applied to prevent it from crystallizing and to give a homogenous amorphous solid material, glass. The first bioactive glasses were designed within the oxide system SiO_2-Na_2O-CaO-P_2O_5. Today, two melt-derived compositions are accepted for certain clinical used by the US Food and Drug Administration (FDA): the original bioactive glass 45S5 Bioglass® developed by Professor Hench et al. [5] and S53P4 BonAlive® developed by Andersson et al. [22]. The oxide compositions of these glasses are given in Table 8.1. Both glasses are low in SiO_2, which makes them sensitive to crystallization during the cooling and restricts the manufacture of special-shaped products from the melt. Accordingly, the commercial products of these glasses are based on powdered glass, particles, or small monoliths (Fig. 8.1).

Considerable research efforts have been put to find compositions that enable versatile manufacturing of bioactive glass fibers or porous implants and tissue engineering scaffolds. Bioactive glasses suitable for continuous fibers and sintered porous scaffolds have been reported, for example, by Brink et al. [23, 24] and Vedel et al. [6, 9, 25]. Some formulations that contained also K_2O, MgO, and B_2O_3 showed widened working properties and desired in vivo bioactivity. Among these, glass 13-93 [23] and 1-98 [26] have been studied extensively in vitro and in vivo [24, 27–38]. The compositions of 13-93 and 1-98 are given in Table 8.1.

Table 8.1 Oxide compositions of 45S5, S53P4, 13-93, and 1-98 in wt%

Glass	SiO_2	Na_2O	K_2O	MgO	CaO	B_2O_3	P_2O_5	Reference
45S5	45	24.5			24.5		6	[5]
S53P4	53	23			20		4	[22]
13-93	53	6	12	5	20		4	[23]
1-98	53	6	11	5	22	1	2	[26]

Over the years, bioactive glass research has progressed from implant material development to the utilization of glasses in tissue engineering scaffolds and in other products that support the

human body's natural tissue regenerative capability. Within these applications the influence of ions releasing from the glass on tissue regeneration is of major interest. Several studies deal with the effect of replacing CaF_2 or SrO for CaO in 45S5 [39–41]. Substituting B_2O_3 for SiO_2 in the 13-93 formulation enables tailoring of the bioactivity and dissolution rate for porous bone repair and regeneration scaffold tissue [42].

8.4 Surface Reactions of Bioactive Glasses

8.4.1 Reaction Steps at the Glass Surface

The first bioactive glasses were designed to release calcium and phosphate ions in the body environment. These ions are essential components of HAP, the main inorganic component of the bone apatite. Thus, the glasses were thought to supply ions to supersaturate the interfacial solution and to promote HAP precipitation on the glass surface. The precipitation requires not only high enough ion concentrations but also favorable sites for nucleation. The bioactive glasses with low network connectivity form at their surfaces a silica-rich gel as the mobile ions of alkaline and alkaline earths leach out. According to Karlsson [43], the floppy structure of the silica gel with high water content facilitates precipitation of highly dispersive apatite crystals with a size in the nanometer scale. The size of the biological apatite crystals in skeletal bone tissue and dentine is approximately 5 × 30 nm, while the needle-shaped crystals in tooth enamel have an approximate size of 30 × 90 nm. Compared to other bioactive materials such as tricalcium phosphate–based ceramics or calcium hydroxyapatite, the silica gel structure provides flexible nucleation sites for the apatite crystallites to adapt the size and orientation of the crystals in the biological apatite. The silica gel also supplies OH groups in the same way as the main organic component of bone, collagen, does. Accordingly, formation of the silica gel structure is essential for bioactive glasses.

The reactions of bioactive glasses in body fluids leading to chemical bonding of the glass surface to the apatite in living tissue are often described as several successive and partly overlapping reactions steps taking place at the glass surface [1]. These reactions

are summarized below. Figure 8.3 gives a schematic description of the reaction steps taking place at the glass surface. The scanning electron microscopy (SEM) images in the figure give the layer development on the top surface of a bioactive glass in vitro.

1. The reactions commence with a rapid ion exchange of the network modifiers from the glass (Na^+ and Ca^{2+}) with H^+ (or H_3O^+) from the body solution. These ion exchange reactions form silanols (Si-OH) at the glass surface. As H^+ is consumed in the alkali dissolution, the OH^- concentration and pH of the interfacial solution increase:

   $$\text{Si-O-Na}^+ \text{ (glass)} + \text{H}^+\text{(aq)} \rightarrow \text{Si-OH (glass)} + \text{Na}^+\text{(aq)}$$

2. The increase in pH of the interfacial solution leads to the breakup of the silica glass network and to the loss of soluble silica, $Si(OH)_4$. Simultaneously, more silanols are formed at the glass surface:

   $$\text{Si-O-Si(glass)} + \text{H}_2\text{O} \rightarrow \text{Si-OH (glass)} + \text{OH-Si(glass)}$$

3. Condensation and polymerization of the silanol groups to a gel-like silica-rich layer on the glass surface takes place.
4. Migration of Ca^{2+} and PO_4^{3-} groups from the glass through the silica-rich layer and from the solution gives rise to the formation of an amorphous $CaO\text{-}P_2O_5$-rich film on top of the silica-rich layer. This reaction step also results in the growth of the silica-rich layer.
5. The glass continues to dissolve, and the $CaO\text{-}P_2O_5$-rich films grow and crystallize by incorporation of OH^- and CO_3^{2-} ions from the solution to form a carbonate-substituted HAP, a hydroxycarbonate apatite (HCA) layer. This crystallized HCA layer is similar to that in natural bone.

Surface layer formation compatible with the reaction steps has been observed in vivo for bioactive glasses. For the most bioactive glasses the first reactions commence within minutes, while HCA formation takes a few hours. The HCA layer is able to form a chemical bond with natural bone via a series of biological reactions. These include adsorption of growth factors, attachment, proliferation, and differentiation of osteoprogenitor cells [44]. Osteoblasts create the extracellular matrix, collagen, which mineralizes to form a nanocrystalline mineral and collagen on the surface of the glass.

Ideally, new bone tissue forms and conversion reactions of the glass continue at equal rates. A detailed discussion on biomineralization can be found elsewhere in this book.

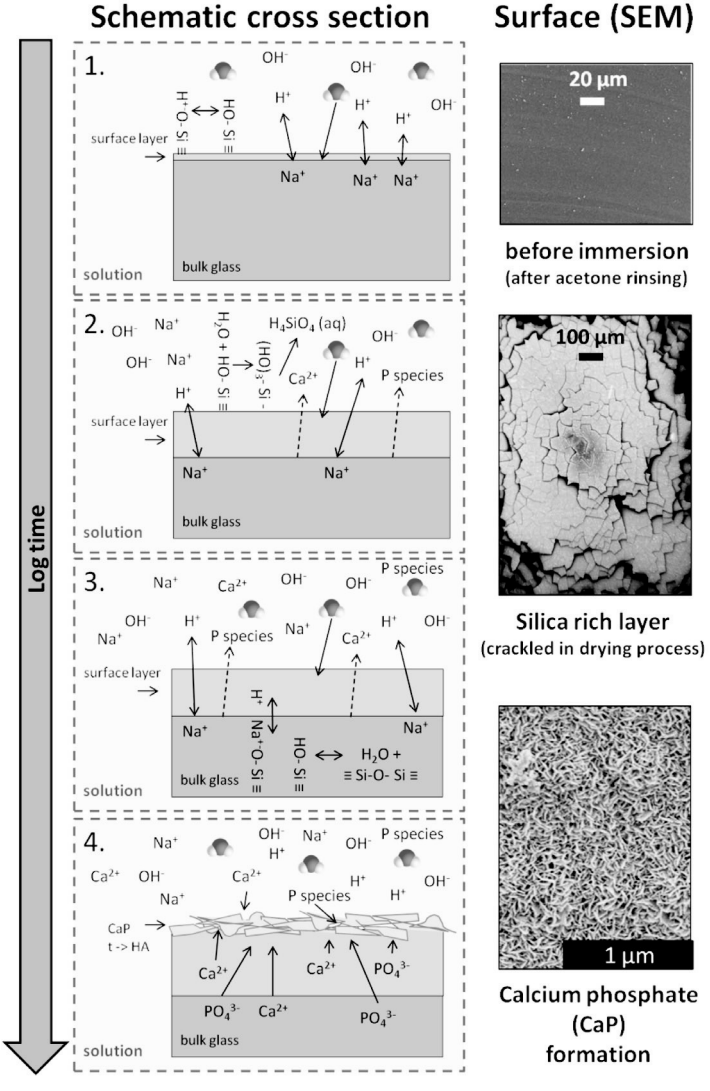

Figure 8.3 Schematic description of the initial reactions at the cross-sectional surface of a bioactive glass in contact with an aqueous solution and SEM images of the top surface of the glass after immersion in simulated body fluid.

8.4.2 In vitro vs. in vivo Surface Layers

The ability of a glass to form an HAP layer at the surface is often studied by immersing it in buffered solutions such as the so-called *simulated body fluid* (SBF). As the HAP formed in SBF has several characteristics similar to the biological apatite, layer formation is often taken as an indication of in vivo bioactivity [45]. The simulated body fluid developed by Kokubo et al. [46] is 2-amino-2-hydroxymethyl-propane-1,3-diol (i.e., Tris) buffer containing all the inorganic components present in human blood plasma. Figure 8.4 shows SEM micrographs of the top surface and cross section of a plate of the bioactive glass 45S5 after the plate has been kept in SBF for two weeks. The top surface shows HAP as a cauliflower-like structure, while in the cross section HAP is seen as a white layer with spherical accumulations. Higher magnification of the top surface in Fig. 8.3 shows the plate-like structure of HAP crystals. The gray-colored layer beneath shows the silica-rich layer, while the intact glass is the undermost layer. The lighter stripe-like formations in the silica-rich layer indicate that HAP precipitation takes place also within the silica-rich gel. The relative amounts of calcium and phosphate in the outer surface correspond to that of HAP.

Similar reaction layers as in SBF form on the glass also in vivo. Figure 8.5 shows the interfacial reaction layer formed between an implant of 45S5 and rat tibia after eight weeks of implantation. The SEM micrographs in Figs. 8.4 and 8.5 nicely show that the in vitro observations are in line with the in vivo reactivity of the glass. It should be pointed out that although the formation of the HAP layer in vitro is an indication of bioactivity, calcium phosphate precipitation may form in SBF also on glasses that do not bond to bone. Factors such as the sample surface area ratio to the solution volume, the agitation of the solution, the duration of the experiment, etc., affect the formation of a calcium phosphate precipitate at the glass surface in SBF. Today, some long-term clinical observations of using bioactive glasses as bone fillers in treatment of fibrous lesions and benign bone tumors are available [48–51].

In general, good bone remodeling was observed. However, still after several years of implantation, remnants of the bioactive glass could be identified in the filled cavities. This suggests that the HCA

layer on the leached silica-rich layer may act as a diffusion barrier that decreases the driving force for further dissolution of the glass. Thus, the glass composition, product form, surface morphology, dosage of the glass, and implantation site should be considered when developing glasses that have dissolution rates compatible with the tissue-remodeling rate.

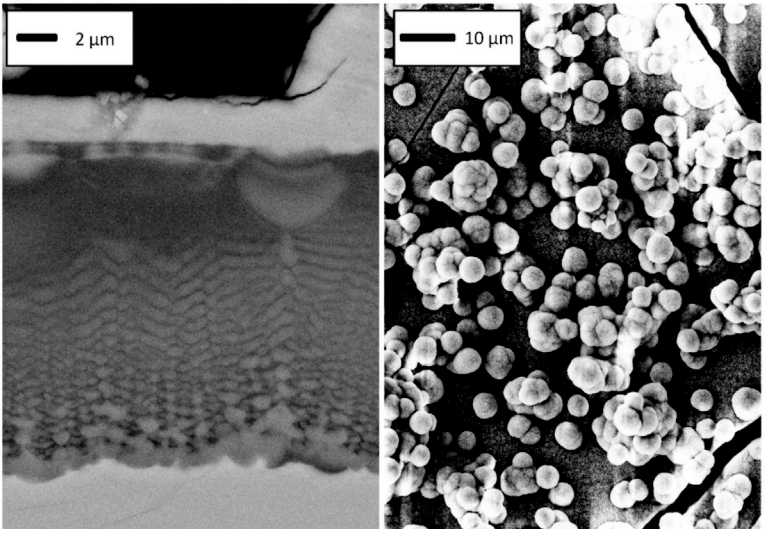

Figure 8.4 SEM micrographs of a 45S5 plate after two weeks in SBF. (a) Cross section and (b) top surface. Experimental details according to Varila et al. [47].

8.5 Ion Dissolution vs. Cellular Response

The bioactive glass research today is increasingly interdisciplinary: biomaterials science, engineering, different branches of medicine, cell-biology, etc. all contribute to our understanding and knowledge on the interactions of the inorganic material glass with living tissues within the human body. Recently, the role of the ions dissolving from the glass in the tissue renewal capability of the body has been emphasized.

Bioactive glasses are developed and studied as third-generation biomaterials that support and stimulate bone cell proliferation, differentiation, and growth. The review paper by Hoppe et al. [53]

summarizes the biological effects of ions released from bioactive glasses on osteogenesis, angiogenesis, and antibacterial activity.

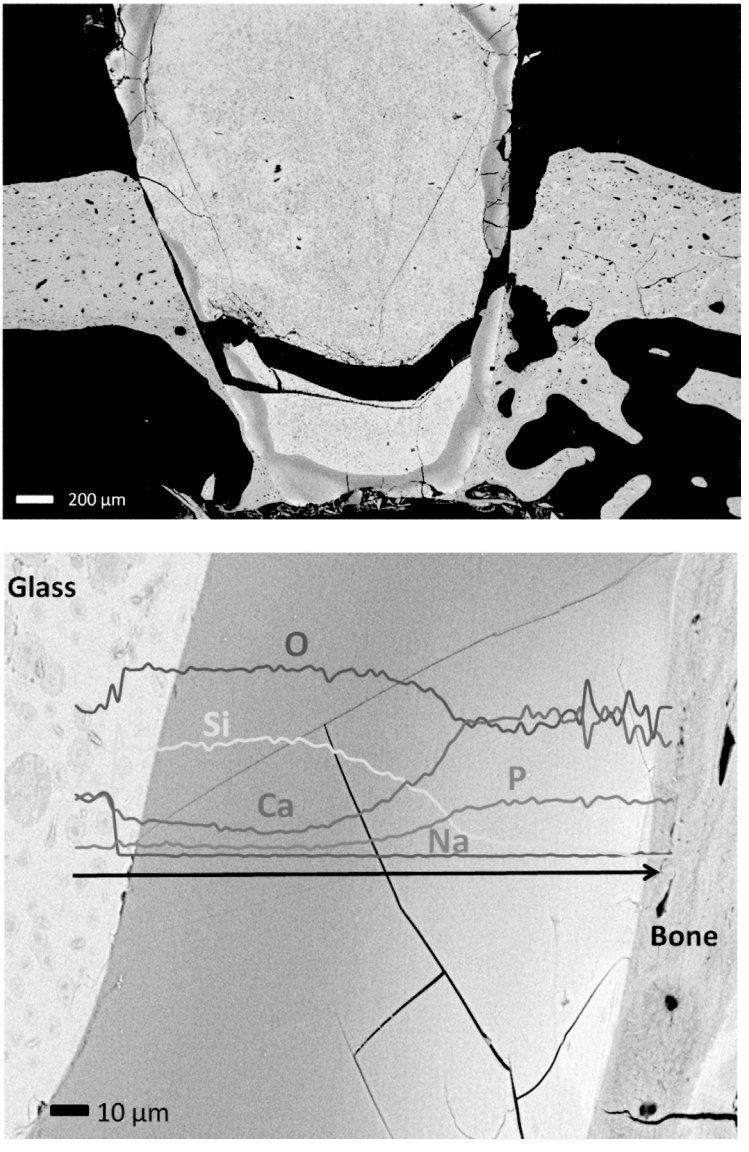

Figure 8.5 SEM micrograph of the interface of 45S5 and rat tibia after eight weeks of implantation (200x). Experimental details according to Hupa et al. [52].

In general, the effect of bioactive glasses on bone growth has been established from the first in vivo tests [5]. Successful bone remodeling is accompanied by proper vascularization of the bone tissue. Basically, porous trabecular bone-like implants favor angiogenesis, that is, the growth of new blood vessels into the biomaterial. The recent research emphasized the role of different therapeutic ions on stimulating bone metabolism as an important criterion for future biomaterials. One of the key questions is to find optimal dosages for these ions and to develop materials that are capable of delivering optimal concentrations into the target tissue over a desired period of time. Several ions affect both osteogenesis and angiogenesis: Si, Mg, Ca, Sr, Cu, Zn, B, and P favor or stimulate biological processes on cellular or genetic levels [53]. The ions released may also have therapeutic effects on treatment of diseases: Sr is promising in treatment of osteoporosis [54–56], while F favors the formation of fluoride-substituted HAP, showing good durability in the occlusion of dental tubules to decrease dental hypersensitivity [39, 40]. Some effects of ions on the healing and repairing of tissue, as well as other therapeutic effects, are given in Table 8.2.

The ion release from bioactive glasses induces antibacterial activity in the interfacial solution around dissolving particles of bioactive glasses. The antibacterial effects of bioactive glasses were observed for the first time when cultivating pathogens typical in enamel caries (*Streptococcus mutans*), root caries (*Actinomyces naeslundii*, *Streptococcus mutans*), and periodontitis (*Actinobacillus actinomycetemcomitas*, *Porphyromonas gingivalis*, *Prevotella intermedia*) in a solution with a high concentration of fine-grained bioactive glass S53P4 [57, 58]. The high pH of the interfacial solution caused by high concentrations of alkali ions dissolving from bioactive glasses was assumed to kill several aerobic and anaerobic bacterial species, typically causing infections on the surfaces of prostheses in the body after implantation [59–61]. Also silver ions released from silver-doped glasses provide an effective way to enhance the antimicrobial activity [62–64].

The various effects of the ions dissolved from bioactive glasses on human cells are not fully understood. Depending on the dosage of the glass in a particular environment the concentration of the ions dissolving from the glass may affect the HCA formation but also induce cell cytotoxicity if the concentration is too high [71, 72].

Accordingly, one challenge to be resolved is to compose a glass composition that releases an optimal concentration per certain dosage and fluid flow environment needed to stimulate cellular responses. The human body is a dynamic environment; the product form of the glass, the surface area of the glass, the flow of the solution, etc., should be taken into account. When using acellular fluids to study ion release, the effect of proteins and other biological moieties on the dissolution is neglected. However, in vitro studies may give essential information needed to adjust the glass composition to a specific cellular response.

Table 8.2 Therapeutic effects of some ions dissolving from bioactive glasses

Ion	Effect	Reference
Ag	Antibacterial effect	[62–64]
B	Stimulation of bone formation	[65]
Ca P	Main components of biological apatite ($Ca_{10}(PO_4CO_3)_6OH_2$) Stimulation of bone formation	[53, 66–68]
Cu	Stimulation of angiogenesis	[44, 53]
F	Caries inhibition, antibacterial effect, antigingivitis effect, dental hypersensitivity, increase of bone density	[39, 40, 69]
K	Nerve-desensitizing effect, treatment of dentine hypersensitivity Side effect on nerve cell functions	[39, 70]
Mg	Stimulation of bone formation	[53]
Si	Essential for metabolic processes related to formation and calcification of bone	[53, 66–68]
Sr	Treatment of osteoporosis, stimulation of bone formation Favorable regeneration of alveolar bone, root cementum, and periodontal ligaments	[44, 54–56]
Zn	Stimulationn of bone formation, anti-inflammatory effect	[44, 53]

Most in vitro studies are conducted by immersing the glass in a certain volume of solution, with or without solution agitation, for various periods of time. The glass surface and the solution are analyzed to give information on layer formation and ion dissolution. The solution should be frequently replenished to avoid saturation or too high pH values. A more sophisticated online analysis method utilizing an inductively coupled plasma optical emission spectrometer (ICP-OES) and a flow-through microvolume pH electrode was recently utilized to study the initial dissolution of bioactive and biocompatible glasses [73–75]. Figure 8.6 shows the principle of ion release measurement. Fresh TRIS solution is fed continuously through a bed of glass particles, and the ion concentrations and pH of the solution are measured online with an ICP-OES. Figure 8.7 shows initial concentrations of the ions of silicon, calcium, magnesium, sodium, potassium, and phosphorus released from 315–500 μm particles of the bioactive glasses 45S5, S53P4, and 13-93 in 0.2 mL/min TRIS buffer at 40°C. The effect of the ion dissolution on the pH of the solution is also indicated. As a comparison, the figure also shows the dissolution profile for an aluminum borosilicate glass (E-glass). E-glass fibers are utilized in denture composites; they are supposed to be inert and provide the composite with the mechanical properties needed for several loading cycles and for a long time [76–78].

Figure 8.7 shows that after the first dissolution peaks of the alkalis the concentration and pH approach constant values that can be used to compare the ion dissolution rate from the different glasses. Clearly different dissolution profiles were measured for the four glasses. For 45S5, the first dissolution peak of sodium ions was higher than the sensitivity of the method. In practice, the first pulse of ion alkali release may be easily eliminated by pretreating the glass before implantation. After the minor initial alkali release, E-glass showed only minor dissolution as presumed. The obtained ion dissolution trends are in agreement with results obtained from conventional dissolution studies.

The dissolution patterns suggested also similar trends as those reported in vivo: glass 45S5 is very bioactive, while S53P4 and 13-93 are both slower albeit bioactive. The online in vitro method is promising for rapid screening of the dissolution mechanism of glasses in different experimental conditions. It also offers a

possibility to determine the dissolution rate parameters in various in vitro conditions. This type of measurement may be of interest in the future when tailoring glasses for controlled ion release needed to activate genes and cells to remodel tissue.

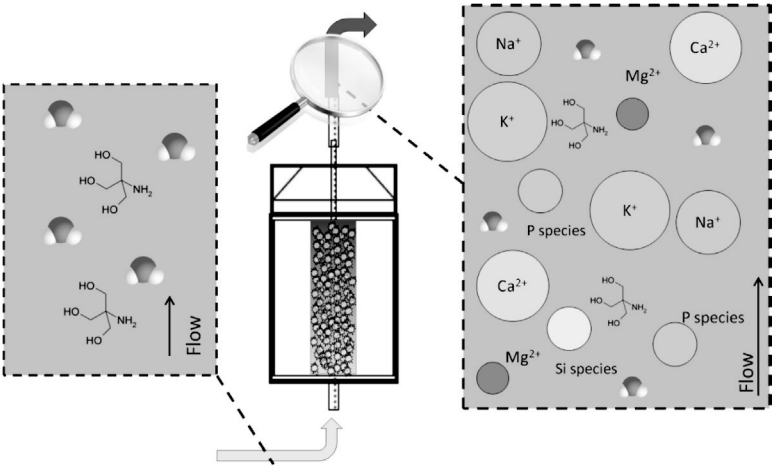

Figure 8.6 Principle of ion release measurement.

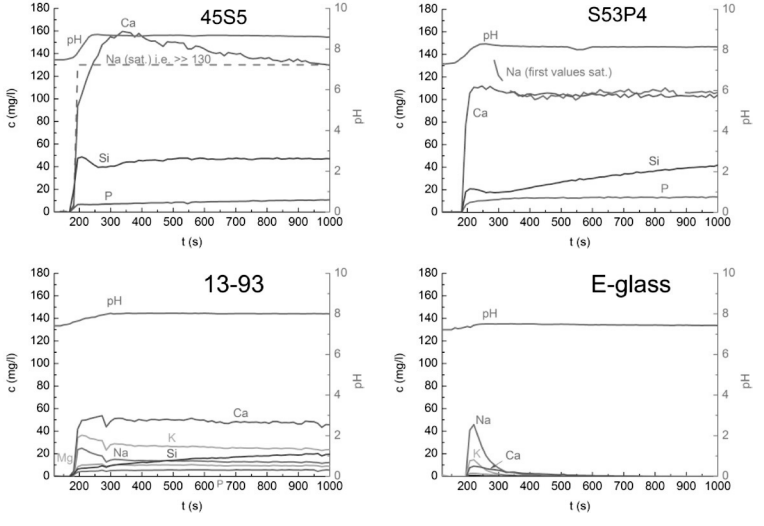

Figure 8.7 Initial dissolution profile of 45S5, S53P4, 13-93, and E-glass (0.2 mL/min, 40°C) in TRIS. Experimental conditions according to Fagerlund et al. [73].

8.6 Applications in Dentistry

The oral cavity is a challenging environment for any biomaterial; the material might be in contact with both hard and soft tissues in an environment where several microorganisms are present. The ability to support adherence and firm bonding to biological tissue, to stimulate tissue growth, but to prevent the growth of microorganisms make bioactive glasses promising materials for dentistry. In addition, the material is expected to have appropriate biomechanical properties strength, stiffness, and hardness. In most of the researched applications bioactive glasses are used as powdered fractions, often combined with other materials in such a way that the brittle nature of glass is not of primary concern.

8.6.1 Bone Regeneration

Bioactive glass materials have been studied in vivo in respect to different bone regeneration applications:

- Graft material preventing loss of bone after removal of tooth
- Graft material with the capability to regenerate tissue in periodontal disease–induced defects around roots of healthy teeth and metal implants
- Graft material guiding and inducing bone regeneration before denture replacement
- Filling materials for voids in implant placement
- Components in glass ionomer cement to remineralize damaged and decayed dentine

In general, research results support the potential of bioactive glasses in bone grafting. Currently, the commercial ready-to-use products available for dentists are all based on the 45S5 Bioglass® formulation.

Grafting with a bioactive glass has successfully been used to guide and induce bone growth needed for stable anchorage of implants in the jaw. After removal of a tooth, the bone around the cavity starts to resorb as it is not mechanically stressed. The first commercial application of bioactive glasses in dentistry was cones of 45S5 Bioglass® used to prevent resorption of alveolar bone. The cones were inserted into fresh cavities, and after a few weeks dentures could successfully be implanted [79, 80].

Periodontal disease may lead to extensive resorption of the bone around the root of a healthy tooth or a denture. Particles of both 45S5 and S53P4 have been found to heal the bone in periodontitis [81]. Particles of 45S5 are commercially available as PerioGlass® for treatment of periodontitis. These particles are also suitable for bone grafting in anchorage of dentures.

In general, the more compact cortical bone in the lower jaw, mandible, is easier to graft to support denture anchorage than the porous cancellous bone of the upper jaw, maxilla. The quality and thickness of the bone in the upper jaw to give support for a titanium root may be increased by lifting the maxillary sinus floor. In clinical tests, a mixture of particles of the bioactive glass S53P4 and autologous bone induced thicker bone than grafting with autologous bone only [82]. Histological analyses indicated resorption of autologous bone, while the mixture containing the bioactive glass S53P4 induced new bone formation, likely due to continuous glass dissolution over the observation period of 78 weeks.

Glass ionomer cements are used mainly as liners and fillers in primary teeth or areas not subjected to high loading. In vivo studies of the bioactive glass S53P4 in glass ionomer cements gave indications of its capability to mineralize dentine in vivo [83]. In contrast, the compressive strength and hardness of glass ionomer cements in vitro decreased with increasing amount of the bioactive glass [84]. The poor bonding between the polymer in the ionomer cement and the bioactive glass explained partly the decrease in mechanical properties. Modifications in the structure of the polymer gave better mechanical properties to the bioactive glass containing the glass ionomer cement. The particles of S53P4 in the ionomer cement enhanced the mineralization of dentin in vitro [85].

8.6.2 Treatment of Dental Hypersensitivity

Dental hypersensitivity is experienced as a sharp pain when subjecting the tooth suddenly to hot, cold, bitter, or sweet drinks and food. The phenomenon is believed to depend on fluid flow through exposed and opened dentinal tubules into the pulp of the tooth. The first studies treating hypersensitivity of teeth with a bioactive glass were published by Salonen et al. [86–88]. When

treating hypersensitive teeth with aqueous solutions or pastes containing fine-grained particles of S53P4 bioactive glass, an HAP precipitate sealed the open tubules, thus resulting in teeth that are less hypersensitive. Figure 8.8 shows the structure of dental tubuli and HAP nucleated in both the tubules and the dentine surface in the area that was treated with a paste containing fine-grained S53P4 (Ø ≈ 20 µm). A powdered bioactive glass may also be used to strengthen dentine tubules during the treatment of enamel and root carries [88].

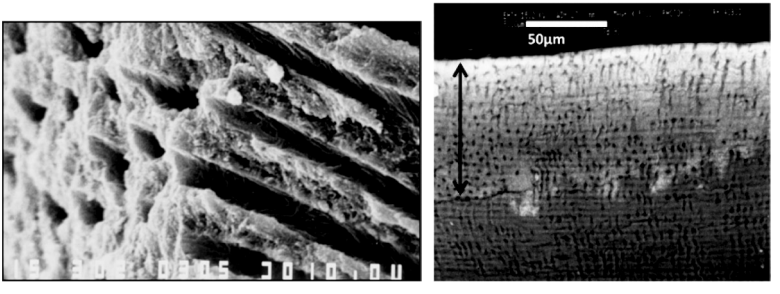

Figure 8.8 Structure of dental tubules (left) and the mineralization of the dentin surface at seven days after treatment with a paste containing the bioactive glass S53P4. The arrow shows the thickness of the mineralized layer. Figure courtesy of Prof. Antti Yli-Urpo.

The effect of the bioactive glass 45S5 on dental hypersensitivity has been reported in several studies. The utilization of microsized particles of bioactive glasses as ingredients in toothpastes lessens the hypersensitivity of teeth [69, 89]. The effect is explained by attachment of glass particles to the dentine with subsequent ion release reactions leading to an increase in the pH of the solution and precipitation of HAP to occlude the tubuli [90]. The HAP precipitation takes place in alkaline environments. As the oral area is often exposed to acidic aqueous solutions such as carbonated and fruit juices, the long-term durability of the HAP crystals formed in the treatment with toothpastes may be limited. Bioactive glasses containing fluoride precipitate fluorapatite crystals that are more stable in acidic solutions [69]. Besides treatment of dental hypersensitivity, the bioactive glass used in toothpastes can be formulated to release therapeutically active ions such as strontium

and fluoride for caries prevention, zinc for antibacterial effects, and potassium to act as a desensitizing agent [39]. A fine-grained bioactive glass in the toothpaste may also aid in remineralization of the apatite in tooth enamel after attack of acidic aqueous solutions or bleaching treatments [91, 92].

8.6.3 Coatings Enhancing Osseointegration

The adhesion and tissue bonding of dental prosthetic devices manufactured using inert biomaterials are crucial for satisfactory performance. Bioactive glass coatings that give chemical bonding to the tissue have been studied as a means of achieving stable attachment of metal and polymer prostheses to the bone. Coating on metal prostheses was one of the first applications of bioactive glasses [93]. Traditional enameling requires careful optimization of the glass coating to match the thermal expansion of the metal to prevent the coating from cracking and peeling off. An additional bond coating with an intermediate thermal expansion between the substrate and the top coating improves adhesion and may also protect the substrate metal from corrosion, thereby decreasing metal ion release from the substrate [94]. Modern techniques, such as the sol-gel route, electrochemical deposition, thermal spray, etc., enable the deposition of thin bioactive glass coatings that attach properly to the metal substrate. The coating composition can also be varied in a controlled manner along the implant surface to give optimal bone and soft tissue responses [95]. A bioactive glass coating on metal has some drawbacks: the brittle glass does not withstand tension or bending and may thus detach easily from the metal surface. As the bioactive glass dissolves gradually, it does not provide permanent fixation. In vivo studies of a bioactive glass 1-98 coating on a titanium implant suggested, however, enhanced initial tissue attachment, supported bone growth, and gave rapid osseointegration [95].

A bioactive glass coating has also been applied on fiber-reinforced polymer composites aimed for dental prosthetic devices [96, 97]. In general, the bioactive glass enhances osseointegration of the fiber-reinforced composite implants [98, 99]. A detailed discussion of fiber-reinforced composites is given elsewhere in this book.

8.7 Scaffolds for Tissue Engineering

Porous bioactive glass–based scaffolds are developed and studied intensively for bone tissue engineering. The scaffolds may be fabricated via sintering of fine particles [100], the salt sintering process [101], porous polymeric templates combined with heat treatment [12, 102–104], unidirectional freezing of camphene-based suspensions [105], the gel-cast foaming technique [106], the sol-gel method [107], ink writing [108], etc.

Often the scaffolds are coated with bioabsorbable polymers for enhanced biomechanical properties. The high porosity enables three-dimensional ingrowth of bone and blood vessels. The bioactive glass surface guides tissue growth and also stimulates tissue remodeling. The applications of tissue engineering scaffolds within dentistry are likely to increase in the future. Recently, a strontium-containing mesoporous bioactive glass scaffold indicated promising results for periodontal tissue engineering. The strontium ions released from the structure improved differentiation of periodontal ligament cells, and the scaffold showed excellent apatite mineralization ability in vitro [54].

Dense scaffolds consisting of bioabsorbable polymers and bioactive glass particles or fibers are of interest for treatment of bone defects around dental implants. The bone cavities can be easily filled by using a composite based on a thermoplastic polymer [109]. Synthetic polymers do not bond to bone but provide a temporary mechanical support to the healing tissue and degrade gradually as the new tissue grows. Most often the composites have been based on polylactic acid or its copolymers. The bioactive glass is thought to provide bone bonding of the composite and to stimulate bone growth. Although the composites are likely to have several interesting properties, the interplay between polymer degradation and glass dissolution is not fully understood. Basically, glass dissolution increases the pH of the interfacial solution, while polymer degradation products are acidic. In dense composites, poor adhesion of the glass to the polymer may lead to cavity and crack formation, which leads to rapid dissolution of the glass and also changes the polymer degradation rate compared to the neat polymer [20].

8.8 Clinical Studies in Head and Neck Surgery

Clinical studies of using plates or particles of the bioactive glass S53P4 in head and neck surgery have been conducted by Aitasalo et al. at the ENT Department of Turku University Hospital, Turku, Finland, over the years 1991–2010. The success rate in reconstruction of craniofacial defects after a five-year follow-up of 271 patients is shown in Table 8.3.

Table 8.3 Success rate of reconstructions of fronto-orbital defects by using the bioactive glass S53P4 after a five-year follow-up of 271 patients. Table courtesy of Prof. Kalle Aitasalo

Operation	Number of patients		Success rate (%)
	Success	Total	
Frontal sinus obliteration (glass granules)	88	91	97
Fonto-orbital trauma reconstruction (glass plates and/or granules)	116	124	94
Fronto-orbital tumor reconstruction (glass plates and/or granules)			
Benign tumor	27	28	96
Malignant tumor	20	28	71

8.9 Commercial Products

The first clinical bioactive glass products were monoliths plates of 45S5 Bioglass® (a device for replacing bones of the middle ear, 1985) and cones (a device designed to support labial and lingual plates in natural tooth roots, 1988), but today most of the applications are based on particulates [5, 68]. One of the challenges has been to develop products that can be handled and used easily in a specific clinical case.

The material must be easy to sterilize, apply in site, and form into any desired shape. If these requirements are satisfied, the material may be attractive, for example, for the dentist in daily practice.

The clinical products and applications of mainly 45S5 Bioglass® have been reviewed by Hench [5, 110, 111] and Jones [10]. Despite

the wide research activities over the decades, bioactive glasses still have only a few commercial applications. Most of the commercial clinical bioactive glass products are based on the FDA-approved compositions 45S5 and S53P4 within bone grafting. The applications of 45S5 range from non-load-bearing bone grafts to treatment of dentinal hypersensitivity with bioactive glasses containing toothpastes (Sensodyne Repair & Protect by GlaxoSmithKline, UK). S53P4 BonAlive® is sold as loose glass granules and an easy-to-use BonAlive® applicator (Fig. 8.9). There are also some new compositions emerging in the market, such as the strontium-substituted 45S5 glass (StronBone™ by RepRegren Ltd., UK) [62].

Figure 8.9 S53P4 BonAlive® as discrete glass granules and an easy-to-use BonAlive® applicator. Pictures provided by courtesy of BonAlive Biomaterials Ltd., copyright (2012) BonAlive Biomaterials Ltd.

8.10 Summary

Bioactive glasses have been studied for more than 40 years as bone-grafting materials. Accordingly, commercial products are found mainly within the utilization of particles of glasses in various bone-grafting applications. Bioactive glasses have been studied widely within the field of dentistry, but the applications are still limited. The most recent research utilizes bioactive glasses as components in highly porous trabecular-like bone tissue engineering scaffolds. These scaffolds are designed to support and guide tissue growth, while releasing therapeutic ions essential for tissue regeneration.

Recently, bioactive glasses have been utilized in special toothpastes to give a therapeutic effect against dental hypersensitivity and to enhance enamel and dentine mineralization. The antibacterial effect of bioactive glasses makes them also interesting candidates for treatment of caries. Increasing utilization and novel applications of bioactive glasses in dentistry require that the glasses be commercially available in packages that are easy to use by dental healthcare professionals.

The active research and development of novel bioactive glass compositions in a variety of product forms suggest that bioactive glasses will find novel medical applications.

References

1. Hench, L. L. (1991) Bioceramics: from concept to clinic, *J. Am. Ceram. Soc.,* **74**(7), 1487–1510.
2. Williams, D. F. (1987) *Definitions in Biomaterials: Proceedings of a Consensus Conference of European Society for Biomaterials*, Chester, England 3-5.1986, Elsevier, Amsterdam.
3. Hench, L. L., Thompson, I. (2010) Twenty-first century challenges for biomaterials, *J. R. Soc. Interface,* **7**, S374–S391.
4. Williams, D. F. (2008) On the mechanisms of biocompatibility, *Biomaterials,* **29**(20), 2941–2953.
5. Hench, L. (2006) The story of Bioglass®, *J. Mater. Sci. Mater. Med.,* **17**(11), 967–978.
6. Arstila, H., Vedel, E., Hupa, L., Hupa, M. (2008) Predicting physical and chemical properties of bioactive glasses from chemical composition II) devitrification characteristics, *Glass Technol.: Eur. J. Glass Sci. Technol., A,* **49**(6), 260–265.
7. Massera, J., Fagerlund, S., Hupa, L., Hupa, M. (2012) Crystallization mechanism of the bioactive glasses, 45S5 and S53P4, *J. Am. Ceram. Soc.,* **95**(2), 607–613.
8. Arstila, H., Vedel, E., Hupa, L., Hupa, M. (2007) Factors affecting crystallization of bioactive glasses, *J. Eur. Ceram. Soc.,* **27**(2–3), 1543–1546.
9. Vedel, E., Arstila, H., Ylänen, H., Hupa, L., Hupa, M. (2008) Predicting physical and chemical properties of bioactive glasses from chemical composition, part I: viscosity characteristics, *Glass Technol.: Eur. J. Glass Sci. Technol., A,* **49**(6), 251–259.

10. Jones, J. R. (2013) Review of bioactive glass: from Hench to hybrids, *Acta Biomater.,* **9**(1), 4457–4486.
11. Cao, W., Hench L. L. (1996) Bioactive materials, *Ceram. Int.* (22), 493–507.
12. Chen, Q. Z., Thompson, I. D., Boccaccini, A. R. (2006) 45S5 Bioglass®-derived glass–ceramic scaffolds for bone tissue engineering, *Biomaterials,* **27**(11), 2414–2425.
13. Hench, L. L. (1998) Bioceramics, *J. Am. Ceram. Soc.,* **81**(7), 1705–1727.
14. Braun, S., Rappoport, S., Zusman, R., Avnir, D., Ottolenghi, M. (1990) Biochemically active sol-gel glasses: the trapping of enzymes, *Mater. Lett.,* **10**(1–2), 1–5.
15. Boccaccini, A. R., Erol, M., Stark, W. J., Mohn, D., Hong, Z., Mano, J. F. (2010) Polymer/bioactive glass nanocomposites for biomedical applications: a review, *Compos. Sci. Technol.,* **70**(13), 1764–1776.
16. Gerhardt, L., Boccaccini, A. R. (2010) Bioactive glass and glass-ceramic scaffolds for bone tissue engineering, *Materials,* **3**(7), 3867–3910.
17. Molin C. (2012) *Electrospinning of Bioactive Glass Nanofibers*, Master's thesis, Åbo Akademi University, Turku.
18. Zhang, D., Jain, H., Hupa, M., Hupa, L. (2012) In-vitro degradation and bioactivity of tailored amorphous multi porous scaffold structure, *J. Am. Ceram. Soc.,* **95**(9), 2687–2694.
19. Arstila, H., Tukiainen, M., Taipale, S., Kellomäki, M., Hupa, L. (2008) Liquidus temperatures of bioactive glasses, *Adv. Mater. Res.,* **39–40**, 287–292.
20. Varila, L., Lehtonen, T., Tuominen, J., Hupa, M., Hupa, L (2012) In vitro behaviour of three biocompatible glasses in composite implants, *J. Mater. Sci. Mater. Med.,* **23**(10), 2425–2435.
21. Fagerlund, S., Massera, J., Moritz, N., Hupa, L., Hupa, M. (2012) Phase composition and in vitro bioactivity of porous implants made of bioactive glass S53P4, *Acta Biomater.,* **8**, 2331–2339.
22. Andersson, Ö. H., Liu, G., Karlsson, K. H., Niemi, L., Miettinen, J., Juhanoja, J. (1990) In vivo behaviour of glasses in the SiO_2-Na_2O-CaO-P_2O_5-Al_2O_3-B_2O_3 system, *J. Mater. Sci. Mater. Med.,* **1**(4), 219–227.
23. Brink, M. (1997) The influence of alkali and alkaline earths on the working range for bioactive glasses, *J. Biomed. Mater. Res.,* **36**, 109–117.
24. Brink, M., Turunen, T., Happonen, R., Yli-Urpo, A. (1997) Compositional dependence of bioactivity of glasses in the system Na_2O-K_2O-MgO-CaO-B_2O_3-P_2O_5-SiO_2, *J. Biomed. Mater. Res.,* **37**, 114–121.

25. Vedel, E., Zhang, D., Arstila, H., Hupa, L., Hupa, M. (2009) Predicting physical and chemical properties of bioactive glasses from chemical composition. Part IV: tailoring compositions with desired properties, *Glass Technol.: Eur. J. Glass Sci. Technol., A*, **50**(1), 9–16.

26. Itälä, A., Koort, J., Ylänen, H., Hupa, M., Aro, H. (2003) Biologic significance of surface microroughing in bone incorporation of porous bioactive glass implants, *J. Biomed. Mater. Res.,* **67A**(2), 496–503.

27. Zhang, D., Vedel, E., Hupa, L., Aro, H., Hupa, M. (2009) Predicting physical and chemical properties of bioactive glasses from chemical composition. Part III. Chemical composition and in vitro reactivity of glasses, *Glass Technol.: Eur. J. Glass Sci. Technol., A,* **50**(1), 1–8.

28. Fagerlund, S., Hupa, L., Hupa, M. (2010) Comparison of reactions of bioactive glasses in different aqueous solutions, in *Advances in Bioceramics and Biotechnologies: Ceramic Transactions,* 101–113 (Ed. Narayan, R., McKittrick, J., Singh, M.), John Wiley & Sons, Hoboken, NJ, USA.

29. Pirhonen, E., Niiranen, H., Niemelä, T., Brink, M., Törmälä, P. (2006) Manufacturing, mechanical characterization, and *in vitro* performance of bioactive glass 13–93 fibers, *J. Biomed. Mater. Res. B,* **77B**(2), 227–233.

30. Itälä, A., Ylänen, H. O., Yrjans, J., Heino, T., Hentunen, T., Hupa, M., Aro H. (2002) Characterization of microrough bioactive glass surface: surface reactions and osteoblast responses in vitro, *J. Biomed. Mater. Res.,* **62**(3), 404–411.

31. Ylänen, H., Karlsson, K. H., Itälä, A., Aro, H. T. (2000) Effect of immersion in SBF on porous bioactive bodies made by sintering bioactive glass microspheres, *J. Non-Cryst. Solids,* **275**(1–2), 107–115.

32. Fu, Q., Rahaman, M. N., Bal, B. S., Kuroki, K., Brown, R. F. (2010) In vivo evaluation of 13–93 bioactive glass scaffolds with trabecular and oriented microstructures in a subcutaneous rat implantation model, *J. Biomed. Mater. Res. A,* **95A**(1), 235–244.

33. Rahaman, M. N., Brown, R. F., Bal, B. S., Day, D. E. (2006) Bioactive glasses for nonbearing applications in total joint replacement, *Semin. Arthroplasty,* **17**(3–4), 102–112.

34. Arstila, H., Tukiainen, M., Hupa, L., Ylänen, H., Kellomäki, M., Hupa, M. (2006) In vitro reactivity of bioactive glass fibers, *Adv. Sci. Tech.,* **49**, 246–251.

35. Arstila, H., Hupa, L., Karlsson, K., Hupa, M. (2007) In vitro bioactivity of partially crystallised glasses, *Glass Technol.: Eur. J. Glass Sci. Technol., A,* **48**(4), 196–199.

36. Fu, Q., Rahaman, M. N., Sonny Bal, B., Brown, R. F., Day, D. E. (2008) Mechanical and in vitro performance of 13–93 bioactive glass scaffolds prepared by a polymer foam replication technique, *Acta Biomater.,* **4**(6), 1854–1864.

37. Liu, X., Rahaman, M. N., Fu, Q. (2013) Bone regeneration in strong porous bioactive glass (13–93) scaffolds with an oriented microstructure implanted in rat calvarial defects, *Acta Biomater.,* **9**(1), 4889–4898.

38. Alm, J. J., Frantzén, J. P. A., Moritz, N., Lankinen, P., Tukiainen, M., Kellomäki, M., Aro, H. (2010) In vivo testing of a biodegradable woven fabric made of bioactive glass fibers and PLGA80: a pilot study in the rabbit, *J. Biomed. Mater. Res. B: Appl. Mater.,* **93B**(2), 573–580.

39. Lynch, E., Brauer, D. S., Karpukhina, N., Gillam, D. G., Hill, R. G. (2012) Multi-component bioactive glasses of varying fluoride content for treating dentin hypersensitivity, *Dent. Mater.,* **28**(2), 168–178.

40. Brauer, D. S., Karpukhina, N., O'Donnell, M. D., Law, R. V., Hill, R. G. (2010) Fluoride-containing bioactive glasses: effect of glass design and structure on degradation, pH and apatite formation in simulated body fluid, *Acta Biomater.,* **6**(8), 3275–3282.

41. O'Donnell, M. D., Hill, R. G. (2010) Influence of strontium and the importance of glass chemistry and structure when designing bioactive glasses for bone regeneration, *Acta Biomater.,* **6**(7), 2382–2385.

42. Fu, Q., Rahaman, M. N., Bal, B. S., Bonewald, L. F., Kuroki, K., Brown, R. F. (2010) Silicate, borosilicate, and borate bioactive glass scaffolds with controllable degradation rate for bone tissue engineering applications. II. In vitro and in vivo biological evaluation, *J. Biomed. Mater. Res. A,* **95**(1), 172–179.

43. Karlsson, K. H. (1999) Bone implants: a challenge to materials science, *Ann. Chir. Gynaecol.,* **88**(3), 226–235.

44. Rahaman, M. N., Day, D. E., Sonny Bal, B., Fu, Q., Jung, S. B., Bonewald, L. F., Tomsia, A. P. (2011) Bioactive glass in tissue engineering, *Acta Biomater.*, **7**(6), 2355–2373.

45. Ducheyne, P. (1987) Bioceramics: material characteristics versus in vivo behavior, *J. Biomed. Mater. Res.,* **21**(A2 Suppl), 219–236.

46. Kokubo, T., Kushitani, H., Sakka, S. (1990) Solutions able to reproduce in vivo surface-structure changes in bioactive glass-ceramics A-W, *J. Biomed. Mater. Res.,* **24**, 721–734.

47. Varila, L., Fagerlund, S., Lehtonen, T., Tuominen, J., Hupa, L. (2012) Surface reactions of bioactive glasses in buffered solutions, *J. Eur. Ceram. Soc.,* **32**(11), 2757–2763.

48. Aho, A., Suominen, E., Alanen, A., Yli-Urpo, A., Knuuti, J., Aho, H. (2003) Case report: remodeling of the tibia after grafting of a large cavity with particulate bioactive glass-hydroxylapatite on treatment of fibrous dysplasia with 13 years' follow-up, *Acta Orthop. Scand.,* **74**(6), 766–770.

49. Lindfors, N. C., Koski, I., Heikkilä, J. T., Mattila, K., Aho, H. J. (2010) A prospective randomized 14-year follow-up study of bioactive glass and autogenous bone as bone graft substitutes in benign bone tumors, *J. Biomed. Mater. Res. B: Appl. Mater.,* **94**(1), 157–164.

50. Lindfors, N. C., Hyvönen, P., Nyyssönen, M., Kirjavainen, M., Kankare, J., Gullichsen, E., Salo, J. (2010) Bioactive glass S53P4 as bone graft substitute in treatment of osteomyelitis, *Bone,* **47**(2), 212–218.

51. Lindfors, N. C., Heikkilä, J. T., Koski, I., Mattila, K., Aho, H. J. (2009) Bioactive glass and autogenous bone as bone graft substitutes in benign bone tumors, *J. Biomed. Mater. Res. B: Appl. Mater.,* **90**, 131–136.

52. Hupa, L., Karlsson, K. H., Hupa, M., Aro, H. T. (2010) Comparison of bioactive glasses in vitro and in vivo, *Glass Technol.: Eur. J. Glass Sci. Technol., A,* **51**(2), 89–92.

53. Hoppe, A., Güldal, N. S., Boccaccini, A. R. (2011) A review of the biological response to ionic dissolution products from bioactive glasses and glass-ceramics, *Biomaterials,* **32**, 2757–2774.

54. Wu, C., Zhou, Y., Lin, C., Chang, J., Xiao, Y. (2012) Strontium-containing mesoporous bioactive glass scaffolds with improved osteogenic/cementogenic differentiation of periodontal ligament cells for periodontal tissue engineering, *Acta Biomater.,* **8**(10), 3805–3815.

55. Kendler, D. (2006) Strontium ranelate: data on vertebral and nonvertebral fracture efficacy and safety: mechanism of action, *Curr. Osteoporos. Rep.,* **4**(1), 34–39.

56. Marie, P. J., Ammann, P., Boivin, G., Rey, C. (2001) Mechanisms of action and therapeutic potential of strontium in bone, *Calcif. Tissue Int.,* **69**(3), 121–129.

57. Stoor, P., Söderling, E., Salonen, J. I. (1998) Antibacterial effects of a bioactive glass paste on oral microorganisms, *Acta Odontol. Scand.,* **56**(3), 161–165.

58. Stoor, P., Söderling, E., Grenman, R. (2001) Bioactive glass S53P4 in repair of septal perforations and its interactions with the respiratory infection-associated microorganisms Haemophilus influenzae and Streptococcus pneumoniae, *J. Biomed. Mater. Res.,* **58**(1), 113–120.

59. Munukka, E., Leppäranta, O., Korkeamäki, M., Vaahtio, M., Peltola, T., Zhang, D., Hupa, L., Ylänen, H., Salonen, J., Viljanen M., Eerola, E. (2008)

Bactericidal effects of bioactive glasses on clinically important aerobic bacteria, *J. Mater. Sci. Mater. Med.,* **19**(1), 27–32.

60. Zhang, D., Leppäranta, O., Munukka, E., Ylänen, H., Viljanen, M. K., Eerola, E., Hupa, M., Hupa L. (2010) Antibacterial effects and dissolution behavior of six bioactive glasses, *J. Biomed. Mater. Res. A,* **93A**(2), 475–483.
61. Leppäranta, O., Vaahtio, M., Peltola, T., Zhang, D., Hupa, L., Hupa, M., Ylänen, H., Salonen, J., Viljanen, M., Eerola, E. (2008) Antibacterial effect of bioactive glasses on clinically important anaerobic bacteria in vitro, *J. Mater. Sci. Mater. Med.,* **19**(2), 547–551.
62. Jones, J., Ehrenfried, L., Saravanapavan, P., Hench, L. (2006) Controlling ion release from bioactive glass foam scaffolds with antibacterial properties, *J. Mater. Sci. Mater. Med.,* **17**(11), 989–996.
63. Vernè, E., Nunzio, S. D., Bosetti, M., Appendino, P., Vitale Brovarone, C., Maina, G., Cannas M. (2005) Surface characterization of silver-doped bioactive glass, *Biomaterials,* **26**(25), 5111–5119.
64. Bellantone, M., Coleman, N. J., Hench, L. L. (2000) Bacteriostatic action of a novel four-component bioactive glass, *J. Biomed. Mater. Res.,* **51**(3), 484–490.
65. Jain, R. H., Marzillier, J. Y., Kowal, T. J., Wang, S., Jain, H., Falk, M. M. (2011) Expression of mineralized tissue-associated proteins is highly upregulated in MC3T3-E1 osteoblasts grown on a borosilicate glass substrate, in *Advances in Bioceramics and Porous Ceramics IV: Ceramic Engineering and Science Proceedings*, 111–120, John Wiley & Sons.
66. Xynos, I. D., Edgar, A. J., Buttery, L. D. K., Hench, L. L., Polak, J. M. (2001) Gene-expression profiling of human osteoblasts following treatment with the ionic products of Bioglass® 45S5 dissolution, *J. Biomed. Mater. Res.,* **55**(2), 151–157.
67. Hench, L. L., Polak, J. M., Xynos, I. D., Buttery, L. D. K. (2000) Bioactive materials to control cell cycle, *Mater. Res. Innov.,* **3**, 313–323.
68. Hench, L. L. (2009) Genetic design of bioactive glass, *J. Eur. Ceram. Soc.,* **29**(7), 1257–1265.
69. Mneimne, M., Hill, R. G., Bushby, A. J., Brauer, D. S. (2011) High phosphate content significantly increases apatite formation of fluoride-containing bioactive glasses, *Acta Biomater.,* **7**(4), 1827–1834.
70. Frantzén J. (2012) *Bioactive Glass in Lumbar Spondylodesis, A Pre-Clinical and Clinical Study*, PhD thesis, Turku University, Turku.
71. Labbaf, S., Tsigkou, O., Müller, K. H., Stevens, M. M., Porter, A. E., Jones, J. R. (2011) Spherical bioactive glass particles and their interaction with

human mesenchymal stem cells in vitro, *Biomaterials,* **32**(4), 1010–1018.

72. Jones, J. R., Sepulveda, P., Hench, L. L. (2001) Dose-dependent behavior of bioactive glass dissolution, *J. Biomed. Mater. Res.,* **58**(6), 720–726.
73. Fagerlund, S., Hupa, L., Hupa, M. (2013) Dissolution patterns of biocompatible glasses in 2-amino-2-hydroxymethyl-propane-1,3-diol (Tris) buffer, *Acta Biomater.,* **9**(2), 5400–5410.
74. Fagerlund, S., Ek, P., Hupa, L., Hupa, M. (2012) Dissolution kinetics of a bioactive glass by continuous measurement, *J. Am. Ceram. Soc.,* **95**(10), 3130–3137.
75. Taipale, S., Ek, P., Hupa, M., Hupa, L. (2008) Continuous measurement of the dissolution rate of ions, *Adv. Mater. Res.*, **39–40**, 341–346.
76. Vallittu, P. K. (1996) Comparison of the in vitro fatigue resistance of an acrylic resin removable partial denture reinforced with continuous glass fibers or metal wires, *J. Prosthodont.,* **5**(2), 115–121.
77. Vallittu, P. K. (1999) Flexural properties of acrylic resin polymers reinforced with unidirectional and woven glass fibers, *J. Prosthet. Dent.,* **81**(3), 318–326.
78. Tanner, J., Vallittu, P. K., Söderling, E. (2001) Effect of water storage of E-glass fiber-reinforced composite on adhesion of Streptococcus mutans, *Biomaterials,* **22**(12), 1613–1618.
79. Stanley, H. R., Hall, M. B., Colaizzi, F., Clark, A. E. (1987) Residual alveolar ridge maintenance with a new endosseous implant material, *J. Prosthet. Dent.,* **58**(5), 607–613.
80. Stanley, H. R., Hall, M. B., Clark, A. E., King, C. J.,3rd, Hench, L. L., Berte, J. J. (1997) Using 45S5 bioglass cones as endosseous ridge maintenance implants to prevent alveolar ridge resorption: a 5-year evaluation, *Int. J. Oral Max. Impl.,* **12**(1), 95–105.
81. Larmas, E., Sewón, L., Luostarinen, T., Kangasniemi, I., Yli-Urpo, A. (1995) Bioactive glass in periodontal bone defects. Initial clinical findings of soft tissue and osseous tissue repair, *Bioceramics,* **8**, 279–284.
82. Turunen, T., Peltola, J., Yli-Urpo, A., Happonen, R. (2004) Bioactive glass granules as a bone adjunctive material in maxillary sinus floor augmentation, *Clin. Oral Implants Res.,* **15**(2), 135–141.
83. Yli-Urpo, H., Närhi, M., Närhi, T. (2005) Compound changes and tooth mineralization effects of glass ionomer cements containing bioactive glass (S53P4), an in vivo study, *Biomaterials,* **26**(30), 5934–5941.

84. Yli-Urpo, H., Lassila, L. V. J., Närhi, T., Vallittu, P. K. (2005) Compressive strength and surface characterization of glass ionomer cements modified by particles of bioactive glass, *Dent. Mater.,* **21**(3), 201–209.

85. Xie, D., Zhao, J., Weng, Y., Park, J., Jiang, H., Platt, J. A. (2008) Bioactive glass-ionomer cement with potential therapeutic function to dentin capping mineralization, *Eur. J. Oral Sci.,* **116**(5), 479–487.

86. Forsback, A. P., Areva, S., Salonen, J. I. (2004) Mineralization of dentin induced by treatment with bioactive glass S53P4 in vitro, *Acta Odontol. Scand.,* **62**(1), 14–20.

87. Salonen, J., Tuominen, U., Andersson, Ö. H. (1996) Mineralization of dentin by making use of bioactive glass, *Biomater. Today Tomorrow*: *Proc. Finn. Dent. Soc.*, 25–26.

88. Salonen J., Tuominen U., Yli-Urpo A. (1999) New use of bioactive silicious glass and new compositions containing bioactive silicious glass, WO 9610985 (A1)

89. Bakry, A. S., Tamura, Y., Otsuki, M., Kasugai, S., Ohya, K., Tagami, J. (2011) Cytotoxicity of 45S5 bioglass paste used for dentine hypersensitivity treatment, *J. Dent.,* **39**(9), 599–603.

90. Earl, J. S., Leary, R. K., Muller, K. H., Langford, R. M., Greenspan, D. C. (2011) Physical and chemical characterization of dentin surface following treatment with NovaMin technology, *J. Clin. Dent.,* **22**(3), 62–67.

91. Dong, Z., Chang, J., Zhou, Y., Lin, K. (2011) In vitro remineralization of human dental enamel by bioactive glasses, *J. Mater. Sci.,* **46**(6), 1591–1596.

92. Gjorgievska, E., Nicholson, J. W. (2011) Prevention of enamel demineralization after tooth bleaching by bioactive glass incorporated into toothpaste, *Aust. Dent. J.,* **56**(2), 193–200.

93. Hench, L., Splinter, R., Allen, W., Greenlec, J. T. (1972) Bonding mechanisms at the interface of ceramic prosthetic materials, *J. Biomed. Res. Symp. No. 2*, 117–141.

94. Sola, A., Bellucci, D., Cannillo, V., Cattini, A. (2011) Bioactive glass coatings: a review, *Surf. Eng.,* **27**(8), 560–572.

95. Moritz, N., Vedel, E., Ylänen, H., Jokinen, M., Hupa, M., Yli-Urpo, A. (2004) Characterisation of bioactive glass coatings on titanium substrates produced using a CO2 laser, *J. Mater. Sci. Mater. Med.,* **15**(7), 787–794.

96. Ballo, A., Lassila, L., Vallittu, P., Närhi, T. (2007) Load bearing capacity of bone anchored fiber-reinforced composite device, *J. Mater. Sci. Mater. Med.,* **18**(10), 2025–2031.

97. Ballo, A., Kokkari, A., Meretoja, V., Lassila, L., Vallittu, P., Närhi, T. (2008) Osteoblast proliferation and maturation on bioactive fiber-reinforced composite surface, *J. Mater. Sci. Mater. Med.,* **19**(10), 3169–3177.

98. Tuusa, S. M., Peltola, M. J., Tirri, T., Puska, M. A., Röytta, M., Aho, H., Sandholm, J., Lassila, L., Vallittu, P. (2008) Reconstruction of critical size calvarial bone defects in rabbits with glass-fiber-reinforced composite with bioactive glass granule coating, *J. Biomed. Mater. Res. B: Appl. Biomater.,* **84**(2), 510–519.

99. Nganga, S., Zhang, D., Moritz, N., Vallittu, P. K., Hupa, L. (2012) Multilayer porous fiber-reinforced composites for implants: In vitro calcium phosphate formation in the presence of bioactive glass, *Dent. Mater.,* 28, 1134–1145.

100. Brown, R. F., Day, D. E., Day, T. E., Jung, S., Rahaman, M. N., Fu, Q. (2008) Growth and differentiation of osteoblastic cells on 13–93 bioactive glass fibers and scaffolds, *Acta Biomater.,* **4**(2), 387–396.

101. Liang, W., Rüssel, C. (2006) Resorbable, porous glass scaffolds by a salt sintering process, *J. Mater. Sci.,* **41**(12), 3787–3792.

102. Vitale-Brovarone, C., Verné, E., Robiglio, L., Appendino, P., Bassi, F., Martinasso, G., Muzio, G., Canuto, R. (2007) Development of glass–ceramic scaffolds for bone tissue engineering: characterisation, proliferation of human osteoblasts and nodule formation, *Acta Biomater.,* **3**(2), 199–208.

103. Vitale-Brovarone, C., Miola, M., Balagna, C., Verné, E. (2008) 3D-glass–ceramic scaffolds with antibacterial properties for bone grafting, *Chem. Eng. J.,* **137**(1), 129–136.

104. Fu, Q., Saiz, E., Rahaman, M. N., Tomsia, A. P. (2011) Bioactive glass scaffolds for bone tissue engineering: state of the art and future perspectives, *Mater. Sci.,* **31**(7), 1245–1256.

105. Liu, X., Rahaman, M. N., Fu, Q. (2011) Oriented bioactive glass (13–93) scaffolds with controllable pore size by unidirectional freezing of camphene-based suspensions: microstructure and mechanical response, *Acta Biomater.,* **7**(1), 406–416.

106. Wu, Z. Y., Hill, R. G., Yue, S., Nightingale, D., Lee, P. D., Jones, J. R. (2011) Melt-derived bioactive glass scaffolds produced by a gel-cast foaming technique, *Acta Biomater.,* **7**(4), 1807–1816.

107. Pereira, M. M., Clark, A. E., Hench, L. L. (1995) Effect of texture on the rate of hydroxyapatite formation on gel-silica surface, *J. Am. Ceram. Soc.,* **78**(9), 2463–2468.

108. Fu, Q., Saiz, E., Tomsia, A. P. (2011) Direct ink writing of highly porous and strong glass scaffolds for load-bearing bone defects repair and regeneration, *Acta Biomater.,* **7**(10), 3547–3554.

109. Närhi, T. O., Jansen, J. A., Jaakkola, T., de Ruijter, A., Rich, J., Seppälä, J., Yli-Urpo, A. (2003) Bone response to degradable thermoplastic composite in rabbits, *Biomaterials,* **24**(10), 1697–1704.

110. Hench L. (2012) *Bioactive Glasses: From Concept to Clinic a 45th Year Celebration*, Oral presentation in 11th ESG Conference, Maastricht.

111. Hench, L. L., Day, D. E., Höland, W., Rheinberger, V. M. (2010) Glass and medicine, *Int. J. Appl. Glass Sci.,* **1**(1), 104–117.

This page intentionally left blank

Chapter 9

Biological Activity of Titanium

Yo Shibata and Takashi Miyazaki
Department of Conservative Dentistry, Division of Biomaterials and Engineering, Showa University School of Dentistry, 1-5-8 Hatanodai, Shinagawa-ku, Tokyo 142-8555, Japan
miyazaki@dent.showa-u.ac.jp

Titanium-based metallic biomaterials have become an important area. This chapter focuses mainly on titanium implants as these materials are well suited to the quality and longevity of human life. Implant surfaces should have not only wear and corrosion resistance but also fundamental properties such as biological compatibility in terms of surface chemistry. In addition to acceleration of wound-healing phenomena, titanium implant surfaces should result in the formation of an interfacial layer and a bone matrix with adequate biomechanical properties. Improved fixation of titanium implants needs to be achieved by a healing bone tissue response toward the titanium surface. Moreover, reducing initial bacterial attachment and maintaining long-term antibacterial properties are desirable for future applications.

Handbook of Oral Biomaterials
Edited by Jukka P. Matinlinna

ISBN 978-981-4463-12-6 (Hardcover), 978-981-4463-13-3 (eBook)
www.panstanford.com

9.1 Initial Cell Adhesion

A titanium surface forms a passive and protective surface oxide film as a function of time. A passive titanium dioxide (TiO_2) film on a titanium surface has surface free energy [1]. The surface energy is the result of an electrostatic potential or hydrophilic functional groups on TiO_2. When the TiO_2 is in contact with water, the surface spontaneously generates hydrogen peroxide and its oxidation products such as hydrophilic functional groups, because of trapped electron–hole pairs (Ti^{4+} and e^-) within the TiO_2, according to the following equations [2, 3].

$$TiO_2 \rightarrow TiO_2\ (h_{vb} + e_{cb}) \tag{9.1}$$

$$h_{vb}^{+} + OH^- \rightarrow HO\bullet \tag{9.2}$$

$$e_{cb}^{-} + O_2 \rightarrow O_2\bullet \tag{9.3}$$

$$2O_2\bullet \rightarrow H_2O_2 + O_2 \tag{9.4}$$

$$H_2O_2 + e_{cb}^{+} \rightarrow HO\bullet + OH^- \tag{9.5}$$

The TiO_2 surface reacts under illumination (or even in the dark), which also decomposes surface organic impurities, reducing contamination of the titanium surface [1, 4, 5] (see also Chapter 10).

Hydrophilic surfaces are more desirable than *hydrophobic* ones in view of their interactions with biological fluids, cells, and tissues [6–8]. The event that occurs immediately upon implantation is contact with biological fluids and proteins. Immersion tests on titanium in biological fluids indicate that the sodium ion concentration increases with time, followed by phosphate and calcium adsorption [9]. Calcium adsorption on titanium surfaces may cause later host tissue responses. However, the roles of sodium and phosphate ions are more important than that of calcium ions, at least in the initial stage. Increasing sodium and phosphate adsorption on the titanium surface induces adsorption of *extracellular matrix* (ECM) *proteins*, as shown by the NH^+ and COO^- binding energies, without calcium adsorption in X-ray photoelectron spectroscopy analysis [10].

The adsorption of ECM proteins is crucial in cell adhesion onto titanium surfaces. Many tissue culture cells need focal adhesion initiated by specific binding of ECM proteins and receptors in the integrin superfamily for growth and differentiation. The Arg-Gly-ASP

(RGD) sequence of ECM proteins has been recognized as mediating cell adhesion on titanium surfaces [11]. The RGD sequence has been identified in numerous ECM proteins, including fibronectin, vitronectin, type I collagen, osteopontin, and bone sialoprotein. An in vitro study found selective affinities of fibronectin or vitronectin on titanium, as the most abundant cell-binding proteins in serum proteins [8].

Glow-discharge plasma has been used to investigate the role of electrostatic interactions in biological events such as inorganic adsorption and in cell adhesion properties [8–10, 12]. The surface energy (negative charge) on the titanium surface is increased by the glow-discharge plasma, thereby enhancing the cell adhesion properties associated with inorganic adsorption, which obviously elucidates the initial cell adhesion cascade caused by the titanium surface energy.

One approach to promoting the initial adhesion cascade on the titanium surface uses cell adhesion molecules. Since the identification of the RGD sequence as a mediator of cell adhesion properties, researchers have been depositing RGD-containing peptides on titanium surfaces [13]. Researchers have also attempted to increase the surface energy using ultraviolet illumination [14–16] of titanium surfaces on the basis of Eqs. 9.1–9.5. An ultraviolet-illuminated titanium surface has superior initial adhesion properties as well as glow-discharge plasma, although the efficiency decreases significantly with time. In contrast, anodically oxidized titanium prepared by discharging maintains its hydrophilicity over time [1].

In anodic oxidation, the thickness of the amorphous *anatase* TiO_2 at the phase boundaries of the oxide/electrolyte and oxide/metal is nearly the same because of the simultaneous migration of Ti^{4+} and O^{2-} toward the electrolyte and the metal, respectively. An incompletely crystallized thick oxide layer incorporates trapped electron–hole pairs (Ti^{4+} and e^-) until TiO_2 crystallization is complete. Hydroxyl radicals and superoxide anions, as intermediate products of the trapped electron–hole pairs in an amorphous anatase TiO_2 surface and water, continuously generate oxidation products such as hydrophilic functional groups. Because of its prolonged hydrophilicity, anodically oxidized titanium has high cell adhesion properties and enhances osteoblast phenotypes.

9.1.1 Wound-Healing Phenomena

Bone integration with titanium implants is a complex regenerative process initiated in response to surgical injury. The cells adhered on the materials are subjected to oxidative stress during wound healing at a surgical site, which may delay bone integration onto the surface.

Although titanium is a primary metallic biomaterial in orthopedic or dental implants, a titanium surface does not have antioxidant properties against oxidative stress, as indicated by the decrease in antioxidant defense molecules such as glutathione (GSH) in the adherent cells [17, 18]. Since depletion of antioxidant molecules leads to impaired cell viability and less tolerance against additional oxidative stress, the problem of oxidative stress on titanium needs to be solved. The oxidative stress of adherent cells on material surfaces is associated with insufficient oxygen diffusion as a result of a profound alteration in mitochondrial functions caused by respiratory depression of cell mitochondria [17].

One of the foremost challenges is oxygen diffusion on titanium surfaces, since supplying sufficient oxygen during wound-healing processes is critical for survival and integration of adherent cells. In a biopolymer modification, sustained release of oxygen diffusion by a poly*(*lactic-co-glycolic) acid (PLGA) film incorporating sodium percarbonate was achieved [17]. When the PLGA was placed in contact with ischemic tissue in a mouse model, decreased tissue necrosis was observed. The oxygen-producing element in the PLGA film is the incorporated sodium percarbonate. *Sodium percarbonate* ($Na_2CO_3 \cdot 1.5H_2O_2$) is an adduct of sodium bicarbonate and hydrogen peroxide, which spontaneously decomposes in contact with water to produce oxygen. The results show that peroxidation with hydrogen peroxide of a modified titanium surface might be useful for increasing oxygen diffusion to adherent cells. Peroxidation of a titanium surface can be achieved by generation of hydroxyl radicals and their oxidation products on an anodically oxidized titanium surface prepared by discharging. The anodically oxidized titanium surface can continuously generate hydrogen peroxide and oxygen [1], according to Eqs. 9.1–9.5. As a result, the levels of intracellular antioxidant molecules such as reduced GSH are not decreased in the adherent osteoblasts on an anodically oxidized titanium surface or a typical cell-cultured polystyrene, although

bare titanium and thermally oxidized titanium show decreased GSH levels [2]. However, the cells participating in wound-healing processes are more complex. Because of the observed early adhesion of monocytes/macrophages and endothelial cells on titanium implants, the potential contribution of these cells in wound healing is another advantage worth considering [19, 20]. There have been few investigations of antioxidant effects of titanium implants. Further insights into the wound-healing processes occurring at the cell–implant interface will be useful in understanding the reactions occurring at the interface in implant acceptance or failure.

9.2 Bone Tissue Responses

The bone tissue responses to titanium implants placed at surgical sites involve a series of cell and matrix events, ideally leading to intimate apposition, that is, osseointegration. At this stage, gaps between the bone and the implant surface need to be filled and repaired. During osseointegration, unfavorable conditions such as premature loading and micromotion disrupt formation of the new tissue, and formation of a fibrous capsule occurs [11, 21]. Histological studies have shown the heterogeneity of bone–implant interfaces. Afibrillar interfacial zones have often been reported [11, 22, 23]. The interface has been reported to be rich in glycosaminoglycans [24], and high-resolution immunocytochemical studies have shown that the interfacial layer is rich in noncollagenous proteins such as osteopontin and bone sialoprotein [25, 26]. The absence or relative paucity of serum proteins indicates selective accumulation of noncollagenous bone matrix proteins by a host response. The afibrillar interfacial zone might have a major role in the mechanism of "bonding" between the host bone and the implant surface, but the inherent mechanical weakness of the afibrillar interface argues against this possibility [11, 27].

Osteoblasts, osteoids, and a mineralized matrix are observed adjacent to the interfacial layer [22, 26]. The bone is therefore deposited directly on the surface of the titanium implant and extended outward from the surface. When bone formation occurs, not only does healing approach from the bone, it also extends from the titanium implant toward the healing bone. A study has shown that formation of bone extending away from the implant is about

30% faster than that of bone healing toward the implant surface [11] (see also Chapter 10).

Because of the complexities of in vivo events, the bone–implant interface has not been fully elucidated. In vitro cell culture models have been used to investigate bone–titanium interactions. Most culture cells are osteoblastic cells, and very few use osteoclastic cells [12]. However, recent reports have indicated that continuous balanced osseous remodeling is essential for the successful maintenance of titanium implants [28, 29]. Further work is needed to identify and determine both osteoblast and osteoclast functions at the interface.

9.3 Biomechanical Considerations

The biomechanical stability of osseointegrated titanium implants is of particular importance. Stability is achieved for a range of implant surface topographies as well as physicochemical properties of the mineralized tissues at the interface.

9.3.1 Surface Roughness of Titanium Implants

Various methods have been developed for providing rough surfaces with enhanced bone fixation [7, 30]. Methods for producing surface roughness of titanium are plasma spraying, blasting with ceramic particles, acid etching, and anodizing (Table 9.1).

Table 9.1 Surface roughness of dental implants

Type of implant	Surface Rougness (μm)
Cp Ti (polished)	Ra = 0.22 ± 0.01
W-EDM	Ra = 19.5 ± 0.40
TPS	Ra = 7.01 ± 2.09
Acid etched	Ra = 0.51 ± 0.10

These methods have been used either alone or in combinations such as blasting + acid etching (SLA). Alternatively, wire-electric discharging machining enables processing of titanium materials by a spark discharge generated through running water between

a narrow metal wire and the titanium material [31–33]. This computer-controlled process enables accurate bulk implant shaping and surface microtexturing in parallel.

The macrolevel, for topographical features, is defined as being in the range of millimeters to tens of microns [7]. This scale is directly related to implant geometry for threaded screw and macroporous surface treatments. Both early fixation and long-term mechanical stability of the implanted prosthesis can be improved by using high-roughness surface profiles rather than fine, smooth surfaces [34]. A high roughness profile results in mechanical interlocking between the implant surface and the healing bone, though an increase in peri-implantitis and ionic leakage are major risks [35]. An implant surface with a microtopographic profile maximizes mechanical interlocking between the bone and the implant surface [34, 36]. A surface roughness in this range results in greater bone-to-implant contact and higher resistance to torque removal of bone than are obtained with other types of surface topographies. Nanometer-scale profiles of implant surfaces are increasingly being reported [7, 37].

Nanoscale profiles may play an important role in adsorption of ECM proteins and in cell adhesion properties, thereby increasing the rate of osseointegration. However, reproducibility of nanoscale surface profiles of titanium with chemical modifications such as acid etching is quite difficult to achieve and unreliable, and thus the optimal nanoprofile of titanium surfaces for rapid osseointegration is still uncertain. In addition, inadequate recovery of the passive TiO_2 layer on acid-etched bare titanium surfaces causes much greater surface contamination than that noted in oxidized surfaces; this has been referred to as "time-dependent degradation of titanium"[1, 15, 16].

Numerous studies have demonstrated that the surface roughness of titanium implants affects the rate of osseointegration and biomechanical fixation. Nonetheless, the variety of models used makes it difficult to draw a consensus conclusion as to whether, or to what extent, the surface roughness influences biological responses.

9.3.2 Nanomechanical Evaluation of Biological Tissues

Because mechanical failure of titanium implants is frequently localized within an afibrillar mineralized layer at the bone–implant

interface [11], the biomechanical properties of the mineralized layer on the implant surface play significant roles in the longevity of an implant prosthesis. Bulk mechanical testing has sometimes shown that the biomechanical strength of the interface might be inferior to the intrinsic strength of the host bone [38, 39].

There are still few studies determining the biomechanical properties of the mineralized layer on titanium implants, and more studies are essential. In vitro bone cell behavior on a titanium sample can be similar to that of an in vivo afibrillar mineralized layer, and cell organization is comparable to that in a mineralized matrix on a titanium surface during culture with supplemental ascorbic acid, sodium β-glycerophosphate, and dexamethasone [40]. This is therefore an important consideration as the information obtained reflects in vivo events.

The biomechanical evaluation of such microenvironments is a challenge. Nanobiomechanical testing technology, such as nanoindentation, enables measurements of the mechanical properties of samples of very small volume [41–43]. There are two crucial factors associated with the evaluation of in vitro–mineralized tissue on titanium surfaces. First—and this is central to standard nanoindentation analysis—is the assumption that the surface is in ideal contact with the indenter penetration depth (Fig. 9.1).

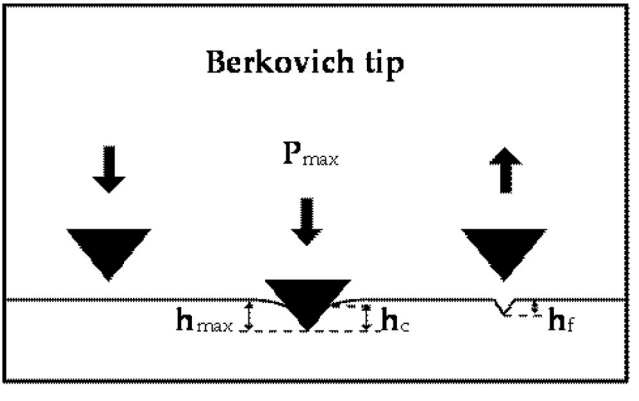

Figure 9.1 Typical nanoindentaton process to a sample surface.

In reality, all biological surfaces are characterized by some degree of roughness or inhomogeneity [44]. Second, the viscoelastic properties of biological tissues cause problems [45]. Figure 9.2 shows

typical load versus indenter displacement data for an indentation experiment. In the nanoindentation, the hardness (H) and elastic modulus (E) can be calculated using the following equations:

$$H = P/A \tag{9.6}$$

$$E = \frac{1}{\beta}\frac{\sqrt{\pi}}{2}\frac{S}{\sqrt{A}} \tag{9.7}$$

*A is the contact area at maximum loading force.
*β is a coefficient where S is contact stiffness calculated by unloading slope (dP/dh).

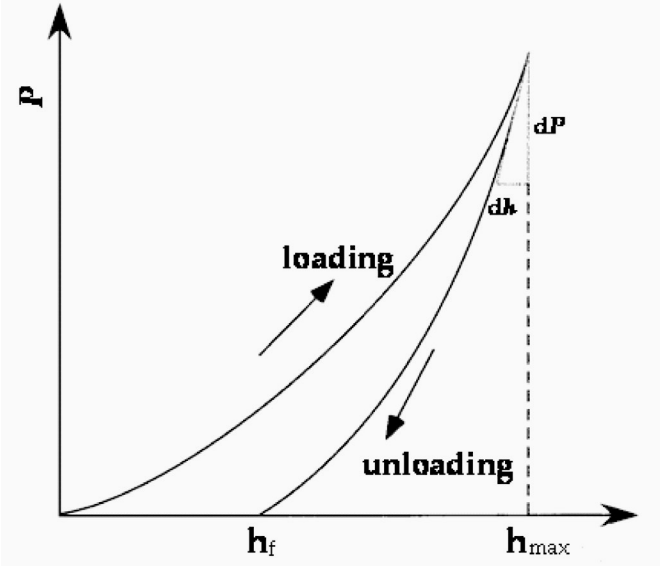

Figure 9.2 A schematic representation of load versus indenter displacement data for an indentation experiment.

In elastic–plastic materials, the obtained values are always constant, regardless of the load function. However, many polymeric biomaterials and biological tissues exhibit time-dependent or viscoelastic behavior [46]. The most readily observed effect of viscoelasticity on indentation is creep, or sinking of the tip into the sample under a constant load function. In such viscoelastic materials, the hardness and moduli usually vary with load function (or loading rate) because different loadings affect the creep or sinking behavior, leading to variations in the contact area (A) and unloading phase shift (dP/dh) in Eqs. 9.6 and 9.7.

A depth-dependent loading/partial unloading function consists of a number of loading/unloading portions (data points) toward the applied final loading force (Fig. 9.3). A partial unloading technique enables ideal contact between the indenter tip and the sample surface as a function of depth, so the depth-dependent mechanical properties of inhomogeneous biological structures can be normalized in the direction perpendicular to the sample surface [2, 44]. An additional holding time at each peak load, followed by an unloading portion, prevents an inappropriate unloading slope because the hold enables relaxation of the initial loading force (Fig. 9.3). Numerous mineralized tissues on titanium surfaces can therefore be compared using average depth-dependent nanomechanical values.

As reported in a previous in vitro study [1], the area of mineralized nodules on anodically oxidized titanium prepared by discharging in an electrolyte was greater than that observed on titanium or thermally oxidized titanium because of the expression of bone matrix proteins such as *Bsp2*, *Ocn*, and *Opn*. The mechanical properties of mineralized tissue are associated with maturation of the extracellular mineralized bone matrix proteins produced by osteoblasts. The higher hardness and elastic modulus of mineralized tissue on anodically oxidized titanium was also evaluated by a nanoindentation test with partial unloading [2].

The values were comparable to those of natural bone or dentine. In the case of metallic or solid elastic–plastic materials, the elastic properties may be related to density or increased hardness. However, in the case of mineralized biocomposites, such as bone or dentine, the elastic modulus does not increase linearly with increasing density or mineralization [45].

The elastic modulus is associated with fluid displacement and inelastic deformation of the collagen/apatite structure. The higher hardness and inelastic properties of mineralized tissues suggest that there is a reduction in permeability and consolidation via cross-linking of the structures. In the living body, oxidation of lysine residues in immature bone matrix proteins such as collagen molecules is the final enzyme reaction for cross-linking between molecules [47, 48].

According to Eqs. 9.1–9.5, generation of hydroxyl radicals or superoxide anions occurs on amorphous anatase on anodically oxidized titanium. Since the enhanced nanobiomechanical properties

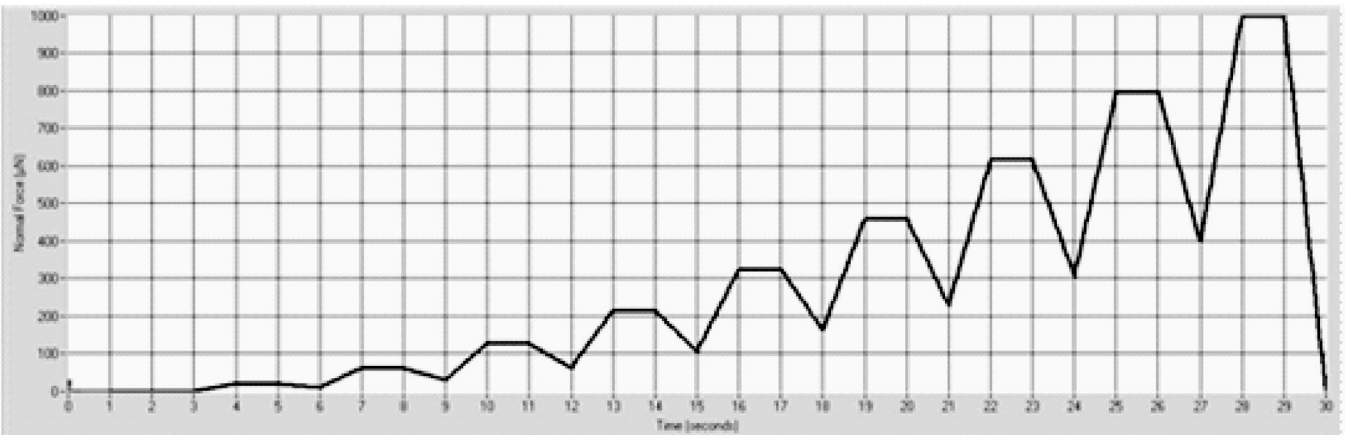

Figure 9.3 A schematic representation of a depth-dependent loading/partial unloading function.

of in vitro–mineralized tissues were only observed on anodically oxidized titanium surfaces, surface hydroxyl radicals enabled oxidation of the lysine residues of immature collagen molecules, in addition to oxidation by natural oxidation enzymes such as lysyl oxidase. Surface radical reactions on titanium may have a key role in biomechanical considerations at the interface of healing bone and titanium implants.

In investigating the above speculation, Raman spectroscopy analyses and alterations in the protein structure are of particular importance in distinguishing mature or immature calcified tissues, since subtle molecular changes often cause detectable vibrational changes [49–52]. The coupling of a Raman spectrometer with an optical microscope allows reduction of the analysis scale to the micrometer scale, with better spatial resolution than that obtained using infrared spectroscopy. There have been several characteristics of Raman spectra of calcified tissues (Fig. 9.4).

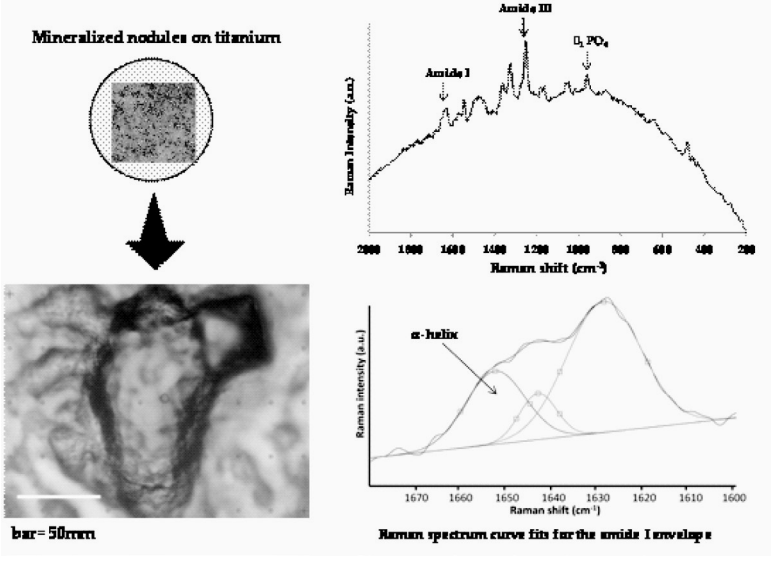

Figure 9.4 Raman spectra of in vitro–mineralized tissue on titanium.

Briefly, the Amide I region between 1600 cm^{-1} and 1700 cm^{-1} revealed the occurrence of three or more bands at 1623 cm^{-1}, 1637 cm^{-1}, and 1656 cm^{-1}, attributable to characteristic collagen

secondary structures [50, 51]. The band at 1637 cm^{-1} is characteristic of a collagen secondary structure and is present as an evident shoulder of the Amide I band in the Raman spectrum of collagen. The increase in the Amide I band shoulder at 1656 cm^{-1} was attributable to the maturity of typical α-helix collagen secondary structures. This was related to hydrogen bonding between collagen molecules and subsequent cross-linking of tissues [53].

The Raman spectra also show bone mineral bands from apatite phosphate at ~960 cm^{-1} and carbonate at ~1070 cm^{-1}. The ratio of mineral bands to the Amide III band at around 1250 cm^{-1}, attributable to disordered and ordered bone matrix proteins, indicates the mineral-to-matrix ratio of the calcified tissues [52]. An inorganic apatite transformation associated with collagen cross-linking plays a key role in the biological stability of the mineralized layer at the interface of bone and titanium implants, thereby increasing the longevity of the implant prosthesis. In the light of these findings, bone tissue engineering on titanium implants needs to be performed at the micro- or nanoscale.

9.4 Bacterial Cell Responses

In addition to surfaces that promote bone growth and adaptation, antimicrobial properties of implant surfaces are highly desirable. The initial adhesion of microorganisms onto an implant surface is an unavoidable event and triggers biofilm formation. Such biofilm formation on implants is a major complication, leading to potential failure of implant bonding [54]. Although it is difficult to obtain quantitative information regarding the prevalence of complications, it was suggested in one study that peri-implantitis was responsible for between 8% and 50% of all implant failures [55]. Another potential problem is the unpredictability of implant integration with the host bone.

In clinical practice, the bonding of dental implants is often incomplete, raising the risk that an implant will loosen over time. The development of antimicrobial implants with excellent osteoconductivity has recently been of substantial interest in orthopedic and dental therapy. However, achieving antimicrobial activity as well as osteoconductivity remains a crucial challenge.

Recent approaches have focused on surface modification techniques for antimicrobial activity of titanium implants, but there are still very few antimicrobially modified titanium surfaces. These can be roughly categorized into two groups according to whether their strategies are aimed at killing adherent bacteria on the surface or preventing adhesion of bacterial cells.

9.4.1 Killing Adherent Bacteria on Titanium Implants

In one approach aimed at killing adherent bacteria, titanium implants with an immobilized disinfectant use an antibiotic, fluorine, or Ag ions to kill bacteria on the surface, with a high local chemical concentration adjacent to the surgical site [56–58]. Nanostructured titanium surfaces can be loaded with an antibiotic or nanoparticles as a coating for implant materials. Nanotubes of size 80–400 nm fabricated on titanium through anodization enable antibiotic loading onto the surfaces [56]. It has been reported that drug-eluting nanotubes decreased initial *Staphylococcus epidermis* adhesion, but such methods lead to burst release of the antibiotic, with more than 80–90% of the antibiotic being released from the coating layer within the first 60 minutes [59, 60]. Nanotubes loaded with Ag nanoparticles killed planktonic bacteria in a culture medium during the first four days [58]. An Ag-incorporated titanium surface prevents bacterial adhesion for 30 days, which might be long enough to prevent infection after surgery in the early and intermediate stages of implantation.

An alternative approach has been developed to confer an implant with strong antimicrobial activity as well as osteoconductivity. A modified titanium surface anodized by discharge in sodium chloride solution (Ti-Cl) is an efficient defensive weapon against oral bacteria [1, 54, 58, 61, 62]. The experimental results showed large decreases in the numbers of different oral pathogens adhering to Ti-Cl, such as *Streptococcus mutans*, *Streptococcus salivarius*, *Streptococcus sobrinus*, *Actinomyces viscosus*, *Aggregatibacter* (*Actinobacillus) actinomycetem-comitans*, *Capnocytophaga ochracea*, and *Porphyromonas gingivalis*, with an increase in contact time of as long as 15 minutes. Furthermore, osteogenic gene expressions and mineralization on Ti-Cl are superior to those on an unmodified titanium surface [1].

$TiCl_3$ formed on the surface is gradually hydrolyzed into perchloric acid (HClO) and Ti-OH. The peroxidation effect of HClO efficiently destroys the bacterial cell surface peptidoglycan structure, while increasing the hydrophilicity, because Ti-OH facilitates adhesion of the osteoblastic cells associated with accumulated cell-binding proteins on the surface.

HClO is known to be an unstable chemical, but it has good antimicrobial activity. Since the HClO generated on the Ti-Cl surface is readily decomposed, particularly when in contact with serum proteins, the peroxidation effects are limited to a region extremely close to the surface. In fact, bacteria can more closely adhere to the Ti-Cl surface through an electrostatic mechanism, whereas the adhesion of osteoblastic cells through a protein-mediated mechanism is much higher than that of bacteria. The differences in each adherence mode may result in the existence of individual territories of osteoblastic cells and bacteria on the Ti-Cl surface. The viability of the adherent osteoblastic cells on the Ti-Cl surface is therefore not inhibited, even if the modified surface generates HClO continuously [54]. Most importantly, the efficiency of the antimicrobial activity does not decrease for at least eight weeks in a culture medium.

9.4.2 Preventing Bacterial Cell Adhesion on Titanium Implants

Another approach to preventing bacterial cell adhesion onto the implant surface, involving polyelectrolyte deposition on the titanium surface, has been reported [63]. The strategies are generally based on the hydrophilicity associated with the higher surface energy of synthetic polypeptides, which leads to a reduction in adhesion of early colonizers within supragingival plaque by increasing the electrostatic (repulsive) forces between the modified implant surface and bacteria. Additionally, osteoblast adhesion is increased with higher surface energy, since this provides a local concentration of cell-binding proteins or other immobilized agents such as RGD peptides or osteogenic proteins to the polypeptides.

Although several hundred bacterial species are associated with plaque biofilms, mitis streptococci, *Streptococcus mitis* (*S. mitis*) and *Streptococcus gordonii* (*S. gordonii*), are generally accepted as early colonizers within supragingival plaque biofilms [64, 65]. The

local accumulation of early colonizer streptococci, followed by late colonizer mutans streptococci, such as *Streptococcus mutans* or *Streptococcus sobrinus*, plays a pivotal role in the maturation of supragingival plaque, which leads to potential infection by subgingival plaque. Thus, prevention of early colonizer adherence might delay infection of a dental implant.

Hydroxyapatite (HA) coatings have been routinely used in bioactive modifications of titanium implants because the coatings enhance bone formation and generally provide early fixation between bone and implant surfaces. Their use is widespread, but the relatively low survival rate of HA-coated titanium implants is of particular concern. This may be a result of the integrity of the bonding between the HA layer and the implant surface and also of the susceptibility of the layer to biofilm formation [66]. The preparation of HA-coated titanium by electrical discharge in a buffered physiological saline solution has several advantages over traditional techniques such as high-temperature plasma spraying. Specifically, it can generate highly crystalline nanoscale HA (approximately 100 nm in diameter) of thickness 1 μm [67, 68]. The HA crystals are incorporated within the developing thickness of the titanium oxide layer that is generated during processing. The thinner coating layer at the bone–titanium interface may reduce its biomechanical integrity over time.

Moreover, the developing thickness of a titanium oxide film results in an electrostatic potential, associated with greater surface hydrophilicity, so the HA-coated titanium surface shows antimicrobial activity, specifically against early colonizers such as *S. mitis* and *S. gordonii*, as a result of a repulsion force, whereas the sintered HA surface is susceptible to early or late colonizers because the pure HA surface is electrostatically stable in biological environments [66].

9.5 Future Challenges and Directions

The biocompatibility of titanium implants is mainly determined by events at the interface between the bone and the implant surface. Many advances have been made in understanding events at this interface and in developing methods for controlling these events. There are a number of surface modifications commercially available for titanium implants. Most of these modified surfaces

have proven to be clinically successful, but the development of these surface modifications has been empirical. The exact role of surface chemistry and topography in the bonding of titanium implants is poorly understood.

The ideal nano- to microscale topography and chemistry should be defined for enhancing implant integration into native tissue. An understanding of the bone–implant interface is critical for the development of proactive titanium implants that can promote desired outcomes. Several important questions still remain; for example, the relationship between titanium surfaces and tissue structure, matrix composition, and biomechanical properties of the interface. Recent in vitro studies have clearly demonstrated that antimicrobially modified titanium surfaces increase osteoblast cell functions, while decreasing bacterial attachment onto surfaces. However, more research is required to understand the underlying factors in osteoblast and bacterial behavior on titanium and to translate that knowledge into commercially available products for dental applications.

References

1. Shibata, Y., et al. (2010) The characteristics of in vitro biological activity of titanium surfaces anodically oxidized in chloride solutions, *Biomaterials,* **31**, 8546–8555.
2. Iwai-Yoshida, M., et al. (2012) Antioxidant and osteogenic properties of anodically oxidized titanium, *J. Mech. Behav. Biomed. Mater.,* **13**, 230–236.
3. Rajagopal, G., Maruthamuthu, S., Mohanan, S., Palaniswamy, N. (2006) Biocidal effects of photocatalytic semiconductor TiO2, *Colloids Surf., B*, **51**, 107–111.
4. Beutner, R., Michael, J., Förster, A., Schwenzer, B., Scharnweber, D. (2009) Immobilization of oligonucleotides on titanium based materials by partial incorporation in anodic oxide layers, *Biomaterials,* **30**, 2774–2781.
5. Tizazu, G., Adawi, A. M., Leggett, G., Lidzey, D. G. (2009) Photopatterning, etching, and derivatization of self-assembled monolayers of phosphonic acids on the native oxide of titanium, *Langmuir,* **25**, 10746–10753.
6. Buser, D., et al. (2004) Enhanced bone apposition to a chemically modified SLA titanium surface, *J. Dent. Res.,* **83**, 529–533.

7. Le, Guéhennec L., Soueidan, A., Layrolle, P., Amouriq, Y. (2007) Surface treatments of titanium dental implants for rapid osseointegration, *Dent. Mater.,* **23**, 844–854.
8. Shibata, Y., Hosaka, M., Kawai, H., Miyazaki, T. (2002) Glow discharge plasma treatment of titanium plates enhances adhesion of osteoblast-like cells to the plates through the integrin-mediated mechanism, *Int. J. Oral Maxillofac. Implants,* **17**, 771–777.
9. Shibata, Y., Miyazaki, T. (2002) Anode glow discharge plasma treatment enhances calcium phosphate adsorption onto titanium plates, *J. Dent. Res.,* **81**, 841–844.
10. Yamamoto, H., Shibata, Y., Miyazaki, T. (2005) Anode glow discharge plasma treatment of titanium plates facilitates adsorption of extracellular matrix proteins to the plates, *J. Dent. Res.,* **84**, 668–671.
11. Puleo, D. A., Nanci, A. (1999) Understanding and controlling the bone-implant interface, *Biomaterials,* **20**(23–24), 2311–2321.
12. Kawai, H., Shibata, Y., Miyazaki, T. (2004) Glow discharge plasma pretreatment enhances osteoclast differentiation and survival on titanium plates, *Biomaterials,* **25**, 1805–1811.
13. Rezania, A., Thomas, C. H., Branger, A. B., Waters, C. M., Healy, K. E. (1997) The detachment strength and morphology of bone cells contacting materials modified with a peptide sequence found within bone sialoprotein, *J. Biomed. Mater. Res.,* **37**, 9–19.
14. Aita, H., et al. (2009) The effect of ultraviolet functionalization of titanium on integration with bone, *Biomaterials,* **30**, 1015–1025.
15. Att, W., et al. (2009) Time-dependent degradation of titanium osteoconductivity: an implication of biological aging of implant materials, *Biomaterials,* **30**, 5352–5363.
16. Hori, N., et al. (2009) Age-dependent degradation of the protein adsorption capacity of titanium, *J. Dent. Res.,* 88(7), 663–667.
17. Harrison, B. S., Eberli, D., Lee, S. J., Atala, A., Yoo, J. J. (2007) Oxygen producing biomaterials for tissue regeneration, *Biomaterials,* **28**, 4628–4634.
18. Sato, N., et al. (2009) N-Acetyl cysteine (NAC) inhibits proliferation, collagen gene transcription, and redox stress in rat palatal mucosal cells, *Dent. Mater.,* **25**, 1532–1540.
19. Lee, K., Lee, H., Lee, K. W., Park, T. G. (2011) Optical imaging of intracellular reactive oxygen species for the assessment of the cytotoxicity of nanoparticles, *Biomaterials,* **32**, 2556–2565.
20. Tsaryk, R., et al. (2007) Response of human endothelial cells to oxidative stress on Ti6Al4V alloy, *Biomaterials,* **28**, 806–813.

21. Szmukler-Moncler, S., Salama, H., Reingewirtz, Y., Dubruille, J. H. (1998) Timing of loading and effect of micromotion on bone-dental implant interface: review of experimental literature, *J. Biomed. Mater. Res.,* **43**, 192–203.
22. Albrektsson, T., Hansson, H. A. (1986) An ultrastructural characterization of the interface between bone and sputtered titanium or stainless steel surfaces, *Biomaterials,* **7**, 201–205.
23. Davies, J. E., Lowenberg, B., Shiga, A. (1990) The bone-titanium interface in vitro, *J. Biomed. Mater. Res.,* **24**, 1289–1306.
24. Linder, L. (1985) High-resolution microscopy of the implant-tissue interface, *Acta Orthop. Scand.,* **56**, 269–272.
25. Ayukawa, Y., et al. (1998) An immunoelectron microscopic localization of noncollagenous bone proteins (osteocalcin and osteopontin) at the bone-titanium interface of rat tibiae, *J. Biomed. Mater. Res.,* **41**, 111–119.
26. Nanci, A., et al. (1994) Tissue response to titanium implants in the rat tibia: ultrastructural, immunocytochemical and lectin-cytochemical characterization of the bone-titanium interface, *Cell. Mater.,* **4**, 1–30.
27. Brunski, J. B. (1999) In vivo bone response to biomechanical loading at the bone/dental-implant interface, *Adv. Dent. Res.,* **13**, 99–119.
28. Moon, H. J., et al. (2011) Effect of heparin and alendronate coating on titanium surfaces on inhibition of osteoclast and enhancement of osteoblast function, *Biochem. Biophys. Res. Commun.,* **413**, 194–200.
29. Zreiqat, H., et al. (2003) Differentiation of human bone-derived cells grown on GRGDSP-peptide bound titanium surfaces, *J. Biomed. Mater. Res., A.,* **64**, 105–113.
30. Cochran, D. L., Schenk, R. K., Lussi, A., Higginbottom, F. L., Buser, D. (1998) Bone response to unloaded and loaded titanium implants with a sandblasted and acid-etched surface: a histometric study in the canine mandible, *J. Biomed. Mater. Res.,* **40**, 1–11.
31. Kataoka, Y., Tamaki, Y., Miyazaki, T. (2011) Synergistic responses of superficial chemistry and micro topography of titanium created by wire-type electric discharge machining, *Biomed. Mater. Eng.,* **21**, 113–121.
32. Otsuka, F., Kataoka, Y., Miyazaki, T. (2012) Enhanced osteoblast response to electrical discharge machining surface, *Dent. Mater. J.,* **31**, 309–315.
33. Yamaki, K., Kataoka, Y., Ohtsuka, F., Miyazaki, T. (2012) Micro-CT evaluation of in vivo osteogenesis at implants processed by wire-type electric discharge machining, *Dent. Mater. J.,* **31**, 427–432.

34. Buser, D., et al. (1991) Influence of surface characteristics on bone integration of titanium implants. A histomorphometric study in miniature pigs, *J. Biomed. Mater. Res.,* **25**, 889–902.

35. Becker, W., et al. (2000) A prospective multicenter clinical trial comparing one- and two-stage titanium screw-shaped fixtures with one-stage plasma-sprayed solid-screw fixtures, *Clin. Implant. Dent. R.,* **2**, 159–165.

36. Wennerberg, A., Hallgren, C., Johansson, C., Danelli, S. (1998) A histomorphometric evaluation of screw-shaped implants each prepared with two surface roughnesses, *Clin. Oral Implants Res.,* **9**, 11–19.

37. Brett, P. M., et al. (2004) Roughness response genes in osteoblasts, *Bone,* **35**, 124–133.

38. Hong, L., Hengchang, X., De Groot, K. (1992) Tensile strength of the interface between hydroxyapatite and bone, *J. Biomed. Mater. Res.,* **26**, 7–18.

39. Wong, M., Eulenberger, J., Schenk, R., Hunziker, E. (1995) Effect of surface topology on the osseointegration of implant materials in trabecular bone, *J. Biomed. Mater. Res.,* **29**, 1567–1575.

40. Irie, K., Zalzal, S., Ozawa, H., McKee, M. D., Nanci, A. (1998) Morphological and immunocytochemical characterization of primary osteogenic cell cultures derived from fetal rat cranial tissue, *Anat. Rec.,* **252**, 554–567.

41. Bolshakov, A., Oliver, W. C., Pharr, G. M. (1996) Influences of stress on the measurement of mechanical properties using nanoindentation: part II. Finite element simulations, *J. Mater. Res.,* **11**, 760–768.

42. Hay, J. C., Bolshakov, A., Pharr, G. M. (1999) Critical examination of the fundamental relations used in the analysis of nanoindentation data, *J. Mater. Res.,* **14**, 2296–2305.

43. Menčík, J., Munz, D., Quandt, E., Weppelmann, E. R., Swain, M. V. (1997) Determination of elastic modulus of thin layers using nanoindentation, *J. Mater. Res.,* **12**, 2475–2484.

44. Shibata, Y., et al. (2008) Micromechanical evaluation of mineralized multilayers, *J. Biomech.,* **41**, 3414–3418.

45. Shibata, Y., He, L. H., Kataoka, Y., Miyazaki, T., Swain, M. V. (2008) Micromechanical property recovery of human carious dentin achieved with colloidal nano-β-tricalcium phosphate, *J. Dent. Res.,* **87**, 233–237.

46. Ebenstein, D. M., Pruitt, L. A. (2006) Nanoindentation of biological materials, *Nano Today.,* **1**, 26–33.

47. Paschalis, E. P., et al. (2001) Spectroscopic characterization of collagen cross-links in bone, *J. Bone Miner. Res.,* **16**, 1821–1828.

48. Vora, S. R., et al. (2010) Lysyl oxidase propeptide inhibits FGF-2-induced signaling and proliferation of osteoblasts, *J. Biol. Chem.,* **285**, 7384–7393.

49. Carden, A., Morris, M. D. (2000) Application of vibrational spectroscopy to the study of mineralized tissues, *J. Biomed. Opt.,* **5**, 259–268.

50. Dehring, K. A., Smukler, A. R., Roessler, B. J., Morris, M. D. (2006) Correlating changes in collagen secondary structure with aging and defective type II collagen by Raman spectroscopy, *Appl. Spectrosc.,* **60**, 366–372.

51. Dehring, K. A., et al. (2006) Identifying chemical changes in subchondral bone taken from murine knee joints using raman spectroscopy, *Appl. Spectrosc.,* **60**, 1134–1141.

52. Xu, C., Karan, K., Yao, X., Wang, Y. (2009) Molecular structural analysis of noncarious cervical sclerotic dentin using Raman spectroscopy, *J. Raman Spectrosc.,* **40**, 1780–1785.

53. Bonifacio, A., et al. (2010) Chemical imaging of articular cartilage sections with Raman mapping, employing uni- and multi-variate methods for data analysis, *Analyst,* **135**, 3193–3204.

54. Omori, S., et al. (2009) Micro-organism and cell viability on antimicrobially modified titanium, *J. Dent. Res.,* **88**, 957–962.

55. Barbour, M. E., Gandhi, N., El-Turki, A., O'Sullivan, D. J., Jagger, D. C. (2009) Differential adhesion of Streptococcus gordonii to anatase and rutile titanium dioxide surfaces with and without functionalization with chlorhexidine, *J. Biomed. Mater. Res. A,* **90**, 993–998.

56. Popat, K. C., Eltgroth, M., LaTempa, T. J., Grimes, C. A., Desai, T. A. (2007) Decreased Staphylococcus epidermis adhesion and increased osteoblast functionality on antibiotic-loaded titania nanotubes, *Biomaterials,* **28**, 4880–4888.

57. Yoshinari, M., Oda, Y., Kato, T., Okuda, K. (2001) Influence of surface modifications to titanium on antibacterial activity in vitro, *Biomaterials,* **22**, 2043–2048.

58. Zhao, L., et al. (2011) Antibacterial nano-structured titania coating incorporated with silver nanoparticles, *Biomaterials,* **32**, 5706–5716.

59. Radin, S., Campbell, J. T., Ducheyne, P., Cuckler, J. M. (1997) Calcium phosphate ceramic coatings as carriers of vancomycin, *Biomaterials,* **18**, 777–782.

60. Yamamura, K., Iwata, H., Yotsuyanagi, T. (1992) Synthesis of antibiotic-loaded hydroxyapatite beads and in vitro drug release testing, *J. Biomed. Mater. Res.,* **26**, 1053–1064.

61. Deng, J. Y., et al. (2010) Role of chloride formed on anodized titanium surfaces against an oral microorganism, *J. Biomater. Appl.,* **25**, 179–189.

62. Shibata, Y., Kawai, H., Yamamoto, H., Igarashi, T., Miyazaki, T. (2004) Antibacterial titanium plate anodized by being discharged in NaCl solution exhibits cell compatibility, *J. Dent. Res.,* **83**, 115–119.

63. Chua, P. H., Neoh, K. G., Kang, E. T., Wang, W. (2008) Surface functionalization of titanium with hyaluronic acid/chitosan polyelectrolyte multilayers and RGD for promoting osteoblast functions and inhibiting bacterial adhesion, *Biomaterials,* **29**, 1412–1421.

64. Medaglini, D., Pozzi, G., King, T. P., Fischetti, V. A. (1995) Mucosal and systemic immune responses to a recombinant protein expressed on the surface of the oral commensal bacterium Streptococcus gordonii after oral colonization, *Proc. Natl. Acad. Sci. U. S. A.,* **92**, 6868–6872.

65. Socransky, S. S., Haffajee, A. D., Cugini, M. A., Smith, C., Kent, R. L., Jr. (1998) Microbial complexes in subgingival plaque, *J. Clin. Periodontol.,* **25**, 134–144.

66. Murakami, A., et al. (2012) Antimicrobial and osteogenic properties of a hydrophilic-modified nanoscale hydroxyapatite coating on titanium, *Nanomedicine,* **8**, 374–382.

67. Toda, Y., Shibata, Y., Kataoka, Y., Kawawa, T., Miyazaki, T. (2008) Interfacial assembly of bioinspired nanostructures mediated by supersensitive crystals, *J. Biomed. Mater. Res. A,* **84**, 869–874.

68. Yamamoto, H., Shibata, Y., Tachikawa, T., Miyazaki, T. (2006) In vivo performance of two different hydroxyapatite coatings on titanium prepared by discharging in electrolytes, *J. Biomed. Mater. Res. Appl. Biomater. B,* **78**, 211–214.

Chapter 10

Titanium in Implant Dentistry

Niklaus P. Lang[a] and Jukka P. Matinlinna[b]
[a]*Faculty of Dentistry, Implant Dentistry, University of Hong Kong, Prince Philip Dental Hospital, 34 Hospital Road, Sai Ying Pun, Hong Kong SAR, People's Republic of China*
[b]*Faculty of Dentistry, Dental Materials Science, University of Hong Kong, Prince Philip Dental Hospital, 34 Hospital Road, Sai Ying Pun, Hong Kong SAR, People's Republic of China*
nplang@switzerland.net, jpmat@hku.hk

Titanium (Ti) is the most widely used metallic material for dental submucosal implants due to its invaluable, unique, and outstanding biomedical and biomechanical properties. These are its great availability, high biocompatibility, high strength and stiffness, and relatively low density. The chemistry of Ti has some special features, such as its rich oxide formation capacity. Ti is abundant in the earth's crust but cumbersome to extract. It has been known for a long time that titanium implants are known to osseointegrate into living bone tissues. Osseointegration is defined as the ability of bone tissues to grow directly and intimately into contact with the surface of the implant without any intermediate soft tissue layer.

Handbook of Oral Biomaterials
Edited by Jukka P. Matinlinna

ISBN 978-981-4463-12-6 (Hardcover), 978-981-4463-13-3 (eBook)
www.panstanford.com

10.1 Titanium, Its Chemistry, and Biomechanics

Titanium (chemical symbol Ti; origin: Titans from Greek mythology) is a so-called transition metal. It is used in technology as an addition to steel to impart great tensile strength and to Al to impart resistance to attack by salt solutions and by organic acids. Ti is recognized for its high strength-to-weight ratio. Titanium is mechanically a strong metal with low density, and especially in oxygen-free circumstances, it is also quite ductile. Ti is lustrous and metallic white in color, and it is paramagnetic, having fairly low thermal and electrical conductivity.

As an element, titanium belongs to the first transition series (Sc, Ti, V, Cr, Mn, Fe, Co, Ni, Cu and Zn) and to group 4 (previously labeled as group IV A), that is, Ti, Zr (zirconium), and Hf (hafnium). These elements have a strong tendency to form chemical compounds with the valence +IV. In other words, ions such as Ti^{4+}, Zr^{4+}, and Hf^{4+} develop. These metals are easily rendered passive so that they are not reactive at room temperature and they have very high resistance to corrosion. Ti is almost as corrosion resistant as platinum (Pt) [1].

Titanium has five naturally occurring isotopes, mostly with mass number 48 (73.94%). Ti is not radioactive. Its highest oxidation state is +4, and all naturally occurring Ti compounds have the metal in this chemical state. However, formal oxidation states of –1 and 0 are found in some complex compounds with the 2,2'-bipyridyl ligand. Ti^{2+}, in Ti(II) compounds, is known as the dichloride, dibromide, and diiodide and in TiO. However, the +2 state is unstable in aqueous solutions, where Ti^{2+} is known to be a strong reducing species. Ti(III) compounds include the oxide, some sulphates, and trihalides [2].

Interestingly, Ti has metallic and ionic radii very close to Hf due to the so-called lanthanide contraction. Ti is abundant, found in around 0.63% of the earth's crust, being the ninth most abundant element, but difficult to extract to pure metal. Titanium is found as the oxide in the minerals *rutile* (TiO_2, tetragonal; the most common Ti mineral), *anatase* (TiO_2, tetragonal), *brookite* (TiO_2, rhombic), *ilmenite* ($FeTiO_3$), and *perovskite* ($CaTiO_3$). Some other minerals include *sphene*, *titanite* ($CaTiSiO_5$), and *benitoite* ($BaTiSi_3O_9$). Reduction of titanium with carbon (C) is unsatisfactory because the very stable (and harmful) carbide, TiC, is also formed. Thus, the commercial production of Ti is by the metallothermic reduction of titanium tetrachloride, $TiCl_4$ [2–4].

Ti is a dimorphic metal: the α-form has a hexagonal structure below 882.5°C, while the β-form stays body-centered cubic (bcc) above 882.5°C. Ti is brittle when cold and malleable when hot; however, it can be ductile only when it is free of oxygen. On the other hand, traces of nitrogen or oxygen increase its strength. At 700°C–800°C, Ti can decompose steam, and at red heat Ti combines with oxygen. To describe the specific properties of Ti, it can burn in an atmosphere of oxygen under certain conditions. It is attacked by acids only on heating, and nitric acid oxidizes Ti to TiO_2. Ti dissolves in hot HCl to give $TiCl_3$ but can resist attack by cold mineral acids. Melting Ti is cumbersome because at 800°C it combines with nitrogen, which sets high requirements for casting Ti—a protective atmosphere is vital. Ti forms alloys with Al, Cr, Co, Cu, Fe, V, Fe, Ni, and Sn (cf Table 10.1) [1, 2, 4] (see also Chapters 9 and 11–13).

10.2 Bonding to Titanium

Ti is a versatile material and recently became a metal of choice in prosthetic dentistry, where it finds its indications as crowns, bridges, fixed partial dentures, and, in particular, subgingival coated dental implant fixtures. Resin titanium bonding may be promoted significantly using silica coating followed by silanization (i.e., using silane coupling agents) and then a resin composite luting cement [7–9] (see also Chapter 11). Extensive research directed toward development of the casting, finishing, and bonding to porcelain has been ongoing for a long while. Yet, many practical problems with the use of Ti and its alloys for crowns and bridges remain to be solved. The high melting temperature and the vigorous chemical reactivity of Ti at high temperatures result in difficulties with casting and Ti porcelain bonding. Porcelain Ti bonding sets certain demands for pretreatment procedures and firing temperatures [10].

10.3 Titanium Alloys

Although Ti has acceptable biomechanical properties and has been widely used for orthopedic and dental implants, for most applications titanium is alloyed with small amounts of aluminum (Al) and vanadium (V), typically 6 wt% and 4 wt%, respectively. Such a Ti alloy is Ti-6Al-4V (aka Ti6Al4V or Ti 6-4), the most commonly used

Ti alloy. It has a chemical composition of 6% Al, 4% V, ≤0.25% Fe, ≤0.2% O_2, and the balance Ti. Commercially pure (c.p.) Ti is available in four grades where the oxygen content varies between 0.18 wt% and 0.40 wt% and the Fe content between 0.20 wt% and 0.50 wt%; grade 4 is the current Ti material of choice in implant dentistry [5, 6].

The apparently slight concentration differences have, however, a substantial effect on the physical and mechanical properties of c.p. Ti. At room temperature, c.p. Ti has a hexagonal close-packed (hcp) crystal lattice and is called the α-Ti (so-called α-phase). On heating, an allotropic phase transformation occurs: at 883°C forms a bcc lattice, labeled as the β-phase [5]. Ti is a reactive metal: in air and aqueous electrolytes, it forms spontaneously a dense oxide film at its surface (see Table 10.1 below).

Table 10.1 Some chemical and physical properties of the group 4 (IV A) elements, titanium, zirconium, and hafnium [1, 3, 6, 12]

	Ti	Zr	Hf
Crystal structure	**Hexagonal**	**Hexagonal close-packed**	**Hexagonal**
Abundance in the earth's crust	0.63%	0.023%	5 ppm
Atomic number	22	40	72
Atomic weight	47.90	91.22	178.49
Electronic configuration	$3d^2 4s^2$	$4d^2 5s^2$	$5d^2 6s^2$
Metallic radius/pm	147	160	158
Ionic radius (+4 ion)/pm	68	80	81
Oxidation states (ions)	–1, 0, +2, +3, **+4**	+2, +3, **+4**	+2, +3, **+4**
Density (g cm^{-3})	4.54	6.53	13.3
Melting point/°C	1677	1857	2227
Boiling point/°C	3277	3577	4603
Young's modulus/GPa	116	88	78
Shear modulus/GPa	44	33	30
Bulk modulus/GPa	110	91.1	110
Vickers hardness/MPa	970	903	1760
Thermal conductivity/ W m^{-1} K^{-1}	21.9	22.6	23.0
Thermal expansion (25°C)/μm m^{-1} K^{-1}	8.6	5.7	5.9

The density of Ti, 4.5 g/cm^3, is only about half the value of many base metal alloys. Interestingly, compared to dental implants made of other materials, those made of Ti are significantly lighter, more durable, and capable of withstanding higher pressure without harmful deformation, such as cracking. Although Ti is also used in manufacturing orthodontic wires, wrought alloys of N and Mo are used in the applications of orthodontics [5].

There are four grades of c.p. Ti, depending on the oxygen and iron concentrations. The slight concentration differences markedly affect the physical and mechanical properties of titanium.

Recently, a new potential binary implant material, Ti-Zr alloy, was introduced. It has been demonstrated that the Ti-Zr alloy would have better mechanical properties than c.p. Ti to a level that makes it qualified to be used in cases of small-diameter implants to withstand the bending moments without fracture. It has been reported that the Ti-Zr alloy has a significantly increased mechanical stability compared to Ti (c.p. grade 4), with respect to fatigue strength and elongation. The ultimate tensile strength of Ti-Zr is observed to be comparable to Ti-6Al-4V [11].

Nickel-titanium, Ni-Ti, is a wrought alloy (55% Ni and 45% Ti) that possesses a shape memory effect that refers to its ability to undergo deformation at one temperature and then recover its original, undeformed shape upon heating above its so-called "transformation temperature." In addition, Ni-Ti is a *superelastic* alloy; this property takes place at a narrow temperature range just above its transformation temperature. No heating is necessary to cause the undeformed shape to recover, and the material exhibits enormous elasticity, some 10–30 times that of ordinary metals. Ni-Ti is used in orthodontics as a wire [5].

10.4 Titanium Oxides

Currently, titanium is the most widely used, leading material for the manufacturing of oral implants [13]. Titanium is highly biocompatible, as a result of low toxicity and a low rate of ion release from its surface, and nontoxic and is not rejected by the body. Such unique properties are unanimously understood to be the consequence of an inert surface oxide film and an unusually high

resistance to corrosion [14]. When pure titanium or its alloys are exposed to air, a layer of titanium dioxide, TiO_2, with a thickness of approximately 2–5 nm is formed within nanoseconds (ns), i.e., in 10^{-9} s [5].

This thin film also protects the titanium materials, making the latter highly resistant to corrosion [6]. TiO_2 is insoluble in water and dilute acids but slowly dissolves in concentrated sulfuric acid. As a compound, TiO_2 is a so-called amphoteric oxide, that is, it reacts with both acids and bases. The onset of amphotersim correlates with a significant degree of covalent character in the bonds formed by Ti [15]. Titanium dioxide has much industrial importance as a white pigment material on account of its high opacity [3].

Several phases of *titanium oxides* have been detected that cover a wide range of O/Ti ratios: Ti_3O, Ti_3O_2, Ti_3O_5, Ti_2O, Ti_2O_3, and TiO_2. These titanium oxides have an influence on the titanium physical properties, such as isoelectric point, charge, and solubility. TiO_2 is the most stable form of titanium oxide. TiO_2 exists in *amorphous* or *crystalline* forms.

Interestingly, several phases containing between 63.6 atom% and 65.5 atom% of oxygen have been identified: these Ti oxides are of the formulae $TiO_{1.752}$ to $TiO_{1.902}$. Titanium(III)oxide, Ti_2O_3, behaves as a basic oxide and is prepared by heating TiO_2 with carbon. Ti_2O_3 is a violet powder. Interestingly, the Ti oxide with the valence of +2, TiO, shows marked *nonstoichiometry* in its composition. At elevated temperatures, at around 1400°C, TiO has a defect crystal lattice over the composition range $TiO_{0.64}$ to $TiO_{1.27}$ and electrical neutrality is preserved in the crystal by changes in the charges on the Ti ions. Also oxides, such as Ti_3O_5 and Ti_2O, have been detected and identified in special circumstances at elevated temperatures [2, 3, 13, 16, 17].

Even in large doses, Ti is nontoxic. It does not play any natural role inside the human body [6]. It has been estimated that a quantity of 0.8 mg of Ti would be ingested by humans each day. However, most of it passes through without being absorbed.

Due to its very special properties, Ti finds with its alloys applications also in endodontics (as files and instruments), the aerospace industry, the automotive industry, sporting goods, industrial processes, biomedicine, etc.

10.5 Titanium Surface Properties and Surface Modifications

In implant dentistry today, Ti implants are surgically inserted inside the jawbone, applying the principle of *osseointegration* (aka osteointegration), where the implant fixture is directly bonded to newly formed bone without the interference of a connective tissue layer. Obviously, the Ti surface is one of the most vital factors that influence the osseointegration process. Adequate Ti surface treatment may achieve faster osseointegration and speed up the overall treatment process and healing (see also Chapter 9).

Techniques to modify Ti surfaces may be classified into topographical and chemical surface modifications. Most techniques that are used to modify surface topography will change simultaneously the surface chemistry—either intentionally or accidently. In the past decade, chemical modification of titanium surfaces has been a target to enhance osseointegration. This was to control the interactions that occur between the implant surface and biological body fluids. There are various protocols that have been developed to produce different Ti surface chemistries, in terms of the titanium/oxygen ratio, thickness of the oxide layer, incorporation of bioactive elements, CaP coatings, crystallization properties, and surface impurities. Commonly used methods to *modify implant surface topography* can be classified into *additive* and *subtractive* processes. *Additive* processes include the addition of a CaP or titanium plasma coating onto the Ti surface to form a convex profile. *Subtractive* processes such as grit blasting, acid etching, blasting and etching, and oxidation cleanse and remove particles from the surface to form a concave profile (see also Chapters 11 and 12). In both processes, the goal is to increase the contact surface with bone.

Surface properties play a vital role in the interaction dynamics that occur between the implant and the biological environment. Implant surface properties, such as topography, roughness, chemistry, surface energy, and charge, and the presence of impurities have a significant impact on bone tissue responses. Ti surface modifications are performed to achieve the optimal surface properties to produce reliable and predictable bone healing. Currently, *acid etching* is widely used to modify many titanium dental implants to produce a roughened surface. It has been proven that implants with

moderately rough surfaces have stronger anchorage and fixation in bone compared to the smooth-surfaced implants [18, 19]. Recently, ultraviolet (UV) treatment of Ti has been introduced as an adjunctive method to enhance surface properties to the implant surface without changing the surface topography [20].

Commonly used methods to modify: *Ti implant surface topography* can be classified into additive and subtractive processes.

Additive processes include addition of CaP or titanium plasma coating onto the Ti surface to form convex profile and thus increase the surface in contact with bone.

Subtractive processes, such as acid etching, grit blasting, blasting and etching, and oxidation, remove particles from the surface to form concave profiles with the same goal of increasing the surface in contact with bone.

In the last decade, combining *sandblasting and acid etching* was a very common Ti surface modification and is currently used for many commercially available dental implants (Fig. 10.1). The so-called widely known "sandblasted, large-grit, acid-etched" (SLA®, by Straumann) surface can be created by grit blasting with *alumina* (Al_2O_3) or *titania* (TiO_2) powder to create the optimal roughness. This is needed for mechanical fixation; then additional etching may smooth out the sharp peaks and cleanse any remaining contaminants on the surface. This process obtains a *moderate* level of roughness that equals 1.19 μm. This, in turn, is suggested to produce strong anchorage and fixation in bone [21]. At present, there is a general consensus that rough-surfaced implants allow for stronger bone anchorage compared to smooth implants. This has been attributed to the rough topographical feature that leads to mechanical interlocking with the growing bone cells [22] (see also Chapter 12).

Ti surface properties such as surface charge, topography, wettability, and chemistry are known to strongly influence implant–bone anchorage.

10.6 Surface Charges on Titanium

The surface energy of any biomaterial can be determined by the material's surface charge density and the net polarity of the charge.

A surface with a net positive or negative charge may be more hydrophilic. The surface charge of a dental implant is understood to be a vital factor to promote bone cells adhesion and early-stage bone mineralization in the bone–implant interface. In this light, surface charge modifications might be a promising new direction for improving the osseointegration of a Ti dental implant. The main challenge in a surface charge lies in effective modification of a long-lasting surface charge of dental subgingival implant materials.

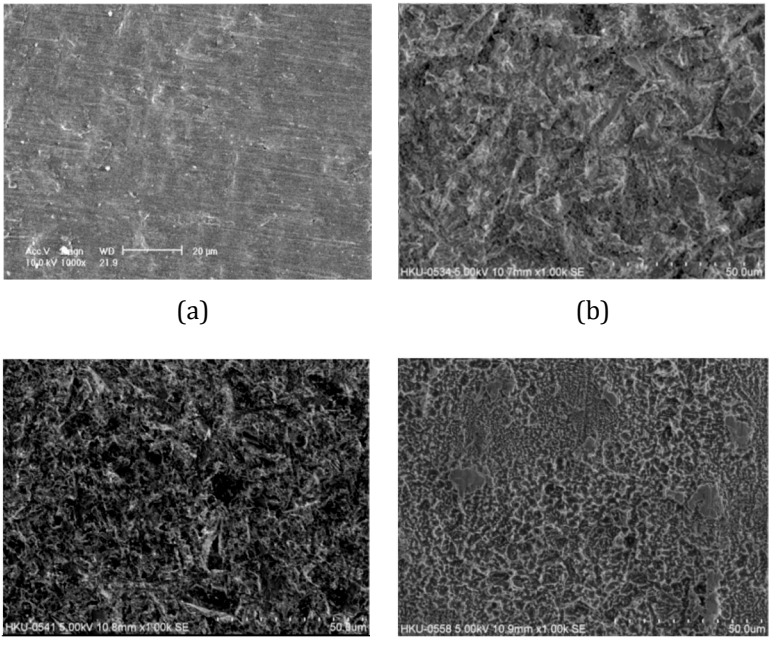

Figure 10.1 Effect of various surface treatments on Ti surfaces. (a) Polished Ti, (b) Ti blasted with Al_2O_3, 110 μm, for 15 s, (c) H_2SO_4 etching and Al_2O_3, and (d) 48% H_2SO_4 etching for 1 h at 60°C. Courtesy of C. Y. Guo, University of Hong Kong.

On the theory side, a deeper understanding of the underlying mechanism for charge generation during sandblasting is of high importance [14, 23]. It was recently concluded that sandblasting is a relatively simple and effective way to increase the static electric charge on a Ti surface. The results confirmed that using alumina (Al_2O_3) powders with various grit sizes, a negative charge was

generated to Ti. On the other hand, the static charges decayed until a stable voltage level (equal to the environment) was reached [24]. However, such findings might help to design and develop surface treatment methods.

10.7 Oral Implants

In modern times, the *first generation* of implants dates back to 1948, when two American dentists, Gershoff and Goldberg, surgically placed a subperiosteal implant that was made of *stainless steel* prefabricated on a study model by Dr. Gustav Dahl from Sweden [25, 26].

This *first generation* of implants had limited success. It was only applicable for the fully edentulous patient. Over time, it had a very high failure rate due to infections spreading through the mucosal seal along the implant frame into the subperiosteal lodge. Needless to say that such failing implant frames left a disastrous situation for future prosthetic treatment, since bone resorption was very extensive. Consequently, subperiosteal implants were soon abandoned and banned from being used in reconstructive dentistry.

The *second generation* of implants is characterized by its incorporation pattern. The healing process followed a *fibrous encapsulation* of the foreign body that was termed *fibro-osseous incorporation* (Fig. 10.2). These implants were placed into a trough prepared into the jawbone of an edentulous ridge [27]. *Stainless steel* was the material of choice. It is noteworthy that these second-generation implants had a limited survival rate over five years. Again, infections spread through the mucosal seal and created enormous bone resorption around the blade implants. Moreover, in the absence of infection, the connective tissue capsule around the blades was 5–10 times the dimension of a natural periodontal ligament, hereby creating increased mobility of the implant. Consequently, blade implants soon became unpopular [28] and gave way to the *third generation* of oral implants.

10.8 Osseointegration

This *third generation* of oral implants is characterized by a healing pattern termed *osseointegration* or *functional ankylosis*. This

healing pattern is based on the biocompatibility of the material used. The material with the highest resistance to corrosion has been documented to be c.p. titanium and titanium alloys followed by zirconia. Hence, titanium became the material of choice for oral implants owing to its high biocompatibility and physicochemical features for turning and manufacturing implants (see Fig. 10.3) [29]. The *steel alloys* used in the era of the *second-generation* implants were well tolerated by the body but healed by *fibrous encapsulation*. Hence, they could not give rise to osseointegration [29]. The latter phenomenon was accidentally discovered in Sweden and in Switzerland in the late 1960s and early 1970s.

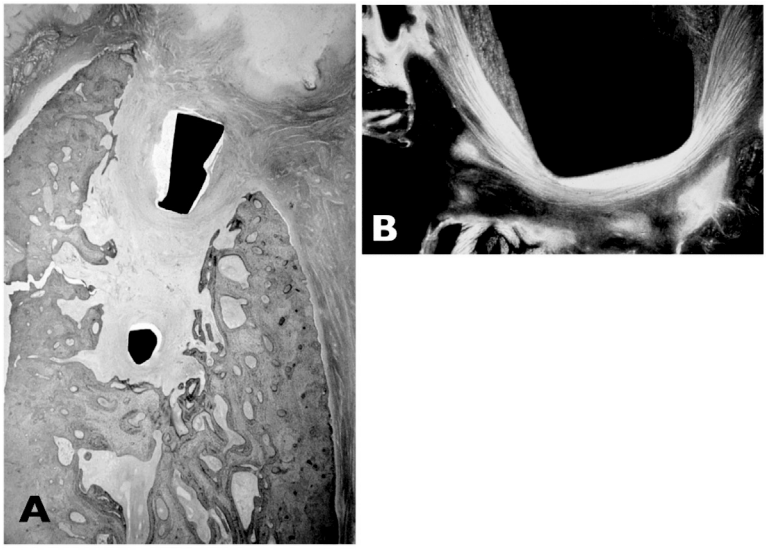

Figure 10.2 Second-generation implants: healing by fibrous encapsulation. (A) A steel blade implant ad modum Linkow is surrounded by a connective tissue capsule. Such an implant is mobile since it is supported by a connective tissue fiber network. (B) A fluorescent photomicrograph yielding a functional orientation of the fibrous encapsulation coping with the occlusal loading of the implant.

In the 1960s, the Swedish orthopedic surgeon P. I. Brånemark (b. 1929) was studying wound- and bone-healing sequences as well as bone regeneration, installing wound chambers made of titanium into long bones of experimental animals. Accidentally, he discovered that

bone was growing on top of and adhered to the titanium. Brånemark subsequently carried out further studies using animal and human subjects to confirm this unique phenomenon of titanium [30].

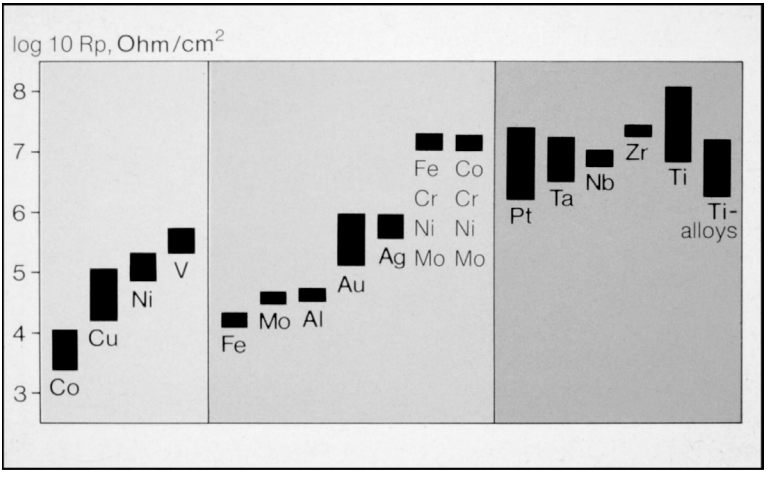

Figure 10.3 Corrosion experiments in vivo for various metals and alloys. Key: CoCrNiMo = a wrought Co alloy; cw316LESR = cold-worked remelted stainless steel; Ti alloys = Ti_4Al_4Mo, Ti_6Al_4V, and $Ti_{15}Mo$. Modified from Ref. [29].

Due to a high rate of edentulism in the general population of that time, Brånemark realized that the incorporation of an implant into the jawbone could dramatically improve denture stability. The term *osseointegration* was defined to mean adherence of bone to metal—in this case titanium. In 1965, Brånemark placed and documented the first titanium dental implant in a human at the University of Göteborg in Sweden [30].

In Switzerland, at the same time, *osseointegration* was discovered in studies of the Association of Internal Fixation (ASIF) of orthopedic surgeons. The stability of fixation screws for orthopedic plates was to be improved. Through the work of metallurgists [29] and bone morphologists [31], it was realized that bone would grow directly on top of c.p. titanium. The dental researcher André Schroeder applied these results and developed oral implants that would *functionally ankylose* ("osseointegrate"), together with the engineer Franz Sutter. The term *functional ankylosis* described the features of *osseointegration* and emphasized the direct bone-to-implant

contact achieved on titanium implants [32] (Fig. 10.4). Later, it has been demonstrated that *osseointegration or functional ankylosis* represents direct bonding of the bone on top of the titanium, not only on the apparent light (visible level), but also on the ultrastructural level [33].

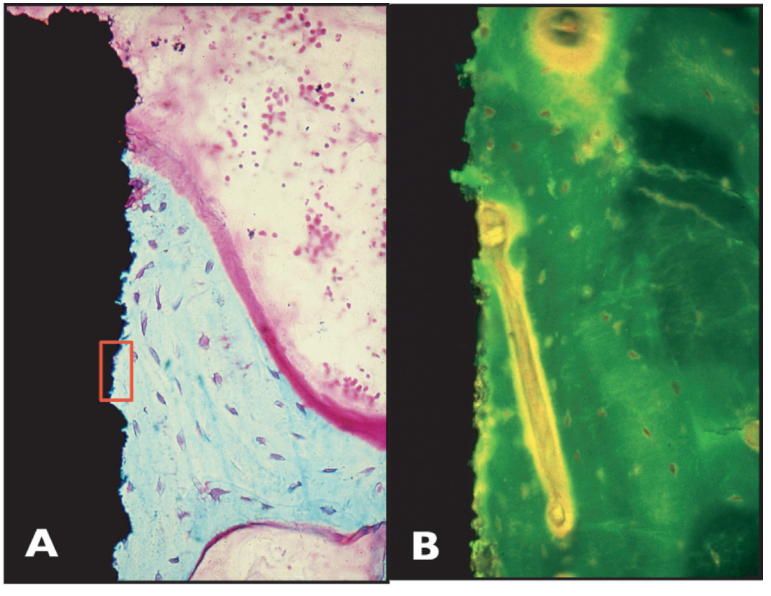

Figure 10.4 Third-generation implants. (A) Incorporation of the implant by direct bone-to-implant contact. This phenomenon was termed "osseointegration" or "functional ankylosis." Red insert: Higher magnification. (B) Fluorecent micrograph documenting osseointegration with a blood vessel "attaching" to the implant surface as a sign of the high biocompatibility of titanium.

Since osseointegrated oral implants came into dental practice in the 1970s [34], implant dentistry has become increasingly popular and indispensible in contemporary oral rehabilitation. Due to high survival rates and high predictability of *third-generation* oral implants, the number of patients seeking implant treatment is increasing continuously year by year [35]. The annual implant instalment rate has been over one million worldwide in the past decade [36]. Thus, dental implants have become a valuable option in comprehensive periodontal treatment plans for both edentulous and partially dentate patients [37].

As implant therapy is an optional treatment for patients in most cases, in-depth evidence on implant provision and alternative treatment options needs to be provided to support patients in their choice of appropriate treatment in terms of longevity of the reconstruction, economic aspects, and risks and complications to be encountered [38, 39]. Furthermore, evidence-based data may guide dental practitioners to render optimal treatment available to patients [40].

Beyond any doubt, titanium has unique properties among all metals in the periodic table. Hence, it truly may be presented as the material of choice for oral implants.

10.9 Clinical Aspects of Dental Implant Surfaces

Most of the third-generation implants were manufactured in a turning or machining process that resulted in a relatively smooth implant surface. Surface roughness R_a was approximately 0.3–0.4 µm. This surface was propagated by industry for many years and was copied on a variety of implants resembling the original Brånemark design. As opposed to machined surface implants, implants with a rough surface made of titanium plasma particles being sprayed on the implant surface with an Argon (Ar) gas carrier and at high temperatures (titanium plasma sprayed, TPS) yielded a surface roughness of R_a = 2.9 µm. Such a TPS surface increased the total contact area of the implant 13–15-fold and, consequently, provided a surface for increased anchorage. However, the manufacturing process of the TPS surface was tiresome, tedious, complicated, and costly. Therefore, attempts were made throughout the 1990s to improve implant surfaces by creating roughened surfaces with optimal characteristics [41]. Out of these studies resulted a roughened surface that was sandblasted with large grit and acid-attacked (SLA). The surface roughness was approximately R_a = 1.9–2.2 µm. The osseointegration appeared to be faster and more pronounced when compared to the TPS surface in a miniature pig model and dramatically superior than with a machined surface [42]. This was reflected in higher removal torques and increased bone-to-implant contact.

It was recognized that moderately rough surfaces yielded higher bone-to-implant contact than either rough or smoother surfaces (Fig. 10.5). Most of the implant surfaces used today have a moderately rough surface topography.

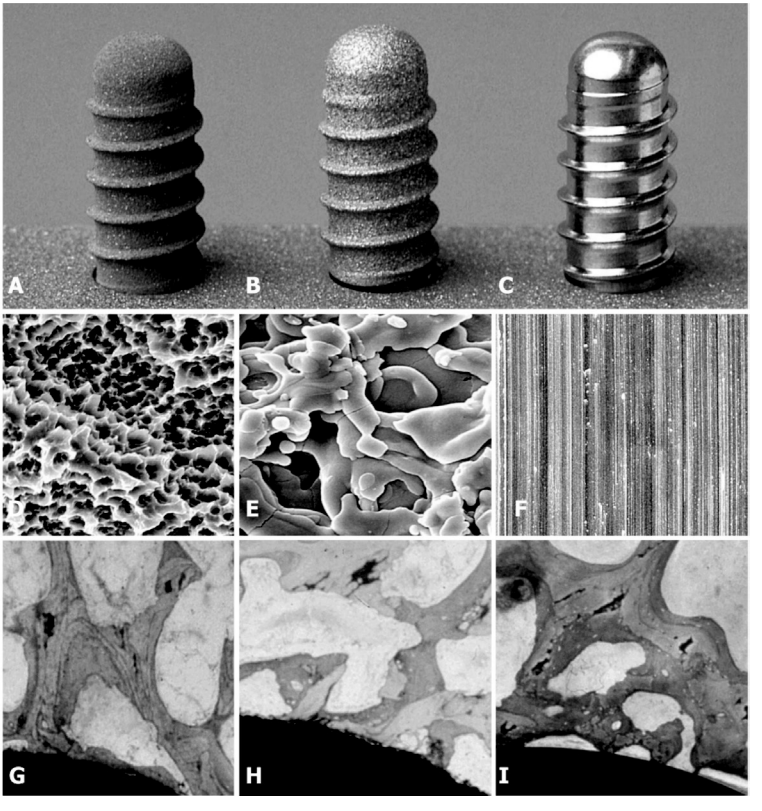

Figure 10.5 Prototype implants of various surface roughness. (A, D, G) SLA (sandblasted with large grit and acid-attacked) surface with a roughness value of approximately R_a = 1.8 µm. (B, E, H) TPS surface with a roughness value of approximately R_a = 2.9 µm. (C, F, I) Machined or turned surface with a roughness value of approximately R_a = 0.4 µm. (D) Subtractive roughness created by sandblasting and acid etching. (E) Additive roughness created by blasting titanium plasma particles onto the surface, resulting in an increase in the surface of approximately 13x. (F) Very minimal roughness of a turned surface. (G) Highest bone-to-implant contact on the SLA surface. (H) Good bone-to-implant contact on the TPS surface. (I) Minimal bone-to-implant contact on the turned surface.

Surface roughness has been identified as a major feature responsible for the osseointegration process. Biomechanical and biochemical bonding mechanisms have been reviewed by Albrektsson and Wennerberg [21].

The surface topographical properties were evaluated and expressed at the micrometer level and categorized into:

(1) smooth or machined surfaces: $R_a < 0.5$ µm
(2) minimally rough surfaces: $R_a = 0.5 – 1.0$ µm
(3) moderately rough surfaces: $R_a = 1.0 – 2.0$ µm
(4) rough surfaces: $R_a > 2.0$ µm

A recent *systematic review* explored possible effects of titanium surface topography on osseointegration [22]. Of 1184 titles found through an electronic search in PubMed, 1064 had to be disregarded owing to the fact that they did not accurately present in vivo data on osseointegration as a response of implant surface topography. After scrutinizing the remaining 120 articles, bone responses to surface topography were evaluated in terms of bone-to-implant contact, removal torques, and push-out tests. Again, the analysis revealed that moderately rough surfaces showed higher bone bonding than rough surfaces or minimally rough or smooth surfaces.

More recently, there is evidence that surface chemical modifications on the nanometer level may improve osseointegration both on a temporal basis as well as on a degree level. Especially two nanotechnological modifications have shown promising results during early phases of osseointegration. Fluoride-modified TiOblast™ implant surfaces showed larger bone-to-implant contact (~13%) after two weeks of healing and more new bone within the voids of the implants compared to their counterparts with a conventional TiOblast™ surface. However, these differences were no longer present after six weeks of healing in the dog model [43]. In addition, early osseointegration to hydrophilic and hydrophobic implant surfaces was studied in a human biopsy model. Again, the nanotechnologically modified SLA surface with hydrophilic properties yielded significantly more bone-to-implant contact (~16%) after four weeks of healing. After six weeks, however, there were no statistically significant differences [44].

These latter studies have demonstrated that surface topography on the nanometer level may positively influence biological bonding

and, thus, provide additional predictability of implant therapy in patients with compromised bone situations (osteoporosis, diabetes mellitus, irradiated bone, etc.) [45]. Recent laboratory studies suggest that novel silane-based [9] coatings on titanium [46], dental porcelain [47], and also zirconia [48] were successfully developed and optimized. Such coatings may significantly promote resin cement adhesion and, in addition, produce hydrophobic surfaces [49–51] without compromising surface roughness.

References

1. Heslop, R. B., Robinson, P. L. (1967) *Inorganic Chemistry*, 3rd ed., Elsevier, Amsterdam.
2. Bell, C. F., Lott, K. A. K. (1972) *Modern Approach to Inorganic Chemistry*, 3rd ed., Butterworths, London.
3. Heslop, R. B., Robinson, P. L. (1976) *Inorganic Chemistry: A Guide to Advanced Study*, Elsevier, Amsterdam.
4. Cotton, F. A., Wilkinson, G. (1988) *Advanced Inorganic Chemistry,* 5th ed., John Wiley & Sons, New York, USA.
5. Powers, J. M., Sakaguchi, R. L. (2006) *Craig's Restorative Dental Materials,* 12th ed., Mosby Elsevier, St. Louis.
6. Emsley, J. (2001) *Titanium. Nature's Building Blocks: An A-Z Guide to the Elements*, Oxford University Press, Oxford.
7. Matinlinna, J. P., Mittal K. L. (2009) *Adhesion Aspects in Dentistry,* VSP/ Brill, Leiden.
8. Matinlinna, J. P., Vallittu, P. K. (2007) Silane based concepts on bonding resin composite to metals, *J. Cont. Dent. Pract.,* **8**(2), 1–8.
9. Lung, C. Y. K., Matinlinna, J. P. (2012) Aspects of silane coupling agents and surface conditioning in dentistry: an overview, *Dent. Mater.,* **28**, 467–477.
10. Könönen, M., Kivilahti, J. (1994) Bonding of low-fusing dental porcelain to commercially pure titanium, *J. Biomed. Mater. Res.*, **28**, 1027–1035.
11. Berner, S., Dard, M., Gottlow, J., Molenberg, A., Wieland, M. (2009) Titanium-zirconium: a novel material for dental implants, *Eur. Cells Mater.*, **17**(Suppl 1), 16.
12. O'Neil, M. J. (2006) *The Merck Index*, 14th ed., Merck, Whitehouse Station.

13. Lindhe, J., Lang, N. P. (2008) *Clinical Periodontology and Implant Dentistry, Vols. 1 and 2*, 5th ed., Blackwell Munksgaard, Oxford.
14. Guo, C. Y., Tang, A. T. H., Matinlinna, J. P. (2012) Insights into surface treatment methods of titanium dental implants, *J. Adhes. Sci. Technol.,* **26**, 189–205.
15. Shriver, D. F., Atkins, P. W. (2001) *Inorganic Chemistry*, 3rd ed., Oxford University Press, Oxford.
16. Clark, R. J. H. (1968) *The Chemistry of Titanium and Vanadium,* Elsevier, Amsterdam.
17. Barksdale, J. (1968) Titanium, in *The Encyclopedia of the Chemical Elements*, 732–738 (Ed. Hampel, C. A.), Reinhold Book Corporation, New York, USA.
18. Elias, C. N., Oshida, Y., Lima, J. H., Muller, C. A. (2008) Relationship between surface properties (roughness, wettability and morphology) of titanium and dental implant removal torque, *J. Mech. Behav. Biomed. Mater.,* **1**, 234–242.
19. Said, M. M. M. (2012) *Characterization of Titanium Surfaces with Different Treatment and Aging Processes,* MPhil thesis, Faculty of Dentistry, University of Hong Kong.
20. Aita, H., Hori, N., Takeuchi, M., Suzuki, T., Yamada, M., Anpo, M., Ogawa, T. (2009) The effect of ultraviolet functionalization of titanium on integration with bone, *Biomaterials,* **30**, 1015–1025.
21. Albrektsson, T., Wennerberg, A. (2004) Oral implant surfaces: part 1: review focusing on topographic and chemical properties of different surfaces and in vivo responses to them, *Int. J. Prosthodont.,* **17**, 536–543.
22. Wennerberg, A., Albrektsson, T. (2009) Effects of titanium surface topography on bone integration: a systematic review, *Clin. Oral Implants Res.,* **20**(Suppl 4), 172–184.
23. Guo, C. Y., Matinlinna, J. P., Tang, A. T. H. (2012) Effects of surface charges on dental implants: past, present and future, *Int. J. Biomater,* **2012**, Article ID 381535, 5 pages. doi:10.1155/2012/381535.
24. Guo, C. Y., Matinlinna, J. P., Tang, A. T. H. (2012) A novel effect of sandblasting on titanium surface: static charge generation, *J. Adhes. Sci. Technol*., **26**(23), 2603–2613.
25. Ring, M. E. (1995) A thousand years of dental implants: a definitive history: part 1, *Compend. Cont. Educ. Dent.,* **16**, 1060–1064.
26. Ring, M. E. (1995) A thousand years of dental implants: a definitive history: part 2, *Compend. Cont. Educ. Dent.,* **16**, 1132–1136.

27. Linkow, L. I., Weiss, J. L. (1969) The endosseous blade. A progress report, *Intl. J. Orthodont.*, **7**, 155–165.

28. Schneider, H. R., Kallenberger, A., Meszaros, J. (1978) Mobility measurements and histological studies on endosseous titanium implants under masticatory stress in the mandibles of adult macacas, *SSO Schweiz. Monatsschr. Zahnh.,* **88**, 815–828.

29. Steinemann, S. G. (1998) Titanium: the material of choice? *Periodontol. 2000*, **17**, 7–21.

30. Brånemark, P. I., Adell, R., Breine, U., Hansson, B. O., Lindström, J., Ohlsson, A. (1969) Intra-osseous anchorage of dental prostheses. I. Experimental studies, *Scand. J. Plastic Reconstr. Surg*., **3**, 81–100.

31. Schenk R. K., Buser D. (1998) Osseointegration: a reality, *Periodontol. 2000*, **17**, 22–35.

32. Schroeder, A., Pohler, O., Sutter, F. (1976) Tissues reaction to an implant of a titanium hollow cylinder with a titanium surface spray layer, *SSO Schweiz. Monatsschr. Zahnh.,* **86**, 713–727.

33. Listgarten, M. A., Buser, D., Steinemann, S. G., Donath, K., Lang, N. P., Weber, H. P. (1992) Light and transmission electron microscopy of the intact interfaces between non-submerged titanium-coated epoxy resin implants and bone or gingiva, *J. Dent. Res.,* **71**, 364–371.

34. Lindh, T., Gunne, J., Tillberg, A., Molin, M. (1998) A meta-analysis of implants in partial edentulism, *Clin. Oral Implants Res.,* **9**, 80–90.

35. Sonoyama, W., Kuboki, T., Okamoto, S., Suzuki, H., Arakawa, H., Kanyama, M., Yatani, H., Yamashita, A. (2002) Quality of life assessment in patients with implant-supported and resin-bonded fixed prosthesis for bounded edentulous spaces, *Clin. Oral Implants Res.,* **13**, 359–364.

36. Brunski, J. B. (1999.) In vivo bone response to biomechanical loading at the bone/dental-implant interface, *Adv. Dent. Res.,* **13**, 99–119.

37. Greenstein, G., Cavallaro, J. R., Tarnow, D. (2010) Dental implants in the periodontal patient, *Dent. Clin. N. Am.,* **54**, 113–128.

38. Brägger, U., Krenander, P., Lang, N. P. (2005) Economic aspects of single-tooth replacement, *Clin. Oral Implants Res.,* **16**, 335–341.

39. Scheuber, S., Hicklin, S., Brägger, U. (2012) Implants versus short-span fixed bridges: survival, complications, patients' benefits. A systematic review on economic aspects, *Clin. Oral Implants Res.,* **23**(Suppl 6), 650–662.

40. Guyatt, G. H., Cook, D. J. (1994) Health status, quality of life, and the individual, *JAMA*, **272**, 630–631.

41. Buser, D., Schenk, R. K., Steinemann, S., Fiorellini, J. P., Fox, C. H., Stich, H. (1991) Influence of surface characteristics on bone integration of titanium implants. A histomorphometric study in miniature pigs, *J. Biomed. Mater. Res.,* **25**, 889–902.

42. Buser, D., Nydegger, T., Oxland, T., Cochran, D. L., Schenk, R. K., Hirt, H. P., Snetivy, D., Nolte, L. P. (1999) Interface shear strength of titanium implants with a sandblasted and acid-etched surface: a biomechanical study in the maxilla of miniature pigs, *J. Biomed. Mater. Res.,* **45**, 75–83.

43. Berglundh, T., Abrahamsson, I., Albouy, J. P., Lindhe, J. (2007) Bone healing at implants with a fluoride-modified surface: an experimental study in dogs, *Clin. Oral Implants Res.,* **18**, 147–152.

44. Lang, N. P., Salvi, G. E., Huynh-Ba, G., Ivanovski, S., Donos, N., Bosshardt, D. D. (2011) Early osseointegration to hydrophilic and hydrophobic implant surfaces in humans, *Clin. Oral Implants Res.,* **22**, 349–356.

45. Albrektsson, T., Wennerberg, A. (2010) On implant surfaces: a review of current knowledge and opinions, *Int. J. Oral Maxillofac. Implant.,* **25**, 63–74.

46. Matinlinna, J. P., Tsoi, J. K. H., de Vries, J., Busscher, H. J. (2013) Characterization of novel silane coatings on titanium implant surfaces, *Clin. Oral Implants Res.,* **24**, 688–697.

47. Hooshmand, T., Matinlinna, J. P., Keshvad, A., Eskandarion, S., Zamani, F. (2013) Microtensile bond strength of leucite-reinforced dental ceramic to a resin cement using different silane coupling agents*, J. Mech. Behav. Biomed. Mater.,* **17**, 327–332.

48. Matinlinna, J. P., Choi, A. H., Tsoi, J. K. H. (2013) Bonding promotion of resin-composite to silica-coated zirconia implant surface using a novel silane system, *Clin. Oral Implants Res.,* **24**, 290–296.

49. Guo, C. Y., Tang, A. T. H., Tsoi, J. K. H., Matinlinna, J. P. (2014) Effects of different blasting materials on charge generation and decay on titanium surface after sandblasting, *J. Mechan. Behav. Biomed. Mater*., **32**, 145–154.

50. Villard, N. M., Seneviratne, C. J., Tsoi, J. K. H., Heinonen, M., Matinlinna, J. P. (2014) Candida albicans aspects of novel silane system coated titanium and zirconia implant surfaces, *Clin. Oral Implants Res*., (in press) doi: 10.1111/clr.12338.

51. Della Bona, A. (2009) *Bonding to Ceramics: Scientific Evidences for Clinical Dentistry*, Artes Medicas, Sao Paulo.

Chapter 11

Surface Pretreatment Methods and Silanization

Christie Ying Kei Lung and Jukka P. Matinlinna
Faculty of Dentistry, Dental Materials Science, University of Hong Kong, Prince Philip Dental Hospital, 34 Hospital Road, Sai Ying Pun, Hong Kong SAR, People's Republic of China
cyklung@hku.hk

The clinical success of dental restorations depends on the adhesive strength and bonding between dental restorative materials and tooth structure. Adhesion occurs when two dissimilar materials are close in a molecular level and contact to form bonds. In general, the adhesion and affinity between dissimilar materials, for example, inorganic and organic materials may be very weak. Adhesion can be significantly increased by application of a mediator, such as a *silane coupling agent*, that contains different functional groups to react and form a linkage to connect them. After surface pretreatment, the surface is more reactive for bond formation. Therefore, the surface treatment of some indirect dental restorative material is an important step in restorative dentistry. This chapter covers (1) the introduction of surface science, (2) basic theories of adhesion and surface characterization, (3) a discussion of several common surface

Handbook of Oral Biomaterials
Edited by Jukka P. Matinlinna

ISBN 978-981-4463-12-6 (Hardcover), 978-981-4463-13-3 (eBook)
www.panstanford.com

treatment methods, (4) some other new surface treatment methods currently under investigation, and (5) explanations for different types of mechanisms for various surface treatments to understand how they achieve the surface modification in question.

11.1 Introduction

In dental indirect restoration, *surface pretreatment*, also called surface conditioning, of dental materials is a vital preliminary step to enhance the adhesion between a luting resin composite and the restoration (resin composite materials are discussed comprehensively in Chapter 6). It is defined as one or a series of steps such as cleaning, removal of loose particles, and modification of a surface to which an adhesive is then applied for bonding.

The purpose of surface treatments is to:

(1) remove or prevent the formation of any weak surface layer on the substrate such as greases and dust particles
(2) maximize the molecular interaction at the interfacial layer between two different substrates, that is, increase the surface free energy
(3) optimize the adhesion at the interface such that sufficient adhesive strength can attain the required strength during the service
(4) create special surface microstructures for retention [1].

In this chapter, some basic principles of surface science, the theory of adhesion, surface characterization, and surface pretreatment methods currently used in dentistry are discussed. Some other new surface treatment methods with application of different techniques are also discussed. The underlying principles of these surface pretreatment methods will be further explained. Dentin bonding is discussed in Chapter 1.

11.2 Surface Science

11.2.1 Interface and Surface Tension

In a system, a surface or an *interface* (interface = a surface forming a common boundary between two regions) exists when there is a

change in the system properties with distance. Properties that show change at the interface are chemical composition, crystal structure, and density [2]. The interfacial particles differ in energy from the bulk of each phase because they are at the boundary region and interact with the particles of the other phases [1].

All molecules in the liquid state are held together with attractive intermolecular forces. The overall attractive force for each molecule in the bulk is zero. However, the resultant force of the molecules at the surface is not zero compared to the bulk liquid molecules. The force, *F*, required to increases the surface by a unit length, *L*, is called surface tension [3]:

$$\gamma = \frac{F}{\delta L} \tag{11.1}$$

More specifically, surface tension can also be defined as the energy required to increase the surface area by a unit of area. This energy is called the *surface free energy* of that liquid to resist the extension of a free surface per unit area [1].

Surface tension is strongly affected by temperature. The intermolecular forces of molecules are weakened when temperature increases. An equation for the relationship between the surface tension of the liquid and temperature is given by Guggenheim's equation:

$$\gamma = \gamma_0 \left(1 - \frac{T}{T_c}\right)^{\frac{11}{9}} \tag{11.2}$$

where γ_0 is the surface tension at absolute zero temperature and T_c is the critical temperature of the liquid [4].

11.2.2 Contact Angle

When liquids are in contact with solid surfaces, wetting occurs at the interface. The contact angle, α, is defined as an equilibrium of a liquid drop on a solid surface under an effect of three surface tensions, as shown in Fig. 11.1 [5].

At equilibrium, the surface tension at the solid–vapor interface is balanced by the sum of surface tensions at the solid-liquid and liquid-vapor interfaces. This relationship is given by Young's equation [6]:

$$\gamma_{sv} = \gamma_{sl} + \gamma_{lv}\cos\alpha \tag{11.3}$$

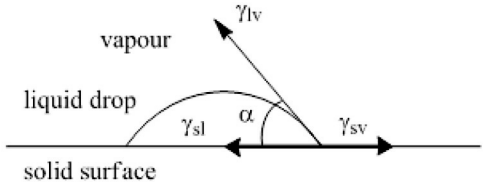

Figure 11.1 Contact angle of a liquid drop in contact with a solid surface.

The ability of a liquid to keep in contact with a solid surface is called wetting. The degree of wetting depends on the adhesive force between liquid and solid surfaces and the cohesive force within the liquid molecules. It can be determined by the equilibrium contact angle, γ. For, γ = 0, it is complete wetting of the liquid on the solid surface. For, 0 < γ < 90°, the wetting of the liquid on the solid surface is high. For 90° < γ < 180°, the wetting of the liquid on the solid surface is low [3].

11.2.3 Critical Surface Tension

In the early 1950s, Zisman and Fox studied the contact angle of various liquids on different solid surfaces and measured the surface tension of the liquids. From the plot of cos α against γ_{lv}, a straight line is always obtained for homologous liquids and a curved line is obtained for nonhomologous liquids, as shown in Fig. 11.2 [6].

From the plot of cos α against γ_{lv}, the extrapolation of cos α to 1 gives the value of the **critical surface tension** (γ_c) of the solid (Fig. 11.2). It varies with different solid surfaces. Therefore, from Eq. 11.3, when cos α = 1, $\gamma_c = \gamma_{sv} - \gamma_{sl}$. An explanation for this curvature of the Zisman plot is the interactions such as hydrogen bonding between the liquid and the solid surface.

NB: We have *two terms*, an interface (*see above*) and an interphase. An interphase is defined as a region between the unambiguous boundaries of two phases and characterized by distinct properties—actually it is a third phase [7].

11.3 Theories of Adhesion

Some theories are used to explain the mechanisms of adhesion [1, 7–9]. In most of the cases, adhesion between the adhesive and the

substrate surface is a combination of different mechanisms.

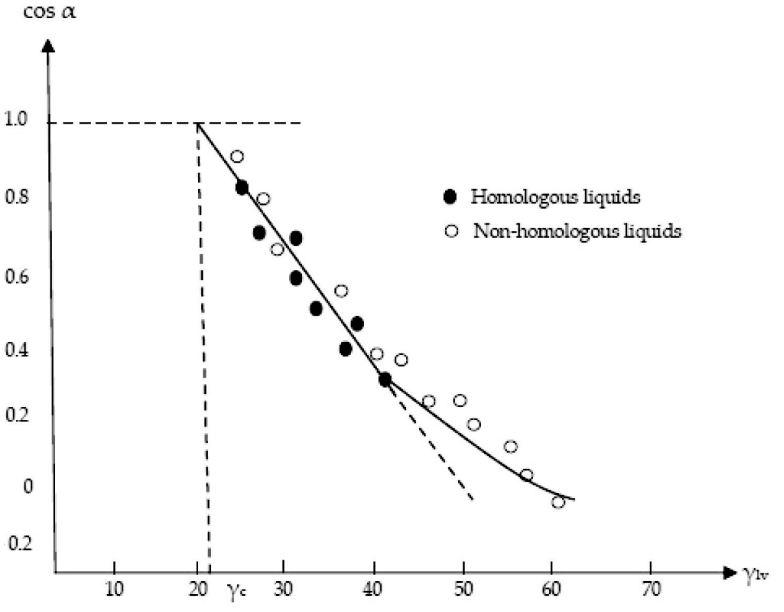

Figure 11.2 Zisman plot of contact angle and surface tension. Modified from Ref. [6].

Currently, there are six dominating theories of adhesion to describe the *nature of adhesion* [1, 7–9]:

1. Mechanical interlocking theory
2. Wetting theory
3. Diffusion theory
4. Weak boundary layer theory
5. Electrostatic theory
6. Chemical bonding theory

11.3.1 Mechanical Interlocking Theory

For an irregular and rough substrate surface, the adhesive penetrates the cavities and pores. After hardening, the adhesive locks mechanically (micromechanically) to the substrate surface, provided that good wetting is achieved with the rough surface. Otherwise, the

presence of voids at the interface lowers the adhesion. In general, adhesive bonds form better in a more irregular and porous surface than a smooth surface. The increase in surface roughness of a substrate enhances adhesion by mechanical interlocking.

11.3.2 Wetting Theory

This theory is based on the fact that adhesion occurs through molecular interaction and surface forces developed between the adhesive and the substrate surface. First, interfacial forces are developed between the adhesive and the substrate. Then, the process of continuous contact, that is, *wetting*, is established. To have good wetting of the adhesive on the substrate surface, the surface tension of the adhesive should be lower than the critical surface tension of the substrate surface.

11.3.3 Diffusion Theory

This theory applies to adhesion with long-chain-length polymer molecules. It involves the *interdiffusion* of polymer molecules across the interfacial layer. The interdiffusion occurs when the temperature is above the glass transition temperature such that the polymer chains are mobile. Adhesion by means of diffusion can be described by this relationship:

$$\delta = \sqrt{\frac{E_{\text{coh}}}{V}} \tag{11.4}$$

where δ is the solubility parameter, E_{coh} is the energy required to separate the molecules to infinite separation, and V is the molar volume. High adhesion is achieved when solubility parameters between the adhesive and the substrate are similar. This theory applies to adhesion of the same polymer or chemically very similarly polymers because of the same solubility or similar mutual solubility.

An example of diffusion bonding is solvent welding of thermoplastics. The solvent lowers the glass transition temperature of the polymer, and interdiffusion of polymer molecules across the interfacial layer takes place. The interdiffusion also increases at an elevated temperature, which leads to increased adhesive strength.

11.3.4 Weak Boundary Layer Theory

In this theory, weak boundary layers are present in the adhesive or the substrate surface and the adhesion is weakened. When failure takes place, breaking at the weak boundary layers occurs first. The presence of weak boundary layers at the interface is due to the substrate surface being exposed before adhesion and so being contaminated, for example, by dust or grease. Moreover, if the adhesive does not wet the substrate surface completely, air is trapped at the interface. This causes the decrease of adhesive strength. Therefore, surface pretreatments before bonding are necessary to remove surface contamination.

11.3.5 Electrostatic Theory

The basis of this theory is that *free charges* exist to a different extent in any material. There is an electrochemical potential difference between two different materials when in contact. A *charge transfer* takes place, and free-charge carriers move across the interfacial region. An *electric double layer* is formed. This theory is used to explain the polymer–metal adhesion where charge transfer occurs between polymer and metal and an electric double layer is formed in the interfacial layer.

11.3.6 Chemical Bonding Theory

This theory states that a chemical bond is formed between the adhesive and the substrate surface. Examples of chemical bonds are covalent, ionic, ion–dipole, dipole–dipole, and hydrogen bonds and van der Waals (aka London) forces. Covalent and ionic bonds are the strongest chemical bonds that can be formed between the adhesive and the substrate surface. Other weak chemical bonds include hydrogen bonds, dipole–dipole attraction, van der Waals forces. In a real situation, the adhesion between the adhesive and the substrate surface involves a *combination* of other adhesion mechanisms: mechanical interlocking (retention), wetting, or diffusion. This depends on the functional groups of the adhesive, the chemical composition, and the surface properties of the substrate surface.

11.4 Surface Characterization Techniques

The importance of surface characterization is that it can provide valuable information of surface topography, chemical composition, and the amount of trace impurities. Some common surface characterization techniques used in dental materials research are discussed concisely in this section [1, 10, 11].

11.4.1 Infrared Spectroscopy

All molecules are capable of vibrating above 0 K, that is, –273.15°C, and the more complicated a molecule is, the more the amount of different possible modes is. In general, the molecular vibration modes are stretching, rocking, wagging, and bending. The vibrational transitions of inorganic and organic molecules take place in the infrared (IR) region of light. The typical excitation energy, ΔE, is between 10^{-12} J and 10^{-19} J, and the corresponding frequency (f) is about the magnitude of 10^{13}–10^{14} Hz (1 Hz = 1 s^{-1}):

$$\Delta E = hf \tag{11.5}$$

where h is p (Planck's constant) = 6.626×10^{-34} Js.

In IR spectroscopy transitions are usually expressed in terms of their *wavenumbers,* $\bar{\nu}$, which are reciprocals of the wavelength, λ. The wavenumber region is typically in the scale of 3000–300 cm^{-1} for the majority of organic molecules. Given this, the principle of IR spectroscopy is based upon the absorption of particles in the IR region. Absorption occurs when the energy of IR is equal to the molecular vibration. The absorption frequency is specific for various functional groups of the molecule as the amount of energy absorbed is different. The relationship between absorbance and the sample concentration is given by Beer's law:

$$A = \varepsilon bc \tag{11.6}$$

where A is absorbance, ε is the extinction coefficient, b is the sample thickness, and c is the sample concentration (in a selected solvent).

Silane coupling agents are important hybrid inorganic-organic molecules that are applied to some dental materials. They absorb IR light in the mid-IR region, namely, between 4000 cm^{-1} and 600 cm^{-1} [12, 13].

For analysis of the sample surface, the attenuated total internal reflectance (ATIR) IR technique is used. In this technique, the sample is in close contact with both surfaces of a high refractive index crystal. A multiple internal reflectance of the IR beam on the sample surface is achieved. The IR spectrum gives information regarding the *chemical structure* of the sample surface.

Another very widely used technique that is based on interference is Fourier transform infrared (FTIR) spectroscopy. An IR beam is split by a beam splitter, which is positioned 45° to the incident beam. The two beams are reflected by a fixed and a movable mirror to recombine the resultant beam. The interference pattern is analyzed by a mathematical model called Fourier transform. It may be used effectively since the siloxane groups (…–Si–O–Si–…) yield very strong (and complex) absorbance signals [13].

The FTIR method produces fingerprint spectra for every compound that is prone to the method. The modern computational spectral subtraction capability of FTIR spectrometers enables selective monitoring of the structure of the coupling agent. The FTIR method is convenient, fast, and widely applied, for example, in silane research. The spectra can be mathematically processed to minimize noise and also to make the spectra comparable. The hydrolysis and condensation reactions usually can be followed with FTIR analysis [12–14].

11.4.2 Scanning Electron Microscopy

Scanning electron microscopy (SEM) is an important technique to analyze the material surface topography. The material surface is sputtered with a thin layer of gold metal so that the surface is conductive before SEM analysis. A beam of electrons is focused onto the sample surface. The interaction of the electron beam and the sample surface produces excited secondary electrons, back-scattered electrons, and X-ray photon energy. A detector collects the emitted particles to produce the image of the sample surface.

11.4.3 Energy Dispersive X-Ray Spectroscopy

Energy dispersive X-ray spectroscopy (EDX or EDS) is a very useful technique to identify and quantify the chemical composition of

the material surface structure. When electrons of the atoms on the sample surface are excited by a high-energy electron beam, an emission of photon energy with wavelengths of X-rays is detected. An energy-dispersive detector analyzes the corresponding elements. This gives the chemical composition of the sample surface.

11.4.4 Transmission Electron Microscopy

The basic principle of transmission electron microscopy (TEM) is the scattering or diffraction of electrons. This occurs upon interaction with the crystalline planes of the sample when a high voltage of focused electron beams is passed through a thin solid sample. A TEM system comprises three sections:

1. An illumination system
2. A sample stage
3. An imaging system

The illumination system has an electron gun and condenser lenses to focus the electrons onto the sample. The sample stage is used to position the sample in the TEM system. The imaging system has three or more lenses to produce a magnified image of the sample on the screen.

11.4.5 Atomic Force Microscopy

The first commercially available atomic force microscope (AFM) was introduced in 1989. The instrument is very useful as it can be applicable to both conductive and nonconductive material surfaces. The basic principle of atomic force microscopy is the measurement of intermolecular forces between the AFM tip and the sample surface. An AFM can be used to image and manipulate atoms and structures on a variety of material surfaces.

There are *three AFM operational modes* for surface topographic imaging, depending on the application: 1. *noncontact mode*, 2. *contact mode*, and 3. *tapping mode*. In noncontact mode, the cantilever tip is above the sample surface to detect the intermolecular forces between the tip and the sample. Surface topographic images are acquired by scanning the tip across the sample surface. In contact mode, the cantilever tip is in close contact with the sample surface.

However, the tip may damage the sample surface due to the lateral movement of the tip and the image is distorted. Thus, this mode is not suitable for biological and polymer surfaces. In tapping mode, the cantilever tip is oscillated at the resonant frequency. Then, the vibrating tip is moved close to the sample surface until it taps lightly the surface. There is energy loss of the tip due to contact with the surface. The change in the amplitude of vibration is measured to plot the surface topography of the sample [10, 13].

11.5 Surface Pretreatment Methods Used in Dental Laboratories

Some of the common surface pretreatment methods used in dental laboratories for *indirect restorations* are:

- hydrofluoric acid (HF) etching;
- grit blasting;
- pyrochemical silica coating;
- tribochemical silica coating.

These treatment methods can alter the surface properties of dental restorations, physically, chemically, or both ways, such that strong and durable bonding may be established between resin composites and these surface-treated materials. These surface treatment methods have been demonstrated to improve bonding and are well documented in the literature [7, 15–17].

11.5.1 Hydrofluoric Acid Etching

HF has wide applications in many areas such as glass etching and oxide removal from metals [18]. As a matter of fact, hydrogen fluoride is a colorless gas, and it fumes in humid air. It is very soluble in ethanol and water, and its *solution with water* is called *hydrofluoric acid*. It is strongly corrosive, and it is an excellent ionizing solvent and dissolves many inorganic and organic compounds [7, 19].

In dental laboratories, HF is used to etch porcelain veneers/crowns/onlays and, in principle, in intraoral repair the fractured porcelain restoration surface. However, *intraoral use should be*

avoided [17, 19]. When the porcelain veneer surface is treated with HF etching gel, the HF dissolves the glass matrix of the porcelain (no other mineral acids dissolve that effectively). After rinsing the acid-etched surface with water and air-drying, a microporous structure on the porcelain veneer surface is obtained. These porosities enhance micromechanical interlocking retention for durable bonding [7, 17, 20, 21].

Although HF is a *weak acid*, it is highly corrosive and toxic to humans. It penetrates skin tissues much more quickly than other inorganic acids due to its low ionization constant. This results in causing extensive internal tissue damage [18]. In a typical dental HF gel the actual HF content is around 4% to 10% and so can be used safely. Definitely the best advice is to follow the manufacturer's recommendation, or if no specific instruction is given, a good rule of thumb is to etch for between one and two minutes to obtain adequate roughness [17, 19].

11.5.2 Grit Blasting

In this methodology, the surface of materials is blasted usually with alumina powder of an average particle size of, for example, 50 μm under compressed air, for example, at a pressure of 380 kPa. Usually the blasting time is around 10–15 seconds at a perpendicular distance of about 10 mm from the nozzle to a surface area of ca. 1 cm^2 [15, 16]. Grit blasting increases the surface roughness of the materials that would thereby enhance the mechanical interlocking for bonding [7, 21–23]. Inevitably, a layer of alumina, Al_2O_3, particles may be embedded onto the substrate surfaces after grit blasting. The amount of alumina embedded and the degree of surface roughness depend on the grit size, nozzle distance to the surface, blasting time, and applied pressure [15, 24–26]. The presence of alumina particles, however, may deteriorate the ceramic–metal and resin–metal bonding [27, 28].

11.5.3 Pyrochemical Silica Coating

In this method, a silica (SiO_2) layer is deposited onto the substrate surface by means of pyrochemical processes. From the historical point of view, there are several pyrochemical silica-coating sys-

tems (aka thermal silica-coating systems) that have been utilized in dental laboratories: Silicoater™ Classical, Silicoater MD and Siloc™ (Heraeus-Kulzer, Wehrheim, Germany), and PyrosilPen™ device (SurA Instruments, Jena, Germany) [15–17, 29]. Tetraethoxysilane (TEOS) (aka tetraethylsilicate) solution is injected into a flame and burned with oxygen in the presence of fuel gas butane. The intermediates (–SiO_x–C) formed reach the substrate surface and deposit onto the surface. When the silica-coated substrate surface is cooled to room temperature, a silane coupling agent is applied onto the coated surface and is followed by cementation [30]. This per se chemically interesting surface-conditioning method is not anymore used in dental technology [16].

11.5.4 Tribochemical Silica Coating

A tribochemical Rocatec™ System (3M ESPE, Seefeld, Germany) was introduced in 1989, and it is continuously used for surface treatment of various dental materials such as metals, metal alloys, and ceramics in dental laboratories [15, 28, 31–34]. The silica-coating of the substrate surface can be carried out using Rocatec™ Soft (30 μm silica-coated alumina powder) or Rocatec™ Plus (110 μm silica-coated alumina powder) with defined operational parameters, such as under a compressed air pressure of 280 kPa for 30 s/cm^2 at a perpendicular distance of around 10 mm [31]. Thus, a silica-coated layer is formed on the surface and further treated by silanization. A durable siloxane linkage is formed after drying. The silica-coated and silanized substrate is cemented with a resin composite to complete the restoration [13]. The Cojet™ system (3M ESPE, Seefeld, Germany) is an in-office silica-coating system that employs 30 μm silica-coated alumina powder for sandblasting the substrate surface. It may be used for intraoral repair of fractured metal ceramic (porcelain fused to metal [PFM]), all-ceramic, resin composites, and even amalgam restorations [15, 17, 35].

11.5.5 Silanization

When silanes promote adhesion between dissimilar materials, silanes react to form a siloxane film (sometimes called a silane film) between these materials. It is usually expected that at least one

of the surfaces should be *siliceous* for its chemistry, that is, silica, silicates, or glass should be available on the substrate surface. The silane solutions must be optimized (e.g., silane concentration, solvent consistency, pH, hydrolysis/activation time, etc.) to avoid silane polymerization before the deposition [15, 36].

Silanization (silanation) means application of a silane coupling agent. When deposited on an inorganic surface, silanol oligomers react with each other, forming branched hydrophobic siloxane bonds, –Si–O–Si–. With a surface of an inorganic matrix (e.g., silica and metal oxides containing hydroxyl, –OH, groups), they form metallosiloxane bonds of the type –Si–O–M– (where M = metal). In dentistry and dental technology, silane coupling agents are used to promote adhesion between a luting resin composite cement and a silica-coated base metal and noble metal alloys, Ti, etc. [15, 17]. As a coupling agent, silanes have two different functional groups that react to link them together.

There is a plethora of commercially available dental silane products, and they differ from each other for their formulations and properties [37]. Silane coupling agents for dental use are usually supplied as ca. 1–2 vol% in their prehydrolyzed form in a 90–95% ethanol/water solvent. Ethanol (or some other alcohols) is necessary to use to dissolve *hydrophobic* silane monomers. Silanes have to be *activated* by hydrolysis before application. When activated silane is deposited onto the inorganic substrate surface, a chemical reaction occurs, which allows bonds to be formed between activated silane and the substrate (see also Chapter 3).

In general, various silane coupling agents find numerous applications in *coatings* and adhesion promoters in steel, aluminum, and brass pretreatments (see Fig. 11.3).

Also in these applications, silanes are not supposed to react with the metal substrate in depth but to wet it and deposit as *thin films.* Stable condensation products of silanization, *silane coatings* (also called *polysiloxane coatings*), may alter the wetting and adhesion characteristics of a silanized substrate surface [36].

There are also some silanes, such as methyltrichlorosilane and trimethylchlorosilane (including their alkoxy derivatives), that are employed to render materials (e.g., masonry, laboratory glassware) water repellent. In these cases, silanes change the wettability characteristics of a substrate surface. In general, it can be stated that

low surface energy results in low adhesion and high surface energy in high adhesion [7, 38].

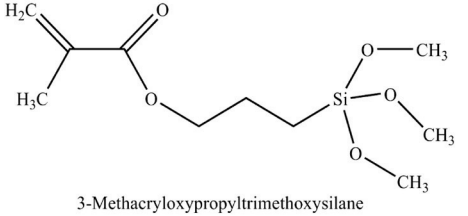

3-Methacryloxypropyltrimethoxysilane

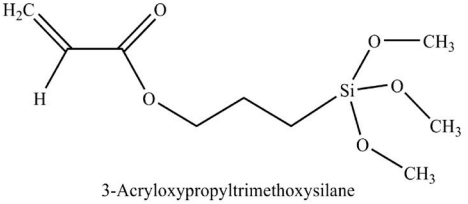

3-Acryloxypropyltrimethoxysilane

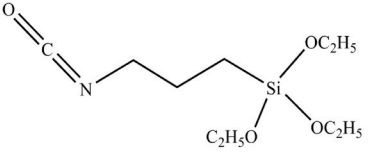

3-Isocyanatopropyltriethoxysilane

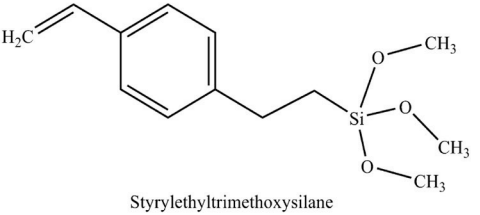

Styrylethyltrimethoxysilane

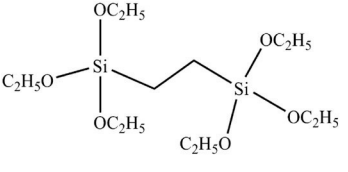

Bis-1,2-(triethoxysilyl) ethane

Figure 11.3 Some silane coupling agents. BTSE is a so-called cross-linking silane. *Abbreviation*: BTSE, bis-1,2-(triethoxysilyl) ethane.

Silanes are characterized by direct silicon–carbon (Si–C) bonds, which are calculated to be as strong as, and in some cases even stronger than, the analogous C–C bonds. Chemically, silanes are hybrid inorganic-organic compounds that are synthesized by reduction of silica (SiO_2). Silica is abundant on the earth. Silica reacts with carbon at high temperatures to produce silicon (Eq. 11.7). In the case of a *trialkoxysilane* (Fig 11.3.), those with methoxy groups, $-OCH_3$, may be effective without catalysis. The degree of silane polymerization is determined by the amount of water that is available and also by the *organofunctional* moiety [36].

The silicon (Si) produced from silica reacts with hydrogen chloride (HCl) in the presence of a Cu catalyst to produce trichlorosilane. Coupling of trichlorosilane with haloalkene followed by alcoholysis gives the alkoxysilane [36], as presented below:

$$SiO_2 + C \rightarrow Si + CO_2 \quad (11.7)$$

$$Si + 3\ HCl \rightarrow HSiCl_3 + H_2 \quad (11.8)$$

$$ClH_2RCH{=}CH_2 + HSiCl_3 \rightarrow ClH_2RCH_2CH_2SiCl_3 \quad (11.9)$$

$$ClH_2RCH_2CH_2SiCl_3 + 3\ R'OH \rightarrow ClH_2RCH_2CH_2Si(OR')_3 + 3\ HCl \quad (11.10)$$

When talking about *stability* it is noteworthy that elements other than C or Si bonded directly to Si generally undergo somewhat rapid hydrolysis. Water necessary for hydrolysis can originate from various sources: it may be present originally on the surface, it may be added, or it may come from the atmosphere. However, most bonds to Si oxidize slowly, and protecting silanes from moisture is more important than protecting them from O_2.

3-Methacryloxypropyltrimethoxysilane (MPS) is commonly used in clinical commercial silane products. This silane monomer is prehydrolyzed in an acidified solvent mixture of ethanol and water before its use on a restoration surface [15, 36]. Several factors determine the silane reactivity, for example, the drying time on a substrate surface prior to cementation, in this case [39].

In dental laboratories, the standard procedure of the surface treatment of some indirect dental restorative materials such as metal alloys and, for example, Ti [12–15], zirconia [40, 41], or porcelain [17, 26, 42], is first sandblasting or HF etching, rinsing, and drying. Then, a solution of the silane coupling agent is applied onto the treated surface with one thin coating using a clean fine bush. The silane is

then allowed to dry and react: in chair-side clinical applications the curing is expected to happen at room temperature in a few minutes. On the other hand, when dental restorations are made in the dental laboratory, prolonged curing times and higher temperatures can be used [16]. The step of applying a silane coating is called *silanization* (or silanation). Cementation should then follow immediately after silanization.

> Silane coupling agents should be activated because the condensation between hydrolyzed silane, that is, silanols (–SiOH), and surface hydroxyl groups on the substrate surface is fast at room temperature through hydrogen bond formation.
>
> The condensation between unhydrolyzed silane monomers and surface hydroxyl groups is slow at a reduced temperature.

11.6 Current Studies on Other Surface Pretreatment Methods

Many laboratory studies show bond degradation over time under artificial aging with the conventional surface treatments discussed above [41, 43]. Moreover, surface treatment by grit blasting and tribochemical silica-coating may introduce *surface flaws* that will affect long-term performance of, for example, ceramics [44]. As a result, other surface pretreatment methods are developed to increase bond durability under artificial aging. In these methods, substrate surfaces are modified *physically* or *chemically*. All methods have different mechanisms of treatment to activate surfaces, and these will be discussed in section 11.7.

11.6.1 Chemical Treatment

At room temperature, the surfaces of metal oxides, metals, and metal alloys are partially *hydroxylated*. For some metals, such as Cr, Al, and Ti, and some metal alloys, a passive oxide layer is formed. The presence of hydroxyl groups (–OH) will favor the interaction with silane coupling agents by forming hydrogen bonds first. This is followed by condensation to form a linkage and finally covalent bonds. The extent of condensation depends on the surface

hydroxyl group density and the nature of substrates. The degree of hydroxylation is different between ceramic and metal surfaces. The density of hydroxyl groups can be increased by treatment with acids. In this method, the substrate surface is first sandblasted, rinsed, and dried. Then, the substrate surface is immersed in a strong acid solution such as hydrochloric acid. After the hydroxylation process, the number of hydroxyl groups is increased, which depends on the types of acids and the processing temperature [45, 46].

11.6.2 Selective Infiltration Etching

The selective infiltration etching (SIE) method is a specifically developed novel pretreatment method for zirconia-based surface treatment to enhance resin zirconia bonding. A special glass powder conditioning agent containing SiO_2, Al_2O_3, Na_2O, TiO_2, and K_2O is mixed with water to form a paste. The zirconia surface is coated with a thin layer of this paste and cured at high temperature. Next, the coated zirconia is cooled to room temperature. This glass-conditioning agent is etched away with dilute HCl and then rinsed with deionized water. This creates a highly reactive and retentive surface. After silanization (or without it) a resin cement is used for bonding the zirconia surface [47–49]. The SIE method is also covered in Chapter 14.

11.6.3 Laser Treatments

Three types of lasers are used for surface treatment of different dental materials:

(1) Erbium: yttrium-aluminum-garnet (Er:YAG)
(2) Neodymium: yttrium-aluminum-garnet (Nd:YAG)
(3) Carbon dioxide (CO_2)

Different types of lasers are used for different dental materials and *dental tissues* as the emission wavelength of absorption varies with different materials. During laser treatment, the substrate surface is irradiated with a laser beam. This produces surface irregularities that increase the mechanical interlocking, retention [50]. The main drawback of this method is that too high a power setting of laser irradiation would create surface cracks [51]. Therefore, it is very

important that appropriate laser operating parameters be used for different materials to minimize crack formation.

11.6.4 Nanostructured Alumina Coating

In this specific coating method, a dilute suspension of aluminum nitride (AlN) in deionized water is prepared and heated to 75°C. Then, zirconia specimens are immersed in the suspension. Aluminum nitride undergoes hydrolysis to form *boehmite* (γ-AlOOH), which deposits onto the zirconia surface. A nanostructured alumina coating is thereby formed on the zirconia surface. The coated zirconia surfaces are air-dried in an oven and thermally treated in a furnace in air at 900°C. During the heat treatment, the boehmite undergoes phase transformation through two stages to δ-alumina [52]. A large microretentive area is created on the zirconia surface, which increases the micromechanical interlocking (retention) for resin bonding.

11.6.5 Internal Porcelain Coating

In this technique, zirconia surfaces are coated with silica-based ceramics by *fusion*. The surfaces are first polished and then air-abraded with alumina powder to increase surface roughness. Then, the treated zirconia surface is coated with fusing porcelain, which is prepared by stirring the porcelain powder with distilled water. The porcelain powder is mainly composed of SiO_2 and with a small amount of Al_2O_3, Na_2O, and K_2O. The thickness of the porcelain layer is about a hundred micrometers. The coated porcelain layer is fired at temperatures higher than 800°C in vacuum for one minute. After the firing, the surface is cleaned, air-abraded, and then followed by silanization. Thus, a highly retentive and silica-based coated zirconia surface is obtained for resin bonding [53].

11.6.6 Chemical Vapor Deposition

The zirconia surface can be pretreated with *oxygen plasma* to remove organic contaminants and increase the degree of surface hydroxylation. In the molecular vapor deposition system, a pretreated

zirconia specimen is fixed in position in a vacuum chamber. A mixture of tetrachlorosilane ($SiCl_4$) and water is heated. The vapor mixture is passed onto the zirconia surface. The silane undergoes hydrolysis to form silanols (–SiOH), which react with the surface hydroxyl groups of zirconia. A silica seed layer (Si_xO_y) is deposited on the zirconia surface and a by-product HCl gas produced. The layer thickness is controlled by the deposition time [54]. The presence of the Si_xO_y seed layer is reported to form durable siloxane bonds with a silane coupling agent, and this improves adhesion to zirconia.

11.6.7 Plasma Fluorination

This is another advanced technique in which the zirconia surface is chemically modified to be more reactive by means of plasma treatment. In an inductively coupled *plasma reactor*, zirconia samples are exposed to a continuous flow of sulfur hexafluoride (SF_6) gas at a constant pressure for a certain period of time. Plasma is generated when an electric current is applied. The sulfur hexafluoride forms a highly reactive species and reacts with zirconia. After plasma fluorination, an oxyfluoride surface layer is formed. When a silane coupling agent is applied onto this active layer, a reaction occurs such that surface silanation is achieved. However, the mechanism of bond formation between silane and the oxyfluoride layer remains still unknown [55].

11.7 Mechanisms of Surface Pretreatment Methods

In this section, the mechanisms of each surface pretreatment method introduced above are discussed to help the readers to understand the underlying principles. Each method has a different mechanism to achieve surface modification such that strong adhesion is attained. In principle, a surface is more reactive after treatment by (a) increasing the surface roughness for mechanical interlocking or (b) increasing the surface chemical reactivity for chemical bonding formation or both [7].

11.7.1 Hydrofluoric Acid Etching

There is a general agreement that HF etching followed by silanization generates higher bond strengths than either treatment alone [17]. Application of a silane coupling agent is a procedure called *silanization*. It is understood to create hydrogen and covalent bonds between the luting resin cement and the ceramic substrate, while etching per se provides micromechanical interlocking [15–17, 26]. When HF is applied on the surface of a porcelain veneer, a series of reactions (Eqs. 11.11–11.13) occur:

$$SiO_2\,(s) + HF\,(aq) \rightarrow SiF_4\,(ad) + H_2O\,(l) \quad (11.11)$$

$$SiF_4\,(ad) + 2F^-\,(aq) \rightarrow SiF_6^{2-}\,(aq) \quad (11.12)$$

$$SiF_4\,(ad) + 2HF_2^-\,(aq) \rightarrow HSiF_6^-\,(aq) \quad (11.13)$$

where HF_2^- is formed from HF and dissociated F^- [56]. The SiF_4 formed is adsorbed (= ad) on the surface and then further reacts with F^-. The etching rate depends on the surface structure, HF concentration, and which types of dental porcelain are used [57]. The etching of the *amorphous state* is *faster* than the crystalline state as the former is in a higher energy state than the latter. In clinical practice, the HF etching of a porcelain veneer is to remove the amorphous silica structure in order to increase the surface roughness and thus the micromechanical interlocking retention [42, 58].

Some other reagents, such as ammonium hydrogen difluoride (NH_4HF_2), may also etch porcelain [17]. It was suggested that HF etching might be substituted by grit blasting using alumina powder, followed by so-called modified silanization, that is, an idea to utilize hot air to cure the siloxane film [59].

11.7.2 Pyrochemical Silica Coating

A *pyrochemical reaction* is defined as the process of chemical reactions at high temperatures. For pyrochemical silica coating, the silane, in this case tetraethoxysilane (i.e., tetraethylsilicate), $Si(OCH_2CH_3)_4$, is injected into the flame. The fuel gas is butane and is burned in atmospheric oxygen, that is, a combustion reaction. The

reaction mechanism is a series of free-radical reactions. The initial step is hydrogen abstraction of tetraethoxysilane by oxygen to form reactive free radicals [60]. Then, a series of free-radical reactions proceed, and e.g., SiO_x-C species are formed. These reactive species deposit and condense onto the substrate surface to form a glass-like layer [29].

11.7.3 Grit Blasting and Tribochemical Silica-Coating

The principles of grit blasting and sandblasting are basically the same [15, 34]. Sand (actually, we should use the word *powder*) particles are projected under compressed air from a nozzle onto the substrate surface. The impact of the particles on the substrate surface causes *kinetic energy* transfer. The energy is transformed into heat energy. The energy absorbed by the substrate surface results in melting. The powder particles are partially incorporated into the substrate surface [61]. A suggested mechanism for grit blasting and tribochemical silica coating is shown in Fig. 11.4.

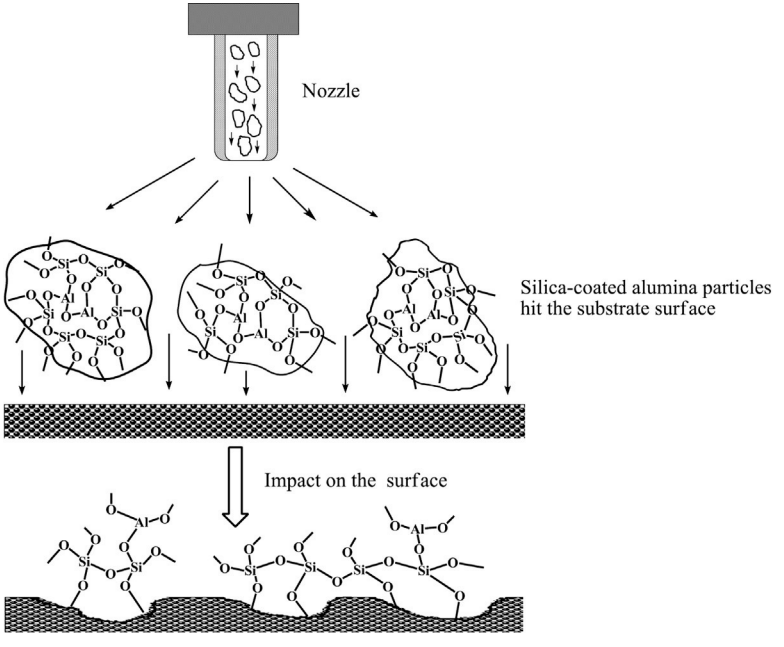

Figure 11.4 A schematic diagram of sandblasting on a substrate surface.

11.7.4 Silanization

A silane coupling agent (silane) contains two functional groups, with the general formula of Z-$(CH_2)_k$-Si-$(OR')_3$: Z is an organofunctional group, –$(CH_2)_k$– is a linker (connector) segment, and –OR' is a hydrolyzable group. Silanes can react with the resin composite and inorganic dental restorative materials to join together. Silanes have to be activated such that free silanol groups are produced that react with the hydroxyl groups on inorganic substrate surfaces [15, 36].

When the silanes undergo hydrolysis, the alkoxyl group is protonated at pH 3–5. A bimolecular nucleophilic substitution takes place at the central silicon atom. A backside attack of a nucleophile, water, to the silicon atom, an electrophile, gives a pentavalent transition state. A new covalent bond is formed, and a covalent bond is cleaved between the silicon and the leaving group [36]. The silane hydrolysis mechanism is shown in Fig. 11.5.

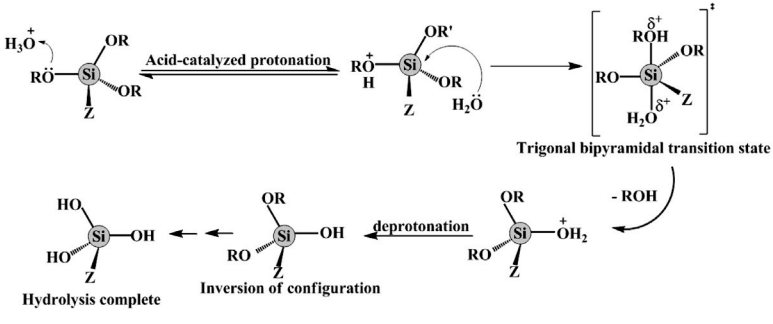

Figure 11.5 A reaction mechanism of silane hydrolysis.

The rate of silane hydrolysis is affected by *steric and inductive effects* of alkoxy groups. The steric effect is the major factor that affects the reaction rate [62]. If the alkoxy group (–OR') is large in size, it is more difficult for the nucleophile (water) to approach the silicon central atom. The activation energy of the transition state formation is increased, and the hydrolysis rate is thus decreased [7, 36].

In use, silane monomers are usually strongly diluted in a solvent that is usually ethanol (plus some water). The final silane concentration may be somewhere in the range of 0.1–5 vol% for coupling purposes. When the silane coupling agent is applied

onto a silica-coated substrate surface, the silanol groups (–SiOH) interact with the surface hydroxyl groups of the substrate by forming hydrogen bonds. This is followed by condensation to form a siloxane (…–Si–O–Si–…) linkage. The silane monomers react with other silane monomers through the silanol groups to form a 3D polysiloxane network. The degree of polymerization of silane monomers is controlled e.g., by the amount of water available and also the organofunctional moiety [15, 36]. After the process of silanization of the restoration, a resin composite cement is applied onto the silanized substrate surface, fitted on the prepared tooth, and finally light-cured.

The actual thickness of a silane coating (polysiloxane layer) is determined by several factors, such as silane concentration, drying (reaction) time, solvent used, pH, deposition technique, and temperature [36]. In practice, silane coatings are extremely thin 3D multilayer systems.

Figure 11.6 demonstrates how *initially hydrophobic* silanes first turn *hydrophilic* during hydrolysis—and they condense to form dimers, oligomers, etc. Next, silanes deposit onto the surface, and after curing (setting), they form a *hydrophobic* siloxane layer [36].

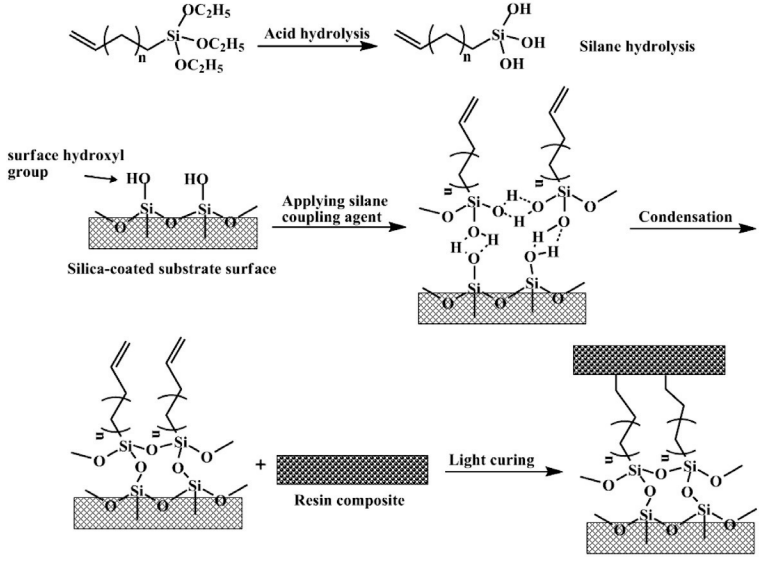

Figure 11.6 The processes of silane hydrolysis, silanization, and setting reaction with a resin composite luting cement.

Interestingly, *silane blends*, that is, combinations of functional silanes and *cross-linker silanes* (e.g., BTSE) in a solvent (see Fig. 11.3) may have a significant impact on bonding to a substrate, increasing mechanical strength and hydrolytic stability in many coatings and composite systems. Some silane blends containing BTSE can provide excellent protection for corrosion in applications where steel sheets are silanized and then finally painted. It is noteworthy that cross-linker silanes are strongly diluted and blended at the ratio of 1:10–1:5 to an organofunctional silane [38].

A so-called *novel silane system* concept for resin-bonding promotion in dental applications was introduced by Matinlinna et al. [63]. Laboratory studies suggest a significant growth in shear bond strength for resin Ti bonding [63–67], resin porcelain bonding [68], and resin zirconia bonding [69, 70] when the control has been a commercially available dental silane [37]. To demonstrate a novel silane system in dentistry, we may have a look at silica-coated and silanized zirconia substrates (Fig. 11.7).

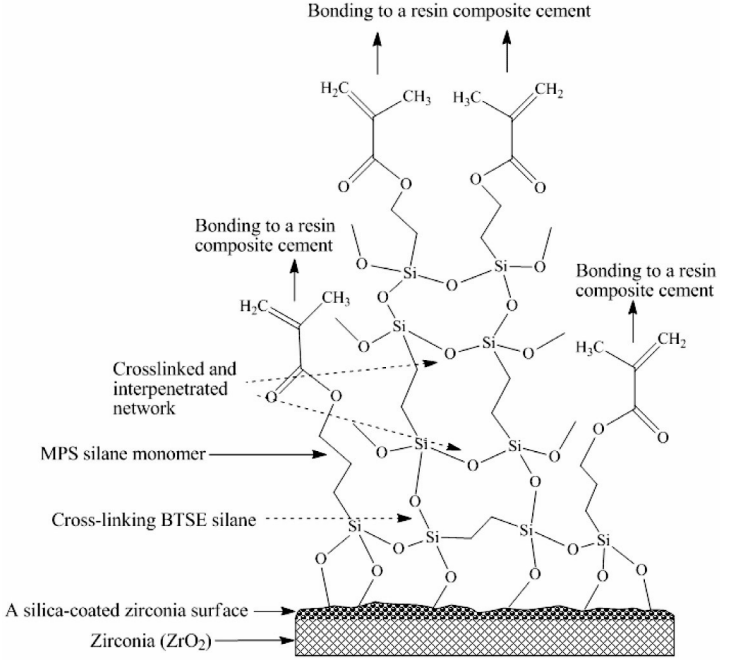

Figure 11.7 An illustration of a novel silane system applied in resin zirconia bonding.

A functional silane, in this case MPS, is blended with BTSE, and they form a durable, hydrolytically stable 3D siloxane film to connect the silica-coated zirconia surface to a resin composite luting cement. This novel silane system approach in resin bonding might have clinical success (durable cementation) when meticulously optimized.

In addition to a novel silane system, the use of some other functional silane monomers on bonding resin to silica-coated substrates may be a key for durable bonding [71–75].

When speaking about silane-aided bonding in conjunction with resin composites, we may notice the role and importance of chemistry. The resin composites used in dentistry are predominantly methacrylate monomers such as 2,2-bis[4(2-hydroxy-3-methacryloxypropyloxy)-phenyl] propane (bis-GMA) and urethane dimethacrylate (UDMA or UEDMA) that contain the polymerizable >C=C< functional groups.

The *initiators* in the resin composite decompose by blue visible light to form energetic free-radical species. These reactive species react with the >C=C< groups in resin monomers. This process generates other reactive free radicals. These free radicals react with resin monomers to form new C–C single bonds. After the light-curing process, the resin composite and the inorganic substrate are connected by the silane coupling agents [36, 75]. A suggested mechanism of the whole process is shown above in Fig. 11.6. More about resin composites in dentistry is found in Chapter 6.

11.7.5 Chemical Treatments

On a metal oxide surface, the outermost surface layer is composed of *oxide ions.* These are very reactive sites for surface chemical reactions. When the oxide surface is treated with an *acid*, the dangling oxygen atoms form intermolecular hydrogen bonds with the acid. After rinsing with deionized water, surface hydroxyl groups are formed after hydroxylation [45]. A suggested mechanism of hydroxylation of metal oxide by acid treatment is shown in Fig. 11.8.

The degree of hydroxylation depends on the acid concentration and what type of acid is used and on the time and temperature of the treatment [76]. For metals/metal alloys, a layer of passive oxide layer is formed at ambient temperature. The presence of this oxide layer favors the formation of hydroxyl groups after acid treatment.

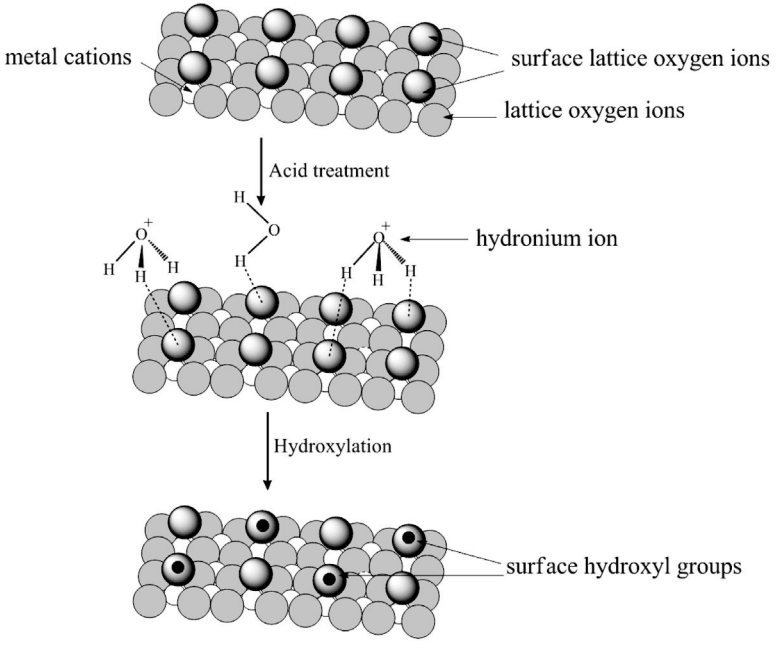

Figure 11.8 The process of hydroxylation on a metal oxide surface by acid treatment. Modified from Ref. [45].

11.7.6 Selective Infiltration Etching

One of the most interesting new openings in zirconia surface pretreatments is SIE (see also Chapter 14). The basics for this treatment are heat-induced structural maturation and grain boundary diffusion to transform the relatively smooth nonretentive surface of yttria-stabilized zirconia into a highly retentive surface [47, 77]. As described above, when a zirconia surface is coated with a special glass-conditioning agent and heated above its glass transition temperature, the molten glass particles infiltrate into the surface grain boundaries and induce surface tension, which results in movements of the surface grains. This creates an intergrain porosity. Finally, the glass infiltration agent is removed by acid-etching treatment with HF and rinsing with water. The zirconia surface is thereby transformed into a highly reactive and retentive surface [49].

11.7.7 Laser Treatments

The acronym "laser" stands for ***l****ight* ***a****mplification by* ***s****timulated* ***e****mission of* ***r****adiation*. It is a process of optical amplification from stimulated emission of photons absorbed by atoms or molecules [78]. When a laser beam hits a substrate surface, there are *four ways* of interaction.

The first one is *reflection*: the beam bends back from the surface and causes no effect. The second one is *scattering*, in which the beam is deflected in different directions. The third one is *transmission*, during which the beam passes through the surface without any interaction. The fourth one is *absorption*: the laser energy is absorbed when the laser beam interacts with the material [79]. Absorption of the laser energy leads to conversion into heat energy. This causes melting of the material and change of surface morphology. However, when the laser intensity increases, more heat is generated, and thus microcracks are formed (Fig. 11.9). One approach to minimize microcrack formation is to use a lower laser power setting [80].

11.7.8 Nanostructured Alumina Coating

Aluminum nitride can undergo hydrolysis to form *boehmite* and ammonia (Eqs. 11.14 and 11.15). At the initial stage of hydrolysis of aluminum nitride, there is an increase in the concentration of aqueous aluminum (poly)cations in the suspension. This leads to supersaturation that allows the *heterogeneous nucleation* of lamellar boehmite on the substrate surface immersed in the suspension. After the coating process, the coated surface is heat-treated. The boehmite-coated layer then undergoes a series of phase transformations accordingly [81]:

$$AlN + H_2O \longrightarrow \gamma\text{-}AlOOH + NH_3 \quad (11.14)$$

$$\gamma\text{-}AlOOH \xrightarrow{300\text{-}500^\circ C} \gamma\text{-}Al_2O_3 \xrightarrow{700\text{-}800^\circ C} \delta\text{-}Al_2O_3 \xrightarrow{900\text{-}1100^\circ C} \theta\text{-}Al_2O_3 \xrightarrow{1000\text{-}1100^\circ C} \alpha\text{-}Al_2O_3 \quad (11.15)$$

The alumina-coated layer is heat-treated up to 900°C. The reason for this heat treatment is that during phase transformation from γ-AlOOH to α-Al_2O_3, the surface area of the alumina particles increases from γ-AlOOH to a maximum at δ-Al_2O_3 and then decreases

to a minimum at α-Al_2O_3 [82]. A large surface area is obtained after heat treatment to 900°C. This increases the micromechanical interlocking (retention) for resin bonding.

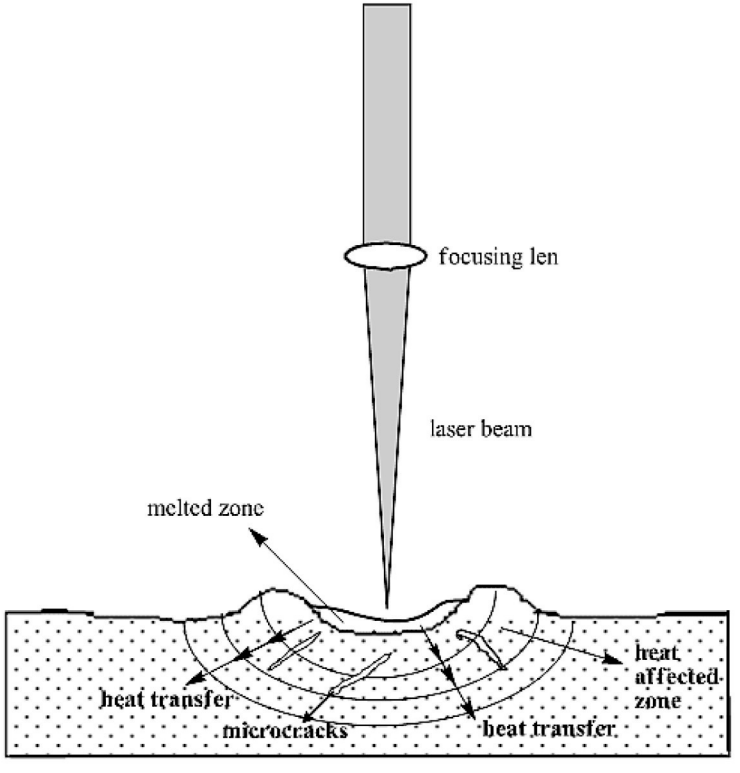

Figure 11.9 A schematic diagram of the effect of laser treatment. Modified from Ref. [79].

11.7.9 Internal Porcelain Coating

The mechanism of *internal coating* is similar to SIE: a zirconia surface is coated with a fusing porcelain powder, a ceramic veneering material that is suspended in distilled water. During the firing of the porcelain coating on zirconia at high temperature, the porcelain particles infiltrate into the grain boundaries of the zirconia surface layer. A thin layer of porcelain is finally fused on the zirconia surface. The composition of the ceramic veneering material is similar to

the glass-conditioning agent used in the SIE technique [47, 49] (see above).

The main difference between these two techniques is that a silica-based coating is formed for the internal porcelain coating, whereas a highly retentive surface is created after removal (etching) of the glass infiltration agent by HF [83].

11.7.10 Chemical Vapor Deposition

Chemical vapor deposition (CVD) is defined as a process in which a thin film is deposited on a substrate by means of chemical reactions of the *gaseous reactants at a high temperature* near or on a heated substrate [84]. CVD is a chemical process used to produce high-performance and high-purity solid materials. The process often finds applications in the semiconductor industry to produce specific thin films.

The process of CVD involves several steps [85]:

1. Flow of gaseous reactants into the system
2. Diffusion of gaseous reactants through the boundary layer to the substrate
3. Adsorption of gases onto the substrate surface
4. Chemical reactions of the adsorbed species with the substrate at the surface layer
5. Desorption of by-products from the substrate surface
6. Diffusion of gaseous by-products through the boundary layer to the bulk gas
7. Exit of gases from the system

The actual process is shown below in Fig. 11.10.

11.7.11 Plasma Fluorination

The main advantage of this method over CVD is that the reaction activated by plasma could be processed at a lower deposition temperature. Plasma is an active species, which is composed of highly excited ionic and free-radical species. It is produced when reactant gases are excited into energetic states by microwave, radio frequency, or electrons from a hot filament discharge [86]. When atoms or molecules gain enough energy, ionization occurs.

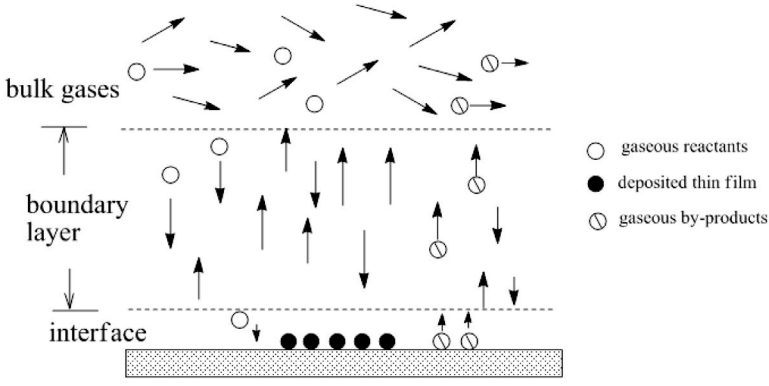

Figure 11.10 A schematic diagram of the CVD process. Modified from Ref. [85].

A mechanism suggested by Hodak et al. [87] for the plasma fluorination of silk fabrics, using sulfur hexafluoride (SF_6) as the source gas, is:

$$SF_6 \rightarrow SF_5\cdot + F \quad (11.16)$$

$$SF_5\cdot \rightarrow SF_4 + F \quad (11.17)$$

$$SF_5\cdot + SF_6 \rightarrow S_2F_{10} + F \quad (11.18)$$

$$S_2F_{10} \rightarrow 2\ SF_5\cdot \quad (11.19)$$

The fluorine atoms generated react with the fabric surface to form a fluorinated layer. The $SF_5\cdot$ radicals generated would either decompose into SF_4 and F or combine with SF_6 to form S_2F_{10} and F, since no sulfur is detected on the modified silk fabric surface from X-ray photoelectron spectroscopy (XPS) analysis [87]. This reaction mechanism can be used to explain the fluorination of zirconia surfaces in resin zirconia bonding reported by Piascik et al. [55].

These surface treatment methods, with different approaches, modify the surface properties of some dental materials (e.g., zirconia) in order to enhance adhesion. However, some of them employ toxic precursors such as sulfur hexafluoride and other use expensive instruments such as a molecular vapor deposition system. Further laboratory studies of these treatment methods are necessary. These are important factors to consider before these methods are fully implemented in dental practice.

11.8 Conclusions

The surface pretreatment methods of dental indirect restorative materials are discussed thoroughly in this chapter. These methods are currently in use, either at dental laboratories or under intensive development in research laboratories. This research takes place in vitro, in vivo, and in silico. In the future, validation of these new methods in clinical practice will be carried out. On the other hand, other new surface treatment methods will obviously emerge and be investigated globally [88].

We may conclude that an *ideal surface treatment method* should:

1. be nondestructive to substrate surfaces;
2. provide strong and durable bonding;
3. be sustainable in the oral environment for long-term performance; and
4. be convenient to use for dental technicians and/or dentists.

References

1. Ebnesajjad, S., Ebnesajjad, C. F. (2006) *Surface Treatment of Materials for Adhesion Bonding*, William Andrew, USA.
2. Hudson, J. B. (1998) *Surface Science: An Introduction*, 3, John Wiley & Sons, USA.
3. Barnes, G. T., Gentle, I. R. (2005) *Interfacial Science: An Introduction*, Oxford University Press, UK.
4. Guggenheim, E. A. (1945) The principle of corresponding states, *J. Chem. Phys.*, **13**, 253–261.
5. Frederick, M. F. (1964) *Contact Angle, Wettability and Adhesion*, 1–51, American Chemical Society, USA.
6. Johnson, R. E. (1959) Conflicts between Gibbsian thermodynamics and recent treatments of interfacial energies in solid-liquid–vapour systems, *J. Phys. Chem.*, **65**, 1655–1658.
7. Darvell, B. W. (2009) *Materials Science for Dentistry*, Woodhead Publishing, UK.
8. Comyn, J. (1997) *Adhesion Science*, Royal Society of Chemistry, UK.
9. M da Silva, L. F., Öchsner, A., Adams, R. D. (2011) *Handbook of Adhesion Technology*, Springer-Verlag, Germany.

10. Jalili, N., Laxminarayana, K. (2004) A review of atomic force microscopy imaging systems: application to molecular metrology and biological sciences, *Mechatronics*, **14**, 907–945.
11. Egerton, R. F. (2005) *Physical Principles of Electron Microscopy: An Introduction to TEM, SEM, and AEM*, Springer Science+Business Media, USA.
12. Matinlinna, J. P., Laajalehto, K., Laiho, T., Kangasniemi, I., Lassila, L. V. J., Vallittu, P. K. (2004) Surface analysis of Co-Cr-Mo-alloy and Ti substrates silanated with some trialkoxysilanes and silane mixtures, *Surf. Interface Anal.,* **36**, 246–253.
13. Matinlinna, J. P., Areva, S. J., Lassila, L. V. J., Vallittu, P. K. (2004) Characterization of siloxane films on titanium substrates derived from three aminosilanes, *Surf. Interface Anal.,* **36**, 1314–1322.
14. Sheehan, D. (2009) *Physical Biochemistry: Principles and Applications*, John Wiely & Sons, UK.
15. Lung, C. Y. K., Matinlinna, J. P. (2012) Aspects of silane coupling agents and surface conditioning in dentistry: an overview, *Dent. Mater.*, **28**, 467–477.
16. Matinlinna, J. P., Vallittu, P. K. (2007) Bonding of resin composites to etchable ceramic surfaces: an insight review to the chemical aspects on surface conditioning, *J. Oral. Rehabil.,* **34**, 622–630.
17. Matinlinna, J. P. (2013) Processing and bonding of dental ceramics, in *Non-Metallic Biomaterials for Tooth Repair and Replacement*, 129–160 (Ed. Vallittu, P. K.), Woodhead, Cambridge, UK, ISBN 978-0-85709-244-1.
18. Genuino, H. C., Opembe, N. N., Njagi, E. C., McClain, S., Suib, S. L. (2012) A review of hydrofluoric acid and its use in the car wash industry, *J. Ind. Eng. Chem.*, **18**, 1529–1539.
19. Alex, G. (2008) Preparing porcelain surfaces for optimal bonding, *Comp. Cont. Educ. Dent.*, **29**, 324–335.
20. Della Bona, A. (2009) *Bonding to Ceramics: Scientific Evidences for Clinical Dentistry*, Artes Medicas, Sao Paulo.
21. Ho, G. W., Matinlinna, J. P. (2011*)* Evaluation of the microtensile bond strength between resin composite and hydrofluoric acid etched ceramic in different storage media, *J. Adhes. Sci. Technol.,* **25**, 2671–2685.
22. Heikkinen, T. T., Lassila, L. V. J., Matinlinna, J. P., Vallittu, P. K. (2007) Effect of operating air pressure on tribochemical silica-coating, *Acta Odontol. Scand.,* **65**, 241–248.

23. Stewardson, D, Shortall, A., Marquis, P. (2012) The bond of different post materials to a resin composite cement and a resin composite core material*, Oper. Dent.*, **38**, E1-E12.

24. Al Jabbari, Y. S., Zinelis, S., Eliades, G. (2012) Effect of sandblasting conditions on alumina retention in representative dental alloys, *Dent. Mater. J.*, **31**, 249–255.

25. Kern, M., Thompson, V. P. (1993) Sandblasting and silica-coating of dental alloys: volume loss, morphology and change in the surface composition, *Dent. Mater.*, **9**, 155–161.

26. Ho, G. W., Matinlinna, J. P. (2011) Insights on porcelain as a dental material. Part II: chemical surface treatments, *Silicon,* **3**, 117–123.

27. Cai, Z., Bunce, N., Nunn, M. E., Okabe, T. (2001) Porcelain adherence to dental cast CP titanium: effects of surface modifications, *Biomaterials*, **22**, 979–986.

28. Kern, M., Thompson, V. P. (1994) Effect of sandblasting and silica-coating procedures on pure titanium, *J. Dent.*, **22**, 300–306.

29. Janda, R. (1992) Kleben und Klebetechniken, *Dent. Lab.,* **40**, 615–628 (in German).

30. Janda, R., François, J. F., Wulf, M., Tiller, H. J. (2002) Resin/resin bonding: a new adhesive technology, *J. Adhes. Dent.*, **4**, 299–308.

31. Guggenberger, R. (1989) Das Rocatec System: Haftung durch tribochemische Beschichtung, *Dtsch. Zahnarztl. Z.,* 44, 874–876 (in German).

32. Matinlinna, J. P., Lassila, L, V, J., Vallittu, P. K. (2007) The effect of five silane coupling agents on the bond strength of a luting cement to a silica-coated titanium, *Dent. Mater.*, **23**. 1173–1180.

33. Matinlinna, J. P., Lassila, L. V. (2011) Enhanced resin-composite bonding to zirconia framework after pretreatment with selected silane monomers, *Dent. Mater.*, **27**, 273–280.

34. Matinlinna, J. P., Vallittu, P. K. (2007) Silane based concepts on bonding resin composite to metals, *J. Cont. Dent. Pract.,* **8**, 1–8.

35. Frankenberger, R., Krämer, N., Sindel, J. (2000) Repair strength of etched vs. silica-coated metal-ceramic and all-ceramic restorations, *Oper. Dent.*, **25**, 209–215.

36. Lung, C. Y. K., Matinlinna, J. P. (2013) Silanes for adhesion promotion and surface modification, in *Silanes: Chemistry, Applications and Performance*, 87–109 (Ed. Moriguchi, K., Utagawa, S.), Novapublishers, USA, ISBN 978-1-62257-432-2.

37. Matinlinna, J. P., Lassila, L. V., Vallittu, P. K. (2006) Evaluation of five dental silanes on bonding a luting cement onto silica-coated titanium, *J. Dent.*, **34**, 721–726.

38. Seth, A., van Ooij, W. J., Puomi, P., Yin, Z., Ashirgade, A., Bafna, S., Shivane, C. (2007) Novel, one-step, chromate-free coatings containing anticorrosion pigments for metals: an overview and mechanistic study, *Prog. Org. Coat.*, **58**, 136–145.

39. Özcan, M., Matinlinna, J. P., Vallittu, P. K., Huysmans M.-C. (2004) Effect of drying time of 3-methacryloxyproyltrimethoxysilane on the shear bond strength of composite resin to silica-coated base/noble alloys, *Dent. Mater.,* **20**, 586–590.

40. Matinlinna, J. P., Heikkinen, T., Özcan, M., Lassila, L. V. J., Vallittu, P. K. (2006) Evaluation of resin adhesion to zirconia ceramic using some organosilanes, *Dent. Mater.,* **22**, 824–831.

41. Wolfart, M., Lehmann, F., Wolfart, S., Kern, M. (2007) Durability of the resin bond strength to zirconia ceramic after using different surface conditioning, *Dent. Mater.*, **23**, 45–50.

42. Ho, G. W., Matinlinna, J. P. (2011) Insights on porcelain as a dental material. Part I: ceramic material types in dentistry, *Silicon*, **3**, 109–115.

43. Kawaguchi, T., Shimizu, H., Lassila, L. V. J., Vallittu, P. K., Takahashi, Y. (2011) Effect of surface preparation on the bond strength of heat-polymerized denture base resin to commercially pure titanium and cobalt-chromium alloy, *Dent. Mater. J.*, **30**, 143–150.

44. Zhang, Y., Lawn, B. R., Rekow, E. D., Thompson, V. P. (2004) Effect of sandblasting on the long-term performance of dental ceramics, *J. Biomed. Mater. Res. B: Appl. Biomater.*, **71B**, 381–386.

45. Lung, C. Y. K., Matinlinna, J. P., Kukk, E., Hägerth, T. (2010) Surface modification of zirconia by various chemical treatments, *Appl. Surf. Sci.*, **257**, 1228–1235.

46. Lohbauer, U., Zipperle, M., Rischka, K., Petschelt, A., Müller, F. A. (2008) Hydroxylation of dental zirconia surfaces: characterization and bonding potential, *J. Biomed. Mater. Res. B: Appl. Biomater*., **87B**, 461–467.

47. Aboushelib, M. N., Feilzer, A. J., Kleverlaan, C. J. (2010) Bonding to zirconia using a new surface treatment, *J. Prosthodont.*, **19**, 340–346.

48. Aboushelib, M. N., Matinlinna, J. P., Salameh, Z., Ounsi, H. (2008) Innovations in bonding to zirconia based materials. Part I, *Dent. Mater.,* **24**, 1268–1272.

49. Aboushelib, M. N., Matinlinna, J. P. (2011) Combined novel bonding method to zirconia ceramics in dentistry: a pilot study, *J. Adhes. Sci. Technol.,* **25**, 1049–1060.
50. Akyil, M. Ş., Uzun, I. H., Bayindir, F. (2010) Bond strength of resin cement to yttrium-stabilized tetragonal zirconia ceramic treated with air abrasion, silica coating, and laser irradiation, *Photomed. Laser Surg.*, **28**, 801–808.
51. Akova, T., Yoldas, O., Toroglu, M. S., Uysal, H. (2005) Porcelain surface treatment by laser for bracket-porcelain bonding, *Am. J. Orthod. Dentofacial Orthop.*, **128**, 630–637.
52. Jevnikar, P., Krnel, K., Kocjan, A., Funduk, N., Kosmač, T. (2010) The effect of nano-structured alumina coating on resin-bond strength to zirconia ceramics, *Dent. Mater.*, **26**, 688–696.
53. Kitayama, S., Nikaido, T., Maruoka, R., Zhu, L., Ikeda, M., Watanabe, A., Foxton, R. M., Miura, H., Tagami, J. (2009) Effect of internal coating technique on tensile bond strengths of resin cements to zirconia ceramic, *Dent. Mater. J.*, **28**, 446–453.
54. Piascik, J. R., Swift, E. J., Thompson, J. Y., Grego, S., Stoner, B. R. (2009) Surface modification for enhanced silanization of zirconia ceramics, *Dent. Mater.*, **25**, 1116–1121.
55. Piascik, J. R., Wolter, S. D., Stoner, B. R. (2011) Development of a novel surface modification for improved bonding to zirconia, *Dent. Mater.*, **27**, e99–e105.
56. Levitin, G., Hess, D. W. (2011) Surface reactions in microelectronics process technology, *Annu. Rev. Chem. Biomol. Eng.*, **2**, 299–324.
57. Della Bona, A., Anusavice, K. J., Mecholsky, J. J., Jr. (2006) Apparent interfacial fracture toughness of resin/ceramic systems, *J. Dent. Res.*, **85**, 1037–1041.
58. Chaiyabutr, Y., McGowan, S., Philips, K. M., Kois, J. C., Giordano, R. A. (2008) The effect of hydrofluoric acid surface treatment and bond strength of a zirconia veneering ceramic, *J. Prosthet. Dent.*, **100**, 194–202.
59. Hooshmand, T., van Noort, R., Keshvad, A. (2002) Bond durability of the resin-bonded and silane treated ceramic, *Dent. Mater.,* **18**, 179–188.
60. Koshi, M., Nishida, N., Murakami, Y., Matsui, H. (1993) Measurements of the absolute concentrations of H and OH produced in the $SiH_3 + O_2$ reactions: determination of the product branching ratios, *J. Phys. Chem.*, **97**, 4473–4478.

61. Gbureck, U., Masten, A., Probst, J., Thull, R. (2003) Tribochemical structuring and coating of implant metal surfaces with titanium oxide and hydroxyapatite layers, *Mater. Sci. Eng.*, **23**, 461–465.

62. Chambers, R. C., Jones, W. E., Haruvy, Y., Webber, S. E., Fox, M. A. (1993) Influence of steric effects on the kinetics of ethyltrimethoxysilane hydrolysis in a fast sol-gel system, *Chem. Mater.*, **5**, 1481–1486.

63. Matinlinna, J. P., Lassila, L. V. J., Vallittu, P. K. (2006) The effect of a novel silane blend system on resin bond strength to silica-coated Ti substrate, *J. Dent.*, **34**, 436–443.

64. Matinlinna, J. P., Lassila, L. V. J., Vallittu, P. K. (2006) The effect of three silane coupling agents and their blends with a cross-linker silane bonding on bis-GMA resin to silicatized titanium (a novel silane system), *J. Dent.*, **34**, 740–746.

65. Matinlinna, J. P., Lassila, L. V. J., Vallittu, P. K. (2009) Experimental novel silane system in adhesion promotion between dental resin and pretreated titanium, *Silicon*, **1**, 249–254.

66. Matinlinna, J. P., Özcan, M., Lassila, L. V. J., Kalk, W., Vallittu, P. K. (2008) Effect of the cross-linker silane concentration in a novel silane system on bonding resin-composite cement, *Acta Odontol. Scand.,* **66**, 250–255.

67. Matinlinna, J. P., Tsoi, J. K. H., de Vries, J., Busscher, H. J. (2013) Characterization of novel silane systems on titanium implant surfaces, *Clin. Oral. Implants Res.,* **24**(6), 688–697.

68. Hooshmand, T., Matinlinna, J. P., Keshvad, A., Eskandarion, S., Zamani, F. (2013) Bond strength of a dental leucite-based glass ceramic to a resin cement using different silane coupling agents, *J. Mech. Behav. Biomed. Mater.,* **17**, 327–332.

69. Matinlinna, J. P., Lassila, L. V. J., Vallittu, P. K. (2007) Pilot evaluation of resin composite cement adhesion to zirconia using a novel silane system, *Acta Odontol. Scand.,* **65**, 44–51.

70. Matinlinna, J. P., Choi, A. H., Tsoi, J. K. H. (2013) Bonding promotion of resin-composite to silica-coated zirconia implant surface using a novel silane system, *Clin. Oral. Implants Res.,* **24**, 290–296.

71. Matinlinna, J. P., Lassila, L. V. J., Kangasniemi, I., Vallittu, P. K. (2005) Isocyanato- and methyacryloxysilanes promote bis-GMA adhesion to titanium, *J. Dent. Res.,* **84**, 360–364.

72. Matinlinna, J. P., Heikkinen, T., Özcan, M., Lassila, L. V. J., Vallittu, P. K. (2006) Evaluation of resin adhesion to zirconia ceramic using some organosilanes, *Dent. Mater.,* **18**, 179–188.

73. Matinlinna, J. P., Lassila, L. V. J., Vallittu, P. K. (2006) The effect of five silane coupling agents on the bond strength of a luting cement to a silica-coated titanium, *Dent. Mater.,* **23**, 1173–1180.

74. Lung, C. Y. K., Matinlinna, J. P. (2010) Resin bonding to silicatized zirconia with two isocyanatosilanes and a cross-linking silane. Part I: experimental approach, *Silicon*, **2**, 153–161.

75. Lung, C. Y. K., Matinlinna, J. P. (2010) Resin bonding to silicatized zirconia with two isocyanatosilanes and a cross-linking silanes. Part II: mechanistic approach, *Silicon*, **2**, 163–169.

76. Uchida, M., Kim, H. M., Kokubo, T., Nawa, M., Asano, T., Tanaka, K., Nakamura, T. (2002) Apatite-forming ability of a zirconia/alumina nano-composite induced by chemical treatment, *J. Biomed. Mater. Res. A*, **60**, 277–282.

77. Aboushelib, M. N., Kleverlaan, C. J., Feilzer, A. J. (2007) Selective infiltration-etching technique for a strong and durable bond of resin cements to zirconia-based materials, *J. Prosthet. Dent*., **98**, 379–388.

78. Coluzzi, D. J. (2008) Fundamentals of lasers in dentistry: basic science, tissue interaction, and instrumentation, *J. Laser. Dent.*, **16**(Spec Issue), 4–10.

79. Kaldos, A., Pieper, H. J., Wolf, E., Krause, M. (2004) Laser machining in die making: a modern rapid tooling process, *J. Mater. Process Technol*., **155–156**, 1815–1820.

80. Akova, T., Yoldas, O., Toroglu, M. S., Uysal, H. (2005) Porcelain surface treatment by laser for bracket-porcelain bonding, *Am. J. Orthod. Dentofacial Orthop.*, **128**, 630–637.

81. Levin, I., Brandon, D. (1998) Metastable alumina polymorphs: crystal structures and transition sequences, *J. Am. Ceram. Soc.,* **81**, 1995–2012.

82. Kiyohara, P. K., Santos, H. S., Coelho, A. C. V., Santos, P. D. S. (2000) Structure, surface area and morphology of aluminas from thermal decomposition of $Al(OH)(CH_3COO)_2$ crystals, *An. Acad. Bras. Ciênc.*, **72**, 471–495.

83. Liu, D., Matinlinna, J. P., Pow, E. H. N. (2012) Insights into porcelain zirconia bonding, *J. Adhes. Sci. Technol.*, **26**, 1249–1265.

84. Pierson, H. O. (1999) *Handbook of Chemical Vapour Deposition: Principles, Technology and Applications,* 2nd ed., Noyes Publications, New York, USA.

85. Spear, K. E. (1982) Principles and applications of chemical vapour deposition (CVD), *Pure Appl. Chem*., **54**, 1297–1311.

86. Chu, P. K., Chen, J. Y., Wang, L. P., Huang, N. (2002) Plasma-surface modification of biomaterials, *Mater. Sci. Eng. R*, **36**, 143–206.

87. Hodak, S. K., Supasai, T., Paosawatyanyong, B., Kamlangkla, K., Pavarajarn, V. (2008) Enhancement of the hydrophobilicity of silk fabrics by SF_6 plasma, *Appl. Surf. Sci.,* **254**, 4744–4749.

88. Lung, Y. K. C., Kukk, E., Matinlinna, J.P. (2013) The effect of silica-coating on zirconia by sol-gel process on resin zirconia bonding, *Dental Mater. J*., **32**(1), 165–172.

This page intentionally left blank

Chapter 12

Sol-Gel Coatings on Titanium

Andy H. Choi[a,b] and Besim Ben-Nissan[b]
[a]*Faculty of Dentistry, Dental Materials Science, University of Hong Kong, Prince Philip Dental Hospital, 34 Hospital Road, Sai Ying Pun, Hong Kong SAR, People's Republic of China*
[b]*School of Chemistry and Forensic Science, Faculty of Science, University of Technology, Sydney, Australia*
ahchoi@hotmail.com

Nanocoatings present the possibility of altering the surface properties of medical-grade materials to achieve improvements in biocompatibility, reliability, and performance. Sol-gel processing is a versatile and attractive technique since it can be used to fabricate ceramic coatings from solutions by chemical means. The sol-gel process is relatively easy to perform, and complex shapes can be coated, and it has also been demonstrated that the nanocrystalline grain structure of sol-gel coatings produced results in improved mechanical properties.

12.1 Introduction

A material containing delicate structures and sizes that fall within the range of 1 nm to 100 nm is referred to as a *nanostructured material.*

Handbook of Oral Biomaterials
Edited by Jukka P. Matinlinna

ISBN 978-981-4463-12-6 (Hardcover), 978-981-4463-13-3 (eBook)
www.panstanford.com

As a result of this size, extensive development of nanotechnology has taken place during the past decade in the fields of materials science and engineering.

The improvement of interface bonding by nanoscale coatings, depending on biomimetics, has been of worldwide interest during the past two decades, and today several companies are in early commercialization stages of new-generation, nanoscale-modified implants for orthopedic, ocular, and maxillofacial surgery, as well as for hard- and soft-tissue engineering. Modeling and analysis of these nanoscale structures are current interests in both engineering and clinical science. Tissue–implant interactions are generated in the nano- and the mesoscale, and mathematical analyses of these are also current interests.

Nanotechnology has opened up novel techniques for the production of bone-like synthetic nanopowders and coatings of bone-like hydroxyapatite (HAp) on titanium substrates. Titanium is discussed also in Chapters 9, 10, and 13.

The microstructure and properties of nanostructured materials are dependent on their chemistry and method of synthesis, in addition to their processing route. Consequently, it is extremely important to select the most appropriate technique when preparing *nanomaterials* with desired properties and property combinations. The most widely employed synthesis techniques for the production of advanced ceramics include pressing, as well as wet-chemical processing techniques such as coprecipitation and sol-gel processing, some of which have been used to produce nanostructured solid blocks and shapes, nanocoatings, and nanoparticles.

Bone mineral is composed of nanocrystalline platelets, referred to originally as HAp. It is now agreed that bone apatite can be better described as carbonate HAp (CHA) and approximated by the formula $(Ca,Mg,Na)_{10}(PO_4CO_3)_6(OH)_2$. The composition of commercial CHA is similar to that of bone mineral inorganic component apatite. Bone pore sizes range from 1 nm to 100 nm in normal cortical bone and from 150 microns to 400 microns in trabecular bone tissue, and the pores are interconnected.

It has been well proven that porous bulk HAp cannot be used for load-bearing applications. As a result, HAp has been employed as a coating for dental and orthopedic applications.

Coatings offer the possibility of altering the surface properties of dental and surgical-grade materials to achieve improvements in properties and performance. Coating is a technique for modifying the surface of the base material in order to improve the mechanical and/or physical performances of implants and devices. Techniques such as chemical vapor deposition (CVD), physical vapor deposition (PVD), electrochemical vapor deposition, metal–organic chemical vapor deposition (MOCVD), thermal or diffusion conversion, plasma and fusion coating, and sol-gel processing have been used to produce coatings on both the micro- and the nanoscale.

Four general conventional industrial coating techniques have been anticipated for the manufacture of bioactive HAp coatings during the past 30 years for clinical applications. The first technique was developed by Ducheyne et al. This method utilizes the spray-coating method that employs relatively thick calcium phosphate coatings with thickness ranging from 100 μm to 2 mm for bone ingrowth [1]. The second technique was developed by Hench et al. [2] for the fabrication of thick bioglass coatings with surface bioactivity.

During the early 1990s, the third technique was developed by Kokubo et al. [3], and the method was based on self-assembly by precipitation in a simulated body fluid (SBF) solution. At a later stage this method was applied and still utilized to investigate the biocompatibility in a range of new materials. The forth technique developed by Ben-Nissan et al. for calcium phosphate nanocoatings [4, 5] is much newer and shows very promising signs, and the method involves dipping in sol-gel-derived HAp solutions to produce strong 70–100 nm thick single or multilayered nanocoatings.

While coatings based on self-assembly and thick bioglass coatings are effective, spray coating is the only coating technique that has been commercially applied to orthopedic and dental implants.

The present focus is on the production of new nanoceramics that are relevant to a wide range of applications, including modeling and finite-element analysis (FEA), increased bioactivity for tissue regeneration and engineering, and implantable surface-modified dental and medical devices for better hard- and soft-tissue attachment.

The process of biomimetics is based on, at the molecular level, the ability of the biological systems to process and store information,

and during the past decade, the extension of this concept has been brought out to the processing of nanocomposites for biomedical devices and tissue engineering, for example, scaffolds for bone regeneration [6].

By definition, a nanocomposite is a heterogeneous combination of two or more materials in which at least one of those materials should be on a nanoscale. Using the composite approach and with the aid of secondary substitution phases, the mechanical properties of composites, such as the Young's modulus, can be manipulated closer to those of natural bone.

For biomedical applications, another form of nanocomposites developed is the gel system. A gel system can be considered as a three-dimensional network immersed in a fluid and nanomaterials can be entrapped in the gel. A nanogel, which is a nanosized, flexible, hydrophilic polymer gel [7], is an example of a gel that can be used in drug delivery carriers.

The aim of this chapter is to provide a brief background on currently used coating methods and further detailed information relating to our choice of sol-gel-derived nano-HAp coatings for dental and biomedical applications.

12.2 Coating Techniques for Dental and Biomedical Applications

Even though trials were carried out on various oxides and mixed oxides, research and development of HAp nanocoatings did not commence until the early 1990s [5]. Meanings of the terms of "macrofilm," "microfilm," "thin film," and "nanothickness," or more generally, thin films, in biomedical applications, have been employed wrongly and/or interchangeably within the literature, so the authors of this chapter believe that coatings greater than 1000 μm should be classed as thick or macrocoatings, 1–1000 μm should be classed as thin-film coatings or microcoatings, and below 1 μm should be classed as nanocoatings.

12.2.1 Plasma Spraying

Techniques such as plasma spraying, flame spraying, detonation gun spraying, and high-velocity oxygen flame spraying can be classified

under the definition of the term "thermal spraying." Plasma spraying uses a direct current arc or other sources such as radio frequency (RF) to produce gas plasma and is capable of producing coatings with thicknesses ranging from a few microns to a few millimeters [8].

On a commercial scale, plasma spraying is the only extensively used technique to generate coatings on medical implants. Plasma spraying can be carried out under vacuum (vacuum plasma spraying [VPS]), under controlled atmospheres, such as nitrogen, or in an ambient atmosphere (atmospheric plasma spraying [APS]). Plasma spraying uses an electrical discharge to convert a carrier gas (such as argon) into plasma. The expansion of rapid gas induces speeds of up to 800 m/s. The powder is heated by the plasma into a partially liquid form, and it is propelled toward the substrate.

12.2.2 Chemical Vapor Deposition

The process of producing coatings and films with CVD involves the chemical reactions of gaseous reactants on or near the vicinity of a heated substrate surface. CVD can be employed to manufacture single-layer, multilayer, composite, nanostructured, and functionally graded coating materials with well-controlled dimensions and a unique structure at low processing temperatures.

This atomistic deposition method can offer highly pure materials with structural control at atomic or nanoscale levels, in addition to a coating of complex-shaped biomedical prostheses and the fabrication of nanodevices and composites [1, 9]. See also Chapter 11.

12.2.3 Physical Vapor Deposition

PVD is a flexible synthesis method, and the technique involves the generation of vapor-phase species via laser ablation, ion beams, sputtering, or evaporation. It is capable of preparing thin-film materials with structural control at the atomic or nanometer scale. This control can be accomplished by carefully controlling the processing conditions.

In most PVD-based processing approaches, it is not possible to generate a uniform coating on nonplanar substrates without the use

of multiple, spatially distributed sources or sophisticated substrate translation/rotation. This is due to the fact that the vapor atoms are produced in high vacuum, which results in nearly collisionless vapor transport to the substrate. Therefore, only regions in the line of sight of the vapor source are coated [10].

12.3 The Sol-Gel Technique

The sol-gel technique is an attractive and versatile method and is relatively easy to perform, and complex shapes can be coated. It can be employed to fabricate ceramic coatings from solutions by chemical means, and it has also been demonstrated that the nanocrystalline grain structure of coatings produced results in an improvement in mechanical properties [11–14].

The sol-gel technique dates back to the genesis of chemistry. In 1846, it was first discovered as an application technology, when Ebelmen [15] observed the hydrolysis and polycondensation of tetraethylorthosilicate (aka tetraethoxysilane [TEOS]). The first sol-gel patent was published in 1939, which covers the preparation of SiO_2 and TiO_2 coatings [16].

Roy and Roy [17] recognized the potential in 1955 for the production of high-purity glasses using methods not possible with traditional ceramic-processing techniques. As a result, the first report on the application of sol-gel technology to produce homogeneous multicomponent glasses was born.

Schroeder [18] reported the first investigation conducted by Schott glass involving sol-gel-synthesized coatings in 1965. Mixed-oxide coatings were developed, although they were mainly interested in single-oxide optical coatings of SiO_2 and TiO_2.

During the late 1980s and 1990s, sol-gel technology also found uses in a variety of technology fields, such as biomedical applications [5, 19]. There are a number of excellent books, book chapters, and review articles that cover the basic science and technology of sol-gel technology for various ceramic oxide systems [3, 20–27].

By definition, a sol is a suspension of colloidal particles in a liquid [28]. The difference between a sol and a solution is that a sol is a two-phase, solid–liquid system, while a solution is a single-phase system. The size of the colloidal particles can range from approximately 1 nm to 1000 nm. Consequently, gravitational forces on these colloidal

particles are negligible, and interactions are dominated by surface charges and short-range forces such as van der Waals forces.

Diffusion of the colloids by Brownian motion leads to a low-energy arrangement, thus imparting stability to the system [29]. Reducing surface charges can improve the stability of the sol particles. Gelation is induced if the surface charge is significantly reduced, and the resultant product is able to maintain its shape without the assistance of a mold.

Since gels consist of a solid skeleton or network that encloses a liquid phase or excess of solvent, they considered as composites. Gels can be soft and have a low elastic modulus, depending on their chemistry. This can be accomplished through controlling the polymerization of the hydrolyzed starting compound. In this case, a three-dimensional network forms, resulting ultimately in a high-molecular-weight polymeric gel. The resultant gel can be considered as a macroscopic molecule that extends throughout the solution. The time taken for the last bond in this network to form is referred to as the gelation point. Depending on the process applied, this gelation can be used to produce a nanostructured monolith or nanosized coatings [8].

The sol-gel technique can be classified as aqueous or alcohol based. Aqueous-based systems generally are carried out in the presence of water, whereas alcohol-based systems exclude water buildup until the hydrolysis stage. On the other hand, there are also nonhydrolytic sol-gel processes that do not require the presence of solvents at all.

Correspondingly, *sol-gel precursors* can be categorized as either alkoxides or nonalkoxides. While alkoxides are the preferred precursors for sol-gel production due to their volatility, other compounds, such as metal salts, can also be used. This is often the case for group I and II elements whose alkoxides are solid and nonvolatile and in many cases have low solubility [29].

The use of *solvents* is needed in the preparation of sol solutions, which are usually organic alcohols. Although the main purpose of using solvents is to dissolve solid precursors, they are also used to minimize the effect of concentration gradients and dilute liquid precursors. The particular solvent employed can influence factors such as crystallization temperature [30] and particle morphology [31].

Cracking during the production stages—such as fast drying—can be a problem due to the large amount of organic material needed in the processing of sol-gel-derived forms. It is common in the case of monoliths that shrinkage occurs during drying. On the other hand, cracking in thicker coatings is often a result of phenomena such as inhomogeneities resulting from thermal mismatch with the substrate used, phase separation, or various factors related to the drying process.

The synthesis of a sol involves the preparation of a solution from precursors. Coatings are fabricated using various deposition techniques from the solutions. The coated substrate is then exposed to water for hydrolysis. During this process, hydroxides or hydrated oxides form and gelation occurs to form a three-dimensional network.

The gelation process can be pictured as clusters grown by aggregation of particles or condensation of polymers until the clusters collide. The gel point can only be determined by an increase in viscosity as no latent heat is released. The gel is composed of a solid skeleton surrounding a continuous liquid phase.

The next stage is the drying and firing of the gel. During drying, excess solvents are removed from the pore network. A significant amount of shrinkage takes place during the drying and firing processes. Firing, also referred to as sintering, is the final stage in the production of ceramic materials via the sol-gel process. By heating dried gels to elevated temperatures, any remaining organic materials are combusted.

12.4 Sol-Gel Synthesis of Nanohydroxyapatite

Nanocrystalline HAp can be manufactured using a number of different production techniques, and it can be used as nanocoatings, monolithic solid ceramic products, or nanosized powders and platelets for a number of applications.

Although not all completely satisfactory, various methods have been employed for the preparation of nanocrystalline apatites. These methods include mechanical alloying, vibromilling, coprecipitation, hydrothermal synthesis, sol-gel synthesis, wet-chemical precipitation, mechanochemical synthesis, ball milling,

liquid-solid-solution synthesis, RF induction plasma, flame spray pyrolysis, electrocrystallization, microwave processing, hydrolysis of other calcium orthophosphates, double step stirring, and emulsion-based or solvothermal syntheses, and several other techniques are known. Continuous preparation procedures are also available [8, 10, 32].

Since the early 1990s, a number of sol-gel routes have been employed for the production of synthetic HAp powders. Ben-Nissan et al. introduced alkoxide-based nanocoatings as early as in 1989, and since then a number of excellent studies has been conducted on a range of precursors to produce pure nanocrystalline apatite powders, solid products, or coatings for medical and engineering applications [8, 32, 33].

The *major precursors* include calcium acetate, calcium alkoxide, calcium chloride, calcium hydroxide, calcium nitrate, and dicalcium phosphate dihydrate. A number of investigators has reported the thickness of the sol-gel-derived HAp coatings produced are in the 70–100 nm range [8, 32, 33].

12.5 Sol-Gel Synthesis of Hydroxyapatite Micro- and Nanocoatings

A number of calcium phosphate coatings at the nanoscale were introduced since the early 1990s. These included mixed calcium phosphates to 100% pure HAp from amorphous to finely crystalline structures. Their thickness varied according to the chemistry and hence the viscosity to the application methods used. Although many attempted high-purity HAp nanocoatings, many investigators concentrated in research to improve properties by the addition of numerous compounds and chemical modifications.

HAp coatings loaded with nanosilver particles is an attractive method to impart HAp coatings with antibacterial properties, although the method of adding silver has been controversial. Qu et al. [34] produced porous Ti scaffolds with high porosity and interconnected structures using the polymer-impregnating method. A sol-gel process was then used to produce uniform Ag/HAp composite coatings on the surfaces of porous Ti substrates. Calcium nitrate tetrahydrate, $Ca(NO_3)_2{\cdot}4H_2O$, and phosphoric

pentoxide (P_2O_5) were dissolved in 65 mL of absolute ethyl alcohol. After stirred vigorously for six hours, a HAp sol with a Ca/P molar ratio of 1.67 was prepared by mixing the two precursors. After the sol was kept statically (aged) for 48 hours, absolute ethyl alcohol solution with $AgNO_3$ was added to it and stirred enough to guarantee homogeneity. Ti substrates were immersed in the sol with a fixed dipping/withdrawing speed of 3 cm/min in an ambient atmosphere and dried at 80°C for 12 hours, followed by sintering at 300°C for 15 minutes. This step was repeated several times to meet the requirement of the thickness of the composite coatings before they were finally sintered at 600°C for 10 minutes. The average thickness of the coatings was estimated to be 30 μm on the basis of the back-scattering electron (BSE) micrograph.

Li et al. [35] investigated the effects of strontium-substituted HAp coatings with 10 mol% Ca^{2+} replaced by Sr^{2+} (10% Sr-HAp) on implant fixation in ovariectomized (OVX) rats. Coatings of HAp and 10% Sr-HAp were prepared on the surface of titanium implants using sol-gel dip methods. Analytical grade $Ca(NO_3)_2{\cdot}4H_2O$, $Sr(NO_3)_2$, and P_2O_5 were dissolved in absolute alcohol in two sets of beakers to form the Ca+Sr precursor and the P precursor, which were then mixed in a (Ca+Sr)/P molar ratio of 10/6 and refluxed for 24 hours to form dipping sols. Subsequently, the prepared Ti implants were immersed into the dipping sols and withdrawn at a speed of 8 cm/min. After 15-minute drying at 150°C and 15-minute firing at 700°C, a single layer of 10% Sr-HAp was obtained. Such a dipping-drying-firing process was repeated twice to increase coating thickness. The thickness of coatings measured by scanning electron microscopy (SEM) from cross sections was 955 ± 105 nm for HAp and 898 ± 102 nm for 10% Sr-HAp coatings.

Un and Durucan [36] established sol-gel processing routes for the development of HAp-titania (TiO_2) hybrid coatings on Ti-6Al-4V by dip coating. To produce the TiO_2 sol, Ti-isopropoxide was dissolved in ethanol under vigorous stirring. Nitric acid, ethanol, and deionized (DI) water were mixed and then added to the Ti-isopropoxide:ethanol solution to catalyze the sol-gel reactions. HAp powder, 1.000 g, was added to ethanol, and this HAp suspension was poured into the TiO_2 sol to obtain the HAp-TiO_2 coating. The dip-coating process was employed to apply HAp-TiO_2 sols to metallic substrates. A dip-coating speed of 16 cm/min was chosen. Coated

samples were first dried at around 70°C. This was followed by oven drying at 100°C for 1.5 hours to remove the organics. Finally, the coated samples were heat-treated at 500°C for 30 minutes for calcination and to mature the TiO_2-based coating. The reported thickness ranged from 0.120 μm for a single layer to 0.810 μm for multilayered (three-time-coated) film.

Wu et al. [37] used novel sphene ($CaTiSiO_5$) ceramics as coatings for Ti-6Al-4V. Sphene coatings were prepared by the sol-gel spinning method using tetraethyl orthosilicate, $(C_2H_5O)_4Si$; titanium (IV) butoxide, $Ti(O(CH_2)_3CH_3)_4$; and calcium nitrate tetrahydrate, $Ca(NO_3)_2{\cdot}4H_2O$, as raw materials. Tetraethyl orthosilicate and titanium (IV) butoxide were mixed with ethanol and HNO_3. The calcium nitrate tetrahydrate was added to the mixture, and reactants were stirred for five hours and then aged for one day at room temperature for coating. Ti-6Al-4V disks were fixed on the spinning machine with a controllable spinning speed, and a sol solution was dropped to the substrate and spin-coated at 2000 rpm for 10 seconds. After drying at 60°C for 24 hours, samples were heated at 875°C for 10 minutes in air with a heating rate of 4°C min^{-1}. A uniform structure of the sphene coating was found across the Ti-6Al-4V surface, with a thickness and surface roughness of the coating of about 0.5–1 μm and 0.38 μm, respectively.

A biphasic layer with a Zn-containing β-tricalcium phosphate (ZnTCP) phase and a fluoridated HAp (FHAp) phase on a titanium alloy substrate was prepared by Miao et al. [38] using the sol-gel technique. The colloidal solution for dip coating was prepared by mixing ethanol solutions of $Ca(NO_3)_2{\cdot}4H_2O$ and P_2O_5 in a Ca/P molar ratio of 1.67, and a desired amount of hexafluorophosphoric acid (HPF_6) was added. After the mixture was refluxed for 24 hours to form an FHAp precursor solution, equivalent amounts of β-TCP and ZnTCP powder were added to form colloidal solutions. The ratio of Ca in the powders to that in FHAp precursor solution is 1/2. Ti-6Al-4V substrates were first ground with 1000-grit silicon carbide paper, and ultrasonically rinsed in acetone and DI water and then immersed into the dipping solutions and withdrawn at a speed of 8 cm min^{-1}. After drying at 150°C for 15 minutes, the layers were fired at 600°C for 15 minutes. This deposition procedure was repeated twice to obtain a zinc-release FHAp layer (ZnTCP/FHAp).

An effective colloidal-sol-gel method was developed by Cheng et al. [39] to prepare biphasic calcium phosphate coatings. Calcium nitrate tetrahydrate, $Ca(NO_3)_2{\cdot}4H_2O$, and phosphor pentoxide (P_2O_5) were dissolved in ethanol to form a Ca solution and a P solution. After the P solution was refluxed for 24 hours, a designed amount of HPF_6 was added. Then, the Ca solution was added to form the FHAp precursors with a Ca:P:F ratio of 5:3:1 and 15:9:2. Commercial HAp powders were added to the FHAp precursors. After 20-minute ultrasonic dispersing, colloidal sols were obtained. Ti-6Al-4V substrates were dipped in the colloidal sols and withdrawn at a speed of 15 cm/min. After 15-minute drying in the oven at 150°C and 15-minute firing at 600°C, a single layer of the coatings was obtained.

A simple sol-gel method was developed by Wen et al. [40] for HAp/TiO_2 coatings on a titanium-zirconium (Ti-Zr) alloy for biomedical applications. The sol-gel process started with the preparation of a TiO_2 sol. Tetrabutylorthotitanate ($C_{16}H_{36}TiO_4$) was first diluted with absolute ethanol, and then a small amount of distilled water mixed with diethanolamine ($NH(CH_2\text{-}CH_2OH)_2$), which was used as a catalyst, was added for hydrolysis. For the preparation of the HAp sol, triethyl phosphite, $(C_2H_5O)_3P$, diluted with anhydrous ethanol was first hydrolyzed for 24 hours with distilled water under vigorous stirring. A stoichiometric amount of calcium nitrate, $Ca(NO_3)_2{\cdot}4H_2O$, dissolved in anhydrous ethanol was added to the hydrolyzed phosphite sol (molar ratio Ca:P = 1.67). The HAp/TiO_2 layers were spin-coated on the surface of the Ti-Zr alloy at a speed of 3000 rpm for 15 seconds, followed by heat treatment at 600°C for 20 minutes in an argon atmosphere sequentially. Extensive observations revealed that the average thicknesses of both the TiO_2 and the HAp layer were approximately 25 μm and the total thickness of the HAp/TiO_2 coatings was 50 μm.

HAp-based coatings on Ti-6Al-4V were attempted by Balamurugan et al. [41] using the sol-gel process. Phosphoric acid ester $(C_2H_5O)_3PO$ was hydrolyzed for 24 hours with a fixed amount of distilled water in a sealed container under vigorous stirring. A stoichiometric amount of 4 M ethanol solution of calcium nitrate, $Ca(NO_3)_2{\cdot}4H_2O$, was added drop wise to the hydrolyzed sol. The mixed sol solution was then continuously agitated for an additional 30 minutes and kept static at an ambient duration time for 24 hours.

Ti-6Al-4V substrates were dip-coated with the sol solution with a withdrawal speed of 10 mm/s. The coatings were then dried at 80°C, followed by annealing in vacuum; the temperature ranges between 200°C and 900°C with a dwelling time of five hours.

Silicon-substituted HAp has been deposited by Hijón et al. [42] onto Ti-6Al-4V substrates by sol-gel technology. Triethyl phosphite, $P(OCH_2CH_3)_3$, was hydrolyzed in water for 24 hours. After that, tetraethyl orthosilane, $Si(OCH_2CH_3)_4$, was added. The reaction was carried out maintaining a molar ratio of $H_2O/(P + Si) = 4$. A 4 M aqueous calcium nitrate solution, $Ca(NO_3)_2{\cdot}4H_2O$, was poured into the sol-containing phosphorus and silicon. The amounts of reagents were calculated considering a $Ca/(P + Si)$ molar constant ratio, equal to HAp stoichiometry (1.67). The mixed sol was stirred for 15 minutes and aged at 60°C in an oven for 6 hours. Ti-6Al-4V discs were dip-coated into the precursor sol and extracted with a withdrawal speed of 2500 μm/s. After the deposition, the coatings were dried at 100°C for 1 hour, annealed in air at 550°C for 10 minutes, and then cooled to room temperature. Finally, the coatings were washed with ethanol in an ultrasonic bath for two minutes. The reported thickness of the coating was around 600 nm.

Bioactive calcium phosphate (Ca-P) coatings were produced by Kim et al. [43] on Ti by using phosphate-based glass (P glass) and HAp. To prepare the HAp sol, triethyl phosphite, $P(C_2H_5O)_3$, was hydrolyzed for 24 hours in ethanol with the addition of distilled water. Separately, calcium nitrate, $Ca(NO_3)_2{\cdot}4H_2O$, was dissolved in ethanol. The Ca-containing solution was added slowly to the P-containing solution, and the mixture sol was aged at room temperature for 7 days and then at 40°C for another 24 hours. The Ti disk was dip-coated with the glass and glass-HAp slurries and dried at room temperature for 3 hours and then at 80°C for another 24 hours. After repeating the coating-drying process twice, the samples were heat-treated at 600°C for one hour. The coating layer had a thickness of approximately 30–40 μm and adhered to the Ti substrate tightly.

The interface shear strength of calcium phosphate (Ca-P) thin films applied to Ti-6Al-4V substrates has been evaluated by Gan et al. [44]. The Ca-P films were synthesized using sol-gel methods from both an inorganic and an organic precursor solution. For the inorganic route–formed films, calcium nitrate tetrahydrate and ammonium dihydrogen phosphate were used as calcium and

phosphorous precursors, and the molar ratio of Ca/P in these starting reactants was set equal to 1.67. Five separate film layers were applied using a substrate withdrawal rate of 30 cm/min and relatively low temperature anneals (~210°C) between dippings in order to develop a final film thickness ≈ 1 μm. A final anneal at 500°C for 10 minutes in air was used to consolidate the Ca-P film, followed by sample furnace cooling to room temperature. For the organic route–formed film, calcium nitrate tetrahydrate and triethyl phosphite were selected as the calcium and phosphorous precursors. The calcium nitrate tetrahydrate was dissolved in absolute anhydrous ethanol, which was then added drop-wise to the hydrolyzed phosphorus solution, again at a Ca/P ratio equal to 1.67. This clear solution was aged in a 40°C water bath for four days. A diluted sol from the mother solution was further aged for two days at room temperature to form the film for substrate coating. A single dipping treatment was used with the organic route solution. The substrates were withdrawn from the solution at a rate of 20 cm/min and the resulting coating annealed at 500°C for 20 minutes in air and then furnace-cooled to room temperature.

12.6 Cell Responses and Hydroxyapatite Coatings on Titanium

Coating characteristics such as composition, crystallite features, and topography collectively impact the cell response. The influence of splat size and morphology has not been properly assessed for HAp thermal spray coatings on titanium substrates. Gross et al. [45] determined the osteoclast resorption pattern on a topographically refined coating compared to dentine. Human-derived osteoclasts were placed on a coating and compared to dentine, a polished coating, and polished sintered HAp. The results revealed osteoclasts showing a clear preference for activity on coatings with refined topography. The resorption of human-derived osteoclasts revealed a tenfold greater number of resorption pits on dentine and the thermally sprayed coating compared to polished coatings. The pit diameter is larger for coatings with splats compared to polished coatings. The pit depth is shallower for coatings than dentine. They suggested that HAp coatings with splat topography undergo active remodeling like

dentine and bone and provide a useful topographical feature for the design of implant surfaces.

The time required for osseointegration with a metal implant having a smooth surface ranges from three to six months. Ravichandran et al. [46] hypothesized that biomimetic coating surfaces with poly(lactic-co-glycolic acid) (PLGA)/collagen fibers and nano-HAp on the implant would enhance the adhesion of mesenchymal stem cells (MSCs). Therefore, this surface modification of dental and bone implants might enhance the process of osseointegration. In their study, they coated PLGA or PLGA/collagen fibers on Ti disks by modified electrospinning for five seconds to two minutes; after that, they further deposited nano-HAp on the fibers. The cell attachment efficiency was tested on all the scaffolds for different intervals of time (10, 20, 30, and 60 min). Alkaline phosphatase (ALP) activity, cell proliferation, and mineralization were analyzed on all the implant surfaces on days 7, 14, and 21. Results of the cell adhesion study indicated that cell adhesion was greatest on the implant surface coated with PLGA/collagen fibers deposited with nano-HAp compared to other scaffolds. Within a short span of 60 minutes, 75% of the cells adhered onto the mineralized PLGA/collagen fibers. Similarly by day 21, the rate of cell proliferation was significantly higher on the mineralized PLGA/collagen fibers owing to enhanced cell adhesion on these fibers. This enhanced initial cell adhesion favored higher cell proliferation, differentiation, and mineralization on the implant surface coated with mineralized PLGA/collagen fibers.

Zhao et al. [47] compared magnesium-substituted and pure HAp coatings on the promotion of osteogenesis in vitro and on osseointegration in vivo. Electrochemically deposited pure HAp (EDHAp) or electrochemically deposited magnesium-substituted HAp (EDMHAp) coatings was formed on the surface of pure titanium disks or implants. MC3T3-E1 preosteoblasts were cultured in the EDHAp- and EDMHAp-coated disks, and cell growth, ALP activity, and osteocalcin (OC) secretion were measured at various time points. For studies on osseointegration, 30 roughened implants coated either with EDHAp or EDMHAp were implanted in the femurs of 15 New Zealand White rabbits. After two, four, and eight weeks, femurs were retrieved and prepared for histomorphometric evaluation. MC3T3-E1 cells cultured on EDMHAp-coated disks

showed increased cell numbers, ALP, and OC secretion compared to EDHAp-coated disks at all time points. Histologic observation of the coated implants showed woven bone in direct contact with both implant surfaces after two weeks and mature bone after eight weeks.

Chung and Long [48] evaluated the effect of strontium substitution for calcium in HAp coatings on titanium via microarc treatment (MAT) on the microstructure and osteoblast/osteoclast responses. The results indicated Sr-HAp coatings possess better osteoblast compatibility than raw titanium and non-Sr-HAp coatings. The difference becomes significant after 48-hour incubation. Furthermore, Sr-HAp coatings promote later cell growth stages than a non-Sr-HAp coating and form a much firmer connection between the Sr-HAp coating and osteoblasts. A Sr content in the Sr-HAp coatings exceeding 38.9 at% significantly affects the ability to inhibit the differentiation of osteoclasts.

Roy et al. [49] fabricated strontium (Sr)- and magnesium (Mg)-doped HAp coatings on commercially pure titanium substrates using inductively coupled RF plasma sprays. In vitro cell–material interactions using human fetal osteoblasts (hFOBs) showed better cell attachment and proliferation on Sr-HAp coatings compared to HAp or Mg-HAp coatings. Presence of Sr in the coating also stimulated hFOB cell differentiation and ALP expression.

Dimitrievska et al. [50] fabricated a TiO_2 nanostructure-based coating charged with 10 wt% HAp (TiO_2-HAp) sprayed by high-velocity oxyfuel on Ti64 substrates. In their study, they elucidated the TiO_2-HAp nanocomposite coating surface chemistry and in vitro osteoinductive potential by culturing human MSCs (hMSCs) in a basal and in an osteogenic medium (hMSC-ob). The results revealed hMSCs and hMSC-ob demonstrated increased proliferation and osteoblastic differentiation on nanostructured TiO_2-HAp coatings, suggesting TiO_2-HAp coating nanostructure surface properties induce osteogenic differentiation of hMSCs and support hMSC-ob osteogenic potential better than our current gold-standard HAp coatings.

A sputtering technique followed by low-temperature hydrothermal treatment has been demonstrated to produce a dense and bioactive HAp thin-film coating. Hao et al. [51] investigated osteoblast and osteoclast responses to HAp-coated plates and

titanium plates with similar roughness. Rat bone marrow stromal cells were cultured on these plates to induce osteoblasts. The cells showed significantly enhanced proliferation on the HAp surface, accompanied by an increase of osteoblastic phenotypes. The cocultured osteoclasts exhibited a significantly different cell number and morphology between the HAp and titanium surfaces. A series of osteoclast marker genes were more stimulated on HAp, and 32% of the HAp surface area could be resorbed by osteoclasts. They concluded that thin-film sputtered HAp could provide a favorable surface for both osteoblast and osteoclast formation and their function, indicating its good osteoconductivity and biodegradability.

Hirota et al. [52] evaluated human osteoblast activity on thin HAp-coated three-dimensional scaffolds made of a titanium fiber web. A thin HAp film was coated on a titanium fiber web by the molecular precursor method. Human osteoblasts were disseminated onto the uncoated and HAp-coated titanium fiber web, and osteoblast activity was observed at days 3, 7, 14, and 21 of culture. Proliferation activities of osteoblasts were significantly higher in the uncoated titanium fiber web. Osteoblasts in the uncoated titanium fiber web showed a typical expression pattern, but those in the HAp-coated titanium fiber web showed rapid OC expression and calcification at an early stage of culture. Moreover, OC expression per osteoblast was significantly higher in the HAp-coated group.

Bodhak et al. [53] examined the influence of surface charge and polarity on in vitro bone cell adhesion, proliferation, and differentiation on electrically polarized HAp-coated Ti. Uniform and crack-free thin-film HAp coatings of 20+/–1.38 μm thickness were polarized by application of an external direct current (DC) field at 400°C for one hour. In vitro bioactivity of polarized HAp coatings was evaluated by soaking in SBF, and bone cell–material interactions were studied by culturing with hFOBs for a maximum period of 11 days. SEM observation showed that accelerated mineralization on negatively charged surfaces favored rapid cell attachment and faster tissue ingrowth over nonpolarized HAp coating surfaces, while a positive charge on HAp coating surfaces restricted apatite nucleation with limited cellular response. Immunochemistry and confocal microscopy confirmed that cell adhesion and early-stage differentiation were more pronounced on negatively charged coating surfaces as hFOB cells expressed higher vinculin and ALP

proteins on a negatively charged surface compared to cells grown on all other surfaces.

The effect of nano-HAp coatings on the in vitro proliferation of SaOS-2 osteoblast-like cells was investigated by Xiong et al. [54] on the surface of a titanium-niobium shape memory alloy. The results showed that in vitro proliferation of the osteoblast-like cells was significantly enhanced on the nano-HAp-coated titanium-niobium alloy compared to the titanium-niobium alloy without a coating. They reported that the cell numbers on the nano-HAp-coated titanium-niobium alloy changed consistently with the surface energy of the HAp coatings. They further postulated that surface energy as a characteristic parameter influencing the in vitro proliferation of osteoblast-like cells was predominant over the crystallinity and surface micro-roughness of the nano-HAp coatings.

Jensen et al. [55] explored the osseointegrational effect of a 50/50 vol% composite of HAp nanoparticles and poly-D,L-lactic acid (PDLLA) coated on model titanium bone implants in an in vivo animal model. The aim is to evaluate how the addition of HAp to PDLLA may improve the bone formation and initial fixation of the implant. Two titanium implants coated with the PDLLA/HAp composite and pure PDLLA, respectively, were implanted bilaterally in the proximal part of humeri with a 2 mm peri-implant gap in 10 sheep. After 12 weeks, the remains of the coatings were present on 20.3% and 19.8% of PDLLA/HAp composite- and PDLLA-coated implants, respectively. It was observed that newly formed bone (39.3%) and fibrous tissue (58.3%) had replaced the PDLLA/HAp composite, whereas pure PDLLA was replaced almost completely by fibrous tissue (96.2%). Consequently, the PDLLA/HAp composite-coated implants were better fixated as confirmed by push-out tests. Using quantification of peri-implant tissue and implant fixation as parameters, the present findings, therefore, clearly reveal that the addition of nanoparticulate HAp to a PDLLA coating on titanium implants increases osseointegration.

Human bone marrow–derived osteoblastic cells were used by Gomes et al. [56] to assess the in vitro biocompatibility of silicon-substituted HAp (Si-HAp) coatings plasma-sprayed over Ti-6Al-4V. Cells attached and grew well on the Si-HAp coatings, putting in evidence increased metabolic activity and ALP expression compared to the control, that is, titanium substrates plasma-sprayed

with HAp. Further, a trend for increased differentiation was also verified by the upregulation of osteogenesis-related genes, as well as by the augmented deposition of globular mineral deposits within established cell layers. The authors concluded that on the basis of the present findings, plasma spraying of Si-HAp coatings over titanium substrates demonstrates improved biological properties regarding cell proliferation and differentiation, comparing to only plasma-coated HAp.

Inoue et al. [57] developed a novel biomaterial called a calcium titanate-amorphous carbon ($CaTiO_3$-aC) coating prepared by a modified thermal decomposition method. They evaluated the effect of $CaTiO_3$-aC and HAp coatings (positive control) and Ti (negative control) on osteoblastic (MT3T3-E1) cell responses. The results showed an increase in cellular proliferation was observed in the $CaTiO_3$-aC coating compared to the HAp coating. The maximum expressions of ALP activity, Col I, and ALP mRNA were higher and achieved in a shorter period of time in the $CaTiO_3$-aC coating compared to others. They concluded that $CaTiO_3$-aC promoted better cell attachment, cellular proliferation, and osteoblastic differentiation compared to HAp, although they ignored that different routes, surface topographies, structures, and chemistries of HAp exist and influence cell differentiation.

Czarnowska et al. [58] examined the properties, bioactivity, and biocompatibility of HAp islets deposited on a new composite layer, Ti_3P+Ti_2Ni type, produced by a duplex method on a Ti-6Al-4V titanium alloy. Their bioactivity were examined in SBF and analyzed with XPS. Biocompatibility was investigated in an osteoblast SaOS-2 line culture in contact with the tested material. Cell proliferation and activity were determined by the 3-[4,5-dimethylthiazol-2-yl]-2,5 diphenyltetrazolium bromide (MTT) test and measurement of ALP activity, respectively. Cell distribution was analyzed under a confocal microscope. The results revealed higher bioactivity and biocompatibility of Ti_3P in comparison to the reference titanium alloy. Biocompatibility analyzed under a confocal microscope in the range of cell adhesion with osteoblast cells of the SaOS-2 line revealed initially the highest osteoblast adhesion on Ti_3P between HAp islets and increasing on HAp during the following days. Cells were characterized by high proliferation and ALP activity.

Zhang et al. [59] determined material and cytocompatibility properties (with osteoblasts) of helical rosette nanotubes (HRNs)/HAp composites on titanium. The results demonstrated enhanced osteoblast adhesion on the HRN/nanocrystalline HAp-coated titanium compared to conventional uncoated titanium. Among all the HRN/nanocrystalline HAp coatings tested, osteoblast adhesion was the greatest when the HAp nanometer particle size was the smallest.

Human osteoprogenitor (HOP) cell adhesion on different titanium surfaces functionalized with HAp, type I collagen (Coll), or Arg-Gly-Asp (RGD)-containing peptides was studied by Le Guillou-Buffello et al. [60] using quartz crystal resonators and by confocal laser scanning microscopy (CLSM) for the imaging of focal contact formation. Data obtained by the quartz crystal resonator technique revealed that RGD-containing peptides alone increase HOP cell adhesion in an early time period of culture. Moreover, association of RGD-containing peptides with either type I collagen or with HAp layers induces an additive effect on HOP cell adhesion compared to Ti-Coll or Ti-HAp. CLSM shows both the area of focal contact by cell unit and the cytoskeleton network organization to differ according to the surfaces. Association of RGD-containing peptides with HAp layers induces an additive effect on focal contact formation on HOP cells compared to Ti-HAp alone. The authors concluded this data confirms that an RGD peptide effect occurs in the early time of culture, which is beneficial for osteoblast spreading, differentiation, and survival.

Nanocomposites consisting of HAp and a sodium maleate copolymer (maleic polyelectrolyte), synthesized by the hydrothermal method and deposited on titanium substrates by the matrix-assisted pulsed laser evaporation (MAPLE) technique, were tested by Negroiu et al. [61] for biological properties. Coating bioanalysis was carried out by triple staining of actin, microtubules, and nuclei, followed by immunofluorescence microscopy. Within 24 hours cells that occupied the biomaterial surface displayed a morphology and cytoskeleton pattern similar to controls. Cells grown on nanocomposite-coated surfaces had a higher proliferation rate than their counterparts grown on Ti coated with HAp alone, indicating that the maleic polyelectrolyte improved surface bioadhesive characteristics.

Zinc-containing fluoridated HAp (ZnFHAp) films on Ti-6Al-4V substrates were prepared by Miao et al. [62] using the sol-gel dip-coating method. The release of zinc ions from the ZnFHAp film was controlled mainly by the zinc content in the film. The release behavior showed an initial rapid increase release followed by a tapering off and directed to a constant value at a longer time. After soaking in SBF for eight days, a layer was deposited and it completely covered the original surface of the ZnFHAp film, indicating good in vitro "bioactivity." The osteoblast-like MG63 cells were seeded on the ZnFHAp films; an FHAp film and a Ti-6Al-4V substrate were used as controls. The cell culture result showed that cell adhesion and proliferation on ZnFHAp films were significantly increased compared to the controls.

Balamurugan et al. [41] investigated the biocompatibility of HAp-based coated titanium implants by implantation studies in a rabbit's tibia for a period of eight weeks. Bone remodeling and inflammatory responses of the implants were studied during the implantation period. Better tissue–implant interaction of coated implants with respect to uncoated implants was observed after a defect-healing period of eight weeks. A coated implant with no evidence of rejection is a further advantage of the sol-gel-derived HAp coating.

Iezzi et al. [63] conducted a histologic and histomorphometric examination of two HAp-plasma-coated titanium implants, retrieved after a loading period of 14 years due to a fracture of the abutment screws. At low-power magnification, it was possible to observe that the HAp coating was in contact with mature bone. No gaps or connective fibrous tissue was found at the implant–bone interface. No epithelial downgrowth was present. No acute or chronic inflammatory cell infiltrate was present at the implant–bone interface. No foreign body reaction was present in the peri-implant tissues. Some osteocytes were in direct contact with the coating. The authors concluded that the HAp coating may produce improved initial stability, an increase in bone–implant contact, and a better load–stress distribution to peri-implant bone.

Sol-gel coatings were developed by Harle et al. [64] on Ti substrates of pure HAp and TiO_2 and two composite forms, HAp+10% TiO_2 and HAp+20% TiO_2, and the biological properties of the coatings were evaluated. All the coating layers exhibited thin and homogeneous structures and phase-pure compositions (either HAp or TiO_2).

Primary human osteoblast cells showed good attachment, spreading, and proliferation on all the sol-gel-coated surfaces, with enhanced cell numbers on all the coated surfaces relative to the uncoated Ti control at day 1, as observed by the MTT assay and SEM. Cell attachment rates were also enhanced on the pure HAp coating relative to control Ti. The pure HAp and HAp+10% TiO_2 composite coating furthermore enhanced proliferation of osteoblasts at four days. Moreover, the gene expression level of several osteogenic markers, including bone sialoprotein and osteopontin, as measured by reverse transcription–polymerase chain reaction (RT-PCR) at 24 hours, was shown to vary according to coating composition.

Zhu et al. [65] investigated cell responses to nano-HAp, nano-HAp/collagen, native, and anodized titanium surfaces. The in vitro studies showed that porous structures produced by anodic oxides on titanium served as positive anchorage sites for cell filopodia to connect, and nano-HAp decreased cell attachment of osteoblasts and induced well-developed long filopodia and broad lamellipodia, thereby enhancing cellular motility. Collagen involvement enhanced cell adhesion to nano-HAp.

Sohn et al. [66] determined the effects of various thin-layer HAp coatings on anodized Ti surfaces on the biological responses of a human osteoblast-like cell line (MG63). MG63 cells were cultured on 100 nm HAp, 500–700 nm HAp, 1 μm Hap, and only anodized Ti. The morphology of these cells was assessed by SEM. The cDNAs prepared from the total RNAs of the MG63 were hybridized into a human cDNA microarray (1152 elements). The appearances of the surfaces observed by SEM were different on each of the four dental substrate types. MG63 cells cultured on 100 nm HAp, 1 μm HAp, and anodized Ti exhibited cell–matrix interactions. It was the 500–700 nm HAp surface showing cell–cell interactions. In the expression of genes involved in osseointegration, several genes, including bone morphogenetic protein 2, latent transforming growth factor beta binding protein 1, catenin (cadherin-associated protein), integrin, PDGFRB, and GDF-1 growth differentiation factor 1, were upregulated on the different surfaces. Several genes, including fibroblast growth factor receptor 3, fibroblast growth factor 12, and CD4, were downregulated on the different surfaces. The attachment and expression of key osteogenic regulatory genes were enhanced by the surface morphology of the dental materials used.

Kim et al. [67] explored properties of films, such as crystallinity and surface roughness, and their effects on the osteoblast-like cell (HOS TE85) responses in vitro. A titanium (Ti) surface was coated with HAp films via the sol-gel method. Their results revealed the attachment, proliferation, and differentiation behaviors of human osteosarcoma HOS TE85 cells were affected by the properties of the films. On films with higher crystallinity, the cells attached and proliferated well and expressed ALP and OC to a higher degree as compared to the poorly crystallized film. On the rough film, cell attachment was enhanced, but the ALP and OC expression levels were similar as compared to smooth films.

Sol-gel processing was used by Sato et al. [68] to coat titanium substrates with HAp, TiO_2, and poly(D,L-lactic-glycolic acid). Coatings were evaluated by cytocompatibility testing with osteoblast-like cells (or bone-forming cells). The cytocompatibility of the HAp composite coatings prepared in the present in vitro study was compared to that of a traditional plasma-sprayed HAp coating. Results showed that osteoblast-like cell adhesion was promoted on the novel HAp sol-gel coating compared to the traditional plasma-sprayed HAp coating. In addition, hydrothermal treatment of the sol-gel coating improved osteoblast-like cell adhesion. They concluded since osteoblast adhesion is a necessary prerequisite for subsequent formation of bone, these results provided evidence that hydrothermally sol-gel-processed HAp may improve bonding of titanium implants to juxtaposed bone.

The biocompatibility of dental implants coated with TiO_2/HAp and TiO_2/bioactive glass (BG) composites obtained via the sol-gel process was examined by Ramires et al. [69] using an in vitro and in vivo model. A device for the in vitro testing of screw-shaped dental implants was developed to well compare the two experimental models studying the behavior of human MG63 osteoblast-like cells seeded onto a particular geometry. The expression of some biochemical parameters of the osteoblastic phenotype (ALP-specific activity, collagen, and OC production) and some indications on cells morphology obtained by SEM were evaluated. The in vitro and in vivo models were compared after implant insertion in rabbit tibia and femur.

The removal torque and histomorphometric parameters (percentage of bone in contact with the implant surface and the

amount of bone inside the threaded area) were examined. The results showed better performance of HAp and BG sol-gel-coated dental implants with respect to uncoated titanium; in particular, it was found that in vitro the HAp coating stimulates osteoblastic cells in producing a higher level of ALP and collagen, whereas in vivo this surface modification resulted in a higher removal torque and a larger bone–implant contact area.

12.7 Mechanical Testing of Thin Films and Coatings

With the ever-increasing demands imposed by the use of implants and devices for dental and medical applications, novel techniques are required to determine their mechanical reliability. Techniques for determining adhesion and mechanical properties have been stimulated by developments of bioinspired coatings such as HAp on metallic substrates. Methods are required to quantitatively determine the mechanical properties of these thin coatings on substrates or freestanding films.

There have been constant improvements and developments in equipment capable of extracting the adhesion of a coating to an underlying substrate, as well as the mechanical properties of the structure or thin films and coatings [70].

12.7.1 Instrumented Nanoindentation

Nanoindentation is the method of choice and starting point of many researchers in the biomedical and dental field for determining the mechanical properties of implants and coatings.

Nanoindentation provides a comprehensive assessment of the mechanical properties of a coating, in addition to the elastic–plastic response from the loading and unloading curves based on the coating–substrate combination (e.g., a soft/hard and rigid/compliant coating on a soft/hard and rigid/compliant substrate). It is now considered a simple and effective way to obtain meaningful values of Young's modulus, E, and hardness, H, coatings at the micro- and nanoscale.

To obtain the best-possible results during nanoindentation, the key requirements are sample preparation, calibration of equipment, and corrections for thermal drift, initial penetration, frame compliance, and indenter tip shape [71–74].

During nanoindentation testing, a set load in the millinewton (mN) range is applied to the indenter in contact with the specimen. As the load is applied, the penetration depth is measured (nanometer range). At maximum load, the area of contact is determined by the depth of the impression and the known angle or radius of the indenter. The result is a load–displacement curve, which yields contact pressure or hardness and Young's modulus from the shape of the unloading curve using software based on the model and indenter type (pointed, i.e., Berkovich, Vickers, Knoop, or spherical) (see Fig. 12.1) [72].

Correspondingly, various kinds of loading and unloading approaches can be employed to extract desired properties as a function of depth of penetration [73–75]. As mentioned by Swain et al. [71–74], the application of nanoindentation can also be directed toward measuring film adhesion and residual stress using direct indentation or transverse scratching.

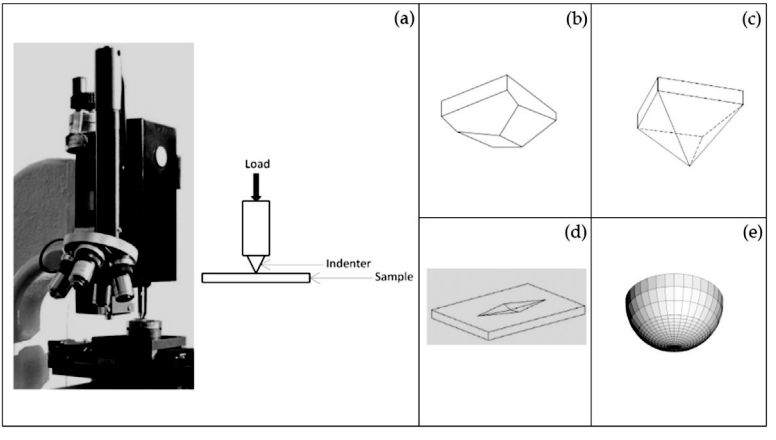

Figure 12.1 (a) Photograph and schematic diagram of a nanoindentation test; (b) a Berkovich indenter; (c) a Vickers indenter; (d) an elongated diamond-shaped indent formed on the sample by a Knoop indenter; and (e) a spherical indenter.

Nanoindenters have been used to determine coating adhesion and residual stress from the load at which delamination occurs (taken from the pop-in that corresponds to a plateau or discontinuity in the load–displacement curve). Nanoindenters can also serve as scratch testers, depending on the capability of the equipment used

[73]. Similarly, creep and viscoelastic behavior can also be examined for softer materials [76, 77] and is particularly appropriate in the study of bone, dental composites/resins, and biological tissues.

The tribomechanical behavior of films produced by alkali treatment (AT) and alkali heat treatment (AHT) on Ti was investigated by de Souza et al. [78] using the instrumented indentation technique. Hardness and elastic modulus profiles were obtained by instrumented indentation. The applied loads ranged from 0.14 mN to 300 mN in 12 successive loading/unloading cycles at increasing loads using a Berkovich diamond indenter. Nanoscratch tests were carried out with the Berkovich tip by the same instrumented indentation device. Ramping loads reached 10 mN, applied for 600 μm following the tip edge direction. Tip penetration profiles were monitored before, during, and after the scratch tests. The profiles during loading and elastic recovery were determined, taking into account the original surface topography.

Diamond-like carbon (DLC) films are favored for wear components because of diamond-like hardness, low friction, low wear, and high corrosion resistance. Hydrogen-free amorphous, tetrahedrally bonded DLC films (ta-C) were deposited by Hinüber et al. [79] at low temperatures by PVD on medical grade Co28Cr6Mo steel and the titanium alloy Ti-6Al-4V. The ta-C coating adhesion to the metal substrates was evaluated using both Rockwell C indentation and scratch testing. During the Rockwell C adhesion test, a cone-shaped diamond tip with a radius of 200 μm and a tip angle of 120° was perpendicularly indented into the coating with a force of 1472 N.

Rau et al. [80] prepared carbonated HAp films on titanium substrates by pulsed laser deposition (PLD) at different substrate temperatures ranging from 30°C to 750°C. Microhardness measurements were performed with a standard Vickers pyramidal indenter (square-based diamond pyramid of a 136° face angle). The loading and unloading speed was 5×10^{-6} m/s, and the time under the peak load was 15 seconds. For hardness measurements on both the carbonated HAp bulk target and the carbonated HAp film/Ti substrate system, indentations were made applying seven loads ranging from 0.2 N up to 9.8 N. For each sample, approximately 10–15 indentations were made at each load.

Micro- and nanotesting methods have been explored by Arias et al. [81] to study thin calcium phosphate coatings with high adhesive strength. The PLD technique was utilized to produce calcium phosphate coatings on metal substrates. Due to the limitations of conventional techniques to evaluate the mechanical properties of these thin coatings (1 μm thick), microscratch testing has been applied to evaluate the coating-to-substrate adhesion and nanoindentation to determine the coating hardness and elastic modulus. The resolutions of load, vertical displacement, and spatial displacement in the *XY* directions were ±75 mN, ±0.04 nm, and ±0.4 μm, respectively. The indentation tests were performed at a constant displacement rate of 20 nm/s under displacement control. The maximum indentation displacement was 0.5 μm. After reaching this maximum value, the load was held constant for 10 seconds before unloading at a rate of 20 nm/s. After unloading 90% of the peak load, the indenter was held for 100 seconds to establish the rate of thermal drift in the machine and in the specimen for the purpose of data correction. Five indentations were performed in each testing area to reduce random errors.

12.8 Concluding Remarks

A major disadvantage of current synthetic implants is their failure to adapt to the local tissue environment. In the dental and orthopedic field, the aim of modifying the surface of metallic materials by coating is to promote biocompatibility and at the same time reduce corrosion and ion release and/or inhibit wear.

Micro- and nanocoatings and surface modification techniques are currently being applied to produce body-interactive materials, which promotes the regeneration of tissues and aids the body in healing, therefore restoring physiological function. Surface coatings offer the possibility of altering the properties of a component and therefore improve both reliability and performance. Currently, various deposition techniques have been used to manufacture bioactive, wear, and/or protective corrosion-resistant coatings on a number of substrates.

During the next decade, there will be an increase in the applications of dental and biomedical materials and devices

containing nanocoatings. These materials and devices containing nanocoatings will be used in implantable materials, bone grafts, biologically active membranes, slow drug delivery systems, and stem cell and biogenic material–containing scaffolds.

The mechanical properties of biomaterial micro- and nanocoatings are strongly governed by the deposition and microstructure of the film, in addition to the influence of interfacial constraints. To determine the properties of the coatings, it is crucial to have accurate nanoscale measurement techniques as these properties can differ from the bulk material. Most of all, better techniques are needed to measure quantitatively the adhesion strength, friction, hardness, and interfacial fracture toughness at the coating–substrate interface.

Instrumented nanoindentation is an essential measuring tool for the characterization of submicron coating properties. A further understanding of mechanical processes involved in these and other tests will help in obtaining valuable information, as well as in identifying the limitations of micro- and nanocoatings.

The relationship between biological responses and surface properties of materials is one of the main issues in biomedical materials research. The modification of surfaces using thin-film deposition has become an important tool for research aimed at understanding how the properties of chemical and structural surfaces influence material–biosystem interactions.

One can expect that surface modifications for the purpose of controlling tissue response will open up avenues for the development of new and superior dental and biomedical implants and devices in a more systematic manner and at a faster rate than at present as better understanding is achieved.

References

1. Ducheyne, P., Radin, S., Heughebaert, M., Heughebaert, J. C. (1990) Effect of calcium phosphate ceramic coatings on porous titanium: effect of structure and composition on electrophoretic deposition, vacuum sintering and in vitro dissolution, *Biomaterials*, **11**, 244–254.
2. Hench, L. L., West, J. K. (1990) The sol–gel process, *Chem. Rev*., **90**, 33–72.
3. Kokubo, T., Kim, H. M., Kawashita, M., Nakamura, T. (2000) Novel ceramics for biomedical applications, *J. Aust. Ceram. Soc.,* **36**, 37–46.

4. Ben-Nissan, B., Choi, A. H. (2010) Nanoceramics for Medical Applications, in *Advanced Nanomaterials*, 523–553 (Ed. Geckeler N.), Wiley-VCH Verlag, Germany.
5. Ben-Nissan, B., Chai, C. S. (1995) Sol–gel derived bioactive hydroxyapatite coatings, in *Advances in Materials Science and Implant Orthopedic Surgery*, 265–275, NATO ASI Series, Series E: Applied Sciences (Ed. Kossowsky R., Kossovsky N.), Vol. 294, Kluwer Academic Publishers.
6. Chang, M. C., Ko, C. C., Douglas, W. H. (2003) Preparation of hydroxyapatite-gelatin nanocomposite, *Biomaterials*, **24**, 2853–2862.
7. Vinogradov, S. V., Bronich, T. K., Kabanov, A. V. (2002) Nanosized cationic hydrogels for drug delivery: preparation, properties and interactions with cells, *Adv. Drug Delivery Rev*., **54**, 135–147.
8. Ben-Nissan, B., Choi, A. H. (2006) Sol–gel production of bioactive nanocoatings for medical applications: part I: an introduction, *Nanomedicine*, **1**, 311–319.
9. Choy, K. L. (2003) Chemical vapour deposition of coatings, *Prog. Mater. Sci.*, **48**, 57–170.
10. Ben-Nissan, B., Latella, B. A., Bendavid, A. (2011) Biomedical thin films: mechanical properties, in *Comprehensive Biomaterials*, 63–73 (Ed. Ducheyne P., Healy K. E., Hutmacher D. W., Grainger D. W., Kirkpatrick C. J.), Elsevier.
11. Kirk, P., Pilliar, R. (1999) The deformation response of sol–gel-derived thin films on 316L stainless steel using a substrate straining test, *J. Mater. Sci*., **34**, 3967–3975.
12. Chen, T. S., Lacefield, W. R. (1994) Crystallisation of ion beam deposited calcium phosphate coatings, *J. Mater. Res*., **9**, 1284–1296.
13. Anast, M., Bell, J., Bell, T., Ben-Nissan, B. (1992) Precision ultra-microhardness measurements of sol–gel derived zirconia thin films, *J. Mater. Sci. Lett.*, **11**, 1483–1485.
14. Roest, R., Eberhardt, A. W., Latella, B. A., Wuhrer, R., Ben-Nissan, B. (2004) Adhesion of sol–gel derived zirconia nano-coatings on surface treated titanium, *Key Eng. Mater.*, **254–256**, 455–458.
15. Ebelmen, J. (1846) Untersuchungen über die Verbindung der Borsaure und Kieselsaure mit Aether, *Ann. Chim. Phys. Ser.*, **57**, 319–355 (in German).
16. Geffcken, W., Berger, E. (1939) Änderung des Reflexionsvermogens Optischer Gläser. German Patent 736411 (in German).

17. Roy, D. M., Roy, R. (1954) An experimental study of the formation and properties of synthetic sepentines and related layer silicates, *Am. Mineral.,* **39**, 957–975.

18. Schroeder, H. (1965) Water-dispersed industrial and architectural coatings, *Paint Varnish Prod.*, **55**, 31–46.

19. Chai, C., Ben-Nissan, B., Pyke, S., Evans, L. (1995) Sol–gel derived hydroxyapatite coatings for biomedical applications, *Mater. Manuf. Process.*, **10**, 205–216.

20. Mazdiyasni, K. S. (1982) Powder synthesis form metal–organic precursors, *Ceram. Int.*, **8**, 42–56.

21. Sakka, S., Kamiya, K., Makita, K., Tamamoto, Y. (1984) Formation of sheets and coating films from alkoxide solutions, *J. Non-Cryst. Solids*, **63**, 223–235.

22. Yoldas, B. E. (1984) Wide-spectrum anti-reflective coatings for fused silica and other glasses, *Appl. Opt.*, **23**, 1418.

23. Roy, R. (1987) Ceramics by the solution–sol–gel route, *Science*, **238**, 1664–1669.

24. Klein, L. C. (1989) *Sol–Gel Technology for Thin Films, Fibers, Preforms, Electronics and Specialty Shapes*, 1st ed., Noyes Publishing, USA.

25. Scriven, L. E. (1988) Physics and application of dip coating and spin coating, *Mater. Res. Soc. Symp. Proc.*, **121**, 717–729.

26. Brinker, C. J., Clark, D. E. (1988) *Better Ceramics Through Chemistry*, 3rd ed., Materials Research Society, USA.

27. Brinker, C. J., Scherer, G. W. (1990) *Sol-Gel Science: The Physics and Chemistry of Sol–Gel Processing*, 1st ed., Academic Press, USA.

28. Floch, H. G., Belleville, P. F., Priotton, J. J., Pegon, P. M., Dijonneau, C. S., Guerain, J. (1995) Sol–gel optical coatings for lasers, *Int. Am. Ceram. Soc. Bull.*, **74**, 60–63.

29. Percy, M. J., Bartlett, J. R., Spiccia, L., West, B. O., Woolfrey, J. L. (2000) The influence of b–diketones on hydrolysis and particle growth from zirconium (IV) N-propoxide in n-propanol, *J. Sol–Gel Sci. Technol.*, **19**, 315–319.

30. de Kambilly, H., Klein, L. C. (1989) Effect of methanol concentration on lithium aluminosilicates, *J. Non-Cryst. Solids*, **109**, 69–78.

31. Harris, M. T., Byers, C. H., Brunson, R. R. (1988) A Study of Solvent Effects on the Synthesis of Pure Component and Composite Ceramic Powders by Metal Alkoxide Hydrolysis, *Mater. Res. Soc. Symp. Proc.,* **121**, 287–292.

32. Choi, A. H., Ben-Nissan, B. (2007) Sol–gel production of bioactive nanocoatings for medical applications: part II: current research and development, *Nanomedicine*, **2**, 51–61.

33. Ben-Nissan, B., Milev, A., Vago, R. (2004) Morphology of sol-gel derived nano-coated coralline hydroxyapatite, *Biomaterials*, **25**, 4971–4976.

34. Qu, J., Lu, X., Li, D., Ding, Y., Leng, Y., Weng, J., Qu, S., Feng, B., Watari, F. (2011) Silver/hydroxyapatite composite coatings on porous titanium surfaces by sol-gel method, *J. Biomed. Mater. Res. B: Appl. Biomater.*, **97**, 40–48.

35. Li, Y., Li, Q., Zhu, S., Luo, E., Li, J., Feng, G., Liao, Y., Hu, J. (2010) The effect of strontium-substituted hydroxyapatite coating on implant fixation in ovariectomized rats, *Biomaterials.*, **31**, 9006–9014.

36. Un, S., Durucan, C. (2009) Preparation of hydroxyapatite-titania hybrid coatings on titanium alloy, *J. Biomed. Mater. Res. B: Appl. Biomater.*, **90**, 574–583.

37. Wu, C., Ramaswamy, Y., Gale, D., Yang, W., Xiao, K., Zhang, L., Yin, Y., Zreiqat, H. (2008) Novel sphene coatings on Ti-6Al-4V for orthopedic implants using sol-gel method, *Acta Biomater.*, **4**, 569–576.

38. Miao, S., Cheng, K., Weng, W., Du, P., Shen, G., Han, G., Yan, W., Zhang, S. (2008) Fabrication and evaluation of Zn containing fluoridated hydroxyapatite layer with Zn release ability, *Acta Biomater.*, **4**, 441–446.

39. Cheng, K., Zhang, S., Weng, W. (2007) Surface characterization of colloidal-sol gel derived biphasic HA/FA coatings, *J. Mater. Sci. Mater. Med.*, **18**, 2011–2015.

40. Wen, C. E., Xu, W., Hu, W. Y., Hodgson, P. D. (2007) Hydroxyapatite/titania sol-gel coatings on titanium-zirconium alloy for biomedical applications, *Acta Biomater.*, **3**, 403–410.

41. Balamurugan, A., Rebelo, A., Kannan, S., Ferreira, J. M., Michel, J., Balossier, G., Rajeswari, S. (2007) Characterization and in vivo evaluation of sol-gel derived hydroxyapatite coatings on Ti6Al4V substrates, *J. Biomed. Mater. Res. B: Appl. Biomater.*, **81**, 441–447.

42. Hijón, N., Victoria Cabañas, M., Peña, J., Vallet-Regí, M. (2006) Dip coated silicon-substituted hydroxyapatite films, *Acta Biomater.*, **2**, 567–574.

43. Kim, H. W., Lee, E. J., Jun, I. K., Kim, H. E. (2005) On the feasibility of phosphate glass and hydroxyapatite engineered coating on titanium, *J. Biomed. Mater. Res. A*, **75**, 656–667.

44. Gan, L., Wang, J., Pilliar, R. M. (2005) Evaluating interface strength of calcium phosphate sol-gel-derived thin films to Ti6Al4V substrate, *Biomaterials*, **26**, 189–196.

45. Gross, K. A., Muller, D., Lucas, H., Haynes, D. R. (2012) Osteoclast resorption of thermal spray hydoxyapatite coatings is influenced by surface topography, *Acta Biomater*., **8**, 1948–1956.

46. Ravichandran, R., Ng, C. C., Liao, S., Pliszka, D., Raghunath, M., Ramakrishna, S., Chan, C. K. (2012) Biomimetic surface modification of titanium surfaces for early cell capture by advanced electrospinning, *Biomed. Mater*., **7**, 015001.

47. Zhao, S. F., Jiang, Q. H., Peel, S., Wang, X. X., He, F. M. (2013) Effects of magnesium-substituted nanohydroxyapatite coating on implant osseointegration, *Clin. Oral Implants Res*., doi: 10.1111/j. 1600–0501.2011.02362.x.

48. Chung, C. J., Long, H. Y. (2011) Systematic strontium substitution in hydroxyapatite coatings on titanium via micro-arc treatment and their osteoblast/osteoclast responses, *Acta Biomater*., **7**, 4081–4087.

49. Roy, M., Bandyopadhyay, A., Bose, S. (2011) Induction plasma sprayed Sr and Mg doped nano hydroxyapatite coatings on Ti for bone implant, *J. Biomed. Mater. Res. B: Appl. Biomater.*, **99**, 258–265.

50. Dimitrievska, S., Bureau, M. N., Antoniou, J., Mwale, F., Petit, A., Lima, R. S., Marple, B. R. (2011) Titania-hydroxyapatite nanocomposite coatings support human mesenchymal stem cells osteogenic differentiation, *J. Biomed. Mater. Res. A*, **98**, 576–588.

51. Hao, J., Kuroda, S., Ohya, K., Bartakova, S., Aoki, H., Kasugai, S. (2011) Enhanced osteoblast and osteoclast responses to a thin film sputtered hydroxyapatite coating, *J. Mater. Sci. Mater. Med*., **22**, 1489–1499.

52. Hirota, M., Hayakawa, T., Ametani, A., Kuboki, Y., Sato, M., Tohnai, I. (2011) The effect of hydroxyapatite-coated titanium fiber web on human osteoblast functional activity, *Int. J. Oral Maxillofac. Implants*, **26**, 245–250.

53. Bodhak, S., Bose, S., Bandyopadhyay, A. (2010) Electrically polarized HAp-coated Ti: in vitro bone cell-material interactions, *Acta Biomater*., **6**, 641–651.

54. Xiong, J., Li, Y., Hodgson, P. D., Wen, C. (2010) In vitro osteoblast-like cell proliferation on nano-hydroxyapatite coatings with different morphologies on a titanium-niobium shape memory alloy, *J. Biomed. Mater. Res. A*, **95**, 766–773.

55. Jensen, T., Jakobsen, T., Baas, J., Nygaard, J. V., Dolatshahi-Pirouz, A., Hovgaard, M. B., Foss, M., Bünger, C., Besenbacher, F., Søballe, K. (2010)

Hydroxyapatite nanoparticles in poly-D,L-lactic acid coatings on porous titanium implants conducts bone formation, *J. Biomed. Mater. Res. A*, **95**, 665–672.

56. Gomes, P. S., Botelho, C., Lopes, M. A., Santos, J. D., Fernandes, M. H. (2010) Evaluation of human osteoblastic cell response to plasma-sprayed silicon-substituted hydroxyapatite coatings over titanium substrates, *J. Biomed. Mater. Res. B: Appl. Biomater.*, **94**, 337–346.
57. Inoue, M., Rodriguez, A. P., Takagi, T., Katase, N., Kubota, M., Nagai, N., Nagatsuka, H., Inoue, M., Nagaoka, N., Takagi, S., Suzuki, K. (2010) Effect of a new titanium coating material ($CaTiO_3$-aC) prepared by thermal decomposition method on osteoblastic cell response, *J. Biomater. Appl.*, **24**, 657–672.
58. Czarnowska, E., Zajaczkowska, A., Godlewski, M. M., Mroz, W., Sobczak, J. W., Wierzchon, T. (2009) Combination of hydroxyapatite islets with Ti3P surface layer produced on titanium alloy for bone implants, *J. Nanosci. Nanotechnol.*, **9**, 3462–3468.
59. Zhang, L., Chen, Y., Rodriguez, J., Fenniri, H., Webster, T. J. (2008) Biomimetic helical rosette nanotubes and nanocrystalline hydroxyapatite coatings on titanium for improving orthopedic implants, *Int. J. Nanomed.*, **3**, 323–333.
60. Le Guillou-Buffello, D., Bareille, R., Gindre, M., Sewing, A., Laugier, P., Amédée, J. (2008) Additive effect of RGD coating to functionalized titanium surfaces on human osteoprogenitor cell adhesion and spreading, *Tissue Eng. A*, **14**, 1445–1455.
61. Negroiu, G., Piticescu, R. M., Chitanu, G. C., Mihailescu, I. N., Zdrentu, L., Miroiu, M. (2008) Biocompatibility evaluation of a novel hydroxyapatite-polymer coating for medical implants (*in vitro* tests), *J. Mater. Sci. Mater. Med.*, **19**, 1537–1544.
62. Miao, S., Weng, W., Cheng, K., Du, P., Shen, G., Han, G., Huang, X., Yan, W., Zhang, S. (2007) *In vitro* bioactivity and osteoblast-like cell test of zinc containing fluoridated hydroxyapatite films, *J. Mater. Sci. Mater. Med.*, **18**, 2101–2105.
63. Iezzi, G., Scarano, A., Petrone, G., Piattelli, A. (2007) Two human hydroxyapatite-coated dental implants retrieved after a 14-year loading period: a histologic and histomorphometric case report, *J. Periodontol.*, **78**, 940–947.
64. Harle, J., Kim, H. W., Mordan, N., Knowles, J. C., Salih, V. (2006) Initial responses of human osteoblasts to sol-gel modified titanium with hydroxyapatite and titania composition, *Acta Biomater.*, **2**, 547–556.

65. Zhu, X., Eibl, O., Scheideler, L., Geis-Gerstorfer, J. (2006) Characterization of nano hydroxyapatite/collagen surfaces and cellular behaviors, *J. Biomed. Mater. Res. A*, **79**, 114–127.

66. Sohn, S. H., Jun, H. K., Kim, C. S., Kim, K. N., Chung, S. M., Shin, S. W., Ryu, J. J., Kim, M. K. (2006) Biological responses in osteoblast-like cell line according to thin layer hydroxyapatite coatings on anodized titanium, *J. Oral Rehabil.*, **33**, 898–911.

67. Kim, H. W., Kim, H. E., Salih, V., Knowles, J. C. (2005) Sol-gel-modified titanium with hydroxyapatite thin films and effect on osteoblast-like cell responses, *J. Biomed. Mater. Res. A*, **74**, 294–305.

68. Sato, M., Slamovich, E. B., Webster, T. J. (2005) Enhanced osteoblast adhesion on hydrothermally treated hydroxyapatite/titania/poly(lactide-co-glycolide) sol-gel titanium coatings, *Biomaterials*, **26**, 1349–1357.

69. Ramires, P. A., Wennerberg, A., Johansson, C. B., Cosentino, F., Tundo, S., Milella, E. (2003) Biological behavior of sol-gel coated dental implants, *J. Mater. Sci. Mater. Med.*, **14**, 539–545.

70. Ben-Nissan, B., Pezzotti, G. (2002) Bioceramics: processing routes and mechanical evaluation, *J. Ceram. Soc. Japan*, **110**, 601–608.

71. Field, J. S., Swain, M. V. (1993) A simple predictive model for spherical indentation, *J. Mater. Res.*, **8**, 297–306.

72. Field, J. S., Swain, M. V. (1995) Determining the mechanical properties of small volumes of material from submicrometer spherical indentations, *J. Mater. Res*., **10**, 101–112.

73. Gan, L., Ben-Nissan, B., Ben-David, A. (1996) Modelling and finite element analysis of ultra-microhardness indentation of thin films, *Thin Solid Films*, **290–291**, 362–366.

74. Fischer-Cripps, A. C. (2002) *Introduction to Nanoindentation*, Springer, New York.

75. Gan, L., Ben-Nissan, B. (1997) The effect of mechanical properties of thin films on nano-indentation data: finite element analysis, *Comput. Mater. Sci.*, **8**, 273–281.

76. Fischer-Cripps, A. C. (2004) A simple phenomenological approach to nanoindentation creep, *Mater. Sci. Eng. A*, **385**, 74–82.

77. Latella, B. A., Gan, B. K., Barbé, C. J., Cassidy, D. J. (2008) Nanoindentation hardness, Young's modulus, and creep behavior of organic–inorganic silica-based sol–gel thin films on copper, *J. Mater. Res.,* **23**, 2357–2365.

78. de Souza, G. B., Lepienski, C. M., Foerster, C. E., Kuromoto, N. K., Soares, P., de Araújo Ponte, H. (2011) Nanomechanical and nanotribological

properties of bioactive titanium surfaces prepared by alkali treatment, *J. Mech. Behav. Biomed. Mater.,* **4**, 756–765.

79. Hinüber, C., Kleemann, C., Friederichs, R. J., Haubold, L., Scheibe, H. J., Schuelke, T., Boehlert, C., Baumann, M. J. (2010) Biocompatibility and mechanical properties of diamond-like coatings on cobalt-chromium-molybdenum steel and titanium-aluminum-vanadium biomedical alloys, *J. Biomed. Mater. Res. A*, **95**, 388–400.
80. Rau, J. V., Generosi, A., Laureti, S., Komlev, V. S., Ferro, D., Cesaro, S. N., Paci, B., Albertini, V. R., Agostinelli, E., Barinov, S. M. (2009) Physicochemical investigation of pulsed laser deposited carbonated hydroxyapatite films on titanium, *ACS Appl. Mater. Interface*, **1**, 1813–1820.
81. Arias, J. L., Mayor, M. B., Pou, J., Leng, Y., León, B., Pérez-Amor, M. (2003) Micro- and nano-testing of calcium phosphate coatings produced by pulsed laser deposition, *Biomaterials*, **24**, 3403–3408.

This page intentionally left blank

Chapter 13

Internal Fixation in Oral and Maxillofacial Surgery

Roger A. Zwahlen
Faculty of Dentistry, Oral & Maxillofacial Surgery, University of Hong Kong, Prince Philip Dental Hospital, 34 Hospital Road, Sai Ying Pun, Hong Kong SAR, People's Republic of China
zwahlen@hku.hk

This chapter provides a survey of titanium, today's most frequently used material in oral and maxillofacial surgery for internal fixation of fractures and osteotomies, as well as to bridge bone defects after tumor resections in the form of plates and screws. The chapter is introduced with a survey of bone morphology, healing, and characteristics of facial bones. Surgical treatment changes due to the advent of plates and screws are highlighted. The development of nonresorbable materials for internal fixation is described in chronological order; their concomitant adverse effects are pointed out. Titanium as the current number one rigid internal fixation material relishes a closer insight. First a summary of its chemical and mechanical properties as well as a brief discussion about

Handbook of Oral Biomaterials
Edited by Jukka P. Matinlinna

ISBN 978-981-4463-12-6 (Hardcover), 978-981-4463-13-3 (eBook)
www.panstanford.com

its biocompatibility are presented. After a survey about clinical applications of titanium plates and screws in oral and maxillofacial surgery, the to date resorbable alternative material poly (α-hydroxyacid) is shortly presented. Plates and screws of this material are mainly used in craniofacial surgery.

13.1 Introduction

Related to reconstructive procedures after fractures and tumor resections, the oral and maxillofacial area represents a challenge both to surgeons and to material.

Due to the following reasons surgeons have to choose the most appropriate biocompatible material for internal fixation: firstly bone structures vary from thin and delicate in the midfacial region to thick and hard in the mandibular cranial regions, secondly biting and chewing forces represent mechanical stresses to materials being used for internal fixation, and thirdly, in many oral and maxillofacial regions internal fixation materials are only covered by thin, soft tissue layers [1].

Due to its mechanical and chemical properties, its relative low toxicity, and sensitization titanium represents since the mid-1980s a reliable and safe material to master these challenges [2, 3].

13.1.1 Bone

Bone is the supporting tissue of our body, which determines its form and size. Its hardness is mainly a result of its 65% nonorganic content of hydroxyapatite. However, due to the high amount of collagen, which accounts to around 95% of the organic matrix, bone is elastic. Every impact of force that exceeds the bone's own elasticity results in a break, called fracture. It is important to know that bone is a dynamic tissue with a usually balanced apposition and resorption rate. This balance is steered by physiological and mechanical factors.

According to their localization, facial bones vary in thickness and strength. Whereas thick in the mandible and frontal areas, lamella-like thin bones are found in the midfacial area; these are integrated in a honeycomb-like framework of bony pillars.

13.1.2 Bone Healing

13.1.2.1 Indirect bone healing

As bone is a dynamic tissue, it can unite without surgical treatment, as long as covering soft tissues, nerves, and blood vessels are intact and the fractured bone ends are not too much dislocated. The initial hematoma in the fracture gap is substituted by fibrous tissue, which later will transform over cartilage into bone. This bone healing by callus formation is called indirect bone healing or "healing by second intention." As no surgical measures are applied to reposition and fix the nondislocated fractured bones, this type of bone healing goes along with temporary impairment of function. Another shortcoming may be deformation due to steady movement caused by muscle pull simultaneously to the healing process [4].

An example of such type of bone healing in the head region is an intracapsular condylar head fracture.

13.1.2.2 Direct bone healing

Surgical fracture management with osteosynthesis tackles the above-mentioned shortcomings inherent to indirect fracture healing. With the patient under general or partial anesthesia open reduction of dislocated fractures with internal fixation is performed.

Thereby two types of bone healing occur:

(1) On site with direct contact via Haversian remodeling
(2) In two steps via sagittal bone apposition and Haversian remodeling at gap sites [5]

This bone healing by the first intention is not quicker than the multiple-step healing on the second intention but is more efficient per unit than a callus [4].

13.1.3 Osteosynthesis

Various auxiliary fixation devices have already been in use in facial fractures to promote bone healing by immobilizing fracture pieces and/or osteotomies.

In the 1970s Halo frames fixed to the outer table of the skull were used as an anchorage platform for vertical rods and cheek wires to

suspend midfacial bones [6, 7]. This extraoral fixation technique has been replaced by frontomaxillary suspensions [8, 9] where partial or total dental splints and/or continuous dental wires were suspended with steel wires to the nonfractured frontal bone or zygomatic arches. Additional mandibulomaxillary fixation (MMF) yielded the basis for the necessary immobilization to promote bone healing within a time frame of six weeks.

The first intraoral internal fixations were performed with steel wire loops [10, 11]. Because wires provided little immobilization, a six-week retention phase had to be granted for adequate bone healing. Wire techniques required a longer hospitalization period and led to longer-lasting postoperative impaired function of patients [12].

Albin Lambotte, a Belgian, was one of the pioneers of internal fixation. In his book [13] he used the term "osteosynthesis" for the first time ever. A closer study of problems related to bone healing, its relation to rigid internal fixation was finally initiated by a group of Swiss orthopedic surgeons in 1958. This group founded the Arbeitsgemeinschaft für Osteosynthesefragen/Association for the Study of Internal Fixation (AO/ASIF).

Their continuous engagement in basic and clinical research regarding bone healing and internal fixation [5, 14, 15], together with pioneers from Germany (Luhr) and France (Michelet, Champy), led in the sixties and seventies of the last century to the two concepts of bone compression responsible for direct fracture healing:

- **Concept of static compression**: The advent of open reduction and rigid internal fixation with compression plates and screws [16, 17] at the mandibular inferior border increased the immobilization degree of fractured mandibles. Prein et al. already in 1976 used successfully noncompression reconstruction plates to bridge and stabilize comminuted, infected, and atrophic mandibular fractures [18].
- **Concept of dynamic compression**: The osteosynthesis technique using miniplates and monocortical screws, first described by Michelet et al. [19] was modified by Champy et al. [20]. The latter applied miniplates on the zero line (Fig. 13.1) of the mandible between strain and pressure forces.

Miniplates further facilitated three-dimensional reconstruction possibilities of struts that compose the honeycomb-like framework of the midface [1].

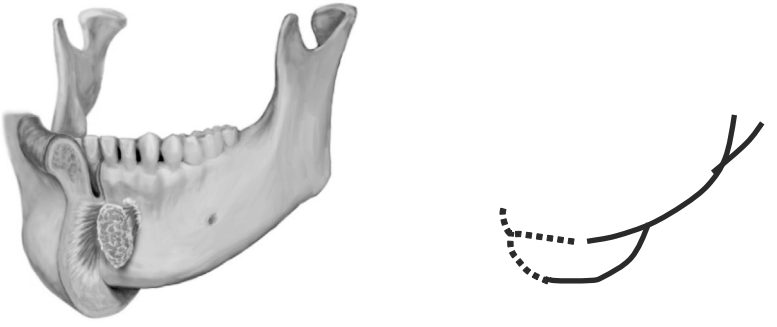

Figure 13.1 Concept of the zero line of the mandible.

Apart from these technical advantages in the midface, the monocortical concept (1) achieves a degree of immobilization that withstands deforming biomechanical forces or can use them to stabilize fracture fragments or osteotomies, (2) allows loading as far as to permit postoperative functional treatment without MMF, and (3) can be used also in areas with rather thin covering soft tissue, such as the frontozygomatic suture or infraorbital rim.

13.2 Titanium

Over time different nonresorbable materials have been used to achieve functionally stable osteosyntheses.

Today titanium alloys represent the most frequently used nonresorbable metal implants for fracture fixation. These alloys provide an almost optimal combination of mechanical properties, corrosion resistance, and biocompatibility. Titanium is also discussed in Chapters 9, 10, and 12.

13.2.1 Mechanical Properties

Three microstructure types of titanium alloys are known [21]:

(1) α-titanium (commercial pure = c.p. titanium): Hexagonal lattice structure, stable up to 882°C; At >882°C this structure turns into a cubic face-centered pattern (=β-titanium). At <882°C this **titanium needs to be stabilized by adding alloying elements**.

(2) α- + β-titanium (Ti-6Al-4V; Ti-6Al-7Nb; Ti-6Al-4V).
(3) β-titanium (Ti-15Mo; Ti-15Mo-5Zr-3Al).

All alloys have outstanding corrosion and erosion resistance as well as excellent strength-to-weight ratios. They all account for good toughness, strength, and high ductility [22].

Whereas tensile properties like ultimate tensile strength, yield strength, elongation, and reduction of area are similar in α- + β-titanium grades, β-titanium alloys are of less strength but of better ductility, providing therefore better contouring to fit shapes [21, 23].

Compared to other nonresorbable materials, titanium exhibits an elastic modulus closer to the one of bone. Due to this material characteristic local intraosseous stress concentrations are reduced [21], resulting in increased fatigue resistance of titanium.

13.2.2 Biocompatibility

Titanium is described to have excellent biocompatibility showing beneficial tissue reactions and being nonallergic. Its exceptional corrosion resistance is based on the titanium dioxide layer, which is formed spontaneously in the presence of oxygen. This titanium dioxide film regenerates instantaneously after mechanical wear, such as plate contouring and screw-to-plate contact while fixing the plate to the bone [21].

To improve its mechanical properties and biocompatibility, titanium has been alloyed with nontoxic and nonallergic metals. Ti-6Al-4V became the primary titanium alloy for trauma and reconstructive procedures. However, already in the 1980s and 1990s reports came up regarding the in vitro and in vivo toxicity of vanadium (V) [24–26], leading to substitution of vanadium by niobium (Nb). Further toxic findings of aluminum in the 1990s [27] brought up the manufacture of Al- and V-free Ti-Zr- or Ti-Sn-based alloys of the group of β-titanium alloys, alloys with a lower modulus of elasticity and improved strength [28] (see also Chapter 10).

13.2.3 Clinical Applications

The electrochemical process of anodization can create protective titanium oxide layers because light diffraction varies as a result of

layer thickness. In their product range, companies use resulting color effects to distinguish plates and screws regarding various sizes and applications [21].

Another advantage lies in the nonmagnetic response of titanium alloys [23], which firstly leads to less artifacts in magnetic resonance imaging (MRI) and secondly is of advantage for the use of titanium alloy instruments for operations using open MRI.

Titanium alloy permits manufacturing of tiny and thin plates and screws that still are strong enough to withstand torsion forces and enable therefore undisturbed bone-healing processes. Clinically this is of importance in children [29] as well as in particular facial areas of adults, such as nasoethmoidoorbital, infraorbital, supraorbital, and the zygomatic arch where bone is covered only with thin soft tissue layers.

The following section 1.3 will highlight shortly the most important application purposes of titanium alloy plates and screws as a means of internal fixation of bones in oral and maxillofacial surgery.

13.3 Oral and Maxillofacial Surgery

13.3.1 Clinical Applications in Oral and Maxillofacial Fractures

A fracture can be defined as a discontinuation of bone due to direct or indirect impact of energy that exceeds the body's own elasticity. Clinically every fracture is characterized by dislocation, pathological mobility, and crepitation. The aim of every open fracture treatment is the anatomically exact reposition of the fracture fragments and their stable internal fixation. In facial fractures extending into tooth-bearing jaws, however, firstly attention has to be paid to reestablish the habitual occlusion by means of, for example, continuous wiring (Fig. 13.2) and MMF. Thereafter open reduction and internal fixation of the bone fragments can be performed.

Fracture dislocation may occur both due to the impact directly and due to muscle pull, especially in the mandible where strong masticatory muscles insert. If reposition is not performed before fixation and retention, bone healing occurs in malposition.

Pathological mobility of the fracture ends will lead to delayed bone healing, sometimes with the development of a pseudoarthrosis, which is a nonosseous healing between the fracture ends.

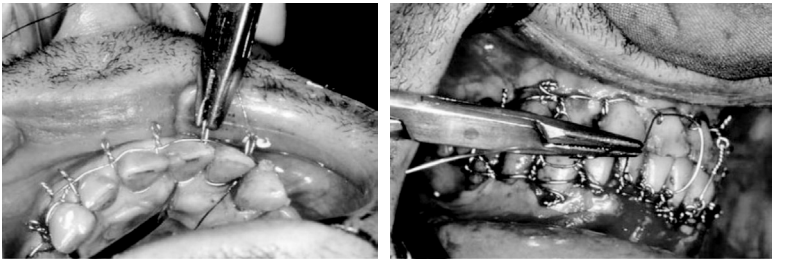

Figure 13.2 (a) Continuous wiring of the upper and lower jaws. (b) MMF before open reduction and internal fixation.

The development of titanium alloy plates and screws has become a capstone in fracture management. After reposition they permit internal rigid or semirigid fixation of fractures, leading to undisturbed bone healing, something especially important in the face, which represents a unique part of the body in interpersonal communication.

13.3.1.1 Mandibular fractures

Due to its location, projection, and mobility the mandible is frequently involved in facial trauma.

Anatomically the mandible is a parabolic tubular bone with a cortical shell and a cancellous core in which lies the inferior alveolar nerve as well as alveolar sockets. It consists of the mandibular body and the alveolar bone on top of it, which is growing cranially during the eruption of permanent teeth.

According to the dimension of impact different fracture patterns of the bone may occur, starting from simple to compound to comminuted, where greater forces lead to multiple fragmentation of the bone.

It goes without saying that plate and screw dimensions need to be chosen according to the particular fracture pattern in order to obtain necessary stabilization to guarantee undisturbed bone healing after open reposition and internal fixation.

- *Simple and compound fractures*
  In these fracture patterns usually the load-sharing concept of internal fixation can be applied. Due to the widely intact bone structure of the mandible near the fracture site the total load during bone healing can be distributed between bone and plate. Therefore smaller-dimensioned plates and screws can be applied via the intraoral approach, such as miniplates and monocortical screws 1.5–2.0 mm in diameter. Whereas Figs. 13.3a and 13.3b highlight the radiographic images of a twofold fracture of the mandible, condylar and parasymphysal, before and after open reposition and internal fixation with 2.0 miniplates, Fig. 13.4 shows a 2.0 miniplate set.

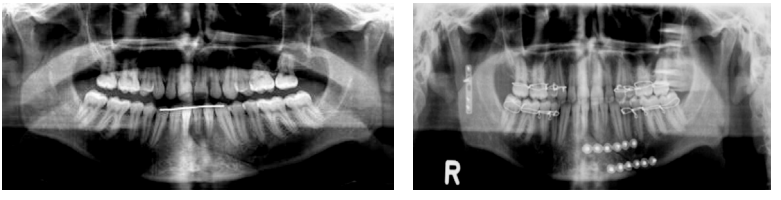

Figure 13.3 Simple and compound fractures of the mandible (a) before and (b) after open reposition and internal fixation.

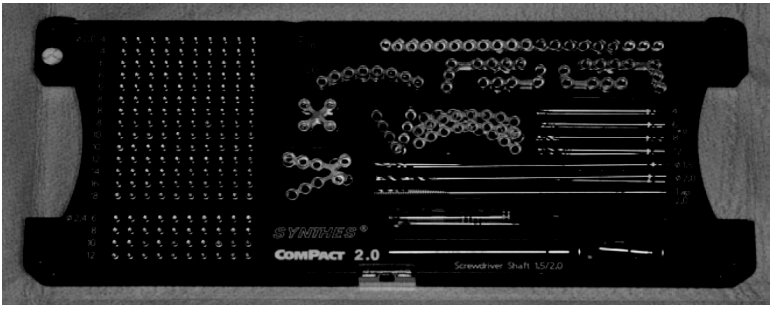

Figure 13.4 Osteosynthesis set with miniplates and screws, system 2.0.

- *Comminuted fractures*
  In these fracture patterns usually the load-bearing concept of internal fixation is applied. Bigger-dimensioned plates, unilock reconstruction plates, with bicortical screws 2.3–3 mm in diameter are used in such situations, fixated with screws conceptualized for bicortical fixation. Such plates and screws bear the whole load during jaw function. The plate holes have internal threads, which match the threads

of the screw heads. Because of this, holes have to be drilled perpendicularly to the plate using a drill guide that is screwed in the plate holes before drilling. The screw length has to be defined using a depth gauge.

Because of the bicortical contact of the screws and the tight fixation between the screw heads within the plate holes, the unilock reconstruction plate does not need to be fully adapted to the bone surface. Therefore this plate system can be considered as an "internal" external fixator. This is especially suitable in comminuted mandibular fractures, as it reduces the plate's pressure onto the periosteal layer over comminuted fractures zones and, therefore, as a consequence, leads to less jeopardize of the perfusion of the comminuted zone. Figure 13.5a,b presents a comminuted mandibular fracture with manifold simple and compound fractures. In the postoperative orthopantomographic (OPT) radiograph, Fig. 13.6a,b a unilock reconstruction plate is visible in situ with several other miniplates and a microplate. The unilock reconstruction plate bridges the comminuted zone in the region of the chin. In this zone the periosteal layer is not detached from the multiple small bone segments, which prevents further compromise of blood perfusion. Figure 13.7a,b shows a survey of a unilock osteosynthesis set and detailed parts of it.

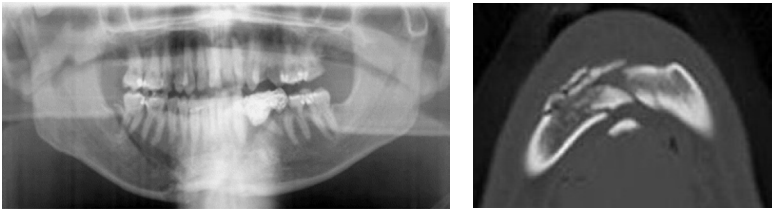

Figure 13.5 A comminuted fracture of the mandible. (a) OPT and (b) axial CT view. *Abbreviation*: CT, computed tomography.

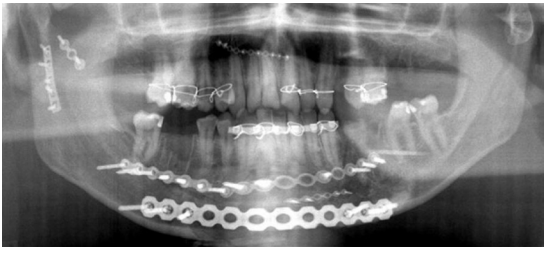

Figure 13.6 Reconstruction plate spanning the comminuted fracture site.

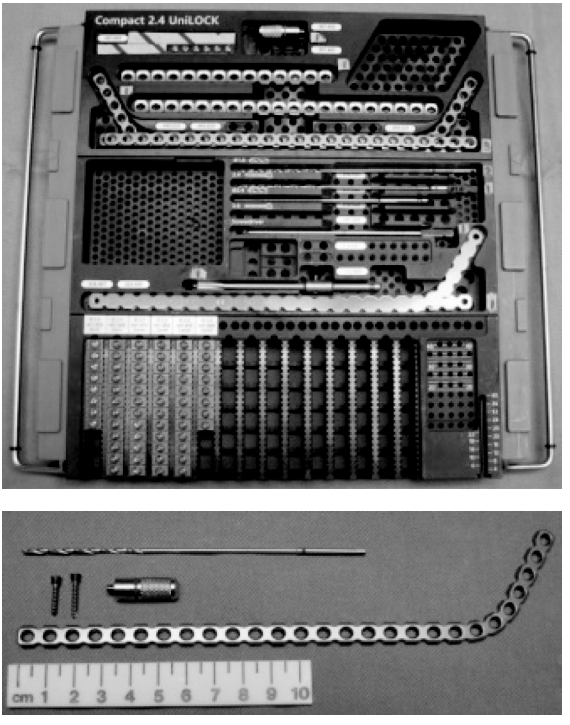

Figure 13.7 (a) Set of reconstruction plates and screws and (b) drill, drill guide, screws, and a sample of a unilock reconstruction plate.

13.3.1.2 Midfacial fractures

Nearly 25% of all fractures in this area occur during sports and leisure activities. Motor vehicle accidents, work accidents, alcohol, and violence may be considered to be additional causes.

Anatomically the midface is compiled of a system of cavities and pillars, similar to a honeycomb, and different bones. As there are only mimic muscles originating and inserting in the midfacial area, dislocation of fractures mainly happens due to impact. Further dislocation because of muscle pull is very unlikely.

After open reposition of fractures, miniplates and their screws are only necessary to guarantee enough stabilization for undisturbed bone healing. It is important to understand that because of the midfacial honeycomb structure, plates and screws have to be applied on the repositioned pillars, as only they offer enough bone volume for the screw retention (Fig. 13.8).

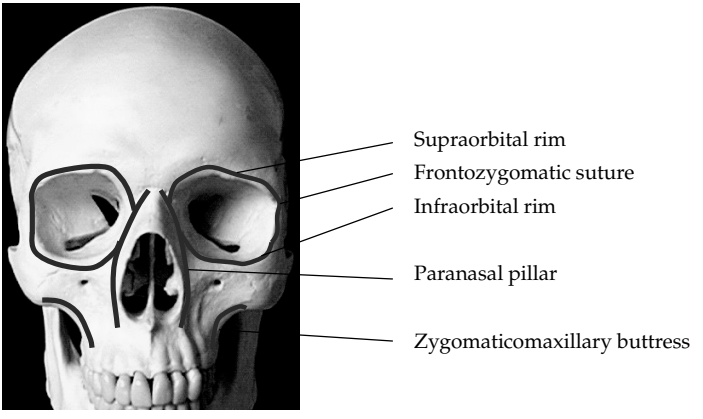

Figure 13.8 Midfacial pillars that are suitable for miniplate fixation.

- *Fractures in the midface area*
  Small-dimension load-sharing plates and monocortical screws provide enough internal retention to guarantee undisturbed bone healing in this area. Special areas of the midface, such as the zygomatic arch and the infraorbital rim, are covered only with a thin layer of skin and subcutaneous tissue. In these particular areas microplates with screws 0.8 mm in diameter provide enough stability for internal fixation, nevertheless remaining inconspicuous below the thin integument (Figs. 13.9 and 13.10).

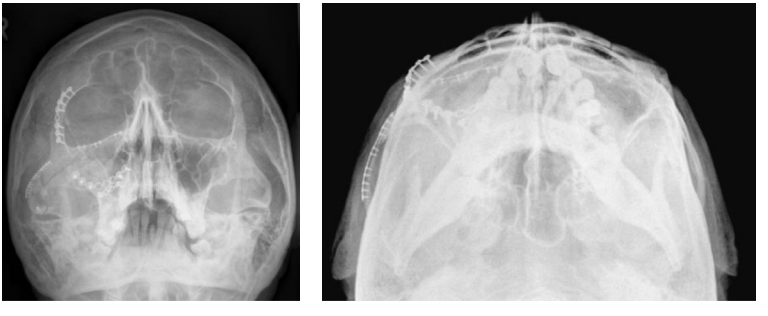

Figure 13.9 (a) Occipitomental radiograph shows microplates at the infraorbital rim and at the zygomatic arch and miniplates at the frontozygomatic suture and the zygomaticomaxillary buttress. (b) Submental vertex radiograph represents the second plane for diagnosis in zygomatic fractures, highlighting the position of the zygomatic arch with the microplate in place.

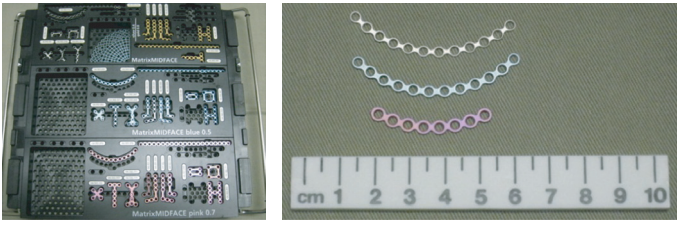

Figure 13.10 (a) Matrix midface system with screws of 0.7 mm and 0.5 mm diameter, as well as microplates at the top of the picture. (b) Comparison of mini- and microplates (microplate in silver color).

13.3.2 Clinical Applications in Orthognathic Surgery

Discontinuation of bone happens not only due to trauma. Many times patients present in oral and maxillofacial surgery with occlusal disturbances due to dentofacial deformities. In such cases it is not possible to achieve stable occlusion performing orthodontic treatment alone, because of incorrect or asymmetric relations of upper and/or lower jawbones. After orthodontic dental decompensation, where the teeth axes are positioned into their ideal angulation regarding the jawbones, the latter have to be osteotomized at defined positions under general anesthesia. After mobilization, the tooth-bearing jawbones are newly positioned according to their preoperatively planned relation to the skull base and the adjusted occlusion. Internal fixation is achieved with load-sharing miniplates. Figure 13.11 gives a survey of the most frequent osteotomies in the upper and lower jaws related to orthognathic surgery.

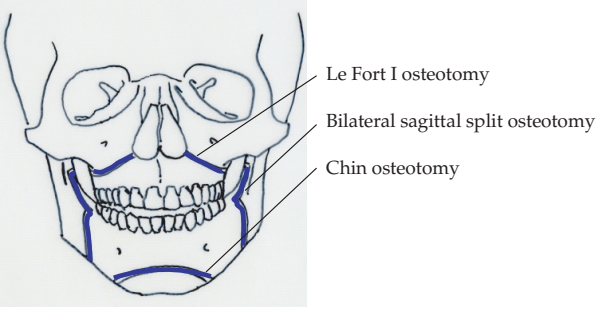

Figure 13.11 Most frequently performed osteotomies related to orthognathic surgery.

X-ray controls depict the location of the miniplates in the upper and lower jaws (Fig. 13.12), whereas Fig. 13.13 presents the screw fixation of a chin segment after reposition in the desired position.

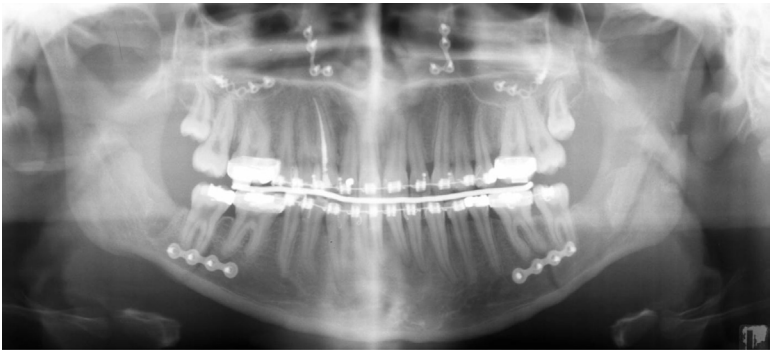

Figure 13.12 Location of the plates after bimaxillary osteotomy.

Figure 13.13 Detailed lateral cephalographic view depicting screw fixation of the osteotomized chin segment.

13.3.3 Titanium Alloy as Substitution for Bone Defects

A titanium alloy mesh or unilock plates are used to bridge bone defects. Whereas the former is used especially in extensive orbital floor defects caused by fractures or tumors, the latter mainly suits patients where due to tumors different types of mandibular resections have to be performed. Both devices serve to re-establish bone continuity and functionality.

The reconstruction of the orbital floor with an orbital titanium mesh after its resection due to a malignant tumor is displayed in Fig. 13.14a. Figure 13.14b illustrates the coronal position control of the titanium mesh in a CT follow-up examination. Titanium meshes usually are fixated to the bone with screws 2.0 mm or 1.5 mm in diameter.

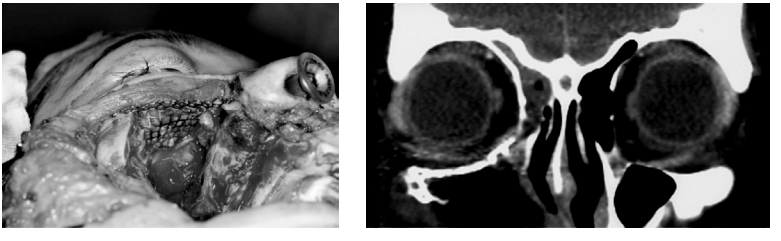

Figure 13.14 (a) Clinical image of an inserted titanium alloy mesh to reconstruct the resected orbital floor. The screws, 1.5 mm in diameter, are fixing the mesh lateral and medial to the defect in place. (b) Coronal CT position control in line with the regular tumor follow-up.

The Unilock reconstruction plate is very suitable to bridge mandibular resection defects to restore continuity and functionality.

Figure 13.15a shows the OPT control of a functional mandibular reconstruction using a unilock plate in a medically compromised patient where simultaneous bone reconstruction was not performed to reduce surgical comorbidities. The same plate system bridging a mandibular resection defect is presented in Fig. 13.15b; in this case a microvascular reanastomised fibula flap was inserted simultaneously and fixated with screws to the unilock plate. Figure 13.16 highlights an orbital titanium mesh, unbent.

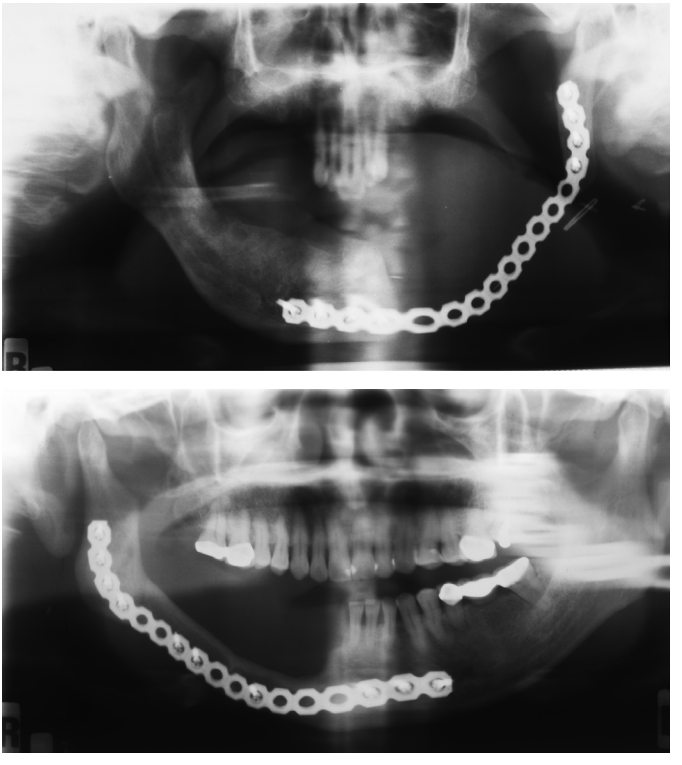

Figure 13.15 (a) Radiographic control of a unilock plate without bone substitution. (b) Unilock plate with additional simultaneous bone substitution using a microvascular reanastomised fibula flap.

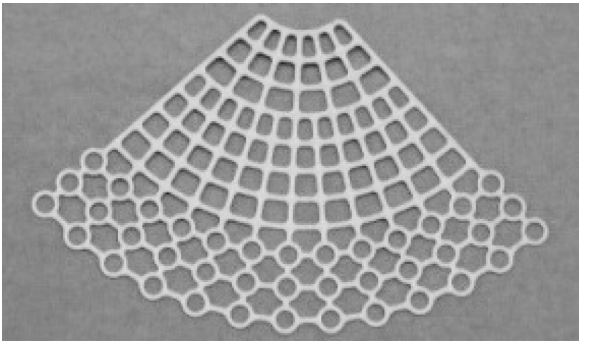

Figure 13.16 Titanium mesh before bending and situational modification.

13.4 Alternatives to Titanium for Internal Fixation

To date osteosynthesis materials on a metallic basis, especially titanium alloys, are considered to be the "gold standard" [29]. Clinicians estimate very much their easy handling and sterilization together with their good mechanical properties. The feasibility to produce small-dimensioned plates and screws in metal processing make them also applicable in facial areas that are prominent and covered by only thin layers of skin and subcutaneous tissue.

13.4.1 Adverse Events of Titanium

Titanium alloys are still considered to be highly biocompatible related to the definition of biocompatibility coined by Williams in 2008 [30]: *The biocompatibility of a long term implantable medical device refers to the ability of the device to perform its intended function, with the desired degree of incorporation in the host, without eliciting any undesirable local or systemic effects in that host.*

Even though titanium alloys are very stable to corrosion due to their superficial titanium oxide layer, soft tissue pigmentations in the proximity of plates might be found during osteosynthesis material removal. It is supposed that such pigmentation, which, however, does not interfere with bone healing, results due to surface defects caused by manipulation of the material at the time of insertion [31]. Examination of such pigmented soft tissue did not show any inflammatory response or giant cell reaction [32]. Recently increased values of titanium were detected in patients' hair and nails after orthognathic surgery [33]; cases of potential allergic reactions related to titanium osteosynthesis come up sporadically. Nevertheless, to date it remains unclear if allergic contact dermatitis and material flaws are increased in patients suffering from metallic allergies [34], especially due to diagnostic uncertainties in titanium testing.

13.4.2 Removal of Titanium Plates after Bone Healing

Many authors have written about removal or nonremoval of nonresorbable metallic internal fixation devices [35, 36]. However,

until today, there is no consensus within the oral and maxillofacial surgery community itself. Mostly, especially titanium alloy plates and screws are left in place if they are clinically asymptomatic [37].

- *Symptomatic internal nonresorbable plates and screws*
  Clinical symptoms like (1) plate and/or screw exposure with or without chronic infection, (2) patients' palpability of plates and screws, and (3) thermal sensitivity often at prominent regions, such as the frontozygomatic suture, may occur. Under these circumstances plates and screws are recommended to be removed. This can be performed under general or if feasible due to the location under local anaesthesia.

  According to personal experience, removal two years and more after insertion is more complicated and associated with a longer operation time because of the plates' and screws' encasement due to bone growth. In such a situation the surgeon often needs a bur, chisel, and hammer to remove the overlying bone in order to approach the plate and screws. Such a surgical procedure might cause longer and increased stretching of the periosteal layer due to retraction purposes, a circumstance that leads to increased postoperative facial swelling.

  Another symptomatic effect is loosening of hardware such as screws. Loose hardware might migrate, become palpable, and may cause chronic infection. Such nonresorbable material is highly recommended to be removed.
- *Asymptomatic internal nonresorbable devices*
  To date, titanium alloy plates and screws without above-mentioned clinical symptoms are not necessarily removed.

  However, children undergoing craniofacial or facial trauma surgery represent somewhat an exception regarding nonresorbable device removal. Even though the effect of rigid osteosynthesis onto growth is not really understood in humans, it is recommended to put plates that do not traverse suture lines and to remove them two to three months after the open reduction and internal fixation [38]. Several authors [37, 39] report about migration of nonresorbable devices due to the appositional resorptive growth of the cranium and facial bones; as headaches may occur due to such an intracranial migration of titanium alloy plates and screws, craniofacial

surgeons and neurosurgeons switched early to the use of resorbable osteosynthesis material [40].

13.4.3 Polyhydroxyacids: Reabsorbable Osteosynthesis Materials

Especially shortcomings of metal implants such as thermal sensitivity, palpation, and the migration of devices in children led already in the 1970s to the introduction of bioresorbable materials. Poly(α-hydroxyacid) osteosynthesis materials have been used since then in trauma and orthognathic surgery with somewhat contradictory results in stability and biocompatibility. Poly(α-hydroxyacids) have been found to be bioabsorble and biocompatible. They are the most widely studied and used bioabsorbable synthetic polymers in medicine today. More specifically and chemically, poly(α-hydroxyacids) are polyglycolide (PGA) and poly-L-lactide (PLLA) homopolymers and their copolymers (poly(lactic-co-glycolic) acid [PLGA]), as well as polylactic acid (PLA) stereocopolymers [41-45].

Application of the material in fracture treatment and orthognathic surgery needs more time as every screw hole has to be drilled and tapped. Omitting tapping will mostly end up in breaking off of the screw head. Expensiveness of the material, length of storage, and the fact that it can be only once sterilized by irradiation or ethylene oxide represent limitations in its use. Figures 13.17a and 13.17b show clinical intraoperative pictures with poly(hydroxyacid) plates and screws in place after trauma and orthognathic surgery, respectively.

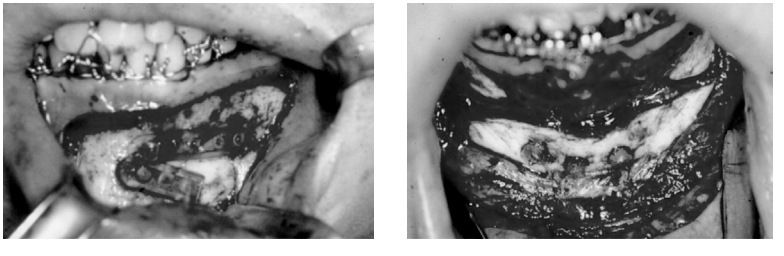

Figure 13.17 (a) Bioresorbable plates fix a mandibular fracture and (b) bioresorbable screws fix the chin after orthognathic genioplasty.

13.5 Epilogue

Future research in the area of osteosynthesis material will comply both with new resorbable materials as well as with novel designs of plates and screws.

As nowadays resorbable materials do not fulfill the expectations that load-bearing situations require, future studies will investigate the mechanical properties and strength of novel materials, such as ceramics or bioactive glasses eventually reinforced with boron or strontium. The latter materials could eventually also be used to coat weaker poly(α-hydroxyacid) plates and screws to improve their mechanical properties.

By now, β-titanium alloys still represent the gold standard for many surgeons due to their excellent mechanical properties and strength, even in small-dimensioned plates and screws, which are frequently used, even in craniofacial surgery.

References

1. Stuck, B. A., Heller, T. (2011) Implant materials for the internal fixation of midfacial fractures, *HNO*, **59**, 1088–1092.
2. Acero, J., Calderon, J., Salmeron, J. I., Verdaguer, J. J., Concejo, C., Somacarrera, M. L. (1999) The behaviour of titanium as a biomaterial: microscopy study of plates and surrounding tissues in facial osteosynthesis, *J. Craniomaxillofac. Surg*., **27**, 117–123.
3. Neumann, A., Kevenhoerster, K. (2009) Biomaterials for craniofacial reconstruction, *GMS Curr. Top. Otorhinolaryngol. Head Neck Surg*., **8**(Doc08), doi: 10.3205/cto000060.
4. Phillips, J. H., Rahn, B. A. (1989) Comparison of compression and torque measurements of self-tapping and pretapped screws, *Plast. Reconstr. Surg.,* **83**, 447.
5. Schenk, R., Willenegger, H. (1964) Zur Histologie der primären Knochenheilung, *Langenbeck's Arch. Surg.,* **308**, 440–452 (in German).
6. Crewe, T. C. (1966) A halo frame for facial injuries, *Br. J. Oral Surg*., **4**, 147–149.
7. Mackenzie, D. L., Ray, K. R. (1970) The Royal Berkshire Hospital "Halo," *Br. J. Oral Surg*., **8**, 27–31.
8. Hardin, J. C., Jr. (1967) Frontomaxillary suspension of comminuted type 3 facial fractures, *Plast. Reconstr. Surg*., **40**, 450–452.

9. Kufner, J. (1970) A method of craniofacial suspension, *J. Oral Surg*., **28**, 260–262.
10. Whinery, G. (1968) An armed atraumatic wire for use in circumferential and internal wiring of fractured facial bones, *J. Oral Surg*., **26**, 188–189.
11. Rudert, H. (1971) Wire suture osteosynthesis in facial and skull traumatology, *Z. Laryngol. Rhinol. Otol*., **50**, 640–646.
12. Schmoker, R., Spiessl, B., Tschopp, H., Prein, J., Jaques, W. (1976) Functionally stable osteosynthesis of the mandible by means of an excentric-dynamic compression plate. Results of a follow-up of 25 cases, *SSO Schweiz. Monatsschr. Zahnheilkd*., **86**, 167–185.
13. Lambotte, A. (1907) L'intervention operatoire dans les fractures recentes et anciennes envisagee particulierement au point de vue de l'osteosynthese. (Lamertin, Brussels) (in French).
14. Matter, P., Brennwald, J., Perren, S. M. (1974) Biological reaction of bones to osteosynthesis plates, *Helv. Chir. Acta*, **0**(Suppl 12), 1–44.
15. Rittmann, W. W., Perren, S. M. (1974) *Cortical Bone Healing after Internal Fixation and Infection. Biomechanics and Biology*, Springer-Verlag, Germany.
16. Luhr, H. (1970) Die Kompressionsosteosynthese bei Frakturen des zahnlosen Unterkiefers, *Dtsch. Zahnaertzl. Z*., **25**, 131 (in German).
17. Champy, M., Wilk, A., Schnebelen, J. (1975) Treatment of mandibular fractures by means of osteosynthesis without intermaxillary immobilization according to FX Michelet's technic, *Zahn Mund Kieferheilkd. Zentralbl*., **63**, 339–341.
18. Prein, J., Eschmann, A., Spiessl, B. (1976) Ergebnisse der Nachuntersuchung bei 81 Patienten mit funktionsstabiler Unterkieferosteosynthese, *Fortschr. Kiefer Gesichtschir*., **21**, 304–307 (in German).
19. Michelet, F. X., Deymes, J., Dessus, B. (1973) Osteosynthesis with miniaturized screwed plates in maxillo-facial surgery, *J. Maxillofac. Surg.,* **1**, 79–84.
20. Champy, M., Lodde, J., Grasset, D., Muster, D., Mariano, A. (1977) Mandibular osteosynthesis and compression, *Ann. Chir. Plast*., **22**, 165–167.
21. Pohler, O. E. M. (2000) Unalloyed titanium for implants in bone surgery, *Injury*, **31**(Suppl 4), 7–13.
22. Niinomi, M. (1998) Mechanical properties of biomedical titanium alloys, *Mater. Sci. Eng. A*, **243**, 231–236.

23. Disegi, J. A., Eschbach, L. (2000) Stainless steel in bone surgery, *Injury*, **31**(Suppl 4), 2–6.

24. Llobet, J. M., Domingo, J. L. (1984) Acute toxicity of vanadium compounds in rats and mice, *Toxicol. Lett.*, **23**, 227–231.

25. Ciranni, R., Antonetti, M., Migliore, L. (1995) Vanadium salts induce cytogenetic effects in in vivo treated mice, *Mutat. Res.*, **343**, 53–60.

26. Cortizo, A. M., Salice, V. C., Vescina, C. M., Etcheverry, S. B. (1997) Proliferative and morphological changes induced by vanadium compounds on Swiss 3T3 fibroblasts, *Biometals*, **10**, 127–133.

27. Domingo, J. (1994) Metal-induced developmental toxicity in mammals: a review, *J. Toxicol. Environ. Health, A*, **42**, 123–141.

28. Niinomi, M., Nakai, M., Hieda, J. (2012) Development of new metallic alloys for biomedical applications, *Acta Biomater.*, **8**(11), 3888–3903.

29. Bos, R. R. M. (2005) Treatment of pediatric facial fractures: the case for metallic fixation, *J. Oral Maxillofac. Surg.*, **63**, 382–384.

30. Williams, D. F. (2008) On the mechanisms of biocompatibility, *Biomaterials,* **29**, 2941–2953.

31. Acero, J., Calderon, J., Salmeron, J. I., Verdaguer, J. J., Concejo, C., Somacarrera, M. L. (1999) The behaviour of titanium as a biomaterial: microscopy study of plates and surrounding tissues in facial osteosynthesis, *J. Craniomaxillofac. Surg.*, **27**, 117–123.

32. Langford, R. J., Frame, J. W. (2002) Tissue changes adjacent to titanium plates in patients, *J. Craniomaxillofac. Surg.*, **30**, 103–107.

33. Bozkus, I., Germec-Cakan ,D., Arun, T. (2011) Evaluation of metal concentrations in hair and nail after orthognathic surgery, *J. Craniofac. Surg.*, **22**, 68–72.

34. Basko-Plluska, J. L., Thyssen, J. P., Schalock, P. C. (2011) Cutaneous and systemic hypersensitivity reactions to metallic implants, *Dermatitis,* **22**, 65–79.

35. Brown, J., Trotter, M., Cliffe, J., Ward-Booth, R., Williams, E. (1989) The fate of miniplates in facial trauma and orthognathic surgery: a retrospective study, *Br. J. Oral Maxillofac. Surg.*, **27**, 306–315.

36. Rauso, R., Tartaro, G., Stea, S., Tozzi, U., Biondi, P. (2011) Plates removal in orthognathic surgery and facial fractures: when and why, *J. Craniofac. Surg.*, **22**, 252–254.

37. Alpert, B., Seligson, D. (1996) Removal of asymptomatic bone plates used for orthognathic surgery and facial fractures, *J. Oral Maxillofac. Surg.,* **54**, 618–621.

38. Zimmermann, C., Troulis, M., Kaban, L. (2006) Pediatric facial fractures: recent advances in prevention, diagnosis and management, *Int. J. Oral Maxillofac. Surg*., **35**, 2–13.

39. Beck, J., Parent, A., Angel, M. F. (2002) Chronic headache as a sequela of rigid fixation for craniosynostosis, *J. Craniofac. Surg*., **13**, 327–330.

40. Eppley, B. L., Sadove, A. M. (1995) A comparison of resorbable andmetallic fixation in healing of calvarial bone grafts, *Plast. Reconstr. Surg*., **96**, 316–322.

41. Bergsma, E. J., Rozema, F. R., Bos, R. R., de Bruijn, W. C. (1993) Foreign body reactions to resorbable poly(L-lactide) bone plates and screws used for the fixation of unstable zygomatic fractures, *J. Oral Maxillofac. Surg*., **51**, 666–670.

42. Bozic, K. J., Perez, L. E., Wilson, D. R., Fitzgibbons, P. G., Jupiter, J. B. (2001) Mechanical testing of bioresorbable implants for use in metacarpal fracture fixation, *J. Hand. Surg. Am.,* **26**, 755–761.

43. Dorri, M., Nasser, M., Oliver, R. (2009) Resorbable versus titanium plates for facial fractures, *Cochrane Database Syst. Rev*., **21**, CD007158.

44. Fedorowicz, Z., Nasser, M., Newton, J. T., Oliver, R. J. (2007) Resorbable versus titanium plates for orthognathic surgery, *Cochrane Database Syst. Rev*., **18**, CD006204.

45. Shetty, V., Caputo, A. A., Kelso, I. (1997) Torsion-axial force characteristics of SR-PLLA screws, *J. Craniomaxillofac. Surg*., **25**, 19–23.

This page intentionally left blank

Chapter 14

Zirconia and Implant Dentistry

Moustafa N. Aboushelib[a] and Jukka P. Matinlinna[b]
[a]*University of Alexandria, Department of Biomaterials, Champolion Street, Azarita, Alexandria, Egypt*
[b]*Faculty of Dentistry, Dental Materials Science, University of Hong Kong, Prince Philip Dental Hospital, 34 Hospital Road, Sai Ying Pun, Hong Kong SAR, People's Republic of China*
info@aboushelib.org, jpmat@hku.hk

The use of zirconia, that is, zirconium dioxide (ZrO_2), as a biomaterial in biomedicine started in the early 1980s. Since then, a growing number of laboratory and clinical studies has been conducted on this special ceramics to assess its unique characteristics. Moreover, zirconia has manifested its extraordinary advantages when used in dental clinical practice since the late 1990s, such as its prominent biocompatibility, satisfactory esthetical performance, and outstanding biomechanical properties. With the development of fabrication methods and more extensive knowledge of this material, zirconia has been employed in more and more dental restorations. Examples are single-crown and root canal posts to long-span fixed dentures and, recently, its use as a subgingival implant material. We discuss among others also alumina (Al_2O_3) as a biomaterial, zirconium metal, and tissue reactions to zirconia.

Handbook of Oral Biomaterials
Edited by Jukka P. Matinlinna

ISBN 978-981-4463-12-6 (Hardcover), 978-981-4463-13-3 (eBook)
www.panstanford.com

14.1 Zirconium, Alumina, and Zirconia

14.1.1 Zirconium Chemistry and Group IV A

The elements of group 4 (or IV A) in the periodic table, that is, *titanium* (^{22}Ti), *zirconium* (^{40}Zr), and *hafnium* (^{72}Hf), are *transition metals* with a strong tendency to exhibit the maximum valence, +IV, in their compounds. Both Ti and Zr, as metals, exhibit unique biocompatibility, that is, they exhibit no adverse reactions with living tissues in humans.

Zirconium (atomic mass: 91.22) has the electron configuration [Kr]$4d^2 5s^2$, and it has five naturally occurring isotopes: ^{90}Zr, ^{91}Zr, ^{92}Zr, ^{94}Zr, and ^{96}Zr. Zirconium is purified from $ZrSiO_4$ mineral. Zirconium is chemically very similar to Hf, due to the almost identical ionic radii for Zr^{4+} and Hf^{4+} (Zr: 80 pm; Hf: 81 pm). Zirconium has the valence +IV, but few compounds are known with the oxidation state +III and +II. As an element, Zr is lustrous, ductile, and silvery white and has a high melting point (1855°C) and boiling point (4409°C).

Zr is extremely resistant to corrosion at ordinary temperatures because it is easily rendered passive by formation of an oxide layer, exactly as Ti. The occurrence of Zr within the earth's crust is 0.023%, that is, around 0.13 g/kg. Sea water contains ca. 0.026 μg/L of Zr^{4+}. On heating Zr, however, reacts with oxygen, nitrogen, hydrogen, carbon, and sulfur. Zirconium can form zirconium dioxide: Zr (s) + O_2 (g) → ZrO_2 (s). Zirconium is highly resistant to acids, alkalis, and brine. Zr reacts with hydrofluoric acid (HF) but is not attacked by nitric acid (HNO_3) or other mineral acids. *Metallic zirconium* is much softer than Ti and used in technology as a neutron capture, opacifier, and refractory material [1, 2].

Zirconum dioxide (zirconia) was introduced for biomedical applications already in the seventies. By then the material was able to be purified through chemical processing and its fabrication process was fully controlled. Zirconia is a trivial name and also the commercial, widely used name given to zirconium dioxide. The zirconia product family comprises zirconia *with different additional constituents* to prevent volume expansion (tetragonal to monoclinic). Such additives are, for example, MgO, CaO, Ce_2O_3, and Y_2O_3, and they

control its mechanical and physical properties (see also Chapter 15).

On the other hand, the *zirconate coupling agents* (*zirconates*), expressed with the general formula of $(RO)_n$-Zr-$(OXR'Y)_{4-n}$, are more universally reactive than silane coupling agents. Synthetic zirconates may be particularly useful on surfaces that do not have reactive surface hydroxyl groups. Zirconate compounds possess the C–Zr bond(s), and the Zr–O bond is capable of dissociation allowing *trans*-esterification, *trans*-alkylation, and repolymerization in some applications. Zirconate coupling agents claim to maintain their coupling capability, even in the presence of water. Zirconates and *titanate coupling agents* have been used to improve the adhesion between inorganic fillers and the organic matrices of some composite materials [3, 4]. It has been claimed that *neoalkoxy zirconate* coupling agents are viable materials in future biomaterials research (about coupling agents, see Chapter 11).

14.1.2 Zirconia and Alumina

Crystalline *zirconium dioxide* (zirconium oxide), ZrO_2, called zirconia (not to be confused with *zircon*, which is a mineral, and Zirkon™, which is a product in the market) is manufactured for use as a white pigment from minerals by conversion to $Zr(SO_4)_2$, followed by hydrolysis. ZrO_2 is used also as a refractory material (crucibles, furnace lining), and it is insoluble in water, only slightly soluble in HCl and HNO_3, and, however, slowly soluble in HF upon heating with 66% H_2SO_4 [1, 2, 5].

Zirconia caught attraction due its *superior mechanical properties* as superior flexure strength (which is 1200 MPa compared to 1000 MPa for steel), high fracture toughness, high hardness, excellent fatigue, and damage resistance. The material is resistant to chemical attacks and does not react easily with strong acids, alkalis, or other corrosive material. Regarding its physical properties, ZrO_2 is a white and opaque material that does not dissolve or react with water and other solvents. It is an excellent thermal and chemical insulator and is used in fuel cells.

The principal natural sources, ores, and minerals of Zr are *zircon*, a silicate mineral chemically named *zirconium orthosilicate* ($ZrSiO_4$), *malacon* (brownish $ZrSiO_4$), *baddeyleite* (ZrO_2), *zirkelite*,

and *eudialyte*. Zircon, $ZrSiO_4$, also called the mineral *jacinth* was said to be adopted as a kind of gem in the Bible. It was actually in 1789 when zirconia was accidently identified by M. H. Klaproth (1743–1817), a German chemist, who was also well known for his discovery of titanium some years after its initial discovery and uranium (^{92}U) as he was investigating a zircon stone found in Sri Lanka. Zirconium silicate ($ZrSiO_4$) toxicity is very low: it is an abrasive irritant for the eyes and skin. Treatment of the above-mentioned minerals with carbon and chlorine at red heat yields $ZrCl_4$, which, after purification, can be reduced (with Mg) to Zr. For high-purity Zr, the decomposition reaction of ZrI_4 is used [1, 2, 5].

Zirconia is considered one of the best currently known biocompatible ceramic materials along with the metallic titanium. It is currently one of the most studied dental biomaterials [6]. It is, however, reported to be sensitive to manufacturing and manipulation processes. Given this, there is also a debate about which processing method is least harmful to the final restoration. Cementation, that is, resin zirconia bonding, is under a vivid discussion, and chipping of the veneering porcelain is reported as a common clinical problem, probably currently the main clinical drawback [7, 8]. The most common oxide of Zr is zirconium dioxide, ZrO_2. This odorless, tasteless, and white solid material has exceptional fracture toughness and chemical resistance, especially when it is in its cubic form (see also Chapter 15).

Pure ZrO_2 has a monoclinic crystal structure at room temperature. Transitions to other possible crystal forms, viz., tetragonal and cubic, take place at elevated temperatures. The actual volume expansion of zirconia caused by cubic to tetragonal to monoclinic transformation induces very large stresses and will cause pure ZrO_2 to crack upon cooling from high temperatures. Several different metal oxides may be added to zirconia to stabilize the phase changes from tetragonal to cubic phases. Such additives are, for example, *magnesia* (magnesium oxide, MgO); *yttria* (yttrium trioxide, Y_2O_3); *lime*, that is, calcium oxide (CaO); and *ceria*, that is, cerium trioxide (Ce_2O_3) [9].

Actually, the use of aluminum trioxide, *alumina* (Al_2O_3), as a biomaterial took place before zirconia. Alumina has good biocompatibility [10]. However, the flexural strength and toughness

of alumina are just moderate. Zirconia is generally supposed to have more clinical benefits compared to alumina because of zirconia's higher flexural strength and higher fracture toughness, which might facilitate the reduction in the risk of failure. Interestingly, when zirconia particles *are added to alumina* and scattered in the matrix, alumina will be toughened with greater hardness. The combination of these two materials is called ZrO_2-toughened alumina (ZTA). Zirconia content in ZTA varies between 10% and 20%, and the tetragonal-phase zirconia remains in the metastable state [11]. ZTA also has high mechanical properties, but further investigation of its performance in its clinical use is needed.

The *crystallographic structures* of zirconia consist of three different forms. At room temperature, zirconia finds its arrangement as the monoclinic (M) phase. When heated above 1170°C, it transforms into the tetragonal (T) phase and finally into cubic (C) form at temperatures above 2370°C. The transformations among these phases will be accompanied with dimensional changes of about 3–5%. The stabilized tetragonal- or cubic-phase zirconia is stiffer due to the stress-induced transformation-toughening effect. Some oxides, such as CeO_2 (^{58}Ce is a lanthanide metal) and Y_2O_3, are added as stabilizers and transform pure zirconia into a multiphase ceramic structure. We then call it partially stabilized zirconia (PSZ). It consists of mainly the cubic phase with a minor diffusion of tetragonal and monoclinic phases [8, 12].

Different PSZ-based materials, such as Mg-PSZ and Y-PSZ, have being developed during the past few years. In general, they are proved to possess some improvements in their biomechanical properties [5]. One partially stabilized type of zirconia is called tetragonal zirconia polycrystal (TZP), and it has become the focus of research. It was reported that the tetragonal phase could be stabilized at room temperature when yttrium oxide in low concentration was added as a stabilizer [13]. The amount of Y_2O_3 in TZP is ca. 2–3% mol, and the microstructure of TZP mainly consists of tetragonal grains. The occurrence of the tetragonal phase is influenced by the grain size, the amount of yttria, and the structure of the zirconia matrix [5, 8]. It has been concluded that yttria-stabilized TZP (i.e., Y-TZP) materials exhibit high flexural strength and fracture toughness, in addition to great hardness [14].

14.2 Biomedical Applications of Zirconia

Zirconia was first used as a *hip joint replacement* material due to its superior strength, which allowed fabrication of ball-and-socket joints with conservative dimensions, in addition to its excellent wear resistance. Autoclaving was the technique used to *sterilize* this material, which resulted in a process of slow surface destruction of the material, known as low-temperature water degradation (LTD), ending in the fracture of many of the inserted joints [5, 8]. Today more is known about the behavior of the material under different conditions, and the material is gaining more attention as a scaffold material, implant, and *bone substitute*.

14.2.1 Tissue Reactions around Zirconia Implants

Cell response to zirconia can be easily evaluated using *cell culture techniques* where cultured cells are grown and monitored over the surface of zirconia discs for a certain period of time. Several parameters such as cell size, shape, excretory functions, metabolism, multiplication, DNA activity, attachment mechanism, and more are used to evaluate the primitive cell response to the implant material [6]. These cells are simple and easy to use, but they are only used for screening purposes and as a reference compared to control material, usually Ti plates (see also Chapter 5).

Different types of *purified bone cells* derived from human or animal source are multiplied in the laboratory until a sufficient number is available. Cells are grown in a special growth medium, and a drop, containing a fixed number of cells, is added on the surface of the plates. After a few minutes the cells establish good contact with the surface of the plates, and a sufficient amount of growth medium is added to the containing wells. The plates are incubated at a fixed temperature and oxygen gradient, and cell growth and viability are monitored regularly.

Cell culture experiments have revealed that zirconia implants had similar or superior results compared to titanium implants. However, results could not be directly compared between different studies as the many variables could influence the results as (a) cell type, (b) incubation condition, and (c) most importantly surface properties of the prepared plates. Surface roughness is one of the

most investigated parameters that had a significant influence on cell growth and attachment mechanism. For biocompatibility aspects, read Chapter 5, and for titanium, read also Chapters 9, 10, 12, and 13.

Today, nanoporous zirconia surfaces have shown improved cell growth, as indicated by a higher cell count and larger cell size compared to polished zirconia and Ti specimens and sandblasted and acid-etched (SLA) titanium specimens. The *selective infiltration etching* (SIE) technique created a nanoporous zirconia surface without increasing the surface roughness of the treated zirconia (R_a = 0.2 ± 0.2 μm). This is a direct advantage when compared to airborne particle abrasion, which is associated with introducing surface and subsurface damage. This would consequently lead to compromising of the fatigue resistance of the abraded zirconia [15, 16].

14.2.2 Zirconia as a Dental Implant Material

Insertion of new implant materials in *animal models* allowed evaluation of the healing mechanism and a better understanding of the *osseointegration* (aka osteointegration) process around implant material. After different time intervals calculated from the time of implant placement, the animal is sacrificed and bone sections containing the implant material prepared for histological evaluation. After fixation and proper embedding of the obtained bony block, serial sections are cut through the implant, allowing proper evaluation of the bone–implant interface. Presence of mineralized bone in direct contact with the implant surface is considered as an indication of successful osseointegration; the higher the percentage, the better the performance of the implant material (see also Chapter 10).

Nevertheless, these studies are very expensive and require investing lots of time and effort dedicated toward delivering proper care to the host animal. Preparing histological sections is not an easy job and requires a well-equipped lab plus expensive processing materials.

Zirconia was first introduced to prosthetic dentistry as a potential *metal-free* framework material, mainly due to its whitish color, which made it esthetically attractive, in addition to its outstanding biomechanical properties. Another advantage of zirconia is the fact that it displays a significantly *reduced plaque affinity*, thus reducing

the risk of inflammatory changes in the surrounding of soft tissue [17]. Histological observations and several animal studies [18, 19] revealed that zirconia implants osseointegrated to the same extent as titanium implants and in some cases were more superior (Fig. 14.1).

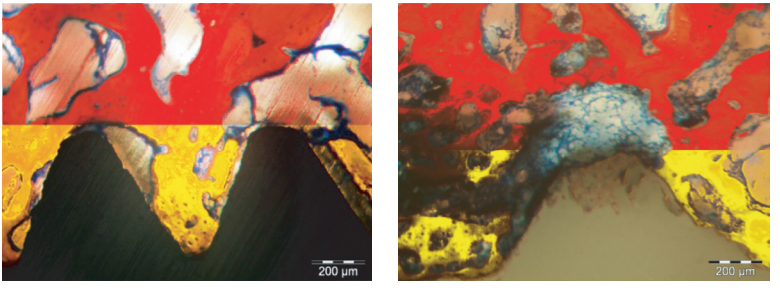

Figure 14.1 Amount of new bone (yellow) between implant threads after two weeks of insertion: titanium (left) and zirconia (right).

As the success of any implant material is interpreted in its *degree of osseointegration*, zirconia surface modifications have been investigated to enhance bone apposition and implant stability. Even though the optimal surface modification has not yet been found, *new approaches* have been used in an effort to improve surface properties of zirconia, such as airborne particle abrasion, acid etching with hydrochloric or hydrofluoric acids, plasma spraying [20], aggregation of bioactive materials such as calcium hydroxyapatite, and, more recently, UV radiation, which has been used to increase the hydrophilic properties of zirconia implants [21].

To improve the surface properties of zirconia implants *two main approaches* were used, (1) through optimizing the micro-roughness of the implant surface by using sandblasting and chemical etching and (2) by applying bioactive coatings such as hydroxyapatite and calcium phosphate salts.

Implants with micro-roughness demonstrated encouraging results compared to implants with smooth surfaces. Gahlert et al. investigated zirconia implants with either a machined or a sandblasted surface and compared them with SLA titanium implant surfaces in the maxilla of miniature pigs. The machined ZrO_2 implants showed statistically significant lower removal torque testing (RTQ) values than the other two implants types. The authors

concluded that roughening the machined zirconia implants enhances their osseointegration [19]. Other animal and clinical studies also reported successful osseointegration of roughened zirconia implant surfaces that was comparable to titanium implants [17, 22–24].

14.2.3 Difficulties Related to Fabrication of Ceramic Implants

Due to the complicated shape of dental implants, relying on computer-assisted design/computer-assisted milling (CAD/CAM) technology has some limitations. Fine reproduction of thread details requires using very fine machining tools, which results sometimes in fracture of the thin thread; thus manufacturers rely on using larger threads with a simplified pattern.

Most commercially available zirconia implants use a simple spiral design with an increase in interthread spacing (thread step and peak) instead of using the common reverse buttress design used with titanium implants (Fig. 14.2). The change in thread design is associated with an increase in peak stresses located inside the supporting bone, which could influence implant initial stability and increase risk when immediately loaded [25]. A direct benefit of CAD/CAM machining is that gingival fibroblasts tend to arrange themselves parallel to surface scratches; thus maintaining a circular machined zirconia neck could help obtain a tight gingival seal [26]. For more about CAD/CAM systems, see Chapter 18.

Figure 14.2 Direct milling and shaping of fine implant threads does not produce expected accuracy compared to machined titanium.

A second major problem is related to the abutment implant connection, as relying on a fixation screw is not applicable with brittle

ceramics. This is due to the difficulty in machining accurate internal threads and the very limited capacity of zirconia to accommodate deformation associated with screw tightening. To solve this problem, manufacturers tend to fabricate single-unit zirconia implants, which are screwed as one piece [27], leaving the prefabricated abutment emerging from the osteotomy site. Reducing the *number of components* in an implant restoration comes with some limitations when the need to have submerged implants presents. There are also some limitations in the implant switch platform design, which may narrow the prosthetic and restorative treatment options.

A major limitation is related to optimizing the *surface* of zirconia implants in order to improve osseointegration. Zirconia has a very hard (13,350 VHN [Vickers hardness number]) and dense surface (6.1 g/cm^3) that is composed of micrograins with an approximate diameter of ca. 0.1–0.5 μm. The micrograins do not react to the SLA (cf. Chapter 10) procedure that is used with Ti implants. Moreover, a dense and smooth zirconia surface will significantly increase the risk of *implant loosening* due to difficulties related to attachment of bone cells to this surface. A few years ago, sandblasting (aka airborne particle abrasion) with coarse alumina particle powder was the standard surface treatment used to roughen zirconia surface [28]. Unfortunately, this aggressive surface treatment was associated with the creation of surface defects in the form of surface and subsurface sharp scratches and defects, which dramatically reduced the fatigue resistance of the material.

Nowadays, new surface treatments are available to improve surface properties of zirconia implants without jeopardizing their mechanical strength. For sandblasting, read more in Chapter 11.

14.2.4 New Surface Treatments of Zirconia Implants

Surface coatings with a bioactive material such as Ca-hydroxyapatite or other calcium salts have been used to enhance cellular response to coated zirconia implants (cf. Chapter 12). Despite promising results, delamination (chipping) of the coat was associated with loss of zirconia implants after long periods of loading time. To solve these problems, trials to reduce coating thickness were conducted, and a nanolayer, which maintains the required chemical effect, is the new trend used to coat zirconia implants. Controlling coating thickness

using plasma spraying or arch induction has become a very simple procedure with accurate and repeatable surface qualities.

Plasma anodization and *fluoridation* are other methods used to control the surface charge and energy of zirconia implants. Long-term exposure to fluoride tends to modify the surface energy of the surface and enhances bone implant contact of zirconia implants.

Application of *laser* to the surface of zirconia has various effects, depending on the type of laser. An erbium-doped yttrium aluminium garnet (Er:YAG) laser has high penetrating power and does not appear to affect surface properties. A carbon dioxide (CO_2) laser can melt the surface and create surface cracks related to fast cooling, and this method thus could not be recommended as a standardized method. On the contrary, a diode laser could be used to clean the surface of the implant in cases of *peri-implantitis* [29].

SIE is a new surface treatment that is used to create a nanoporous surface suitable for cell growth and attachment (Fig. 14.3). The required surface of the implant is coated with a viscous infiltration glass, which is heated above its glass-transition temperature. In the molten state, the glass tends to infiltrate between the surface grains of zirconia and facilitates gain sliding and reorganization. After cooling to room temperature, the glass is dissolved in an acid bath, leaving behind a highly porous surface. The advantage of this method is that only the first few microns on the surface are affected and the interconnected porosity creates an ideal surface for cell attachment and growth [30].

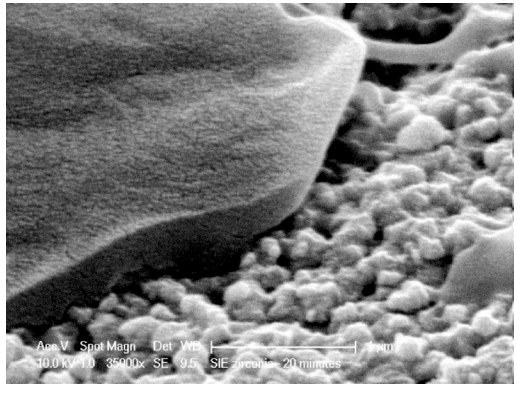

Figure 14.3 Cell membrane of an osteoblast in direct contact with a nanoporous SIE zirconia implant.

Some recent laboratory studies suggest that silica-coating followed by some experimental silane [31] primer formulations [32] might promote significantly durable resin bonding to zirconia [33] and Ti [34] abutment after artificial aging. In vitro studies suggest that SIE combined with new experimental silane primer formulations might significantly enhance resin bonding to zirconia abutments [35, 36].

14.2.5 Future Composite Ceramics for Zirconia Implants

The search for superior materials and improved material properties does not stand satisfied with what is currently present on the bench but seeks greater improvements. A *stronger and more biocompatible material* will always catch the attention of the dentist and thus remain always of a commercial value. The list of ideal material properties cannot be achieved using a single homogenous material.

Today the emphasis has shifted from studying metal alloys to studying composite ceramics and other new composite materials, such as those based on E-glass fibers [37] (see also Chapter 7).

A new breed of zirconia-based ceramics is now being evaluated, waiting for the right time to launch these hybrid products into the market. A high-toughness *alumina–zirconia composite* with twice the flexure strength (2200 MPa) and double the fracture toughness (12 MPa $m^{½}$) is now available with different formulations containing titanium, magnesium, and some other elements [38]. Given this, long-term fatigue resistance tests of these hybrid materials produced promising results. These high-performance composite ceramics might allow the fabrication of a thin structure with more confidence and reduced fracture rate.

14.2.6 Precautions When Using Zirconia Implants and Abutments

We may say that zirconia implants are still in the *maturity phase*, and they will require extensive long-term evaluation before reaching solid recommendations. Most studies so far have been conducted on animal models and have reported basic bone formation around zirconia implants.

Only long-term observation under true clinical conditions could justify its use. Load, moisture, cyclic loading, and thermal and chemical attachment are only some of the parameters that could affect implant success. Moreover, it has to be borne in mind that zirconia implants are supplied as one piece and limited in size and design, which might narrow down treatment possibilities.

Zirconia abutments have caught attention as an esthetic implant superstructure that could improve appearance, especially around thin gingival tissues. Being white and opaque, the color of the cemented porcelain crown was not compromised by the gray effect observed with titanium abutments. Nevertheless, this feature came at the expense of the mechanical integrity of the abutment.

Zirconia abutments are in nature hollow, and these tubes that are fitted with a metallic hex are used to establish connection with the implant and the fixation screw. A major problem with this system is loss of the friction fit between the metallic hex and the zirconia abutment (Fig. 14.4).

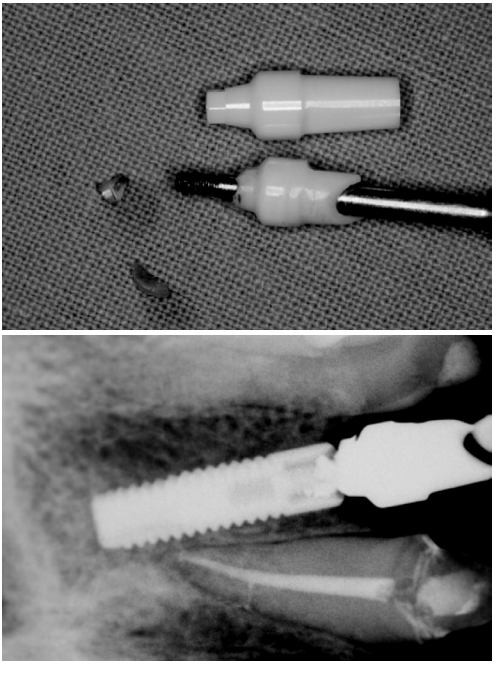

Figure 14.4 A fractured zirconia abutment: this was due to the friction of a fixation screw in the brittle ceramic.

A second problem may be that these abutments are more prone to fracture if overprepared or when used for angle correction. Moreover, there is a significant price difference compared to similar Ti abutments.

Today it is possible to mill your own customized implant zirconia abutments using CAD/CAM systems in your dental office with full control over the emergence profile, soft tissue transfer, and abutment contour. In addition, customized zirconia abutments could directly be covered with a porcelain veneer that could be fused or *directly cemented* on the abutment.

To improve esthetics, a Ti connect system has been introduced to the market (Fig. 14.5.). The titanium connection is screwed on the implant, providing a short cylindrical superstructure. By scanning an implant collar, a customized abutment could be fabricated, veneered, and cemented on the Ti connect, which is finally screwed to the implant. In principle, this system offers simplicity and retrievability of the restoration.

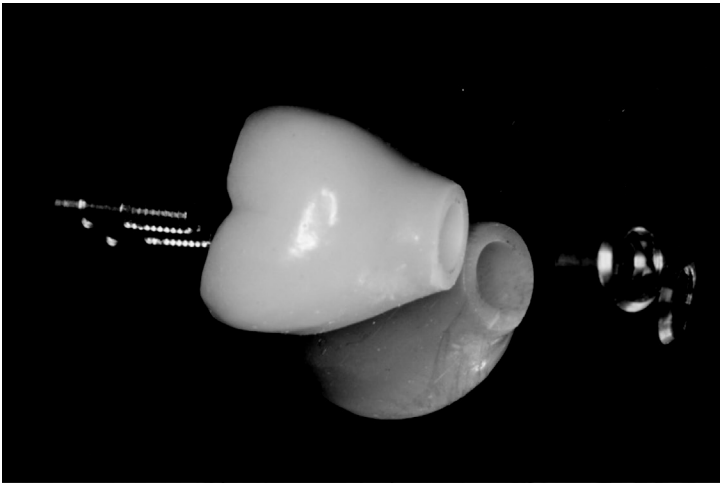

Figure 14.5 Photograph demonstrating a Ti connect, a customized veneered zirconia abutment, and the fixation screw.

References

1. Heslop, R. B., Robinson, P. L. (1976) *Inorganic Chemistry: A Guide to Advanced Study,* 3rd ed., Elsevier, Amsterdam.

2. O'Neil, M. J (Ed.) (2006) *The Merck Index,* 14th ed., Merck, Whitehouse Station, NJ, USA.
3. Monte, S. J. (2002) Neoalkoxy titanate and zirconate coupling agent additives in thermoplastics, *Polym. Polym. Compos.,* **10**(2), 121–172.
4. Cheng, H. C. K., Tsoi, J. K. H., Zwahlen, R. A., Matinlinna, J. P. (2014) Effects of silica-coating and a zirconate coupling agent on shear bond strength of flowable resin-zirconia bonding, *Int. J. Adhes. Adhesiv*., **50**, 11–16.
5. Piconi C., Maccauro, G., Muratori F., Brach del Prever, E. (2003) Alumina and zirconia ceramics in joint replacements*, J. Appl. Biomater. Biomech*., **1**, 19–32.
6. Mallineni, S. K., Nuvvula, S., Matinlinna, J. P., Yiu, C. K. Y., King, N. M. (2013) Biocompatibility of various dental materials of contemporary dentistry: a narrative insight, *J. Invest. Clin. Dent.,* **4**, 9–19.
7. Al-Amleh, B., Lyons, K., Swain, M. (2010) Clinical trials in zirconia: a systematic review, *J. Oral Rehab.,* **37**, 641–652.
8. Liu, D., Matinlinna, J. P., Pow, E. H. N. (2012) Insights into porcelain zirconia bonding, *J. Adhes. Sci. Technol.,* **26**, 1249–1265.
9. Green, D. J., Hannink, R., Swain, M. V. (1989) *Transformation Toughening of Ceramics*, CRC Press, Boca Raton, FL, USA.
10. Hench, L. L., Wilson, J (1999) *An Introduction to Bioceramics*, World Scientific.
11. Claussen, N. (1976) Fracture toughness of Al_2O_3 with an unstabilized ZrO_2 dispersed phase, *J. Am. Ceram. Soc.,* **59**, 49–51.
12. Subbarao, E. C. (1981) *Advances in Ceramics, Vol. 3. Science and Technology of Zirconia*, Elsevier, Amsterdam.
13. Gupta, T. K., Bechtold, J. H., Kuznicki, R. C., Cadoff, L. H., Rossing, B. R. (1977) Stabilization of tetragonal phase in polycrystalline zirconia, *J. Mater. Sci. Med.,* **12**, 2421–2426.
14. Kelly, J. R., Denry, I. (2008) Stabilized zirconia as a structural ceramic: an overview, *Dent. Mater.,* **24**, 289–298.
15. Wang, H., Aboushelib, M. N., Feilzer, A. J. (2008) Strength influencing variables on CAD/CAM zirconia frameworks, *Dent. Mater.,* **24**, 633–638.
16. Hempel, U., Hefti, T., Kalbacova, M., Wolf-Brandstetter, C., Dieter, P., Schlottig, F. (2012) Response of osteoblast-like SAOS-2 cells to zirconia ceramics with different surface topographies, *Clin. Oral Implants Res.*, **21**, 174–81.
17. Akagawa, Y., Hosokawa, R., Sato, Y. K. K. (1998) Comparison between freestanding and tooth-connected partially stabilized zirconia

implants after two years' function in monkeys: a clinical and histologic study, *J. Prosthet. Dent.,* **80**, 551–558.

18. Gahlert, M., Gudehus, T., Eichhorn, S., Steinhauser, E., Kniha, H., Erhardt, W. (2007) Biomechanical and histomorphometric comparison between zirconia implants with varying surface textures and a titanium implant in the maxilla of miniature pigs, *Clin. Oral Implants Res*., **18**, 662–668.
19. Rocchietta, I., Fontana, F., Addis, A., Schupbach, P. M. S. (2009) Surface-modified zirconia implants: tissue response in rabbits, *Clin. Oral Implants Res.,* **20**, 844–850.
20. Langhoff, J. D., et al. (2008) Comparison of chemically and pharmaceutically modified titanium and zirconia implant surfaces in dentistry: a study in sheep, *Int. J. Oral Maxillofac. Surg.,* **37**, 1125–1132.
21. Att, W., Takeuchi, M., Suzuki, T., Kubo, K., Anpo, M. T. O. (2009) Enhanced osteoblast function on ultraviolet light-treated zirconia, *Biomaterials,* **30**, 1273–1280.
22. Sennerby, L., Dasmah, A., Larsson, B., Iverhed, M. (2005) Bone tissue responses to surface-modified zirconia implants: a histomorphometric and removal torque study in the rabbit, *Clin. Implant. Dent. Rel. Res.,* **7**, S13–20.
23. Blaschke, C., Volz U. (2006) Soft and hard tissue response to zirconium dioxide dental implants - a clinical study in man, *Neuroendocrinol. Lett.,* **27**(Suppl 1), 69–72.
24. Depprich, R., Zipprich, H., Ommerborn, M., Naujoks, C., Wiesmann, H. P., Kiattavorncharoen, S. et al. (2008) Osseointegration of zirconia implants compared with titanium: an *in vivo* study, *Head Face Med*., **4**(Paper 30).
25. Caglar, A., Bal, B. T., Aydin, C., Yilmaz, H., Ozkan, S. (2010) Evaluation of stresses occurring on three different zirconia dental implants: three-dimensional finite element analysis, *Int. J. Oral Maxillofac. Impl,* **25**, 95–103.
26. Tete, S., Mastrangelo, F., Bianchi, A., Zizzari, V., Scarano, A. (2009) Collagen fiber orientation around machined titanium and zirconia dental implant necks: an animal study, *Int. J. Oral Maxillofac. Impl.,* **24**, 52–58.
27. Koch, F. P., Weng, D., Kramer, S., Biesterfeld, S., Jahn-Eimermacher, A., Wagner, W. (2010) Osseointegration of one-piece zirconia implants compared with a titanium implant of identical design: a histomorphometric study in the dog, *Clin. Oral Implants Res.,* **21**, 350–356.

28. Bacchelli, B., Giavaresi, G., Franchi, M., Martini, D., De Pasquale, V., Trire, A., et al. (2009) Influence of a zirconia sandblasting treated surface on peri-implant bone healing: an experimental study in sheep, *Acta Biomater.*, **5**, 2246–2257.
29. Stubinger, S., Homann, F., Etter, C., Miskiewicz, M., Wieland, M., Sader, R. (2008) Effect of Er:YAG, CO(2) and diode laser irradiation on surface properties of zirconia endosseous dental implants, *Lasers Surg. Med.,* **40**, 223–228.
30. Aboushelib, M., Salem, N., Abotaleb, A., Abd El Moniem, N. (2011) Influence of surface nano-roughness on osseointegration of zirconia implants in rabbit femur heads using selective infiltration etching technique, *J. Oral Implantol.,* **Sep. 9**, epub ahead of print.
31. Lung, C. Y. K., Matinlinna, J. P. (2012) Aspects of silane coupling agents and surface conditioning in dentistry: An overview, *Dent. Mater.,* **28**(5), 467–477.
32. Hooshmand, T., Matinlinna, J. P., Keshvad, A., Eskandarion, S., Zamani, F. (2013) Bond strength of a dental leucite-based glass ceramic to a resin cement using different silane coupling agents, *J. Mech. Behav. Biomed. Mater.,* **17**, 327–332.
33. Matinlinna, J. P., Choi, A. H., Tsoi, J. K. H. (2013) Bonding promotion of resin-composite to silica-coated zirconia implant surface using a novel silane system, *Clin. Oral Implants Res.*, **24**(3), 290–296.
34. Matinlinna, J. P., Tsoi, J. K. H., de Vries, J., Busscher, H. J. (2013) Characterization of novel silane systems on titanium implant surfaces, *Clin. Oral. Implants Res.,* **24**(6), 688–697.
35. Aboushelib, M. N., Matinlinna, J. P., Salameh, Z., Ounsi, H. (2008) Innovations in bonding to zirconia based materials. Part I, *Dent. Mater.,* **24**, 1268–1272.
36. Aboushelib, M. N., Mirmohamadi, H., Matinlinna, J. P., Kukk, E., Ounsi, H., Salameh, Z. (2009) Innovations in bonding to zirconia based materials. Part II: focusing on chemical interactions, *Dent. Mater.,* **25**, 989–993.
37. Zhang, M., Matinlinna, J. P. (2012) E-glass fiber reinforced composites in dental use, *Silicon*, **4**, 73–78.
38. Kohal, R. J., Wolkewitz, M., Mueller, C. (2010) Alumina-reinforced zirconia implants: survival rate and fracture strength in a masticatory simulation trial, *Clin. Oral Implants Res.,* **21**, 1345–1352.

This page intentionally left blank

Chapter 15

Bonding to Zirconia

Alvaro Della Bona[a] and Jukka P. Matinlinna[b]
[a]*Post-Graduate Program in Dentistry, Dental School, University of Passo Fundo, Campus I, BR285, Passo Fundo, RS 99001-970, Brazil*
[b]*Faculty of Dentistry, Dental Materials Science, University of Hong Kong, Prince Philip Dental Hospital, 34 Hospital Road, Sai Ying Pun, Hong Kong SAR, People's Republic of China*
dbona@upf.br, jpmat@hku.hk

Zirconium dioxide, or zirconia, ZrO_2, is the word in present-day dentistry. We may say that zirconia is a material of choice in contemporary restorative dentistry for several reasons. Moreover, restorative dentistry is about adhesion promotion and about durable bonding of restorations. Zirconia has found wide applications in dental restorations, such as bridges, crowns, dental implant abutments, and full dental implant systems. This is due to its special and unique properties: high fracture toughness, light color, radiopacity, and, most importantly, biocompatibility. Nevertheless, the restoration interfaces, porcelain-to-zirconia and zirconia-to-resin cement systems, have challenged the dental community and are discussed in this chapter, which also presents bonding mechanisms and the mechanical tests to evaluate these adhesive interfaces. With the advance in zirconia research and the development of its medical uses, the prospects of zirconia as a dental biomaterial are auspicious.

Handbook of Oral Biomaterials
Edited by Jukka P. Matinlinna

ISBN 978-981-4463-12-6 (Hardcover), 978-981-4463-13-3 (eBook)
www.panstanford.com

15.1 Introduction: Is It Zirconium or Zirconia?

15.1.1 Zirconium and Its Alloys

Zirconium (Zr) is an element, a *transition metal*, with an atomic number of 40 (atomic mass 91.22) and with a strong tendency for the maximum valence, +IV (Fig. 15.1). Zirconium is a very strong, ductile, malleable, and lustrous silver-gray metal (Fig. 15.2). Interestingly, its chemical and physical properties are similar to those of titanium (Ti). Ti and Zr are the only two metals commonly used in implant dentistry that do not inhibit the growth of osteoblasts, the bone-forming cells that are essential for *osseointegration*. Zirconium found in nature is composed of five isotopes. ^{90}Zr, ^{91}Zr, ^{92}Zr, and ^{94}Zr are stable. ^{94}Zr can undergo so-called double *beta* decay with a half-life of over 1.10×10^{17} years. ^{96}Zr has a half-life of 2.4×10^{19} years, which makes it the longest-lived radioisotope of Zr. Of these natural isotopes, ^{90}Zr is the most common, making up 51.45% of all zirconium. The isotope ^{96}Zr is the least common, comprising only 2.80% of zirconium [1].

Zirconium is extremely resistant to corrosion and heat, it is lighter than steel, and its hardness is similar to copper (Cu). Surprisingly, when Zr is finely divided, the metal can spontaneously ignite in air, especially at elevated temperatures. Zirconium and its salts generally have low systemic toxicity: the estimated dietary intake is about 50 μg. Most passes through the gut without being adsorbed, and that which is adsorbed tends to accumulate in the skeleton. It has been claimed that the strength of pure titanium is insufficient for use as an artificial hip joint as compared to Co-Cr alloys. Ti-Zr binary alloys have been investigated to evaluate their possible use as biomedical materials with promising results [3]. The Ti-40Zr alloy was shown to have better mechanical properties than Ti, excellent elastic recovery capability, and improved grindability at low grinding speed. It was concluded that the Ti-40Zr alloy has a great potential for use as a dental machining alloy [4].

A recently launched Ti-Zr alloy, commercially called Roxolid™, has been claimed to combine high biomechanical strength with excellent osseointegration, and it might be suitable for dental subgingival implants with narrow diameters. As they claim, ". . . the combination

of enhanced strength and osseointegration could open the door for a new generation of smaller, safer implants, which would be particularly advantageous in situations where there is limited space between teeth. A further potential advantage could be the use in thin bone (narrow bone ridge), where wider implants would necessitate bone augmentation and/or grafting procedures" [5].

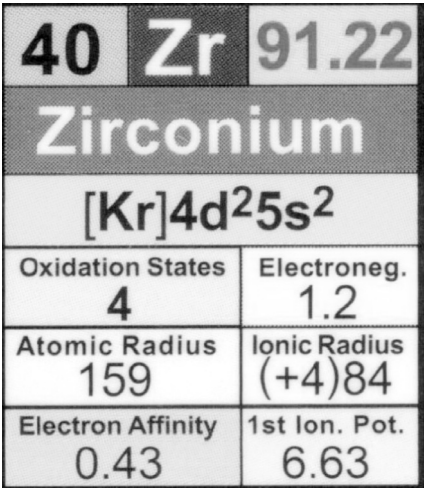

Figure 15.1 Zirconium (Zr) as shown in the periodic table of elements. Some of the important properties are as follows: molar volume is 14.06 cm^3 mol^{-1}, density is 6.5 g cm^{-3}, melting point is 1855°C (1 atm), boiling point is 4409°C (1 atm), specific heat capacity is 0.28 J g^{-1} K^{-1}, and thermal conductivity is 0.23 W cm^{-1} K^{-1}, both at 25°C and 1 atm. Adapted from Ref. [2].

Figure 15.2 From left, blocks of Ti, Zr, and ZrO_2.

It is noteworthy that in some of the marketing materials meant for dental practitioners, we too often read something like ". . . the look of zirconium crowns and bridges is so close to natural teeth that it is hard to tell the difference and it is this quality which makes it very useable within dental work. Zirconium crowns can be fixed using traditional dental cements. Zirconium crowns have quickly become the preferred material for dental crowns. Zirconium is a very strong substance that can endure wear and tear of everyday use. When looking at Zirconium crowns from an aesthetic point it is clear and very similar to a natural tooth and reflects light the same way . . ."

That unfortunate and erroneous extract was read in April 2012 on www.zirconiumcrowns.com, and it tells the plain truth about prevailing confusion in terminology in biomaterials science. Those authors certainly wanted to talk about the zirconia-based ceramic substructure, not zirconium!

15.1.2 Zirconia

Zirconia (zirconium dioxide, ZrO_2) used in dentistry is most often a modified *yttria* (yttrium trioxide, Y_2O_3) tetragonal zirconia polycrystal (Y-TZP). Indeed, yttria is added to stabilize the crystal structure transformation during firing at elevated temperature and improve the physical properties of zirconia [6]. To illustrate this, important zirconia-based ceramic systems are shown in Fig. 15.3A,B. Upon heating, the monoclinic phase (M) in pure zirconia starts transforming to the tetragonal phase (T) at 1187°C (1461 K), peaks at 1197°C (1471 K), and finishes at 1206°C (1480 K). On cooling, the transformation from the tetragonal to the monoclinic phase starts at 1052°C (1326 K), peaks at 1048°C (1322 K), and finishes at 1020°C (1294 K), exhibiting a hysteresis behavior that is well known for this material. As this transformation has many characteristics of *martensitic transformation* in metals, the zirconia tetragonal-to-monoclinic phase transformation is also known as martensitic transformation [2] (see also Chapter 3).

A relatively large volume change accompanies this zirconia phase transformation, with the monoclinic phase occupying about 4% more volume than when tetragonal, which could result in the formation of ceramic cracks if no stabilizing oxides were used. *Ceria*

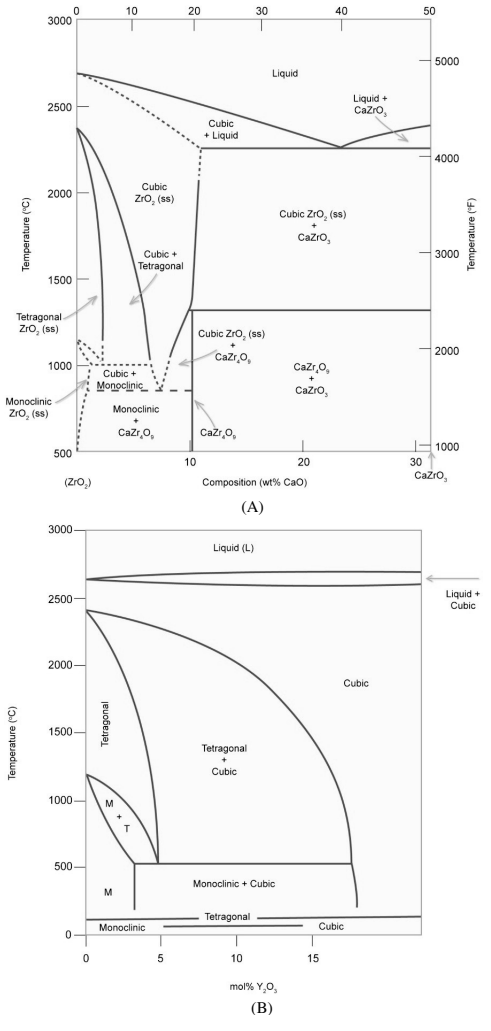

Figure 15.3 (A) A portion of the zirconia–calcia phase diagram (a binary system). The ZrO_2 phases have three different crystal structures: cubic (C), tetragonal (T), and monoclinic (M). NB: The horizontal axis extends to only about 31 wt% CaO (50 mol% CaO), at which $CaZrO_3$ forms. (B) The zirconia-rich end of the yttria–zirconia phase equilibrium diagram. Although pressure is also a parameter that influences the phase structure, it remains virtually constant in most applications; thus these phase diagrams are for a constant pressure of 1 atm. Key: ss = solid solution. Adapted from Ref. [2].

(CeO_2), *yttria* (Y_2O_3), *alumina* (Al_2O_3), *magnesia* (MgO), and *calcia* (CaO) have been used as stabilizing oxides. So, as the monoclinic and $CaZr_4O_9$ phases do not form under normal cooling conditions (as predicted from the phase diagram, Fig 15.3A), consequently, the cubic and tetragonal phases are retained and crack formation due to phase transformation is circumvented [2].

It is also important to consider that stabilization of the tetragonal and cubic structures requires different amounts of dopants (stabilizers). The tetragonal phase is stabilized at lower dopant concentrations than the cubic phase, as shown in the room-temperature region of the ZrO_2–Y_2O_3 phase diagram (Fig. 15.3B). Yet another way of stabilizing the tetragonal phase at room temperature is to decrease the crystal size (the critical average grain size is <0.3 μm). This effect has been attributed to a surface energy difference [2].

Consequently, zirconia-based ceramics used for biomedical purposes typically exist as a metastable tetragonal partially stabilized zirconia (PSZ) at room temperature (Table 15.1). Metastable means that trapped energy still exists within the material to drive it back to the monoclinic state. It turned out that the highly localized stress ahead of a propagating crack is sufficient to trigger zirconia grains to transform in the vicinity of the crack tip. In this case the 4% volume increase becomes beneficial, essentially squeezing the crack to close and increasing toughness [2].

Zirconia, which is sometimes named as "ceramic steel," possesses ideal properties for dental use: superior toughness, strength, and fatigue resistance. Zirconia possesses, in addition, excellent wear properties and is biologically inert—no adverse reactions with tissues are reported. However, its nonreactive surface presents a consistent issue of poor adhesion, that is, low bond strength to other substrates, synthetic or tissues.

Zirconia is currently widely used as a dental biomaterial in frameworks and dental implant fixtures because of its high flexural strength compared to alumina and Co-Cr. Zirconia's compression resistance is ~2000 MPa [7]. Moreover, many investigations on the biocompatibility of zirconia reported no cytotoxic effects on cell culture in vitro tests and no adverse tissue reactions in animals on the basis of in vivo tests [8]. However, the bonding between zirconia and porcelain and, on the other hand, between resin cement and

zirconia, is relatively weak due to the extremely inert, nonreactive character of zirconia. The shear bond strength (SBS) between yttrium-stabilized zirconia and cement reported was only very weak, about 1.5 MPa [9], without any pretreatment on the surface of zirconia.

It is noteworthy that zirconia remains stable even when implanted in the human body, without any adverse reactions. Pure Y-TZP should not cause any concern about its radioactivity [10].

> As a dental biomaterial, zirconia is definitely a material of choice because it has some pronounced advantages. On the other hand, zirconia is chemically inert, leading us to the fact that etching the surface of zirconia with acids is cumbersome.

15.1.3 Alumina

It may be worth taking a brief glance at "aluminum oxide" (Al_2O_3) or *alumina*. Chemically named *aluminum trioxide*, it occurs in nature in corundum as the $Al(OH)_3$ minerals *bauxite* [$Al(OH)_3$], *corundum* [Al_2O_3], *diaspora* [AlO(OH)], and *gibbsite* [$Al(OH)_3$]. Native alumina is very hard, crystalline, and insoluble in water. Alumina is prepared by dehydrating one of the hydrous oxides, which are AlO(OH) and $Al(OH)_3$, which both occur in different crystallographic forms. When heated at ca 850°C, soft and less dense γ-alumina turns to α-alumina, which is insoluble in acids, and perhaps interestingly, its specific gravity increases from 2.8 g cm^{-3} to 4.0 g cm^{-3}. It is noteworthy that alumina in *powder form* is widely used as a grit-blasting material in dental technology. Gems, such as *amethyst, emerald, ruby*, and *sapphire*, are α-alumina with traces of specific metal impurities to give color [11].

Alumina may be called the predecessor of zirconia as a biomaterial in dentistry. Alumina was first introduced in dentistry as a reinforcing inclusion for porcelain in the mid-1960s. However, the inherently low tensile strength of porcelain did not allow it to be used in areas subjected to high stresses. Today, alumina still may find its use as a framework material for the construction of crowns and small all-ceramic fixed restorations. As orthodontic brackets, alumina has also found an application in dentistry. Alumina is used in orthopedics as ball and socket replacements of the hip joint [12].

It is noteworthy that when zirconia particles are added to alumina and mixed properly, alumina will be *toughened* and will thus become harder. The combination of these two materials is called ZrO_2-toughened alumina (ZTA) (Table 15.1) [2]. The zirconia content may vary between 10% and 20% in ZTA [13].

Table 15.1 Some mechanical properties of alumina and zirconia [2, 13]

Property	Alumina	Mg-PSZ	ZTA	Y-TZP	Ce-TZP
Density (g cm^{-3})	3.98	5.7	4.2	6.0	6.1
Vickers hardness (GPa)	24	10	12	11	9
Compr. strength (MPa)	4250	2000	–	2000	–
Young's modulus (GPa)	400	205	380	205	215
Fracture toughness (MN $m^{3/2}$)	5	8...15	4...5	5...9	15...20

Examples of commercially available ceramics: Mg-PSZ = Denzir-M™; ZTA = In-Ceram Zirconia™; Y-TZP = DC Zirkon™, Cercon™, Lava™, and In-Ceram™.

Both alumina and zirconia are single-phase microstructures without a glassy phase, meaning they are real crystalline inorganic ceramic materials. Currently pure alumina core materials on the market contain ca 99.5% alumina, and their flexural strength ranges between 487 MPa and 699 MPa. Alumina's fracture toughness is reported to be around 4.48–6 MPa $m^{1/2}$. In comparison, pure zirconia has a flexural strength of 1000 MPa and a fracture toughness of ca 10.00 MPa $m^{1/2}$ [14, 15].

15.1.4 Zirconia Restorations and Their Preparation

There are in principle *two different ways* to manufacture zirconia structures (frameworks, copings). Both these methods are making use of certain computer-aided design/computer-aided manufacturing (CAD/CAM) technologies. The first way is to machine fully sintered dense blocks of zirconia directly on a specific CAD/CAM system for dental use. It is relatively easy to keep the dimensions of the product without any observable shrinkage.

However, the tools used for grinding may suffer from a high rate of wear. Given this, the flaws produced during machining may lower the mechanical reliability of a zirconia base structure [16].

There is a second way of processing zirconia: the base structure is milled from presintered zirconia blocks, and then a second sintering will be carried out, determining the final mechanical properties of the zirconia structure. Then, the final sintering is accompanied with shrinkage in dimensions that can be compensated with a preadjustment of size at the designing stage (Fig. 15.4). Thus, the fit of the zirconia framework will be warranted [15, 17].

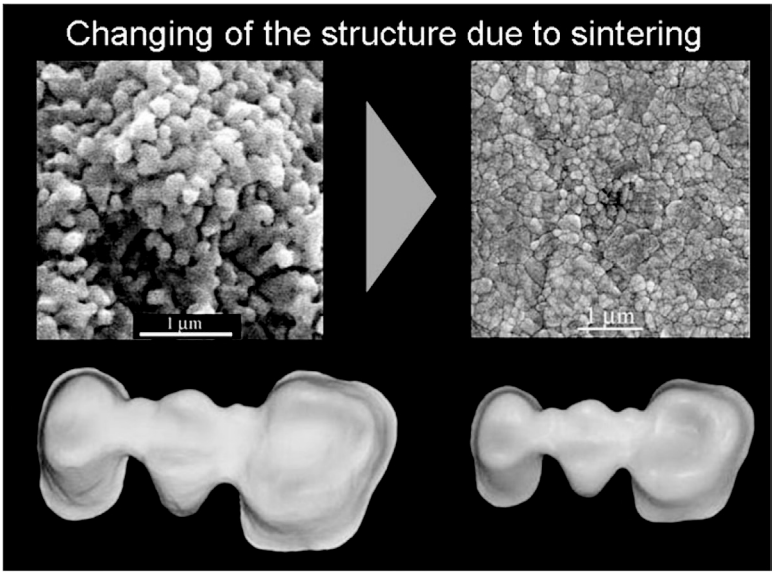

Figure 15.4 Zirconia crystals from Y-TZP contract (shrink) during sintering, resulting in a compact structure. Adapted from Ref. [2].

It has been observed that the CAD/CAM technique has had the ability to produce zirconia restorations with sufficient precision for dental use. A contemporary CAD/CAM system typically consists of three basic parts: a digital scanner, the software for processing obtained data and designing, and the specific technology of production. The use of CAD/CAM technology in the fabrication of zirconia all-ceramic restorations might require less manual work and provide an accurate anatomical appearance (cf. Chapter 18).

Moreover, its effect in improving zirconia–porcelain adhesion has been considered to be significant. There are three main steps in producing a zirconia base: acquisition of digital data, processing and designing, and the fabrication process of the zirconia structure [18].

After the production of a zirconia coping or framework, *veneering porcelain materials* are then fired onto the zirconia base structure with a corresponding anatomical contour. There are two main ways to do it: by using the traditional layering technique (Fig. 15.5) or the hot-pressing method [2, 15].

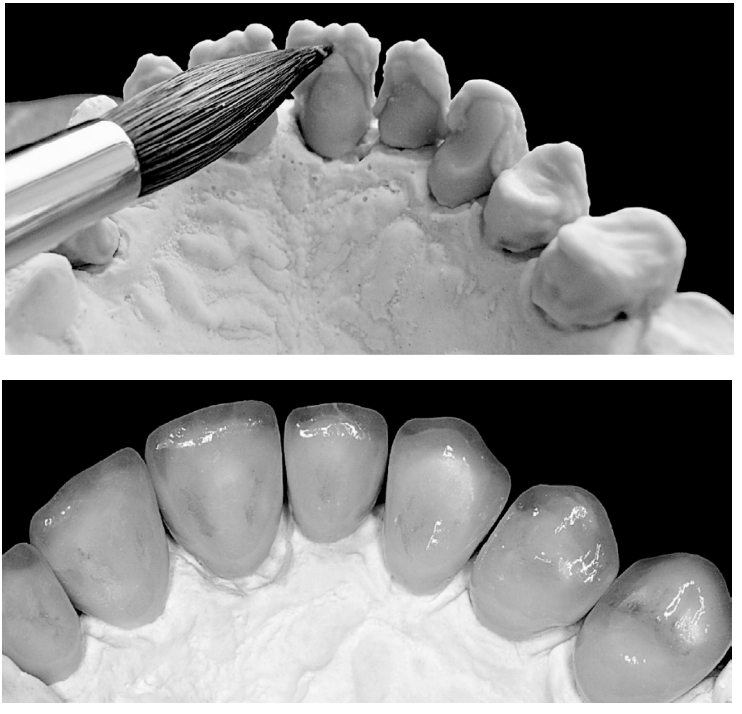

Figure 15.5 Veneering of the zirconia structure: layering technique (above) and hot pressing (below). Adapted from Ref. [2].

15.2 Porcelain–Zirconia Bonding

The mechanisms of porcelain–metal bonding in porcelain fused-to-metal (PFM) restorations are widely understood to consist primarily of chemical bonding between the metal oxide coating on

the framework metal surface and the porcelain, micromechanical interlocking, and compatibility in the coefficient of thermal expansion [19]. As far as the mechanism in porcelain-to-zirconia bonding is concerned, it is still somewhat unclear and not fully understood.

15.2.1 Surface Treatments and Their Effects: Coloring

Regarding its appearance, zirconia is intensively dull white in color and its opacity can mask the tooth substance underneath. In addition, dyeing can be carried out to enhance the esthetic outlook. When the milling process is finished, some manufactures recommend dyeing, coloring, before further steps [15].

Extension of the dyeing time was also reported to be detrimental to the strength and hardness of the frameworks. Hjerppe et al. concluded that the coloring treatment should be performed with great skill and care [20].

15.2.2 Sandblasting

After a zirconia structure is prepared, the veneering porcelain has to be applied and fired onto its surface. As a pretreatment method, sandblasting is often carried out to enhance the bond strength between the zirconia structure and porcelain. However, its benefits are controversial. In one research study, the tensile bond strength between porcelain and zirconia after sandblasting on a zirconia base at different pressures was evaluated and the application of sandblasting at a pressure of 0.4 MPa was recommended as a suitable pretreatment before veneering [21]. On the other hand, it has been reported that the increase in surface roughness could not improve the bonding strength, suggesting that the application of sandblasting and polishing is unnecessary [22–24].

Application of sandblasting was reported to induce a certain amount of the monoclinic phase in zirconia, and this type of transformation would be reversed by the following veneering process. Given this, the variations in dimensions during the course could facilitate the creation of surface flaws [15, 25, 26]. Surface treatments of prosthetic structures in dentistry are also discussed in Chapters 3, 6, and 11.

15.2.3 Some Laboratory Observations

There is some concern about whether the *bonding between porcelain and zirconia* is durable enough for clinical use or whether it is lower than the bonding between porcelain and metal in PFM restorations. Numerous laboratory experiments have been conducted to illuminate this point. One of these studies reported that the difference between porcelain–zirconia bonding and porcelain–metal bonding was not significant. Failures were found to be of a cohesive nature, and they mostly occurred in the veneered porcelain structure near the bonding interface. Thus, it was concluded that the bonding of porcelain and zirconia would not cause a lowering of the clinical performance of zirconia [27]. Moreover, another study on shear bond strength (SBS) testing had confirmed the same findings. In that experiment, the bond strength value of porcelain to zirconia was not significantly different from that of porcelain–metal bonding, while porcelain–alumina bonding appeared to be the weakest one. Furthermore, cohesive failure within the veneered porcelain was observed to be the predominant mode [28].

The relatively strong bonding values have not been confirmed by others. A significant difference on the SBSs was reported when comparing the veneer-to-core interfacial integration between a zirconia-based all-ceramic restoration and a porcelain fused-to-noble-alloy restoration, with the zirconia restoration having the lowest bond strength value. The effect of artificial aging (thermocycling) on the porcelain–zirconia bonding was not confirmed [29]. The same finding was confirmed in a study that explained that the differences among various PFM systems, with both base and noble metal alloys, might not be significant [30]. There is a laboratory study in which SBS tests were carried out assessing the bonding strength values of three different combinations (i.e., study groups): a porcelain–zirconia group, a PFM group, and a porcelain–Li-disilicate group. The porcelain–zirconia group was found to yield the lowest bond strength values [31].

The mode of failure, that is, cohesive, or adhesive, may act as a good assessment tool for the obtained bond strength. The microtensile bond strength (MTBS, μ-TBS) test showed that the interface was the weakest part in porcelain–zirconia bonding and accounted for more than 90% failures [32]. In the SBS test, adhesion

and mixed failures were the predominantly observed modes, while the type of zirconia was not the only factor in determining the failure pattern [33]. Similar failures were found in another laboratory experiment, which also suggested the clinically adequate bond strength in zirconia-based all-ceramics under artificial aging [23].

During production, the veneered porcelain and zirconia substructure goes through firing cycles. The influence of processing may be a potentially detrimental factor to the general reliability of zirconia-based restorations. In a laboratory study, the flexural strength of zirconia specimens was assessed after being veneered under selected firing circles. After mechanical testing, the failure modes were investigated and assessed. The occurrence of *delamination* between porcelain and zirconia was found in some of the specimens with the separation of zirconia and veneered porcelain phases. This might indicate the insufficient bonding strength of porcelain to zirconia [34].

Due to variations in the results of the above-mentioned comparisons, it was suggested that a measurement system for the comparison between different ceramic systems be established [35]. Given this, it was suggested that the test method using so-called *chevron-notch* specimens was an effective way of evaluating the quality of the porcelain–zirconia interface by calculating the interfacial fracture toughness. In one of these tests, the results suggested that porcelain–zirconia bonding appeared to produce a much lower value when compared to the bonding between Li-disilicate and the corresponding veneering porcelain [36].

15.2.4 Porcelain–Zirconia Bonding Mechanism

Various commercial zirconia all-ceramic systems may produce different adhesion strengths in laboratory testing. It has been thought and suggested that the porcelain-veneering procedure produces chemical bonds at the interface between zirconia and porcelain and would form durable bonds [15, 22]. Some studies have observed an exchange of certain chemical elements at the porcelain–zirconia interface, but whether a true chemical bond has formed is to be verified. Yet, some Si-Zr diffusion has been observed with increased firing time, which may contribute to bonding [19].

Nevertheless, it has also been reported that there was no ion change of Si and Zr, which might indicate that the formation of chemical bonds didn't take place [37]. Another study concluded that the molecular deposition of silica on the zirconia surface had no influence on bond strength to porcelain, while the number of porcelain-firing cycles significantly affected the bond strength of the ceramic system [38]. If there is no chemical bonding, how do porcelain and zirconia unite, then?

> Micromechanical (and nanomechanical) interlocking is currently regarded as the major mechanism of porcelain–zirconia bonding.

15.2.5 Laser Methods in Dentistry

Lasers have transformed several areas, including dentistry. Lasers lie very much on the frontier of chemistry and physics. The word *laser* is actually an acronym that is formed from *light amplification by stimulated emission of radiation*. What is stimulated emission, then? A so-called excited state is stimulated to emit a photon by radiation of the same frequency. The more photons that are present, the greater is the probability of the emission. Laser radiation has the following characteristics: it has high power, monochromaticity (one wavelength only), coherence, and collimation and is pulsed [39]. *Dental laser systems* are a family of instruments that can be used for surgery, to cure restorative materials, to assist in tooth bleaching, and to remove decayed tooth structure. Lasers have already been utilized in clinical practice and surface treatment of dental materials for many years [40].

For tooth hard-tissue ablation, the primary mechanism is explained as when the water content in tooth tissue absorbs laser energy, it will be turned into steam instantly. The following volume expansion leads to a microexplosion, which removes ambient tissues and makes surfaces rougher. These properties have made laser irradiation a widely used technique of surface treatment.

In recent years, the use of laser energy in zirconia surface treatment has been reported by several studies. It has been found that the values of zirconia surface roughness had been significantly increased after being processed with an erbium-doped yttrium

aluminum garnet (Er:YAG) laser (i.e., the lasing medium is $Y_3Al_5O_{12}$). The consequent topographical changes of zirconia were observed to be similar to those being air-abraded. Nevertheless, such a high-energy treatment would cause melting and excessive loss of material, generating severe surface damage [41].

Yet, it was claimed that CO_2 laser irradiation at an output power of 3 W could induce higher bond strength of resin to zirconia compared to other surface treatments such as hydrofluoric acid etching and sandblasting with alumina particles. Such improvement was attributed to the appropriate level of output power and microcracks generated on the superficial layer, suggesting that laser treatment could be an alternative to surface treatment of zirconia [42].

The influence of laser surface treatment on porcelain–zirconia bonding still merits further studies—and a deeper understanding.

15.2.6 Zirconia in the Human Body

In dentistry, a strong bond between dental biomaterials and dental tissues is desirable to ensure that a material or a structure, for example, a dental restoration, survives in the oral environment.

On the other hand, there are several studies that have reported that Y-TZP would lose its stability in a wet environment, leading to strength degradation. The crystallographic transformation from the metastable tetragonal phase to the monoclinic phase (T to M transformation) was also observed. Given this, it has been suggested that steam sterilization, at 134°C, should not be carried out when using zirconia as ball-head parts in hip prostheses [2, 7, 17, 43].

Yet another study showed that the microstructure significantly influenced the mechanical and slow crack growth (SCG) behavior of dental ceramics and, consequently, the strength degradation over time (lifetime). The high crystalline content and low porosity found for polycrystalline ceramics (zirconia- and alumina-based ceramics) resulted in high values of flexural strength, low susceptibility to SCG, and low strength degradation over time [44].

The influence of low-temperature degradation (LTD) on dental zirconia is still in need of further and deepening investigation.

15.2.7 Some Zirconia Properties and Their Effects

To understand zirconia's behavior, we have to have a deep look at its properties. There may be mismatch in some mechanical and thermal properties such as fracture toughness, flexural strength, coefficient of thermal expansion, and elastic modulus that affect the bonding between porcelain and zirconia [15]. The results of one study emphasized the effect of misfit in the flexural strength of the veneering material during the development of delamination. Complete interfacial failure was observed between porcelain and zirconia. When another type of porcelain material was used, the flexural strength increased to 300 MPa and then the mode of interfacial failure did not happen. It was proposed that the use of veneering porcelain with high flexural strength, over 300 MPa, could improve the reliability of zirconia-based restorations [45].

The coefficient of thermal expansion was also reported to be one of the critical factors in determining the reliability of zirconia-based restorations [43]. The porcelain will fit well to the zirconia surface when its firing temperature is above its glass transition temperature. On the other hand, when the temperature is below the glass transition temperature, it will be difficult for such an adaptation to be continued due to the high viscosity of porcelain. Thus, residual stresses will be formed in veneering porcelain. When the porcelain goes through a change in temperature through its glass transition temperature, there will be variations in the coefficient of thermal expansion. It is noteworthy that this change has an influence on the residual stress distribution during the cooling process above the glass transition temperature [15]. The residual stresses derived from the coefficient of thermal expansion match between the zirconia core and the porcelain layer were detrimental to the interfacial integration [32]. A study by Aboushelib et al. on SBS testing suggested a detrimental effect of increasing the coefficient of thermal expansion mismatch on porcelain–zirconia bonding [46].

Even so, it has been assumed that there is a high stress area created and concentrated close to the core–veneer interface. With the increase in the coefficient of thermal expansion mismatch between core and veneer materials, the induced high stress would become more pronounced. When the combination of this stress and applied load exceeds the bonding strength, delamination might

happen. The use of a veneering material with a higher coefficient of thermal expansion than the core material would cause immediate failure of the veneered porcelain during cooling [15, 47]. If there was no difference between the zirconia core and porcelain, the highest resistance of delamination would be attained. Moreover, the lower tolerance of shear loading would be produced when using porcelain with a lower coefficient of thermal expansion [26].

A complete match in the coefficient of thermal expansion is very cumbersome in practice. There are also concerns about a suitable level of the difference of the coefficient of thermal expansion between veneer (porcelain) and core (zirconia) materials. One previous study on fracture strength suggested the value of $\Delta\alpha\Delta T$, where $\Delta\alpha$ is referred to as the difference in the coefficient of thermal expansion and ΔT is referred to as the value of the porcelain glass transition temperature over room temperature, to be set at the range between 185×10^{-6} and 1250×10^{-6} for minimizing the residual stress generated in the veneer part [48]. Adoption of a difference at a magnitude of $\Delta\alpha\Delta T \approx 1000 \times 10^{-6}$ would facilitate the highest shear bond strength for porcelain–zirconia bonding [49]. When the mismatch in the coefficient of thermal expansion was within the range $0.75–1.7 \times 10^{-6}$ K^{-1}, its influence was not regarded as significant [23]. These results may give us some indication for further investigations.

The initiation and propagation of delamination were also reported to be related to the misfit in elastic moduli and fracture toughness of porcelain and zirconia [50]. Indeed, such differences might induce crack propagation deflected from the porcelain, to proceed along the veneer-to-core interface.

15.2.8 Cooling Rate

The veneering porcelain will experience a change from a viscoelastic state to a solid form when its temperature is reduced and when it passes through the glass transition temperature, T_g [15]. During cooling after sintering, residual stresses might be generated and influence both the strength of porcelain and interfacial integration. Most of the manufacturers recommend slow cooling [2, 51].

Now, slow cooling after the sintering process of veneering is intended to reduce the chipping rate of zirconia-based restorations. The creation of residual stresses may be administrated by performing

heat treatment near the glass transition temperature and altering the cooling rate, as suggested by Taskonak et al. [52].

However, the slow cooling rate has been questioned by one laboratory study in which the application of slow cooling, that is, in the range between the sintering temperature and the glass transition temperature, was shown to have a negative effect on porcelain–zirconia bonding. It was explained that the compressive stresses produced during the rapid cooling stage might reduce the tensile stresses caused by the applied load. Given this, the slow cooling process might fail to develop such an effect. The results suggested [53] that the slower cooling rate would increase the possibility of chipping, which might be caused by the lack of formation of compressive stresses in the porcelain structure. However, this was one study, and the conclusions need to be proven.

Porcelain–zirconia bonding has been thought to be promoted by using a special *liner material*, which could also mask the bright-white appearance of zirconia. Indeed, such an effect was confirmed in the microtensile strength test with the bond strength being even doubled after applying the liner material. The positive effect was explained to be due to better wetting between porcelain and zirconia [32]. Nevertheless, the results of using a liner (primer) were different from another SBS test report that suggested no positive effect on bond strength [54].

15.2.9 More about Veneering

Pressable veneering porcelains were introduced into the market, claiming that the pressing technology might help to establish better bonding between porcelain and zirconia. As reported before, the adoption of veneering porcelain recommended by the manufacturer would play an important role in the production process [31]. Different effects of several techniques on the impact fracture strength have been evaluated. The results suggested that the difference between the traditional and the pressing method was not significant and the most frequent modes of failure were proved to be delamination and cone cracking within the veneered porcelain body [55].

A combination of hot pressing and manual layering techniques has also been suggested. The use of pressable porcelain aims to achieve a better anatomical appearance of zirconia-based

restorations. It may produce fewer flaws in bulk of the material. The influence of such a veneering technique on the bonding quality of the zirconia–porcelain interface was tested for microtensile strength, and it was shown to produce a negligible effect when compared to the conventional layering method [56].

A high fracture toughness value was produced with a new veneering method using CAD/CAM technology. In this new method, a Li-disilicate ceramic cap is produced by a CAD/CAM system. The ceramic cap is then veneered on the zirconia coping by using certain glass ceramics. Such a combination could improve the wetting between zirconia and porcelain and result in an improvement of bond strength [57]. In addition, the fracture strength was shown to be higher than that produced in a traditional porcelain-layering method.

It was observed that the wet-veneering procedure might be associated with a decrease in the quality of porcelain–zirconia bonding. The first veneering process with minimal moisture composition may be beneficial for the production of zirconia restorations. A survey of the porcelain–zirconia interface has identified that higher moisture content and veneering temperature would facilitate the generation of grain faceting on the zirconia surface [58]. The reasons for this phenomenon and its long-term influence on the reliability and stability of zirconia–porcelain integration are unclear and thus merit further study.

15.2.10 Some Clinical Experience and Observations

There has been some concern about whether the bonding between porcelain and zirconia is durable enough for clinical use or whether it is lower than the bonding between porcelain and metal. This scientific discussion certainly continues when you are reading these lines! Several laboratory experiments have been conducted on certain ways to compare and assess the matter, as described above.

The incidence of veneering porcelain fracture in zirconia-based restorations seems to be at a relatively high level when compared to PFM systems, according to Sailer et al. [59]. The rate of fracture of veneering porcelain from zirconia-based restorations was reported to vary from 6% to 25% after about three years [2, 27, 60–62]. There are some review papers on the fracture rate of all-

ceramic restorations [2, 59]. The fracture of veneering porcelain was reported to be 0.59% and 2.92% per year in PFM and all-ceramic (including zirconia) restorations, respectively [59].

> Delamination (i.e., failure at the porcelain–zirconia interface) and, on the other hand, chipping (i.e., failure within the veneering porcelain) have been reported to be the two most common modes of failure [63, 64].

15.3 Resin–Zirconia Bonding

This part of the chapter introduces adhesion mechanisms used for resin–ceramic bonding, mainly resin bonding to zirconia-based restorations, providing scientific evidence for the clinical procedures.

At first, one could imagine that an all-ceramic restoration would not withstand the intraoral service. It could be true if the restoration was not bonded to the tooth structure or remaining restorative materials (e.g., resin composites and metals), working as an integrated system where diverse stresses, from chewing and parafunctional habits (e.g., bruxism), are distributed throughout the system due to appropriate bonding [2]. This rationale is supported by the ISO 6872:2010 [65] standard that classifies ceramics according to the intended clinical use and makes a distinction between adhesively and nonadhesively cemented restorations.

So, what is *adhesion?* It can be defined as a molecular (or atomic) attraction between two contacting surfaces (substrates) promoted by the interfacial force of attraction from different molecules (or atoms). This is distinct from *cohesion*, which is the attraction between same types of molecules within one substance. The adhesion and cohesion concepts are also important for further distinction between adhesive and cohesive failures, presented later in this chapter. The adhesion phenomenon can occur via (a) *physical*, (b) *mechanical* (structural interlocking), or (c) *chemical* mechanisms or a combination of them. Whenever an adhesive agent is used to bond two materials and it solidifies during bonding, the process is called adhesive bonding.

Therefore, *adhesives* are substances that promote adhesion between two substrates, that is, *adherends.* In addition, an

intermediary substance can be used to enable bonding between the adhesive and the adherend, and such a material is known as a coupling agent (Fig. 15.6), for example, silanes (which are discussed in detail in Chapter 11). Alternatively, the products used to modify the characteristics of a surface facilitating adhesion are known as *primers*, such as phosphoric acid (H_3PO_4) for dental enamel and dentine and hydrofluoric acid (HF) for porcelains (see also Chapters 3, 6, and 11).

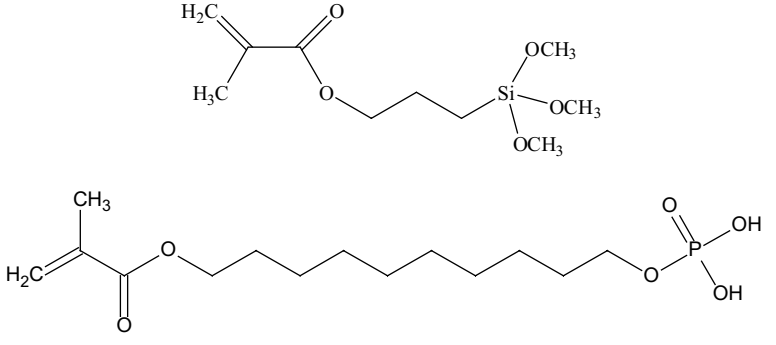

Figure 15.6 Molecular structures of MPS (above) and MDP (below). *Abbreviations*: MPS, 3-methacryloyloxypropyltrimethoxysilane; MDP, 10-methacryloyloxydecyldihydrogenphosphate.

Unfortunately, the *distinction* between primers and coupling agents is rarely made in the dental literature, and the two terms are used interchangeably. Nevertheless, a relatively strong bond can result from the synergistic action of a number of bonding mechanisms, such as a large area of intimate contact providing numerous sites for the creation of weak secondary bonds and the presence of surface undercuts at the microscopic level [2, 66] (see also Chapters 3 and 6).

15.3.1 Adhesion Mechanisms

Adhesion to the tooth structure (enamel, cementum, and dentine) is well explored and explained in the dental literature, and therefore, it is not the primary goal of this chapter (but see Chapter 1). However, ceramic restorations need to be bonded to the tooth structure and/or other remaining restorative materials, and the clinical success of

the restorations also depends on adequate bonding at the cement–tooth structure interface. Nevertheless, different primers and adhesives coupled with specific bonding procedures drastically reduce microleakage and its consequences. Today, glass ionomer cements (GICs) and resin-based cements are primary choices for bonding ceramic restorations to the remaining tooth structure. GICs and resin-modified GICs (RMGICs) are often used to cement acid-resistant ceramics, mostly because these cements are very easy to use. Yet, the most popular and effective cements for all types of ceramic restorations are resin-based composites, especially systems containing 10-methacryloyloxydecyldihydrogenphosphate (MDP) monomers, which are often used to cement acid-resistant ceramics (Fig. 15.6) [2].

Considering the chemical reactivity to acids, ceramics can be either acid sensitive or acid resistant according to the degree of surface degradation produced by acids. Acid-sensitive ceramics (e.g., feldspar-, leucite-, and lithium disilicate–based ceramics) are readily etched, creating micromechanically retentive surfaces (Fig. 15.7A–C). Acid-resistant ceramics (e.g., densely sintered alumina ceramics and Y-TZP ceramics) do not show much surface degradation by etching, preventing a reliable micromechanical bond to resin [2, 17, 67–70].

It has been reported that the clinical success of resin-bonding procedures for ceramic restorations and ceramic repairs depends on the quality and durability of the bond between the ceramic and the resin. The quality of this bond depends upon the bonding mechanisms that are controlled in part by the surface treatment that promotes micromechanical and/or chemical bonds to the substrate [17, 67–78].

Structural and surface analyses of etched acid-sensitive ceramics have shown that different etching patterns are created according to the ceramic microstructure and composition and according to the concentration, application time, and type of etchant [67–70, 72]. Fluoride-containing etchants such as hydrofluoric acid (HF), ammonium hydrogenfluoride, aka ammonium bifluoride (ABF), and acidulated phosphate fluoride (APF) have been used to etch dental ceramics [67, 68].

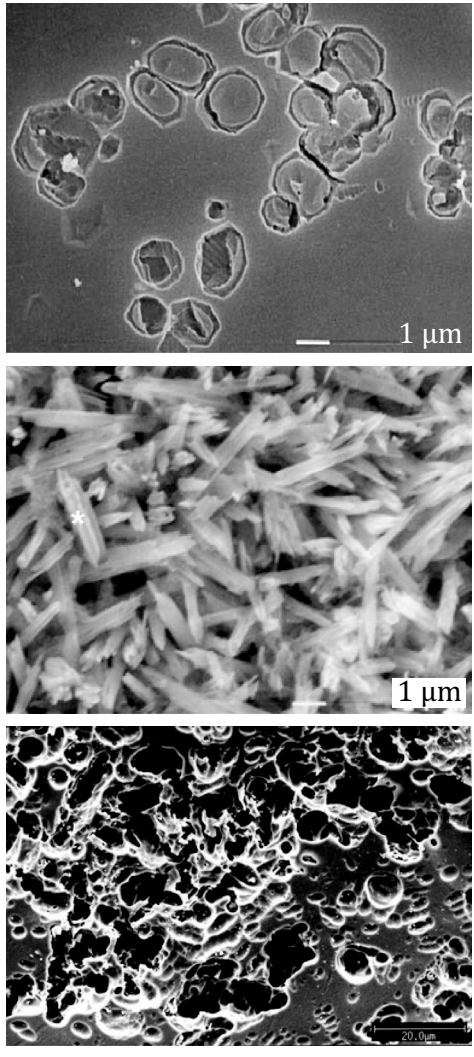

Figure 15.7 SEM photomicrographs in the SEI mode of etched (10% HF for 90 s) ceramic surfaces, showing clinically acceptable retentive surfaces for resin bonding. (Above) Leucite-reinforced glass ceramic (IPS Empress™, Ivoclar-Vivadent) (1000x). **(**Middle) Li-disilicate-based ceramic (IPS Empress 2™, Ivoclar-Vivadent); the Li-disilicate crystals (*) were confirmed by XRD (white bar is 1 µm). (Below) Feldspathic porcelain (Ceramco II™, Dentsply) (1000x). All images adapted from Ref. [2]. *Abbreviations*: SEM, scanning electron microscopy; SEI, secondary electron image.

Alteration of the surface topography results in changes in the surface area and in the wetting behavior of the ceramic [67–70, 71–78]. This also changes the ceramic surface free energy and its adhesive potential to resins [76].

Thus, the ceramic microstructure, composition, and morphology after surface treatment (priming) should yield potentially useful information on the clinical success of the bonding procedures for ceramic restorations and ceramic repairs, justifying the interest of dentists and researchers in potential ceramic surface treatments, which still offer some challenge for acid-resistant ceramics [2].

As *acid etching* is not an effective surface treatment for acid-resistant ceramics, other methods to produce micromechanical retention have been used, including airborne particle abrasion systems and coarse diamond rotary instruments. Several studies [38, 69, 70, 77–79] reported that airborne particle abrasion methods using alumina particles or silica-modified alumina particles (*silica-coating*) produced greater surface roughness (R_a) values and that silica-coated surfaces showed a significant increase (76%) in the concentration of silicon, which should enhance bonding to resins via silane coupling agents (Fig. 15.8) [70, 79]. Therefore, silica-coating (aka silicatization) systems (e.g., Rocatec™ and CoJet™, 3M ESPE, Seefeld, Germany) have been used to create a silica layer on metal and ceramic surfaces through high-speed surface impact of the silica-modified alumina particles that can penetrate up to 15 μm into ceramic and metal substrates (Fig. 15.8).

This *tribochemical effect* may be explained by *two bonding mechanisms*:

(1) The creation of a topographic pattern via airborne particle abrasion, allowing for micromechanical bonding to resins
(2) The promotion of a chemical bond between the silica-coated ceramic surface and the resin-based material via a silane coupling agent (Fig. 15.8) (see also Chapter 11)

Silane bonds to Si-OH on a ceramic surface by condensation reactions, and the methyl methacrylate >C=C< double bonds provide bonding to the adhesive. As long as there are adequate Si-OH sites on the ceramic surface, satisfactory bonding should be achievable [78, 79]. Therefore, if the goal is to obtain a thin silane coating on any ceramic surface, the protocol should consider the various

ceramic microstructures and silane types and mechanisms to reduce the thickness of the silane layer, such as heat treatment [79] (see also Chapter 11 for details).

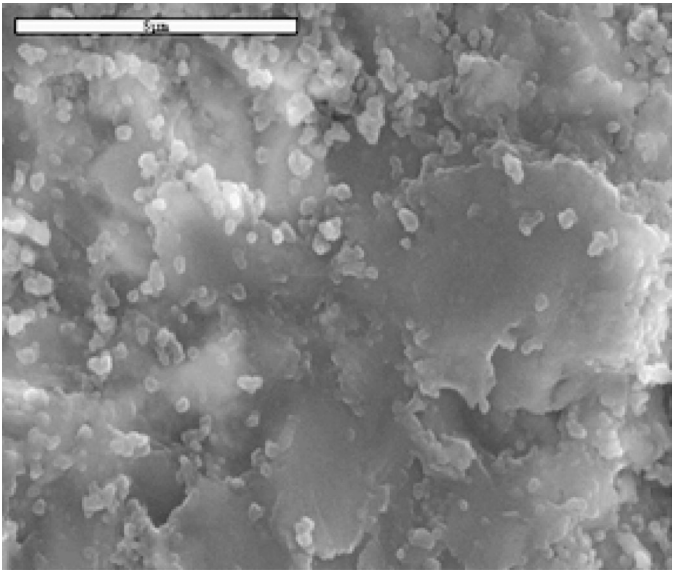

Figure 15.8 SEM photomicrographs in SEI mode of silica-coated zirconia-reinforced alumina (In-Ceram™ Zirconia, Vita™) using 30 μm silica-modified alumina particles (CoJet™, 3M ESPE) blasted for 15 seconds (5000x). Adapted from Ref. [2].

In addition, the *type of resinous adhesive* also plays an important role in the bond to high-crystalline-content ceramics. It has been reported that the chemical bond to these ceramics is improved by using adhesive resin systems containing phosphate monomers, for example, MDP [2, 78] (see also Chapter 6).

Therefore, adhesion between dental ceramics and resin-based composites is the result of a *physicochemical interaction* across the interface between the resin (adhesive) and the ceramic (substrate). The physical contribution to the adhesion process is dependent on the surface treatment and topography of the substrate and can be characterized by its *surface energy*. Alteration of the surface topography by etching or airborne particle abrasion results in changes in the surface area and in the wettability of the substrate, which are related to the surface energy and the adhesive potential.

In addition, the surface energy of a solid is greater than that of its interior, where interatomic distances are equal, and the energy is minimal [2]. Similarly, at the surface of the lattice, the energy is greater because the outermost atoms are not equally attracted in all directions. This increase in energy per unit area of the surface (J m^{-2} or N m^{-1}) is referred to as the surface energy (g), or surface tension for liquids.

Therefore, the surface atoms of a solid tend to form bonds to other atoms in close proximity to the surface, reducing the surface energy of the solid. Again, achieving an energy balance or the lowest energy state is the driving force for the chemical bond between the adhesive and the adherend. Yet, the surface energy and adhesive qualities of a given solid can be reduced by any surface impurity or contaminate, such as human secretions and air voids. The functional chemical groups available or the type of crystal plane of a space lattice present at the surface also affect the surface energy [2].

Nevertheless, a clean (i.e., no contaminants) and dry surface ensures that the adhesive has the best-possible chance of creating a proper bond with the adherent. In addition, the wettability of the adherend by the adhesive, the viscosity of the adhesive, and the morphology of the adherend surface influence the ability of the adhesive to make intimate contact with the adherend. Thus, to succeed in the challenge of resin bonding to any high-crystalline-content ceramic, including zirconia-based ceramics, one should consider all the aspects listed above, which have been discussed in many recent dental publications, including the citations of this chapter.

15.3.2 Bond Strength Tests and Fractography Analysis

Bond strength tests have been used to predict the clinical performance of resin-bonded ceramic restorations. Yet, most of these tests exhibit wide variability in *fracture pattern* and *bond strength value*. The commonly used SBS test is very sensitive to the method of application of the adhesive and design of the testing arrangement, often producing fracture at a distance from the resin–ceramic adhesion zone that may lead to erroneous conclusions on bond quality [73, 78, 80–83].

Such failures of the substrate prevent measurement of interfacial bond strength and limit further improvements in bonding systems. A classic study showed that significant differences in SBSs are obtained for different sample configurations using identical geometric design and adhesive interface [73]. This gives some credence to the expression "Imagine a bond strength value and a test arrangement can be designed to produce such a result . . ."

Yet, many studies using SBS test arrangements suggested a lack of reliability of such measurements and identified nonuniform stress distributions along the bonded interfaces [70, 71, 73, 78, 80–85]. Nevertheless, when they are correctly performed and interpreted using *fractography analysis*, they may adequately rank experimental groups with relevant differences.

In the search for a method that produces uniform stress distribution across the interface, investigators have evaluated similar adhesive systems under different bond test configurations and suggested that a tensile bond strength test would be more appropriate to evaluate the bond strength of adhesive interfaces [2, 70, 73, 74, 78, 80–85].

The MTBS, or μ-TBS, test, which is actually a tensile bond strength test with a reduced testing area, was developed as an attempt to eliminate the nonuniform stress distribution at the adhesive interface and to minimize the influence of interfacial defects. The reduction in the number and size of defects in the adhesion zone is thought to decrease the incidence of bulk cohesive failures and increase the tensile bond strength, regardless of the cross-sectional shape of the specimens. This test has been used to measure the bond strength of resin-based composites to the tooth structure and to restorative materials, including all types of ceramics [2, 70, 74, 78, 84, 85] (see also Chapter 16).

There are *two typical methods* of preparing specimens for the microtensile test, *trimming* (dumbbell shaped) and *nontrimming* (bar shaped). The nontrimming method places less stress on the adhesion zone, and as no specimen finishing is necessary, it also avoids areas of stress concentration produced by polishing materials of different hardness values. The adhesion zone is defined as the region in which the adhesive interacts with the two substrates to promote bonding.

More specifically, the **composite–ceramic adhesion zone** consists of the following:

(1) An interfacial region between the adhesive and the composite within which molecular interaction and chemical bonding occur between the two materials
(2) An adhesive
(3) An interfacial region between the adhesive and the ceramic, including the treated ceramic surface region where micromechanical and/or chemical bonding occurs

Again, the bond strength values resultant from any bond test, including the microtensile bond strength test, can only be considered a reliable indicator of the resin–ceramic bond quality if the fractures occur within the adhesion zone [2, 74, 78].

Although the mode of failure is an important aspect of bond strength tests, it is not commonly reported. A detailed inspection of fractured surfaces can indicate the failure mode of a bonded assembly. The fracture behavior of adhesive interfaces depends on the stress level, flaw distribution, material properties, and environmental effects. Therefore, fracture surface characterization combined with analyses of fracture mechanics parameters is of great importance to understand and predict bonded interface reliability and also to reduce the risk for data misinterpretation such as the inference that the bond strength must exceed the cohesive strength of the ceramic when the fracture initiates within the ceramic material and away from the interface [2, 70, 74, 78].

> Therefore, **failure analysis based on fractographic principles** should assist researchers to correctly interpret the fracture phenomena [2, 74, 78, 83, 86–88].

Yet, *optical microscopy observation* is often not enough to determine the mode of failure of bonding interfaces, and a thorough SEM examination of the fracture surfaces along with a surface composition analysis (e.g., X-ray elemental map analysis) produces a more consistent and complete description of the fracture process and the modes of failure [2, 74, 78, 88].

These analyses would avoid simplistic comments such as the “mixed mode of failure” that often follows “adhesive and/or

cohesive" unscientific observations. Thus, when fractography is correctly used to determine the fracture origin, a proper scientific statement on the mode of fracture can be formulated, improving the quality of the scientific report [2]. Additionally, one can promote crack initiation within the adhesion zone and use an interfacial toughness test coupled with fracture mechanics and fractographic principles to estimate the apparent interfacial fracture toughness [2, 77].

Another appropriate way to assess the interfacial bond is to analyze the energy per unit crack surface area, G_I, that is required for a crack to advance in the bond plane. The toughness is related to the *critical strain energy release rate* (G_{IC}) and is a measure of the resistance of the bond to fracture, since G_{IC} represents the relative energy required to create new surfaces [2, 77].

The above rationale on adhesion to ceramics should develop a fundamental basis to understand the clinical performance of bonded all-ceramic restorations, the possible failure causes, and the principles to improve the adhesion mechanisms of resin-based composites bonded to dental ceramics.

15.3.3 Clinical Considerations for Resin Bonding to Zirconia

Long-lasting esthetics is the main reason for the increasing interest in all-ceramic restorations [2]. The new polycrystalline dental ceramics are stronger and tougher but have to be veneered for pleasant esthetics. Additionally, these restorations have to be bonded to teeth to have a greater survival rate. Failures due to fracture are mostly related to the brittle nature of ceramic materials and inadequate restorative design. Secondary caries and periodontal support are biological responses not related to ceramic materials. In fact, there is no evidence to say that a marginal gap is clinically related to secondary caries.

On the contrary, it is more related to the caries susceptibility of the patient [2, 62]. Additionally, resin bonding decreases the marginal leakage of ceramic restorations, improving the overall strength of the restoration [2, 89–91]. To minimize failures in all-ceramic

restorations, dentists should pay attention to case selection, tooth preparation, material selection, restoration design, cementation technique, occlusion equilibration, and patient preservation [2, 92–96]. Tooth preparation has a major influence on the durability and color (mainly shade and translucency) of the final ceramic restoration, because it will dictate the internal surface contour and the thickness of the ceramic restoration [2, 96, 97]. Analogically to cracks, sharp angles on tooth preparation are stress concentrators and should be always avoided. In addition, the fracture behavior and strength of ceramic restorations change as the ceramic thickness changes, which is theoretically explained by A. A. Griffith (1893–1963) and clinically observed in chipped ceramic restorations [2].

Therefore, the *amount of tooth reduction* should allow for adequate ceramic thickness. Although color is an effect of light and subjective perception, the final shade of the restoration will modify as the thickness of the ceramic layers changes, especially when the thickness of the enamel ceramic layer is altered. As skilled hands can only execute what one's brain perceives visually, clinicians have to be circumspect examining the patient and envisioning the treatment that best encompasses the various aspects of the final restoration: anatomically, biologically, structurally, functionally, and esthetically. However, since tooth preparation often influences the material selection for the final restoration, clinicians should be attentive to the fact that treatment planning may require modification after tooth preparation [2]. The introduction of zirconia-reinforced alumina and zirconia-based structures allowed for the introduction of posterior fixed partial dentures (FPDs) that have shown adequate survival rates [2, 62].

A study evaluated the clinical performance of zirconia-reinforced alumina (In-Ceram™ Zirconia) posterior FPDs (n = 18) after three years of service with a survival rate of 94.5% [98].

Another study showed a success rate of 98% for 33 posterior zirconia-based FPDs (Cercon™), despite the fact that the overall survival rate has been 74% due to other complications, such as secondary caries (22%) and chipping of the veneering ceramic (15%) [199]. In these two clinical studies (n = 51) only one fracture of the zirconia-based framework was reported, which showed a very promising trend for all-ceramic FPDs (Fig. 15.9A–C).

Figure 15.9 (A) A CAD/CAM system (Cerec 3 InLab™, Sirona) was used to scan the cast and fabricate zirconia-based ceramic substructures (In-Ceram YZ, Vita™) that were tried in place. (B) A feldspathic ceramic (VM9, Vita™) was used to veneer the zirconia substructure. (C) The FPD was cemented in place using a self-etching resin-based luting system (RelyX Unicem™, 3M ESPE). Adapted from Ref. [2].

In general, the *most common causes of all-ceramic structural failures* reported from clinical studies are (1) fracture initiated in the connector area of FPDs, either at the core–veneer interface or at the gingival embrasure and (2) chipping of the veneering material [2, 17, 44, 62, 92, 93, 100, 101]. Yet, very few clinical studies suggested some type of adhesion failure, but none could confirm an interfacial bond failure [2, 44].

This fact (i.e., no interfacial bond failure observed) mainly infers two possible explanations:

(1) The current adhesive protocols are clinically reliable.
(2) The all-ceramic restorations structurally fail before interfacial bond failure. Well-designed, long-term clinical trials will enlighten this uncertainty [2].

Currently, the *two most popular clinical strategies* to resin-bond acid-resistant ceramic restorations are [2]:

(1) improving mechanical retention with an airborne particle abrasion system using alumina particles associated with a chemical bond using an adhesive/cement system containing a ceramic primer with a phosphate-based monomer such as MDP [102, 103]
(2) improving mechanical retention with an airborne particle abrasion system using silica-coated alumina particles to introduce an irregular silica layer onto the ceramic surface, followed by a silane coupling agent, which promotes a chemical bond to any resin-based adhesive/cement system [15, 79, 104–107].

It is noteworthy that manufacturers routinely provide cementation recommendations that should be given serious consideration.

Summa summarum: This chapter presented evidence suggesting an acceptable clinical longevity of resin-bonded zirconia-based restorations to go along with their long-lasting esthetics.

References

1. Audi, G., Bersillon, O., Blachot, J., Wapstra, A. H. (2003) Nubase2003 evaluation of nuclear and decay properties, *Nucl. Phys. A,* **729**, 3–128.

2. Della Bona, A. (2009) *Bonding to Ceramics: Scientific Evidences for Clinical Dentistry*, Artes Medicas, Sao Paulo.
3. Kobayashi, E., Matsumoto, S., Doi, H., Yoneyama, T., Hamanaka, H. (1995) Mechanical properties of the binary titanium-zirconium alloys and their potential for biomedical materials*, J. Biomed. Mater. Res.,* **29**, 943–950.
4. Ho, W. F., Chen, W. K., Wu, S. C., Hsu, H. C. (2008) Structure, mechanical properties, and grindability of dental Ti-Zr alloys, *J. Mater. Sci. Med.*, **19**, 3179–3186.
5. Berner, S., Dard, M., Gottlow, J., Molenberg, A., Wieland, M. (2009) Titanium-zirconium: a novel material for dental implants, *Eur. Cells Mater.,* **17**, 16.
6. Lung, C. Y. K., Matinlinna, J. P. (2010) Resin bonding to silicatized zirconia with two isocyanatosilanes and cross-linking silane. Part I: experimental approach, *Silicon*, **2**, 153–161
7. Piconi, C, and Maccauro, G. (1999) Review: zirconia as a ceramic biomaterial, *Biomaterials*, **20**, 1–25.
8. Warashina, H., Sakano, S., Kitamura, S., Yamauchi, K.-I., Yamaguchi, J., Ishiguro, N., Hasegawa, Y. (2003) Biological reaction to alumina, zirconia, titanium and polyethylene particles implanted onto murine calvaria, *Biomaterials*, **24**, 3655–3661.
9. Derand, T., Molin, M., Kvam, K. (2005) Bond strength of composite luting cement to zirconia ceramic surfaces, *Dent. Mater.,* 21, 1158–1162.
10. Vagkopoulou, T., Koutayas, S. O., Koidis, P., Strub, J. R. (2009) Zirconia in dentistry, part 2: evidence-based clinical breakthrough, *Eur. J. Esthet. Dent*., **4**, 130–151.
11. Heslop, R. H., Robinson, P. L. (1967) *Inorganic Chemistry: A Guide to Advanced Study*, 3rd ed., Elsevier, Amsterdam.
12. McLean, J. W. (2001) Evolution of dental ceramics in the twentieth century, *J. Prosthet. Dent.,* **85**, 61–66.
13. Claussen, N. (1976) Fracture toughness of Al_2O_3 with an unstabilized ZrO_2 dispersed phase, *J. Am. Ceram. Soc.*, **59**, 49–51.
14. Hefferman, M. J., Aquilino, S. A., Diaz-Arnold, A. M., Haselton, D. R., Stanford, C. M., Vargas, M. A. (2002) Relative translucency of six all-ceramic systems. Part I: core materials, *J. Prosthet. Dent.,* **88**, 4–9.
15. Liu, D., Matinlinna, J. P., Pow, E. H. N. (2012) Insights into porcelain zirconia bonding, *J. Adhes. Sci. Technol.*, **26**, 1249–1265.

16. Luthardt, R. G., Holzhüter, M., Sandkuhl, O., Herold, V., Schnapp, J. D., Kuhlisch, E., Walter, M. (2002) Reliability and properties of ground Y-TZP-zirconia ceramics, *J. Dent. Res.,* **81**, 487–491.

17. Denry, I., Kelly, J. R. (2008) State of the art of zirconia for dental applications, *Dent. Mater.,* **24**, 299–307.

18. Coli, P., Karlsson, S. (2004) Precision of a CAD/CAM technique for the production of zirconium dioxide copings, *Int. J. Prosthodont.*, **17**, 577–580.

19. Kawai, Y., Uo, M., Watari, F. (2010) Microstructure evaluation of the interface between dental zirconia ceramics and veneering porcelain, *Nano Biomed.,* **2**, 31–36.

20. Hjerppe, J., Närhi, T., Fröberg, K., Vallittu, P. K., Lassila, L. V. (2008) Effect of shading the zirconia framework on biaxial strength and surface microhardness, *Acta Odontol. Scand.,* **66**, 262–267.

21. Nakamura, T., Wakabayashi, K., Zaima, C., Nishida, H., Kinuta, S., Yatani, H. (2009) Tensile bond strength between tooth-colored porcelain and sandblasted zirconia framework, *J. Prosthodont. Res.,* **53**, 116–119.

22. He, S., Chen, J. H., Wang, G. Y., Wang, S. H., Shen, L. J., Wang, H. (2005) The bond properties of Vitadur alpha on dental zirconia framework material, *Shanghai Kou Qiang Yi Xue*, **14**, 397–401.

23. Guess, P. C., Kulis, A., Witkowski, S., Wolkewitz, M., Zhang, Y., Strub, J. R. (2008) Shear bond strengths between different zirconia cores and veneering ceramics and their susceptibility to thermocycling, *Dent. Mater.,* **24**, 1556–1567.

24. Kim, S. T., Cho, H. J., Lee, Y. K., Choi, S. H., Moon, H. S. (2010) Bond strength of Y-TZP-zirconia ceramics subjected to various roughening methods and layering porcelain, *Surf. Interface Anal.,* **42**, 576–580.

25. Guazzato, M., Quach, L., Albakry, M., Swain, M. V. (2005) Influence of surface and heat treatments on the flexural strength of Y-TZP dental ceramic, *J. Dent.,* **33**, 9–18.

26. de Kler, M., de Jager, N., Meegdes, M., van der Zel, J. M. (2007) Influence of thermal expansion mismatch and fatigue loading on phase changes in porcelain veneered Y-TZP zirconia discs, *J. Oral Rehabil.,* **34**, 841–847.

27. Vult von Steyern, P., Carlson, P., Nilner, K. (2005) All-ceramic fixed partial dentures designed according to the DC-zirkon technique. A 2-year clinical study, *J. Oral Rehabil.*, **32**, 180–187.

28. Al-Dohan, H. M., Yaman, P., Dennison, J. B., Razzoog, M. E., Lang, B. R. (2004) Shear strength of core-veneer interface bi-layered ceramic, *J. Prosthet. Dent.,* **91**, 349–355.

29. Ashkanani, H. M., Raigrodski, A. J., Flinn, B. D., Heindl, H., Mancl, L. A. (2008) Flexural and shear strengths of ZrO_2 and ahigh-noble alloy bonded to their corresponding porcelains, *J. Prosthet. Dent.*, **100**, 274–284.

30. Choi, B. K., Han, J. S., Yang, J. H., Lee, J. B., Kim, S. H. (2009) Shear bond strength of veneering porcelain to zirconia and metal cores, *J. Adv. Prosthodont.,* **1**, 129–135.

31. López-Mollá, M. V., Martínez-González, M. A., Mañes-Ferrer, J. F., Amigó-Borrás, V., Bouazza-Juanes, K. (2010) Bond strength evaluation of the veneering-core ceramics bonds, *Med. Oral Patol. Oral Cir. Bucal.,* **15**, e919–e923.

32. Aboushelib, M. N., de Jager, N., Kleverlaan, C. J., Feilzer, A. J. (2005) Microtensile bond strength of different components of core veneere all-ceramic restorations, *Dent. Mater.,* **21**, 984–991.

33. Ozkurt, Z., Kazazoglu, E., Unal, A. (2010) In vitro evaluation of shear bond strength of veneering ceramics to zirconia, *Dent. Mater. J.,* **29**, 138–146.

34. Hjerppe, J., Fröberg, K., Lassila, L. V. J., Vallittu, P. K. (2010) The effect of heat treatment and feldspathic glazing on some mechanical properties of zirconia, *Silicon*, **3**, 171–178.

35. White, S. N., Miklus, V. G., McLaren, E. A., Lang, L. A., Caputo, A. A. (2005) Flexural strength of alayered zirconia and porcelain dental all-ceramic system, *J. Prosthet. Dent.,* **94**, 125–131.

36. Anunmana, C., Anusavice, K. J., Mecholsky, J. J., Jr. (2010) Interfacial toughness of bilayer dental ceramics based on a short-bar, chevron-notch test, *Dent. Mater.,* **26**, 111–117.

37. Kwon, J. E., Lee, S. H., Lim, H. N., Kim, H. S. (2009) Bonding characteristics between zirconia core and veneering porcelain, *Dent. Mater.,* **25**, e42.

38. Queiroz, J. R. C., Benetti, P., Massi, M., Lafayette, N., Della Bona, A. (2012) Effect of multiple firing and silica deposition on the zirconia-porcelain interfacial bond strength, *Dent. Mater.,* **28**, 763–768.

39. Atkins, P., de Paula, J. (2002) *Atkins' Physical Chemistry*, 7th ed., Oxford University Press, Oxford, UK.

40. Green, J., Weiss, A., Stern, A. (2011) Lasers and radiofrequency devices in dentistry, *Dent. Clin. N. Am.*, **55**, 585–597.

41. Noda, M., Okuda, Y., Tsuruki, J., Minesaki, Y., Takenouchi, Y., Ban, S. (2010) Surface damages of zirconia by Nd:YAG dental laser irradiation, *Dent. Mater. J.,* **29**, 536–541.

42. Ural, Ç., Külünk, T., Külünk, Ş., Kurt M. (2010) The effect of laser treatment on bonding between zirconia ceramic surface and resin cement, *Acta Odontol. Scand.,* **68**, 354–359.

43. Swain, M. V. (2009) Unstable cracking (chipping) of veneering porcelain on all-ceramic dental crowns and fixed partial dentures, *Acta Biomater*., **5**, 1668–1677.

44. Borba, M., Araújo, M. D., Fukushima, K. A., Yoshimura, H. N., Cesar, P. F., Griggs, J. A., Della Bona, A. (2011) Effect of the microstructure on the lifetime of dental ceramics, *Dent. Mater.,* **27**, 710–721.

45. Liu, Y., Feng, H., Bao, Y., Qiu, Y., Xing, N., Shen, Z. (2010) Fracture and interfacial delamination origins of bilayeredceramic composites for dental restorations, *J. Eur. Ceram. Soc.,* **30**, 1297–1305.

46. Saito, A., Komine, F., Blatz, M. B., Matsumura, H. (2010) A comparison of bond strength of layered veneering porcelains to zirconia and metal, *J. Prosthet. Dent.,* **104**, 247–257.

47. Aboushelib, M. N., Feilzer, A. J., de Jager, N., Kleverlaan, C. J. (2008) Prestresses in bilayered all-ceramic restorations, *J. Biomed. Mater. Res. B: Appl. Biomater.,* **87**, 139–145.

48. Fischer, J., Stawarczyk, B., Tomic, M., Strub, J. R., Hämmerle, C. H. (2007) Effect of thermal misfit between different veneering ceramics and zirconia frameworks on in vitro fracture load of single crowns, *Dent. Mater. J.,* **26**, 766–772.

49. Fischer, J., Stawarzcyk, B., Trottmann, A., Hämmerle, C. H. (2009) Impact of thermal misfit on shear strength of veneering ceramic/zirconia composites, *Dent. Mater.,* **25**, 419–423.

50. Guazzato, M., Proos, K., Quach, L., Swain, M. V. (2004) Strength, reliability and mode of fracture of bilayered porcelain/zirconia (Y-TZP) dental ceramics, *Biomaterials,* **25**, 5045–5052.

51. Taskonak, B., Mecholsky, J. J., Jr., Anusavice, K. J. (2005) Residual stresses in bilayer dental ceramics, *Biomaterials,* **26**, 3235–3241.

52. Taskonak, B., Borges, G. A., Mecholsky, J. J., Jr., Anusavice, K. J., Moore, B. K., Yan, J. (2008) The effects of viscoelastic parameters on residual stress development in a zirconia/glass bilayer dental ceramic, *Dent. Mater.,* **24**, 1149–1155.

53. Göstemeyer, G., Jendras, M., Dittmer, M. P., Bach, F. W., Stiesch M., Kohorst, P. (2010) Influence of cooling rate on zirconia/veneer interfacial adhesion, *Acta Biomater.,* **6**, 4532–4538.

54. Fischer, J., Grohmann, P., Stawarczyk, B. (2008) Effect of zirconia surface treatments on the shear strength of zirconia/veneering ceramic composites, *Dent. Mater. J.,* **27**, 448–454.

55. Guess, P. C., Zhang, Y., Thompson, V. P. (2009) Effect of veneering techniques on damage and reliability of Y-TZP trilayers, *Eur. J. Esthet. Dent.*, **4**, 262–276.

56. Aboushelib, M. N., Kleverlaan, C. J., Feilzer, A. J. (2008) Microtensile bond strength of different components of core veneered all-ceramic restorations. Part 3: double veneer technique, *J. Prosthodont.,* 17, 9–13.

57. Aboushelib, M. N., de Kler, M., van der Zel, J. M., Feilzer, A. J. (2008) Effect of veneering method on the fracture and bond strength of bilayered zirconia restorations, *Int. J. Prosthodont.,* **21**, 237–240.

58. Tholey, M. J., Swain, M. V., Thiel, N. (2009) SEM observations of porcelain Y-TZP interface, *Dent. Mater.,* **25**, 857–862.

59. Sailer, I., Pjetursson, B. E., Zwahlen, M., Hämmerle, C. H. (2007) A systematic review of the survival and complication rates of all-ceramic and metal-ceramic reconstructions after an observation period of at least 3 years. Part II: fixed dental prostheses, *Clin. Oral Implants Res.,* **18**(Suppl 3), 86–96.

60. Tinschert, J., Schulze, K. A., Natt, G., Latzke, P., Heussen, N., Spiekermann, H. (2008) Clinical behavior of zirconia-based fixed partial dentures made of DC-zircon: 3-years results, *Int. J. Prosthodont.,* **21**, 217–222.

61. Sailer, I., Gottnerb, J., Kanelb, S., Hämmerle, C. H. (2009) Randomized controlled clinical trial of zirconia-ceramic and metal-ceramic posterior fixed dental prostheses: a 3-year follow-up, *Int. J. Prosthodont.*, **22**, 553–560.

62. Della Bona, A., Kelly, J. R. (2008) The clinical success of all-ceramic restorations, *J. Am. Dent. Assoc*., **139**, 8S–13S.

63. Deng, Y., Lawn, B. R., Lloyd, I. K. (2002) Characterization of damage modes in dental ceramic bilayer structures, *J. Biomed. Mater. Res.,* **63**, 137–145.

64. Al-Amleh, B., Lyons, K., Swain, M. (2010) Clinical trials in zirconia: a systematic review, *J. Oral Rehabil.,* **37**, 641–652.

65. International Organization for Standardization. (2010) *ISO 6872: Dental Ceramics*, 3rd ed., International Organization for Standardization, Geneva.

66. van Noort, R. (2007) *Introduction to Dental Materials*, 3rd ed., Mosby, London.

67. Della Bona, A., Anusavice, K. J. (2002) Microstructure, composition, and etching topography of dental ceramics, *Int. J. Prosthodont.*, **15**, 159–167.

68. Della Bona, A., Anusavice, K. J., Hood, J. A. A. (2002) Effect of ceramic surface treatment on tensile bond strength to a resin cement, *Int. J. Prosthodont.*, **15**, 248–253.

69. Della Bona, A., Donassollo, T. A., Demarco, F. F., Barrett, A. A., Mecholsky, J. J., Jr. (2007) Characterization and surface treatment effects on topography of a glass-infiltrated alumina/zirconia-reinforced ceramic, *Dent. Mater.*, **23**, 769–775.

70. Della Bona, A., Borba, M., Benetti, P., Cecchetti, D. (2007) Effect of surface treatments on the bond strength of a zirconia-reinforced ceramic to composite resin, *Braz. Oral Res.*, **21**, 10–15.

71. van Noort, R., Noroozi, S., Howard, I. C., Cardew, G. (1989) A critique of bond strength measurement, *J. Dent.*, **17**, 61–67.

72. Boscato, N., Della Bona, A., Cury, A. A. D. B. (2007) Influence of ceramic pre-treatments on tensile bond strength and mode of failure of resin bonded to ceramics, *Am. J. Dent.*, 20, 103–108.

73. Della Bona, A., van Noort, R. (1995) Shear versus tensile bond strength of resin composite bonded to ceramic, *J. Dent. Res.*, **74**, 1591–1596.

74. Della Bona, A., Anusavice, K. J., Shen, C. (2000) Microtensile strength of composite bonded to hot-pressed ceramics, *J. Adhes. Dent.*, **2**, 305–313.

75. Della Bona, A., Anusavice, K. J., Mecholsky, J. J., Jr. (2003) Failure analysis of resin composite bonded to ceramic, *Dent. Mater.*, **19**, 693–699.

76. Della Bona, A., Shen, C., Anusavice, K. J. (2004) Work of adhesion of resin on treated lithia disilicate-based ceramic, *Dent. Mater.*, **20**, 338–344.

77. Della Bona, A., Anusavice, K. J., Mecholsky, J. J., Jr. (2006) Apparent interfacial fracture toughness of resin/ceramic systems, *J. Dent. Res.*, **85**, 1037–1041.

78. Della Bona, A. (2009) Important aspects of bonding resin to dental ceramics, *J. Adhes. Sci. Technol*., **23**, 1163–1179.

79. Lung, C. Y. K., Matinlinna, J. P. (2012) Aspects of silane coupling agents and surface conditioning in dentistry: an overview, *Dent. Mater.,* **28**, 467–477.

80. van Noort, R., Noroozi, S., Howard, I. C., Cardew, G. (1989) A critique of bond strength measurement, *J. Dent.*, **17**, 61–67.

81. van Noort, R., Cardew, G. E., Howard, I. C., Noroozi, S. (1991) The effect of local interfacial geometry on the measurement of the tensile bond strength to dentin, *J. Dent. Res.*, **70**, 889–893.

82. Versluis, A., Tantbirojn, D., Douglas, W. H. (1997) Why do shear bond tests pull out dentin? *J. Dent. Res.*, **76**, 1298–1307.

83. Kelly, J. R., Benetti, P., Rungruanganunt, P., Della Bona, A. (2012) The slippery slope: critical perspectives on in vitro research methodologies, *Dent.Mater.*, **28**, 41–51.

84. Pashley, D. H., Carvalho, R. M., Sano, H., Nakajima, M., Yoshiyama, M., Shono, Y., et al. (1999) The microtensile bond test: a review, *J. Adhes. Dent.*, **1**, 299–309.

85. Sano, H., Shono, T., Sonoda, H., Takatsu, T., Ciucchi, B., Carvalho, R., Pashley, D. (1994) Relationship between surface area for adhesion and tensile bond strength: evaluation of a micro-tensile bond test, *Dent. Mater.*, **10**, 236–240.

86. Quinn, G. D. (2007) *Fractography of Ceramics and Glasses*, National Institute of Standards and Technology (NIST), WA, USA.

87. Borba, M., Araújo, M. D., Lima, E., Yoshimura, H. N., Cesar, P.,F., Griggs, J.,A., Della Bona, A. (2011) Flexural strength and failure modes of layered ceramic structures, *Dent. Mater.*, **27**, 1259–1266.

88. Della Bona, A., Mecholsky, J. J., Jr., Anusavice, K. J. (2004) Fracture behavior of lithia disilicate- and leucite-based ceramics, *Dent. Mater.*, **20**, 956–962.

89. Albert, F. E., El-Mowafy, O. M. (2004) Marginal adaptation and microleakage of Procera AllCeram crowns with four cements, *Int. J. Prosthodont.*, **17**, 529–535.

90. Magne, P. (2005) Immediate dentin sealing: a fundamental procedure for indirect bonded restorations, *J. Esthet. Restor. Dent.*, **17**, 144–154.

91. Magne, P., So, W. S., Cascione, D. (2007) Immediate dentin sealing supports delayed restoration placement, *J. Prosthet. Dent.*, **98**, 166–174.

92. Kelly, J. R. (2004) Dental ceramics: current thinking and trends, *Dent. Clin. N. Am.*, **48**, 513–530.

93. Kelly, J. R., Denry, I. (2008) Stabilized zirconia as a structural ceramic: an overview, *Dent. Mater.*, **24**, 289–298.

94. Raigrodski, A. J. (2004) Contemporary materials and technologies for all-ceramic fixed partial dentures: a review of the literature, *J. Prosthet. Dent.*, **92**, 557–562.

95. Hidaka,O., Iwasaki, M., Saito, M., Morimoto, T. (1999) Influence of clenching intensity on bite force balance, occlusal contact area, and average bite pressure, *J. Dent. Res.*, **78**, 1336–1344.

96. Summitt, J. B., Robbins, J. W., Hilton, T. J., Schwartz, R. S. (2006) *Fundamentals of Operative Dentistry: A Contemporary Approach*, 3rd ed., Quintessence, Chicago, IL, USA.

97. Heffernan, M. J., Aquilino, S. A., Diaz-Arnold, A. M., Haselton, D. R., Stanford, C. M., Vargas, M. A. (2002) Relative translucency of six all-ceramic systems. Part II: core and veneer materials, *J. Prosthet. Dent.*, **88**, 10–15.

98. Suárez, M. J., Lozano, J. F., Paz Salido, M., Martínez, F. (2004) Three-year clinical evaluation of In-Ceram Zirconia posterior FPDs, *Int. J. Prosthodont.*, **17**, 35–38.

99. Sailer, I., Fehér, A., Filser, F., Gauckler, L. J., Lüthy, H., Hämmerle, C. H. (2007) Five-year clinical results of zirconia frameworks for posterior fixed partial dentures, *Int. J. Prosthodont.*, **20**, 383–388.

100. Benetti, P., Della Bona, A., Kelly, J. R. (2010) Evaluation of thermal compatibility between core and veneer dental ceramics using shear bond strength test and contact angle measurement, *Dent. Mater.*, **26**, 743–750.

101. Rekow, E. D., Harsono, M., Jana, M., Thompson, V. P., Zhang, G. (2006) Factorial analysis of variables influencing stress in all-ceramic crowns, *Dent. Mater.*, **22**, 125–132.

102. Heikkinen,T. T., Lassila, L. V. J., Matinlinna, J P., Vallittu, P. K. (2007) Effect of operating air pressure on tribochemical silica-coating, *Acta Odontol. Scand.,* **65**, 241–248.

103. Heikkinen, T. T., Lassila, L. V. J., Matinlinna, J. P., Vallittu, P. K. (2009) Dental zirconia adhesion with silicon compounds using some experimental and conventional surface conditioning methods, *Silicon*, **1**, 199–201.

104. Matinlinna, J. P., Lassila, L. V. J. (2011) Enhanced resin-composite bonding to zirconia framework after pretreatment with selected silane monomers, *Dent. Mater.,* **27**, 273–280.

105. Heikkinen, T. T., Lassila, L. V. J., Matinlinna, J. P., Vallittu, P. K. (2013) Long term water storage deteriorates bonding of composite resin to alumina and zirconia, short communication, *Open Dent. J.*, **7**, 123–125.

106. Liu, D., Matinlinna, J. P., Tsoi, J. K. H., Pow, E. N. H., Miyazaki, T., Shibata, Y., Kan, C. W. (2013) A new modified laser pretreatment for porcelain zirconia bonding, *Dent. Mater.*, **29**, 559–565.

107. Liu, D., Pow, E. H. N., Tsoi, J. K. H., Matinlinna, J. P. (2014) Evaluation of four surface coating treatments for resin to zirconia bonding, *J. Mechan. Behav. Biomed. Mater.*, **32**, 300–309.

Chapter 16

All-Ceramic Restorations on Implants

Alvaro Della Bona and Marcia Borba
Post-Graduate Program in Dentistry, Dental School, University of Passo Fundo, Campus I, BR285, Passo Fundo, RS 99001-970, Brazil
dbona@upf.br, marciaborba@upf.br

Ceramics show high biocompatibility, chemical stability, and superior esthetics when compared to other restorative dental materials. In addition, the introduction of computer-aided design/computer-aided manufacturing (CAD/CAM) technology to dentistry and the development of high-toughness ceramics improved the range of application of ceramic materials. Thus, ceramics with different compositions and microstructures are available to produce dental restorations and implant abutments. This chapter presents laboratory and clinical studies that estimated the prognosis of these restorative procedures and suggested ways to improve their clinical performance.

16.1 Introduction: Ceramic Materials

Ceramic materials were introduced in dentistry in the 18th century to produce total dentures and individual teeth with the objective of

Handbook of Oral Biomaterials
Edited by Jukka P. Matinlinna

ISBN 978-981-4463-12-6 (Hardcover), 978-981-4463-13-3 (eBook)
www.panstanford.com

reaching the esthetics of a natural tooth. Since then, innumerous ceramic systems were developed [1, 2]. However, the first ceramic materials used for dental restorations had low fracture strength and toughness, due to ceramic's high amorphous content, showing poor clinical behavior [3].

The optical properties of ceramic materials justify their large range of applications in dentistry. The microstructure and composition of dental ceramics result in optical behavior that is similar to the one observed for tooth structures, providing a more natural-looking restoration [1, 4]. In addition, it shows high chemical stability, which is a desired characteristic to produce a biocompatible dental restoration. Ceramic restorations also have low thermal and electric conductivity, preventing pulp aggression [1, 5].

On the other hand, ceramics show brittle mechanical behavior that may limit their indication to produce restorations that are subjected to high tensile stress concentration [5]. As mentioned above, the first ceramic systems introduced in dentistry showed poor clinical performance. To overcome this limitation, a series of mechanisms were considered, which involved strengthening of the ceramic structure using a framework material that presents high fracture strength and an effective bond with other structures, distributing stresses from one substrate to another. The framework material may be a metal alloy, producing a metal–ceramic restoration, or a high-crystalline-content ceramic material, resulting in an all-ceramic restoration [1, 2].

This chapter presents the most popular all-ceramic systems for restorative dentistry and dental implants (see also Chapters 3, 14, and 15).

16.2 All-Ceramic Restorations

The introduction of computer-aided design/computer-aided manufacturing (CAD/CAM) technology to dentistry in the early 1980s and the development of high-toughness ceramics improved the application of all-ceramic restorations. CAD/CAM technology is composed of three steps: (1) data capture, through scanning of the tooth preparation, adjacent and opposing teeth; (2) design of the desired structure using computer software (CAD); and (3) fabrication

of the structure by a milling unit (CAM) using prefabricated blocks. Ceramic blocks are available with a range of compositions, and it is also possible to produce metal and composite structures with this technology [6].

The mechanical and optical behaviors of ceramic structures are strongly related to the fabrication, composition, and microstructure, such as the crystalline content, the chemical nature, the size of the particles, and the presence or absence of an amorphous phase [1, 7]. Ceramic materials with high crystalline content are stronger, although they are highly opaque [7, 8]. Thus, these ceramics are indicated as a framework material and should be veneered with a glass-based ceramic that has superior optical properties, resulting in a bilayered restoration [1, 4, 9]. Although the ceramic framework material is opaque, the esthetics of the all-ceramic restoration is superior to the esthetics achieved with metal–ceramic restorations. The final restoration has a more translucent and natural appearance than the metallic ones [4].

Ceramics can be classified into three major types, according to their microstructure: predominantly glass; particle-filled glass, with low or high glass content; and polycrystalline, which has no glass phase [1]. To reinforce these materials various types of crystals have been used, such as leucite, lithium disilicate, alumina, and zirconia. These crystals present toughening mechanisms that oppose crack propagation when the material is subjected to tensile stresses, increasing its fracture strength [1, 7, 10, 11].

16.2.1 Glasses and Porcelains

Porcelains may be classified as glass ceramics or particle-filled materials with high glass content as the ceramic's microstructure may vary depending on the manufacturer and the materials' indication. The glass phase is constituted mainly by a silica network with sodium and/or potassium oxides [2]. Leucite, alumina, and fluorapatite crystals can be added to the glass matrix with the objective of reinforcing and also matching the coefficient of thermal expansion (CTE) of the porcelain with the CTE of the framework material [1, 2, 12].

Leucite is a potassium-aluminum-silicate crystal ($K_2O \times Al_2O_3 \times 4SiO_2$) that can be added to dental porcelain by

incongruent melting of potash feldspar or as a synthetic powder [13]. The presence of this crystal in the porcelain is associated with a toughening mechanism called crack deflection that could result in increased fracture toughness. Tangential compressive stresses and microcracks in the glass around the leucite crystals may be induced by the large CTE mismatch between leucite and the glassy matrix, when cooled. Such residual stresses may counteract the crack-driving force and act as crack deflectors [10, 14]. In addition, microcrack toughening is related to the creation of a shielding zone that reduces stress intensification at the crack tip and can occur in ceramics that contain high-localized residual stresses, such as the ones induced by the leucite and glass matrix CTE mismatch [10]. However, the addition of leucite to dental porcelain has a strengthening effect on the material only until a certain leucite content, approximately 20%. Above this threshold, the microcracks formed during cooling may act as crack initiators, decreasing the material's fracture strength [14, 15].

Due to the high amorphous content, porcelains have high translucency and are capable of mimicking the optical behavior of the tooth; however, they show poor mechanical behavior [3, 4, 7, 16]. Thus, these materials are indicated to produce laminate veneers, inlays, onlays, and anterior crowns and to veneer metal–ceramic and all-ceramic restorations [1, 14]. The restoration can be produced by a laboratory technician using the layering technique. After sculpting the desired shape, the restoration is sintered to obtain a dense and strong structure [2]. Another technique used to produce these restorations is CAD/CAM technology, in which a presintered porcelain block is milled into the final restoration [1].

16.2.2 Particle-Filled Ceramics

16.2.2.1 Hot-pressed leucite- and lithium disilicate–based ceramics

Ceramics with two different compositions are available for the hot-pressing technique, both constituted by a glass matrix and reinforced either by leucite or by lithium disilicate crystals [1, 17]. The hot-pressing or injection process uses, initially, the lost wax technique to produce restorations. The wax pattern is sculpted,

included in an investment, and burned out in a special furnace. Then, a ceramic ingot is heated with high temperature and pressed into the investment mold, producing the final restoration [2].

One example of a leucite-reinforced ceramic is the IPS Empress Esthetic (previously named as IPS Empress, from Ivoclar, Schaan, Liechtenstein) and is clinically indicated to produce laminate veneers, inlays, onlays, and anterior crowns and to veneer metal–ceramic and all-ceramic restorations [1]. Microstructurally, it shows tetragonal leucite crystals (approximately 1.7 μm in diameter) immersed in a glass matrix [10]. The crystalline content varies around 30% in volume [10, 16]. Thus, its optical and mechanical behaviors are close to the porcelain's [16]. The fracture strength and toughness values are mainly related to the crack deflection and microcrack-toughening mechanisms associated with the leucite crystals, as explained before [10]. Mean values of fracture strength and toughness reported in the literature for hot-pressed leucite-reinforced ceramics and other framework materials are described in Table 16.1.

An example of the lithium disilicate–reinforced ceramic is the IPS e.max Press (previously named as IPS Empress 2, Ivoclar-Vivadent, Schaan, Liechtenstein). This material microstructure presents elongated lithium disilicate ($Li_2Si_2O_5$) crystals (mean length 5.2 μm) and a second phase of lithium orthophosphate crystals (Li_3PO_4) involved by a glass matrix [10, 16, 17]. Lithium disilicate crystals are also associated to crack deflection and microcrack-toughening mechanisms. The crack tip changes its path when reaching the elongated lithium disilicate crystals, causing dispersion of its energy, which results in an increase of fracture toughness. The crystalline content is higher than the leucite-based hot-pressed material, ranging from 58% to 65% in volume [10, 16]. Thus, it is possible to use this ceramic as a framework material for crowns and three-unit fixed partial dentures (FPDs) located up to the pre-molar region [1].

Both ceramics are also available for CAD/CAM technology. The prefabricated blocks are named IPS Empress CAD (leucite) and IPS e.max CAD (lithium disilicate). After milling by the CAM unit, the restoration should be subjected to a crystallization process, in a ceramic furnace, to obtain its final strength and desired esthetic properties.

Table 16.1 Mean fracture strength (σ) and fracture toughness (K_{Ic}) values reported in the literature for ceramics used as frameworks in all-ceramic restoration

Ceramics	σ (MPa)	K_{Ic} (MPa·m$^{0.5}$)
Hot pressed, leucite based (IPS Empress Esthetic, Ivoclar)	85[*w]; 106[§]; 177[§]; 134[β]	1,2[£]; 1,3[#]; 1,7[†]
Hot pressed, lithium disilicate based (IPS e.max Press, Ivoclar)	215[*w]; 306[§]	2,9[£]; 3,4[#]
Glass infiltrated, alumina based (In-Ceram Alumina, Vita)	352[β]; 594[§]; 323[§]	4,4[£]; 4,5[†]
Polycrystalline alumina (Procera AllCeram, Nobelpharma)	464[§]; 687[β]	4,5[†]
Glass infiltrated, alumina based, zirconia reinforced (In-Ceram Zirconia, Vita)	564[*]; 638[§]; 645[β]	4,8[£]
Y-TZP (In-Ceram YZ, Vita)	900[§]	5,9[γ]
Y-TZP (DC-ZirKon, DCS Dental)	840[§]	7,4[£]
Y-TZP (Lava, 3M-Espe)	786[§]; 1267[β]	–
Y-TZP (Prozir, Norton-St. Gobain)	1450[β]	4,9[¨]; 5,4[†]

[§]Three-point flexural strength
[*]Four-point flexural strength
[w]Tested in 37ºC distilled water
[β]Biaxial flexural strength
[£]Indentation strength
[#]Fractography
[†]Indentation fracture
[♦]SEPB
[γ]SEVNB
Abbreviation: Y-TZP; yttria-stabilized tetragonal zirconia polycrystals.
Source: Reproduced from Della Bona, 2009 [1].

16.2.2.2 Glass-infiltrated ceramics

Three systems showing distinct crystal-phase composition represent the glass-infiltrated ceramics. As they show different

types and fractions of crystals they also present different optical and mechanical properties (Table 16.1) and, consequently, distinct clinical indications.

In 1989, an alumina-based glass-infiltrated ceramic named In-Ceram Alumina was developed by Sadoun and introduced in dentistry by Vita Zanhfabrik (Bad Säckingen, Germany). This material consists of a partially sintered alumina structure that gains strength through the infiltration of a lanthanum oxide–based glass [18, 19]. In 2007, the In-Ceram Alumina patent expired, instigating the release of similar ceramics from other manufacturers [19]. The volume fraction of the alumina phase varies from 42% to 75%, depending on the manufacturer and processing method [19]. Several toughening mechanisms were observed for this material, such as grain pull-out, crack bridging and crack deflection [10]. This ceramic is used as a framework material for single-unit crowns located in the anterior and posterior areas of the mouth and for anterior three-unit FPDs [1].

In subsequent years, with the objective of obtaining a more translucent framework material, the In-Ceram Spinell (Vita Zanhfabrik, Bad Säckingen, Germany) system was developed. This glass-infiltrated ceramic is reinforced with approximately 80% in volume of spinel crystals ($MgAl_2O_4$). The mechanical properties are inferior to the alumina-based system, but the system offers better esthetics. In-Ceram Spinell is indicated as a framework material for inlays and anterior crowns [8, 20].

To improve the mechanical properties of alumina-based glass-infiltrated ceramics, approximately 33% of ceria (CeO_2) partially stabilized zirconia was added to this material [21]. Thus, an alumina-based zirconia-reinforced glass-infiltrated ceramic named In-Ceram Zirconia (Vita Zanhfabrik, Bad Säckingen, Germany) was introduced. The material is composed of approximately 33% volume fraction of alumina crystals, 33% of zirconia, and 23% of a glass matrix [11, 21]. Therefore, a combination of several toughening mechanisms related to alumina and zirconia crystals could be acting, such as crack deflection, contact shielding, phase transformation, and microcrack nucleation [11]. This ceramic can be used as a framework material for crowns and FPDs [1]. The manufacturer recommends a minimum connector cross section of 16 mm^2 for posterior FPDs (with a 10 mm span).

The conventional method to produce glass-infiltrated ceramic restoration is the slip-cast technique. Initially, a ceramic slurry is applied over a special plaster die that absorbs the water by capillarity, resulting in a dense structure, which is, subsequently, partially sintered. To reduce the structure porosity and to obtain a strong material, a lanthanum oxide–based paste is applied over the restoration and infiltrated using a special furnace at 1100°C [2]. Different methods can be used to uniformly apply the ceramic slurry over the die, such as the manual technique, electrophoretic deposition, and the vacuum-driven method [19]. For CAD/CAM technology, dry-pressed blocks are available for milling and subsequent glass infiltration [10, 19].

16.3 Polycrystalline Ceramics

16.3.1 Alumina-Based Polycrystalline Ceramics

The introduction of CAD/CAM technology allowed for the use of polycrystalline ceramics to produce dental restorations and implant abutments as it was not possible to fabricate dense and strong polycrystalline structures using only manual techniques (powder technology) [22]. Alumina-based ceramics show a combination of good mechanical properties, biocompatibility, and excellent resistance to corrosion. This material was introduced in medicine to produce orthopedic prosthesis (hip joint implants) and has been applied in dentistry since 1964, when Sanhaus used this ceramic to replace lost teeth [23, 24].

The first alumina-based polycrystalline dental ceramic was produced by Nobel Biocare (Göteborg, Sweden), named Procera AllCeram. The ceramic restoration is manufactured using a laboratory production center model, in which the plaster die reproducing the prepared tooth is scanned and the data sent to a production center where the ceramic framework is fabricated. In the production center, the alumina powder is first dry-pressed over an oversize milled replica of the die. Then, the external surface of the framework is milled and the final structure is sintered at 1550°C for one hour [22]. According to the manufacturer, this material is indicated as a framework material for crowns and up to four-unit FPDs.

Vita also developed an alumina-based polycrystalline material named Vita In-Ceram AL. This ceramic is available as presintered blocks for CAD/CAM processing and subsequent sintering. The restorations should be milled oversized to compensate the, approximately, 15% sintering shrinkage. This materials' indication is restricted to crowns and three-unit FPD frameworks located in the anterior region [1, 7].

16.3.2 Zirconia-Based Polycrystalline Ceramics

Zirconia-based polycrystalline ceramics can be classified into categories according to its microstructure. The most used are (1) fully stabilized zirconia (FSZ), (2) partially stabilized zirconia (PSZ), and (3) tetragonal zirconia polycrystals (TZP). The most popular type of zirconia-based polycrystalline ceramic used in dentistry is TZP, which is constituted predominantly by the tetragonal phase, although small amounts of the cubic phase can also be found, and this material is usually stabilized with yttrium oxide (3–6% in weight) [25].

Yttria-stabilized tetragonal zirconia polycrystals (Y-TZP) are a dental ceramic with a larger range of clinical indications, being used as framework material for crowns and large FPDs located in all areas of the mouth. Compared to other high-crystalline-content ceramics, Y-TZP requires a relatively small connector cross section, around 9 mm^2 for a 12 mm span between abutments. In addition, Y-TZP can be used to produce intra-radicular posts, orthodontic brackets, dental implants, and implant abutments [1, 26].

The restorations are produced using CAD/CAM technology through milling of prefabricated, presintered blocks or densely sintered hot isostatic pressed (HIP) blocks. Although the use of densely sintered blocks may result in restorations with superior adaptation, the process is time consuming and involves high wear of the milling instruments. On the other hand, the milling process of presintered blocks is more efficient. Yet, around 20% sintering shrinkage has to be compensated by milling enlarged restorations to guarantee the precision of adaptation [27, 28].

The superior mechanical behavior of zirconia-based ceramics is related to a well-known toughening mechanism associated with a tetragonal-to-monoclinic phase transformation. When this material

is subjected to external stresses, such as the ones produced during chewing, grinding, and polishing, a crystal-phase transformation is induced, resulting in compressive stresses and microcrack toughening that act opposing the tensile stresses that would lead to crack propagation [1, 11, 25, 29].

However, the same toughness mechanism that improves the mechanical performance of zirconia-based ceramics can also be responsible for the degradation of their properties. Any factor that affects the stability of tetragonal zirconia can induce a phenomenon called low-temperature degradation (LTD). Among these factors are the crystal size, the amount of stabilizer oxide added to the material, and the presence of residual stresses [1, 26, 29]. Residual stresses are a special concern for the dentist because they may be induced during the restoration processing. The effect of milling, thermal changes, finishing, and polishing procedures on the mechanical behavior of Y-TZP was investigated, and results were controversial. Milling and finishing can induce residual compressive stresses in the ceramic surface, improving the material's mechanical properties. On the other hand, large cracks, which overcome the compressive stress layer, may be created, increasing the material's susceptibility to LTD [30–32]. Investigations are still being performed to clarify which processing steps could compromise the mechanical performance of Y-TPZ ceramics.

16.4 Ceramic Implant Abutments

The application of high-crystalline-content and high-toughness ceramics was not restricted to the production of crowns and FPD frameworks but was expanded to dental implantology through the production of implants and implant abutments.

Titanium is the material of choice to produce implant abutments. Titanium abutments provide reliable and biocompatible structures to produce implant-supported restorations [33]. The main challenge of using this type of abutment is the esthetics, especially clinical cases in the anterior area with thin gingival tissue or gingival recession. In addition, restorations are in direct comparison with the natural adjacent teeth, which is critical when the patient has a gingival smile or a high lip line. Esthetics can be compromised by

the gray appearance of the metallic abutment throughout the soft tissues and by direct metal exposure due to gingival recession. A solution to these clinical cases is to use ceramic abutments that can provide adequate optical behavior and result in superior esthetics [34, 35]. Ti is discussed also in Chapters 9, 10, and 13.

Ceramic implant abutments are available as prefabricated or custom structures. Prefabricated abutments can be prepared directly in the mouth, by the dentist, or in a working model, by the laboratory technician. Custom abutments are produced in the dental laboratory by a technician (i.e., glass-infiltrated ceramics/slip-cast technique) or using CAD/CAM technology. For CAD/CAM, two strategies can be used: (1) the abutment shape and finish line is designed using wax or resin, and this model is scanned so that the CAM unit can receive information to produce the custom abutment; and (2) the abutment is completely designed with the CAD software (i.e., material thickness, abutment angle, finish line) and then milled by the CAM unit. Custom abutments can be designed to provide excellent support for the surrounding soft tissues and to obtain a superior esthetic result [34, 35]. One of the commercial systems available to produce custom implant abutments is Procera (Nobel Biocare). This system works using both strategies mentioned above. The virtual design is sent to a production center, where the final abutment is fabricated using one of the three available materials: titanium, alumina-based ceramics, or zirconia-based ceramics [36].

Zirconia- and alumina-based glass-infiltrated and polycrystalline ceramics can be used to produce implant abutments. In 1993, Nobel Biocare introduced a novel alumina-based ceramic abutment, named CerAdapt™. This system is a prefabricated abutment produced with densely sintered aluminum oxide. Alumina-based abutments show advantages such as biocompatibility, low corrosion potential, and low thermal conductivity. In addition, alumina ceramic is easier to prepare, which is important if the abutment reduction is performed intraorally [35, 37]. However, its mechanical performance is limited, and excessive material reduction could result in weakening of the final structure. Thus, alumina-based ceramics should not be used when the abutment height is lower than 7 mm and the thickness of the axial walls is less than 0.7 mm. This ceramic is indicated to fabricate implant-supported single crowns and short-span FPDs in both anterior and premolar regions [32, 37, 38].

Polycrystalline zirconia, as mentioned earlier in this chapter, shows the best mechanical behavior when compared to other dental ceramics, being highly indicated to produce implant abutments. When a zirconia-based abutment is used, the restrictions for material reduction are less conservative than for alumina-based abutments. An in vitro study examined the external axial reduction of zirconia-based abutments and reported no influence on the fracture strength [40]. However, there is concern about the effect of grinding in the LTD of Y-TZP ceramic, and additional investigations concerning this issue should be performed [30]. Considering esthetics, alumina-based ceramic has superior optical behavior, being more translucent than zirconia [8]. To overcome this limitation, some manufacturers developed staining techniques for zirconia structures. In addition, zirconia allows radiographic visualization due to its radiopacity, which is a limitation of alumina, which is radiolucent [35].

In vitro studies investigated the fracture strength of implant-supported restorations produced with titanium (control), alumina-based abutments, and zirconia-based abutments, with and without mechanical aging. When comparing titanium with ceramic abutments, most studies found better results for titanium [39–42]. Due to the different nature of the materials (metal vs. ceramic), the failure mode is also different. Implant-supported restorations combined with titanium abutments show crown fracture or deflection of the abutment–crown assemblies. When ceramic is used, fracture usually involves the abutment or the abutment and the crown [42, 43]. An investigation found similar performance for titanium and zirconia-based abutments; however, these abutments were not all-ceramic as they were combined with a titanium insert (ZirReal, 3i, Palm Beach Gardens, FL, USA). The objective of the association between metal and zirconia is to provide a metal reinforcement at the implant–abutment interface, resulting in a combination of esthetics and increased fracture strength [43].

Even though it seems to be a consensus that, when tested in vitro, titanium abutments show better mechanical behavior than ceramic abutments, studies are still controversial when abutments produced with different types of ceramics are compared. A study showed equal fracture strength values and failure modes for alumina- and zirconia-based abutments [42]. On the other hand, investigations found that zirconia-based abutments were more resistant to fracture

than alumina-based abutments and different failure modes were observed [43, 44]. All tested ceramic abutments showed fracture strength values above the typical physiological loads reported in the premolar region (approximately 400 N). Failure analysis of ceramic abutments revealed that fractures initiated primarily from the cervical part of the abutments, near or at the implant–abutment interface. It was suggested that this area shows the highest tensile stress concentration as a consequence of the torque generated during the placement of the screw [40, 42, 44]. For implant-supported restorations in the anterior region, fractures were located at the internal connections of the zirconia abutments inside the implant bodies, suggesting high stress concentrations in this area during loading [45]. Yet, direct comparison between different in vitro studies or clinical extrapolations should use caution.

Clinical studies that evaluated the performance of ceramic abutments found promising results, besides the differences in the mechanical behavior reported in vitro [33, 36, 38, 46–49]. Zirconia-based abutments showed a cumulative survival rate close to 100% for single-unit implant-supported restorations from one to five years of use [46–48]. Alumina-based abutments were also evaluated up to a three-year period, and the cumulative survival rate ranged from 93% to 100% when combined with single-unit implant-supported restorations [36, 49]. In addition, when comparing alumina-based and titanium single-unit implant abutments, a similar cumulative survival rate was found after a three-year follow-up (100%) [49].

As ceramic abutments are also recommended to produce FPDs, the clinical function of alumina-based and titanium abutments supporting short-span FPDs was evaluated after two and five years. The cumulative survival rate for FPDs supported by alumina ceramic abutments was 94.7% and 100% for titanium in both studies. In addition, the cumulative success rate for ceramic and titanium abutments was 98.1% and 100%, respectively, and remained unchanged from two to five years' follow-up [33, 38].

Technical problems other than abutment fracture were also observed. A clinical study observed only 2% of porcelain veneer chipping after five years of follow-up [46]. Other authors also reported low rates of porcelain chipping [36, 38, 47, 48]. The incidence of abutment screw loosening was either low (1.8% for the first year and 3.7% after four years) [47] or nonexistent [48].

However, there is concern regarding fractures or chipping during individualization or clinical incorporation of ceramic abutments since studies reported failures during these procedures, which suggested that ceramic abutments are more sensitive to handling than titanium [36, 49].

The mean marginal bone loss measured after different periods of functional loading in clinical studies was within the limits set for successful implants [38, 46, 47]. The biological response was positive since the peri-implant mucosa was healthy in all cases. Periodontal examinations showed healthy soft tissues at the neighboring teeth and ceramic abutments [38, 46–49]. A study observed a higher percentage of mucosal bleeding for titanium abutment implant-supported restorations compared to ceramic abutments after two weeks of follow-up but no difference after one year [48].

Therefore, alumina- and zirconia-based ceramic implants have showed adequate functional and biological behaviors to support single-unit restorations and small-span FPDs.

The use of ceramic abutments allows for direct veneering of all-ceramic restorations. Restorations can be cemented in ceramic abutments or veneered with esthetic glass or porcelain and fixed to the implant using a screw [41]. Direct veneering can be performed using layering or hot-pressing techniques. It is easier to remove or replace the abutment crown intraorally when the direct veneering technique is chosen. However, there is concern regarding loosening of abutment screws and ceramic fractures due to the opening access for the screws [36, 45]. In addition, the implant insertion must be carefully planned so that its long axis and the screw access hole are located lingual to the incisal edge, not compromising the esthetic outcome [45, 49].

A clinical study reported on soft tissue recession in association with the crown–abutment margin, suggesting that cement margins could produce unfavorable biologic effects in the implant area [36]. However, a recent one-year cohort prospective study found no differences in soft tissue stability and the peri-implant marginal bone level between cemented and directly veneered crowns [46].

References

1. Della Bona, A. (2009) *Bonding to Ceramics: Scientific Evidences for Clinical Dentistry*, 1st ed., Artes Médicas, São Paulo.

2. Anusavice, K. J. (2005) *Phillips*, *Materiais Dentários*, 11th ed., Elsevier, Rio de Janeiro.
3. Morena, R., Lockwood, P. E., Fairhurst, C. W. (1986) Fracture toughness of commercial dental porcelains, *Dent. Mater.*, **2**(2), 58–62.
4. Heffernan, M. J., Aquilino, S. A., Diaz-Arnold, A. M., Haselton, D. R., Stanford, C. M., Vargas, M. A. (2002) Relative translucency of six all-ceramic systems. Part II: core and veneer materials, *J. Prosthet. Dent.,* **88**(1), 10–5.
5. Callister, W. D., Jr. (2002) *Ciência e Engenharia de Materiais: Uma Introdução*, 5th ed., Livros Técnicos e Científicos Editora S. A., Rio de Janeiro.
6. Strub, J. R., Rekow, E. D., Witkowski, S. (2006) Computer-aided design and fabrication of dental restorations: current systems and future possibilities, *J. Am. Dent. Assoc*, **137**(9), 1289–1296.
7. Borba, M., de Araujo, M. D., Fukushima, K. A., Yoshimura, H. N., Cesar, P. F., Griggs, J. A., Della Bona, A. (2011) Effect of the microstructure on the lifetime of dental ceramics, *Dent. Mater.*, **27**, 710–721.
8. Heffernan, M. J., Aquilino, S. A., Diaz-Arnold, A. M., Haselton, D. R., Stanford, C. M., Vargas, M. A. (2002) Relative translucency of six all-ceramic systems. Part I: core materials, *J. Prosthet. Dent.,* **88**(1), 4–9.
9. Borba, M., de Araujo, M. D., de Lima, E., Yoshimura, H. N., Cesar, P. F., Griggs, J. A., Della Bona, A. (2011) Flexural strength and failure modes of layered ceramic structures, *Dent. Mater.*, **27**(12), 1259–1266.
10. Guazzato, M., Albakry, M., Ringer, S. P., Swain, M. V. (2004) Strength, fracture toughness and microstructure of a selection of all-ceramic materials. Part I. Pressable and alumina glass-infiltrated ceramics, *Dent. Mater.*, **20**(5), 441–448.
11. Guazzato, M., Albakry, M., Ringer, S. P., Swain, M. V. (2004) Strength, fracture toughness and microstructure of a selection of all-ceramic materials. Part II. Zirconia-based dental ceramics, *Dent. Mater.*, **20**(5), 449–456.
12. Mackert Jr., C. M., Russell, J. R. (1996) Leucite crystallization during processing of a heat-pressed dental ceramic., *Int. J. Prosthodont.*, **9**, 261–265.
13. Ong, J. L., Farley, D. W., Norling, B. K. (2000) Quantification of leucite concentration using X-ray diffraction, *Dent. Mater.*, **16**(1), 20–25.
14. Cesar, P. F., Yoshimura, H. N., Miranda Junior, W. G., Okada, C. Y. (2005) Correlation between fracture toughness and leucite content in dental porcelains, *J. Dent.,* **33**(9), 721–729.

15. Kon, M., Kawano, F., Asaoka, K., Matsumoto, N. (1994) Effect of leucite crystals on the strength of glassy porcelain, *Dent. Mater. J.*, **13**(2), 138–147.
16. Gonzaga, C. C., Yoshimura, H. N., Cesar, P. F., Miranda, W. G., Jr. (2009) Subcritical crack growth in porcelains, glass-ceramics, and glass-infiltrated alumina composite for dental restorations, *J. Mater. Sci. Mater. Med.*, **20**(5), 1017–1024.
17. Della Bona, A., Mecholsky, J. J., Jr., Anusavice, K. J. (2004) Fracture behavior of lithia disilicate- and leucite-based ceramics, *Dent. Mater.*, **20**(10), 956–962.
18. Claus, H. (1990) Vita In-Ceram, a new procedure for preparation of oxide-ceramic crown and bridge framework, *Quintess. Zahntech.*, **16**(1), 35–46.
19. Della Bona, A., Mecholsky, J. J., Jr., Barrett, A. A., Griggs, J. A. (2008) Characterization of glass-infiltrated alumina-based ceramics, *Dent. Mater.*, **24**(11), 1568–1574.
20. Jung, Y. G., Peterson, I. M., Pajares, A., Lawn, B. R. (1999) Contact damage resistance and strength degradation of glass-infiltrated alumina and spinel ceramics, *J. Dent. Res.*, **78**(3), 804–814.
21. Della Bona, A., Donassollo, T. A., Demarco, F. F., Barrett, A. A., Mecholsky, J. J., Jr. (2007) Characterization and surface treatment effects on topography of a glass-infiltrated alumina/zirconia-reinforced ceramic, *Dent. Mater.*, **23**, 769–775.
22. Andersson, M., Oden, A. (1993) A new all-ceramic crown. A dense-sintered, high-purity alumina coping with porcelain, *Acta Odontol. Scand.*, **51**(1), 59–64.
23. Hulbert, S., Bokros, J., Hench, L., Wilson, J., Heimke, G. (1987) Ceramics in clinical applications, past, present and future, in *High Tech Ceramics*, 3–27 (Ed. Vincenzinc, P.), Elsevier Science, Amsterdam.
24. De Aza, A. H., Chevalier, J., Fantozzi, G., Schehl, M., Torrecillas, R. (2002) Crack growth resistance of alumina, zirconia and zirconia toughened alumina ceramics for joint prostheses, *Biomaterials*, **23**(3), 937–945.
25. Chevalier, J., Gremillard, L. (2009) The tetragonal-monoclinic transformation in zirconia: lessons learned and future trends, *J. Am. Ceram. Soc.*, **92**(9), 1901–1920.
26. Denry, I., Kelly, J. R. (2008) State of the art of zirconia for dental applications, *Dent. Mater.*, **24**(3), 299–307.
27. Borba, M., Cesar, P. F., Griggs, J. A., Della Bona, A. (2011) Adaptation of all-ceramic fixed partial dentures, *Dent. Mater.*, **27**(11), 1119–1126.

28. Tinschert, J., Natt, G., Hassenpflug, S., Spiekermann, H. (2004) Status of current CAD/CAM technology in dental medicine, *Int. J. Comput. Dent.,* **7**(1), 25–45.

29. Piconi, C., Maccauro, G. (1999) Zirconia as a ceramic biomaterial, *Biomaterials*, **20**(1), 1–25.

30. Kosmac, T., Oblak, C., Jevnikar, P., Funduk, N., Marion, L. (1999) The effect of surface grinding and sandblasting on flexural strength and reliability of Y-TZP zirconia ceramic, *Dent. Mater.*, **15**(6), 426–433.

31. Guazzato, M., Quach, L., Albakry, M., Swain, M. V. (2005) Influence of surface and heat treatments on the flexural strength of Y-TZP dental ceramic, *J. Dent.,* **33**(1), 9–18.

32. Kim, J. W., Covel, N. S., Guess, P. C., Rekow, E. D., Zhang, Y. (2010) Concerns of hydrothermal degradation in CAD/CAM zirconia, *J. Dent. Res.*, **89**(1), 91–95.

33. Andersson, B., Glauser, R., Maglione, M., Taylor, A. (2003) Ceramic implant abutments for short-span FPDs: a prospective 5-year multicenter study, *Int. J. Prosthodont.*, **16**(6), 640–646.

34. Blatz, M. B., Bergler, M., Holst, S., Block, M. S. (2009) Zirconia abutments for single-tooth implants: rationale and clinical guidelines, *J. Oral Maxillofac. Surg.*, **67**(11 Suppl), 74–81.

35. Kohal, R. J., Att, W., Bachle, M., Butz, F. (2008) Ceramic abutments and ceramic oral implants. An update, *Periodontol. 2000*, **47**, 224–243.

36. Henriksson, K., Jemt, T. (2003) Evaluation of custom-made procera ceramic abutments for single-implant tooth replacement: a prospective 1-year follow-up study, *Int. J. Prosthodont.*, **16**(6), 626–630.

37. Prestipino, V., Ingber, A. (1996) All-ceramic implant abutments: esthetic indications, *J. Esthet. Dent.,* **8**(6), 255–262.

38. Andersson, B., Scharer, P., Simion, M., Bergstrom, C. (1999) Ceramic implant abutments used for short-span fixed partial dentures: a prospective 2-year multicenter study, *Int. J. Prosthodont.*, **12**(4), 318–324.

39. Cho, H. W., Dong, J. K., Jin, T. H., Oh, S. C., Lee, H. H., Lee, J. W. (2002) A study on the fracture strength of implant-supported restorations using milled ceramic abutments and all-ceramic crowns, *Int. J. Prosthodont.*, **15**(1), 9–13.

40. Adatia, N. D., Bayne, S. C., Cooper, L. F., Thompson, J. Y. (2009) Fracture resistance of yttria-stabilized zirconia dental implant abutments, *J. Prosthodont.*, **18**(1), 17–22.

41. Sadoun, M., Perelmuter, S. (1997) Alumina-zirconia machinable abutments for implant-supported single-tooth anterior crowns, *Implant Rep.*, **9**, 1047–1054.

42. Att, W., Kurun, S., Gerds, T., Strub, J. R. (2006) Fracture resistance of single-tooth implant-supported all-ceramic restorations: an in vitro study, *J. Prosthet. Dent.,* **95**(2), 111–116.

43. Butz, F., Heydecke, G., Okutan, M., Strub, J. R. (2005) Survival rate, fracture strength and failure mode of ceramic implant abutments after chewing simulation, *J. Oral Rehabil.*, **32**(11), 838–843.

44. Yildirim, M., Fischer, H., Marx, R., Edelhoff, D. (2003) In vivo fracture resistance of implant-supported all-ceramic restorations, *J. Prosthet. Dent.,* **90**(4), 325–331.

45. Albrecht, T., Kirsten, A., Kappert, H. F., Fischer, H. (2011) Fracture load of different crown systems on zirconia implant abutments, *Dent. Mater.*, **27**(3), 298–303.

46. Ekfeldt, A., Furst, B., Carlsson, G. E. (2011) Zirconia abutments for single-tooth implant restorations: a retrospective and clinical follow-up study, *Clin. Oral Implants Res.*, **22**(11), 1308–1314.

47. Glauser, R., Sailer, I., Wohlwend, A., Studer, S., Schibli, M., Scharer, P. (2004) Experimental zirconia abutments for implant-supported single-tooth restorations in esthetically demanding regions: 4-year results of a prospective clinical study, *Int. J. Prosthodont.*, **17**(3), 285–290.

48. Canullo, L. (2007) Clinical outcome study of customized zirconia abutments for single-implant restorations, *Int. J. Prosthodont.*, **20**(5), 489–493.

49. Andersson, B., Taylor, A., Lang, B. R., Scheller, H., Scharer, P., Sorensen, J. A., Tarnow, D. (2001) Alumina ceramic implant abutments used for single-tooth replacement: a prospective 1- to 3-year multicenter study, *Int. J. Prosthodont.*, **14**(5), 432–438.

Chapter 17

Finite-Element Analysis in Dentistry

Andy H. Choi,[a,b] Besim Ben-Nissan,[b] and Richard Conway[b]
[a]*Faculty of Dentistry, Dental Materials Science, University of Hong Kong, Prince Philip Dental Hospital, 34 Hospital Road, Sai Ying Pun, Hong Kong SAR, People's Republic of China*
[b]*School of Chemistry and Forensic Science, Faculty of Science, University of Technology, Sydney, Australia*
ahchoi@hotmail.com

The finite-element method (FEM) was first introduced in 1956 and was extensively used in the fields of civil and mechanical engineering and in the 1970s in orthopedic biomechanics to evaluate stresses in human bones during functional loadings. Its application to implant design and analysis and in dentistry related to the deformations under functional loadings accelerated after the 1980s. Since then, this method has widely been accepted in engineering and in biomedical systems and applied with increasing frequency for stress analyses of bone and bone-prosthesis structures, dental implants and devices, fracture fixation devices, and soft and hard tissues. FEM has also been accepted in nanoindentation and nanomechanical testing to evaluate the biomechanical properties of nanocoatings such as hydroxyapatite on metallic implants and devices.

Handbook of Oral Biomaterials
Edited by Jukka P. Matinlinna

ISBN 978-981-4463-12-6 (Hardcover), 978-981-4463-13-3 (eBook)
www.panstanford.com

17.1 Introduction

The finite-element method (FEM) is a numerical procedure for analyzing structures and continua. Usually the problem addressed is too complicated to be solved satisfactorily by classical analytical methods. The problem may concern stress analysis, heat conduction, or any of several other areas. The finite-element (FE) procedure produces many simultaneous algebraic equations, which are generated and solved by computational analysis. FE calculations are performed on personal computers, mainframes, and all sizes in between. In early days the results were rarely exact; however, errors have decreased by processing more equations, and results accurate enough for engineering purposes are obtainable at reasonable costs.

Finite-element analysis (FEA) solves a complex problem by redefining it as the summation of the solutions of a series of interrelated simpler problems. The first step is to subdivide (i.e., discretize) the complex geometry into a suitable set of smaller "elements" of "finite" dimensions, which, when combined, form the "mesh" model of the investigated structure.

Each element can adopt a specific geometric shape (i.e., cube, triangle, square, tetrahedron, etc.) with a specific internal strain function. Using these functions, a set of boundary conditions such as constraint points and the actual geometry of the element, one can write the equilibrium equations between the external forces acting on the element and the displacements occurring as its corner points or "nodes." There will be one equation for each DOF for each node of the element. These equations are most conveniently written in matrix form for use in a computer algorithm (see also Chapter 4).

17.1.1 Element Type and Number

The choice of an appropriate element type will depend on the expected response of the model and thus the accomplishment of the objectives of the analysis. FEA offers a wide variety of different element types, which can be categorized by family, order, and topology.

The element family refers to the characteristics of geometry and displacement that the element models. Among the most common families used for typical structural models are one-dimensional (1D)

beam elements, two-dimensional (2D) plane stress and plane strain elements, axisymmetric elements, and three-dimensional (3D) shell and solid elements (Fig. 17.1). Beam elements are useful for modeling beam-like structures, where length is much greater than other dimensions and the overall deflection and bending moments can be predicted. However, this type of model will not be able to predict local stress concentrations at the point of application of a load or at joints.

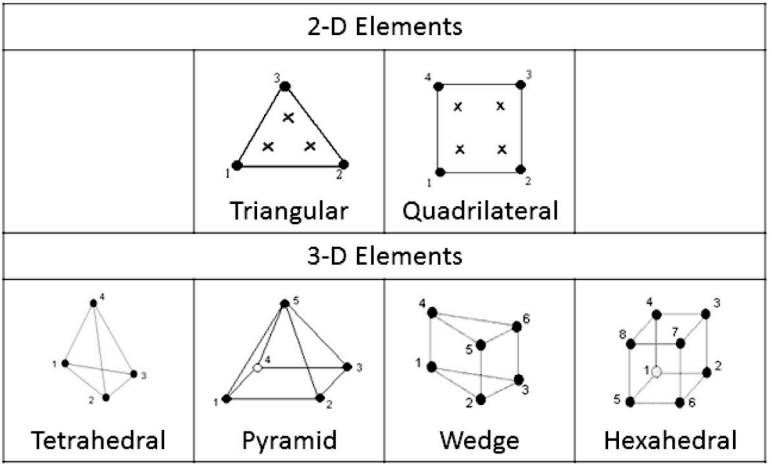

Figure 17.1 FEA element types.

Axisymmetrical elements model 3D stress fields under 2D conditions using well-defined characteristics of an axisymmetric geometry. Shell elements can be effectively used for 3D structures that are thin with respect to other dimensions, such as sheet metal parts where bending and in-plane forces are important. These elements, however, will not predict stresses that vary through the thickness of the shell due to local bending effects. Ideally, all 3D conditions are modeled by means of solid elements. However, because the computational effort of most FE solvers is roughly proportional to the number of equations and the square of the band width, the order of magnitude of such a solid model may impose practical limits on the choice of those elements. Therefore, in each FE analysis, an acceptable reduction of a 3D situation should be seriously considered.

Elements can also be categorized by order. Linear elements have two nodes along each edge; parabolic have three. Higher-order elements are less stiff than lower-order elements (this is related to bending) because additional nodes provide more degrees of freedom (DOFs). A DOF represents the liberty of translatory or rotational motion of a particular node in space. For example, shell elements have six DOFs at each of their unrestrained nodes: three translations (*x*, *y*, and *z*) and three rotations (around the *x*, *y*, and *z* axes). In contrast, the unrestrained nodes in 3D (solid) elements have only three translational DOFs, and 2D elements have only two. A higher number of DOFs means more variables in the stiffness formulation, which is more computer intensive. Higher-order elements offer more accurate results for an equal mesh grid, but a finer grid of lower-order elements can turn out to be more efficient with the same accuracy.

Element topology refers to the general shape of the element (e.g., triangular or quadrilateral). The topology also depends on the family of the element (e.g., 2D or 3D). In general, quadrilateral elements may be considered more suitable than triangular in complex structural models, since the quadrilateral can match the true displacement function more accurately due to a higher number of DOFs. Furthermore, the number of elements in meshes built from triangular elements tends to be larger. On the other hand, the simplicity of triangular elements makes them very attractive, for example, for automatic mesh generation. Triangular-shaped elements are easier to fit to geometrically complex structures. Combining different element topologies and element orders, such as triangular and parabolic, could increase the accuracy of a topologically lesser element.

The shapes of the elements will affect the predictive accuracy of the model, since any deviation in shape from the "ideal" internal elemental strain function will contribute to mathematical inaccuracies. Since FEA offers an approximation to the exact solution, a numerical result closer to this true value will be achieved if the displacements in an FE model become increasingly continuous. An important ingredient in FEA is the behavior of individual elements. A few good elements may produce better results than many poorer elements.

17.1.2 General Principles

Typically, FEA involves the following seven steps. Steps 1, 4, and 5 require decisions by the analyst and provision of input data for the computer program. Steps 2, 3, 6, and 7 are carried out automatically by the FEA computer program used [1–4].

1. Divide the structure or continuum into FEs. Mesh generation programs, called "preprocessors," help the user in doing this work.
2. Formulate the properties of each element. In stress analysis, this means determining nodal loads associated with all element deformation states that are allowed. In biomedical bone modeling it involves a number of parameters such as density and mechanical properties of both trabecular and cortical bones.
3. Assemble elements to obtain the FE model of the structure, such as a long bone or the mandible.
4. Apply the known loads: nodal forces and/or moments in stress analysis, musculature, bite, and reaction forces in mandibular modeling.
5. In stress analysis, specify how the structure is supported. This step involves setting several nodal displacements to known values (which are often zero).
6. Solve simultaneous linear algebraic equations to determine the nodal DOF (nodal displacements in stress analysis).
7. In stress analysis, calculate element strains from the nodal DOF and the element displacement field interpolation and finally calculate stresses from strains. Output interpretation programs, called "postprocessors," help the user sort the output and display it in graphical form.

The power of FEM resides principally in its versatility. The method can be applied to various physical problems with the use of existing commercial FEA packages. The body analyzed can have an arbitrary shape, loads, and support conditions. The mesh can mix elements of different types, shapes, and physical properties. This great versatility is contained within a single computer program. User-prepared input data controls the selection of problem type, geometry, boundary conditions, element selections, etc.

Another attractive feature of FEs is the close physical resemblance between the actual structure and its FE model (Fig. 17.2). The model is not simply an abstraction. This seems especially true in structural mechanics and may account for FEM having its origins there.

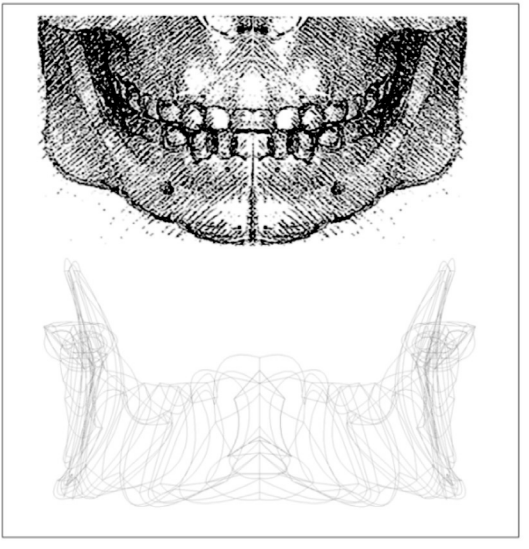

Figure 17.2 Comparison of the anatomical structure of an average mandible (top) and an FE meshed model (bottom).

FEM also has disadvantages. FEA requires special care to be taken during the formation of the wireframe model in step 1, because mesh volumes should be created that provide a reasonable geometric aspect ratio and behavior for the derived elements. To minimize geometric approximation and thus to maximize model accuracy, one could theoretically subdivide a mesh volume into a large number of very small elements. However, this would greatly increase computer memory requirements and processing time. Another option is to manipulate the geometry by dividing contoured curves into smaller ones, thus creating more detailed mesh volumes. This option is, however, feasible only in regions with complex shapes or anticipated high gradients of material deformation. In doing so, one attempts to build mesh volumes where the creation of a smaller number of elements will provide sufficient accuracy without loss of structural response.

17.1.3 Material Properties

The assignment of proper material properties to an FE model is a necessary step to ensure predictive accuracy. Stress and strain in a structure are derived on the basis of material properties. These properties can be classified as **isotropic**, **transversely isotropic**, **orthotropic**, and **anisotropic**.

For an **isotropic** material, the properties are the same in all directions, and since Young's modulus (or modulus of elasticity), shear modulus (or modulus of rigidity), and Poisson's ratio are interrelated, only two out of the three variables need to be determined for the elastic behavior to be completely characterized.

Transversely isotropic materials behave similarly in every direction about a single axis of symmetry.

A material is **anisotropic** if its properties are different when measured in different directions.

An **orthotropic** material is an anisotropic material that displays extreme values of stiffness in mutually perpendicular directions. These directions are called principal directions of the material. Good examples are bone and wood—for example, wood cut from a log, which is stiffest in the axial direction, least stiff in the circumferential direction, and of intermediate stiffness in the radial direction. The Young's modulus for an orthotropic material contains only nine independent coefficients.

17.1.4 Nonlinear Analysis

In structural mechanics, a problem is nonlinear if the force–displacement relationship depends on the current state of the displacement, force, and stress–strain relations [5].

Nonlinearity in structures can be classed as **material nonlinearity**, **geometric nonlinearity**, and **boundary conditions**.

A **material** is called nonlinear if stresses and strains are related by a strain-dependent matrix rather than a matrix of constants. Thus the computational difficulty is that equilibrium equations must be written using material properties that depend on strains but strains are not known in advance. Plastic flow is often a cause of material nonlinearity.

Geometric nonlinearity occurs if the relationships of strains and displacements are nonlinear with the stresses and forces. This can lead to changes in structural behaviour and loss of structural stability. Examples are buckling and large displacement problems.

A **boundary condition** is the load and the resistance to the deformation induced by the load that represent the effects of the surrounding environment on the model. Boundary conditions can cause nonlinearity if they vary with displacement of the structure. Many of these nonlinear boundary conditions have a discontinuous character, which makes them some of the most severe nonlinearities in mechanics. Examples are contact and frictional slip effects.

The main difference between linear and nonlinear FEA lies in the solution of the algebraic equations. Nonlinear analysis is usually more complex and expensive than linear analysis. Nonlinear problems generally require an iterative incremental solution strategy to ensure that equilibrium is satisfied at the end of each step. Unlike linear problems, nonlinear results are not always unique.

In many biomechanical modeling, both in maxillofacial and orthopedic applications, it has been easier to assume that materials used are considered isotropic, homogeneous, and linearly elastic. This is not an accurate assumption but a practical one.

17.1.5 Convergence Test

The accuracy of FEM—measuring how well the mathematics has been approximated—can only be objectively established and verified by a convergence test. As a series of meshes get more refined, that is, more nodes and elements are used, the approximate solution generally improves (a process called h-convergence) and the calculated displacement at any particular node approaches the exact displacement solution.

17.2 Finite-Element Analysis in Dentistry

FEA was first introduced in the fields of engineering in the late 1970s in orthopedic biomechanics to evaluate stresses in human bones during functional loadings and at a later stage in the design and analysis of implants for both dental and orthopedic applications during loading.

Since then, FEA has widely been accepted in biomedical systems and applied with increasing frequency for the analyses of stresses in dental implants and devices, fracture fixation devices, bone and bone-prosthesis structures, and in soft tissues. In addition FEA has been applied in theoretical considerations in biomechanics and other biomaterial modeling and analysis, such as nanoindentation and nanomechanical testing, to determine the properties of nanocoatings such as bioactive hydroxyapatite (HAp) on metallic dental and orthopedic implants and devices.

A few recent examples of the application of FEA in dental and maxillofacial field are given below.

A computed tomography (CT) image-based approach, combined with FEM, has been used by Frisardi et al. [6] to investigate the effect of drill size on the dental implant technique. An edentulous bone segment of the right molar mandibular area has been acquired using high-resolution micro-CT. The images from the micro-CT have been processed to obtain 3D models of the bone segments using the software ScanIP. The drill has been modeled assuming a cylindrical shape with different diameter values. The edentulous drilled bone has been automatically meshed using the software ScanFE. The meshing process has been carried out using the enhanced volumetric marching cubes (EVoMaCs) approach, providing meshes of approximately 3 million elements (8-node brick elements and 4-node tetrahedral elements) and 900,000 nodes. The numerical analyses have been carried out by using the Comsol Multiphysics Analysis simulation software.

Ferraz et al. [7] evaluated stress distribution in peri-implant bone by simulating the effect of an implant with microthreads and platform switching on angled abutments through 3D FEA. Four mathematical models of a central incisor supported by an implant were created. All materials were considered isotropic, homogeneous, and linearly elastic. A distributed load, in approximately 10 mm^2 of 100 N, was applied to the lingual surface of the crown, near the incisal edge, 45° to the long axes of the tooth for all models. The boundary conditions were constrained on the external surface of the maxilla bone segment. Parabolic tetrahedral elements were used for meshing. The models presented a number of elements, ranging from 106,237 to 116,868, and a number of nodes, ranging from 170,880 to 189,786. The analysis was performed using the ANSYS® Workbench FEA software.

May et al. [8] determined the influence of cement thickness and ceramic/cement bonding on stresses and failure of computer-aided design/computer-aided manufacturing (CAD/CAM) crowns, using both multiphysics FEA and monotonic testing. Axially symmetric FEA models were created for stress analysis of a stylized monolithic crown having resin cement thicknesses from 50 μm to 500 μm under occlusal loading. The ceramic–cement interface was modeled as bonded or not bonded (cement-dentin as bonded). Cement polymerization shrinkage was simulated as a thermal contraction. Loads necessary to reach stresses for radial cracking from the intaglio surface were calculated by FEA. Triangular second-order elements were used. Meshing was controlled through free mesh parameters, and the final mesh size was determined by convergence testing. Maximum element sizes for the cement varied from 0.025 mm to 0.20 mm in order to obtain three layers of elements for each cement thickness. COMSOL Multiphysics was the software used for the isotropic, linear, and elastic FEA.

Watanabe et al. [9] used 3D FEA to evaluate the mechanical behavior of a maxillary central incisor with three types of dowels with variable heights of the remaining crown structure. On the basis of micro-CT images, the 3D models were reconstructed using 82 micro-CT sections and finalized on the SolidWorks 2007 software. All tooth structures (enamel, crown and root dentin, dental pulp, and the periodontal ligament) were included in the solid model. To achieve convergence of analysis, the mesh was composed of 3 mm tetrahedral elements. The models had up to 64,650 elements and up to 115,881 nodes. Numerical analysis was performed using the ANSYS Workbench FEA software to obtain stress fields.

Bacchi et al. [10] evaluated the influence of mucosal properties and relining material on the stress distribution in peri-implant bone tissue during masticatory function with a conventional complete denture during the healing period through FEA. Three-dimensional FE models reproducing a severely resorbed jaw with two submerged titanium implants in the anterior region and a conventional complete denture seated on the mucosa were modeled. All materials used in the models were considered to be isotropic, homogeneous, and linearly elastic. The total numbers of elements generated in the FE models were 354,417 for the control group and 355,140 for the relined dentures. The shape of the element was tetrahedral with 10

nodes. The base of the mandible was set to be the fixed support, and loads were applied separately in the lower-right canine (35 N) and the lower-right first molar (50 N).

Miyashita et al. [11] evaluated the biomechanics of an Aramany Class IV obturator prosthesis with FEA and a digital 3D model developed from a CT scan; bone stress was evaluated according to the load placed on the prosthesis. To generate the FE mesh, the contact between the surfaces of interest was determined for the root surfaces and the alveolar bone surfaces, the hard palate mucosa and the hard palate bone, the hard palate mucosa and the palatal plate of the prosthesis, and the dental crown surfaces and the retention clasps of the prosthesis. The geometry of the FE generated in the present study reached 166,046 elements and 281,928 nodes. A force of 120 N was applied to the occlusal (representing the posterior teeth) and incisal platforms (representing the anterior teeth) of the obturator prosthesis.

Schuller-Götzburg et al. [12] performed FEA of a modified sinus elevation procedure involving additional implantation of a cortical bone graft block for stabilization of an implant. A secondary aim was to compare the modified sinus augmentation with the standard technique and to determine whether the FE model to replace a dental implant can be simplified into a cylinder without compromising the accuracy of the outcome. On the basis of CT data, 3D FE models of half of a maxilla were created. A basic model was generated to analyze a conventional sinus elevation procedure, and another was created for the modified version, which involved insertion of a cortical bone graft block. Two implant models were used in the premolar region. Occlusal loads were applied in axial, mediotrusive, and laterotrusive directions, and perfect bonding was assumed to be present at all interfaces.

Sadrimanesh et al. [13] comparatively assessed the masticatory stress distribution in bone around implants placed in the anterior maxilla with three different labial inclinations. Three-dimensional FE models were fabricated for three situations in anterior maxilla. Complete osseointegration at the fixture–bone interface was simulated by sharing the nodes of the fixture and bone elements at this interface. The elements were Solid185-3D, 8-Node Structural (ANSYS SOLID185) with three translational DOFs at each node. All the materials used in the models were assumed to have isotropic,

homogenous and linearly elastic properties. A load of 146N was applied 3 mm below the incisal edge.

Yokoyama et al. [14] investigated the effects of the mechanical properties of adhesive resin cements on stress distributions in fiber-reinforced resin composite (FRC) adhesive fixed partial dentures (AFPDs) using FEA. Two adhesive resin cements were compared. The AFPD consisted of a pontic to replace a maxillary right lateral incisor and retainers on a maxillary central incisor and canine. The FRC framework was made of isotropic, continuous, unidirectional E-glass fibers. Ten-node tetrahedral elements were selected for the hybrid composite, abutment teeth, and adhesive resin cements. Twenty-node hexagonal elements were selected for the anisotropic fiber framework, generating an FE model that consisted of 77,157 elements with 120,084 nodes in total. A concentrated load of 154 N was applied at the center of the pontic's cutting edge at an angle of 135° from the lingual side. FEA was presumed to be linear static. FE model construction and FEA were performed using the ANSYS FEA software.

Kasai et al. [15] examined the influence of occlusal forces during occlusal adjustment on the distribution of forces on combinations of implants and teeth during intercuspal clenching by means of FEA. Three-dimensional FE models of the mandible, one with two implants in the molar region and the other with four implants in the premolar and molar regions, were constructed. The implants were modeled in hexagonal prisms to reduce an FE mesh. Linearly elastic material properties were defined for all elements except the periodontal ligament, which was defined as nonlinearly elastic. The temporomandibular joints and antagonists were simplified and replaced with nonlinear springs. Each model was evaluated under loads of 100 N, 200 N, and 800 N for the distribution of occlusal forces on the teeth and implants. The FE models consisted of approximately 42,000 nodes and 210,000 tetrahedral elements.

Lee et al. [16] evaluated the fatigue limits of poly(etheretherketone) (PEEK) and the effects of the low-elastic-modulus PEEK in relation to existing dental implants using 3D FEA. The bone model consisted of cancellous bone coated with a 1 mm cortical bone layer. The model was meshed with tetrahedral elements. Four-node linear cells were used to simplify the computation of contact pressure, and a finer meshing was generated around the implant. Models were composed

of 428,466 elements and 79,067 nodes. Static forces of 100 N and 30 N within the physiological range were applied vertically on top of the abutment and buccolingually, respectively. The marginal bone loss around the implant was predicted by applying the calculated strain energy density (SED) values by the FEA of each group to the lazy zone range.

Ormianer et al. [17] determined whether one-piece and two-piece implants with equivalent geometries exhibited stresses and strains differently under applied loading conditions. The FE models consist of four-node tetrahedron elements. For the boundary conditions, the outer surface of the bone block was modeled as fixed, and all interfaces between components were modeled as bonded, except the interface between the implant and the abutment that was modeled as a sliding contact. To simulate occlusal loading, 222 N of occlusal force was applied to the implant model at a 30° angle with a 1.5 mm buccolingual offset from the vertical axis of the implant.

Dejak et al. [18] compared the strength of thin-walled molar crowns made of various materials under simulation of mastication. Five 3D FE models of the first lower molar with the use of contact elements were created. It was assumed that the crowns were perfectly luted to molar teeth. The upper and lower teeth models were 3D-positioned in lateral occlusion using reference points from the scan of the lateral occlusal record and separated vertically. The models were fixed in the nodes on the upper surface of the maxillary tooth crown and on the external surface of the periodontium around the mandibular molar roots. In this way the computer 3D model of an intact lower molar tooth and two opposing teeth during the initial phase of chewing movement was created. The vertical movements were chosen to produce a maximum of 200 N reaction forces for each model. The models were considered to be linear, elastic, homogeneous, and isotropic. Contact simulation of FEA was a nonlinear analysis that required the load and displacement to be applied in a number of steps using the ANSYS FEA software.

Möllers et al. [19] calculated the stress distribution of an all-ceramic, fully anatomical, three-unit, inlay-retained dental prosthesis. The commercial FEA software package ANSYS was used for analysis. The FE model was generated by 170,000 ten-node tetrahedral solid elements. The loads were applied to three contact

points on the occlusal surface in the center of the pontic. A total load of 600 N was applied. The FEA type was linear and quasi-static.

Choi et al. [20] compared the differences in stress between Ti-6Al-4V and PS-ZrO_2 dental implants during clenching using 3D FEA. Ti-6Al-4V and PS-ZrO_2 dental implants modeled as a cylindrical structure with a diameter of 3.26 mm and a length of 12.00 mm were placed in the first molar region on the right hemimandible. FEA was performed under nonlinear static conditions, which is programmed automatically using a commercially available FEA package STRAND7®.

Ammar et al. [21] demonstrated the potential of 3D modeling and FEA as clinical tools in treatment planning for orthodontic tooth movement. A cone-beam computed tomography (CBCT) scan of a patient's maxilla and mandible was acquired in vivo. A volumetric mesh was then created and optimized by using tetrahedral elements. The cortical layer at this location was also clearly defined in the CBCT images so that patient-specific geometric accuracy would be preserved. The model input files were read into the ANSYS FEA software as volumetric element meshes by using four-noded six-DOF tetrahedral elements. All materials used in this study were defined as homogeneous, isotropic, and linearly elastic.

Savoldelli et al. [22] analyzed the stress distributions in the temporomandibular joint using a complete high-resolution FE mode. The contours of the skull, compact and cancellous parts of the mandible, and mandibulary and maxillary teeth were obtained from axial, coronal, and sagittal CT images. The FE model consisted of 386,092 tetrahedral elements. The volume meshes were exported into the FEA program FORGE®. The mechanical properties of bone mandibular components, skull, teeth, and articular disc and connective tissue with capsule were assumed to be homogeneous and isotropic. Force vectors were applied to the model to account for the bilateral masticatory muscles (masseter, temporalis, and medial pterygoid). Loading conditions were the same on both sides, and the different forces were applied linearly.

Ausiello et al. [23] examined the mechanical behavior of a maxillary canine adhesively restored by different material post and crown combinations under functional loading by means of 3D FEA. A linear static structural analysis was performed to calculate the stress distribution in different restoration configurations. All numerical

simulations were performed within COMSOL Multiphysics®. A load of 50 N (63° angle with respect to the longitudinal axis of the tooth), acting on the palatal surface of the crown, was applied. For every tooth preparation a suitable FE model was generated. Tetrahedral elements were adopted. Quadratic shape functions (Lagrangian elements) were implemented to achieve more accurate results.

Spazzin et al. [24] evaluated the influence of horizontal misfit change and bar framework material on the distribution of static stresses in an overdenture-retaining bar system using FEA. The anterior part of a severely resorbed jaw and an overdenture-retaining bar system above two osseointegrated implants were modeled using Rhinoceros, a 3D parametric solid modeler. The geometry of the modeled jaw portion was obtained starting from CT data with type III bone. The FE model was obtained by importing the solid model into the mechanical simulation software NEiNastran. All materials were presumed to be linear elastic, homogenous, and isotropic. The 3D FE model contains 13,272 elements and 15,152 nodes.

Rungsiyakull et al. [25] investigated biomechanics with respect to the effect of cusp inclination and occlusal loading on the mandibular bone remodeling. Three different cusp inclinations of a ceramic crown and different occlusal loading locations were taken into account to explore the stresses and strains transferred from the crown to the surrounding dental bone through the implant. The SED obtained from 2D plane strain FEA was used as the mechanical stimulus to drive cancellous and cortical bone remodeling in a buccolingual mandibular section.

Occlusal fingerprint analyses were carried out by Benazzi et al. [26] to identify the contact areas of the teeth. The lower first molar and the antagonistic upper second premolar and first molar were considered in the analysis. The surface models were then imported into STRAND7 FEA software, where volumetric meshes were created initially using four-noded tetrahedral elements. The specimens were analyzed, and then reanalyzed using 10-noded tetrahedral elements to ensure convergence in the pattern of stress. As a result, the first specimen was meshed with a total of 692,732 nodes and 482,962 ten-noded tetrahedral elements, and the second specimen with a total of 775,442 nodes and 536,769 ten-noded tetrahedral elements. All materials used in the models were considered homogeneous, linearly elastic, and isotropic. Boundary constraints were applied to

the lower border of the mandible, and all the associated nodes were fully restrained.

Lin et al. [27] investigated the micromechanical behavior associated with enamel damage at an enamel–adhesive interface for different bracket bases subjected to various detachment forces using 3D FE submodeling analysis. Two FE macromodels using triangular and square bracket bases subjected to shear, tensile, and torsional debonding forces were established using micro-CT images. Six enamel–adhesive interface submodels with micro–resin tag morphology and enamel rod arrangement were constructed at the corresponding stress concentrations in macromodel results. The boundary conditions for the submodels were determined from the macromodel results and applied in submodeling analysis.

Kimsal et al. [28] employed FEA to biomechanically evaluate different fixation schemes used to fixate mandibular angle fractures. A fracture was simulated by dividing the mandibular corpus with a plane at the angle of the mandible. The bite force used for the model is a unilateral molar clench. Each bite force is simulated by restraining the mandible from displacement in all directions at the point of contact of the bite and then applying experimentally derived muscle force vectors for that specific bite. These forces pull the mandible into the constraint, which acts as a fulcrum for the mandible to bend around, simulating the bite. Each force has a direction, area of attachment, and magnitude.

Cheung et al. [29] evaluated the bending fatigue lifetime of a nickel-titanium alloy (Ni-Ti) and stainless steel endodontic files using FEA. The strain–life approach was adopted, and two theoretical geometry profiles, the triangular and the square cross sections, were considered. A fully reversed displacement was applied to the tip of geometrical model, and another tip was fixed in the ANSYS FEA software, known as a cantilever beam model for this analysis. The applied displacement ranged from 0 mm to 2.0 mm. There are 3216 elements with 17,344 nodes for the triangular FE model and 3624 elements with 18,983 nodes for the square FE model.

Lin [30] utilized a quadratic remodeling formula to determine bone resorption as a result of occlusal overload. A 2D FE model with a single-unit implant in the mesiodistal section is considered in this study. The model was derived from a CT scan. A highly dense FE mesh was generated to better capture bone resorption

progressing in detail. The FE model comprises in total 62,884 three-node triangular elements, featuring 60,170 three-node triangular elements in the cortical regions. The loading applied to the implant was 402 N at an inclination angle of 1.32° to simulate the scenario of occlusal overload. The ABAQUS FEA software was employed for FE calculation, and a user subroutine in Python script was used for the bone remodeling calculations.

The distributions of stresses in the cartilaginous temporomandibular joint disc and articular cartilage were analyzed by Mori et al. [31] during prolonged clenching. The number of nodes and elements for the model was 44,856 and 26,728, respectively. The cortical bone was assumed to be linearly elastic. The material properties of the fibrocartilaginous disc and cartilage and connective tissue were modeled using a Kelvin model. The model of the temporal bone was restrained for all DOFs at its superior, anterior, lateral, medial, and posterior margins. The mandible was modeled as a rigid body and constrained at the rearmost point of occlusal contact and at the central point of the anterior teeth on the mandible for mediolateral displacements. Stress analysis was executed by the FEA program NASTRAN.

Lin et al. [32] developed a systematic protocol to assess mandibular bone remodeling induced by dental implantation, which extends the remodeling algorithms established for the long bones into dental settings. A 3D FE model was developed, representing a segment of the human mandible with a number of adjacent teeth. The model was constructed from in vivo CT scan images and processed in Rhinoceros 3.0. The FEA mesh was generated in 10-node tetrahedral elements using MSC PATRAN®, comprising totally 109,020 elements after a convergence test, including 58,885 elements assigned to the cancellous bone and 20,747 elements to the cortical bone. The cortical bone has a thickness of around 2 mm, representing a class 2 bone. The loading condition was chosen to simulate a patient with reduced periodontal tissue and conventional diet; the chewing and swallowing durations are 223 ms and 642 ms, respectively. The bone remodeling equations were formulated using Euler's forward integration method by relating bone density increment to time increment in three different phases as bone apposition, bone equilibrium, and bone resorption.

Thermomechanical FEA in 3D models were described by Cornacchia et al. [33] for determination of stress levels due to thermal and mechanical loads in a healthy and restored tooth. Transient thermomechanical analysis simulating the ingestion of cold and hot drinks was performed to determine the temperature distribution in the models of teeth, followed by linear elastic stress analyses. The thermal loads were applied on the occlusal and lingual surfaces. Subsequently, coupled variation of the temperature and mastication loading was considered. The vertical loading was distributed at occlusal points, adding up to 180 N. The FE used for the determination of the heat distribution was a quadratic 10-node tetrahedron with temperature as the only DOF, due to its flexibility in meshing complex geometries. The total number of elements was 78,079 elements and 107,792 nodes.

Cheng et al. [34] studied the effect of high-performance polyethylene (HPPE) fibers on stress distributions in a maxillary denture and the influence of fiber position on improving denture performance. Fiber lamella reinforcement was incorporated into the denture at different positions (fitting side, midpalatal plane, polished side) with the SolidWorks software. Boundary conditions were constrained at the top of the basal bone, while a bite force of 230 N was applied to the posterior teeth on both sides. The numerical models were meshed with a total of 56,085 nodes and 256,431 tetrahedral elements. Different mesh sizes had been used to obtain converged results. The denture models were analyzed with the ABAQUS FEA software.

Kashi et al. [35] analyzed stresses in a commercially available temporomandibular joint implant, the bone (i.e., mandible), and the bone–implant interface using an FE software package. Both titanium and Co-Cr-Mo/vitallium metals as well as bones with various degrees of osteoporosis were studied. The total number of elements and nodes generated in the FE model were 78,244 and 122,833 for the combined mandible and the temporomandibular joint implant model, respectively. The shape of the element was tetrahedral with 10 nodes, that is, each side had a midside node, and each node had 3 DOFs.

Tu et al. [36] evaluated the effects of cortical bone thickness and implant length on strain in the surrounding bone and micromotion at the bone–implant interface in single, immediately loaded

implants. Experiments with the rapid prototyping technique and FE simulations were performed to evaluate bone strain and micromotion at the bone–implant interface. Implants were embedded into models with three thicknesses of cortical bone, and implants with different lengths were inserted into models with 1.7 mm of thickness of cortical bone. Vertical and lateral loads of 130 N were applied to the models. All models were imported into the ANSYS Workbench FEA software to generate the FE model using 10-node tetrahedral h-elements (ANSYS SOLID187 elements).

Han et al. [37] investigated the displacement and stress distributions during surgically assisted rapid maxillary expansion under different surgical conditions. A 3D FE model of a maxilla with a Hyrax appliance was constructed, and an expansion force of 6000 g was applied using the expansion screw. The model was analyzed with the ANSYS MULTIPHYSICS FEA software. Individual simulations were made after assignment of the corresponding material properties and boundary conditions. In each 3D model, the stress and displacement produced in maxilla was analyzed when there was one turn of the screw.

Verhulp et al. [38] examined the effects of element size, order, and material models on the results of postyield trabecular bone simulations. Four different FE meshes were generated from the first 3D scan using a simple conversion of bone voxels to hexahedral elements using a fixed global threshold value. To achieve sufficient numerical accuracy and to limit computational costs, three meshes were produced. This resulted in high-resolution FE meshes with 539,793, 156,007, and 63,933 elements and 772,328, 254,539, and 117,387 nodes, respectively. Three different isotropic material models were used to describe trabecular tissue yield and postyield behavior. All the micro-FE analyses were performed using the MSC. Marc FEA software.

Basciftci et al. [39] evaluated the biomechanical effects of chincup treatment by using a 3D FE model. The final mesh consisted of 1572 solid elements with 5432 nodes. The chincup with 500 g of force was applied in a direction from the chin toward the mandibular condyle, the coronoid process, and a point anterior to the coronoid process.

Boryor et al. [40] examined how much expansion force is needed during maxillary expansion and where the bony reaction takes place. An FE model of a dry human male skull was generated

from CT scans. All boundary surfaces of cortical bone, cancellous bone, and teeth were then slightly smoothened and represented by 649,000 triangular areas. Tetrahedrons were generated, filling the surrounding triangular surfaces defining the respective regions. The FE model, which consists of cortical and cancellous bone and teeth, was loaded with the same force magnitudes, directions, and working points as in rapid maxillary expansion.

The fracture toughness of dental nanocomposites fabricated by various methods of mixing, silanization, and loadings of nanoparticles had been characterized by Chan et al. [41] using fatigue-precracked compact-tension specimens. FEA was utilized to analyze the growth of an interface crack around an elastic particle embedded within an elastic/plastic matrix.

Huang et al. [42] evaluated the effects of damping on stress concentration in an impacted incisor. An FE model of the upper central incisor was established for dental trauma analysis. ANSYS, the FEA software, was used to perform the transient dynamic analysis on a personal computer. A 2D plane strain FE model of the human maxillary central incisor, containing enamel, dentine, pulp, periodontal membrane, alveolar bone, compact bone, and spongy bone, was built. The dynamic properties of the model, including damping ratio and resonance frequency, were input according to the in vivo tests in this study. The model had a total of 5310 2D quadrilateral elements. A sinusoidal force with a peak of 800 N at 2 ms, and a total duration of 4 ms, was applied to the model in a direction of 45° labial to the incisal edge.

Choi et al. [43] analyzed the distortion and stresses acting on the human mandible during clenching using 3D FEA. The model geometry was derived from position measurements taken from 28 diamond blade cut cross sections of an average size human adult edentulous mandible and generated using a special sequencing method. Data on the material properties of mandibular cortical and cancellous bones were taken from published data. The cortical and cancellous bone of the mandible can be considered to be transversely isotropic with a higher elastic modulus in the longitudinal direction and a lower elastic modulus in all transverse directions. All the muscle forces were assumed to be symmetrical and had equal magnitude on the left and right sides of the mandible. The forces exerted by contracting muscles were represented by vectors in all

three directions. During clenching, all muscles were assumed to be active. The completed model consisted of 258 brick FEA elements and 1635 nodes. FEA was performed under nonlinear static conditions due to the complex constitutive laws of material behavior, which is programmed automatically using a commercially available package, STRAND7.

Using FEA, Lanza et al. [44] carried out a comparative study on stress distribution in the dentine and cement layer of an endodontically treated maxillary incisor. A 3D FEM model consisting of 13,272 elements and 15,152 nodes of a central maxillary incisor was developed. A chewing static force of 10 N was applied at a 125° angle with the tooth longitudinal axis at the palatal surface of the crown. Steel, carbon, and glass fiber posts have been considered.

A 3D FE model of the human mandible was developed by Gallas Torreira and Fernandez [45] to simulate and analyze biomechanical behavior in two standard trauma situations. This computer-based study was made to assess the stress patterns within human mandibles generated by impact forces. The surface mesh was achieved by means of a scanner with laser technology. A load of magnitude 10^7 N/m^2 was simulated either in the symphysis region or in the horizontal ramus of the mandible. The mesh had 7073 nodes and 30,119 elements (tetrahedra), and the MODULEF program was used to solve the 3D elasticity problem.

A 3D FEA model was designed by Tepper et al. [46] to show which surgical procedure and which amount of peri-implant packing yields the best bony support for dental implants. The geometry of the maxilla was defined by a parasagittal section through a highly atrophic edentulous maxilla of a normal individual. The residual ridge height used for modeling was 5.3 mm. The cortical thickness was assumed to be 0.5 mm. In all models, the implants were loaded at their points of emergence with an assumed force of 100 N. The vector of the loading force was inclined 30° posteriorly relative to the implant axis and 30° away from the sagittal plane. The bone–implant interface was assumed to be perfect, simulating full osseointegration. Cortical bone areas were modeled with 3D triangular shell elements. Three-dimensional continuum elements (linear tetrahedrons) were used for modeling cancellous bone and titanium implants.

Akça et al. [47] evaluated the compatibility of 3D FE stress analysis and in vitro strain gauge analysis in the measurement

of strains on a dental implant. Two vertically placed implants embedded in a poly(methyl methacrylate) model were used. Strain gauges were bonded to the cervical parts of the implants, and seven cement-retained fixed partial dentures were fabricated. A 3D model of the strain gauge analysis model was constructed, and an additional model in which human bone simulation was provided was also constructed. A static vertical load of 50 N was applied at certain locations to simulate centrally positioned axial and laterally positioned axial loading for strain gauge analysis and 3D FEA.

O'Mahony et al. [48] compared implant–bone interface stresses and peri-implant principal strains in anisotropic versus isotropic 3D FE models of an osseointegrated implant in the posterior mandible. They obtained anisotropic (transversely isotropic) elastic constants for mandibular bone and derived equivalent isotropic constants by averaging over all possible spatial orientations. An FE model was constructed using 10-node tetrahedral p-elements, providing curved edges, where necessary, and increasing the accuracy of the results in regions of high stress gradients. Perfect bonding was assumed at the implant–bone interface. An oblique load was applied at the coronal aspect of the crown with 100 N vertical and 20 N bucco-to-lingual components.

A technique to simulate the tensile fatigue behavior of human cortical bone was developed by Taylor et al. [49]. A combined continuum damage mechanics and FEA approach was used to predict modulus degradation, accumulation of permanent strain, and the number of cycles to failure of human cortical bone specimens. A 3D FE model of a dumbbell specimen of human cortical bone was created. The model consisted of 599 eight-noded reduced integration elements and 910 nodes. The cortical bone was assumed to be isotropic, homogeneous, and linearly elastic, with a Poisson's ratio of 0.35. No attempt was made to simulate the cyclic viscoelastic properties of cortical bone. All analyses were performed using the Marc FEA software.

Vaillancourt et al. [50] investigated the relationship between stress state and bone loss. A 2D FE model corresponding to buccolingual and mesiodistal sections of canine mandibles with one of two designs of porous-coated dental implants were analyzed. A fully porous-coated design consisting of a solid Ti-6A1-4V core had a porous coating over the entire outer surface of the implant

component, while a partially porous-coated design had the porous coating over the apical two-thirds of the implant surface only. Occlusal forces with axial and transverse components were assumed to act on the implant with interface bonding and effective force transfer at all porous coat–bone interfaces and no bonding for the non-porous-coated regions.

Korioth et al. [51] developed two 3D FE models of a human mandible reconstructed from tomographs of a dry dentate jaw. The total length of a dentate dry human mandible was scanned in the frontal plane at 2 mm intervals by means of CT. The final FE model of the mandible consisted of 4572 elements and 5580 nodes with 16,740 DOFs. Cortical and cancellous bones were considered to behave orthotropically. The periodontal space of each tooth was divided into apical, middle, and coronal thirds, and each third was assigned a different elastic stiffness. The model was loaded with multiple force vectors to simulate muscle forces over wide areas of attachment. The model was restrained from movement at the labial and central occlusal thirds of the right first lower molar.

A 3D FE model of a partially edentulated human mandible was generated by Hart et al. [52] to calculate the mechanical response to simulate isometric biting and mastication loads. No details were supplied on the musculature or the boundary condition. The human mandible was digitized. The data files corresponding to each slice were read by the PATRAN FE pre- and postprocessing program. The level of mesh refinement was established via a convergence test and showed that a model with over 30,000 DOFs was required to obtain analysis accuracy. The material properties for every element were chosen to be isotropic. Four functional load cases were created. In each case, the total applied load on the teeth was 100 N.

Tanne et al. [53] investigated the biomechanical effect of protractive maxillary orthopedic forces on the craniofacial complex by use of 3D FEM. The model was developed on the basis of a dry skull of a young human being. The model consisted of 2918 nodes and 1776 solid elements. Eighteen cranial and facial sutural systems were integrated in the model. An anteriorly directed 1 kg force was applied on the buccal surfaces of the maxillary first molars in both a horizontal parallel direction and a 30° obliquely downward direction to the functional occlusal plane.

The first anatomically correct model of the mandible was created by Ben-Nissan et al. [54]. The model contained all appropriate musculature with correct insertion and origins. FEA was utilized by NASTRAN/PATRAN, and constraining was carried out correctly at the symphysis. The work proposed application of CT scan digitization, which has become the norm in biomechanical modeling and analyses.

Three-dimensional FEA was used by Cook et al. [55] to study the effects that implant neck geometry and the tissue properties at the implant–bone interface have on the stress distribution around free-standing blade- and post-type low-temperature isotropic (LTI) carbon and aluminum oxide dental implants. Implants having neck flares of 13° and 26° were studied. In addition, to simulate fibrous encapsulation of the implant as opposed to a direct bone apposition retention mechanism, a soft-tissue interposing layer between implant and bone was also modeled.

A 3D FE representation of one-half of a dried in vitro mandible symmetric about the symphysis was attempted by Knoell [56]. This model contains an anatomical description of the full mandibular dentition, including third molars and the ramus region. The materials simulated in the model include dentin and cortical and cancellous bone. The properties of cancellous bone were developed by scaling the properties of cortical bone on the basis of porosity, as determined from void area measurements taken of the mandible sections. The materials were idealized as homogeneous, isotropic, and linearly elastic solids. The finite-element model of the mandibular structure consists of 674 nodes and 941 solid elements. The elements were hexagonal, tetrahedronal, and wedge-type constant-strain element discretizations.

17.3 Finite-Element Analysis and Indentation in Dentistry

Nanoindentation has been used to examine dental hard tissues [57] since the early 1990s. Nanoindentation permits the determination of mechanical properties, such as elastic modulus and hardness, at the surface of a material. The procedure for the nanoindentation

technique is much simpler, especially on small complex-shaped samples such as enamel, dentine, and cementum [58].

Zhang et al. [59] explored the feasibility and validity of measuring residual stress of zirconia and porcelain in ceramic crowns by nanoindentation and FEA. The commercial FEA software ABAQUS was used to simulate the Berkovich nanoindentation response at different residual stresses for zirconia. A 2D axisymmetric model with 30 × 50 μm dimensions was used. A conical tip with a 70.3° including angle was used to simulate the pyramid-shaped Berkovich indenter. Edge-biased meshing was applied so that the area directly under the indenter tip had a much finer mesh to better capture surface deformation. The element size under the tip was less than 30 nm. The material was assumed elastic and perfectly plastic.

Adam and Swain [60] explored the effect of friction in simulations of bone nanoindentation. Two-dimensional axisymmetric FE simulations were performed using a spheroconical indenter of tip radius 0.6 μm and angle 90°. The total FE domain was 60 × 60 μm (100 times the indenter tip radius). A graded mesh of reduced integration, linear four-node axisymmetric elements (ABAQUS CAX4R) was used to discretize the domain. The model was loaded in two steps. The indenter was firstly subjected to a ramped 5 mN compressive load, followed by unloading to zero indenter force, to observe the indentation left in the bone upon removal of the load.

Nanoindentation experimental tests and FE simulations were employed by Carnelli et al. [61] to investigate the elastic–inelastic anisotropic mechanical properties of cortical bone. An axisymmetric, spheroconical indenter with an internal angle of 70.3°, a 300 nm end radius, and the same area-to-depth ratio as a three-sided Berkovich pyramid was employed in the model. The tip is modeled as a rigid body. The model allows for anisotropic elastic and postyield behavior of the tissue. A tension–compression mismatch and direction-dependent yield stresses are allowed for. Indentation experiments along the axial and transverse directions were simulated with the purpose to predict the indentation moduli and hardnesses along multiple orientations. Suitable mesh refinement was applied under the indenter tip. The commercial FE code ABAQUS/Standard was used to conduct the analyses.

Using ABAQUS/CAE® FE code, a 3D model for spherical nanoindentation of bone was developed by Paietta et al. [62].

Contact between the analytically rigid half spherical tips and an elastic quarter-space was modeled using hard, frictionless contact along with large deformation theory. A typical mesh consisted of approximately 30,000 eight-noded hexahedral elements. Simulations were performed to explore the contribution of tip location, where indentation tests were placed starting at the centre of a lamella and progressively moved toward the centre of the interlamellar region. Investigation of tip size employed indentation tests to from 100 nm to 500 nm depths, with the indenter tip located at the centre of a single lamella.

FEM was applied by Toparli and Koksal [63] for studying the hardness and yield strength of dentin subjected to a nanoindentation process. FEA was used for the nanoindentation test under the loading and unloading condition. This test with a spherical indenter was modeled as a contact problem between two axisymmetric bodies. Three different samples of dentin were used. The specimen was modeled with 4950 four-node axisymmetric elements. The indenter was modeled as an undeformable surface, and the radius of indenter was 10 μm. The simulations were performed using the ABAQUS® FEA software.

FEA was used by Ford et al. [64] to assess contact damage in dental prostheses, using a Hertzian contact model, consisting of a spherical tungsten carbide indenter contacting a porcelain layer over a palladium alloy substrate. Using the ABAQUS FEA software, a 2.38 mm indenter was modeled to match the experimental conditions. The refinement along the vertical axis of symmetry of the block was necessary to calculate the substrate plastic deformation with sufficient accuracy, while the refinement on the layer surface was for accuracy in calculating contact radii and stress locations. The mesh in these regions was consequently reduced to an element size of 3.125 microns, while in areas away from the contact it increased to 100 microns to reduce computation time and output file size. The block was assumed to be sitting on a frictionless flat surface, with the nodes along the base only permitted radial movement in the axisymmetric model. The nodes on the vertical axis of symmetry were constrained to remain on the axis (maintaining a solid block), and the contact faces between the block and the indenter were frictionless. The hemispherical indenter was pushed downward by a frictionless, rigid, horizontal, flat surface.

A 3D FEA model with elastic–plastic anisotropy was built by Fan et al. [65] to investigate the effects of anisotropy on nanoindentation measurements for cortical bone. The 3D model was simulated with the cyclic symmetric characteristic of a Berkovich indenter. The specimen was represented by 25,066 elements. Eight-node linear brick, reduced-integration elements (C3D8R) were used. The area just under the tip was also meshed with small elements with characteristic length 20 nm, and the area away from the contact area was modeled with a coarser mesh to reduce model size and calculation time. The indenter was modeled as a rigid body. The indentation procedure was simulated by two subsequent steps, loading and unloading. During loading, the rigid indenter was moved in the vertical direction and penetrated into the specimen by applying load; during unloading, the load returns to zero. The FEA studies were conducted using the commercial FEA software ABAQUS.

Dong and Darvell [66] investigated the clinically relevant failure of the ceramic in ceramic–cement–substrate structures under Hertzian indentation, including the effects of supporting the substrate modulus and ceramic thickness on the stress distribution in the ceramic. An axisymmetric model was created on the basis of the dimensions and structure of the experimental specimens with the cement film thickness set at 50 μm and meshed with triangular elements. To simplify the FEM computation, the interfaces were bonded perfectly (no delamination); there was frictionless contact between the ceramic and the indenter. It was also assumed that the indenter was rigid enough and that all materials were isotropic, linear, and homogeneous.

A combined experimental and computational study was conducted by Shrotriya et al. [67] to determine the influence of indenter ball size on contact damage in model multilayered structures with equivalent elastic properties to bonded dentin/crown structures. FE simulations of the Hertzian contact-induced deformation were carried out using the ABAQUS software package. These utilized axissymetric idealizations of the ball/multilayer configurations, and six-node quadratic triangular elements.

17.4 Finite-Element Analysis of Thin-Film Coatings

Nanocoatings, as an approach, present the possibility of altering the surface characteristics and properties of dental and orthopedic implant materials to achieve improvements in bioactivity and clinical performance. The common approaches for the characterization of materials at the nanometer scale have been the nanoindentation or nanohardness test. FEM has been widely adopted to simulate the elastic and plastic deformations beneath a pointed indenter in the nanoindentation test.

Choi et al. [68] examined variations in tensile and compressive stresses and deformation in the nanocoating under a microindentation simulated using 3D FEA. The effects of the radius of indenter, thickness of the nanocoating, and Young's modulus of the coating material were analyzed. The nanoindentation with a spherical indenter was modeled as a 3D contact problem between two axisymmetric bodies, with an assumption that the dimension of the specimen to be indented is large compared to that of the deformed volume. For simplicity, the indenter was modeled as a rigid surface. Diamond was chosen as the indenter material as its Young's modulus is much higher than that of nanocoating materials and the stainless steel substrate. Loading and unloading are the two subsequent steps used to simulate the whole nanoindentation process. During loading, the spherical indenter moves downward along the y axis and penetrates the nanocoating. The depth of penetration is determined by the load applied. During unloading, the indenter returns to its initial position and the load applied is removed. The specimen was represented by a cylinder with such a large dimension that any further increase in its dimension made no significant change in the stress distribution. In the vicinity of the contact region, a fine FE mesh was employed to capture the localized stresses and deformation underneath the indenter. To reduce the computational stress and work for the FE software, the fineness of the FE mesh decreases away from the contact region. Both the coating and the substrate are considered to be homogeneous and isotropic. As strain hardening is not considered in this study, the coating and substrate are also considered to be linearly elastic/

perfectly plastic materials. It is also assumed that a perfect bonding condition occurs between the nanocoating and the substrate. Nanoindentation simulations were carried out using a commercially available FEA package, STRAND7.

A titanium nitride (TiN) coating has been recently introduced in the field of dental titanium implants [69]. Indentation tests carried out on a TiN film were simulated by Gîrleanu et al. [70] using FEM. The FEA software ABAQUS was employed. The Vickers indentation tests performed on a TiN coating–steel substrate were simulated using a 2D axisymmetric model. To keep the same conditions as in experiments, a 500 mN load was applied on a TiN film with a thickness of 1200 nm. The coatings were considered perfectly adherent to the steel substrate; both film and substrate were assumed free of initial stresses. The indenter was modeled as a rigid cone with an angle of 70.3°, which gives the same contact-area-to-depth ratio as a perfect Vickers pyramid.

Rungsiyakull et al. [71] established a relationship between surface morphology–induced micromechanics and bone-remodeling responses to a solid titanium bead–coated porous implant. The FE model consists of a dental implant fixture, an implant abutment, an all-ceramic crown, and a section of bone. A mechanical load of 202.23 N was applied on the top of the crown at 2 mm offset horizontally from the center to the buccal side. Bone remodeling is considered over the two length scales. The macroscopic level generates global responses of bones, while the microscopic level quantifies the change in the apparent bone density of the representative volume elements (RVEs). The FEA software ABAQUS was employed with three-node linear triangular plain strain elements (CPE3).

The mechanical behavior of porous titanium coatings was tested by Schiefer et al. [72] under static and dynamic conditions and was compared to human bone tissue. The fatigue test was statically modeled using FEA. For the calculations, the FEA software ANSYS workbench was used. Meshing was automatically done by the program. On the edge between the implant head and the shaft the mesh was additionally refined. Calculations were performed for an implant load of 200 N at the edge of the massive titanium core at an angle of 30°. This force simulated a typical load for incisors. A bonded contact was assumed between the infiltrated titanium and polymer resin.

Predictions of bone ingrowth into an implant porous coating were investigated by Liu and Niebur [73] using mechanoregulatory models. The mechanoregulatory tissue differentiation algorithm and a modified version that enforces a tissue differentiation pathway by transitioning from differentiation to bone adaptation were investigated. The algorithms were further compared using a micromechanical FE model of a beaded porous scaffold. Predictions of bone and fibrous tissue formation were compared between the two algorithms and to clinically observed phenomena. A 2D model of a beaded scaffold adjacent to bone tissue and filled with granulation tissue was modeled with four-node plane strain elements (ABAQUS element CPE4P). The model simulated a plane cut through a body-centered-cubic unit cell with 200 μm diameter beads, which has a similar volume fraction to real sintered bead porous coatings.

Panich et al. [74] examined factors that affect the nanoindentation process and the determination of mechanical properties of coating films using FEA. A 2D axisymmetric model has been developed to study how the indenter tip radius affects the FEA of hard/soft coatings on a hard substrate using the capacities of the ABAQUS FEA software. Titanium was used as as oft coating on a high-speed steel substrate, while titanium diboride was used as a hard coating. The hard/soft coating perfectly adhered to the substrate. Indentation was carried out using a rigid conical indenter under conditions of frictionless contact. The indenter has the same projected area–depth function as the standard Berkovich as it has a half angle of 70.3°. Since strain hardening is not considered in this case, both the coating and the substrate are considered to be isotropic, which is supposed to be linearly elastic, perfectly plastic material.

Hedia [75] designed a new functionally graded dental implant coating, as well as studying the effect of coating thickness on the maximum von Mises stresses in bone adjacent to the coating layer. A coated titanium-threaded Brånemark-type dental implant was used in this analysis. The coating thickness was changed from 25 μm to 150 μm. An axisymmetric eight-node harmonic element was used to form the mesh. FEA was carried out using the ANSYS package. A fully bonded interface between the implant, coating, and bone was assumed. An axial loading condition on the implant of a magnitude of 100 N was assumed.

Nanoindentation of TiN coatings on ductile substrates was simulated using FEA by Tilbrook et al. [76]. Specimens were modeled axisymmetrically in 2D. A large substrate area was modeled to avoid any artificial constraints or edge effects. The combined thickness of the substrate and the coating was 50 μm, and the width was 50 μm. Mapped meshing with significant refinement around the contact region resulted in approximately 2500 isoparametric quadrilateral elements. In the nanoindentation experiments, the indenter tip is rounded and properties are those of diamond. Loading and unloading processes were modeled through a series of load steps. Nonlinearity associated with contact and plastic deformation necessitates an iterative solution technique. Each load step was applied in a series of substeps, and the Newton–Raphson algorithm was used to obtain convergence for each substep. Simulation was conducted using the ANSYS FEA software.

Three-dimensional FEA was performed by Aoki et al. [77] for thin plasma–coated hydroxyapatite (HAp) and titanium dental implants to study the effects on stress/strain distribution in the mandible with application of axial and oblique loads. The implants were of screw and cylinder types. The model of an implant in the mandible was developed using an FEA program ANSYS. The thickness of the HAp coating was set to 1 μm. The implants were inserted into a simplified mandible segment. All materials used in the models were considered to be isotropic, homogeneous, and linearly elastic. The implant and bone were divided with a 10-node tetrahedral structure solid (ANSYS SOLID92). Forces of 100 N were applied axially and obliquely to the occlusal node at the centre of the abutment. The oblique load was 45° to the vertical axis of the implant. The models were constrained in all directions at the node on the surface of the bone segment.

The indentation of coated systems was studied by Piana et al. [78] in terms of the effect of the mechanical properties of the substrate on film fracture behavior. Both experimental and FE modeling analyses were conducted to study the phenomena that occur when an indenter with Rockwell C geometry applies normal loads of 400 N and 1500 N on TiN films deposited onto different steel substrates. The indentation procedure was simulated using the FEA software ABAQUS. The indenter was assumed to be rigid and to apply normal loads on the coated system. The dimensions of the indenter were

those of a standard Rockwell C test. The indenter was conical with a 120° angle and presented a spherical tip with diameter of 0.2 mm. Normal loads of 1500 N were considered in the analyses. Additionally, simulations with loads of 400 N were also conducted as an attempt to evaluate results at an earlier stage of the indentation. The material of the wear-resistant film was assumed to be elastic. In the simulations the total thickness of the coating was 2.1 μm.

Synchrotron radiation has been used by Cofino et al. [79] to determine local stresses near the interface between a plasma-sprayed HAp coating and a titanium alloy substrate. This experimental determination is compared with the results found by an FEA modeling the thermal effects of the plasma-spraying process. A thin mesh is realized in the interfacial area to determine residual stresses. The coating is constituted by three HAp layers 40 μm thick. The properties of the interface are defined as a 15 μm thick layer with an average value of the characteristics of the two materials. This thickness is equal to the elements' thickness normal to the coating surface and also the elevation of the average substrate's asperities. The second FEA model takes into account the discontinuous morphology of the ceramic coating.

Shan and Sitaraman [80] presented a methodology that combines the nanoindentation technique and FE modeling to characterize the mechanical (elastic and plastic) properties of a titanium thin film. The indentation loading and unloading process is simulated by an FE model with commercial software, ANSYS. Contact elements are placed on the surface of the nanoindenter tip and the surface of the titanium thin film. The bodies of the thin film and the silicon substrate are modeled with a 3D eight-node structural solid element. The elements in the areas with large deformation, that is, areas close to the indenter tip, are refined with a high mesh density to obtain accurate results. The titanium thin film is assumed to be homogeneous and isotropic.

Zhang et al. [81] characterized the elastic/plastic deformation of plasma-sprayed HAp coatings quantitatively. Noting that the Hertzian indentation on coating/substrate systems can be simulated by FEM, they developed a method to obtain the elastic/plastic constitutive equations of plasma-sprayed HAp coatings on a Ti-6Al-4V substrate by combining the indentation tests with nonlinear FEM. For the indentation simulation, 2D axisymmetric modeling was employed

under axially symmetric loading conditions, and no friction was assumed. The four-node bilinear axisymmetric quadrilateral (CAX4) elements were used in the analysis. To obtain the contact impression accurately, elements with fine size were used in the areas near the expected contact region. Linearly elastic deformation was considered for the tungsten carbide indenter. Simulations for the Hertzian indentation on HAp-coated Ti alloy implants were conducted by using the ABAQUS FEA software.

A bioactive glass (BAG) coating has high potential as an implant material. This coating is only functional if it adheres well to the metal substrate and if it is strong enough to transfer all loads. To examine these two properties an appropriate mechanical adhesion test, the moment test, was developed by Schrooten and Helsen [82]. To evaluate the moment test and to simulate the stress distribution a 3D FE model of the test setup was made. The FE grid is loaded with an evenly distributed moment that generates a shear stress of 40 MPa at the coating–substrate interface. All materials are assumed to behave in a linearly elastic manner. The dimensional design of the test setup is made up in such a way that all stresses in both metals (Ti-6Al-4V substrate and stainless steel counterpart) are limited within the elastic deformation area. For more about BAGs, see Chapter 8.

Vaillancourt et al. [83] determined the effect of varying three characteristics of the porous coating dental implant system on crestal bone loss. Two 2D FE models were used to represent orthogonal sections through the buccolingual and mesiodistal directions after implant fixation had occurred through bone ingrowth into the zones with a porous coating of the porous coating implants.

17.5 Concluding Remarks

FEM is used to precisely calculate local stress–strain distributions in geometrically complex structures. The predictive accuracy of the FE model is influenced by the geometric detail of the object to be modeled, the material properties, and the applied boundary conditions.

FEA has become widely used in all biomechanics, especially for assessing stresses and strains in dental implants and the surrounding bone structures, as well as for normal bone remodeling.

The use of computerized modeling methodology such as FEA will have innumerable applications in both dentistry and oral and maxillofacial surgery, not only at a research level, but also at a clinical level. For instance, the ability to take CT scan data or other appropriate imaging of an individual patient to generate his or her own model is already a common practice. By integrating CT/computer-aided design (CAD) and FEA it will be possible to evaluate the correct location, configuration, size, and number of implants needed to address that individual's functional and restorative needs. This integrated system can be coupled with modern rapid prototyping such as laser sintering and ink-printing processes to produce superstructures and patient-matched dental devices and guides.

Similarly, various options for tooth restoration can be examined under simulated functional loading, such as clenching and opening, and designed to resist these loads prior to production.

Accurate 3D modeling and FEA will enable clinicians to best address the form and engineering requirements of implants and prostheses, which are employed to treat mandibular and maxillary fractures, so that both fixation and reduction of the fracture can be obtained, whilst minimizing osteosynthesis plate bulk, number, and size.

Recently, the temporomandibular joint prosthesis has received intense scrutiny as a result of failure primarily due to material failure. It is anticipated that the life quality of patients requiring temporomandibular joint replacement can be benefited through improvements in the design and selection of materials. FEA may also play a role in perfecting the design and be used to assist in vitro testing so that the damages caused in the past generated by numerous material failures can be avoided.

All metallic dental and orthopedic implants and prostheses are bioinert and do not bond chemically to bone—save Ti. Surface coatings present the possibility of altering the properties of a component and, therefore, improve both performance and reliability. More recently, FEM has also been accepted to nanoindentation and nanomechanical testing to evaluate the biomechanical properties of nanocoatings on metallic implants and devices.

Theoretical modeling approaches such as FEA are vital for the advancement in gaining an in-depth understanding in the

interfacial behavior of thin films and substrates. This may lead to better selection in the design and choice of thin-film and substrate materials.

Our drive to determine and measure mechanical properties of thin films at the nanoscale using FEA will inevitably open new avenues in understanding the influence of stresses and deformations in both the micro- and the nanoscale in the growth and repair mechanisms of biologic systems to allow us to use new materials, systems, and tools in tissue regeneration.

References

1. Cook, R. D. (1981) *Concepts and Applications of Finite Element Analysis*, 2nd ed., John Wiley & Sons, New York.
2. Cook, R. D., Malkus, D. S., Plesha, M. E. (1989) *Concepts and Applications of Finite Element Analysis*, 3rd ed., John Wiley & Sons, New York.
3. Gallagher, R. H. (1975) *Finite Element Analysis: Fundamentals*, 1st ed., Prentice-Hall, NJ, USA.
4. Rockey, K. C. (1983) *The Finite Element Method: A Basic Introduction*, 2nd ed., John Wiley & Sons, New York.
5. Zienkiewicz, O. C., Taylor, R. L. (1991) *The Finite Element Method*, 4th ed., McGraw-Hill Book, London, UK.
6. Frisardi, G., Barone, S., Razionale, A., Paoli, A., Frisardi, F., Tullio, A., Lumbau, A., Chessa G. (2012) Biomechanics of the press-fit phenomenon in dental implantology: an image-based finite element analysis, *Head Face Med.*, **8**, 18.
7. Ferraz, C. C., Anchieta, R. B., de Almeida, E. O., Freitas, A. C., Ferraz, F. C., Machado, L. S., Rocha, E. P. (2012) Influence of microthreads and platform switching on stress distribution in bone using angled abutments, *J. Prosthodont. Res.*, **56**, 256–263.
8. May, L. G., Kelly, J. R., Bottino, M. A., Hill, T. (2012) Effects of cement thickness and bonding on the failure loads of CAD/CAM ceramic crowns: Multi-physics FEA modeling and monotonic testing, *Dent. Mater.*, **28**, e99–e109.
9. Watanabe, M. U., Anchieta, R. B., Rocha, E. P., Kina, S., Almeida, E. O., Junior, A. C., Basting, R. T. (2012) Influence of crown ferrule heights and dowel material selection on the mechanical behavior of root-filled teeth: a finite element analysis, *J. Prosthodont.*, **21**, 304–311.

10. Bacchi, A., Consani, R. L., Mesquita, M. F., Dos Santos, M. B. (2012) Influence of different mucosal resiliency and denture reline on stress distribution in peri-implant bone tissue during osseointegration. A three-dimensional finite element analysis, *Gerodontology*, **29**, e833–e837.
11. Miyashita, E. R., Mattos, B. S., Noritomi, P. Y., Navarro, H. (2012) Finite element analysis of maxillary bone stress caused by Aramany Class IV obturator prostheses, *J. Prosthet. Dent.*, **107**, 336–342.
12. Schuller-Götzburg, P., Entacher, K., Petutschnigg, A., Pomwenger, W., Watzinger, F. (2012) Sinus elevation with a cortical bone graft block: a patient-specific three-dimensional finite element study, *Int. J. Oral Maxillofac. Implants*, **27**, 359–368.
13. Sadrimanesh, R., Siadat, H., Sadr-Eshkevari, P., Monzavi, A., Maurer, P., Rashad, A. (2012) Alveolar bone stress around implants with different abutment angulation: an FE-analysis of anterior maxilla, *Implant Dent.*, **21**, 196–201.
14. Yokoyama, D., Shinya, A., Gomi, H., Vallittu, P. K., Shinya, A. (2012) Effects of mechanical properties of adhesive resin cements on stress distribution in fiber-reinforced composite adhesive fixed partial dentures, *Dent. Mater. J.*, **31**, 189–196.
15. Kasai, K., Takayama, Y., Yokoyama, A. (2012) Distribution of occlusal forces during occlusal adjustment of dental implant prostheses: a nonlinear finite element analysis considering the capacity for displacement of opposing teeth and implants, *Int. J. Oral Maxillofac. Implants*, **27**, 329–335.
16. Lee, W. T., Koak, J. Y., Lim, Y. J., Kim, S. K., Kwon, H. B., Kim, M. J. (2012) Stress shielding and fatigue limits of poly-ether-ether-ketone dental implants, *J. Biomed. Mater. Res. B: Appl. Biomater.*, **100**, 1044–1052.
17. Ormianer, Z., Ben Amar. A., Duda, M., Marku-Cohen, S., Lewinstein, I. (2012) Stress and strain patterns of 1-piece and 2-piece implant systems in bone: a 3-dimensional finite element analysis, *Implant Dent.*, **21**, 39–45.
18. Dejak, B., Młotkowski, A., Langot, C. (2012) Three-dimensional finite element analysis of molars with thin-walled prosthetic crowns made of various materials, *Dent. Mater.*, **28**, 433–441.
19. Möllers, K., Parkot, D., Kirsten, A., Güth, J. F., Edelhoff, D., Fischer, H. (2012) Influence of tooth mobility on critical stresses in all-ceramic inlay-retained fixed dental prostheses: a finite element study, *Dent. Mater.*, **28**, 146–151.

20. Choi, A. H., Matinlinna, J. P., Ben-Nissan, B. (2012) Finite element stress analysis of Ti-6Al-4V and partially stabilized zirconia dental implant during clenching, *Acta Odontol. Scand*., **70**, 353–361.
21. Ammar, H. H., Ngan, P., Crout, R. J., Mucino, V. H., Mukdadi, O. M. (2011) Three-dimensional modeling and finite element analysis in treatment planning for orthodontic tooth movement, *Am. J. Orthod. Dentofacial. Orthop*., **139**, 59–71.
22. Savoldelli, C., Bouchard, P. O., Loudad, R., Baque, P., Tillier, Y. (2011) Stress distribution in the temporo-mandibular joint discs during jaw closing: a high-resolution three-dimensional finite-element model analysis. *Surg. Radiol. Anat.*, **34**, 405–413.
23. Ausiello, P., Franciosa, P., Martorelli, M., Watts, D. C. (2011) Mechanical behavior of post-restored upper canine teeth: a 3D FE analysis, *Dent. Mater*., **27**, 1285–1294.
24. Spazzin, A. O., Dos Santos, M. B., Sobrinho, L. C., Consani, R. L., Mesquita, M. F. (2011) Effects of horizontal misfit and bar framework material on the stress distribution of an overdenture-retaining bar system: a 3D finite element analysis, *J. Prosthodont*., **20**, 517–522.
25. Rungsiyakull, C., Rungsiyakull, P., Li, Q., Li, W., Swain, M. (2011) Effects of occlusal inclination and loading on mandibular bone remodeling: a finite element study, *Int. J. Oral Maxillofac. Implants*, **26**, 527–537.
26. Benazzi, S., Kullmer, O., Grosse, I. R., Weber, G. W. (2011) Using occlusal wear information and finite element analysis to investigate stress distributions in human molars, *J. Anat*., **219**, 259–272.
27. Lin, C. L., Huang, S. F., Tsai, H. C., Chang, W. J. (2011) Finite element sub-modeling analyses of damage to enamel at the incisor enamel/adhesive interface upon de-bonding for different orthodontic bracket bases, *J. Biomech*., **44**, 134–142.
28. Kimsal, J., Baack, B., Candelaria, L., Khraishi, T., Lovald, S. (2011) Biomechanical analysis of mandibular angle fractures, *J. Oral Maxillofac. Surg*., **69**, 3010–3014.
29. Cheung, G. S., Zhang, E. W., Zheng, Y. F. (2011) A numerical method for predicting the bending fatigue life of NiTi and stainless steel root canal instruments. *Int. Endodont. J.*, **44**, 357–361.
30. Lin, C. F. (2010) *A Computational Protocol to the Prediction of Dental Implant Induced Bone Remodelling and Its Material Design: A Novel Approach*, PhD dissertation, University of Sydney, Australia.
31. Mori, H., Horiuchi, S., Nishimura, S., Nikawa, H., Murayama, T., Ueda, K., Ogawa, D., Kuroda, S., Kawano, F., Naito, H., Tanaka, M., Koolstra,

J. H., Tanaka, E. (2010) Three-dimensional finite element analysis of cartilaginous tissues in human temporomandibular joint during prolonged clenching, *Arch. Oral Biol*., **55**, 879–886.

32. Lin, D., Li, Q., Li, W., Duckmanton, N., Swain, M. (2010) Mandibular bone remodeling induced by dental implant, *J. Biomech*., **43**, 287–293.
33. Cornacchia, T. P., Las Casas, E. B., Cimini, C. A. Jr and Peixoto, R. G. (2010) 3D finite element analysis on esthetic indirect dental restorations under thermal and mechanical loading, *Med. Biol. Eng. Comput*., **48**, 1107–1113.
34. Cheng, Y. Y., Li, J. Y., Fok, S. L., Cheung, W. L., Chow, T. W. (2010) 3D FEA of high-performance polyethylene fiber reinforced maxillary dentures, *Dent. Mater*., **26**, 211–219.
35. Kashi, A., Chowdhury, A. R., Saha, S. (2010) Finite element analysis of a TMJ implant, *J. Dent. Res*., **89**, 241–245.
36. Tu, M. G., Hsu, J. T., Fuh, L. J., Lin, D. J., Huang, H. L. (2010) Effects of cortical bone thickness and implant length on bone strain and interfacial micromotion in an immediately loaded implant, *Int. J. Oral Maxillofac. Implants*, **25**, 706–714.
37. Han, U. A., Kim, Y., Park, J. U. (2009) Three-dimensional finite element analysis of stress distribution and displacement of the maxilla following surgically assisted rapid maxillary expansion, *J. Craniomaxillofac. Surg*., **37**, 145–154.
38. Verhulp, E., Van Rietbergen, B., Muller, R., Huiskes, R. (2008) Micro-finite element simulation of trabecular-bone post-yield behaviour: effects of material model, element size and type, *Comput. Methods Biomech. Biomed. Eng*., **11**, 389–395.
39. Basciftci, F. A., Korkmaz, H. H., Uşümez, S., Eraslan, O. (2008) Biomechanical evaluation of chincup treatment with various force vectors, *Am. J. Orthod. Dentofacial. Orthop*., **134**, 773–781.
40. Boryor, A., Geiger, M., Hohmann, A., Wunderlich, A., Sander, C., Martin Sander, F., Sander F. G. (2008) Stress distribution and displacement analysis during an intermaxillary disjunction: a three-dimensional FEM study of a human skull, *J. Biomech*., **41**, 376–382.
41. Chan, K. S., Lee, Y. D., Nicolella, D. P., Furman, B. R., Wellinghoff, S., Rawls, H. R. (2007) Improving fracture toughness of dental nanocomposites by interface engineering and micromechanics, *Eng. Fract. Mech.*, **74**, 1857–1871.
42. Huang, H. M., Tsai, C. Y., Lee, H. F., Lin, C. T., Yao, W. C., Chiu, W. T., Lee, S. Y. (2006) Damping effects on the response of maxillary incisor subjected

to a traumatic impact force: a nonlinear finite element analysis, *J. Dent.*, **34**, 261–268.

43. Choi, A. H., Ben-Nissan, B., Conway, R. C. (2005) Three-dimensional modelling and finite element analysis of the human mandible during clenching, *Aust. Dent. J.*, **50**, 42–48.
44. Lanza, A., Aversa, R., Rengo, S., Apicella, D., Apicella, A. (2005) 3D FEA of cemented steel, glass and carbon posts in a maxillary incisor, *Dent. Mater.*, **21**, 709–715.
45. Gallas Torreira, M., Fernandez, J. R. (2004) A three-dimensional computer model of the human mandible in two simulated standard trauma situations, *J. Craniomaxillofac. Surg.*, **32**, 303–307.
46. Tepper, G., Haas, R., Zechner, W., Krach, W., Watzek, G. (2002) Three-dimensional finite element analysis of implant stability in the atrophic posterior maxilla: a mathematical study of the sinus floor augmentation, *Clin. Oral Implants Res.*, **13**, 675–665.
47. Akça, K., Cehreli, M. C., Iplikçioglu, H. (2002) A comparison of three-dimensional finite element stress analysis with in vitro strain gauge measurements on dental implants, *Int. J. Prosthodont.*, **15**, 115–121.
48. O'Mahony, A. M., Williams, J. L., Spencer, P. (2001) Anisotropic elasticity of cortical and cancellous bone in the posterior mandible increases peri-implant stress and strain under oblique loading, *Clin. Oral Implants Res.*, **12**, 648–657.
49. Taylor, M., Verdonschot, N., Huiskes, R., Zioupos, P. (1999) A combined finite element method and continuum damage mechanics approach to simulate the in vitro fatigue behaviour of human cortical bone, *J. Mater. Sci. Mater. Med.*, **10**, 841–846.
50. Vaillancourt, H., Pilliar, R. M., McCammond, D. (1995) Finite element analysis of crestal bone loss around porous-coated dental implants, *J. Appl. Biomater.*, **6**, 267–282.
51. Korioth, T. W. P., Romilly, P., Hannam, A. G. (1992) Three-dimensional finite element stress analysis of the dentate human mandible, *Am. J. Phys. Anthropol.*, **88**, 69–96.
52. Hart, R. T., Hennebel, V. V., Thongpreda, N., Van Buskirk, W. C., Anderson, R. C. (1992) Modeling the biomechanics of the mandible: a three-dimensional finite element study, *J. Biomech.*, **25**, 261–286.
53. Ben-Nissan, B., Svensson, N. L., Kelly, D. W., Vajda, T. T. (1987) Computer aided three-dimensional modelling and finite element analysis of the mandible [online], *Finite Element Methods Eng.: Proc. 5th Int. Conf. Aus. Finite Element Methods*, 290–294.

54. Tanne, K., Hiraga, J., Kakiuchi, K., Yamagata, Y., Sakuda, M. (1989) Biomechanical effect of anteriorly directed extraoral forces on the craniofacial complex: a study using the finite element method, *Am. J. Orthod. Dentofacial. Orthop*., **95**, 200–207.

55. Cook, S. D., Weinstein, A. M., Klawitter, J. J. (1982) Parameters affecting the stress distribution around LTI carbon and aluminum oxide dental implants, *J. Biomed. Mater. Res.*, **16**, 875–885.

56. Knoell, A. C. (1977) A mathematical model of an in vitro human mandible, *J. Biomech.*, **10**, 159–166.

57. Van Meerbeek, B., Willems, G., Celis, J. P., Roos, J. R., Braem, M., Lambrechts, P., Vanherle, G. (1993) Assessment by nano-indentation of the hardness and elasticity of the resin-dentin bonding area, *J. Dent. Res*., **72**, 1434–1442.

58. Waters, N. E. (1980) Some mechanical and physical properties of teeth, *Symp. Soc. Exp. Biol.*, **34**, 99–135.

59. Zhang, Y., Allahkarami, M., Hanan, J. C. (2012) Measuring residual stress in ceramic zirconia-porcelain dental crowns by nanoindentation, *J. Mech. Behav. Biomed. Mater*., **6**, 120–127.

60. Adam, C. J., Swain, M. V. (2011) The effect of friction on indenter force and pile-up in numerical simulations of bone nanoindentation, *J. Mech. Behav. Biomed. Mater*., **4**, 1554–1558.

61. Carnelli, D., Lucchini, R., Ponzoni, M., Contro, R., Vena, P. (2011) Nanoindentation testing and finite element simulations of cortical bone allowing for anisotropic elastic and inelastic mechanical response, *J. Biomech.*, **44**, 1852–1858.

62. Paietta, R. C., Campbell, S. E., Ferguson, V. L. (2011) Influences of spherical tip radius, contact depth, and contact area on nanoindentation properties of bone, *J. Biomech.*, **44**, 285–290.

63. Toparli, M., Koksal, N. S. (2005) Hardness and yield strength of dentin from simulated nano-indentation tests, *Comput. Meth. Prog. Biomed.*, **77**, 253–257.

64. Ford, C., Bush, M. B., Hu, X. Z., Zhao, H. (2004) A numerical study of fracture modes in contact damage in porcelain/Pd-alloy bilayers, *Mater. Sci. Eng. A*, **364**, 202–206.

65. Fan, Z., Rho, J. Y., Swadener, J. G. (2004) Three-dimensional finite element analysis of the effects of anisotropy on bone mechanical properties measured by nanoindentation, *J. Mater. Res*., **19**, 114–123.

66. Dong, X. D., Darvell, B. W. (2003) Stress distribution and failure mode of dental ceramic structures under Hertzian indentation, *Dent. Mater*., **19**, 542–551.

67. Shrotriya, P., Wang, R., Katsube, N., Seghi, R., Soboyejo, W. O. (2003) Contact damage in model dental multilayers: an investigation of the influence of indenter size, *J. Mater. Sci. Mater. Med*., **14**, 17–26.

68. Choi, A. H., Matinlinna, J. P., Ben-Nissan, B. (2012) Three-Dimensional Finite Element Nanoindentation Analysis of Sol-Gel Derived Nanocoatings, *Comp. Meth. Biomech. Biomed. Eng.,* (submitted).

69. Annunziata, M., Oliva, A., Basile, M. A., Giordano, M., Mazzola, N., Rizzo, A., Lanza, A., Guida, L. (2011) The effects of titanium nitride-coating on the topographic and biological features of TPS implant surfaces, *J. Dent*., **39**, 720–728.

70. Gîrleanu, M., Pac, M. J., Louis, P., Ersen, O., Werckmann, J., Rousselot, C., Tuilier, M. H. (2011) Characterisation of nano-structured titanium and aluminium nitride coatings by indentation, transmission electron microscopy and electron energy loss spectroscopy, *Thin Solid Films*, **519**, 6190–6195.

71. Rungsiyakull, C., Li, Q., Sun, G., Li, W., Swain, M. V. (2010) Surface morphology optimization for osseointegration of coated implants, *Biomaterials*, **31**, 7196–7204.

72. Schiefer, H., Bram, M., Buchkremer, H. P., Stöver, D. (2009) Mechanical examinations on dental implants with porous titanium coating, *J. Mater. Sci. Mater. Med*., **20**, 1763–1770.

73. Liu, X., Niebur, G. L. (2008) Bone ingrowth into a porous coated implant predicted by a mechano-regulatory tissue differentiation algorithm, *Biomech. Model Mechanobiol*., **7**, 335–344.

74. Panich, N., Wangyao, P., Surinphong, S., Tan, Y. K., Sun, Y. (2007) Finite element analysis study on effect of indenter tip radius to nanoindentation behavior and coatings properties, *J. Metals Mater. Miner*., **17**, 43–49.

75. Hedia, H. S. (2007) Effect of coating thickness and its material on the stress distribution for dental implants, *J. Med. Eng. Technol*., **31**, 280–287.

76. Tilbrook, M. T., Paton, D. J., Xie, Z. H., Hoffman, M. (2007) Microstructural effects on indentation failure mechanisms in TiN coatings: finite element simulations, *Acta Mater*., **55**, 2489–2501.

77. Aoki, H., Ozeki, K., Ohtani, Y., Fukui, Y., Asaoka, T. (2006) Effect of a thin HA coating on the stress/strain distribution in bone around dental implants using three-dimensional finite element analysis, *Biomed. Mater. Eng*., **16**, 157–169.

78. Piana, L. A., Perez, E. A., Souza, R. M., Kunrath, A. O., Strohaecker, T. R. (2005) Numerical and experimental analyses on the indentation of

coated systems with substrates with different mechanical properties, *Thin Solid Films*, **491**, 197–203.

79. Cofino, B., Fogarassy, P., Millet, P., Lodini, A. (2004) Thermal residual stresses near the interface between plasma-sprayed hydroxyapatite coating and titanium substrate: finite element analysis and synchrotron radiation measurements, *J. Biomed. Mater. Res. A*, **70**, 20–27.
80. Shan, Z. H., Sitaraman, S. K. (2003) Elastic-plastic characterization of thin films using nanoindentation technique, *Thin Solid Films*, **437**, 176–181.
81. Zhang, C., Leng, Y., Chen, J. (2001) Elastic and plastic behaviour of plasma-sprayed hydroxyapatite coatings on a Ti-6Al-4V substrate, *Biomaterials*, **22**, 1357–1363.
82. Schrooten, J., Helsen, J. A. (2000) Adhesion of bioactive glass coating to Ti6A14V oral implant, *Biomaterials*, **21**, 1461–1469.
83. Vaillancourt, H., Pilliar, R. M., McCammond, D. (1996) Factors affecting crestal bone loss with dental implants partially covered with a porous coating: a finite element analysis, *Int. J. Oral Maxillofac. Implants*, **11**, 351–359.

Chapter 18

Digital Dentistry and Dental Informatics

James Kit-Hon Tsoi
Faculty of Dentistry, Dental Materials Science, University of Hong Kong, Prince Philip Dental Hospital, 34 Hospital Road, Sai Ying Pun, Hong Kong SAR, People's Republic of China
jkhtsoi@hku.hk

Digital dentistry and *dental informatics* are the emerging fields in dentistry, particularly in modern dental biomaterials. The importance of these fields is vital for dental biomaterials research, teaching, and applications. It seems that in the future, digital dentistry and dental informatics will be heavily relied upon. In this chapter, the correlation between digital dentistry and dental informatics, with emphasis on dental biomaterials, will be discussed.

18.1 Digital Dentistry: Introduction

What is "digital dentistry"? To understand the term, we first need to know what "digital" is. According to the *Oxford English Dictionary*, "digital" is the adjective of the word "digit," which means any numeral from 0 to 9. Essentially, a numeral is a "code," which is countable and computable. The concept of "digit" further implies the discrete and

Handbook of Oral Biomaterials
Edited by Jukka P. Matinlinna

ISBN 978-981-4463-12-6 (Hardcover), 978-981-4463-13-3 (eBook)
www.panstanford.com

finite nature of the numeral. Therefore, the term "digital" can simply be defined as "code expressive," in which the information, system, signal, or data is represented by using some codes.

Often, the opposite of digital is "analog," which describes the continuous function of a system, data, signal, or information. "Analog" could be defined as "function expressive." If discrete data items are joined together (i.e., digital to analog), then a continuous function (which may not be a simple one) might form. Conversely, data abstraction, that is, sampling, of the continuous function will yield discrete data (i.e., analog to digital). In such data conversion, a kind of error could result in which data could be lost. Thus, in theory, more samples are needed to describe the complete story. However, depending on cases and situations, a large amount of samples may not be immediately available and the time of sampling will become longer. Therefore, in usual practice, sufficient samples should be obtained.

Digital and analog situations are all around us in our daily life, and they present as a *system*. Analog systems include, but are not limited to, physical parameters, such as lights and sounds; chemical parameters, such as materials and states; biological parameters, such as mitosis and life; and psychological parameters, such as sense and logic. All these parameters exhibit the continuous nature and could be functionalized as such. Another noteworthy point is the process of these parameters. For example, a lightbulb emits light and our eyes receive "light" signals, which are then sent to our brain through the nervous system (Fig. 18.1). Thus, we see light from a lightbulb. This is one of the examples showing "analog transmission," which does not involve any discrete data transformation. In brief, light is a continuous waveform. Our eyes are visual detectors of continuous wavelengths, and nerves are continuous signal transmission lines to the brain, which is a centralized analog processor.

Digital systems are usually more device oriented. Some devices such as calculators, computers, and CD players are some examples to illustrate the importance of digital systems. A modern calculator can be used to enumerate mathematical operations by inputting digits and the results are also in digits. The electronics within the calculator are digitalized in 0 and 1 only. This is a good illustration of complete "digital transmission" with the involvement of digits only (Fig. 18.2).

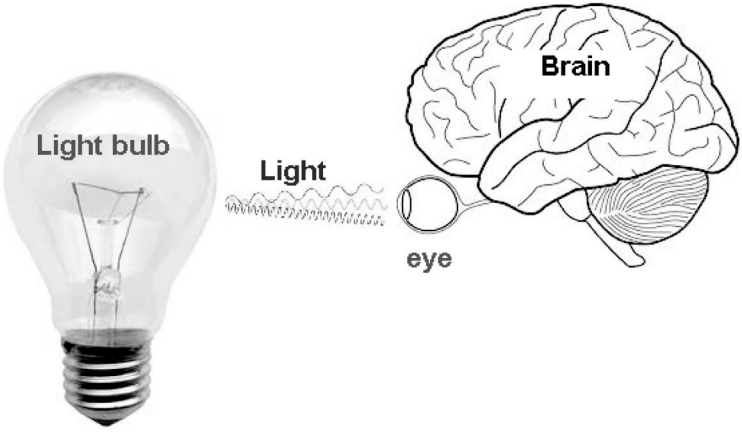

Figure 18.1 Signal transmission of light.

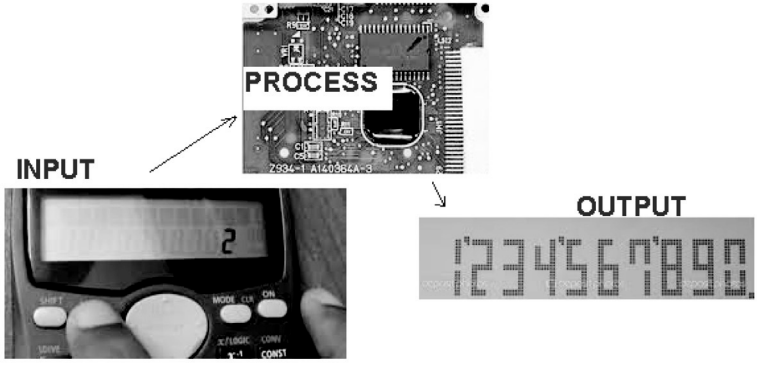

Figure 18.2 Signal transmission of a modern electronic calculator.

In all situations, the transmission process involves input, process, and output (IPO). IPO can be an analog, a digital, or a blended process. Take the following example as an illustration of what a blended process is. A student looks at a mathematical problem and solves it with a calculator. Then, the "looking" process is an analog process. The hand movement of digit inputting into a calculator is another analog process. Further, the use of a calculator to solve the problem is a digital process. Finally, the student reads and writes the calculated answer, which is another analog process. From this example, you can see humans do have the wisdom to transform such digital-to-analog and analog-to-digital processes smoothly.

The process in CD players is more complicated. Sound is an analog source that appears in the form of continuous waves. In a traditional sound storage medium, such as a gramophone record**,** sound is stored in modulated spiral grooves that have variation in 3D orientation parameters (e.g., depth and angles) such that the electromagnetic stylus/pickup could detect a vibration and convert it into an electrical signal, which is a continuous signal for the amplifier. Figure 18.3 shows a scanning electronic microscopy (SEM) image of the surface of a gramophone record.

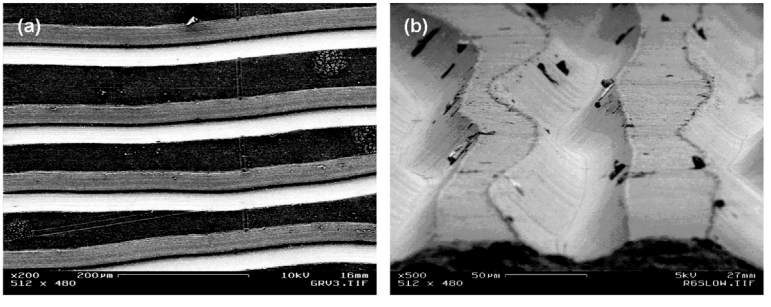

Figure 18.3 SEM image of the surface of a gramophone record. (a) Top view 200× (b) Side view 500×. Notice the changes of depth and angle to produce various vibration signals [1].

In the case of CDs, sound is stored in a digitalized format, which means sound is firstly being transformed from analog to digital (in this case, a signal of 0 and 1 only) with a suitable and proper sampling rate. Then, a code will be obtained. The CD player picks up the code from the CD and decodes it under a suitable algorithm within the chipset. Thus, the discrete code will join together to form a pseudocontinuous signal, which is then output to an amplifier. Figure 18.4 shows an SEM image of the surface of a CD.

So far, some definitions and terms are described and introduced. But, how can these relate to dentistry?

18.2 Digital Dentistry: Systems and Devices

In modern dentistry, dentists use many digital devices to assist in dental treatment. Dental systems are also set up to make dental

practice easier and more professional. Some commercial devices and systems are:

- computer patient record system
- computer-aided design/computer-aided manufacturing (CAD-CAM)
- dental imaging system
- dental laboratory management system
- digital impression
- digital 3D printing
- digital radiography

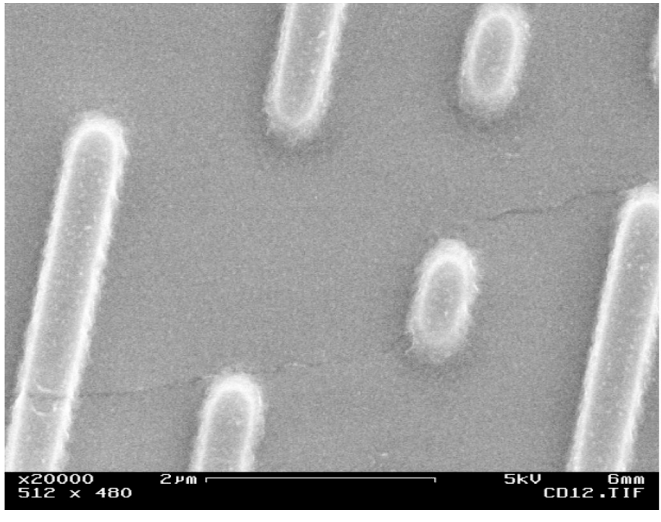

Figure 18.4 SEM image of the surface of a CD (top view 20,000×). Notice the pits depth are uniform to form 0/1 signals with the nonpit area [1].

All examples above share a similarity. They utilize a core device in the IPO: the computer. As the focus of this chapter is oral biomaterials, let us first take a look at computer operations in some illustrated systems that interact with biomaterials.

18.2.1 CAD-CAM

CAD-CAM, as the name implies, makes use of the computer to aid the design and manufacturing process. In the dental field, CAD-CAM can

be used to produce various dental products/devices, such as crowns, crownlays, veneers, inlays and onlays, fixed bridges, dentures, dental implant restorations, and orthodontic appliances.

Dental CAD-CAM systems (Fig. 18.5) are usually installed at dental laboratories or dental clinics, depending on the applications and the scale.

Figure 18.5 A typical dental CAD-CAM system.

Traditionally, the processing of all these materials requires intensive and skilled labor work. For example, in making a porcelain crown, the labor and the respective work required are:

(1) *Dentist*: To take the impression from the patient's mouth, determine the tooth color, and test-try the crown in the patient's mouth. Some dentists may even need to pour the gypsum cast model themselves.
(2) *Dental surgery assistant*: To assist in the mixing of the impression and gypsum materials and to perform other administrative tasks such as proper storage of cast models and patient-contacting matters.
(3) *Dental technician*: To pour the porcelain crown from the cast and to color.

It is generally understood that every kind of material may be adversely affected by various internal factors, for example, the type of material, and external factors, for example, temperature and humidity, which will affect the properties of the material, such as a change of dimension and occurrence of porosity. Further, human factors might also create errors such as incorrect use and handling of materials, which may result in a certain inferior structure of the materials. In addition, time is always tight because dentists, dental technicians, and patients may not be easily available to each other, and the materials also have their best-performance duration. Therefore, such a process, which can also be described as an "analog process" owing to its streamlined nature, may have a high failure rate due to all kinds of errors.

In the case of CAD-CAM, although some human processes are still unavoidable, for example, the dentist's job of taking the impression and try-in, some processes are simplified. The IPO components are:

- I: This involves 3D scanning of the gypsum mold or impressed tray (this is a process of digitalization).
- P: The computer reads through the 3D images and designs a feasible crown solution to the, say, milling machine (this is a CAD process). At this stage, the computer operator could adjust and fine-tune the computer design manually.
- O: The milling machine read the signals and starts to process the crown preparation (this is a CAM process) (Fig. 18.6).

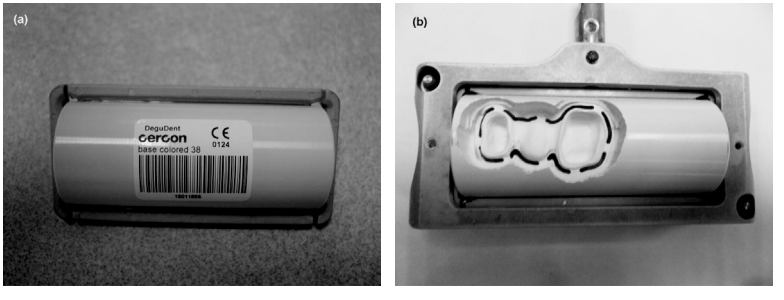

Figure 18.6 Zirconia block (a) before CAM milling and (b) after milling. Courtesy of Jonathan Wong, MSc(DMS) Hong Kong.

Obviously, the advantages of using CAD-CAM in dentistry are (1) reduced labor, (2) cost-effectiveness, (3) timing, and (4) choice of

materials. The reduced labor, in fact, could reduce the human error that might occur during every process. This also directly affects the cost and time as every step it time consuming and the cost of labor is high. Although time is needed for training labor to use the CAD-CAM system, the training time is much less than the time saved.

Another important aspect is the *choice of materials*. For example, it is much more desirable to use sturdier materials in making a crown. The traditional metal (e.g., stainless steel) crown, despite its relatively good mechanical properties, is not esthetically acceptable. Some porcelain materials, such as feldspathic porcelain and metal-bonded ceramics, have excellent esthetics but also have their instinct problems. Feldspathic porcelain is poor in fracture toughness, and it has low thermal conductivity due to the glass nature that generates internal surface cracks easily and eventually fracture. Metal-bonded ceramics (porcelain fused to metal [PFM]) are using two materials—ceramic and metal—to provide extra strength. These two materials, however, usually do not have the same thermal conductivity and thus induce residual stress thermally. Therefore, with the aid of CAD-CAM, high-strength materials are developed.

One of the noteworthy abilities of CAD-CAM is the machining of high-strength materials, which traditional techniques such as die casting or hand craving are not able to achieve. Certain kinds of high-strength materials that CAD-CAM can produce are:

- pure alumina
- zirconia
- leucite-reinforced glass ceramics
- fluormica glass ceramics
- feldspathic glass ceramics
- lithium disilicate glass ceramics

In fact, CAD-CAM technology opens up a new opportunity for dental (bio)materials scientists in the research field. Newer and improved materials are available at every moment. Thanks should be given to the digital era that has changed the world. These materials are discussed in detail elsewhere in this book.

With an understanding of the input process in CAD-CAM above, we notice that dentists still need to take impression materials and cast models. So, is there any possible way to deal with that?

18.2.2 Dental Imaging and Digital Impression

Dental imaging is the representation or reproduction of mouth or stomatological objects via a visual representation (i.e., image/video formation). In digital dentistry, the images and/or videos are digital. Again, IPO components are digitalized:

- I: The sensor of the camera takes images/videos.
- P: The images/videos from the sensor are processed, that is, digitalization.
- O: They are viewed and stored as files/data.

Traditionally, X-ray radiographic films were taken of the patient's mouth and they needed to be viewed from a light box (Fig. 18.7). X-ray films usually consist of an emulsion-gelatin that contains radiation (gamma-rays and X-rays)-sensitive chemicals, such as silver bromide (AgBr) or silver chloride (AgCl), and a flexible, transparent, blue-tinted base. The emulsion is coated on one or both sides of the base in very thin layers (~10 mm). Such a thin layer lets the developing, fixing, and drying process to be accomplished within a reasonable time.

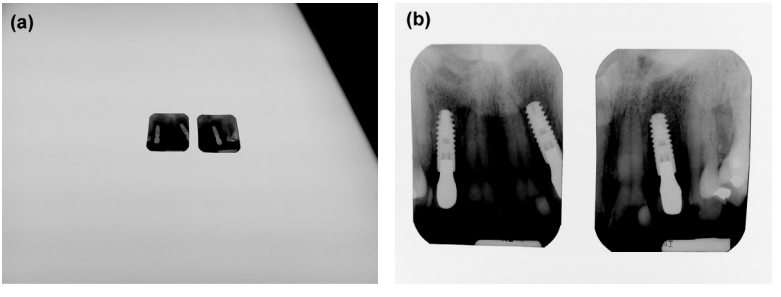

Figure 18.7 Radiographs (a) from a light box and (b) close-ups.

In brief, the principle of radiation-sensitive chemicals is that the radiation waves strike on the emulsion, and then some of the Cl^- or Br^- ions are liberated and captured by the Ag^+ ions. This tiny change produces a latent image. In image processing, the developer converts the latent image to dark metallic silver, which is suspended in gelatin, in the exposed area. A dark environment is required in the *processing* as the chemicals are very sensitive to light. In terms of occupational safety, good ventilation is needed in the processing

because of the toxicity of the chemicals and the uncomfortable smell. Extra care is also highly recommended in handling and storing the X-ray film because all sorts of pressure, creasing, buckling, friction, etc. could damage the film.

To minimize the risk and trouble in handling and storage, digital X-ray radiographic systems (Fig. 18.8) were invented, and this should be a favorable option to dental operators. Firstly, no film, darkroom, and film storage are needed. This does not only save space, but there is no need in handling the hazardous developing solution. Ventilation would also be easy. In this circumstance, no waste is produced other than the radioactive source and a cleaner environment is obtained. Further, time is saved as there is no need to develop the film; all data is immediately obtained from the system computer. The data can be linked with the patient data management system so that, in principle, the data can be stored and transferred without lost.

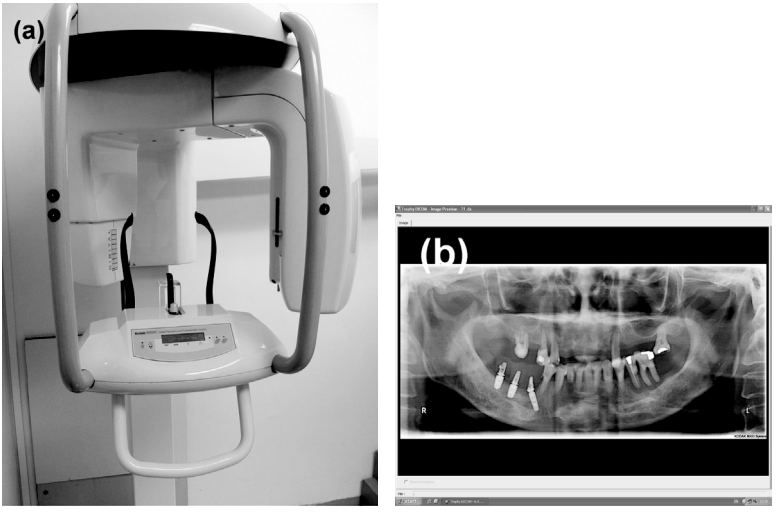

Figure 18.8 Digital panoramic system (a) outlook and (b) digital image from the software.

Digital radiographic technology also promoted the advancement of imaging. Computer tomography (CT) is one of the advanced techniques in using the computer to process digital X-ray images to produce tomographic images. In dentistry, the generated images can

be viewed in three dimensions and in specific curve tomographic planes by using software (Fig 18.9). These volumes of information could be particularly useful during treatment planning and the treatment process that enables dentists to see some nonviable conditions, such as jawbone conditions, providing them the means to make possible judgments and adjustments.

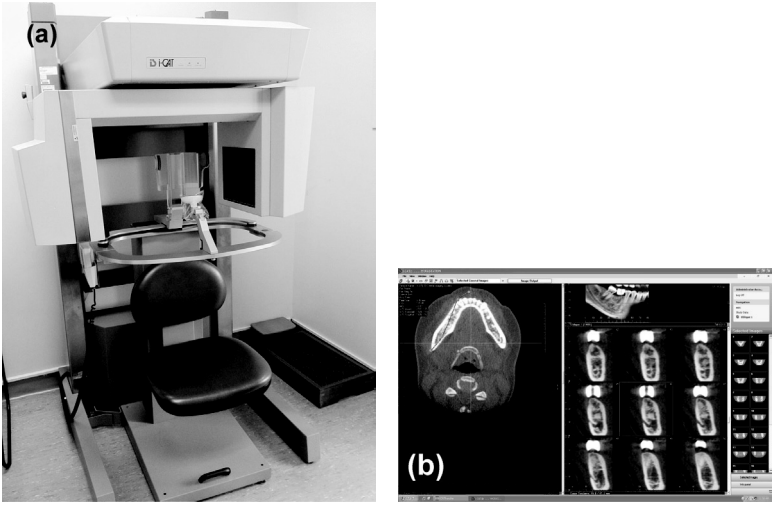

Figure 18.9 Cone beam CT system (a) outlook and (b) digital image from the software.

Another digital imaging device that is commonly used in dentistry is an intraoral camera (Fig. 18.10). The intraoral camera is a very simple device. It comprises a handle, a tiny camera with high resolution, a light, and a transmission medium (could be cable or wireless through WiFi or bluetooth) to connect with the computer. Usually, dentists hold the camera and the patients observe the images from the monitor. In this way, some tooth conditions can be illustrated to patients. This device can be used to enhance the communication and mutual trust between dentists and patients, as the patients could understand better about the oral conditions, while the dentists communicate in pictorial form rather than in words.

The intraoral camera can take photos or videos (depending on product models), and some software programs may enable the export of photo or video data to the patient management system.

All this data has a clearer image and better resolution in yielding successful imaging. A charge-coupled device (CCD) is one of the camera mechanisms that are dominated in the intraoral camera area.

Figure 18.10 A generic intraoral camera.

As mentioned above, even by using CAD-CAM, dentists still need to use impression materials to take teeth impressions from patients. Therefore, with the aid of software and intraoral cameras, digital impression systems were invented and launched in the market (Fig. 18.11). In this case, the intraoral camera is actually a scanner. Different digital impressions may have various operations, but in general, dentists need to select specific teeth from the software first and then the selected teeth are scanned by the dentists. The scanner would take many images at various angles, and these images produce a 3D virtual model. Several times of scanning are needed to obtain the most accurate and precise virtual model. Further, some systems may require the spraying of specific chemicals or another bite scan in order to obtain the finest details. Finally, this data is stored in the computer from which the data can be transferred to a dental laboratory or the clinics' in-house CAD-CAM for further processing digitally, such as for the preparation of a crown.

This digital impression system is an inline design, in which one system manufacturer is responsible for taking care of the materials in both hardware and software. Thus, all materials in the hardware and software are not interchangeable. This can be advantageous because the system manufacturer could control and manage quality easier. Manufacturing high-quality materials benefits patients. However, it

could be disadvantageous for those dental laboratories that are not equipped with the same system as the dentist. These laboratories would lose their business. Further, if some bugs or errors exist in the system, there is no turning point that can reverse the process. Thus, qualified system compliance is necessary. System verification and validation are essential. International standards on such a system are highly demanded.

Figure 18.11 Digital impression system.

Another noteworthy point is data quality and security. While data is being transferred in, for example, an Internet environment from dental clinics to dental laboratories, some data might be lost due to a variation of computer settings in different workplaces. Furthermore, private patient data might be disclosed to some other nonrelated parties due to human error. Therefore, data should be properly encrypted and transferred with high security.

18.2.3 Digital 3D Printing

The 3D printing technique is a rather new concept, and the function may be similar to CAM. CAM is a traditional machining technique that is a subtractive process. However, 3D printing, also called additive manufacturing, is a different manufacturing process that makes 3D solid objects from a digital model, such as from CAD. It is achieved by using successive additive processes. An additive process creates an object, in principle, by adding successive layers of material. Such a process benefits small-scale production that is faster and less expensive than injection molding, which is a method to produce polymer products in large quantities. Thus, 3D printing is also a rapid prototyping technique. In particular, the 3D printing technique is very suitable for dental use as nearly all dental sizes for restorative materials vary from person to person. As such, this technique would give personalized service, which is hoped to benefit dentists, patients, and dental technicians.

The 3D printing technique can be utilized by a 3D printer (Fig 18.12). The software from the 3D printer can read the data from CAD and lays down successive layers of liquid, powder, or sheet material. These layers are usually very thin, and as a result, objects build up the model from a series of cross sections and layers. Various methods are available, namely:

- selective laser sintering (SLS)
- direct metal laser sintering (DMLS)
- fused deposition modeling (FDM)
- stereolithography (SLA)
- laminated object manufacturing (LOM)
- electron beam melting (EBM)
- powder bed and inkjet head 3D printing
- plaster-based 3D printing (PP)

In the current dental field, some commercial printers have been launched. Those printers usually print prothosdontics materials, such as wax-ups, acrylics crowns and bridges, orthodontic baseplates, and partial denture frameworks. These materials are usually softer and are able to use FDM and SLA with direct UV-curing techniques. For some harder materials for bridge frameworks, such as titanium,

cobalt, chromium, and precious metals, DMLS and EBM are required and these machines are not compatible with the former one.

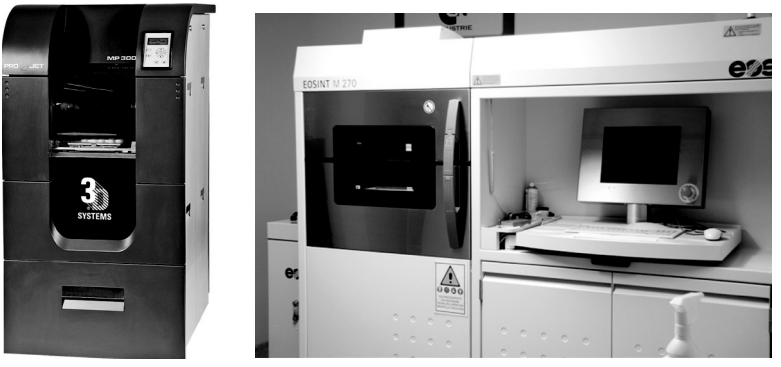

Figure 18.12 3D printer for (left) dental wax-up and acrylics and (right) DMLS implant fabrication.

In other applications such as jawbone reconstruction and implant manufacturing, some manufacturers have utilized SLS and DMLS techniques to produce unique sizes according to the individual patient's need (Fig 18.12). Some implant manufacturers also utilized these techniques to apply on titanium implant surfaces and create nanosized titania (TiO_2) coatings. The surface area and roughness are increased, and better osseointegration might be obtained. Other techniques are still in research stages on applications of, for example, printing zirconia materials for crown and implant materials and polymeric scaffold materials. Therefore, a promising future can be seen for such techniques with new biomaterials.

18.2.4 Digital Dental Biomaterials

A dental biomaterial can be broadly defined as a substance or partial substance that is compatible with the body's living systems, specifically used in the oral environment. During the processing of dental biomaterials, we can name the materials as "digital dental biomaterials" if such a digital process is used. As mentioned above, some digital dental biomaterials are, for example, CAD-CAM crowns, 3D printed wax-ups, jawbones and prostheses, milled implants, and digital radiographs/intraoral pictures/videos. All these materials

are viable and touchable. What about materials that are nonviable and untouchable?

During the digital process, information and data are something that are not viable and touchable. Shall we also call these digital dental biomaterials? As these data and information are the made-up constituents of the ultimate touchable biomaterials, thus without doubt these data and information are the partial substance of dental biomaterials. Therefore, we should include data and information as a key part of digital dental biomaterials.

With advancement of technology, more and more digital dental biomaterials are coming in and the human–computer interaction is one of the key cognitive aspects that we should be aware of. The handling or treatment of data/information is not simply information technology (IT), which is a parameter related to computer literacy, but it is rather a specific subject—dental informatics—which requires suitable and knowledgeable personnel and expertise.

18.3 Dental Informatics

As the name implies, dental informatics is the informatics in dentistry. So, what is informatics? The answer could be:

- application of information
- management of information
- treatment of information
- science

Thus, dental information that is being treated, managed, and/or applied in scientific logic and ways forms the core of dental informatics. Whenever you are handling information, IPO models apply (Fig. 18.13).

A large amount of information has been input into a processing system. An ideal processing system could process the input data in a cognitive way such that the system will manage, treat, and analyze manually or automatically. The system should also contain a database, which is actually an information storage system to store permanently and temporary information and data. Finally, treated information is produced as some reading, figures, etc. It is worth to note that, in many dental informatics applications, the computer is one of the (digital) tools to carry on this IPO model because of its

simplicity. The actual input, for example, patient image taking, is done by humans, and the algorithm, which is the processing brain, is written by humans. The computer at this stage does not have any diagnostic knowledge yet, so the output is to be read and determined by dentists. Thus, this brings a lot of interaction between humans and tools. Therefore, to successfully and correctly make use of the convenience that is brought about by informatics, cooperation is needed between the user and the tool.

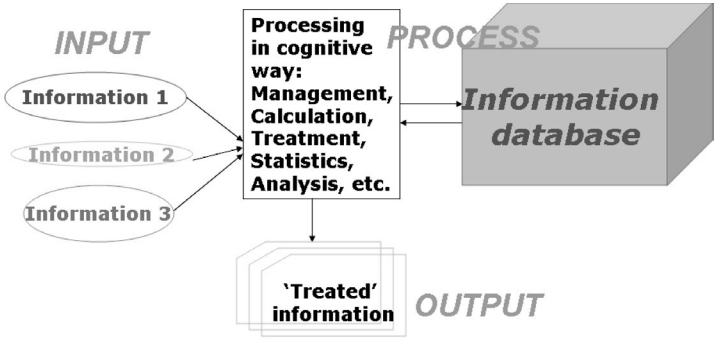

Figure 18.13 IPO model for dental informatics [2].

The prerequisites for successful cooperation between users and tools, probably include (1) a careful sense, (2) an analytical mind, (3) knowledge, and (4) training in computer skills, that is, IT. We know that all hardware and software are not bug free, and erroneous input and output may happen due to human errors as well. Dealing with patient or dental information is not easy, and extra care should be taken. Dentists and dental information handlers should have an analytical mind in order to make any judgment on and adjustment to treated data in the case of an occurrence of error. An analytical mind also relates to the professional knowledge that users have. For the case of software and hardware developers, they should know how to minimize bugs in the system. For information handlers, training is needed to enable them with expertise on how to handle data correctly. Finally, adequate IT skills are essentially important because this helps to run computer jobs seamlessly and could maximize the benefit from information. If someone does not know how to operate the computer, how can he/she be able to input and read the output from the data?

Attention should also be drawn here: IT is not equivalent to informatics [3]. One with high IT skills does not mean being successful in informatics. To excel in dental informatics, not only adequate IT skills are important, but also teamwork is required to ensure, for example, that bugs in the hardware and software are minimized, all data/information is correctly input, treated data is read and interpreted without loss, and data is safely stored in devices. Therefore, to successfully operate dental informatics, the quality of the user is still a dominant factor.

There are many fields for dental informatics, such as research, teaching, digital imaging and image processing, computer-based dental records, clinical decision support, and teledentistry. All these fields involve handling information. In fact, the American Dental Association (ADA) has created certain specifications and technical reports on various digital systems and devices. Such regulatory events recognize the formality of dental informatics and also set criteria for data management, which is beneficial to both patients and dental information handlers.

In the field of dental biomaterials science, we may deal with dental informatics in certain aspects, such as scientific investigation on formulation, system development, system implementation, and study of effects by simulation. All these may require a suitable computer program written in an appropriate computing language, which is properly equipped with a logical algorithm to provide a suitable mathematical process. For example, in Microsoft Excel™, the common standard deviation that is being used in the STDEV command is:

$$\sqrt{\frac{n\sum x^2-\left(\sum x\right)^2}{n(n-1)}} \tag{18.1}$$

However, in our schools and some professional statistics program, such as in Statistical Packages for Social Science (SPSS; IBM, USA), the standard deviation for a sample is:

$$\sqrt{\frac{1}{N}\sum_{i-1}^{N}(x_{\mathrm{i}}-\bar{x})^2} \tag{18.2}$$

Obviously, Eqs. 18.1 and 18.2 are different. Hence, such a small algorithm difference of standard deviation may affect data quality

and the results, especially in some research articles. Therefore, extra care should be taken.

18.3.1 Quality Assurance for Information

Another aspect of dental informatics models and/or systems is quality assurance (QA). To perform QA, two ways are possible:

- Validation
- Verification

Validation is defined as "a process of checking that the model behaviour corresponds to what was originally required, and whether that behaviour corresponds to that of the real system" [4]. The model behavior is important because it affects the real system as for output. As for the specific compliance for software, the FDA stated that "software validation is confirmation by examination and provision of objective evidence that software specifications conform to user needs and intended used, and that the particular requirements implemented through software can be consistently fulfilled" [5]. Specific requirements are needed to be complied with to perform as the objective ascribed. Unlike validation, verification "implies that the logical reliability of the computer model should be confirmed . . .," that is, "there are no 'bugs' in the code" [4]. To show that the system/model is reliable for users to use, the FDA also commented that "software verification looks for consistency, completeness, and correctness of the software . . ." [5], which further implies the minimization of error in the software.

Performing validation and verification is difficult because it is always hard to know how much evidence is enough [5]. Thus, developing a validation/verification model is an art, in which the piece of art should be able to develop a level of confidence to fit for specification and user expectation. Nevertheless, specifications may contain defects, and the defects might induce risks and hazards. Therefore, validation/verification should take risks and hazards into account, which would effectively affect the confidence levels of such process.

There are some general criteria in performing validation, namely, accuracy, precision, linearity, and robustness. *Accuracy* is the closeness of mean test results obtained by the method to the

true value, while *precision* describes the closeness of agreement (degree of scatter) between a series of measurements obtained from multiple samplings of a homogeneous sample under the prescribed conditions (Fig. 18.14).

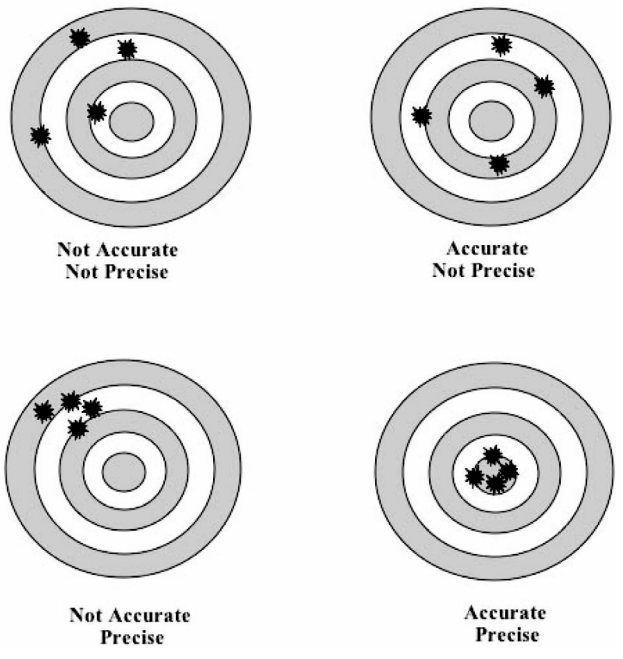

Figure 18.14 Precision and accuracy illustration. The centre is the true value, and the circles are the outliners [6].

Several samples are needed to find true values. Good precision can be achieved if the samples are repeatable under the same operating conditions over a short interval of time. Intermediate precision and reproducibility are measured between the variations of systems at the same location and different locations, respectively.

Another perspective is the *linearity* of the system, which shows the linear relationship between dependent and independent variables within a given range. Further, a system may not be used under a normal condition. Thus, *robustness* is tested by using a measure of its capacity to remain unaffected by small, but deliberate, variations in method parameters. Therefore, this could provide an indication of its reliability during normal usage.

Make sure the specification is carefully done, and an update of test methods on validation and verification are always essential.

18.3.2 Real and Digital Dental Biomaterials: Interaction

Dental biomaterials are handled by dentists, dental researchers, technicians, teachers, and surgery assistants every day. All these biomaterials need handling, caring, storage, mixing, etc. These are, as described before, analog processes. Digital dental biomaterials are information that is in digital form. Thus, analog-to-digital and digital-to-analog conversion takes place inevitably in all situations. We have discussed in previous sections digital dentistry applications, which are all dental informatics clinical and daily examples. Some chapters of this book have also discussed some digital dental biomaterials such as finite-element analysis (FEA). Hence, the following examples will illustrate some other interaction between these systems for teaching, research, and scientific fields.

18.3.2.1 Case 1: Impression materials simulation

Dental impression materials are a system with a polymer network. They are usually composed of a two-paste system, in which the polymer network is developed from a prepolymer. The study of polymer networks would be important due to mechanical properties depending on the network formation and constituents. Thus, some condensational types of impression materials (e.g., polysulphide and condensation silicone) were studied [4].

Firstly, an algorithm was carefully designed with full consideration of emulating actual chemical reactions. Numerical simulation with the Monte Carlo technique (i.e., random numbers) and a sample size of 10 million was chosen to simulate the whole situation (Fig. 18.15) in a high-performance cluster computer (a kind of supercomputer). Then, the prepolymer, which is what actual products are using, was presented by some values (i.e., turning the polymer into digitals). Finally, the polymer networks were enumerated by depolymerization and polymerization.

To check the validity of results, first, accuracy and precision were compared with chemical experimental data from others. The same pattern and finding such as cyclic species and predominant small molecules were matched. For immediate precision and

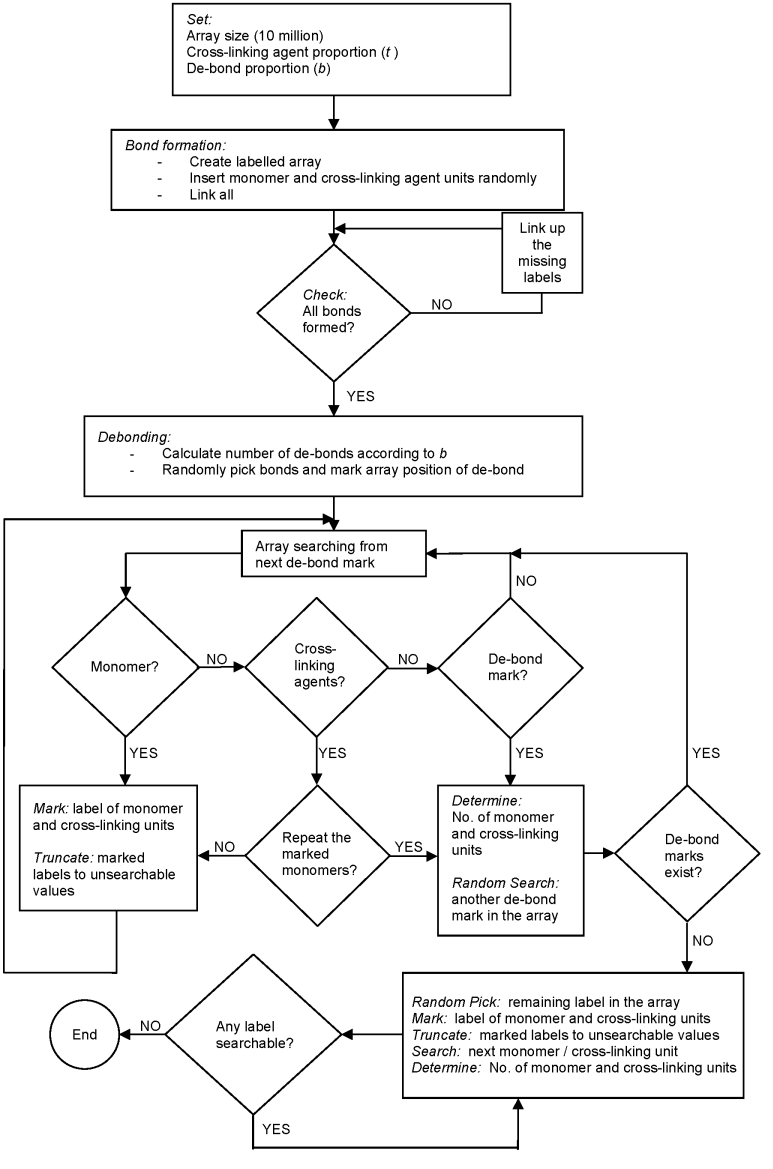

Figure 18.15 Algorithm in polymer network simulation [4].

reproducibility, the same computer program was run on different computers and kernels to ensure the same results are obtainable. The program, due to a random number nature, was also run in

various random seeds to generate different sets of random numbers to show the program could repeat the results. To show the linearity of results, fragments of data were generated and the patterns of all data behaved similarly. Certain changes were also done in the program, for example, to prove that the program maintains in other situations, the program is switched to perform equiprobable reactions to illustrate the robustness of the computer program. For verification, all results were manually checked, while making sure that the program had no bugs.

After validation and verification, a mathematical expression, which is sufficient to describe a condensation polymer network system, was developed.

18.3.2.2 Case 2: Dental biomaterials science education

In the traditional mode of learning, such as in large class lectures, students learn passively and there is nearly no interaction between the teacher and students. This may be effective for primary and secondary school education in which students are learning facts that may not be disputable. *Dental biomaterials science*, however, is a university-level course where presumably all students are equipped with high school or university level of basic science. Thus, such a traditional learning mode may not address the students' need and demand for the fast-changing dental world that requires students (who may be future dentists or dental-related workers) to think and judge on dental biomaterials. Active learning is necessary. Therefore, using informatics might be a good option to enlighten, educate, and equip the students' mentality to think critically and choose correctly the best dental biomaterials for patients.

An e-learning application and a platform such as iClass could be one of the innovative education software programs that encourage interactivity between teachers and students and should be adoptable in undergraduate and postgraduate levels of teaching in dental biomaterials science [7]. iClass is an award-winning application and platform, which was developed by Dr. Wilton Fok et al., Department of Electrical and Electronic Engineering, University of Hong Kong. It utilizes cloud-computing technology and thus real-time responses can be shown immediately. Teachers can set questions and problems in the iClass teacher platform (Fig. 18.16) online before or during class. Then, students can input their comments/answers through

the iClass application. One of the advantages of this platform is that all input will be transparent. In such a circumstance, all students are required to contribute equally and are able to see others' comments/answers. Further, teachers can engage in mental and knowledge exchange with their students, gather all the answers, and arrange them logically in real time. Thus, the interactivity between teachers and students is enhanced. A noteworthy point is not only teachers are influencing students, but also students are interacting with teachers. If the teachers are well prepared, equipped, and trained in dental biomaterials, students could learn and enjoy much in such an active and interactive learning environment (Fig. 18.17).

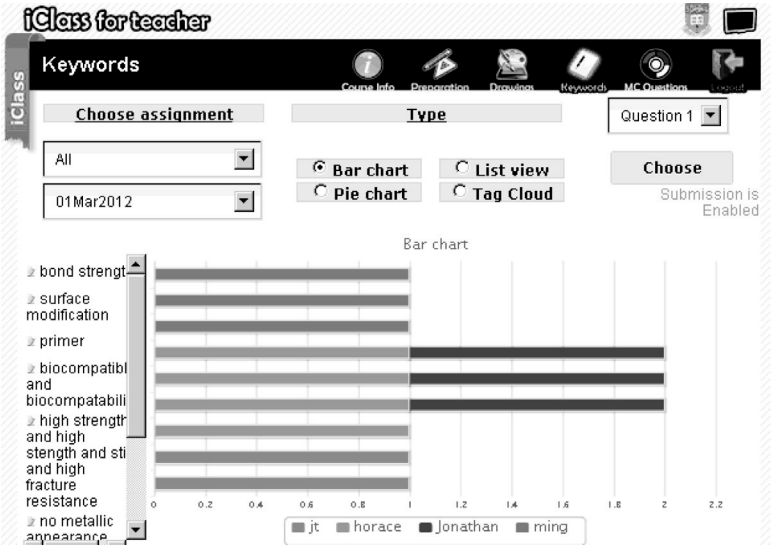

Figure 18.16 iClass (teachers' version) during teaching about dental biomaterials.

18.3.2.3 Case 3: Dental drug discovery

It seems that dental drugs are limited, and nearly all dental drugs share with medicinal drugs. The drug molecules may be effective. However, without specificity in the oral environment and diseases, the drug molecules, dosage, and formulation may not have the best performance and might induce more side effects than expected. Therefore, specific drugs in dentistry are essential. In *dental drug discovery*, there are two aspects that can use informatics as an aid—

(1) discovery of active pharmaceutical ingredients (APIs) and (2) drug formulation. For the discovery of APIs, the traditional stages are:

(i) target identification (0.5–1 year)
(ii) target validation (0.5–1 year)
(iii) lead identification (0.5–1 year)
(iv) candidate optimization (2–3 years)
(v) preclinical trial (1–2 years)
(vi) clinical trial (4–6 years)

Figure 18.17 Teaching dental biomaterials using iClass at the Faculty of Dentistry, University of Hong Kong. The author of this chapter is standing at the podium. The editor of this book is sitting in the front row, second from left.

Apart from the exorbitant amount of money, developing a new drug needs at least 10 years from target identification to clinical trial. Although the clinical trial stage seems the most time-consuming stage, stages (i) to (v) are robust and complicated. Furthermore, the prospected drug molecules may not be immediately synthesizable, even though the mechanism is conceptually correct. Much work is

needed for the preparation. Do note that most drug manufacturers only find a drug for commercial purposes. Thus, due to the limited market size in dentistry, the drug manufacturer is not interested in developing dental-specific drugs. To help the research, academic, and industrial needs, informatics helps dentistry by finding some prospected drugs, saving time and money. With the aid of informatics, the traditional steps (i) to (v) could be saved by using data mining to search drug molecules, to dock and snore the molecules in the database *in silico*, and finally to screen several target drugs for in vivo studies (Fig. 18.18). All these processes could be done within one year and therefore save time and money.

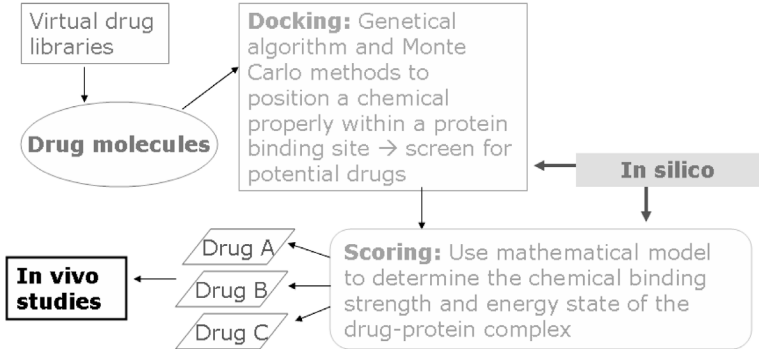

Figure 18.18 Dental drug discovery by informatics [2].

Docking is the screening for potential drug molecules from drug libraries, which is essentially a genetical algorithm and some Monte Carlo methods to simulate the proper chemical within a protein site. Then, the potential drugs need to be scored by using a mathematical model to determine the chemical binding strength and energy state of the drug–protein complex. One of the usual techniques for this modeling is performed by *ab initio* calculation, which is a method from computational quantum chemistry. However, to precisely and accurately perform these in silico processes, the algorithm should be validated and backed up with proteomics.

Another factor is the time in the *in silico* process. Due to the large amount of data for computation, the higher the computation power and the cleaner the algorithm, the faster the data generation. Some types of computers, such as high-performance-cluster computers, are definitely helpful in such a computation. Further, the algorithm

for the cluster can also be written in parallel form, which can then split the algorithm into several subroutines and various data items can be fitted simultaneously and continuously. Nevertheless, with "garbage in and garbage out," extra care of data and algorithm should be taken. Skillful and knowledgeable personnel are necessary for dental informatics.

For the case of drug formulation, emphasis has been placed on the chemistry of oral products. In principle, the drug molecules need to be formulated in a suitable dosage base or carrier in order to confer the best performance, stability, release rate, etc. For dental drugs, such as oral gels, the formulation is very important as the ideal gels need to be sustained in the salivary oral environment, whilst the drug release rate cannot be altered. Despite many kinds of polymeric gels obtain good physical performance, biocompatibility and toxicity are a concern. Moreover, the adhesion of such a gel on the oral mucosa membrane is also a challenge. Therefore, using informatics could help in such a formulation design.

The gels that are being used in dentistry are usually hydrogels, which are gels consisting of water and a gel base. Except APIs, some excipients, such as sucrose and glycerol, are added to improve the taste and smoothness, respectively. To increase the amount of monomer, the polymer gel will have higher viscosity (η) and molecular weight (MW). When the drug molecules are released (i.e., absorbed by the mucosa), the saliva will replace the drug and, on the other hand, will dissolve the gel. Thus, viscosity will decrease overall:

$$\text{API} + \text{Gel} \rightarrow \text{API-gel}\ (\eta + \text{MW}) \tag{18.3}$$

$$\text{API-gel} + \text{Mucosa} \rightleftarrows \text{API-mucosa} + \text{API-gel*}\ (\downarrow\eta + \downarrow\text{MW}) \tag{18.4}$$

$$\text{API-gel} + \text{Saliva} \rightleftarrows \text{API-saliva} + \text{API-gel\^{}}\ (\downarrow\eta + \downarrow \text{MW}) \tag{18.5}$$

All Eqs. 18.3–18.5 are in equilibrium by the nature of the hydrogel. The viscosity decrease in API-gel^ is more than in API-gel*. Further, API-saliva is not absorbed, whilst only API-mucosa is the absorbable content of drug molecules. By carefully simulating and emulating the above equilibrium equations, we can calculate the amount of monomer needed for constituting the polymer gel and the amount of API absorbable by the mucosa.

With the aid of informatics, dental drugs and their formulations can be well designed and be specific for oral use. This does not

only benefit the development of dental-based medicine but also increases the dental successful rate. A patient-driven incentive is always the scope of dentistry, and the discovery of dental drugs by dental informatics is probably the best way.

18.4 Conclusions

The development of digital dentistry and dental informatics is never ending. Likewise in some dental biomaterials, for example, addition polymerized dental acrylics, the radical makes the polymer "ever living" in which the polymer is readily reactive when the new component is added. Digital dentistry and dental informatics are always "living" because new information and data bloom with the existing and change in the dental world. The reactions between digital and analog dental biomaterials always take place, and eventually equilibrium will be established and thus harmonious coexistence will occur.

References

1. Supranowitz, C. *General Topics in Electron Microscopy: Micrograph Acquisition*, http://www.optics.rochester.edu/workgroups/cml/opt307/spr05/chris/.
2. Tsoi, J. K. H. (2011) *Dental Informatics: A Key for Future Dentistry*, Oral Health & Science Seminar, Faculty of Dentistry, University of Hong Kong.
3. Schleyer, T. K. (2003) Dental informatics: an emerging biomedical informatics discipline, *J. Dent. Educ.*, **67**(11), 1193–1200.
4. Tsoi, J. K. H. (2007) *Aspects of Statistics of Condensation Polymerization Networks*, PhD thesis, University of Hong Kong.
5. Food and Drug Administration. (2002) *General Principles of Software Validation; Final Guidance for Industry and FDA Staff*.
6. National Oceanic and Atmospheric Administration. *Accuracy Versus Precision*, http://celebrating200years.noaa.gov/magazine/tct/accuracy_vs_precision.html.
7. Tsoi, J. K. H. (2012) Using iClass as a tool for journal-based learning (JBL) in teaching dental materials science at MSc level, in *The New Era of e-Learning*(Ed. Fok, W. W. T.), University of Hong Kong, ISBN 978-988-15045-3-1.

Chapter 19

Barrier Membranes for Periodontal Guided Tissue Regeneration Applications

Zeeshan Sheikh,[a,d] Mohamed-Nur Abdallah,[a] Nader Hamdan,[b] Mohammad Ahmad Javaid,[c] and Zohaib Khurshid[d]

[a]*Division of Biomedical Sciences, Faculty of Dentistry, McGill University, 3640 University Street, Montreal, QC H3A 0C7, Canada*

[b]*Division of Periodontics, Dental Diagnostic & Surgical Sciences: Faculty of Dentistry, University of Manitoba, Winnipeg, MB R3E 0W2, Canada*

[c]*Division of Periodontics, Faculty of Dentistry, University of British Columbia Nobel Biocare Oral Health Centre, University of British Columbia, Vancouver, BC V6T 1Z3, Canada*

[d]*Department of Materials Sciences & Preclinical Dentistry, Altamash Institute of Dental Sciences, Karachi, Pakistan*

zeeshan.sheikh@mail.mcgill.ca, mohamed.abdallah@mail.mcgill.ca, hamdann@myumanitoba.ca, mohammad.javaid2@mail.mcgill.ca, drzohaibkhurshid@gmail.com

Strategies for periodontal therapy are aimed toward elimination of etiological factors, prevention of spread and elimination of symptoms of disease, correction of anatomical defects, and regeneration of periodontal tissues. Various regenerative surgical techniques are frequently utilized for the augmentation of deficient ridges with decreased bone height prior to placement of dental

Handbook of Oral Biomaterials
Edited by Jukka P. Matinlinna

ISBN 978-981-4463-12-6 (Hardcover), 978-981-4463-13-3 (eBook)
www.panstanford.com

implants. Such regenerative treatments can include the utilization of barrier membranes. Certain cell populations residing in periodontal tissues have the potential to reverse periodontal destruction by creating new cementum, alveolar bone, and the PDL, provided they have the opportunity to populate the periodontal wound or defect. Two surgical techniques, guided tissue regeneration and guided bone regeneration, have been extensively used to regenerate different periodontal tissues. Various barrier membranes have been developed and tested as part of these two procedures to prevent epithelial and connective tissue cells from invading the deficient space, while allowing PDL cells to selectively migrate into the defect.

19.1 Preamble

Periodontitis is an inflammatory disease of the supporting tissues of teeth caused by specific microorganisms or groups of specific microorganisms, resulting in progressive destruction of the periodontal ligament (PDL) and alveolar bone with an increase in probing depth, recession, or both [1]. The different strategies of periodontal therapy are aimed toward elimination of etiological factors, prevention of spread and elimination of symptoms of disease, correction of anatomical defects, and regeneration of periodontal tissues [2–5]. During the last decade, various regenerative surgical modalities have been tried for the regeneration of periodontal tissues; that is, alveolar bone, cementum, PDL, and gingiva [2, 6, 7]. These surgical techniques are also frequently utilized for the augmentation of deficient ridges with decreased bone height prior to placement of dental implants. Such regenerative treatments include the utilization of a wide variety of surgical approaches, barrier membranes, a series of bone grafts and other osteoconductive/inductive materials or protein mixtures, exogenous growth factors, cell-based technology, and genes from recombinant technology.

Certain cell populations residing in periodontal tissues have the potential to reverse periodontal destruction by creating new cementum, alveolar bone, and PDL, provided they have the opportunity to populate the periodontal wound or defect. Collagen fibers are required to be inserted into the newly formed cementum and regenerated alveolar bone in order to restore the normal function and anatomy of the periodontium. Results are variable and reliant

on patient age, general health, defect size, and other demographic effects [8, 9]. Two surgical techniques, guided tissue regeneration (GTR) and guided bone regeneration (GBR), have been extensively used to regenerate different periodontal tissues [4, 10–18].

Various barrier membranes have been developed and tested as part of these two procedures to prevent epithelial and connective tissue cells from invading the deficient space, while allowing PDL cells to selectively migrate into the defect. These membranes will be the main focus of this chapter.

19.2 Guided Tissue/Bone Regeneration

GTR is essentially the use of an occlusive membrane interfacing with the gingival connective tissue/epithelium on one side and PDL/alveolar bone tissues on the other side. It maintains space for clot stabilization and to promote periodontal tissue regeneration, while preventing postsurgical epithelial cell migration to the wound site (Fig. 19.1). Thus, GTR is based on the principle of exclusion of gingival connective tissue cells from the wound and prevention of epithelial downgrowth. This procedure allows cells with regenerative potential to selectively invade the wound site [19]. Progenitor cells located in the remaining PDL, adjacent alveolar bone, or blood are then able to recolonize the root area and differentiate into a new periodontal supporting apparatus with the formation of new bone, PDL, and cementum [20]. Indications of GTR therapy include:

- narrow two- or three-walled intrabony defects;
- class II molar furcation involvement;
- defects with no tooth mobility;
- circumferential defects;
- class I or II gingival recession; and
- presence of thick gingiva [21].

The concept of guided regeneration that concerns the augmentation and restoration of deficient alveolar ridges and extraction sites is known as GBR (Fig. 19.2). Regenerative procedures can be carried out prior to, or in some cases along with, dental implant placement. Mostly, the main purpose is to increase bone volume where deficiency would compromise the function or esthetics of the dental implant restoration [22]. Also, effective results

have been achieved when using membranes for the treatment of furcations and intrabony defects, as well as for the repair of marginal tissue recession defects [5, 23].

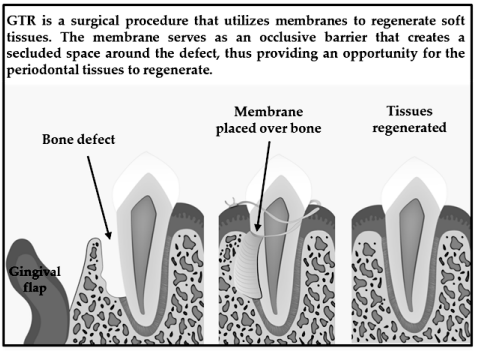

Figure 19.1 Illustration showing periodontal guided tissue regeneration (GTR) technique using a barrier membrane. Courtesy of Ms. Esraa Khalil, Graphic Designer, Amman, Jordan.

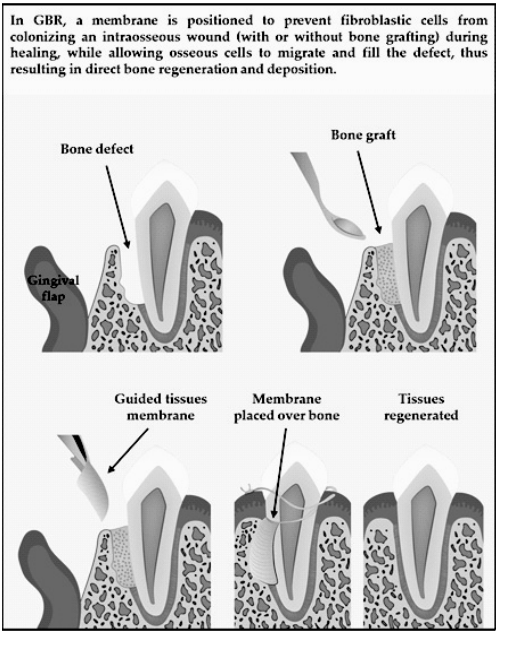

Figure 19.2 Illustration showing guided bone regeneration (GBR) technique using bone graft and a barrier membrane. Courtesy of Ms. Esraa Khalil, Graphic Designer, Amman, Jordan.

Recent systematic reviews have demonstrated the clinical advantages of guided regeneration procedures as opposed to conventional open-flap debridement for treating furcation and intrabony defects [24]. The rationale for bone augmentation procedures primarily relates to the improvement in function and esthetics and may also be used to enhance conventional dental prosthetics such as fixed partial dentures. This improves the deficient contours beneath the pontic (artificial tooth replacement), providing a more natural emergence profile as well as preventing altered phonetics due to the space left between the restoration and gingival tissues [22]. The principles of successful GBR therapy include:

- **Cell exclusion**: In GBR, the barrier membrane is used to prevent gingival fibroblasts and epithelial cells from gaining access to the wound site and forming fibrous connective tissue.
- **Tenting**: The membrane is fitted, and a space is created beneath the membrane, completely isolating the defect from the overlying soft tissue.
- **Scaffolding**: The tented space initially becomes occupied by a fibrin clot, which later serves as a scaffold for the ingrowth of progenitor cells.
- **Stabilization**: The membrane ideally protects the clot from being disturbed by movement of the overlying flap during the healing phase. It is therefore often fixed into position with sutures, mini bone screws, or bone tacks.
- **Framework**: In non-space-maintaining defects such as dehiscences or fenestrations, the membrane is supported to prevent collapse [25].

The *various indications* for GBR essentially involve alveolar bone defects, such as furcation defects (grade II or grade III); extraction sockets requiring future implant placement; dehiscence and fenestration defects; periapical pathologies, which require or have undergone treatment by apicoectomy; ridge augmentation; and sinus lift procedures [26].

The *contraindications* for GBR include any medical condition contraindicating surgery, poor oral hygiene, heavy smoking, infection at the defect site, generalized horizontal bone loss, and advanced lesions with little remaining support and multiple defects.

19.3 Rationale, Biologic Interactions and Advantages of Barrier Membranes for Guided Regeneration Therapy

As previously outlined, the rationale for guided regeneration is to impede apical migration of the epithelium by placing a barrier membrane, which potentially allows PDL cells to repopulate onto the root surface of teeth. Periodontal tissue engineering is an interdisciplinary area of applied biomedical research that attempts to develop techniques and biomaterials for the regeneration of these new tissues on principles of developmental biology, cell biology, and biomaterials science. The main requirements for producing an engineered tissue are appropriate levels and sequencing of regulatory signals, the presence of an adequate number of responsive progenitor cells, an appropriate extracellular matrix or carrier construct (a biomaterial scaffold), and an adequate blood supply [27].

The utilization of barrier membranes for guided regeneration of periodontal tissues serves three functions. Firstly, they act as a biocompatible physical barrier preventing the ingrowth of competing soft-tissue cells from the overlying mucosa. This allows preference to be given to angiogenic and osteogenic cells to migrate into the blood clot (from the opened bone marrow cavity or directly from blood) in the membrane-protected defect. Secondly, the membranes stabilize bone graft materials (if used in conjunction with barrier membranes) and the blood clot, since bone grafts are often affixed to the bone with screws (usually titanium miniscrews). These screws can facilitate easier surgical handling of the membrane and its close adaptation to the bone surface, ensuring a sealing effect (space maintenance/tent formation). Thirdly, the membranes serve as graft preservation devices (reduce in the rate of graft resorption) [22]. This clinical observation of graft preservation was made in an experimental study by Jensen et al. [28] testing expanded polytetrafluoroethylene (e-PTFE) membranes and autografts in the mandible. The control group with autografts alone showed significant graft resorption, whereas the test group with autografts protected by membranes demonstrated efficacious bone augmentation results [22].

After placement of the barrier membrane, the first biological interaction that occurs is the adsorption of plasma proteins at the

membrane–tissue interface. Proteins, generally, demonstrate a preference toward aqueous environments. However, when a protein solution comes into contact with another phase, the proteins have more affinity to accumulate at the interface. The interaction of proteins with the surface of the membrane is not only dependent on the protein structural and chemical properties but is also dependent upon the chemistry, morphology, and surface charge of the barrier membrane [29]. Surface wettability (generally referred to as hydrophobicity/hydrophilicity) is one of the important parameters affecting the protein adsorption on barrier membranes. Wettability affects protein adsorption, platelet adhesion/activation, blood coagulation, and cell and bacterial adhesion [30].

Generally, hydrophobic surfaces are considered to be more protein adsorbent than hydrophilic surfaces because of the strong hydrophobic interactions occurring at the hydrophobic surfaces in contrast to the repulsive solvation forces arising from strongly bound water at the hydrophilic surfaces (Fig. 19.3) [31]. Proteins adsorbed onto the barrier membranes after implantation attract specific growth factors and progenitor cells, which play a vital role toward tissue regeneration/repair.

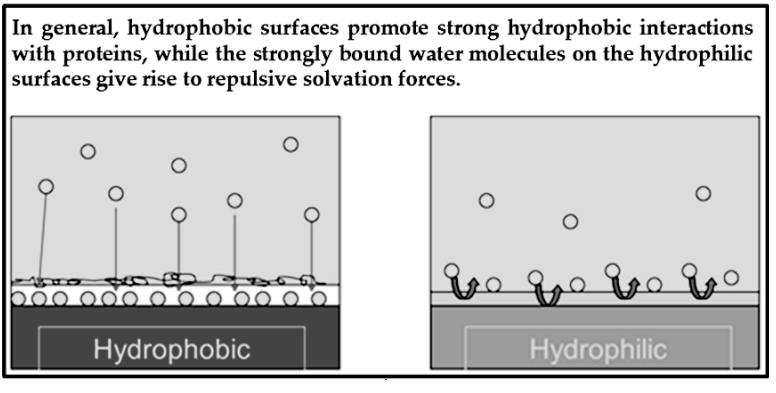

Figure 19.3 Illustration showing comparison between hydrophobic and hydrophilic surfaces in terms of protein adsorption.

In barrier membrane–protected defects, the vascular supply of newly formed tissue (soft or osseous) relies entirely on marrow-derived blood vessels (Fig. 19.4) [32, 33]. Thus, the preparation

of numerous perforations in cortical bone, which is also known as intramarrow penetration, is important to open the marrow cavity as a source of angiogenic and osteogenic cells. This ensures not only bleeding in/or at the defect site to achieve a blood clot around the applied grafts but also the activation of bone formation by the release of local and other bone-inducing factors [34].

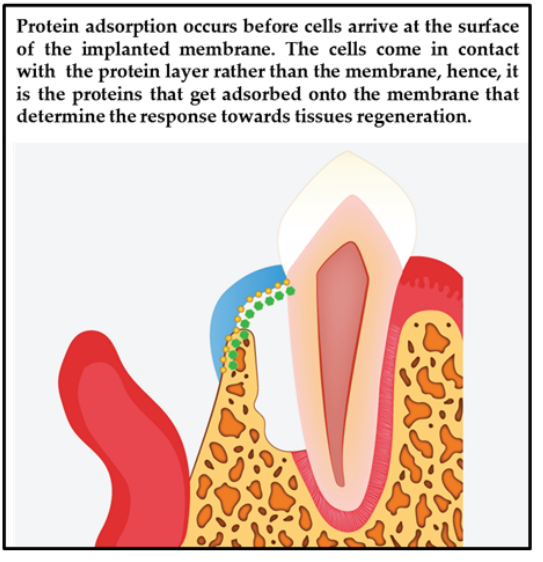

Figure 19.4 Illustration showing a barrier membrane placed around the periodontal defect. Yellow circles: proteins, green circles: cells. Courtesy of Ms. Esraa Khalil, Graphic Designer, Amman, Jordan.

19.4 Ideal Properties of Barrier Membranes

There are some important factors that need to be considered in the design of barrier membranes. These include biocompatibility, cell occlusivity, bioresorption, tear strength, stiffness, biological activity, and clinical manageability.

19.4.1 Biocompatibility

The material out of which the barrier membrane is made should elicit biofunctionality as well as maintain biosafety. It should not

evoke cytotoxicity, immune reactions, and/or cell lysis. The material should also not cause any metaplastic or neoplastic changes [35].

19.4.2 Cell Occlusivity

The membrane should function as a physical barrier against epithelial cells; otherwise, these faster-growing cells would populate the wound space and inhibit the regeneration of the periodontium. Hence, the membrane should enable cell exclusion, separate the gingival flap from the fibrin clot, and maintain space for the new alveolar bone and PDL [36].

19.4.3 Bioresorption

Ideally, the membrane should degrade after its functionality has been achieved, without leaving any residues. The degradation rate should match the physiological tissue formation rate [37].

19.4.4 Tear Strength

The material of the membrane should have high tear resistance so that it would have the ability to resist tearing and rupture that might occur during surgical handling and placement [38].

19.4.5 Stiffness

The membrane should be stiff enough to withstand the pressures exerted by overlying flaps and external forces like mastication, until the blood clot forming underneath the membrane has matured enough to provide support [39].

19.4.6 Biological Activity

Ideally, the barrier membrane should facilitate cell growth of PDL and bone. It should elicit biomimicry (imitate models and systems of natural biology) and be bioactive. Incorporation or contact of growth factors with the membrane should stimulate and enhance the regenerative potential of tissues. Potential release of antimicrobial substances could minimize the effects of microbial

contamination on regenerative outcomes. The membrane should have osteoconductive properties along with the bone graft, affecting bone formation toward the membrane surface and ultimately along the graft [40].

19.4.7 Clinical Manageability

The membrane should be moldable (yet stiff enough) and be easy to adapt by the clinician at the defect site [41].

19.5 Types of Barrier Membranes for Periodontal Guided Tissue Regeneration

The strategy to isolate a periodontal defect with a material (resorbable or nonresorbable) that will function as a physical barrier to avoid gingival cell invasion led toward the development of GTR/GBR membranes [13, 14, 42]. Various types of materials have been developed and explored for the preparation of barrier membranes (Fig. 19.5). Barrier membranes can be grouped together as either nonresorbable or resorbable membranes (Table 19.1). The words "biodegradable," "bioresorbable," and "bioabsorbable" are often used synonymously with each other in the scientific literature. However, according to definitions given by Vert [43, 44]:

Biodegradable refers to solid polymeric materials and devices that break down as a result of macromolecular degradation with dispersion in vivo, but there is no proof of elimination from the body. Biodegradable polymeric systems or devices can be attacked by biologic elements, which affects their stability and breaks them down into smaller fragments that can move away from their site of action but not necessarily from the body.

Bioresorbable refers to solid polymeric materials and devices that can degrade and further resorb in vivo, that is, that are eliminated through natural pathways either because of simple filtration of degradation by-products or after being metabolized. Thus, bioresorption is a concept that reflects total elimination of the initial foreign material and of degradation by-products (lower-molecular-weight compounds) with no residues. The use of the words *completely bioresorbable* assumes that elimination is shown conclusively and completely.

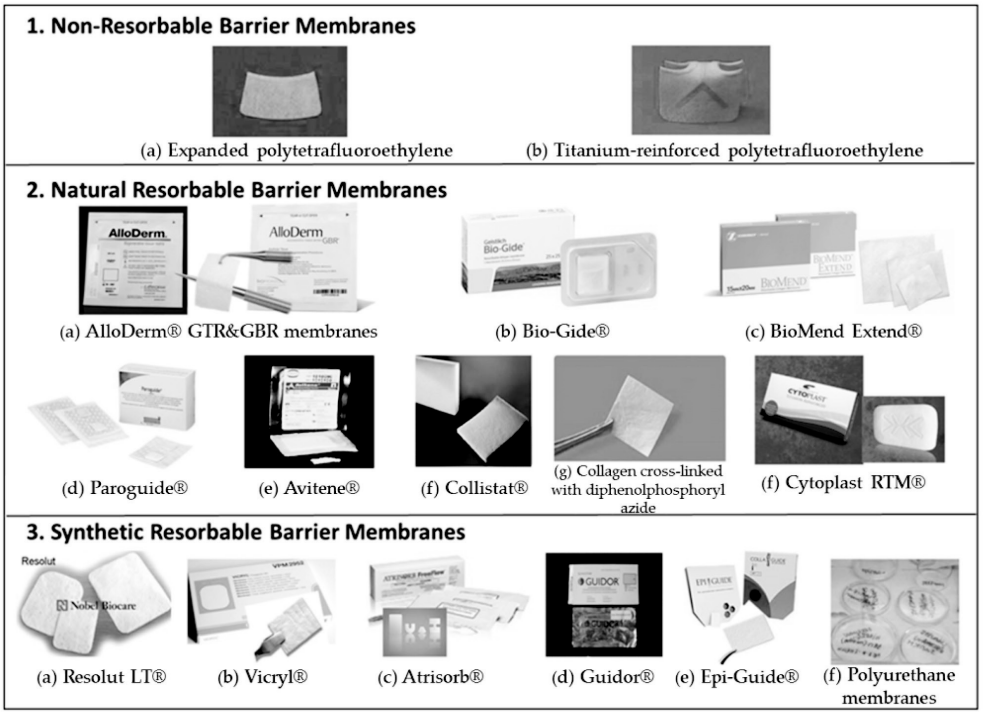

Figure 19.5 Nonresorbable and resorbable barrier membranes available for periodontal GTR and GBR therapy.

Table 19.1 List of some commonly used barrier membranes for GTR/GBR therapy

Resorbability	Barrier membrane	Composition
(a) Nonresorbable	Gore-Tex®	e-PTFE
	Cytoplast® TXT-200	d-PTFE
	Cytoplast® Ti-250	Ti-d-PTFE
(b) Resorbable: natural	AlloDerm®	Collagen type I derived from cadaveric human skin
	Bio-Gide®	Collagen derived from porcine skin (types I and III)
	BioMend Extend®	Collagen type I derived from bovine tendon
	Paroguide®	Collagen type I enriched with chondroitin sulphate
	Avitene®	Microfibrillar hemostatic collagen type I derived from bovine corium
	Collistat®	Hemostatic collagen type I material
	Collagen membrane (modified)	Collagen type I cross-linked by diphenolphosphorylazide
	Cytoplast RTM®	Collagen type I derived from bovine tendon
(c) Resorbable: synthetic	Resolut LT®	Poly-D,L-lactic/co-glycolic acid
	Vicryl Periodontal Mesh®	Polyglactin 910 Polyglycolide/polylactide (9:1, w/w)
	Atrisorb®	Double-layered poly-D,L-lactide and solvent (*N*-methyl-2-pyrrolidone)
	Guidor®	Three-layered polylactic acid and a citric acid ester acetyl tributylcitrate
	Epi-Guide®	D,D-L,L-polylactic acid
	Polyurethane-based barrier membrane	Polyetherurethane (-NH-CO-O-)
	Mempol®	PDS

Abbreviations: d-PTFE, high-density polytetrafluoroethylene; Ti-d-PTFE titanium-reinforced high-density PTFE; PDS, polydioxanon.

Bioabsorbable refers to solid polymeric materials or devices that can dissolve in body fluids without any polymeric chain cleavage or decrease in the molecular mass. Slow dissolution of water-soluble implants in body fluids is an example of this phenomenon. A bioabsorbable polymer can be considered bioresorbable if the dispersed macromolecules are excreted from the body.

For maintaining continuity and ease of reading the terms "nonresorbable" and "resorbable" will be used when discussing barrier membranes with respect to their in vivo degradation properties.

19.5.1 Nonresorbable Barrier Membranes

The first nonresorbable membranes that were used experimentally were constructed from Millipore® (cellulose acetate) filters. As this technique became more prevalent, commercial membranes were produced from Teflon® (PTFE). Successful use of nonresorbable membranes in GTR therapy led to the application of these membranes also in GBR procedures. Nonresorbable barriers maintain their structural integrity for as long as they are left in the tissues. The function of such barrier membranes is temporary, and once their function is completed, they are retrieved via surgery. This compositional and design stability of these nonresorbable membranes provides periodontists and trained clinicians with complete control over the time of application, with the potential to minimize variation in effectiveness.

Nonresorbable barrier membranes require a second surgical procedure for their removal, which raises concerns of patient acceptance, time, and possibility of surgical site morbidity. The regenerated tissues are susceptible to damage due physical trauma and risk of latent or postsurgical bacterial contamination [45]. Also, membrane exposure caused by variable amounts of flap sloughing during healing has been a frequent postsurgical complication associated with the use of nonresorbable membranes [46, 47]. The exposure of barrier membranes allows a communication between the oral environment and newly forming tissues, increasing the potential for infection and decreasing the likelihood of regeneration [26]. Although nonresorbable membranes are superior to open-flap debridement, they do not appear to be superior to demineralized

freeze-dried bone grafts as a stand-alone therapy [48]. Today, as evidence of the effectiveness of resorbable membranes increases, nonresorbable membranes are losing the importance in clinical practice that they once enjoyed, and their use is becoming limited [49].

Examples of two commonly used nonresorbable membranes in dentistry are e-PTFE and titanium-reinforced polytetrafluoroethylene (Ti-PTFE).

19.5.1.1 Expanded polytetrafluoroethylene

e-PTFE is a nonporous fluorocarbon polymer with exceptional inertness and biocompatibility. Hence, it prevents tissue ingrowth and does not elicit a foreign-body response after implantation. e-PTFE is chemically identical to PTFE and has been used in vascular surgeries for several decades. When PTFE is subjected to high tensile stresses, it expands, forming a porous microstructure known as e-PTFE. It is a polymer with high stability in biological systems that resists breakdown by host tissues and also by microbial species and does not elicit immunologic reactions. The e-PTFE membrane used for periodontal GTR (Cytoplast® TXT-200 high-density d-PTFE) consists of two parts, a collar portion (1 mm thick and 90% porous [11], with open pores that allow the ingrowth of connective tissue and prevent epithelial migration) and an occlusive portion (0.15 mm thick and 30% porous [50], which prevents flap tissues from coming into contact with the tooth root surface.

Effectiveness of e-PTFE membranes has been investigated in numerous clinical studies [14–17]. Some studies showed significant periodontal regeneration when e-PTFE membranes were used [15], whereas other studies showed no significant differences in the regeneration outcome between using e-PTFE membranes and conventional flap surgery with open debridement [18]. With successful GBR procedures, e-PTFE membranes became a standard for bone regeneration in the past [49].

19.5.1.2 Titanium-reinforced polytetrafluoroethylene

In situations where bone formation is desired in large defects or in supracrestal areas in the oral cavity, conventional e-PTFE membranes do not adequately maintain space unless supported by

bone graft materials. Because the space defined and protected by the membrane ultimately determines the volume of tissue that can potentially be regenerated, e-PTFE membranes were redesigned with a stiff central portion reinforced with titanium to treat both periodontal and osseous defects [50, 51]. This alternative approach, Ti-PTFE, involves the use of a double layer of PTFE with a titanium framework interposed (Cytoplast® Ti-250). Recent research has demonstrated the successful use of these membranes in vertical ridge augmentation and treatment of large defects in the alveolar process [52–54].

19.5.2 Resorbable Barrier Membranes

Due to the limitations of nonresorbable barrier membranes research in the last few decades has focused on the development of resorbable membranes suitable for clinical applications. Both natural and synthetic polymers have been used to fabricate bioresorbable materials used in the preparation of resorbable barrier membranes. The best-known groups of polymers used for this purpose are collagen and aliphatic polyesters. Currently tested and used membranes are made of collagen or of polyglycolide and/or polylactide or copolymers of them. Results of clinical applications in the early 1990s and thereafter reported (cases and case series) successful use of resorbable membranes for GBR [55–62]. However, clinical studies have revealed incidences of complications involving inflammation of the flap covering the site of regeneration and membrane exposure [63, 64].

Unfortunately, most of the available resorbable membranes are not capable of maintaining space as a stand-alone treatment modality due to their lack of rigidity. This limitation was overcome by supporting these membranes with autogenous or synthetic bone graft substitutes [56, 65, 66]. Other means of support such as screws, reinforcements, and pins have also been investigated with reasonable success [40, 67].

19.5.2.1 Natural resorbable barrier membranes

These membranes are produced using natural tissues from human or animal sources. Collagen has been used extensively for preparation of various biomedical devices because of its biologic

and physical properties [42, 54]. Collagen can be acquired from animal skin, tendons, or intestines. After isolation and purification by means of enzymatic preparation or chemical extraction, it is further processed to various forms [57]. The most common chemical modification is cross-linking, usually by aldehyde treatment, resulting in reduced absorption of water, decreased solubility, and increased tensile strength. Collagen has many desirable biological activities: it has low immunogenicity, attracts and activates PDL and gingival fibroblast cells, is hemostatic, and can potentially augment tissue thickness. Furthermore, it interacts with various cell types during wound healing [34, 40]. All these biological properties make collagen an attractive biomaterial for use in the synthesis of barrier membranes for guided regeneration applications. Some properties of collagen that are desirable for its use in the preparation of barrier membranes are that it:

- **Is hemostatic**: Collagen is a hemostatic agent and possesses the ability to stimulate platelet attachment and to enhance fibrin linkage, which facilitates initial clot formation and stabilization, leading to enhanced tissue regeneration [28].
- **Is easily manipulated and placed**: Collagen can be easily manipulated and adapted at the defect site by clinicians who increase the chance of successful GTR therapy (Fig. 19.6) [28].
- **Is well tolerated**: Barrier membranes made from bovine collagen do not elicit an antibody response when used in GTR therapy, because collagen has been demonstrated to be a weak immunogen and is therefore well tolerated by patients after placement [28].
- **Is chemotactic**: Collagen has been shown to be chemotactic for fibroblasts in vitro. This property could potentially enhance cell migration in vivo as well and promote regeneration [28].
- **Is bioresorbable**: Because collagen is bioresorbable, during enzymatic degradation it incorporates with the flap to support new connective tissue attachment [68]. This results in augmenting tissue/flap thickness to protect further bone formation.
- **Degrades slowly**: Membranes must remain in place until cells capable of regeneration are established at the wound site. Cross-linked collagen membranes have been shown to

last six to eight weeks before being absorbed, whereas non-cross-linked membranes lose their structural integrity within seven days [69].

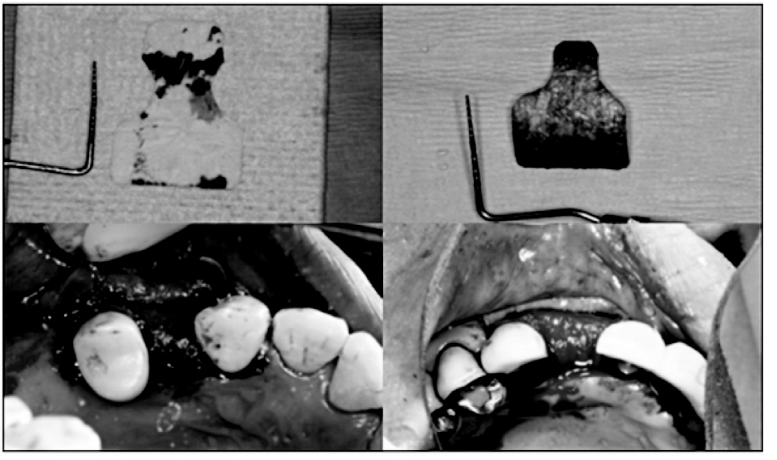

Figure 19.6 Bioresorbable collagen membrane being used in the GBR procedure. The membrane can be tailored and cut to exactly suit the defect before it is well adapted. Also noted is the high wettability of the membrane. Courtesy of Dr. Tom Wierzbicki, periodontist, Calgary, AB, Canada.

When it comes to biocompatibility, it was observed that PTFE inhibits gingival fibroblast DNA synthesis, while collagen membranes stimulate proliferation of these cells [59]. Moreover, osteoblasts show higher levels of adherence to surfaces of collagen than non-collagen-based barrier membranes. In terms of occlusivity, the period in which cross-linked collagen membranes remain intact and prevent apical proliferation of epithelium suffices, as the critical epithelial proliferation time is approximately 14 days [62].

Degradation of implanted resorbable barrier membranes is accomplished by various mechanisms present within the periodontal tissues. The primary structural component of most commercially available collagen membranes is degraded by endogenous collagenases into carbon dioxide and water. These enzymes are produced by macrophages and polymorphonuclear leukocytes. Moreover, some periodontal pathogens like *Porphyromonas gingivalis* also produce collagenases [15]. Cross-linking of collagen fibers is

inversely proportional to the rate of degradation in vivo, and the extent of resorption is greatly dependent on the collagen source and modifications. Collagenases initiate barrier membrane resorption at specific sites. The resulting fragments denature and become gelatin, which is further degraded to amino acids by gelatinases and other enzymes. Examples of some collagen-based resorbable membranes include:

- *AlloDerm*®: The AlloDerm® regenerative tissue matrix (RTM) is basically collagen type I derived from cadaveric human skin. Since its introduction to dentistry in 1994, it has been accepted as an acellular dermal matrix (ADM) for soft-tissue applications. AlloDerm® supports tissue regeneration by allowing rapid revascularization, white cell migration, and cell population. This results in the transformation into host tissue for a strong, natural repair. The thickness of this barrier membrane ranges from 0.9 mm to 1.6 mm. Applications include root coverage, gingival augmentation, soft-tissue ridge augmentation, and soft-tissue augmentation around implants [60]. AlloDerm GBR® RTM is manufactured utilizing the same process used for AlloDerm® RTM; however, AlloDerm GBR® RTM is used as an effective barrier membrane that transitions into the patient's own bone tissue. The thickness ranges from 0.5 mm to 0.9 mm, and applications include graft protection and containment and flap extension to achieve primary closure [63].
- *Bio-Gide*®: This is a barrier membrane synthesized from collagen types I and III derived from porcine skin. Several experimental studies have evaluated the regenerative potential of these collagen membranes. Bio-Gide® has been shown to resorb in eight weeks [65]; however, there was some evidence of a chronic inflammatory infiltrate present around the membrane, which disappeared after resorption, leading ultimately toward periodontal regeneration [43].
- *BioMend Extend*®: This GTR membrane is manufactured from type I collagen derived from the bovine Achilles tendon. The membrane is semiocclusive (pore size 0.004 μm) and resorbs in four to eight weeks. Clinical studies have revealed limited clinical effectiveness, which is seemingly dependent upon the form and size of the defect. The lack of success of guided

regeneration procedures using this membrane is probably due to the inadequate space maintenance that it provides [26, 28].

- *Paroguide*®: Paroguide® is a collagen type I membrane enriched with chondroitin sulphate. Parodi et al. [58] have reported regenerated PDL (which was verified through histology), cementum, and alveolar bone regeneration, with no signs of inflammation after insertion of this barrier membrane [42].
- *Avitene*®: This is a microfibrillar hemostatic collagen type I membrane derived from bovine corium. Histological evaluation after a clinical study has shown that this membrane was not very effective and is difficult to handle during the surgery [47].
- *Collistat*®: This is another hemostatic collagen type I material in which clinical evaluation has demonstrated guided regeneration outcomes similar to control treatment (without barrier membranes). Histological evaluation has indicated that the material completely resorbs seven days after implantation [5].
- *Collagen membrane cross-linked by diphenolphosphoryl azide*: Another type I collagen membrane, derived from the calf pericardium and cross-linked by diphenolphosphoryl azide, has been evaluated for GTR therapy. A histologically significant inflammatory reaction has been observed [36], but clinical studies have indicated effective GTR outcomes [42].
- *Cytoplast RTM*®: It is a barrier membrane synthesized with collagen type I derived from a bovine tendon. It is a multilayered long-lasting membrane with a resorption profile of 26–38 weeks. It has a fiber orientation that provides adequate handling and good tensile strength [43, 44].

19.5.2.2 Synthetic resorbable barrier membranes

Synthetic resorbable materials used in medical devices are usually organic aliphatic thermoplastic polymers. The most commonly used materials in the preparation of barrier membranes are poly-α-hydroxy acids, which include polylactic polyglycolic acid and their copolymers. One of the advantages of polyhydroxy acid is the

complete hydrolysis to the final products, water and carbon dioxide, which facilitates efficient clearance from the placement site. Usually, the degradation time varies and is dependent upon the presence of lactides or glycols [31]. Although high concentrations of degradation products can be toxic for cells, sufficient biocompatibility has been reported in the in vitro tests. Significant foreign-body reactions to porous polylactide polymer implants, interfering with alveolar bone formation, have also been observed [45]. Examples of some synthetic resorbable membranes are:

- *Resolute*®: Resolute® consists of an occlusive barrier membrane of glycolide and a lactic copolymer and a porous web of polyglycolide fiber (poly-D,L-lactic/co-glycolic acid). The occlusive membrane prevents cellular ingrowth, while the porous part promotes tissue integration. Histological studies have demonstrated similar effectiveness to nonresorbable membranes with a mean clinical attachment gain of 2 mm and with a gain of 4 mm or more in more than 85% of treated sites. It also showed structural retainment for four weeks and complete resorption five to six months after placement [4].
- *Vicryl Periodontal Mesh*®: Fibers of polyglactin 910, a copolymer of glycolide and l-lactide (polyglycolide/polylactide, 9:1, w/w), form a tightly woven mesh and are used to manufacture Vicryl Periodontal Mesh®. It has been reported that the membrane starts resorbing after two weeks of placement and loses its structural integrity, whereas it completely resorbs after four or more weeks [22, 39, 44]. Although animal studies indicate a lack of tissue integration and recession formation, clinical evaluation suggests effectiveness equal to that of other GTR barrier membranes [64, 40].
- *Atrisorb*®: The Atrisorb® membrane is the only barrier membrane that is prepared chair-side during the surgical procedure. A polylactic polymer is present in flowable form, dissolved in *N*-methyl-2-pyrrolidone (poly-D,L-lactide and solvent). The membrane is obtained by placing the polylactic polymer in a special cassette containing 0.9% saline for ~4–6 minutes. The resultant membrane has an irregular shape and is cut to the desired shape. Membrane thickness is approximately 600–750 μm, with limited adherence properties, and is placed

into the defect by applying gentle pressure. Histologically complete resorption has been observed 6–12 months after implantation [57, 60]. Clinical studies of guided regeneration have reported its efficacy in the treatment of periodontal defects [64].

- *Guidor*®: This is a double-layered resorbable membrane made of both polylactic acid and a citric acid ester known as acetyl tributylcitrate. The external layer of the barrier membrane is designed with rectangular perforation (400–500/cm^2), allowing the integration of the overlying gingival flap. This surface design successfully promotes tissue integration, and only limited gingival recession after usage has been reported [48, 64]. Between the internal and external layers, internal spacers are present that create space for tissue ingrowth. The internal layer has smaller circular perforations (4000–5000/cm^2) and outer spacers for maintaining the space between the membrane and the root surface. Clinical studies have proved the efficacy of this membrane in the treatment of various periodontal defects [64].
- *Epi-Guide*®: It is a porous three-layered and three-dimensional barrier membrane made of polylactic acid polymers (D-, D-L-, L-polylactic acid). It is designed to stop proliferation and migration of epithelial cells and fibroblasts into the defect. The three-layered construction of the membrane attracts, traps, and retains fibroblasts and epithelial cells, while maintaining space around a bony defect to develop bone and periodontal support tissues. The membrane maintains its structure for 20 weeks and is fully resorbed by 6–12 months. The Epi-Guide® barrier is a self-supporting membrane and can be used in many guided regeneration situations without support from bone-grafting materials [52, 56].
- *Polyurethane-based barrier membranes*: Polyurethanes are organic polymers containing multiple urethane groups (-NH-CO-O-) and are materials with diverse properties. Polyetherurethanes are degraded through enzymatic and oxidative degradation. The use of polyurethanes for barrier membrane production has been evaluated, and animal experiments have shown that polyurethane membranes tend to swell up after placement [28, 69]. There are also reports of

inflammation at the flap margins and recession being more pronounced than with polylactic membranes.

- *Mempol®*: The experimental Mempol® membrane is manufactured from PDS and has a bilayer structure. The first layer is completely nonpermeable, covered with PDS loops that are 200 μm long on the gingival side and facilitate integration with connective tissue. Using Mempol® membranes results in more frequent recession during the healing phase compared to using polylactic membranes, such as Guidor®; however, both types of membranes demonstrate comparable clinical efficacy for GTR [46].

19.6 Factors Influencing Success of Guided Regeneration Therapy Using Barrier Membranes

A number of factors have been reported to affect the success of periodontal regeneration.

19.6.1 Plaque Control and Microbial Contamination

It is well established that plaque control is a critical determinant in the success or failure of periodontal therapy [70]. Barrier membranes after implantation encourage bacterial contamination at the local site [71] and appear to harbor periodontal pathogens on a frequent basis. Clinical studies have found relatively high levels of bacterial contamination of e-PTFE membranes [72]. Even with regular antimicrobial chlorhexidine rinses, gram-negative anaerobic rods, commonly associated with adverse periodontal conditions, are detected. During the active healing phase, it has been observed that GTR sites are more likely to be colonized by periodontal bacteria than sites treated without membranes. The detrimental effects of plaque accumulation have been well described in longitudinal studies of GTR procedures [73].

The presence and accumulation of plaque in the local area of GTR therapy are associated with significantly less gain in the clinical attachment levels and decreased bone fill [74]. Therefore, it is absolutely essential to inform and instruct patients undergoing

the periodontal regeneration procedure about of the importance of maintaining excellent oral hygiene.

19.6.2 Defect Morphology and Tooth Anatomy

The morphology of periodontal defects and tooth anatomy have a significant influence on the success of guided regeneration procedures. The overall defect depth and the number of associated bony walls are critical to the success of regenerative therapy. Studies focused on factors affecting healing of intraosseous defects treated by GTR have identified that increased total depth of the intraosseous component of a defect tends to affect the success of guided regeneration therapy. Greater distances required for cellular repopulation of the wound lead to higher possibility of incomplete bone fill. Enamel projections, lingual grooves, irregularities in root morphology, bifurcation ridges, and other factors related to tooth anatomy have been implicated in periodontal disease, primarily because they favor plaque accumulation [75]. Such factors adversely affect the success of regenerative procedures.

19.6.3 Membrane Exposure

Complete primary closure is crucial for preventing early exposure. However, one of the most frequent postoperative complications of guided regeneration therapy is the exposure of barrier membranes to the oral cavity [49]. Barrier membrane exposure usually occurs due to postoperative soft-tissue dehiscence. Another cause of early exposure is necrosis of a thin flap of gingival tissue covering the barrier membrane and closure of the defect with an overly thick flap, which may result in tissue tension and subsequent dehiscence. In the case of an exposure, it is imperative that thorough debridement and plaque control of the exposed area are exercised to avoid infection. Membrane exposure reduces bone fill remarkably, and less bone regeneration around immediate implants sites is observed when exposed membranes are compared to nonexposed membrane sites [76]. Frequent patient follow-up sessions and thorough management of the exposed area are essential in early membrane exposure. Intensive professional postoperative oral hygiene helps counter the problem because it reduces the likelihood of infection [77].

19.6.4 Defect Space Maintenance

Space maintenance is a desirable property in a barrier membrane, and nonrigid membranes reinforced with titanium strips or meshes can be shaped to conform to the desired ridge morphology with the purpose of preventing membrane collapse within the defect [78]. In addition to membrane rigidity, other means of providing space maintenance include the use of tenting screws, corticocancellous osseous block grafts, osseous particulate grafts, and binding agents in combination with osseous graft materials [77, 78].

19.6.5 Diabetes

Although many systemic diseases can affect tissue regeneration directly or indirectly, uncontrolled diabetic patients with elevated glucose levels increase the risk for failure of regenerative procedures. A delayed wound-healing response is most likely the result of poor control and regulation of glucose metabolism on the inflammatory process. Improved serum glucose–level control is currently the only practical approach to managing this risk factor [79].

19.6.6 Gingival Flap Thickness

The thickness of the gingival flap covering the membrane is critical for the success of guided regeneration procedures. In GTR therapy, blood supply to the flaps depends on their thickness. Blood supply from the bone to the flap is usually impeded by the barrier membrane, and to maintain blood supply to the flaps, and to prevent flap necrosis, more than 1.5 mm gingival thickness is a prerequisite. If GTR or GBR is performed in deep osseous defects with thin gingival flaps in the maxillary anterior region, recession of the interdental papilla or gingival tissue can frequently occur [80].

19.6.7 Smoking

Smoking adversely affects the success rate of guided regeneration procedures. Retrospective analyses of longitudinal studies of GTR procedures in class II furcations have reported a 42% failure rate after at least four years. Of those failures, 80% were in patients

who smoked at least 10 cigarettes per day for five years, indicating a potential dose–response relationship [81]. It has been observed that one year after a GTR procedure, smokers (~10 cigarettes per day) possess a significantly less favorable gain in probing the attachment level when compared to nonsmokers. GTR therapy has also been compared to root-planing therapy alone in smokers versus nonsmokers. In most cases, both the GTR site and the root-planing site in patients respond concordantly. Sites treated with both techniques remained stable in nonsmoking patients who also have good oral hygiene and are compliant with recall visits. Those patients in whom both sites deteriorate are smokers with compromised oral hygiene during the follow-up period [81].

19.7 Summary and Future Considerations

The concepts of GTR and GBR, along with the incorporation of barrier membranes in clinical practice, have changed the outlook for periodontal regeneration and bone augmentation therapeutics significantly. The use of barrier membranes can lead to marked periodontal regeneration, although complete regeneration has never been reported. Current resorbable and nonresorbable membranes act as a physical barrier to avoid connective and epithelial tissue downgrowth into the defect, favoring the regeneration of periodontal tissues. These conventional membranes possess many structural, mechanical, and biofunctional limitations. The main advantage of resorbable membranes is avoiding a second surgical procedure, which is required when nonresorbable membranes are employed. Considerations of material properties and design should be important to the clinician in choosing a particular device; however, the ultimate test for the success or failure of any device is clinical outcome. The treatment of furcation defects with a combination of barrier membranes and bone replacement grafts appears to produce greater clinical improvements than GTR alone.

Nonresorbable membranes are superior to open-flap debridement but are not superior to demineralized freeze-dried bone grafts as a stand-alone therapy. Due to the inherent limitations of nonresorbable barrier membranes, recent research has been focused on the development of resorbable membranes suitable for

clinical applications. Both natural and synthetic polymers are used to fabricate bioresorbable barrier membranes. The best-known groups of polymers used for this purpose are collagen and aliphatic polyesters. Further investigations highlighting factors influencing the regenerative procedure will improve predictability of therapies of bone defects around natural teeth and dental implants.

In conclusion, the future appears exciting for periodontal tissue engineering, and barrier membranes promise to continue playing a critical role. It will require a team effort engaging the expertise of biomaterials scientists/engineers, cell biologists, matrix biologists, microbiologists, molecular biologists, nanotechnologists, immunologists, pharmacologists, and of course periodontists toward the development of more efficacious membranes, graft materials, and surgical techniques.

References

1. Newman, M. G., Takei, H. H., Carranza, N. T. (2012) *Carranza's Clinical Periodontology*, 11th ed., Saunders Elsevier, St-Louis, MO, USA.
2. Giannobile, W. V., Somerman, M. J. (2003) Growth and amelogenin-like factors in periodontal wound healing. A systematic review, *Ann. Periodontol.*, **8**, 193–207.
3. Taba, M., Jr., Jin, Q., Sugai, J. V., Giannobile, W. V. (2005) Current concepts in periodontal bioengineering, *Orthod. Craniofac. Res.*, **8**, 292–312.
4. Sculean, A., Nikolidakis, D., Schwarz, F. (2008) Regeneration of periodontal tissues: combinations of barrier membranes and grafting materials-biological foundation and preclinical evidence: a systematic review, *J. Clin. Periodontol.*, **35**, 106–123.
5. Wang, H. L. (2005) Periodontal regeneration, *J. Periodontol.*, **76**, 1601–1624.
6. Yang, F., Both, S. K., Yang, X. C., Walboomers, X. F., Jansen., J. A. (2009) Development of an electrospun nano-apatite/PCL composite membrane for GTR/GBR application, *Acta Biomater*., **5**, 3295–3319.
7. Nakashima, M., Reddi, A. H. (2003) The application of bone morphogenetic proteins to dental tissue engineering, *Nat. Biotech*., **21**, 1025–1040.
8. Trombelli, L. (2005) Which reconstructive procedures are effective for treating the periodontal intraosseous defect? *Periodontol. 2000*, **37**, 88–103.

9. Jung, E. R., Glauser, R., Scharer, P., Hammerle, C. F. H., Sailer, F. H., Weber, E. F. (2003) Effect of rhBMP-2 on guided bone regeneration in humans-a randomized, controlled clinical and histomorphometric study, *Clin. Oral Implants Res*., **14**, 556–571.
10. Nyman, S., Lindhe, J., Karring, T., Rylander, H. (1982) New attachment following surgical treatment of human periodontal disease, *J. Clin. Periodontol.*, **9**, 290–306.
11. Nyman, S., Gottlow, J., Karring, T., Lindhe, J. (1982) The regenerative potential of the periodontal ligament. An experimental study in the monkey, *J. Clin. Periodontol.*, **9**, 257–271.
12. Nyman, S., Gottlow, J., Lindhe, J., Karring, T., Wennstrom, J. (1987) New attachment formation by guided tissue regeneration. *J. Periodont. Res.*, **22**, 252–268.
13. Karring, T., Nyman, S., Gottlow, J., Laurell, L. (1993) Development of the biological concept of guided tissue regeneration-animal and human studies, *Periodontol. 2000*, **1**, 26–41.
14. Linde, A., Alberius, P., Dahlin, C., Bjurstam, K., Sundin, Y. (1993) Osteopromotion: a soft-tissue exclusion principle using a membrane for bone healing and bone neogenesis, *J. Periodontol.*, **64**, 1116–1133.
15. Geurs, N. C., Korostoff, J. M., Vassilopoulos, P. J., Kang, T. H., Jeffcoat, M., Kellar, R. (2008) Clinical and histologic assessment of lateral alveolar ridge augmentation using a synthetic long-term bioabsorbable membrane and an allograft, *J. Periodontol.*, **79**, 1133–1148.
16. Piattelli, A., Scarano, A., Russo, P., Matarasso, S. (1996) Evaluation of guided bone regeneration in rabbit tibia using bioresorbable and non-resorbable membranes, *Biomaterials*, **17**, 791–807.
17. Behring, J., Junker, R., Walboomers, F. X., Chessnut, B., Jansen, A. J. (2008) Toward guided tissue and bone regeneration: morphology, attachment, proliferation, and migration of cells cultured on collagen barrier membranes. A systematic review, *Odontology*, **96**, 1–13.
18. Polimeni, G., Koo, K. T., Pringle, G. A., Agelan, A., Safadi, F. F., Wikesjo, E. (2008) Histopathological observations of apolylactic acid-based device intended for guided bone/tissue regeneration. *Clin. Implant Dent. Res*., **10**, 99–112.
19. Position paper: periodontal regeneration. (2005) *J. Periodontol.*, **76**, 1601–1622.
20. Hitti, A. R., Kerns D. G. (2011) Guided bone regeneration in the oral cavity: a review, *Open Pathol. J*., **5**, 33–45.
21. Frank, A. Scannapieco. (2005) Periodontal regeneration techniques for treatment of periodontal diseases, *Dent. Clin. N. Am*., **49**, 637–659.

22. Buser, D., Dula, K., Belser, U., Hirt, H. P., Berthold, H. (1993) Localized ridge augmentation using guided bone regeneration. Surgical procedure in the maxilla, *Int. J. Periodont. Restorative Dent.*, **13**, 29–37.

23. Retzepi, M., Donos, N. (2010) Guided bone regeneration: biological principle and therapeutic applications, *Clin. Oral Implants Res.*, **21**, 567–581.

24. Murphy, K. G., Gunsolley, J. C. (2003) Guided tissue regeneration for the treatment of periodontal intrabony and furcation defects. A systematic review, *Ann. Periodontol.*, **8**, 266–281.

25. Sander, L., Karring, T. (1995) New attachment and bone formation in periodontal defects following treatment of submerged roots with guided tissue regeneration, *J. Clin. Periodontol.*, **22**, 295–299.

26. Wang, H. L., Carroll, M. J. (2001) Guided bone regeneration using bone grafts and collagen membranes, *Quintess. Int.*, **32**, 504–515.

27. Slavkin, C. H., Bartold, B. H. (2006) Challenges and potential in tissue engineering, *Periodontol. 2000*, **41**, 9–15.

28. Jensen, O. T., Greer, R. O., Johnson, L., Kassebaum, D. (1995) Vertical guided hone-graft augmentation in a new canine mandibular model, *Int. J. Oral Maxillofac. Implants*, **10**, 335–344.

29. McClellan, J. S., Franses, E. I. (2005) Adsorption of bovine serum albumin at solid/aqueous interfaces, *Colloids Surf. A: Physicochem. Eng. Aspects*, **260**, 265–275.

30. Vogler, A. E. (1999) Water and the acute biological response to surfaces, *J. Biomater. Sci. Polym. Ed.*, **10**, 1015–1045.

31. Israelachvili, J., Wennerstrom, H. (1996) Role of hydration and water structure in biological and colloidal interactions, *Nature*, **379**, 219–225.

32. Schenk, K. R., Buser D., Hardwick R. W., Dahlin, C. (1994) Healing pattern of bone regeneration in membrane-protected defects. A histologic study in the canine mandible, *Int. J. Oral Maxillofac. Implants*, **9**, 13–29.

33. Buser, D., Dahlin, C., Schenk, R. K. (1994) *Guided Bone Regeneration in Implant Dentistry*, Quintessence, Chicago, IL, USA.

34. Buser, D., Dula, A. K. (1999) Localized ridge augmentation with autografts and barrier membranes, *Periodontol. 2000*, **19**, 151–163.

35. DeSanctis, M., Clauser, C., Zucchelli, G. (1996) Bacterial colonization of resorbable barrier materials and periodontal regeneration, *J. Periodontol.*, **67**, 1193–1200.

36. Minabe, M. (1991) Article review of biologic rationale for guided tissue regeneration, *J. Periodontal*., **62**, 171–179.

37. Gary, H. T. (2002) Biodegration of polyurethanes: a review, *Int. Biodeg. Bio.*, **49**, 245–252.

38. Gotfredsen, K., Nimb, L., Hansen, E. H. (1994) Immediate implant placement using a biodegradable barrier, polyhydroxybutyrate-hydroxyvalerate reinforced with polyglactin 910, *Clin. Oral Implants Res*., **5**, 83–91.

39. Mellonig, J. T., Triplett, G. R. (1993) Guided tissue regeneration and endosseous dental implants, *Int. J. Periodont. Restorative Dent*., **13**, 108–19.

40. Selvig, A. K., Nilveus, E. R., Fitzmorris, L., Khorsandi, S. S. (1990) Scanning electron microscopic observations of cell population and bacterial contamination of membranes used for guided periodontal tissue regeneration in humans, *J. Periodontol.*, **61**, 515–520.

41. Robert, M. P., Frank M. R. (1994) Periodontal guided tissue regeneration with a new resorbable polylactic acid membrane, *J. Periodontol.*, **65**. 414–422.

42. Magnusson, I., Batich, C., Collins, B. R. (1998) New attachment formation following controlled tissue regeneration using biodegradable membranes, *J. Periodontol.*, **59**, 1–13.

43. Vert, M. (1989) Bioresorbable polymers for temporary therapeutic applications, *J. Periodontol.*, **167**, 155–168.

44. Vert, M., Li, M. S., Spenlehauer, G., Guerin, P. (1992) Bioresorbability and biocompatibility of aliphatic polyesters, *J. Mater. Sci. Mater. Med.*, **3**, 432–446.

45. Dimitrin, S., Tatkias, N., Anaypr, O., Wikesjo, E. (1999) Devices for periodontal regeneration, *Periodontol. 2000*, **19**, 59–73.

46. Lang, N. P., Hammerle, C. H., Bragger, U., Lehmann, B., Nyman, R. S. (1994) Guided tissue regeneration in jawbone defects prior to implant placement, *Clin. Oral Implants Res.*, **5**, 77–92.

47. Murphy, K. G. (1995) Postoperative healing complications associated with Gore-Tex periodontal material. Part I. Incidence and characterization, *Int. J. Periodont. Restorative Dent*., **15**, 363–375.

48. Laurell, L., Gottlow, J., Zybutz, M. (1998) Treatment of intrabony defects by different surgical procedures. A literature review, *J. Periodontol.*, **69**, 303–313.

49. Hammerle, C. F., Jung, E. R. (2003) Bone augmentation by means of barrier membranes, *Periodontol. 2000*, **33**, 36–53.

50. Scantlebury, T. V. (1993) 1982–1992: a decade of technology development for guided tissue regeneration, *J. Periodontol.*, **64**, 1129–1137.

51. Hardwick, R., Hayes, B.K, Flynn, C. (1995) Devices for dentoalveolar regeneration: an up-to-date literature review, *J. Periodontol.*, **66**, 495–505.

52. Jovanovic, A. S., Nevins, M. (1995) Bone formation utilizing titanium-reinforced barrier membranes, *Int. J. Periodont. Restorative Dent.*, **15**, 57–69.

53. Simion, M., Jovanovic, A. S., Trisi, P., Scarano, A., Piattelli, A. (1998) Vertical ridge augmentation around dental implants using a membrane technique and autogenous bone or allografts in humans, *Int. J. Periodont. Restorative Dent.*, **18**, 9–23.

54. Tinti, C., Parma-Benfenati, S., Polizzi, G. (1996) Vertical ridge augmentation: what is the limit? *Int J. Periodont. Restorative Dent.*, **16**, 220–229.

55. Zitzmann, N. U., Naef, R., Schiipbach, P., Scharer, P. (1996) Sofortoder verzogertes Sofortimplantat versus Spatimplantat bei Anwendung der Prinzipien der gesteuerten Knochenregeneration, *Acta Med. Dent. Helv.*, **1**, 221–227.

56. Parodi, R., Santarelli, G., Carusi, G. (1996) Application of slow-resorbing collagen membrane to periodontal and peri-implant guided tissue regeneration, *Int. J. Periodont. Restorative Dent.*, **16**, 174–185.

57. Pajarola, F. G., Sailer, E. H. Studer, S. (1993) Steuerung der Knochenregeneration um Implantatpfeiler durch eine resorbierbare Folie, *Z. Zahnarztl. Implantol.*, **9**, 181–183.

58. Mayfield, L, Nobreus N, Attstrom R, Linde A. (1997) Guided bone regeneration in dental implant treatment using a bioabsorbable membrane, *Clin. Oral Implants Res.*, **8**, 10–17.

59. Lundgren, D., Sennerby, L., Falk, H., Friberg, B., Nyman, S. (1994) The use of a new bioresorbable barrier for guided bone regeneration in connection with implant installation, *Clin. Oral Implants Res.*, **5**, 177–184.

60. Hurzeler, B. M., Weng, D., Hutmacher, D. (1996) Knochenregeneration um Implantate-eine klinische Studie mit einer neuen resorbierbaren Membran, *Dtsch. Zahnarztl. Z.*, **51**, 2–7.

61. Hurzeler, B. M, Strub, J. R. (1995) Guided bone regeneration around exposed implants: a new bioresorbable device and bioresorbable membrane pins, *Pract. Periodont. Aesthet. Dent.*, **7**, 37–47.

62. Balshi, J. T, Hernandez, E. R, Cutler, H. R., Hertzog, C. E. (2002) Treatment of osseous defects using Vicryl mesh (polyglactin 910) and the Branemark implant: a case study, *J. Periodontol.*, **86**, 215–235.

63. Zitzmann, N., Naef, R., Scharer, I. (1996) Gesteuerte Knochenregeneration und Augmentation in der Implantatchirurgie mit Bio-Oss und Membrantechniken, *Dtsch. Zahnarztl. Z.*, **2**, 35–52.

64. Simion, M., Misitano, U., Gionso, L., Salvato, A. (1997) Treatment of dehiscences and fenestrations around dental implants using resorbable and nonresorbable membranes associated with bone autografts: a comparative clinical study, *Int. J. Oral Maxillofac. Implants*, **12**, 159–167.

65. Schliephake, H., Neukam, F. W., Hutmacher, D., Becker, J. (1994) Enhancement of bone ingrowth into a porous hydroxylapatite- matrix using a resorbable polylactic membrane. An experimental pilot study, *J. Oral Maxillofac. Surg.*, **52**, 25–42.

66. Avera, I. S., Stampley, A. W, McAllister, B. S. (1997) Histologic and clinical observation of resorbable and nonresorbable barrier membranes used in maxillary sinus graft containment, *Int. J. Oral Maxillofac. Implants*, **12**, 88–94.

67. Kostopoulos, L., Karring, T. (1994) Augmentation of the rat mandible using guided tissue regeneration, *Clin. Oral Implants Res.*, **5**, 75–82.

68. Pitaru, S., Tal, H., Soldinger, M., Noff, M. (1989) Collagen membranes prevent apical migration of epithelium and support new connective tissue attachment during periodontal wound healing in dogs, *J. Periodontal Res.*, **24**, 247–253.

69. Blumenthal, N. M. (1988) The use of collagen membranes to guide regeneration of new connective tissue attachment in dogs, *J. Periodontol.*, **59**, 830–836.

70. Kornman, K. S., Robertson, P. B. (1999) Fundamental principles affecting the outcomes of therapy for osseous lesions, *Periodontol. 2000*, **22**, 22–43.

71. Passariello, C., Thaller, M. C., Selan, L., Berlutti, F., Renzini, G. (1991) Periodontal regeneration procedures may induce colonization by glycocalyxproducing bacteria, *Med. Microbiol. Immunol.*, **180**, 67–72.

72. Simion, M., Trisi, P., Maglione, M., Piattelli, A. (1994) A preliminary report on a method for studying the permeability of expanded polytetrafluoroethylene membrane to bacteria *in vitro*: a scanning electron microscopic and histological study, *J. Periodontol.*, **65**, 755–761.

73. Mombelli, A., Zappa, U., Bragger, U., Lang, N. P. (1996), Systemic antimicrobial treatment and guided tissue regeneration. Clinical and microbiological effects in furcation defects, *J. Clin. Periodontol.*, **23**, 386–396.

74. Hugoson, A., Ravald, N., Fornell, J., Johard, G., Teiwik, A., Gottlow, J. (1995) Treatment of class II furcation involvements in humans with bioresorbable and non-resorbable guided tissue regeneration barriers. A randomized multi-center study, *J. Periodontol.*, **66**, 624–634.

75. Tonetti, M. S., Pini-Prato, G., Cortellini, P. (1993) Periodontal regeneration of human intrabony defects. IV. Determinants of healing response, *J. Periodontol.*, **64**, 934–940.

76. Becker, W., Dahlin, C., Becker, B. E. (1994) The use of e-PTFE barrier membranes for bone promotion around titanium implants placed into extraction sockets: a prospective multicenter study, *Int. J. Oral Maxillofac. Implants*, **9**, 31–40.

77. Shanaman, R. H. (1994) A retrospective study of 237 sites treated consecutively with guided tissue regeneration, *Int. J. Periodont. Restorative Dent.*, **14**, 292–301.

78. Schwartz-Arad, D., Levin, L., Sigal, L. (2005) Surgical success of intraoral autogenous block onlay bone grafting for alveolar ridge augmentation, *Implant Dent.*, **14**, 131–138.

79. Kramer, G. M. (1992) Surgical alternatives in regenerative therapy of the periodontium, *Int. J. Periodont. Restorative Dent.*, **12**, 10–31.

80. Rosenberg, E. S., Cutler, S. A. (1994) The effect of cigarette smoking on the longterm success of guided tissue regeneration: a preliminary study, *Ann. R. Australas. Coll. Dent. Surg.*, **12**, 89–93.

81. Tonetti, M. S., Pini-Prato, G., Cortellini, P. (1995) Effect of cigarette smoking on periodontal healing following GTR in infrabony defects. A preliminary retrospective study, *J. Clin. Periodontol.*, **22**, 229–234.

This page intentionally left blank

"*This is a comprehensive textbook covering all currently used materials in dentistry, including the recent methodology used to develop and evaluate these materials.* Handbook of Oral Biomaterials *is a timely contribution for all clinicians.*"

Prof. Nabil Samman
Editor in Chief, *International Journal of Oral and Maxillofacial Surgery*

"*With the fast pace of new discoveries and development of new oral biomaterials, there are great need and demands from dental students, faculty staff, and clinicians for a comprehensive textbook which compiles the updated scientific evidence on oral biomaterials and provides guidance on their appropriate applications. This book responds well to the above need and contributes greatly to the dissemination of useful knowledge in the field.*"

Prof. Edward C. M. Lo
University of Hong Kong, Hong Kong

"*There has been an obvious gap in having a comprehensive and easy-to-read textbook of biomaterials for dental education. I am delighted to see that the needs for this have now been satisfied. I strongly believe that with this book, thanks to its editor Dr. Matinlinna, the readers will gain a deep insight into modern dental bio- and other materials used in dentistry today.*"

Prof. Jukka H. Meurman
University of Helsinki, Finland

"*This book provides a good update on the properties and behavior of materials used in dentistry. It will be useful for undergraduate and postgraduate students in dentistry, and it is also handy for academics involved in the teaching of dental materials. The chapters on implants, membranes for GTR, titanium, and zirconia will certainly benefit clinicians.*"

Prof. Mohamed Ibrahim Abu Hassan
Universiti Teknologi MARA, Malaysia

This book introduces the latest advances in dental materials and biomaterials science. It contains a comprehensive introduction and covers ceramic, metallic, and polymeric oral biomaterials. It is addressed to teachers, instructors, tutors, undergraduate students, and postgraduate students of dental and medical schools and provides a deep insight into the materials being taught for use in clinical practice. The contributing authors are from all over the world and are distinguished in their disciplines. A solid primer for dental students, the book is also highly recommended for students of engineering and basic science who want to gain an insight in contemporary biomaterials science. For medical practitioners, the book offers an invaluable opportunity to learn about the latest steps in dental biomaterials.

Jukka P. Matinlinna is associate professor in dental materials science at the University of Hong Kong. His main field of activity, in addition to undergraduate and postgraduate dental teaching, is dental biomaterials with regard to adhesion and system simulations, with special focus on contemporary dental biomaterials in prosthetic dentistry and implant dentistry; silane chemistry; adhesion promotion; saliva chemistry; dentin bonding; porcelain and resin bonding to zirconia, other ceramic materials, and Ti; experimental primers and resins; E-glass fiber–reinforced restorations; and finite element analysis. Since 2004 he has contributed to more than 200 publications and has been a member of the editorial boards of several scientific journals.

V387
ISBN 978-981-4463-12-6
9 789814 463126

PAN STANFORD PUBLISHING
www.panstanford.com